



TNF
Workshop

PTF
Workshop

22-23 July 2022 Vancouver, Canada





SPONSORS



SFB/Transregio 150
Turbulente, chemisch reagierende
Mehrphasenströmungen in Wandnähe



TECHNISCHE
UNIVERSITÄT
DARMSTADT





TNF15/PTF17 Workshop Proceedings – Table of Contents

Cover Page	1
Workshop Sponsors	2
Table of Contents	3
Workshop Summary	6
TNF Registration List	9
PTF Registration List	11
PTF Workshop Presenters and Titles	12
Workshop Organizers	13
Agenda - Friday	15
Agenda - Saturday	16
TNF Session: Modeling Turbulent H₂ Flames	17
<i>Coordinators: Heinz Pitsch, Lukas Berger, Andy Aspden and Antonio Attili</i>	
Summary	17
Slides – Introduction – <i>Pitsch</i>	18
Slides – Thermodiffusive Instabilities in H ₂ Flames – <i>Berger</i>	19
Slides – Thermal Leading Points in Lean Premixed H ₂ Flames – <i>Howarth</i>	31
Slides – Pressure Effects in Hydrogen-Enriched Flames – <i>Rieth</i>	36
Slides – Available Experimental and Numerical Data Sets – <i>Pitsch</i>	45



TNF Session: Combustion of Ammonia as Energy/Hydrogen Carrier	51
<i>Coordinators: Andrea Gruber and Gaetano Magnotti</i>	
Summary	51
Slides – DNS of Ammonia Combustion Configurations – <i>Gruber</i>	54
Slides – Canonical Turbulent Jet Flames Fueled by Ammonia/Hydrogen/Nitrogen Blends – <i>Magnotti</i>	73
PTF Contributed Talks: Ammonia	94
Slides – Combustion characteristics of ammonia/air premixed turbulent flame at high pressure and high temperature – <i>Hayakawa</i>	95
TNF Session: Multi-Regime Burner (MRB)	99
<i>Coordinators: Dirk Geyer, Robert Barlow, Christian Hasse and Benoit Fiorina</i>	
Summary	99
Slides – Introduction to the burner and measurements – <i>Geyer</i>	101
Slides – Experimental Flame Regime Analysis – <i>Barlow</i>	110
Slides – Numerical Flame Regime Analysis – <i>Hasse</i>	113
Slides – Joint numerical-experimental comparison and analysis – <i>Fiorina</i>	117
PTF Contributed Talks: Flame Structure and Speed	157
Slides – Turbulent Premixed Flames in a Box – <i>Hamlington</i>	158
Slides – How Different is Burning Turbulence? – <i>Steinberg</i>	163
Slides – Role of Non-Flamelets in Estimating How Fast Turbulent Premixed Flames Burn – <i>Kheirkhah</i>	169
Slides – Turbulent Flames Speed Based on the Mass Flow Rate – <i>Chaudhuri</i>	183
Summary & Slides– Closing the Balance of Progress of Reaction on a Turbulent Bunsen Flame & Adaptive PIV Interogation for Spherical Propagation – <i>Hochgreb</i>	191
Friday Panel Discussion: Topics of Interest	203
<i>Panel: Peter Hamlington, Heinz Pitsch, Adam Steinberg, Fabian Hampp</i>	
<i>Moderator: Sina Kheirkhah</i>	
Slides – Engineering Relevance & Community-Wide Code Dev. – <i>Hamlington</i>	204
Slides – Low and Zero Impact Energy Transformation – <i>Pitsch</i>	205
Slides – Flames that Keep Me Awake at Night – <i>Steinberg</i>	208
Slides – Fuel Flexibility – <i>Hampp</i>	209



TNF Session: Flame-Wall Interaction	211
<i>Coordinators: Christian Hasse and Andreas Dreizler</i>	
Summary	211
Slides – Experiments – <i>Dreizler</i>	217
Slides – Modeling and Simulation – <i>Hasse</i>	238
Slides – Papers (since 2018)	257
Slides – Additional Contributed Slides	258
 PTF Contributed Talks: Low Swirl, Instability, Modeling, Liquid Fuels, ML Manifolds	 275
Slides – DNS of Laboratory Lean CH ₄ /H ₂ Low-Swirl Flame Impinging on an Inclined Wall – <i>Savard</i>	276
Slides – Nonlinear Heat Release Characteristics for Triggering of Combustion Instabilities – <i>Acharya</i>	285
Slides – Probability density function modelling in the flamelet regimes of premixed combustion – <i>Cleary</i>	293
Slides – Turbulent Liquid Fuel Flame Topologies via CH and OH PLIF – <i>Allison</i>	301
Slides – Machine Learning Techniques for Manifold-based Models – <i>Yellapantula</i>	315
 TNF Session: Combustion Machine Learning – Principles, Progress, Perspective	 325
<i>Coordinators: Matthias Ihme and Tarek Echehki and Luc Vervisch</i>	
Summary	325
Slides – Overview – <i>Ihme</i>	327
Slides – Contributed Slides – (<i>from nine groups</i>)	333
Slides – Discussion Issues – <i>Ihme</i>	366
 Saturday Panel Discussion: Key Points, Opportunities, and Priorities	 371
<i>Kareem Ahmed, Andreas Dreizler, Matthias Ihme, Hong Im</i>	
<i>Moderator: Christian Hasse</i>	
Summary	371



Summary

The 15th TNF Workshop (International Workshop on Measurement and Computation of Turbulent Flames) and the 17th PTF (Premixed Turbulent Flames) Workshop were held as a combined event on July 22-23, 2022 at the Coast Cole Harbor Hotel in Vancouver, Canada. Traditionally, TNF and PTF have used different formats, with PTF consisting of relatively short, contributed presentations and TNF consisting of longer “curated” sessions on pre-selected focus topics. Overall participation (roughly 80) was lower than expected, due to lingering effects of the corona virus pandemic. This prompted the organizers to combine and blend the programs and presentation styles of the normally-separate workshops. Feedback on this combined approach was generally very favorable, and the PTF and TNF Organizers have discussed the possibility of using a similar approach for at least a part of 2024 workshops in Milan, Italy. These Proceedings follow the format for past TNF Workshops but include information and presentations from the full TNF/PTF program. Slides from PTF contributors are also available from the [PTF web site](#).

A key part of each TNF Workshop has been to present collaborative comparisons of experimental and computational results for selected target flames that are intended to challenge the state-of-the-art in turbulent combustion simulations, while sticking to relatively simple burner geometries and fuels. For 2022, the comparisons were coordinated by Benoit Fiorina and targeted selected cases from the Darmstadt multi-regime burner (MRB). There were also TNF-style sessions on: modeling challenges associated with combustion of hydrogen; combustion of ammonia as an energy/hydrogen carrier; flame-wall interaction; combustion machine learning; and compressible/supersonic combustion. Contributed PTF talks on topics related to these TNF sessions were grouped accordingly in the agenda, while PTF contributions on other topic were grouped into separate PTF-style sessions.

A summary of each TNF-style session (except supersonic combustion) is included in the Proceedings, along with presentation slides. Only a few points from those summaries are listed here.

- **Hydrogen Flames:** Present combustion models do not capture the effects of thermo-diffusive instabilities in turbulent H_2 flames. Predictive and validated models are required in view of the transition toward sustainable fuels. Currently available DNS and experimental databases, as well as needs for new cases, were discussed, and it was proposed that all those interested in collaborating hydrogen combustion should contact Heinz Pitsch (h.pitsch@itv.rwth-aachen.de) to be added to the e-mail list.
- **Ammonia Combustion:** There is growing interest in ammonia as carbon-free energy carrier, but there are many open questions regarding its deployment in combustion devices, including challenges related to flame stability and pollutant formation. Recent DNS results from SINTEF, Sandia, and KAUST on turbulent combustion of pure or partially-cracked ammonia were reviewed, with emphasis on the importance of thermo-diffusive instabilities in $NH_3/H_2/N_2$ flames, sensitivity to equivalence ratio of the formation of NO_x and N_2O , the need for accurate chemical kinetic mechanisms for use in DNS and LES, and pressure effects on $NH_3/H_2/N_2$ flames. Progress on diagnostic developments for ammonia flames, experiments on the resilience to blowout of laminar and turbulent premixed flames of partially cracked ammonia, and initial comparisons of measured and simulated results on turbulent non-premixed jet



flames of partially cracked ammonia at 5-bar pressure was outlined. Three potential test cases for were proposed for measurement campaigns at KAUST to provide datasets for TNF16.

- **Multi-Regime Combustion:** The session consisted of a brief overview of the Darmstadt multi-regime burner (MRB) and available experimental data, a brief review of the Gradient Free Regime Identification (GFRI) approach as applied to experimental data and LES data, and collaborative comparisons of simulation results on selected MRB cases from ten contributing groups. The objective of the joined numerical study is to give a state-of-the-art of turbulent combustion modeling community. Causes of significant differences among predictions of CO were discuss, and possibilities for new target cases emphasizing stratified or multi-regime combustion hydrogen were discussed.
- **Flame-Wall Interaction:** Flame-wall interaction (FWI) has been a TNF topic since 2014. This session provided updates on recent numerical progress (six contributing groups) and experimental progress (four contributing groups), conclusions regarding common challenges and findings from the different FWI studies, and recommendations on future research needs and priorities.
- **Combustion Machine Learning:** This session was organized to provide the TNF community with an overview of ML techniques and their application to TNF/PTF-related problems in combustion. To this end, this session solicited and reviewed contributions from the TNF/PTF research community, resulting in a total of eleven contributions. The discussion session evolved around four main topics: i) data and how TNF/PTF existing database can be leveraged for CombML applications; ii) the integration of ML into TNF and PTF workshops; iii) pathways for establishing ML-models, best practice, and benchmarks for ML training and ML evaluation; and iv) the integration of domain knowledge into CombML.

The workshop concluded with a **panel discussion** and general discussion on “**Key Points, Opportunities, and Priorities.**” Excerpts from the summary of that discussion session (written by K. Ahmed, A. Dreizler, C. Hasse (chair), M. Ihme, and H. Im) are included below.

In the final discussion, we took up the key points of the two days. The challenges for the future are especially new fuels for CO₂-neutral/CO₂-free combustion (H₂, NH₃, and blends, MeOH, EtOH, OME, DMC, SAF). Secondly, physical phenomena or conditions of turbulent flames, including high Ka, high pressure, turbulent flames close to the stability limit, and flame wall interactions are of particular interest. As a starting point for the discussion, three possible targets for the next 2 years were formulated:

1. Consolidated chemistry for NH₃ – use in DNS and LES
2. Transport processes/differential diffusion in turbulent flames (esp. new fuels)
3. Experimental and DNS configurations that build on TNF heritage

The key outcomes of the discussion were:

There is a great need for NH₃ kinetics, so kinetics experts from our community should be integrated into the workshop. The goal is to have a common mechanism for DNS and LES.



Reference configurations for the new fuels will be defined, with two possible options:

1. Some blends can probably be investigated in known reference burners. For this purpose, planning is currently underway at the various locations, including Darmstadt and KAUST. The big advantage for the modeling is that simulation setups are available, and several groups worldwide have experience regarding the specifics of the respective configurations. From previous TNF workshops there is extensive knowledge regarding the comparison of the simulations.
2. New burners, e.g. for pure H_2 or NH_3/H_2 mixtures, are currently under development. These can be either a new design or a modification of previous configurations. One example is the stratified/steam diluted H_2 burner (CORIA, EM2C) as a further evolution of the previous burner from T. Schuler. Depending on the funding opportunities in the respective countries, several new configurations are expected to become available in the next few years.

Regarding the quantities to be quantified experimentally, the discussion participants emphasized that NO is a crucial quantity for the validation of the model. This should be measured locally in laminar and turbulent flames.

DNS should be integrated into the investigations from the beginning and provide further information that the experiments and LES cannot deliver. As far as possible, phenomena such as flame stabilization and ignition should also be investigated. LES of the DNS configuration could become a part of the model comparisons like the reference experiments.

The participants in the discussion were in favor of having a TNF 15.5 in about a year's time, in preparation for TNF16 in Milan.

Thanks to all who contributed.

TNF15 Organizing Committee:

Robert Barlow, Andreas Dreizler, Benoit Fiorina, Christian Hasse, Matthias Ihme, Andreas Kempf, Peter Lindstedt, Gaetano Magnotti, Assaad Masri, Joseph Oefelein, Heinz Pitsch, Zhuyin Ren, Luc Vervisch

PTF17 Organizing Committee:

Andy Aspden, Aaron Skiba, Sina Kheirkhah



TNF Workshop Participants

July 22-23, 2022

Coast Coal Harbor Hotel

Vancouver, Canada

Last Name	First	Affiliation
Abdelwahid	Suliman	KAUST
Ahmed	Umair	Newcastle University
Albalawi	Alfaisal	KAUST
Angelilli	Lorenzo	KAUST
Attili	Antonio	University of Edinburgh
Barlow	Robert	Barlow Combustion Research
Berger	Lukas	ITV, RWTH Aachen University
Bourque	Gilles	Siemens Energy
Breicher	Adrian	University of Applied Sciences and Technical University of Darmstadt
Chen	Jacqueline	Sandia
Darabiha	Nasser	EM2C Lab, CNRS, Centralesupelec
Dieter	Kevin	University of Applied Sciences and Technical University of Darmstadt
Dreizler	Andreas	Technical University of Darmstadt
Engelmann	Linus	Universität Duisburg-Essen
Elbaz	Ayman	KAUST
Fiorina	Benoît	Université Paris-Saclay, CentraleSupélec, EM2C-CNRS
Geyer	Dirk	University of Applied Sciences, Darmstadt
Gruber	Andrea	SINTEF
Guiberti	Thibault	KAUST
Hampp	Fabian	University of Stuttgart
Hasse	Christian	Technical University of Darmstadt
Hawkes	Evatt	UNSW Sydney
Hernandez-Perez	Francisco	KAUST
Hewson	John	Sandia National Laboratories
Hochgreb	Simone	University of Cambridge
Ihme	Matthias	Stanford University
Jones	Bill	Imperial College London
Kempf	Andreas	University Duisburg-Essen
Li	Jiajun	KAUST
Lindstedt	Peter	Imperial College
Luu	Tien Duc	University of Stuttgart
Magnotti	Gaetano	KAUST
Masri	Assaad	University of Sydney
Massey	James	University of Cambridge



Last Name	First	Affiliation
Mercier	Renaud	Safran Tech
Moureau	Vincent	CORIA, CNRS
Nicolai	Hendrik	Technical University of Darmstadt
Niemietz	Kai	ITV, RWTH Aachen University
Pequin	Arthur	Université Libre de Bruxelles
Peterson	Brian	University of Endinburgh
Peterson	David	US Air Force Research Laboratory
Pitsch	Heinz	ITV, RWTH Aachen University
Richter	Martin	Norwegian University of Science and Technology
Rieth	Martin	Sandia National Laboratories
Scholtissek	Arne	Technical University of Darmstadt
Shamooni	Ali	University of Stuttgart
Stein	Oliver	University of Stuttgart
Steinhausen	Matthias	Technical University of Darmstadt
Tang	Hao	KAUST
van Oijen	Jeroen	Eindhoven University of Technology
Wang	Guoping	KAUST
Yu	Tao	KAUST



PTF Workshop Participants

July 22-23, 2022

Coast Coal Harbor Hotel

Vancouver, Canada

Last Name	First	Affiliation
Acharya	Vishal	Georgia Institute of Technology
Ahmed	Kareem	University of Central Florida
Allison	Patton	Michigan State University
Chaudhuri	Swetaprovo	University of Toronto
Cleary	Matthew	University of Sydney
Dinkelacker	Fredrich	ITV, Leibniz Universität Hannover
Driscoll	James	University of Michigan
Fan	Luming	National Research Council Canada
Hamlington	Peter	University of Colorado, Boulder
Hayakawa	Akihiro	Tohoku University
Howarth	Thomas	Newcastle University
Im	Hong	KAUST
Kheirkhah	Sina	The University of British Columbia
Minamoto	Yuki	Tokyo Institute of Technology
Mohammadnejad Daryani	Sajjad	The University of British Columbia
Nozari	Mohammadreza	Polytechnique Montreal
Perry	Bruce	National Renewable Energy Laboratory
Salehi	M. Mahdi	Sharif University of Technology
Savard	Bruno	Polytechnique Montreal
Sharma	Priybrat	KAUST
Steinberg	Adam	Georgia Institute of Technology
Vabre	Martin	Polytechnique Montreal
Yao	Matthew	California Institute of Technology
Yellapantula	Shashank	National Renewable Energy Laboratory
Zimmerman	Paul	ITV, Leibniz Universität Hannover



TNF and PTF Workshops

July 22-23, 2022

Coast Coal Harbor Hotel

Vancouver, Canada

PTF TITLES

Acharya	Nonlinear Heat Release Characteristics for Triggering of Combustion Instabilities
Ahmed	The Compressibility of Highly-Turbulent Premixed Flames
Allison	Turbulent Liquid Fuel Flame Topologies via CH and OH PLIF: Two Truths and One Lie
Chaudhuri	Turbulent flame speed based on mass flow rate of reactants - theory and its validation
Chen	Spectral Analysis of Premixed Ammonia/Hydrogen/Nitrogen-Air Flames in Sheared Turbulence
Cleary	Probability density function modelling in the flamelet regime using multiple mapping conditioning
Dinkelacker	Flame stability measurements for H ₂ -NH ₃ flames - flashback and liftoff-limits**
Hamlington	What do we get wrong (and right) when we study turbulent premixed flames in a box?
Hayakawa	Combustion characteristics of ammonia/air premixed turbulent flame at high pressure and high temperature
Hochgreb	(Difficulties in) closing the balance for progress of reaction in turbulent premixed Bunsen flames
Howarth	Thermal leading points in lean premixed hydrogen
Kheirikhah	What is the role of non-flamelets in estimating how fast turbulent premixed flames burn?
Salehi	Conditional Expansion Methods for Turbulence-Chemistry Interaction Modelling in Highly-Turbulent Premixed Flames
Savard	DNS of a laboratory lean CH ₄ /H ₂ low-swirl flame impinging on an inclined wall
Steinberg	How different is turbulence when burning (and does it matter)?
Yao	Using tabulated chemistry and LES to capture non-unity Lewis number effects in turbulent premixed flames
Yellapantula	Co-Optimized Machine Learned Manifolds: Relearn FGM or FGM with major improvements
Zimmermann	Search for sustainable liquid fuels for clean aviation

TNF15 Organizing Committee



Robert Barlow
Barlow Combustion Research
USA



Andreas Dreizler
Technical University of
Darmstadt
Germany



Benoît Fiorina
Ecole CentraleSupélec
France



Christian Hasse
Technical University of
Darmstadt
Germany



Matthias Ihme
Stanford University
USA



Andreas Kempf
University Duisburg-Essen
Germany



Peter Lindstedt
Imperial College London
UK



Gaetano Magnotti
King Abdullah University
of Science and Technology
Saudi Arabia



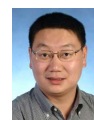
Assaad Masri
University of Sydney
Australia



Joseph Oefelein
Georgia Tech
USA



Heinz Pitsch
RWTH Aachen University
Germany



Zhuyin Ren
Tsinghua University
China



Prof. Luc Vervisch
INSA Rouen, CORIA
France

TNF/PTF Workshop

Vancouver, Canada 22-23 July 2022

PTF Workshop

- First workshop – Berkeley 1988
- Current PTF organizers
 - Andy Aspden, Newcastle University, UK
 - Aaron Skiba, Air Force Research Laboratory, USA
 - Sina Kheirkhah, University of British Columbia, Canada
- Thank you to our past PTF organizers
 - Jim Driscoll
 - Ömer Gülder
 - Fredrich Dinkelacker



<https://sites.google.com/view/ptf-workshop/home>



TNF/PTF Workshop

Vancouver, Canada 22-23 July 2022

TNF/PTF Workshops

Blank Page



TNF and PTF Workshops

July 22-23, 2022

Coast Coal Harbor Hotel

Vancouver, Canada

AGENDA

Friday			
8:30-8:45	Badge Pickup On-site Registration	Foyer and Ballroom A	Chair/ Moderator
8:45-9:00	Introduction	Barlow/Kheirkhah -- Ballroom A	
9-10:30	Premixed H ₂	H. Pitsch (30), Discussion (10), Howarth(10), Rieth (10), Discussion (30)	E. Hawkes
10:30-11:00	Coffee Break	Foyer and Ballroom B	
11:00-12.30	Ammonia	Magnotti/Gruber (40), Discussion (20), Dinkelacker (10), Hayakawa (10), Discussion (10)	T. Guiberti
12:30-1:30	Lunch Buffet	Ballroom B	
1:30-2:40	Multi-regime	Geyer/Barlow/Hasse/Fiorina (50), Discussion (20)	A. Kempf
2:40-3.10	Flame Structure	Chen (10), Hamlington (10), Discussion (10)	M. Rieth
3:10-3:40	Coffee Break	Foyer and Ballroom B	
3:40-4.40	Flame Structure & Speed	Steinberg (10), Kheirkhah (10), Discussion (10) Chaudhuri (10), Hochgreb (10), Discussion (10)	P. Allison
4:40-5:40	Panel Discussion	Hamlington, Pitsch, Steinberg, Hampp	S. Kheirkhah
5:40-7:00	Reception & Host Bar	Ballroom B	



TNF and PTF Workshops

July 22-23, 2022

Coast Coal Harbor Hotel

Vancouver, Canada

AGENDA

Saturday, July 23, 2022			
9:00	Announcements	Ballroom A	Chair/ Moderator
9:00-10:00	Flame-Wall Interaction	Dreizler/Hasse	B. Peterson
10:00-10:30	Low-Swirl & Instability	Savard (10), Acharya (10), Discussion (10)	B. Peterson
10:30-11:00	Coffee Break	Foyer and Ballroom B	
11:00-12:45	Modelling & Liquid Fuels	Cleary (10), Salehi (10), Discussion (10) Yao (10), Discussion (5) Zimmerman (10), Allison (10), Discussion (10)	A. Attili
12:45-1:45	Lunch Buffet	Ballroom B	
1:45-3:15	Machine Learning	Ihme, Yellapantula	M. Cleary
3:15-3:45	Coffee Break	Foyer and Ballroom B	
3:45-4:45	Compressible Combustion	Oefelein, Ahmed	G. Magnotti
4:45-5:30	Key Points, Opportunities & Priorities	Dreizler, Ihme, Ahmed, Im	C. Hasse

TNF Session: Modeling Turbulent Hydrogen Flames

Coordinators: Heinz Pitsch, Lukas Berger, Andy Aspden, Antonio Attili,

Agenda

1. *Thermodiffusive Instabilities in Hydrogen Flames*
(Lukas Berger, Antonio Attili, Heinz Pitsch)
2. *Thermal Leading Points in Lean Premixed Hydrogen*
(Thomas Howarth)
3. *DNS of Premixed H_2*
(Martin Rieth)
4. *Available Experimental and Numerical Datasets*
(Heinz Pitsch)
5. Discussion

Summary

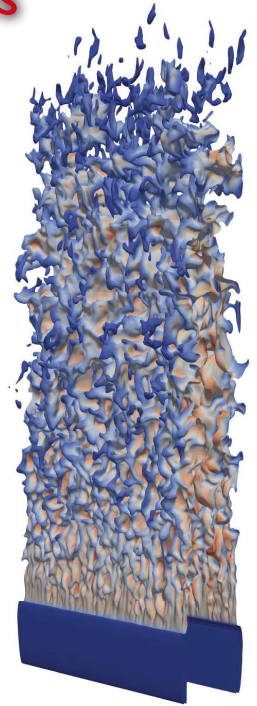
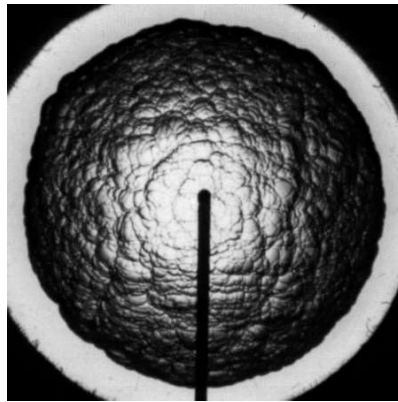
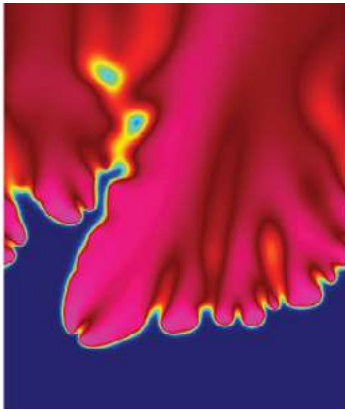
This TNF session aimed to foster the discussion and improve the state of modeling of premixed hydrogen flames. Premixed hydrogen/air flames feature thermodiffusive instabilities, due to the low Lewis number of hydrogen, which significantly affect the flame dynamics. As these effects are not adequately captured by present combustion models, predictive and validated combustion models are required in view of the ongoing energy transition towards sustainable fuels, such as hydrogen. To open the discussion and define the problem, three overview talks were given. The presentations have been shared with the organizers for further distribution.

In the second part, Heinz Pitsch presented a specific selection of currently available experimental and numerical datasets to initiate a discussion for the identification of suitable validation cases or possible new validation configurations. The presentation has been shared with the organizers for further distribution. In the subsequent discussion, the following points were mentioned to be considered for the design of adequate validation cases:

1. While H_2/CH_4 blends are important from an application point of view, it was agreed that in a first step a validation case should be designed for pure hydrogen flames.
2. The effects of confined and swirled flames and their stabilization are important and should be considered.
3. The importance of analyses at high pressures was stressed, as challenges, e.g., thermodiffusive instabilities, become more pronounced at these conditions.
4. It is challenging to stabilize premixed turbulent flames at very turbulent conditions/high power due to flashback, consequently Bunsen flames may only work at weakly turbulent conditions.
5. It needs to be clarified what measurements are exactly needed for validation, e.g., boundary conditions, velocity measurements, NO, and OH were mentioned.
6. For LES, small-scale configurations are not useful due to the small resulting filter sizes, so large-scale applications should be considered.

Finally, it was proposed to collect contact information from everyone interested in hydrogen combustion model validation and/or in sharing experimental and numerical data. Interested researchers, who want to join, can contact Heinz Pitsch (h.pitsch@itv.rwth-aachen.de) to be added to the e-mail list.

TNF Session: Modeling Turbulent Hydrogen Flames



Andy Aspden, Heinz Pitsch
Lukas Berger, Antonio Attili

Outline of Session

Focus of this session: *Thermodiffusive Instabilities in Pure Premixed Hydrogen Flames*

Key Problem: Leading order effect of thermodiffusive instabilities in hydrogen/air flames

- Flame speed increase by factor of 4
- Super-adiabatic temperatures of 400K
- Molecular effects are exacerbated by turbulence (instead of mitigated)
 - lots of non-linear interactions
 - no models yet available

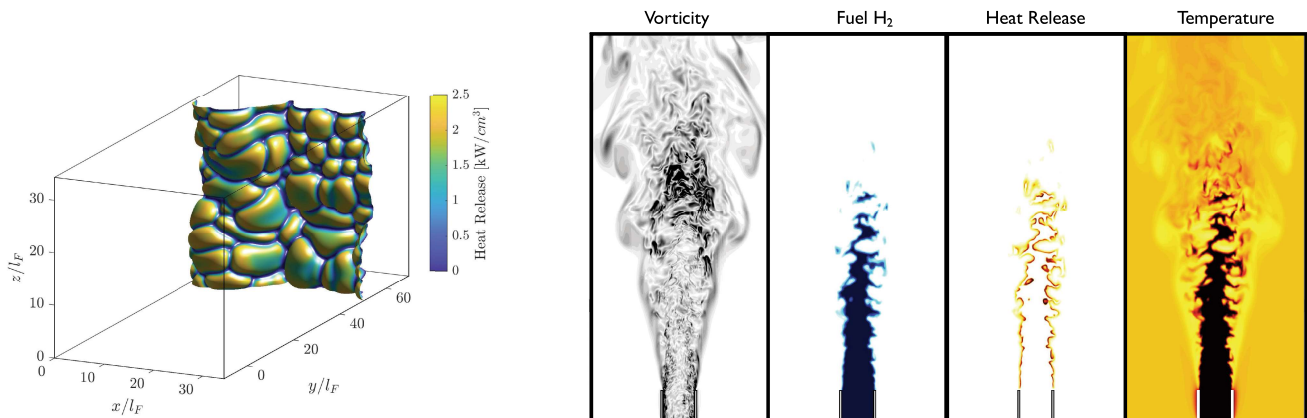
Key Discussion Points:

- Identification of target datasets
- Identification of relevant conditions

Agenda

1. *Thermodiffusive Instabilities in Hydrogen Flames*
(Lukas Berger, Antonio Attili, Heinz Pitsch)
2. *Thermal leading points in lean premixed hydrogen*
(Thomas Howarth)
3. *DNS of premixed H_2*
(Martin Rieth)
4. *Available Experimental and Numerical Datasets*
(Heinz Pitsch)
5. Discussion

Thermodiffusive Instabilities in Hydrogen Flames



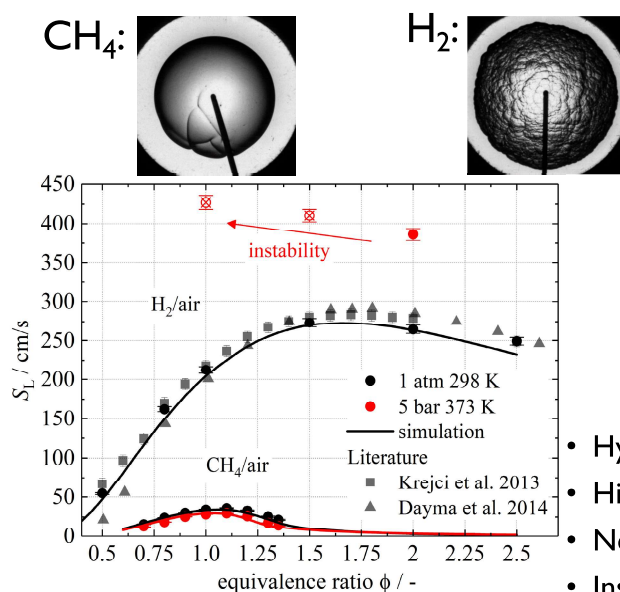
Lukas Berger^a, Antonio Attili^b, Heinz Pitsch^a

^aInstitute for Combustion Technology, RWTH Aachen University

^bInstitute for Multiscale Thermofluids, University of Edinburgh



Hydrogen Combustion – Fuel Properties

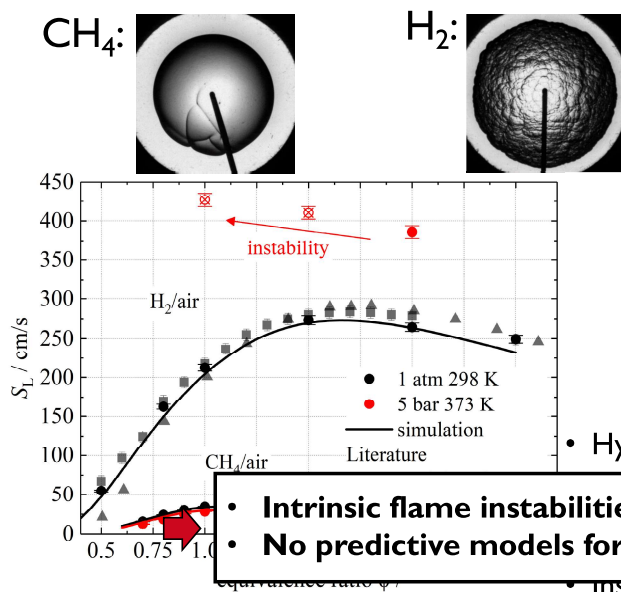


Fuel	H ₂	CH ₄	C ₈ H ₁₈
LHV [MJ/kg]	120	50	44.3
Energy Density [MJ/m ³]	9.6	32.5	30656
Fuel-vol%*	29.5	9.5	1.65
T _{ad} [K]*	2390	2226	2276
RON	130**	120	100
T _{auto-ignition} [K]	858	813	690
Lewis-Number***	~0.3	~1.0	~2.0

*Conditions: $\phi = 1$, $T_u = 300$ K, 1 atm **Diverging RON reported in literature
*** Lewis number = Ratio of thermal to mass diffusivity

- Hydrogen burns entirely differently (different fuel properties)
- High unstretched laminar burning velocity
- Negative Markstein numbers lead to thermodiffusive instabilities
- Instabilities can easily enhance flame speed by 400%

Hydrogen Combustion – Fuel Properties



Fuel	H ₂	CH ₄	C ₈ H ₁₈
LHV [MJ/kg]	120	50	44.3
Energy Density [MJ/m ³]	9.6	32.5	30656
Fuel-vol%*	29.5	9.5	1.65
T _{ad} [K]*	2390	2226	2276
RON	130**	120	100
T _{auto-ignition} [K]	858	813	690
Lewis-Number***	~0.3	~1.0	~2.0

*Conditions: $\phi = 1, T_u = 300K, 1 atm$ **Diverging RON reported in literature
*** Lewis number = Ratio of thermal to mass diffusivity

- Hydrogen burns entirely differently (different fuel properties)

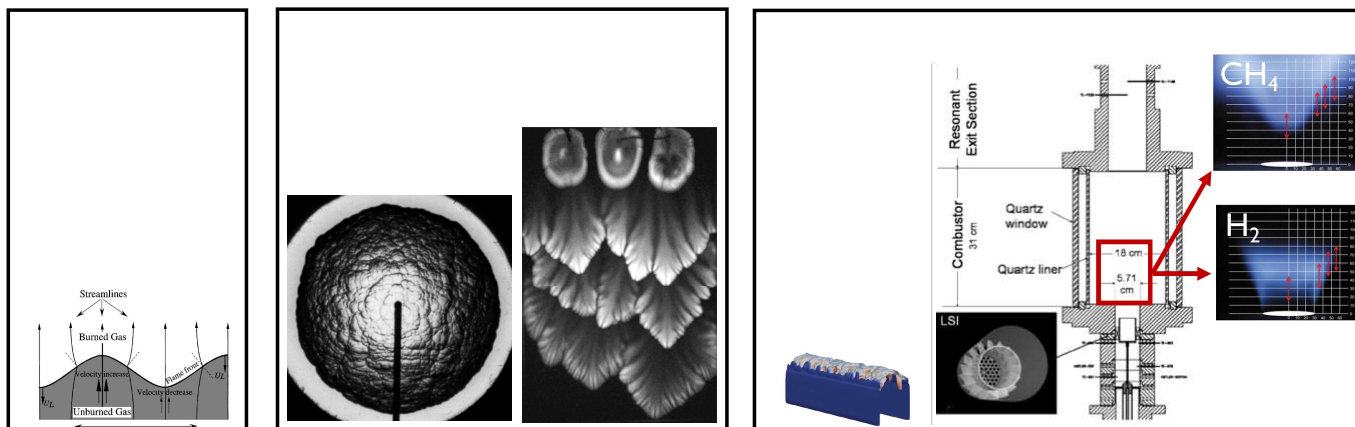
- Intrinsic flame instabilities tremendously affect flame dynamics
- No predictive models for complex combustion behavior

modiffusive instabilities

- instabilities can easily enhance flame speed by 400%

Outline

For lean hydrogen combustion, instabilities are omnipresent!



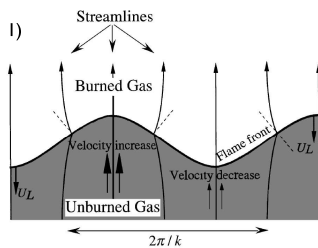
Theory

Laminar
Combustion

Turbulent
Combustion

Flame Intrinsic Instabilities – Theoretical Background

Hydrodynamic (DL) Instability



- Arises from density jump across flame
- Always destabilizing

Perturbation of Planar Flame

- Growth rate of perturbation³:

$$\bar{\omega} = \underbrace{\omega_{DL} \bar{k}}_{\text{DL instability}} - \underbrace{\delta[B_1 + \beta(Le_{eff} - 1)B_2 + PrB_3] \bar{k}^2}_{\text{Stability of thermodiffusive processes depends on Lewis number}}$$

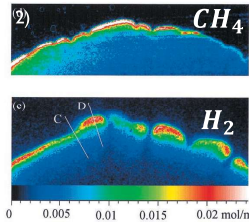
DL instability

$$\omega_{DL} = f(\sigma) > 0$$

Stability of thermodiffusive processes depends on Lewis number

Thermodiffusive Instability (TD)

- Lewis number of H_2 is very low
 $Le = \frac{\text{thermal diffusivity}}{\text{hydrogen mass diffusivity}} \ll 1$
- Strong differential diffusion leads to variations of ϕ and s_L



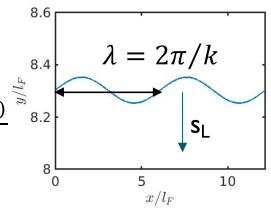
- Intrinsic Flame Parameters:

- Expansion ratio $\sigma = \rho_u / \rho_b$

- Zeldovich number $\beta = \frac{E(T_b - T_u)}{R T_b^2}$

- Lewis number

$$Le_{eff} = 1 + \frac{(Le_{O_2} - 1) + (Le_{H_2} - 1) \cdot A}{1 + A}$$



7

Institute for Combustion Technology | Lukas Berger – TNF Workshop 2022, Vancouver

¹⁾C. Clanet, S. Searby, Phys. Rev. Lett. 80 (1998) 17 ²⁾Bradley et al., Combust Flame 122 (2000) 195-209

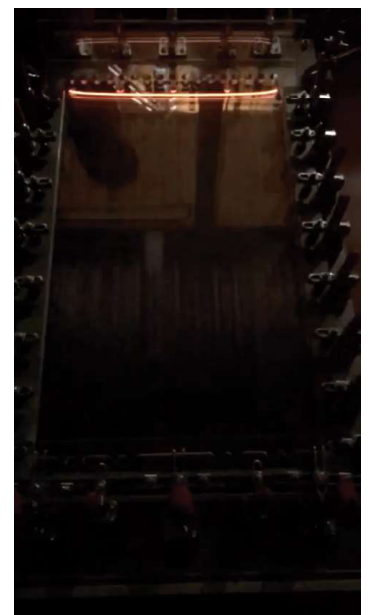
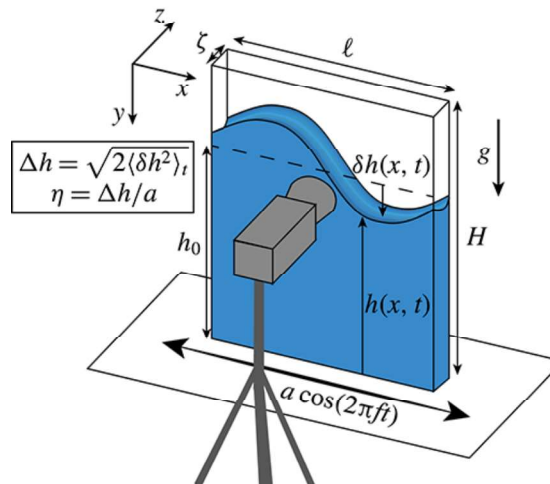
³⁾M. Matalon, C. Cui, J. K. Bechtold, J. Fluid Mech., 487:197–210, 2003.



Laminar Hydrogen Flames

Hele-Shaw cells

- Quasi-2D flow
- Optical accessible
- Well-defined boundary conditions



8

Institute for Combustion Technology | Lukas Berger – TNF Workshop 2022, Vancouver

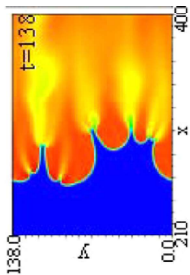
¹⁾F. Viola et al., J. Fluid Mech. 831 (2017)

²⁾Experiments by M.S. Sanchez, Universidad Carlos III de Madrid

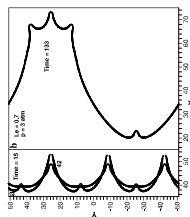


Laminar Hydrogen Flames

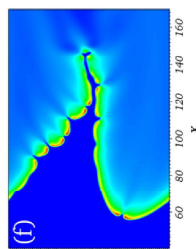
Simulations of laminar hydrogen flames in Hele Shaw cell



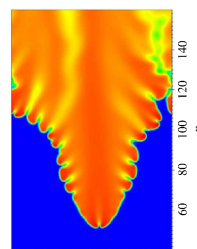
Kadowaki et al., Proc. Comb. Inst. 30 (2005), pp. 169-176



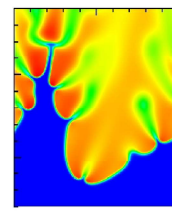
Yuan et al., Proc. Combust Inst. 31 (2007), pp. 1267-1274



Altantzis et al., Proc. Comb. Inst. 33 (2011), pp. 1261-1268



Altantzis et al., J. Fluid Mech. 700 (2012), pp. 329-361



Fernandez-Galisteo et al., Combust Flame 190 (2018), pp. 133-145



Howarth et al. Combust. Flame 237 (2022) 111805

2005

2007

2011

2012

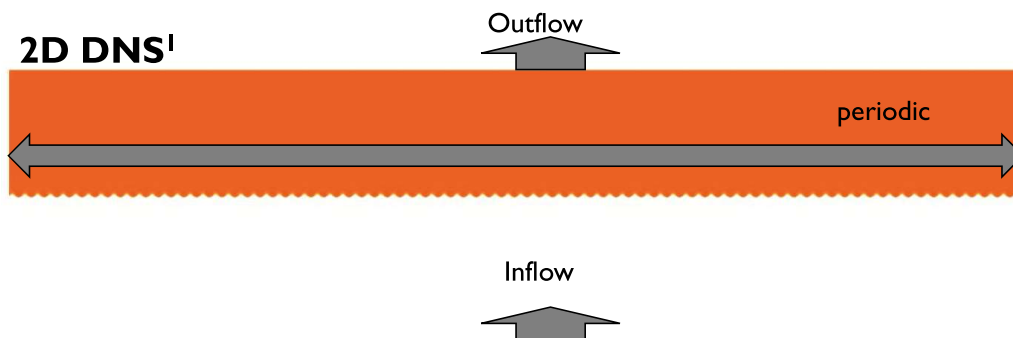
2018

2022

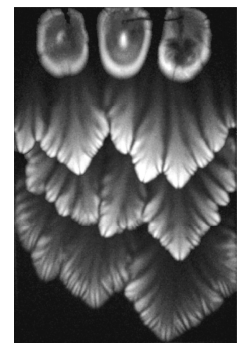
- Formation of small cellular structures
- Formation of large scale finger structures

Laminar Hydrogen Flames

2D DNS¹



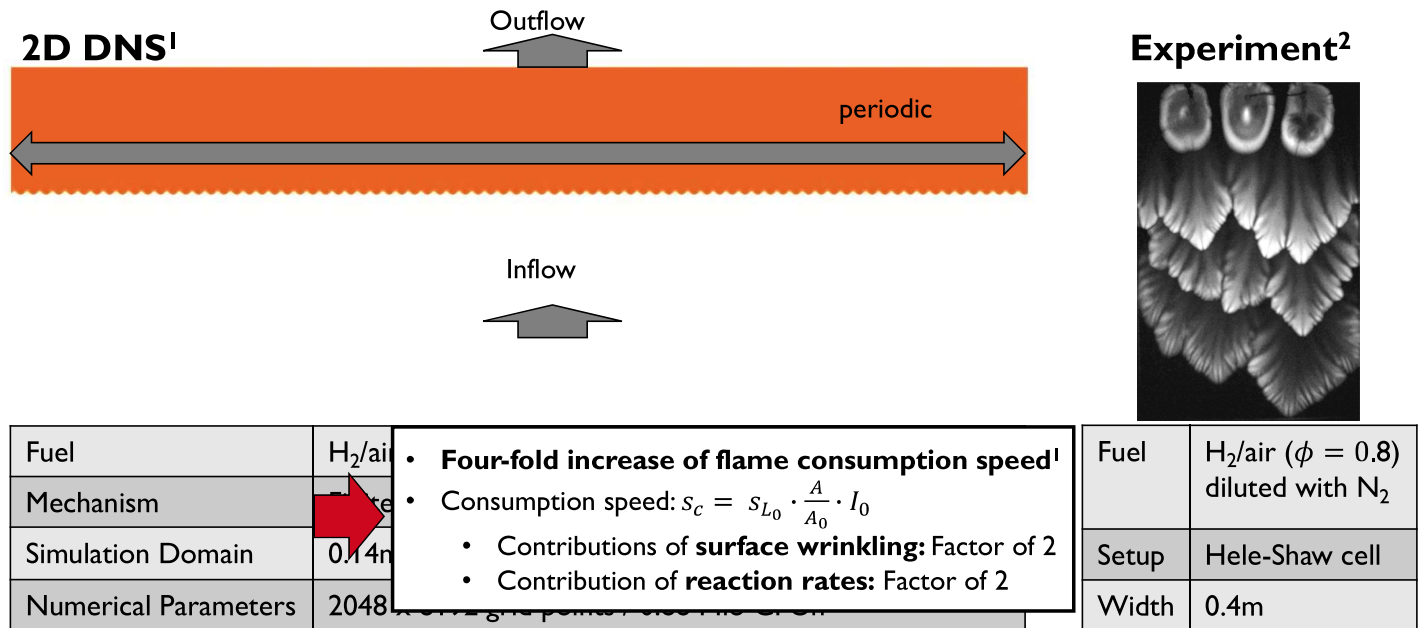
Experiment²



Fuel	H ₂ /air with $\phi = 0.4$, $T_u = 298K$, $p = 1bar$
Mechanism	Finite rate chemistry ¹
Simulation Domain	0.14m x 0.56m (200 _F x 800 _F) / 0.9sec (173 $\tau_{F,laminar}$)
Numerical Parameters	2048 x 8192 grid points / 0.88 Mio CPUh

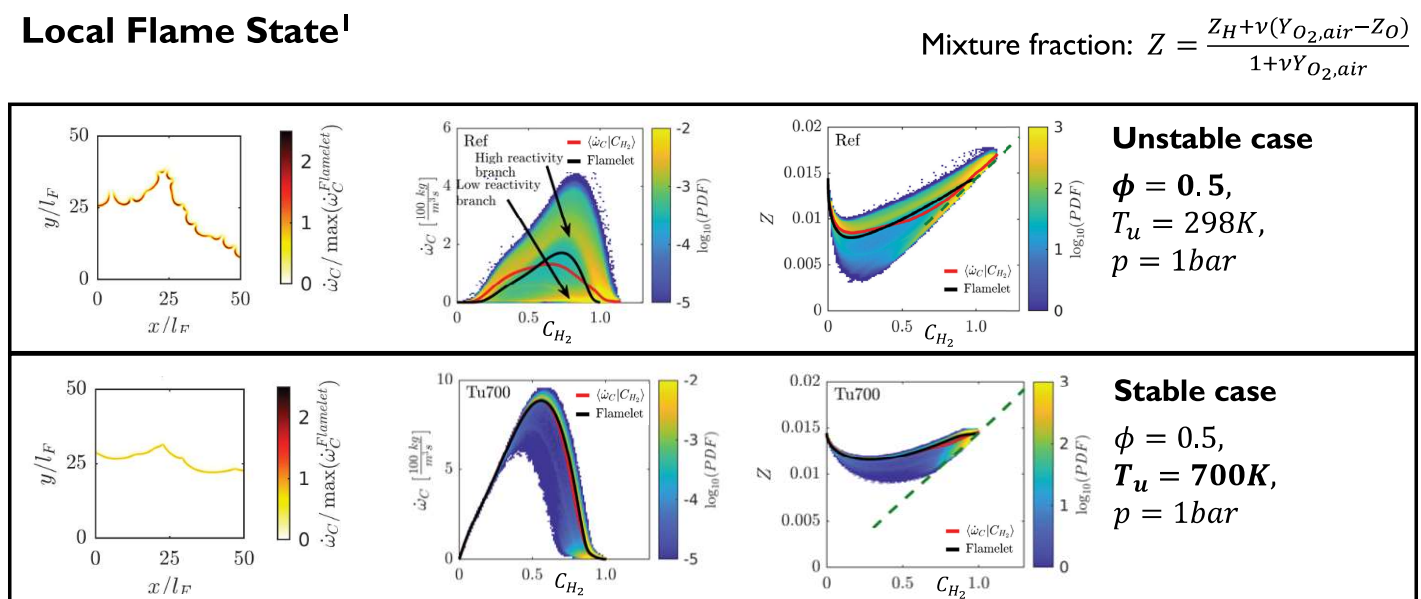
Fuel	H ₂ /air ($\phi = 0.8$) diluted with N ₂
Setup	Hele-Shaw cell
Width	0.4m

Laminar Hydrogen Flames



¹Institute for Combustion Technology | Lukas Berger – TNF Workshop 2022, Vancouver
²L. Berger et al., Proc. Comb. Inst. 37 (2019) 1879-1886
³Wongwiwat et al., 25th intern. colloquium on the dynamics of explosions and reactive systems (2015), Technical Report, No. 258

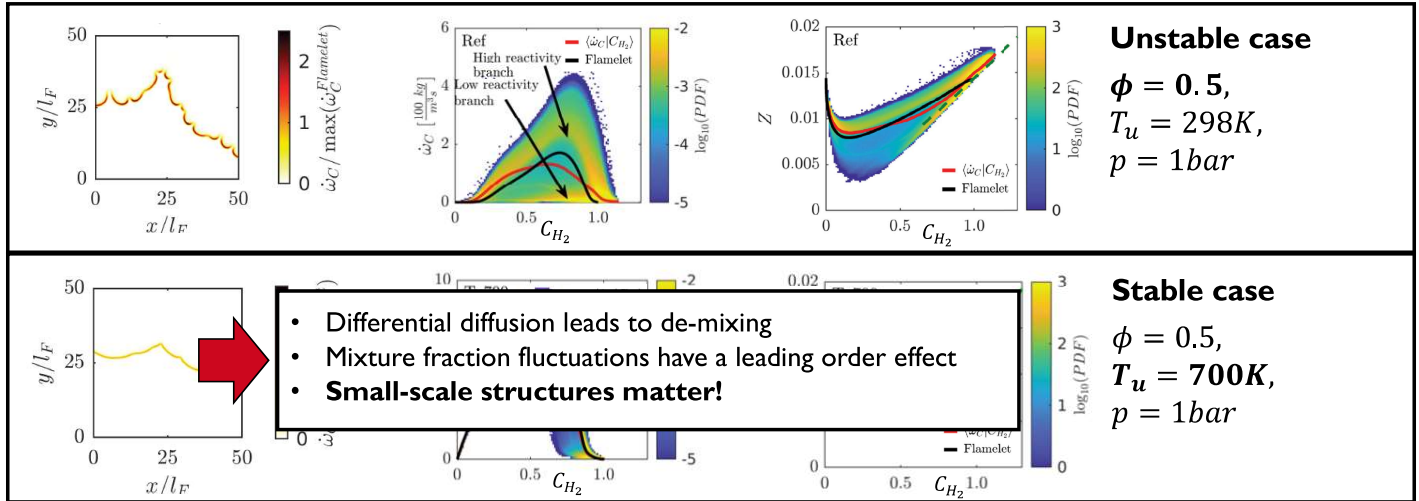
Laminar Hydrogen Flames



Laminar Hydrogen Flames

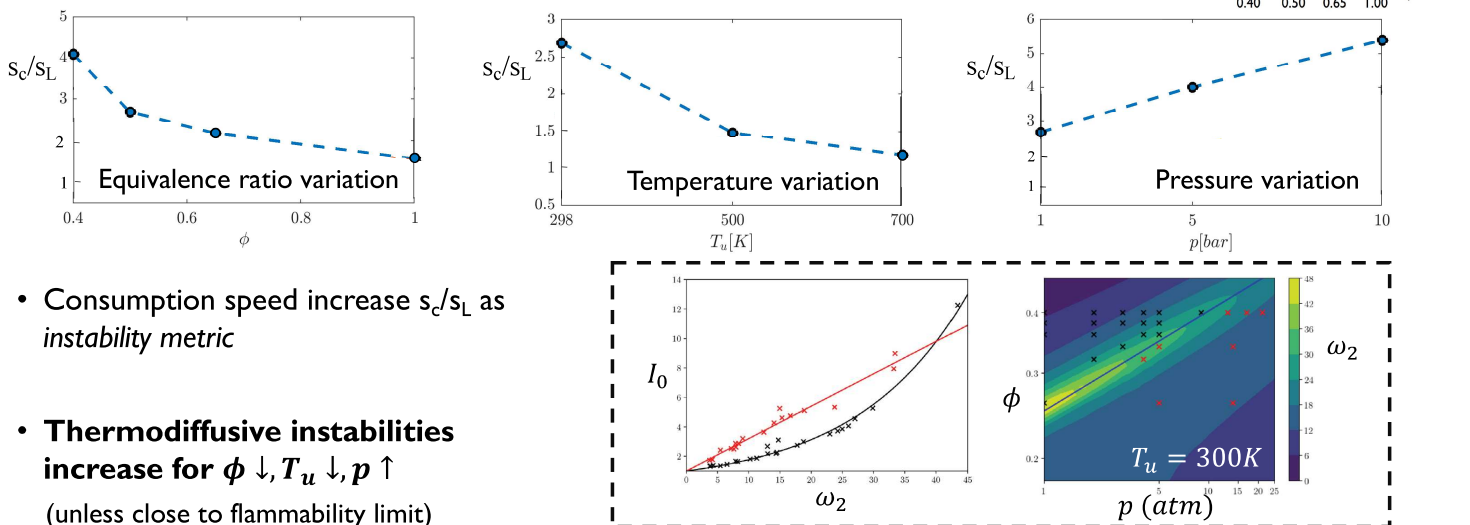
Local Flame State¹

$$\text{Mixture fraction: } Z = \frac{Z_H + \nu(Y_{O_2,air} - Z_O)}{1 + \nu Y_{O_2,air}}$$

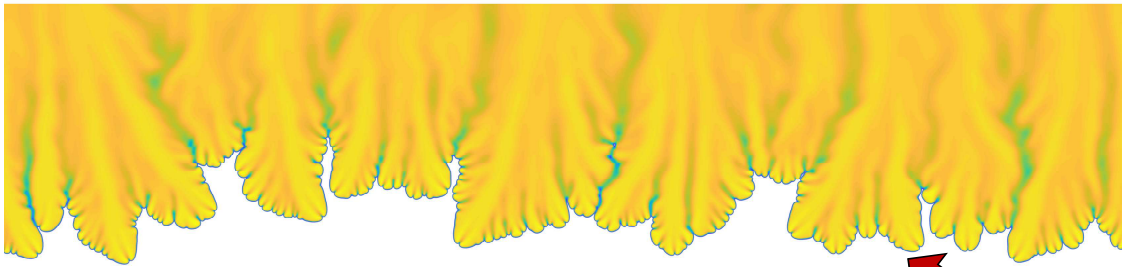


Laminar Hydrogen Flames

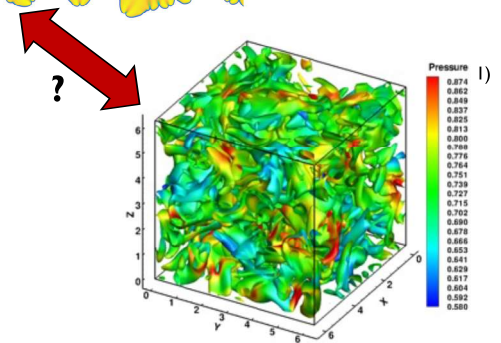
Relevant Conditions for Instabilities¹



Turbulent Hydrogen Flames



How do Thermodiffusive Instabilities Interact with a Turbulent Flow?



16

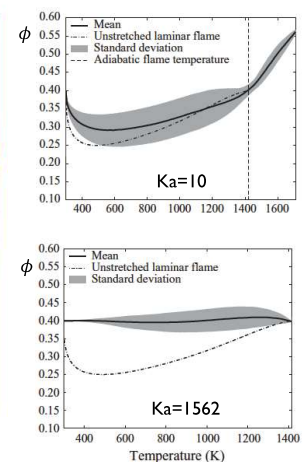
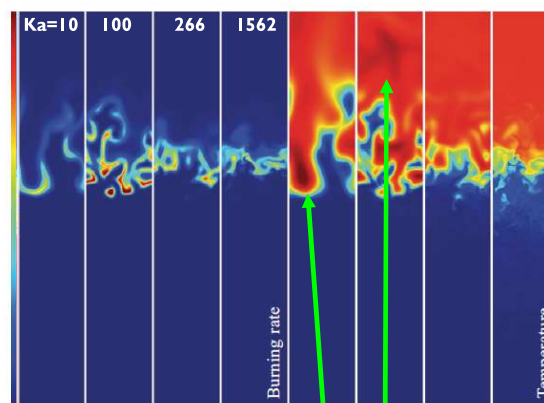
Institute for Combustion Technology | Lukas Berger – TNF Workshop 2022, Vancouver
¹http://debog.github.io/CRWENO/Turbulent_Flows.html



Turbulent Hydrogen Flames

DNS of Hydrogen Flames in Homogeneous Isotropic Turbulence¹

- Expectation:
Instabilities relevant at “low” Karlovitz numbers^{2,3}
- DNS in HIT with forced turbulence
- Observation:
 - Instabilities & ϕ -variations vanish at $Ka = 1562$
 - Instabilities still sustained at $Ka = 100$
- **Molecular effects do not vanish in turbulent environment!**



17

Institute for Combustion Technology | Lukas Berger – TNF Workshop 2022, Vancouver

¹A.J. Aspden, M.S. Day, J.B. Bell, J. Fluid Mech., 680:287–320, 2011. ²H. Boughanem, A. Trouvé, Proc. Comb. Inst., 27:971–978, 1998.

³S. Chaudhuri, V. Akkerman, C.K. Law, Phys. Rev. E, 84, 2011.



Turbulent Hydrogen Flames

Flame Kernels in Homogeneous Isotropic Turbulence¹

- Spherical flame kernels in homogeneous isotropic turbulence

CH₄-IV

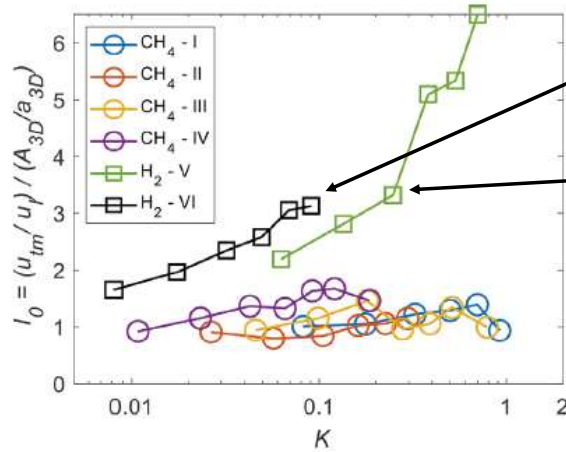


H₂-VI



- Consumption speed: $s_c = s_{L0} \cdot \frac{A}{A_0} \cdot I_0$

- Unity stretch factor in methane/air flames
- Stretch factor significantly enhanced in hydrogen/air flames



Hydrogen/air:
 $\phi = 0.4, T_u = 365K,$
 $p = 5bar$

Hydrogen/air:
 $\phi = 0.3, T_u = 365K,$
 $p = 5bar$

Methane/air flames at different conditions

18

Institute for Combustion Technology | Lukas Berger – TNF Workshop 2022, Vancouver

¹P. Ahmed, B. Thorne, M. Lawes, S. Hochgreb, G.V. Nivarti, R.S. Cant, Combust. Flame 233 (2021) 111586

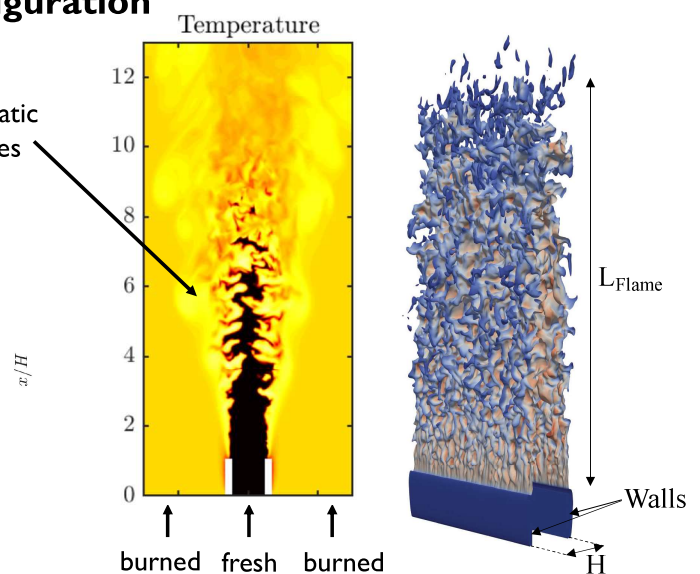
itv | RWTH AACHEN UNIVERSITY

Turbulent Hydrogen Flames

Hydrogen/air Flame in Slot Burner Configuration

- Conditions: $\phi = 0.4, T_u = 298K, p = 1bar$
- Detailed chemical mechanism¹
- Two flames at $Re = 11,000$ & $Ka \approx 15$
- Super-adiabatic temperatures due to instabilities (+400K / in laminar flame “only” +300K)

Super-adiabatic temperatures



19

Institute for Combustion Technology | Lukas Berger – TNF Workshop 2022, Vancouver

¹Berger et al., Combust. Flame 244 (2022) 112254

itv | RWTH AACHEN UNIVERSITY

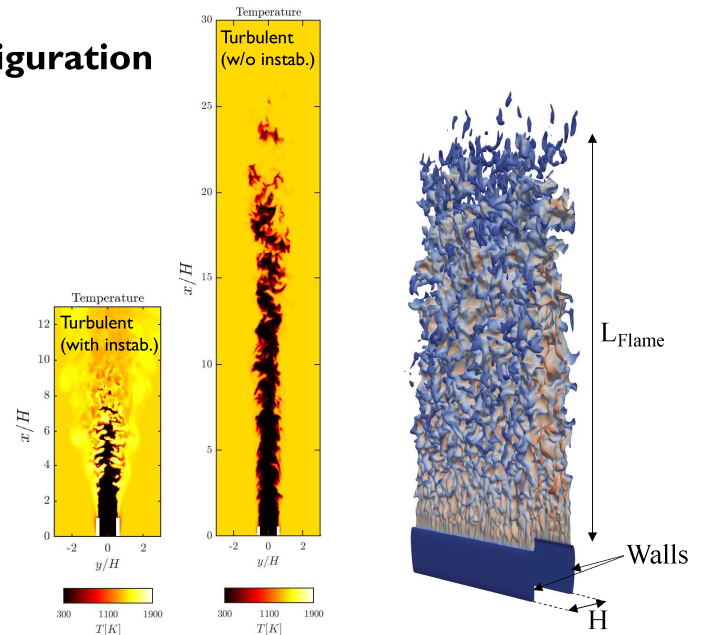
Turbulent Hydrogen Flames

Hydrogen/air Flame in Slot Burner Configuration

- Conditions: $\phi = 0.4$, $T_u = 298\text{K}$, $p = 1\text{bar}$
- Detailed chemical mechanism¹
- Two flames at $Re = 11,000$ & $Ka \approx 15$
- Super-adiabatic temperatures due to instabilities (+400K / in laminar flame "only" +300K)



Instabilities lead to shorter flame / higher turbulent flame speed



20

Institute for Combustion Technology | Lukas Berger – TNF Workshop 2022, Vancouver
¹Berger et al., Combust. Flame 244 (2022) 112254



Turbulent Hydrogen Flames

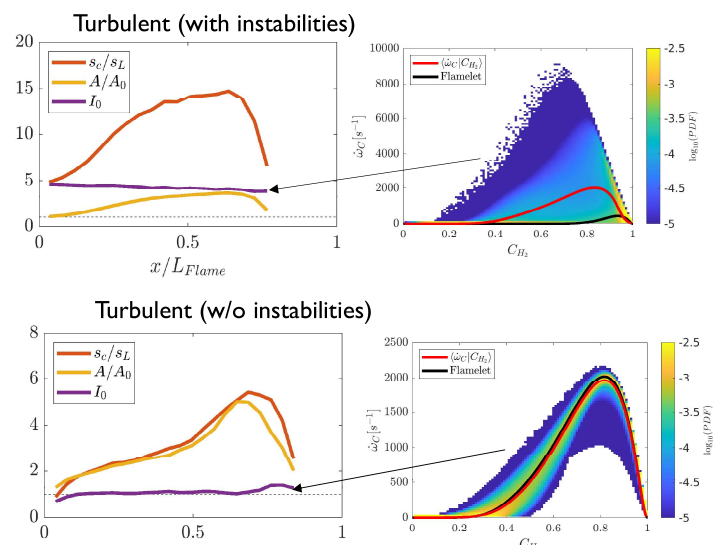
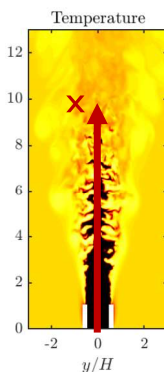
Consumption Speed¹:

$$s_{cons} = - \frac{1}{\rho_u Y_{H_2, u} A_0} \int \dot{\omega}_{H_2} dV$$

$$s_{cons} = s_L \cdot \frac{A}{A_0} \cdot I_0 \leftarrow \text{Stretch Factor}$$

↑
Flame Wrinkling

- Three-fold enhanced flame speed
- Significantly enhanced stretch factor
 - Turbulent (no instab.)²: $I_0 = 1$
 - Turbulent (with instab.): $I_0 = 4$
 - Laminar (with instab.): $I_0 = 2.6$



- **Molecular effects (differential diffusion) do not vanish in turbulent flow**
- **TD instability and turbulence feature synergistic effects ($I_{0,turb.} \gg I_{0,lam.}$) due to higher curvature and strain rate**

21

Institute for Combustion Technology | Lukas Berger – TNF Workshop 2022, Vancouver
¹Berger et al., Combust. Flame 244 (2022) 112254
²Attili et al., Proc. Combust. Inst. 38 (2021) 2939-2947

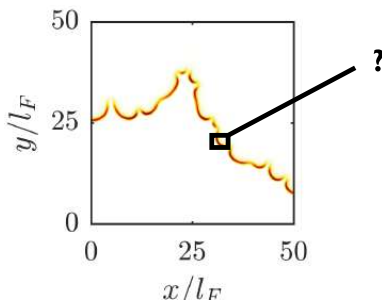


Modeling of Instabilities

Modeling Challenges

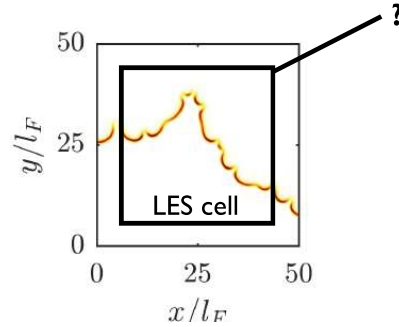
Modeling flame state manifold

How to model variations of local equivalence ratio / flame speed?



Sub-filter modeling

What if not or only partially resolving flame structure?



Modeling of Instabilities

Modeling Flame Intrinsic Instabilities (Laminar Flames)

• Flamelet Models

- Solving two scalar transport equations to account for differential diffusion, e.g. $(C_{H_2O} \text{ \& } Z_{mix})^1$ or $(C_{H_2} \text{ \& } T)^2$
- Example $(C_{H_2O} \text{ \& } Z_{mix})^1$:

$$\begin{aligned}\partial_t \rho + \nabla \cdot (\rho \mathbf{u}) &= 0, \\ \partial_t (\rho \mathbf{u}) + \nabla \cdot (\rho \mathbf{u} \mathbf{u}) &= -\nabla p + \nabla \cdot \tau, \\ \partial_t (\rho Z) + \nabla \cdot (\rho \mathbf{u} Z) &= \nabla \cdot (\rho D_Z \nabla Z) + \dot{\omega}_Z, \\ \partial_t (\rho C) + \nabla \cdot (\rho \mathbf{u} C) &= \nabla \cdot (\rho D \nabla C) + \dot{\omega}_C.\end{aligned}$$

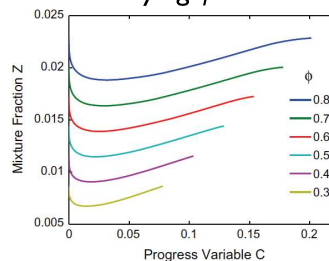
Source term of Z_{mix} :

$$\begin{aligned}\dot{\omega}_Z &= -\nabla \cdot \left[\rho D \left(\frac{1}{v+1} \right) \left(\frac{1}{Le} - 1 \right) (1-Z) \nabla C \right] \\ D_Z &= D \left[1 + \left(\frac{1}{Le} - 1 \right) (1-Z) \right]\end{aligned}$$

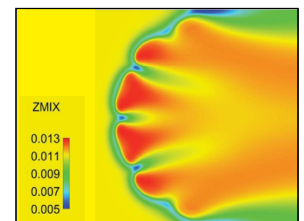


- Reduced order manifolds predict the effects of instabilities
- Turbulence interactions and sub-filter models not yet available
- What if structures are not resolved?

Tabulation by flamelets with varying ϕ



Laminar 2D flames with FGM model



Modeling of Instabilities

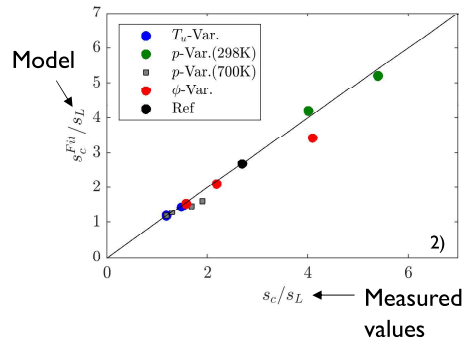
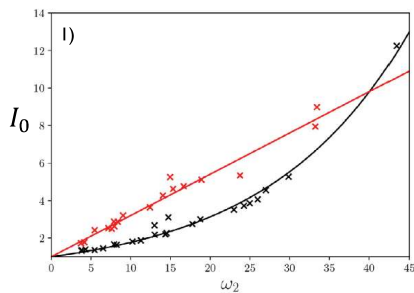
Empirical Modeling Approaches

- Turbulent flame locally corresponds to unstable laminar flame

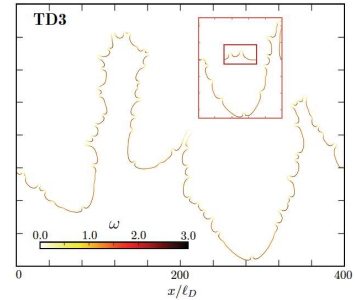
$$\frac{S_F}{S_L} = I_0 = f(\omega_2)$$

$$\frac{S_C}{S_L} \propto \left(\frac{\phi}{\phi_{Ref}} \right)^{\alpha_1} \left(\frac{T_u}{T_{u,Ref}} \right)^{\alpha_2} \left(\frac{p}{p_{Ref}} \right)^{\alpha_3}$$

$$\omega_2 = B_1 + \beta(Le_{eff} - 1)B_2 + PrB_3$$



Data driven modeling³



Modeling of Instabilities

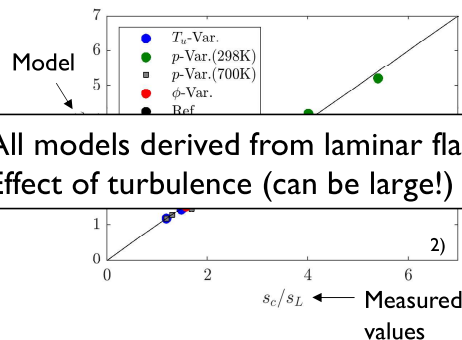
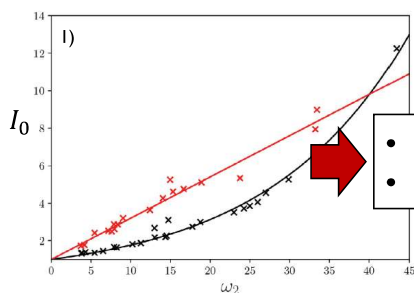
Empirical Modeling Approaches

- Turbulent flame locally corresponds to unstable laminar flame

$$\frac{S_F}{S_L} = I_0 = f(\omega_2)$$

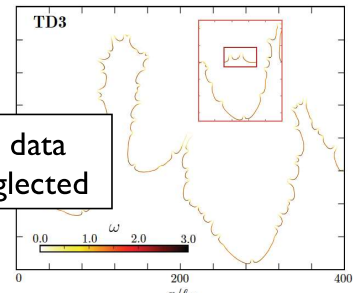
$$\frac{S_C}{S_L} \propto \left(\frac{\phi}{\phi_{Ref}} \right)^{\alpha_1} \left(\frac{T_u}{T_{u,Ref}} \right)^{\alpha_2} \left(\frac{p}{p_{Ref}} \right)^{\alpha_3}$$

$$\omega_2 = B_1 + \beta(Le_{eff} - 1)B_2 + PrB_3$$



- All models derived from laminar flame data
- Effect of turbulence (can be large!) neglected

Data driven modeling³



Conclusions

- **Thermodiffusive (TD) instabilities have a tremendous effect on flame dynamics**

- Four-fold increase of flame speed in laminar flames
- Two-fold increased stretch factor

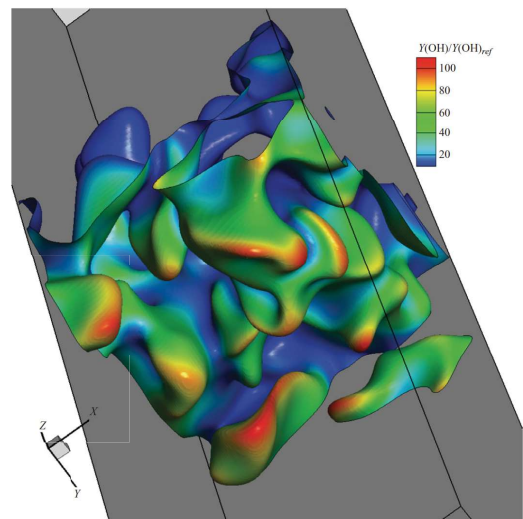
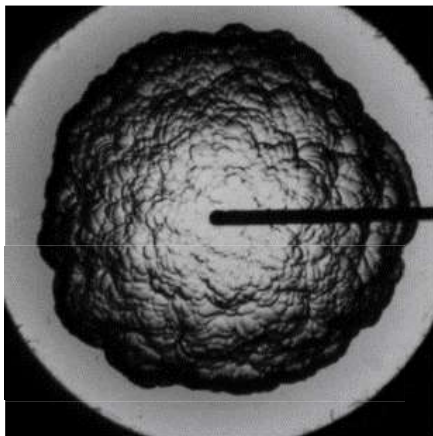
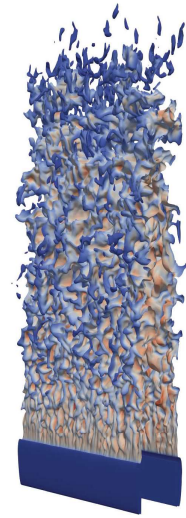
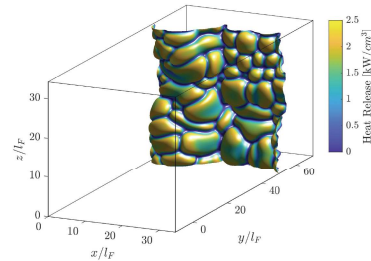
- **TD instabilities feature synergistic interactions with turbulent flow**

- Stretch factor $I_0 = 4$ (turbulent) vs. $I_0 = 2.6$ (laminar)
- Molecular effects do not vanish in turbulent flame

- **Predictive models are yet not available!**

- **Modeling challenges**

- Small-scale structures matter
- How to model if not resolved or partially resolved?



Thank you for your attention

Agenda

1. *Thermodiffusive Instabilities in Hydrogen Flames*
(Lukas Berger, Antonio Attili, Heinz Pitsch)
- > 2. *Thermal leading points in lean premixed hydrogen*
(Thomas Howarth)
3. *DNS of premixed H_2*
(Martin Rieth)
4. *Available Experimental and Numerical Datasets*
(Heinz Pitsch)
5. Discussion

Thermal leading point phenomena in lean premixed H_2 flames

Thomas Howarth

(PhD Sponsor: Reaction Engines & EPSRC)

Edward Hunt

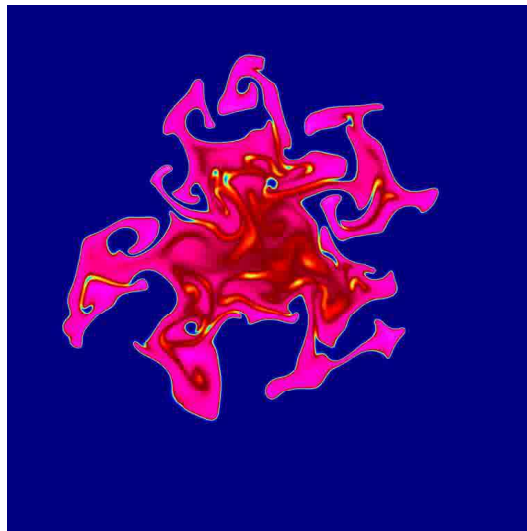
(PhD Sponsor: Ricardo UK & EPSRC)

Andy Aspden

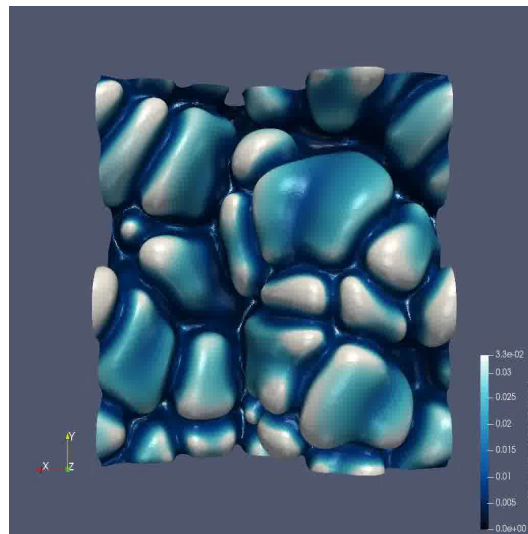
School of Engineering
Newcastle University, UK

PTF Workshop July '22

2D “turbulent” flame kernel

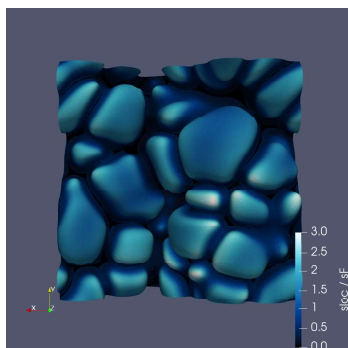


3D freely-propagating flame

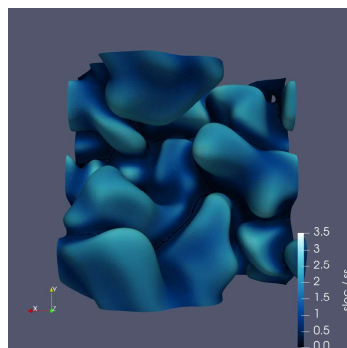


3D DNS canonical flame-in-a-box

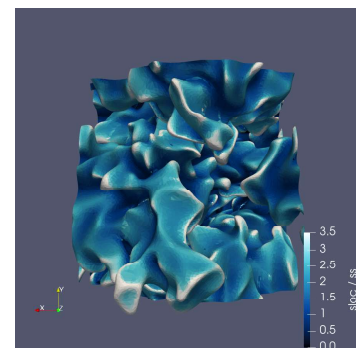
- Example conditions $p = 10\text{atm}$, $T_u = 300\text{K}$, $\phi = 0.4$
- Flame isosurface coloured by normalised local flame speed
 - Direction of propagation out-of-page



$Ka = 0$



$Ka = 4$

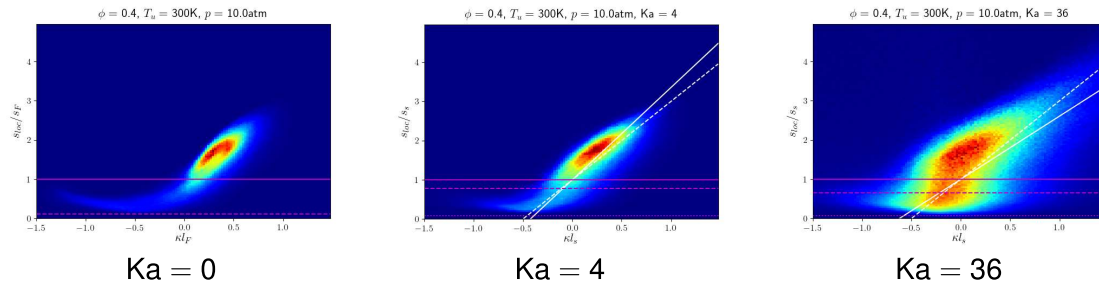


$Ka = 36$

- Clear change in shape of flame surface

Curvature-flame speed JPDFs

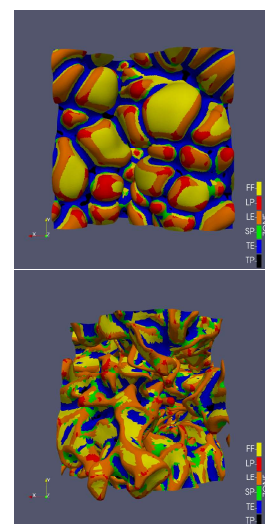
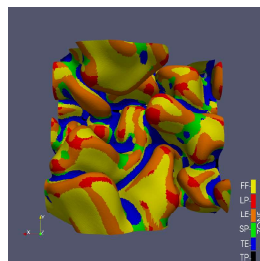
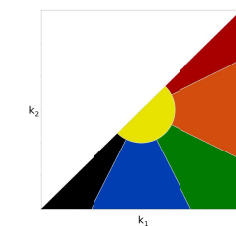
- First moment represents consumption (rather than probability)



- Bulk consumption occurs at
 - Low curvature (flat flame regions)
 - Local flame speed far in excess of laminar value (s_L)
 - Also higher than freely-propagating characteristic value (s_F)
- Contrary to conventional description of thermodiffusively-unstable flames

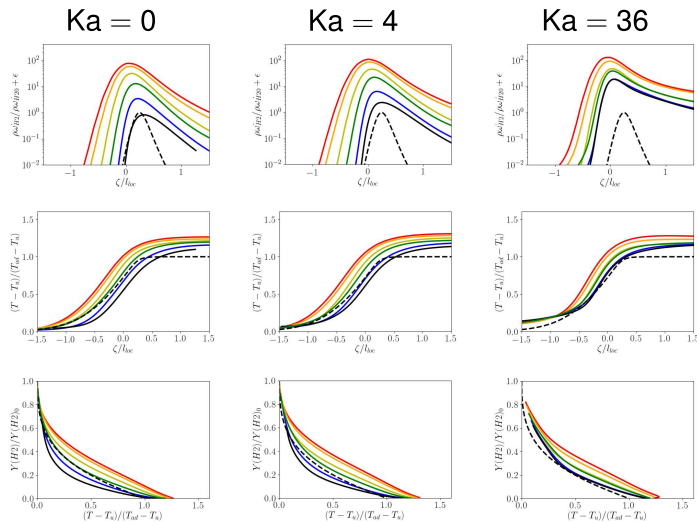
Principal curvature zones (PKZ)

- Consider principal curvatures
- Classify different zones
 - FF: Flat flame (yellow)
 - LP: Leading point (red)
 - LE: Leading edge (orange)
 - SP: Saddle point (green)
 - TE: Trailing edge (blue)
 - TP: Trailing point (black)



Surface normal profiles conditioned on PKZ

- Profiles along surface normals
- Conditioned on PKZ
- Length normalised by mean local thermal thickness
- Higher temperature and reaction rates
- Increasingly so with turbulence
- By $Ka = 36$, close to the flame
 - ▶ Everywhere hotter/faster
 - ▶ Even trailing points



Thermal leading point interpretation

- Observations contrary to conventional description of TD unstable flames
 - ▶ Bulk of fuel consumption occurs at speeds far in excess of laminar/FP reference
 - ▶ Importantly, happens at low curvature (nearly flat flame regions)
- We contend that this behaviour can be explained by thermal leading points
 - ▶ Conventional description is appropriate at leading points
 - ▶ Strong but relatively-low probability
 - ▶ Leave behind regions with low curvature but superadiabatic temperatures
 - ▶ This excess temperature supports high reaction rates in flat regions
- Challenge to demonstrate causality “chicken and egg”
 - ▶ Do higher temperatures result from higher reaction rates?
 - ▶ Do higher reactions result from higher temperatures?

Agenda

1. *Thermodiffusive Instabilities in Hydrogen Flames*
(Lukas Berger, Antonio Attili, Heinz Pitsch)
2. *Thermal leading points in lean premixed hydrogen*
(Thomas Howarth)
- > 3. *DNS of premixed H_2* **Pressure Effects in Hydrogen-Enriched Flame**
(Martin Rieth)
4. *Available Experimental and Numerical Datasets*
(Heinz Pitsch)
5. Discussion

Pressure effects in hydrogen-enriched flames

Martin Rieth¹, Andrea Gruber², Jackie Chen¹

¹Sandia National Laboratories, ²SINTEF Energy Research

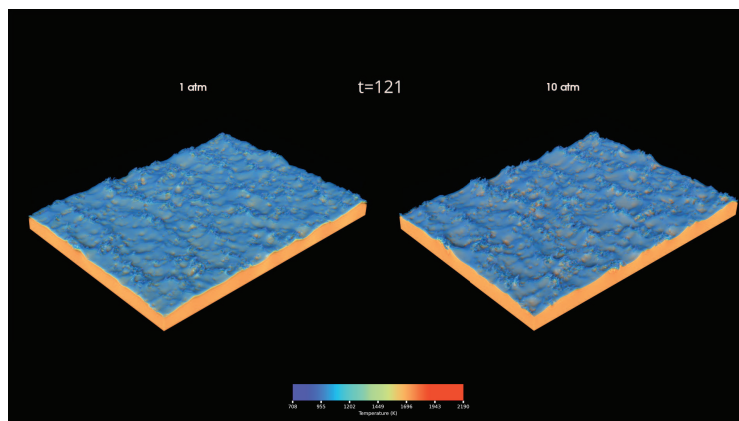
07/22/2022



Navigation icons and page number 1/15

$\text{NH}_3/\text{H}_2/\text{N}_2\text{-air}$, $\phi = 0.45$, $T_u = 750 \text{ K}$, $Ka \sim 600$, $Re_t \sim 1000$, 1 & 10 atm

How does pressure affect preferential diffusion effects?



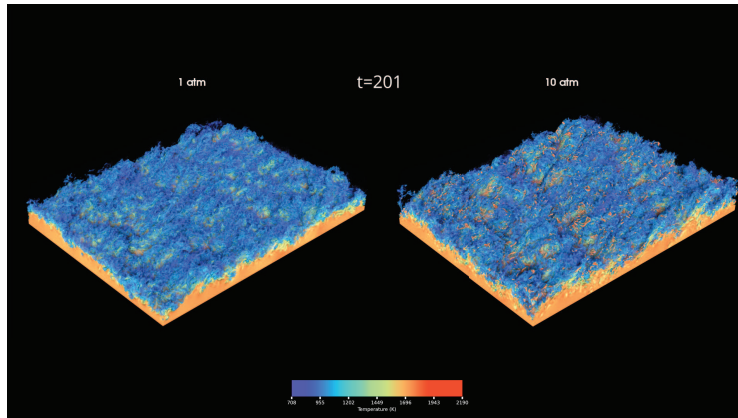
Same turbulence-flame interaction properties for 1 and 10 atm (Re does not increase with pressure here)

- Strong shear-driven turbulence disrupts the flame front
- More wrinkling and cellular structures at 10 atm, disrupted preheat layer at 1 atm
- Strong super-adiabaticity at 10 atm

Navigation icons and page number 2/15

$\text{NH}_3/\text{H}_2/\text{N}_2\text{-air}$, $\phi = 0.45$, $T_u = 750 \text{ K}$, $Ka \sim 600$, $Re_t \sim 1000$, 1 & 10 atm

How does pressure affect preferential diffusion effects?



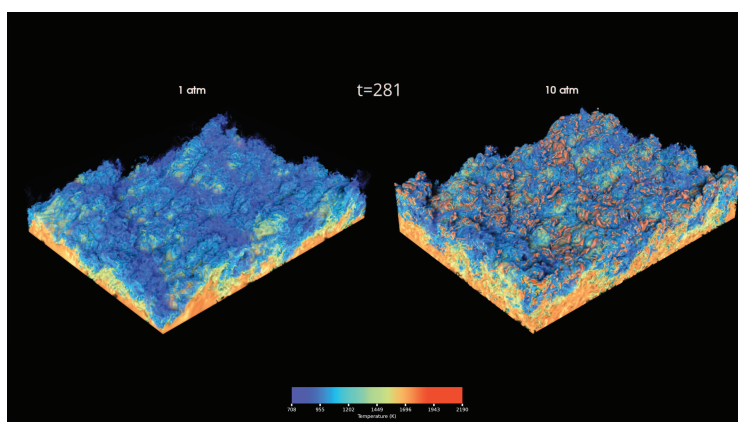
Same turbulence-flame interaction properties for 1 and 10 atm (Re does not increase with pressure here)

- Strong shear-driven turbulence disrupts the flame front
- More wrinkling and cellular structures at 10 atm, disrupted preheat layer at 1 atm
- Strong super-adiabaticity at 10 atm

3/15

$\text{NH}_3/\text{H}_2/\text{N}_2\text{-air}$, $\phi = 0.45$, $T_u = 750 \text{ K}$, $Ka \sim 600$, $Re_t \sim 1000$, 1 & 10 atm

How does pressure affect preferential diffusion effects?

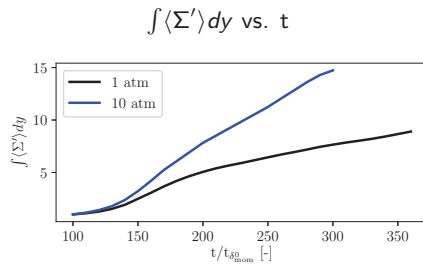


Same turbulence-flame interaction properties for 1 and 10 atm (Re does not increase with pressure here)

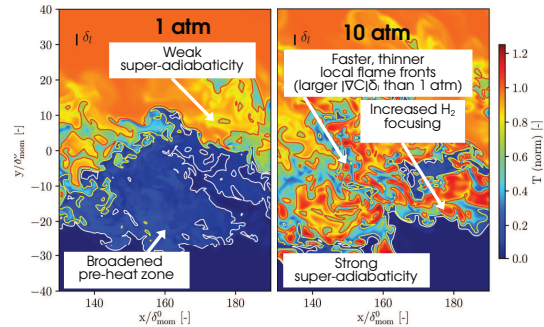
- Strong shear-driven turbulence disrupts the flame front
- More wrinkling and cellular structures at 10 atm, disrupted preheat layer at 1 atm
- Strong super-adiabaticity at 10 atm

4/15

$\text{NH}_3/\text{H}_2/\text{N}_2\text{-air}$, $\phi = 0.45$, $T_u=750$ K, $Ka \sim 600$, $Re_t \sim 1000$, 1 & 10 atm



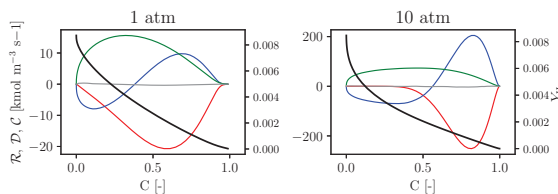
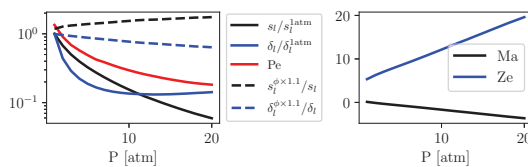
Rieth et al., C&F 2022



- Turbulent flame propagates through shear layer faster at 10 atm, flame surface generation is strongly amplified
- There are clear differences in how 1 and 10 atm flames look like qualitative (stronger super-adiabaticity and flame thinning at 10 atm)
- The decrease in flame thickness with pressure does not explain observed effects because its ratio to all other timescales stays the same

5/15

$\text{H}_2\text{-air}$, $\phi = 0.3$, $T_u=750$ K, effect of pressure on 1D unperturbed flames

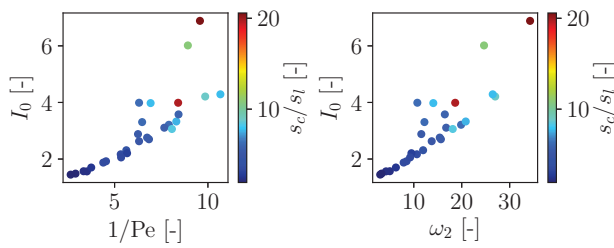


Reaction (red), diffusion (blue), convection (green)
balance for the fuel species (H_2)

- Ze increased, Ma decreases with pressure; equivalence ratio sensitivity increases
- Fuel supply in reaction zone more dependent on diffusion as pressure increases
- 10 atm flame becomes 'weaker' through amplified chain-terminating three-body reactions ($\text{H}+\text{O}_2+\text{M}=\text{HO}_2+\text{M}$)
- Differences in relative importance of convection and diffusion motivates Peclet number definition to model/understand pressure effects

6/15

H₂-air freely propagating flames (2D) at various T_u , p and ϕ



$$\omega = \omega_{DL} k - \underbrace{[B_1 + Ze(Le_{eff} - 1)B_2 + PrB_3]}_{\omega_2}$$

$$Pe = \frac{|\mathcal{C}_{H_2}|_{1D,max}/|\mathcal{D}_{H_2}|_{1D,max}}{|\frac{\partial Y_{H_2}}{\partial x} u|_{1D,max}} = \frac{|\frac{1}{\rho} \frac{\partial}{\partial x} (\rho \frac{W_{H_2}}{W_m} D_{H_2} \frac{\partial X_{H_2}}{\partial x})|_{1D,max}}{|\frac{\partial Y_{H_2}}{\partial x} u|_{1D,max}}$$

- ω_2 comes from dispersion model by Matalon et al. (2003) and is used by Howarth & Aspden (2021) to predict s_c/s_l
- Pe works very similarly, is easy to compute from 1D unperturbed flames
- Can pressure effects purely be described by non-dimensional numbers? Are 'pressure effects' actually unique to pressure?

Rieth et al., C&F 2023.

Navigation icons and page number 7/15

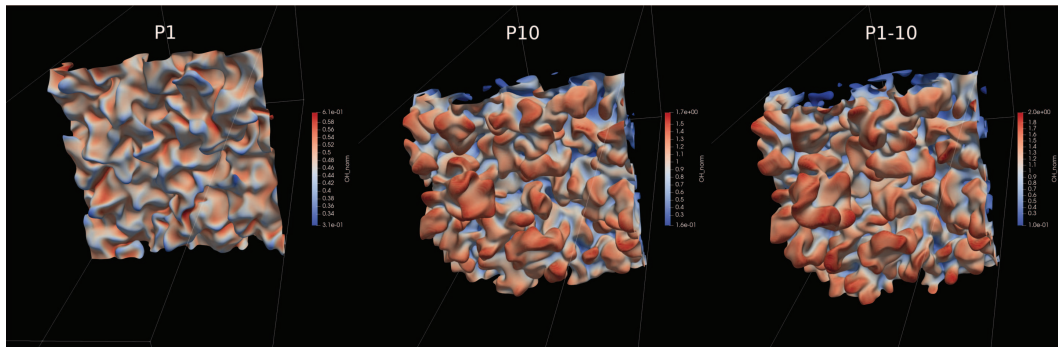
2-D/3-D H₂-air flame parameters

Case	P1	P10	P20	P1-10	P1-20	P10-1	P20-1
P	1	10	20	1	1	10	20
T_u	750	750	750	560.6	486.67	1057.5	1097.5
ϕ	0.3	0.3	0.3	0.23125	0.2235	0.31	0.37
s_l	3.50	0.54	0.21	0.23	0.06	8.71	9.85
δ_l	5.0E-04	6.8E-05	7.1E-05	1.0E-03	2.4E-03	3.54E-05	1.67E-05
Le_{eff}	0.43	0.39	0.38	0.37	0.36	0.44	0.46
Ze	5.3	12.1	19.6	12.1	20.1	4.8	5.1
Ma	0.13	-1.67	-3.63	-1.67	-3.65	0.12	0.12
Pe	1.35	0.30	0.18	0.29	0.15	1.64	1.58
ω_2	0.20	3.91	8.07	4.43	10.06	-0.02	0.00
l_0 (free)	1.00	1.52	2.05	1.59	2.21	0.99	0.87
δ/δ_l (free)	1.39	0.70	0.47	0.72	0.51	1.17	1.53
u'/s_l	21.31	46.55	51.86	45.89	51.73	21.41	21.62
l_t/δ_l	2.25	4.91	5.47	4.84	5.45	2.26	2.28
η_K/δ_l	0.013	0.028	0.031	0.027	0.031	0.013	0.013

Table: Overview of 2-D/3-D DNS cases. The parameters l_0 (free) and δ/δ_l are obtained from freely propagating 2-D flames, ω_2 is calculated using the model by Matalon et al. (2003). All cases feature $Ka = 300$, $Re_t = 1000$ and $Da = 0.1$ (based on thermal flame thickness).

Navigation icons and page number 8/15

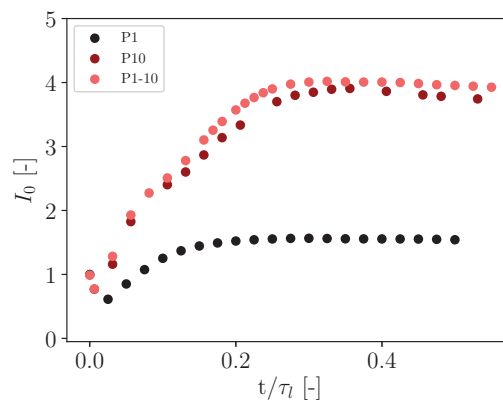
Lean 3-D H₂-air flames with homogeneous turbulence



- P10 (750 K, $\phi = 0.3$) and P1-10 (561 K, $\phi = 0.23$) show stronger flame response
- P1-10 matches conditions of P10 (10 atm) at atmospheric pressure
- Pressure effects can be mimicked by 'weakening' the flames via temperature and equivalence ratio (previous work has shown that lowering temperature amplifies instabilities, e.g., Berger, C&F 2022)

9/15

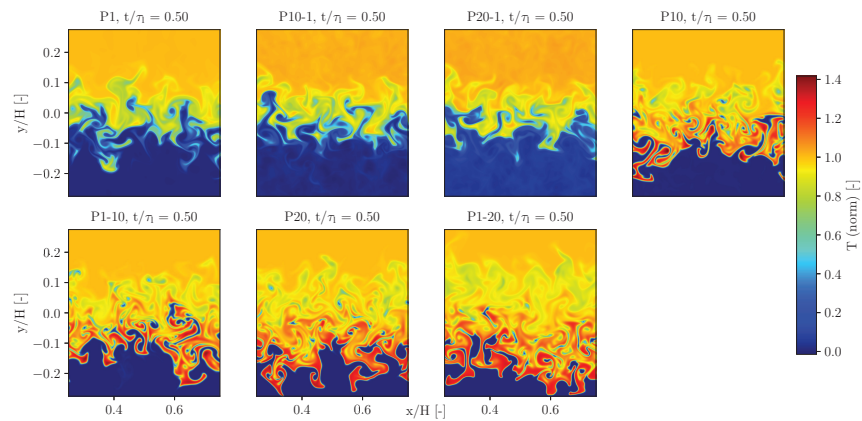
Lean 3-D H₂-air flames with homogeneous turbulence



- Quantitative comparison shows again same trends for P10 and P1-10
- Much amplified flame response for P10 and P1-10 compared to P1

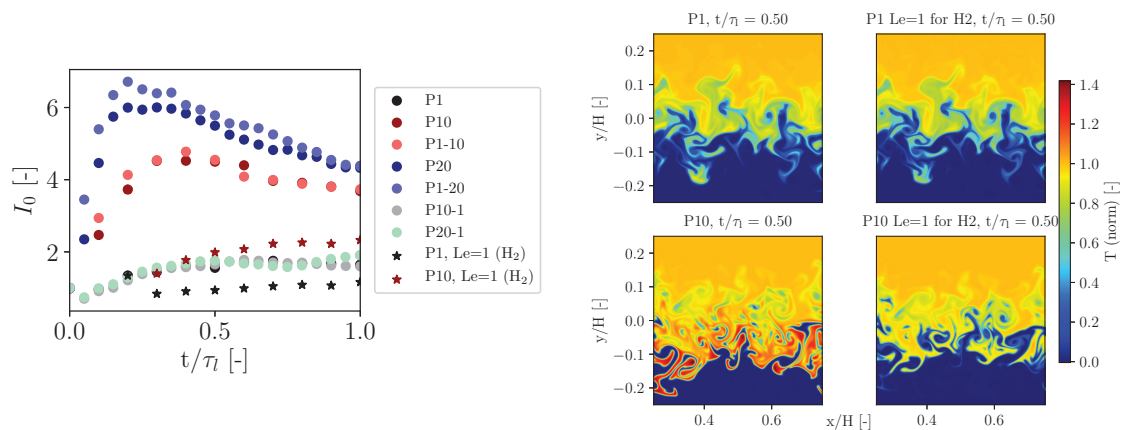
10/15

Lean 2-D H₂-air flames with pseudo-turbulence



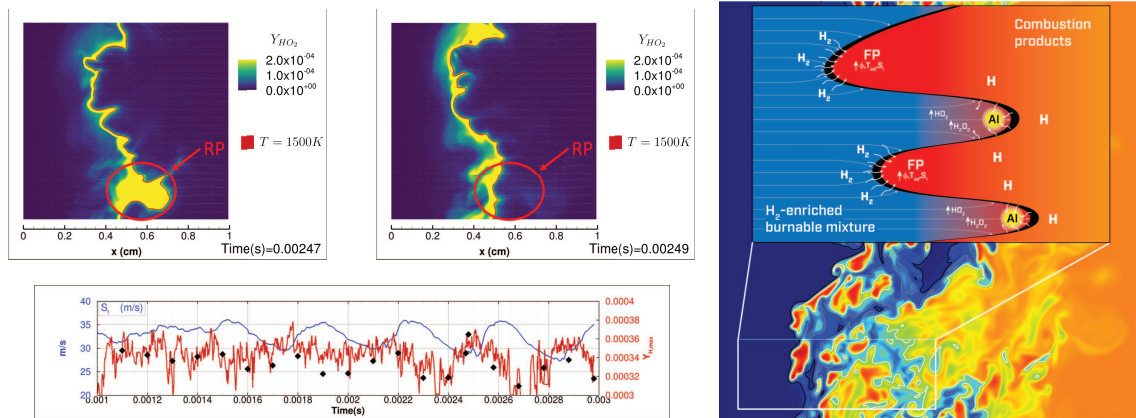
- More cases tested in 2D, same conclusions extending study to 20 atm (with corresponding matching cases)

Lean 2-D H₂-air flames with pseudo-turbulence



- Disabling preferential diffusion cancels I_0 amplification
- Disabling preferential diffusion has smaller effect at lower pressure

Lean reheat hydrogen-air flames ($T \sim 1100$ K, pressure of 5 bar, $\phi = 0.35$)



- Reheat flame at 5 atm shows intermittent instabilities/auto-ignition events
- Reheat flame dynamics are governed by atomic H rather than molecular H_2 diffusion (in regions with negative curvature - concave towards reactants)

Rieth et al., C&F 2022; Gruber et al., C&F 2021

13/15

Conclusions & Outlook

- Lean $NH_3/H_2/N_2$ -air flames show amplified thermo-diffusive instabilities at high pressure - despite high turbulence level
- Increased role of diffusion at elevated pressure observed in canonical cases with lean hydrogen-air mixtures (e.g., 2D flame subject to monochromatic shear)
- Peclet number definition offers potential to model pressure effects
- 3D lean hydrogen-air flames at atmospheric and elevated pressure show similar qualitative features as $NH_3/H_2/N_2$ -air flames - stronger thermo-diffusive effects
- Pressure effects can be mimicked at atmospheric pressure - potential avenue for experiments?

14/15

Acknowledgments

The work at Sandia National Laboratories was supported by the US Department of Energy, Office of Basic Energy Sciences, Division of Chemical Sciences, Geosciences, and Biosciences. Sandia National Laboratories is a multimission laboratory managed and operated by National Technology and Engineering Solutions of Sandia, LLC., a wholly owned subsidiary of Honeywell International, Inc., for the U.S. Department of Energy's National Nuclear Security Administration under contract DE-NA-0003525.

The research work performed in Norway was supported by the CLIMIT-Demo program of the Research Council of Norway, Project Number 617137 (BIGH2/Phase III), Siemens Energy AG, Equinor ASA and by the NCCS Centre, performed under the Norwegian research program Centres for Environment-friendly Energy Research (FME). The authors acknowledge the following partners for their contributions: Aker Solutions, ANSALDO Energia, CoorsTek Membrane Sciences, Gassco, KROHNE, Larvik Shipping, Norcem, Norwegian Oil and Gas, Quad Geometrics, Equinor, TOTAL, and the Research Council of Norway (257579/E20).

An award of computer time on Summit at OLCF was provided by the Innovative and Novel Computational Impact on Theory and Experiment (INCITE) program. This research also used resources of the Oak Ridge Leadership Computing Facility, which is a DOE Office of Science User Facility supported under Contract DE-AC05-00OR22725. We also thank for computing time granted on Betzy.

Thank you for your attention!

Agenda

1. *Thermodiffusive Instabilities in Hydrogen Flames*
(Lukas Berger, Antonio Attili, Heinz Pitsch)
2. *Thermal leading points in lean premixed hydrogen*
(Thomas Howarth)
3. *DNS of premixed H_2*
(Martin Rieth)
- > 4. *Available Experimental and Numerical Datasets*
(Heinz Pitsch)
5. Discussion

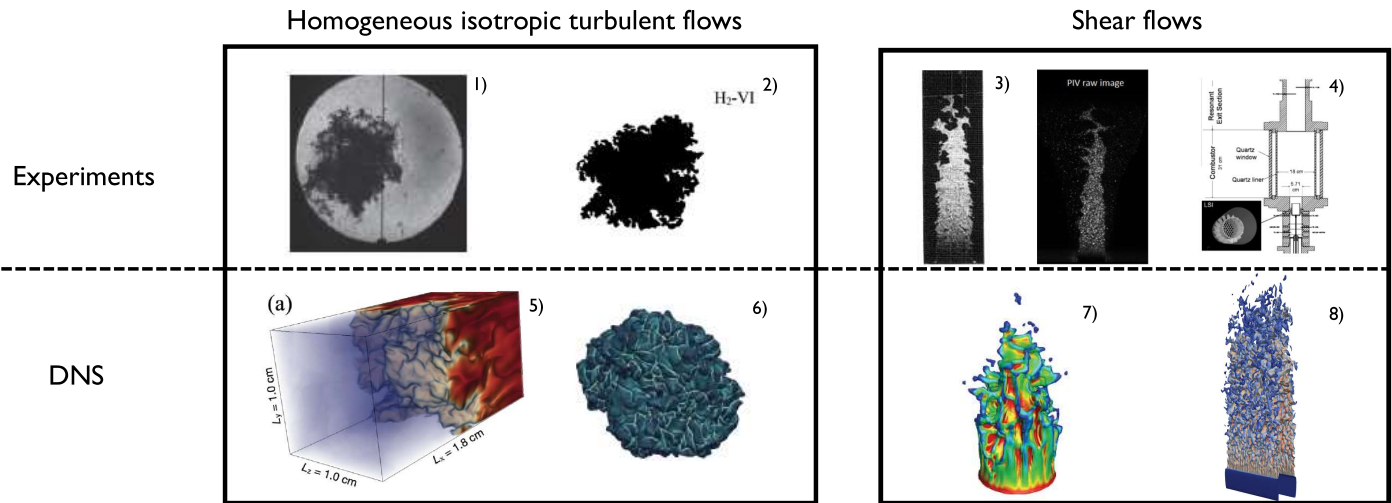
What Datasets/Flames Exist or Should be Targeted to Advance Modeling of Hydrogen Flames?

Key discussion points:

- Hypothesis and validation of turbulent hydrogen combustion models
- Are there any particular advantages of a configuration for hydrogen combustion?
- Who is interested in modeling which experiment/DNS?
- Who is planning any suitable validation experiments?
- Which conditions are of interest?

What Data Exist?

Overview of Experimental Data (Pure Hydrogen)



31

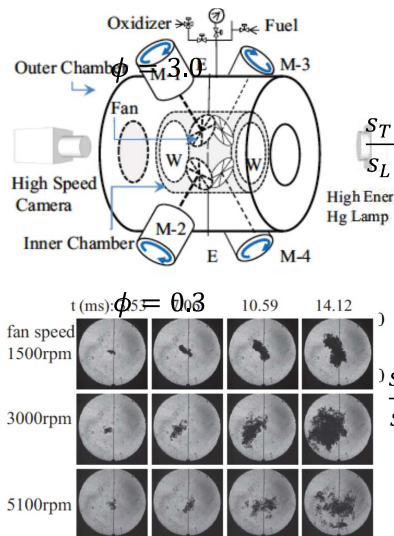
Institute for Combustion Technology | Lukas Berger – TNF Workshop 2022, Vancouver

¹⁾Yang et al., Combust. Flame 188 (2018) 498-504 ²⁾Ahmed et al., Combust. Flame 233 (2021) 111586 ³⁾M.S. Wu et al., Combust. Sci. and Tech. 73 (1990) 327-350 ⁴⁾Cheng et al., Proc. Combust. Inst. 32 (2009) 3001-3009 ⁵⁾Song et al., Combust. Flame 232 (2011) 111523 ⁶⁾Chu et al., Proc. Combust. Inst. 29 (2022) ⁷⁾Rocco et al. Flow Turb. Combust. 94 (2015) 359-379 ⁸⁾Berger et al., Combust. Flame 244 (2022) 112254



Experimental Data

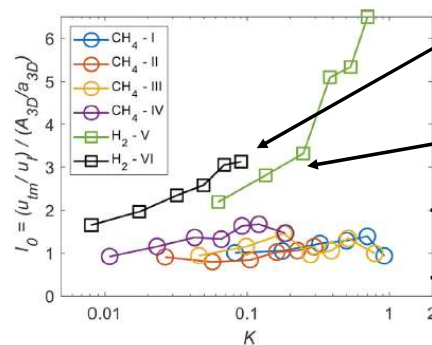
Cylindrical Vessel¹



$$\frac{S_T}{S_L} \bigg|_{\phi=3.0} \ll \frac{S_T}{S_L} \bigg|_{\phi=0.3}$$

→ Clear effects of TD instabilities

Spherical Vessel²



Hydrogen/air:
 $\phi = 0.4, T_u = 365K,$
 $p = 5bar$

Hydrogen/air:
 $\phi = 0.3, T_u = 365K,$
 $p = 5bar$

Methane/air flames at different conditions

- Unity stretch factor in methane/air flames
- Stretch factor significantly enhanced in hydrogen/air flames
- Clear effects of TD instabilities

32

Institute for Combustion Technology | Lukas Berger – TNF Workshop 2022, Vancouver

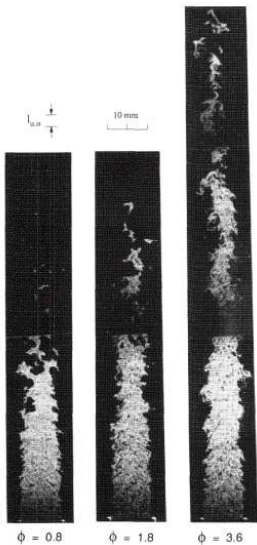
¹⁾S. Yang, A. Saha, W. Liang, F. Wu, C.K. Law, Combust. Flame 188 (2018) 498-504

²⁾P. Ahmed, B. Thorne, M. Lawes, S. Hochgreb, G.V. Nivarti, R.S. Cant, Combust. Flame 233 (2021) 111586



Experimental Data

Turbulent Round Jet^{1,2}

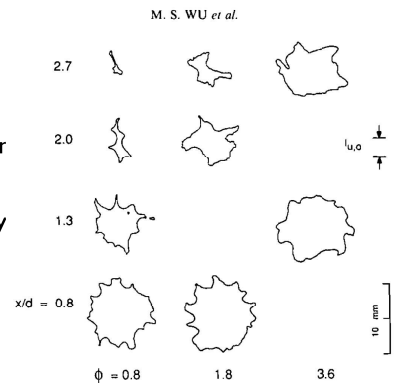


- Coaxial premixed jet with co-flow of burned gas
- Operating conditions:
 - $Re_{pipe} = [7,000 - 40,000]$
 - $\phi = [0.3 - 3.57]$
- Lean cases:
 - Higher turbulent burning velocity even though laminar flame speed lower
 - Higher distortion of flames

→ Effects of TD instabilities

Experimental data

- Lots of data from velocity measurements
 - Mean and fluctuation for nozzle exit velocity
 - Velocity profiles
 - Velocity energy spectra
 - Progress variable
 - Cross-sectional images
 - Statistics on flame position
 - But, no stretch factor or turbulent burning velocity



33

Institute for Combustion Technology | Lukas Berger – TNF Workshop 2022, Vancouver

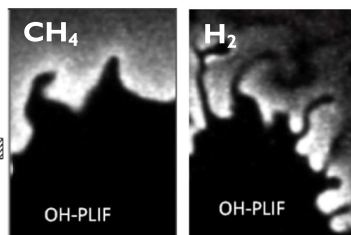
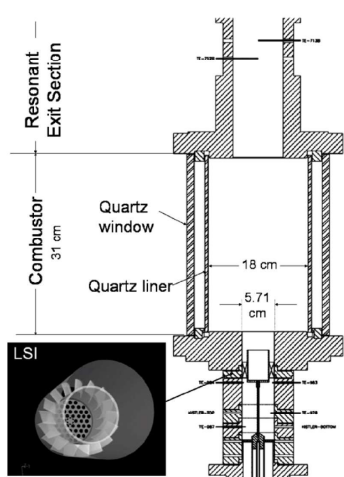
¹M.S. Wu, S. Kwon, J.F. Driscoll, G.M. Faeth, Combust. Sci. and Tech. 73 (1990) 327-350

²M.S. Wu, S. Kwon, J.F. Driscoll, G.M. Faeth, Combust. Sci. and Tech. 78 (1991) 69-96



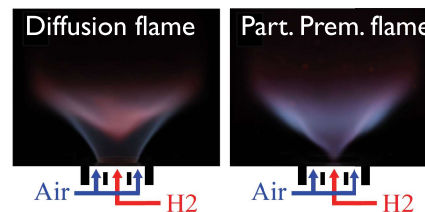
Experimental Data

Low Swirl Injector¹



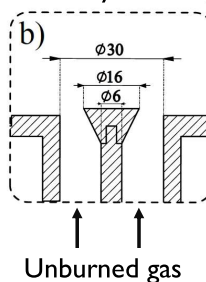
- Stable operation with H_2/air at $\phi = 0.5$ possible
- Comparison H_2 vs. CH_4
 - Different local flame shape & flame stabilization
 - Increased turbulent kinetic energy

Swirl- or Bluff Body-Stabilized Flames^{2,3}



Swirl-Stabilized Flame²

Bluff Body-Stabilized³



- Flame type/stabilization depends on operating conditions
- Difficult to achieve fully premixed flame
- Fully premixed flame can be stabilized by bluff body
- Flashback possible

34

Institute for Combustion Technology | Lukas Berger – TNF Workshop 2022, Vancouver

¹R.K. Cheng, D. Littlejohn, P.A. Strakey, T. Sidwell, Proc. Combust. Inst. 32 (2009) 3001-3009

²S. Marragou, H. Magnes, A. Aniello, L. Selle, T. Poinso, T. Schuller, Proc. Combust. Inst. 39 (2022)

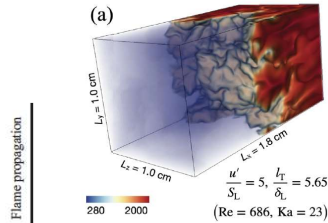
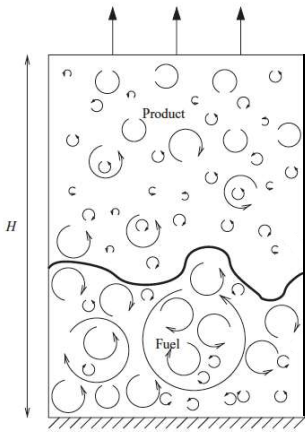
³T. Yaghi, J.R. Dawson, T. Schuller, Proc. Combust. Inst. 39 (2022)



DNS Data

Forced Homogeneous Isotropic Turbulence

Forced HIT^{1,2}

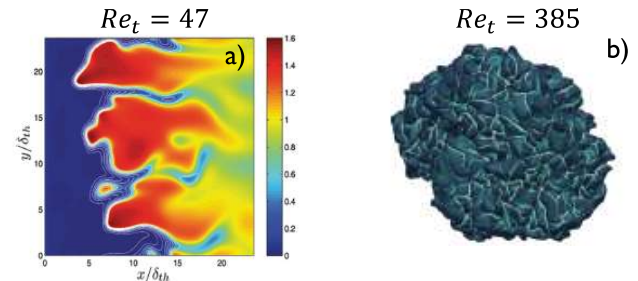


Parametric range explored for hydrogen flames

- $Ka \approx 1 - 1500$
- $Re_t \approx 1 - 700$

Either forcing term required or decaying turbulence

Decaying HIT^{3,4}



- a) Enhancement of turbulent kinetic energy in low Lewis number flames
- b) Four-fold increase of I_0 due to TD instabilities

35

Institute for Combustion Technology | Lukas Berger – TNF Workshop 2022, Vancouver

¹A.J. Aspden, M.S. Day, J.B. Bell, J. Fluid Mech. 680 (2011) 287–320 ²W. Song, F.E.H. Pérez, E.-A. Tingas, H.G. Im, Combust. Flame 232 (2011) 111523

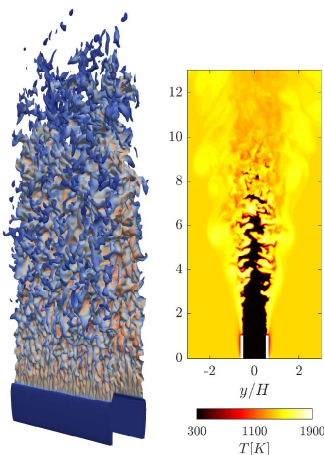
³N. Chakraborty, M. Katragadda, R.S. Cant, Phys. Fluids 23 (2011) 075109 ⁴H. Chu, L. Berger, T. Grenga, Z. Wu, H. Pitsch, Proc. Combust. Inst. 29 (2022)



DNS Data

Shear Driven Turbulent Flows

Slot Burner¹

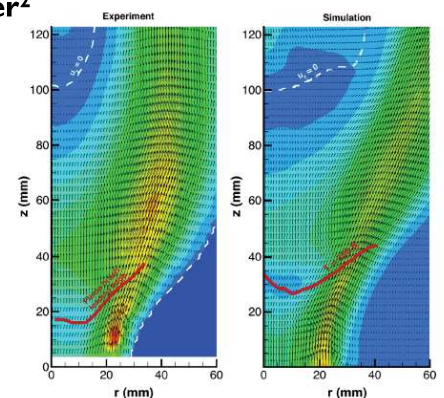


- Operating conditions
 - $Ka \approx 15$
 - $Re_{jet} \approx 11,000$
- Cost: 15Mio. CPUh
- Simplified analysis
 - Periodic direction
 - Stationary flame
- High Karlovitz numbers lead to long flames

Low-NOx burner²



- H_2/air at $\phi = 0.37$
- Comparison of experiments and DNS
- Strong effects of instabilities on local flame structure



36

Institute for Combustion Technology | Lukas Berger – TNF Workshop 2022, Vancouver

¹L. Berger, A. Attili, H. Pitsch, Combust. Flame 244 (2022) 112254

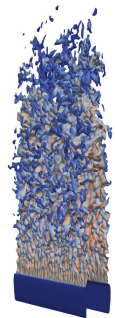
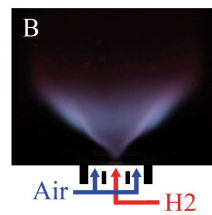
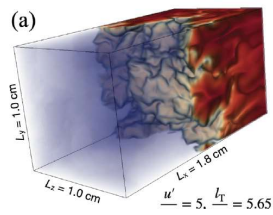
²M. Day, S. Tachibana, J. Bell, M. Lijewski, V. Beckner, R.K. Cheng, Combust. Flame 162 (2015) 2148–2165



Discussion

Key discussion points:

- Hypothesis and validation of turbulent hydrogen combustion models
- Are there any particular advantages of a configuration for hydrogen combustion?
- Who is interested in modeling which experiment/DNS?
- Who is planning any suitable validation experiments?
- Which conditions are of interest?



TNF/PTF Workshops

Blank Page

Summary: Combustion of ammonia as energy/hydrogen carrier

Coordinators: Andrea Gruber and Gaetano Magnotti

Growing interest has recently emerged in the utilization of ammonia as carbon-free energy carrier in thermal energy conversion devices, i.e. gas turbines and reciprocating engines, for power generation and propulsion applications. In this context, several combustion research groups worldwide have initiated research activities to investigate the fundamental characteristics of turbulent combustion of pure ammonia (and of its blend with hydrogen and natural gas) in premixed and non-premixed configurations. Therefore, in true “TNF spirit”, a session on the topic of turbulent combustion of ammonia (pure or blended) was arranged with emphasis on detailed measurements and direct numerical simulation (DNS). The aim is to gain fundamental insights about combustion of this relatively new and unexplored fuel and to provide good numerical and experimental data, using flames that are relatively simple in terms of both chemistry and flow geometry, for benchmarking of turbulence-chemistry interaction models.

Andrea Gruber of SINTEF started the session providing a brief general introduction to the topic of ammonia utilization as carbon-free energy carrier, highlighting the (many) open questions about its deployment in combustion devices and related challenges with flame stability and emissions of undesired atmospheric pollutants (NO_x) and greenhouse gases (N_2O). A crucial point, of relevance to the mission of the TNF workshop, is the present uncertainty in the chemical kinetics of ammonia combustion with a significant spread still observed among the chemical kinetics schemes presently available in the open literature.

In the first part of the session, contributions on DNS of turbulent combustion configurations of pure or partially decomposed ammonia (ammonia/hydrogen/nitrogen fuel blends) at atmospheric and elevated pressure were presented. These included: “SINTEF/Sandia Collaboration on DNS of $\text{NH}_3/\text{H}_2/\text{N}_2$ -air premixed flames” from SINTEF and Sandia; “Structure and propagation characteristics of premixed ammonia flames under different turbulent conditions” from KAUST; “A DNS study of a freely propagating premixed ammonia/air flame under homogeneous turbulence” from Zhejiang University. The main findings from the DNS studies can be summarized as follows:

- In premixed combustion of partially decomposed ammonia, at fuel-lean conditions and for the relatively high decomposition rate investigated (40% ammonia, 45% hydrogen and 15% nitrogen), important local effects of thermo-diffusive instabilities are observed at the small scales with significant increase of the overall turbulent burning rate, ultimately resulting in acceleration of the whole flame front. This behavior, i.e. the global effect of local small-scale processes, represents a challenge for turbulent combustion models.
- NO_x and N_2O formation is greatly affected by the equivalence ratio with large amounts of the unwanted nitrogen species produced at oxygen-rich conditions (fuel-lean combustion). The formation of these compounds is dramatically reduced at fuel-rich conditions but the presence of unburnt fuel (mostly hydrogen, following ammonia pyrolysis by the high temperature of the flame) would require the utilization of longitudinally staged (rich-lean) systems in practical applications.
- On the one side, increasing the pressure level at which combustion takes place, further augments the strength of the thermo-diffusive instabilities and the turbulent flame acceleration. On the other side, the pressure increase leads to a significant decrease in nitric oxides (NO_x) formation and to an increase in nitrous oxide (N_2O).
- Turbulent premixed flames of pure ammonia in air are not affected by thermo-diffusive instabilities and behave very similarly to methane-air flames (stretch factor $I_0 \sim 1$).

Accordingly, these flames are not expected to present significant challenges for turbulent combustion models.

Gaetano Magnotti presented the experimental component of the ammonia session, which consisted of three sections. The first section focused on collaborative work from SINTEF, NTNU, and TU Darmstadt to investigate the resilience to strain-induced blowout (RSIB), defined as the product of the laminar flame time and local extinction strain rate, in laminar premixed counterflow twin flames.[1] Local extinction strain rates were derived from the maximum gradient of the axial velocity measured from particle tracking velocimetry (PTV). Experimental results show the RSIB decreases monotonically with increasing equivalence ratio for $0.6 \leq \phi \leq 1.1$. For all equivalence ratios tested the RSIB, shows a non-monotonic behavior with the H_2 mole fraction, reaching a peak for $x_{H_2} = 0.27$. The effect is very pronounced (3x increase in RSIB) for lean flames, and becomes weaker with increasing equivalence ratio. Comparisons with simulations using the Han kinetic model show good agreement with experimental results for $\phi > 0.8$ but show some deviation at leaner equivalence ratios, underlying the need for detailed measurements in laminar flames to validate kinetic models.

The second section of the experimental presentation provided an overview of the recent development in laser diagnostics for ammonia combustion, including contributions from Lund university (simultaneous OH+NH) [2], SUSTECH (single excitation frequency for simultaneous Rayleigh, NH and NH_3 PLIF measurements) [3]. The session then focused on recent developments at KAUST enabling Raman+NO LIF for line measurements of temperature, major species and NO — a critical diagnostic capability to build the experimental datasets typically featured in the TNF [4]. Intense chemiluminescence and laser-induced fluorescence were highlighted as major challenges in Raman spectroscopy of ammonia combustion, and operation at high pressure was proposed as a strategy to minimize the effects of these interferences. Measurements in a series of laminar premixed and non-premixed counterflow flames revealed a linear relationship between the NH_2 number density and the fluorescence interference signal integrated over the 620-630 nm spectral range. A single calibration factor, obtained by matching the peak NH_2 concentration to predictions using the Otomo chemical kinetics model, lead to an agreement within 5% over a wide range of fuel compositions and strain rates, with a COV < 10%, making the approach suitable for measurements in turbulent flames.

The third and last section of the presentation focused on a comparison between measurements (Raman [5] and NO-LIF, PIV) and simulations (flamelet progress variable (FPV) and Principal Component analysis+Deep Neural Network (PC-DNN) using $Le=1$, from Hong Im, KAUST) of turbulent cracked ammonia (14% and 28%) jet-flames in an air co-flow at 5 bar, with $Re=11200$. The main findings are summarized below:

- The measurements show that in the near field, Lewis number and differential diffusion effects are important, and the temperature and H_2O profiles follow that predicted using the multi-component model. The NH_3 and H_2 profiles are in between the $Le=1$ and the multi-component transport predictions. The differential diffusion effects are overcome by turbulent mixing downstream, but the NH_3/H_2 ratio is increased as a consequence of the diffusion and consumption of H_2 ahead of NH_3 closer to the nozzle.
- The scatterplots in mixture fraction space highlight the presence of localized extinction for the CAJF14 flame, but not for the more stable CAJF28. Further analysis of the extinguished samples, identified by a mixture fraction close to stoichiometry but a low temperature, indicates the presence of unburnt ammonia, but hydrogen mole fraction is within the range found in fully burnt samples
- Both simulations overpredict the NH_3 consumption and underpredict the H_2 consumption, underlying the need to include preferential diffusion and non-unity Le number in the simulation.

- Raman data are already published and accessible [5]. The remaining experimental data (NO [6] and PIV) will be added to the TNF website.


The presentation ended with an overview of potential test cases for measurement campaigns at KAUST to provide datasets for TNF16. Three flames were proposed:

- A variation of the Sandia/Sydney piloted flame, with simulated cracked ammonia as fuel. Measurements will be taken for varying Re numbers ranging from laminar to 80% of the extinction value and will be completed by Summer 2023.
- Sydney/Sandia inhomogeneous burner, (KAUST/Sydney collaboration), with varying NH_3/H_2 ratio and Re. The measurements were completed in October 2022 and be available by the second quarter of 2023.
- Bluff-body stabilized jet flames (KAUST, Magnotti-Dally), with fuel composition ranging from 100% to 20% cracking. Two series, one with constant Re, the other with constant jet velocity.
- Additional test cases may be available from TU Darmstadt, as their Raman instrument for ammonia combustion becomes operational.

Data will be made available to the TNF community by Summer 2023, following an ad-hoc meeting, tentatively scheduled for May 2023 where the experimental results will be presented.

References

- [1] M. Richter, R. Schultheis, J.R. Dawson, A. Gruber, R.S. Barlow, A. Dreizler, D. Geyer, Extinction strain rates of premixed ammonia/hydrogen/nitrogen-air counterflow flames, Proceedings of the Combustion Institute, doi:[https://doi.org/10.1016/j.proci.2022.09.011\(2022\)](https://doi.org/10.1016/j.proci.2022.09.011(2022)).
- [2] Q. Fan, X. Liu, L. Xu, A.A. Subash, C. Brackmann, M. Aldén, X.-S. Bai, Z. Li, Flame structure and burning velocity of ammonia/air turbulent premixed flames at high Karlovitz number conditions, Combustion and Flame 238 (2022) 111943.
- [3] Z. Wang, X. Li, L. Li, Z. Zhao, B. Zhou, X. Gan, Strategy for simultaneous multi-scalar imaging in turbulent NH_3/H_2 premixed flames using a single laser system, Combustion and Flame 242 (2022) 112185.
- [4] H. Tang, C. Yang, G. Wang, T.F. Guiberti, G. Magnotti, Raman spectroscopy for quantitative measurements of temperature and major species in high-pressure non-premixed $\text{NH}_3/\text{H}_2/\text{N}_2$ counterflow flames, Combustion and Flame 237 (2022) 111840.
- [5] H. Tang, C. Yang, G. Wang, Y. Krishna, T.F. Guiberti, W.L. Roberts, G. Magnotti, Scalar structure in turbulent non-premixed $\text{NH}_3/\text{H}_2/\text{N}_2$ jet flames at elevated pressure using Raman spectroscopy, Combustion and Flame 244 (2022) 112292.
- [6] G. Wang, H. Tang, C. Yang, G. Magnotti, W.L. Roberts, T.F. Guiberti, Quantitative laser-induced fluorescence of NO in ammonia-hydrogen-nitrogen turbulent jet flames at elevated pressure, Proceedings of the Combustion Institute, doi:[https://doi.org/10.1016/j.proci.2022.08.097\(2022\)](https://doi.org/10.1016/j.proci.2022.08.097(2022)).



Combustion of ammonia as energy/hydrogen carrier



Gaetano Magnotti (KAUST) & Andrea Gruber (SINTEF/NTNU)
TNF and PTF Workshops - July 22-23, 2022 Coast Coal Harbor Hotel Vancouver, Canada



 SINTEF  NTNU



Outline

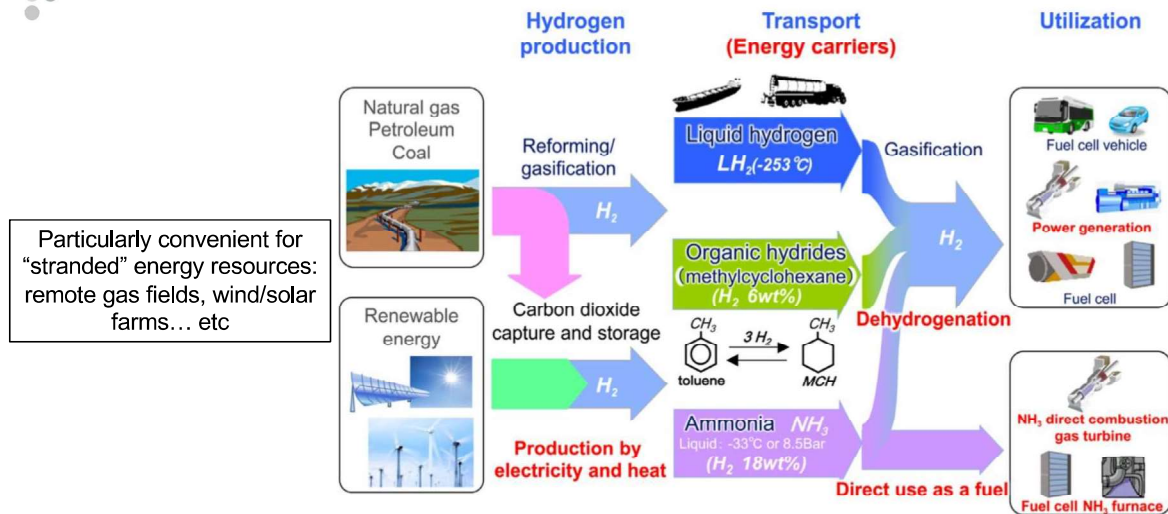
- Intro
- DNS of ammonia combustion configurations
- Detailed experimental measurements of ammonia flames (Gaetano)

 SINTEF  NTNU



Background

Ammonia is emerging as a convenient energy (and hydrogen) carrier

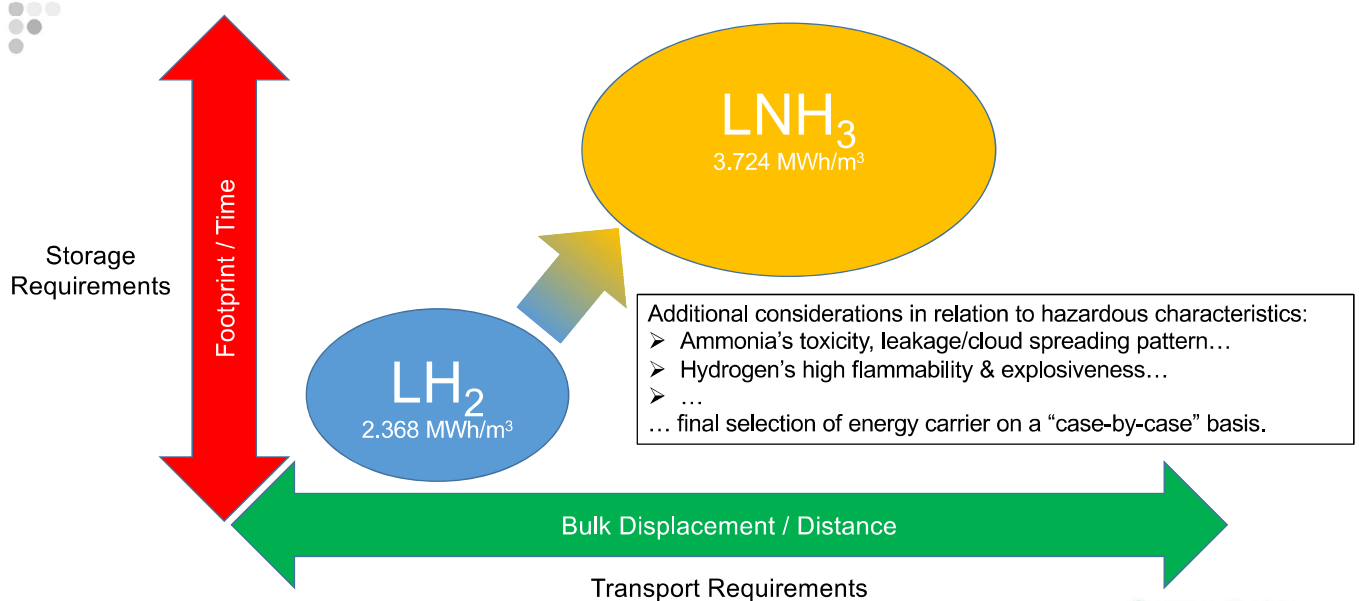


Courtesy of Japan Science and Technology Agency (JST)

SINTEF NTNU



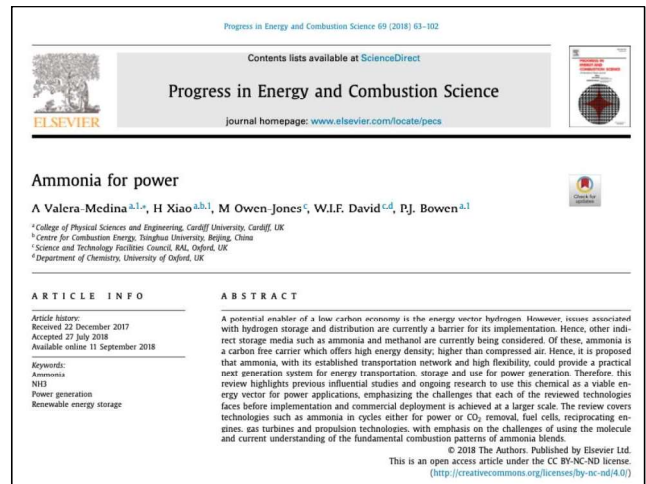
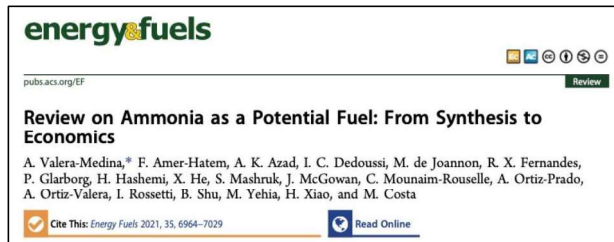
NH_3 vs H_2 as C-free Energy Carriers



Significantly simpler logistics of ammonia vs hydrogen

SINTEF NTNU

Renewed/Recent Interest in Ammonia by Research & Industry



Ammonia Combustion Research (infancy of a fuel 😊)

Several decades of combustion research on conventional hydrocarbons:

- detailed insights about local (structure) and global flame characteristics (TCI)
- this is not the case for ammonia!

”Early” recent work in Japan and UK on ammonia combustion:

- Public funded research at Tohoku U / AIST (post Tohoku earthquake, ~2012)
- Public/private funded research at Cardiff U (~2015)
- Initial focus in Japan and UK on pure ammonia or ammonia/methane blends

Research activity in Norway from 2017 (w/Sandia NL):

- Focus on partially-decomposed ammonia (H₂/N₂/NH₃ blends)
- Inspired by the paper of Verkamp et al. Proc Combust Inst (1966)
- Aim is to optimize the NH₃ decomposition rate to create a C-free fuel that “mimics” natural gas combustion properties (fuel switch on existing assets)

Barely started “scratching the surface” of a vastly unknown topic...



Combustion, Stability & Emissions: Open Questions with Ammonia

Applications-related challenges are the “usual suspects”:

- Static (flashback/blow-out) & dynamic (TA) flame stabilization (GTs)
- Reliable ignition and complete fuel consumption (ICEs)
- Pollutants (NO_x) and greenhouse gases (N_2O) emissions (GTs and ICEs)

Best approach / combustor design strategy? Yet to be found:

- Direct NH_3 combustion or (partial) decomposition to $\text{NH}_3/\text{H}_2/\text{N}_2$ mixtures?
- Gaseous or liquid NH_3 injection, vaporization & combustion?
- Premixed or non-premixed combustion?
- Longitudinal fuel staging (e.g. RQL) seems a promising approach for GTs...
- ... what about ICEs?



Ammonia and Combustion Research

Ammonia-fired GTs and ICEs will likely address niche applications only and industrial R&D efforts will probably focus on fuel-flexible equipment...

Main role of the combustion research community:

- Provide industry with the fundamental and applied knowledge needed to develop reliable, clean and efficient fuel-flexible combustion systems

Where to start? Some suggestions:

- Development & validation of chemical kinetics schemes (a significant spread is presently observed)
- Detailed measurements (e.g. Raman) and simulations (DNS) of laminar and turbulent flames for validation of chemical kinetics schemes and TCI-models
- Effect of pressure is a key aspect (often neglected...)



Direct Numerical Simulation of Turbulence-Chemistry Interaction in Ammonia Flames

Contributions from 3 research groups:

- SINTEF/Sandia NL
 - $\text{NH}_3/\text{H}_2/\text{N}_2$ -air lean premixed flames in temporally-evolving jet (**Ka~160**) and shear layer (**Ka~620**) configurations
 - $\text{NH}_3/\text{H}_2/\text{N}_2$ -air stoichiometric premixed flames in constant volume vessel (**FWI session tomorrow**)
- KAUST
 - NH_3 -air (lean & rich) vs H_2 -air premixed flames (constant S_L) at one selected combustion regime (**Da=0.1, Ka~80**)
 - NH_3 -air (rich) premixed flames across a range of combustion regimes (**Da=0.1-0.5, Ka~30-80**)
- Zhejiang University
 - NH_3 -air (lean & rich) premixed flames comparison in intense turbulence (**Ka~287**)



SINTEF/Sandia NL Collaboration on DNS of $\text{NH}_3/\text{H}_2/\text{N}_2$ -air premixed flames

- Part of larger initiative (BIGH2/Phase III) aimed at improving fuel flexibility of Siemens 4th Gen DLE burner for the SGT750 industrial gas turbine
- Research work started in Q4 of 2017 and ended in Q4 of 2021
- UCSD was involved early in the project for the development of a short mechanism for hydrogen/ammonia combustion usable in large-scale LES/DNS
- Sandia NL contributed to the project with the setup, execution and analysis of the DNS



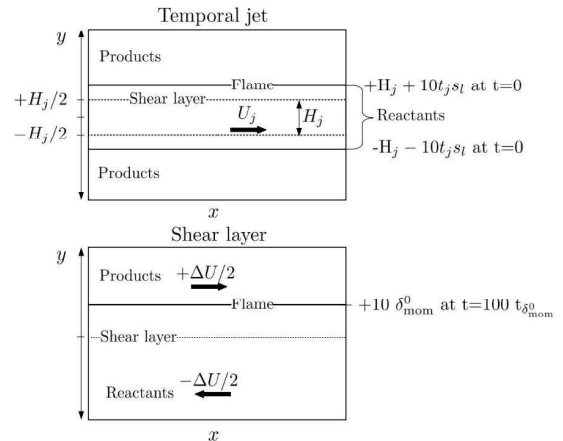
DNS Configurations

	Temporal jet			Shear layer	
Cases:	A	B	C	D	E
ϕ	0.45	0.9	1.1	0.45	0.45
p	1.0	1.0	1.0	1.0	10.0
s_l	0.86	2.28	2.49	0.86	0.19
δ_l	526	342	339	526	188
δ_{mom}^0	0.375	0.1915	0.1841	0.1875	0.075
$U_j, \Delta U$	150	311	331	300	75
$Da_{\delta_{mom}^0}$	0.008	0.008	0.008	0.002	0.002
Re_t	1061	1003	944	1102	1080
Ka	159	166	167	626	613

Effect of equivalence ratio

Effect of pressure

$NH_3/H_2/N_2$ (40/45/15% vol) – air mixture @ 750K



- DNS code: S3D-Legion
- Chemical kinetics: short San Diego (19 species & 63 reactions)*

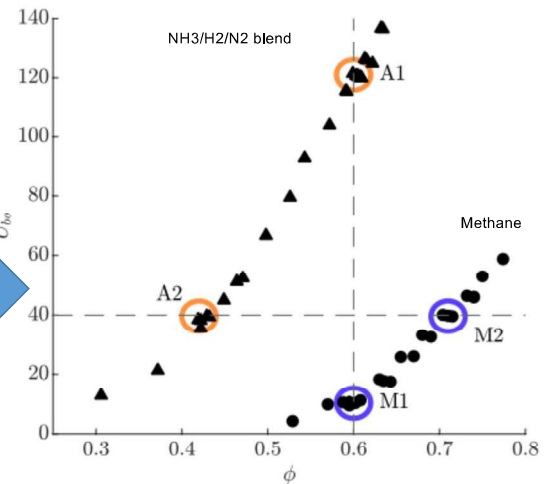
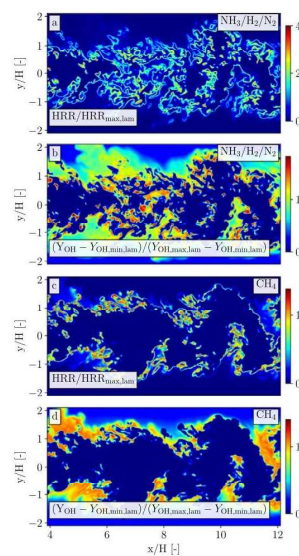
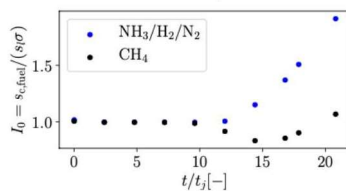
SINTEF NTNU

*Jiang et al, "An updated short chemical-kinetic nitrogen mechanism for carbon-free combustion applications", *Int J Energy Res* vol. 44, pp. 795-810 (2020).



Temporal Jet «A» & Comparison w/ CH_4 *

Cases:	A
ϕ	0.45
p	1.0
s_l	0.86
δ_l	526
δ_{mom}^0	0.375
$U_j, \Delta U$	150
$Da_{\delta_{mom}^0}$	0.008
Re_t	1061
Ka	159



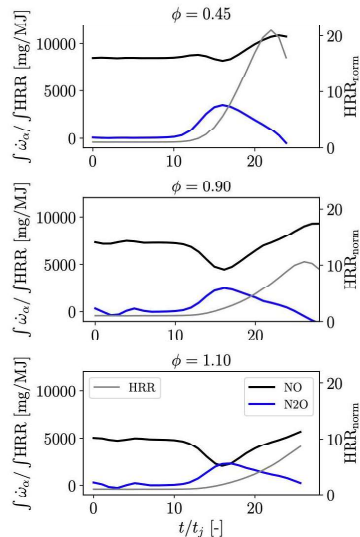
- Significant role of molecular diffusion in highly turbulent flames!

SINTEF NTNU

*Wiseman et al, "A comparison of the blow-out behaviour of turbulent premixed ammonia/hydrogen/nitrogen-air and methane-air flames", *PCI* vol. 38, pp. 2869-2876 (2021).



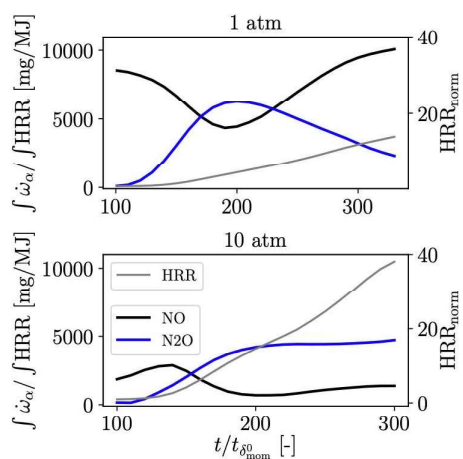
Temporal Jet «A», «B» & «C»: Effect of Equivalence Ratio on Emissions



- Volume-integrated NO and N₂O production normalized by the heat release rate
- Lean cases consistently exhibit higher NO production than rich case at all times during the turbulence-flame interaction
- While NO production is sustained in time, N₂O production peaks (when interaction starts) and then decreases to low (even negative) values towards the end of the interaction



Shear Layer «D» & «E»: Effect of Pressure on Emissions



- Volume-integrated NO and N₂O production normalized by the heat release rate
- High-pressure case consistently exhibit lower NO production than atmospheric case
- N₂O production monotonically increases at high pressure while it decreases to (relatively) low values at atmospheric pressure



Ongoing Investigations and Further Work

- Extension of pressure scaling study to 20 bar
- Investigation of premixed flames for low NH_3 decomposition rates (10-20%)
- Investigation of non-premixed flames (for low- NO_x performance)
- Investigation of second-stage flame in a RQL staging arrangement
- Re-assessment and update/improvement of chemical kinetics scheme
- Open for discussion and suggestions...

SINTEF NTNU



جامعة الملك عبد الله
للعلوم والتقنية
King Abdullah University of
Science and Technology

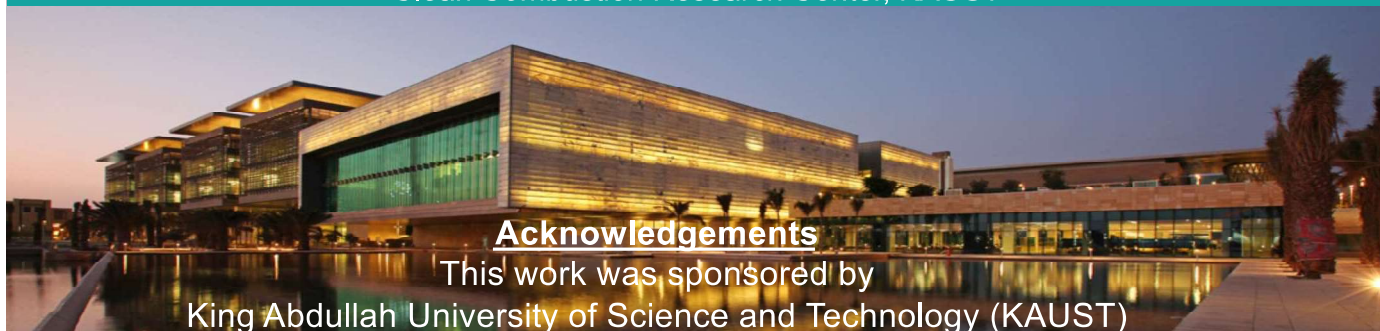
TNF and PTF Workshops
July 22-23, 2022
Vancouver, Canada

Structure and propagation characteristics of premixed ammonia flames under different turbulent conditions

Ruslan Khamedov, Wonsik Song, Francisco E. Hernández Pérez, Hong G. Im
Computational Reacting Flows Laboratory (CRFL)
Clean Combustion Research Center, KAUST

Acknowledgements

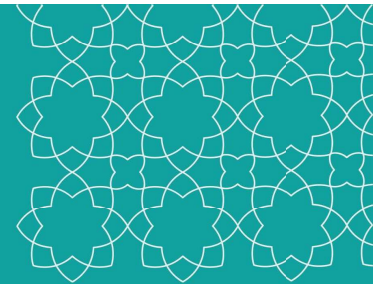
This work was sponsored by
King Abdullah University of Science and Technology (KAUST)





KARFS (KAUST Adaptive Reacting Flow Solver)

- Fully compressible Navier-Stokes, energy, and species equations
 - 8th order central difference scheme for spatial discretization
 - 4th order explicit Runge-Kutta method for time integration
 - 10th order filter
 - Nonreflecting NSCBC (Navier-stokes Characteristic Boundary Conditions)
 - Turbulent forcing: Bassenne et al. (2016) Phys. Fluids
-
- Hydrogen kinetic mechanism by Burke et al. (9 species and 23 reactions)
 - Ammonia kinetic mechanism from KAUST (25 species and 178 reactions)

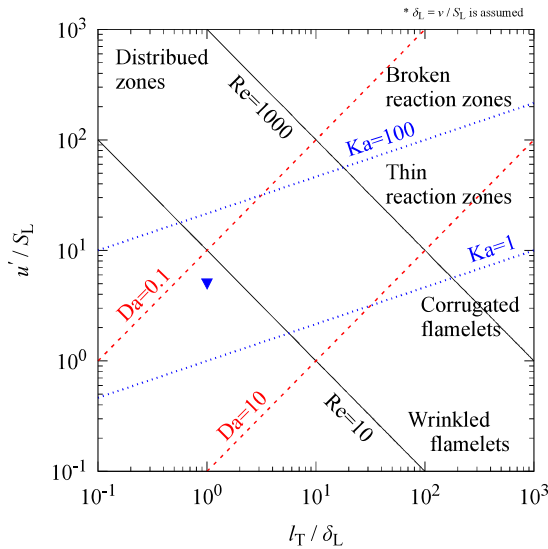


**Comparison of turbulence-flame interaction
between lean H₂/air, and lean and rich NH₃/air
flames at a similar turbulent condition**

Selected conditions for freely propagating turbulent flames



Borghi diagram



Case	l_T / δ_L [-]	u' / S_L [-]	Re [-]	Da [-]	Ka [-]
H2	1	10	78	0.1	88
AL	1	10	56	0.1	75
AR	1	10	72	0.1	85

H2: H₂/air premixed flame

$\varphi = 0.41$, $T = 300$ K ($S_L = 0.211$ m/s), $Le = 0.36$

AL (lean ammonia): NH₃/air premixed flame

$\varphi = 0.81$, $T = 600$ K ($S_L = 0.211$ m/s), $Le = 0.90$

AR (rich ammonia): NH₃/air premixed flame

$\varphi = 1.2$, $T = 500$ K ($S_L = 0.211$ m/s), $Le = 1.12$

19

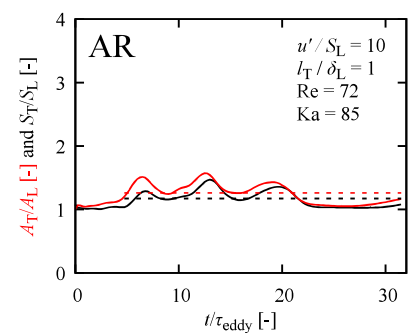
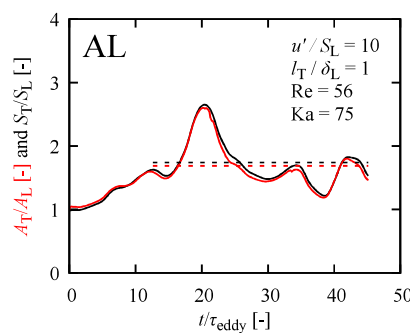
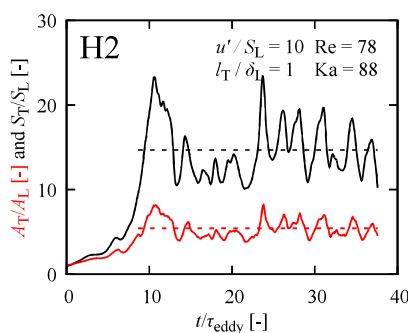
Turbulent flame speed variation

$$S_T = \frac{1}{\rho_u A_0 (Y_{u,F} - Y_{b,F} A_0)} \int_V \dot{\omega}_F dV$$



Poinsot et al. (1992) CST

Temporal evolution of S_T/S_L and A_T/A_L



- Large stretch factor for H2 but close to unity for AL and AR
- Despite the same l_T/δ_L and u'/S_L , A_T/A_L and thereby S_T/S_L are very different
- AR has significant reduction of surface area as compared to the lean ammonia flame (AL)

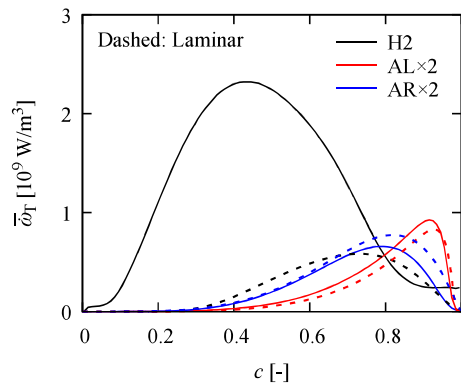
20

Conditional average of heat release rate (HRR)



- Conditional averages of HRR overlaid with laminar counterpart in progress variable space (c)

c for H2: T
 c for AL and AR: Y_{H_2O}



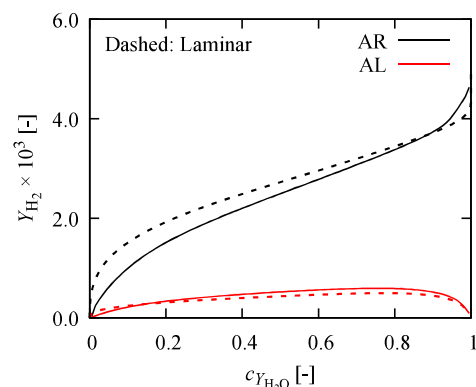
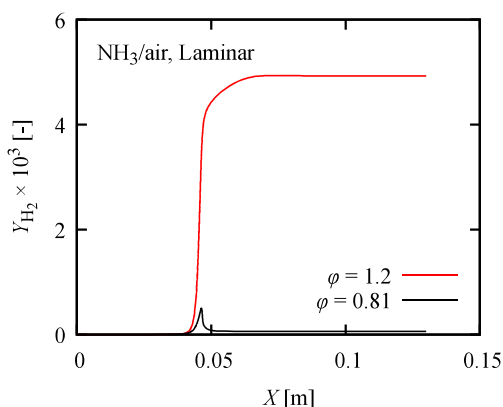
- HRR for turbulent H2:
 - 1) peak lies more upstream
 - 2) small bump upstream
 - 3) larger peak
- HRR for turbulent ammonia:
 - 1) peak lies more downstream
 - 2) AL shows higher peak
 - 3) AR shows broader distribution

21

H₂ mass fraction in ammonia flame



- Going back to the laminar flame...
- Conditional averages of mass fraction of H₂ for ammonia flames (lean vs. rich)



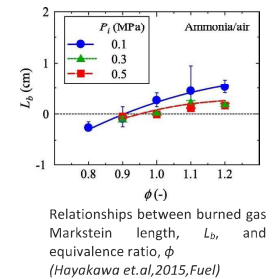
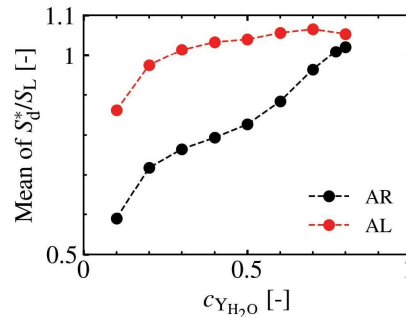
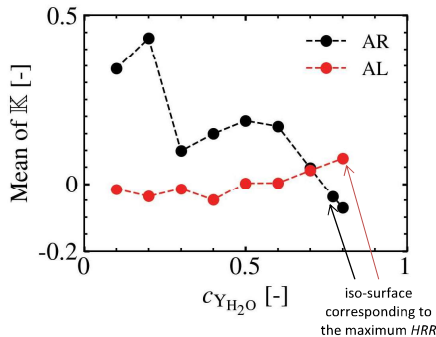
- Lean NH₃ flames, H₂ profile is similar to “intermediate” species
- Rich NH₃ flames, H₂ profile is similar to “product” species
- How does this affect turbulence-flame interaction?
- H₂ diffusion can take place reversely from down- to upstream direction for ammonia
- Local propagation speed may be affected by H₂ along the “**negatively**” curved regions

22

Stretch factor of lean and rich ammonia flame



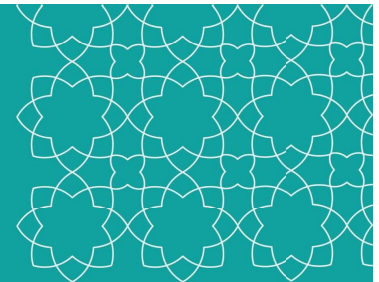
- Mean displacement speed (S_d^*) and stretch (K) along the iso-surfaces of $c_{Y_{H_2O}}$



- For the rich ammonia flame, the mean stretch is positive in the preheated zone and negative in the intense reaction zone
- The decrease of S_d is a result of stretch, which is responsible for the lower values of $\frac{S_T}{S_L}$ compared to $\frac{\bar{A}_T}{\bar{A}_L}$ for the rich ammonia flame $\rightarrow \frac{S_T}{S_L} = \frac{\bar{A}_T \bar{S}_d}{\bar{A}_L \bar{S}_L} \approx (1 - \frac{L \bar{K}}{S_L}) \frac{\bar{A}_T}{\bar{A}_L}$
- For rich ammonia flame ($Le > 0$), the Markstein number is positive

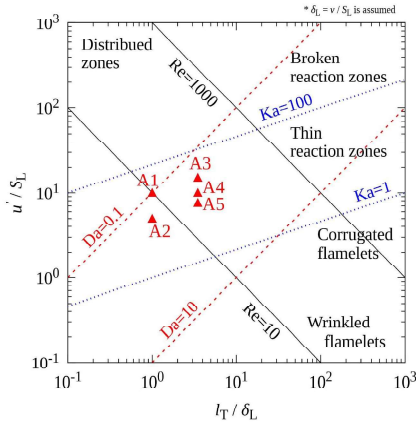
23

Global and local characteristics of premixed rich NH_3 /air flame for a wide range of turbulent conditions



Selected cases for a range of turbulent conditions

Borghi diagram



Turbulent cases

- A1 vs. A2: same l_T/δ_L (= 1.0)
- A3 vs. A4 vs. A5: same l_T/δ_L (= 3.5)
- A1 vs. A4: same u'/S_L (= 10)
- A1 vs. A3: same Ka (= 85)
- A2 vs. A5: same Ka (= 30)

- **Only rich ammonia/air flame is considered:** NH_3/air premixed flame $\varphi = 1.2$, $T = 500 \text{ K}$ ($S_L = 0.211 \text{ m/s}$)
- The effect of different turbulent conditions is analyzed

Case	l_T/δ_L [-]	u'/S_L [-]	Re [-]	Da [-]	Ka [-]
A1	1	10	72	0.1	85
A2	1	5	36	0.2	30
A3	3.5	15.2	386	0.2	85
A4	3.5	10	254	0.4	45
A5	3.5	7.6	192	0.5	30

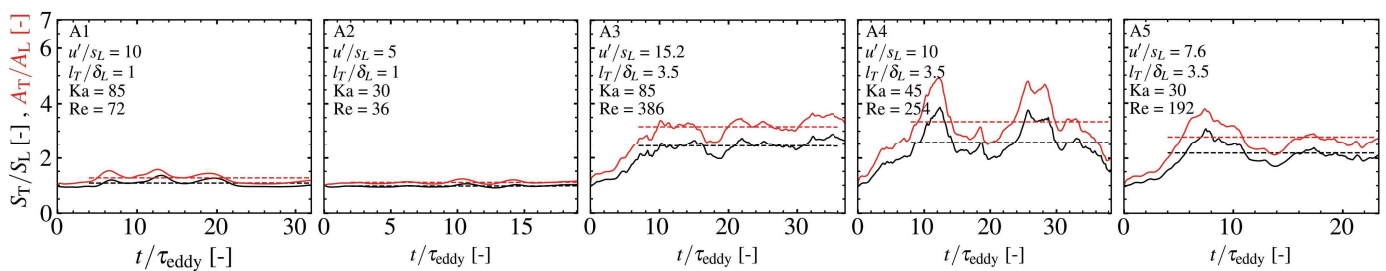
25

Turbulent flame speed

$$S_T = \frac{1}{\rho_u A_0 (Y_{u,F} - Y_{b,F} A_0)} \int_V \dot{\omega}_F dV$$

Poinsot et al. (1992) CST

- Temporal evolution of S_T/S_L and A_T/A_L



- The mean of the turbulent flame speed is increased with higher l_T/δ_L
- Less than unity stretch factor is observed regardless of the turbulent conditions
- The stretch factor for high l_T/δ_L flames is decreasing, i.e. the gap between flame area and flame speed enhancement is getting larger

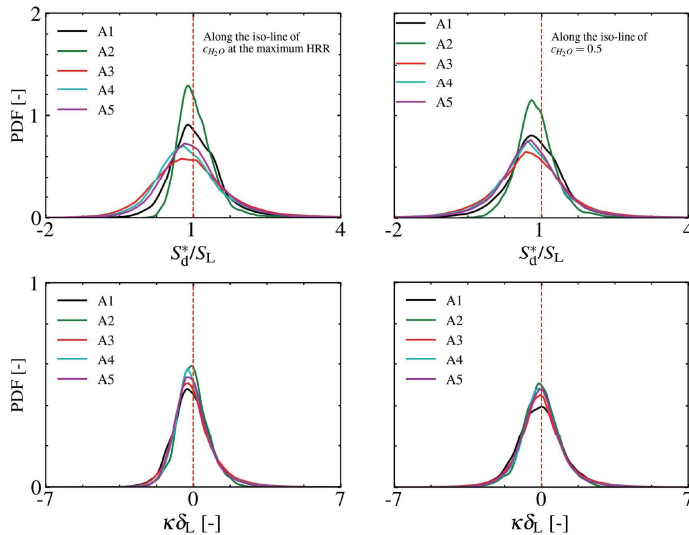
26

Statistics of S_d^* and flame curvature

$$S_d^* = \frac{\rho S_d}{\rho_u} = \frac{1}{\rho \nabla Y_k} [\dot{\omega}_k - \nabla \cdot \mathbf{J}_k]$$

Im and Chen (1999) CNF

- Probability density function for S_d^* and flame curvature (κ) along the iso-surface of $c_{Y_{H_2O}}$ at the maximum HRR

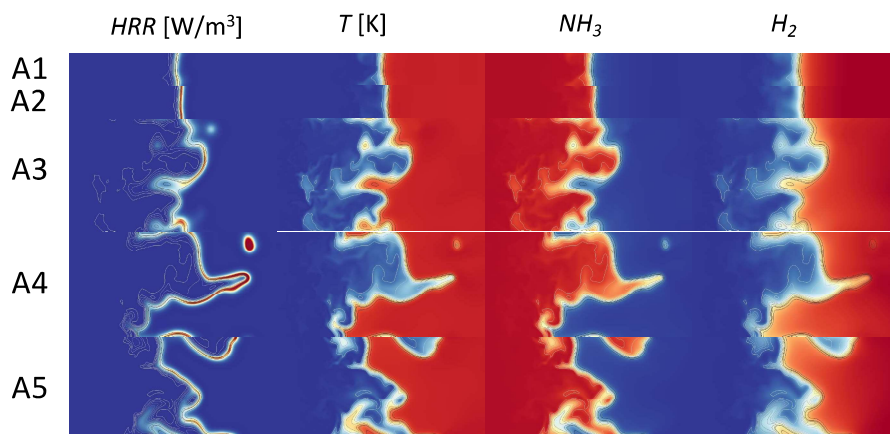


- The shape of the PDF of S_d^* follows a normal-like distribution with the peak at a value of S_d^* lower than S_L
- The flame curvature is mostly negative, which decreases the flame surface

27

Flame structure: representative instantaneous snapshot

- Key variables overlaid with the progress variable iso-lines



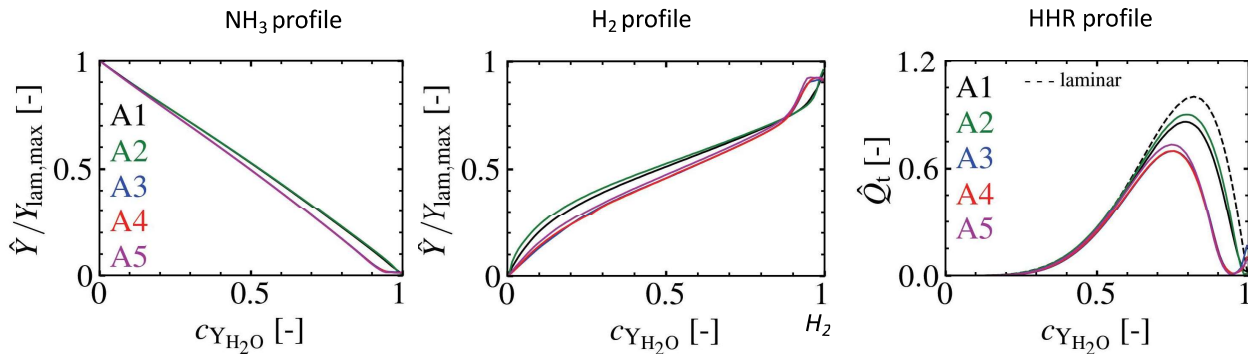
- Qualitative broadening of the flame zone is observed for flames with high l_T/δ_L
- The preheat zone is more disturbed for flames with high l_T/δ_L

28

Flame structure: conditional averages



- Additional observations on conditional averages of normalized mass fractions and HRR



- Peculiar behavior of mass fraction for high l_T/δ_L flames at the downstream zone
- More hydrogen cracking is expected for flow with larger turbulent eddies
- The peak of HRR for high l_T/δ_L flames is diminished and shifted towards unburned gas
- Effect of u'/S_L : the peak is diminished with increasing turbulent RMS velocity for a given l_T/δ_L

29

Conclusions



- Varied response of the flame stretch factor is observed for different equivalence ratios (lean vs. rich)
- The stretch factor ($\bar{I}_0 = (\bar{S}_T/S_L)/(\bar{A}_T/A_L)$) is less than unity for fuel-rich ammonia flame, and for larger integral length scale, the stretch factor decreases more**
- The rich ammonia flame exhibits flame surface area reduction, which may be partly due to the H₂ diffusion from down- to upstream direction
- The turbulent flame speed displays a strong correlation with the size of the most energetic turbulent eddies**
- For the rich ammonia flames, the PDF of S_d^* peaks at a value smaller than the one from 1D laminar flame, and flames have mostly negative curvature

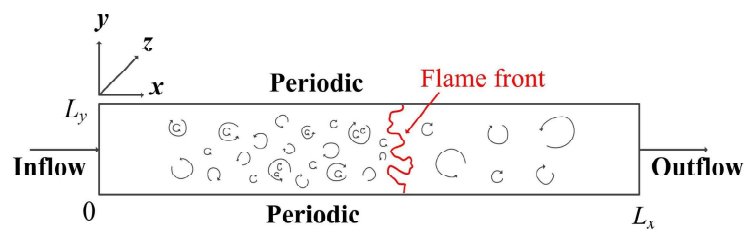
30

A DNS study of a freely propagating premixed ammonia/air flame under homogeneous turbulence

Tingquan Tian^a, Chengbin Song^a, **Haiou Wang^{a,*}**, Kun Luo^a, Jianren Fan^a

^a State Key Laboratory of Clean Energy Utilization, Zhejiang University, Hangzhou 310027, PR China

Configuration set-up



Schematic of the turbulent premixed flame configuration.

- The configuration of a freely-propagating turbulent premixed flame is considered.
- The reactant consists of ammonia/air mixture with a temperature of 300 K and the pressure is 1 atm. Two equivalence ratios of 0.9 and 1.1 are considered.

Configuration set-up



- **Homogeneous isotropic turbulence** based on a Passot-Pouquet kinetic energy spectrum is used as the initial turbulence field. The turbulence parameters are illustrated in Table 1.
- A **linear forcing method** was applied to maintain a statistically steady turbulence field.

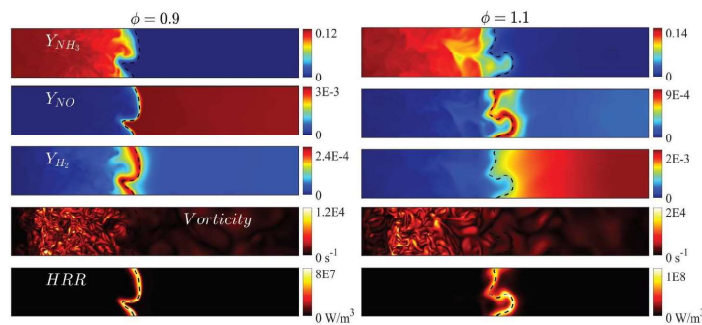
Table 1: Simulation parameters

ϕ	u' (m/s)	l_t (mm)	τ_e (ms)	Re_t	Ka
1.1	1.18	2.00	1.69	157	287
0.9	0.767	3.09	4.03	157	287

- Domain Size: $L_x \times L_y \times L_z = 10.57 \times 1.76 \times 1.76 \text{ cm}^3$ in the lean case and is $L_x \times L_y \times L_z = 6.85 \times 1.14 \times 1.14 \text{ cm}^3$ in the rich case. **Grid number is: $1008 \times 168 \times 168$.**
- More than 10 grid points across flame thickness δ_L are obtained. The criteria, $\eta/\Delta x > 1$, for turbulence is satisfied in all region of the domain
- A skeletal mechanism of ammonia/air combustion, including **20 species and 113 elementary reactions**, is developed for the DNS study, which is **derived from the Mathieu mechanism**.
- The simulation was performed using the DNS code 'S3D'. The DNS code has been used widely in studies of turbulent flames.

33

General flame structure

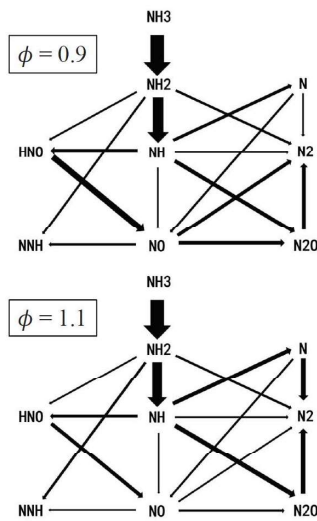


Contours of NH_3 , H_2 and NO mass fractions, vorticity magnitude and HRR in a typical x-y plane

- In the lean case NH_3 is consumed completely, while in the rich case the excess NH_3 is pyrolyzed to H_2 .
- NO mass fraction is the highest in the product for the lean case, while it is the highest in the reaction zone for the rich case.

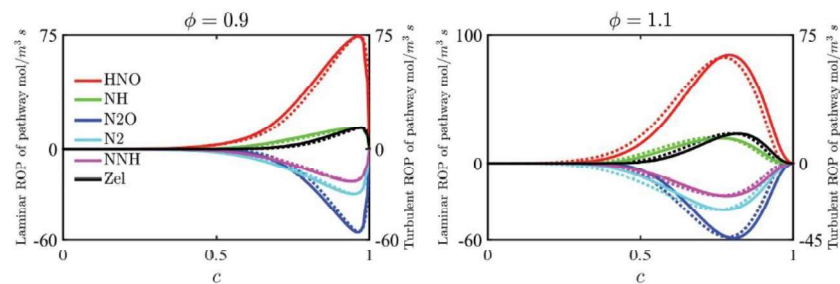
35

NO pathways: effect of TCI



The global nitrogen flow diagrams for the laminar flames. The thickness of the arrows indicates the fraction of the nitrogen flow.

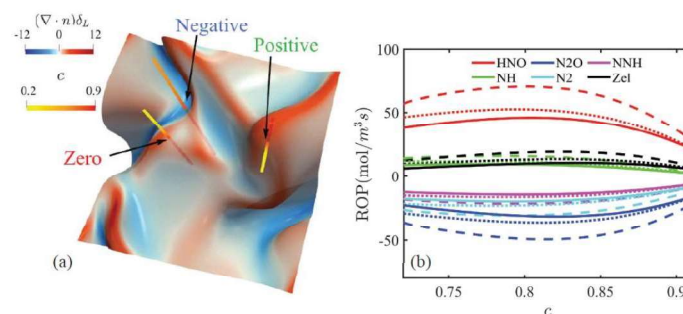
- NH_3 is consumed and converted to NH_2 , and NH_2 is attacked by radicals to produce HNO , NH , NNH and N_2 .
- Six NO pathways**, i.e. HNO , NH , N_2O , N_2 , NNH and Zeldovich (thermal) pathways, are defined based on the diagram.
- HNO pathway** and **N_2O pathway** play the most important role in the **formation** and **consumption** of **NO**, respectively.
- The relative contributions from various NO pathways, however, remain **unchanged between the turbulent and laminar flames**.



The conditional means of the rates of production (ROP) of various NO pathways for the lean and rich cases. The solid line and dotted line denotes the turbulent and corresponding laminar results respectively.

36

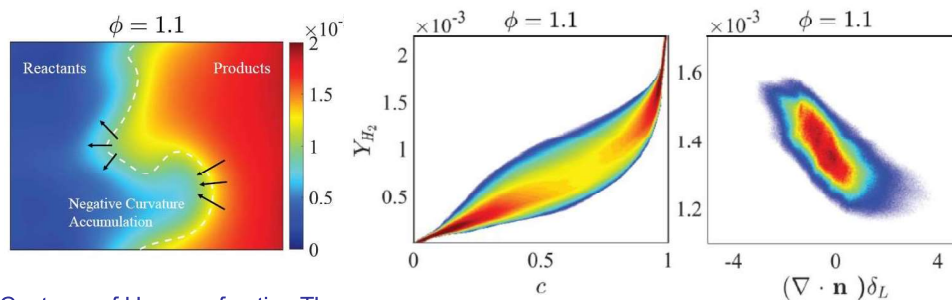
NO pathways: curvature dependence



(a) Schematic diagram of the flame surface colored by curvature. Three lines vertically across the flame surface with positive, negative and zero curvatures. (b) The profiles of various NO pathways along the three lines as a function of c near the reaction zone. (Positive : '—' ; negative: '---' ; and zero : '...' .)

- The magnitude of NO pathways is the highest in negatively curved regions, and the lowest in the region with positive curvature.
- The relative importance of various NO pathways rarely changes with curvature.

38



Contours of H_2 mass fraction The white dashed line indicates the flame front. The arrows denote the directions of H_2 diffusion.

(a) JPDF of Y_{H_2} and progress variable. (b) JPDF of Y_{H_2} and curvature conditioned on the flame front.

- H_2 diffuses from the product side to the reactant side, and is concentrated in negative curvature regions.
- The NO reactions in negative curvature regions are enhanced by the accumulations of radicals such as H_2 due to the preferential diffusion effects.

40

Conclusions, Open Questions & Discussion Items

- **NH_3 -air (both lean & rich) premixed flames** behave like “conventional” turbulent flames: “surface-area controlled” turbulent burning rate ($I_0 \sim 1$)
- **Lean $NH_3/H_2/N_2$ -air premixed flames** are rate-controlled by **molecular diffusion of hydrogen** and local enrichment/acceleration of the leading points ($I_0 > 1$), **more so at high pressure**
- High pressure conditions are beneficial in respect to NO formation, not so much for N_2O formation (abated at fuel-rich conditions)
- In rich NH_3 -air and $NH_3/H_2/N_2$ -air excess ammonia is pyrolyzed to hydrogen (providing optimal RQL conditions)
- Proceed past the conventional “DLE paradigm”: lean premixed flames → low flame temperature → low emissions? – not true for NH_3 flames!
- What is the “optimal” NH_3 decomposition rate in $NH_3/H_2/N_2$ -air flames?
- ...

Canonical turbulent jet flames fueled by ammonia/hydrogen/nitrogen blends

Gaetano Magnotti
KAUST, Clean Combustion Research Center



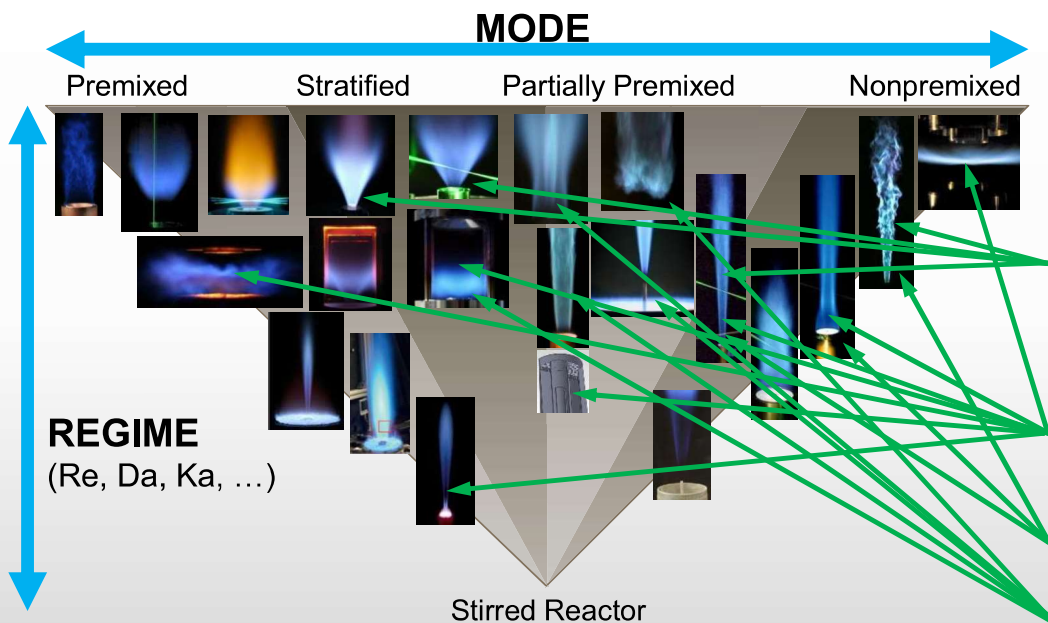
TNF and PTF Workshops - July 22-23, 2022
Coast Coal Harbor Hotel Vancouver, Canada



Clean Combustion
Research Center



Insights from TNF Workshop target flames



- Interactions of turbulence, molecular transport, and chemistry are expressed differently in the different combustion modes and regimes
- Effects of **differential diffusion** in turbulent flames
 - Non-premixed jet flames
 - Premixed and stratified flames
- Characterization of **local extinction and blowout**
- Formation/emission of **NO_x**
- Structure of local reaction zones in **multi-regime flames**



Clean Combustion
Research Center

<https://tnfworkshop.org/>

Canonical turbulent flames for ammonia combustion

• Key phenomena to be investigated

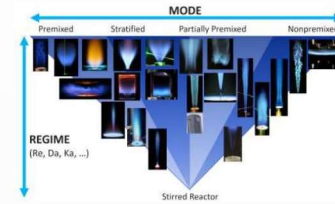
- Stabilization, local extinction, blowout
- NO_x formation and emissions
- Differential diffusion effects
- Pressure effects

• Measurement needs and diagnostic challenges

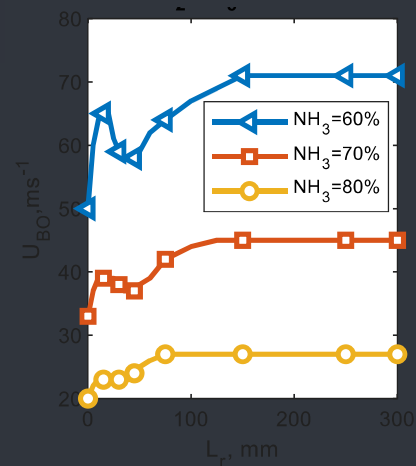
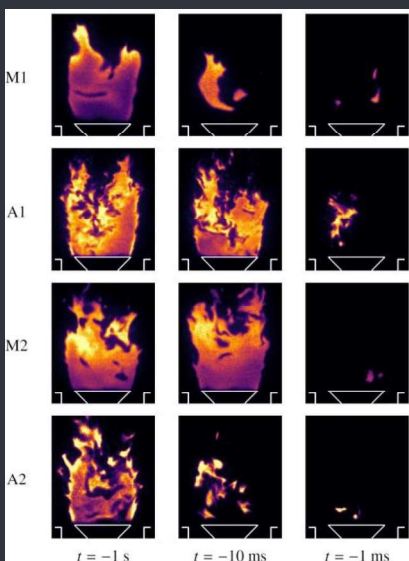
- Extend Raman methods to ammonia/hydrogen flames
- Combine with quantitative measurements of NO , OH , NH , NH_2
- Baseline experiments and simulations on laminar flames (κ_{ext} , minor species)
- 2D and high-speed PIV/LIF imaging of turbulent reaction zone structure, blowout dynamics, etc.

• Selection of turbulent target cases

- Computationally accessible geometries with well-defined bc's and inflows
- Large variety of burners already available that can be operated with ammonia
- Collaboration on experimental design, common burners, comparison with simulations



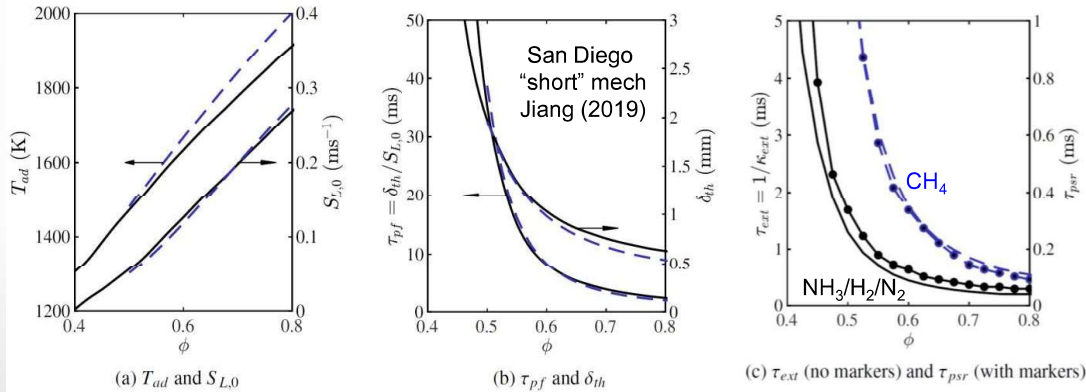
Stability of ammonia/hydrogen/nitrogen flames



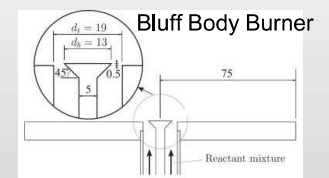
Lean premixed blowoff – NH₃/H₂/N₂ vs CH₄

Laminar premixed flame properties:
NH₃/H₂/N₂ – solid; CH₄ – dashed

Extinction time
(laminar twin flame and PSR)

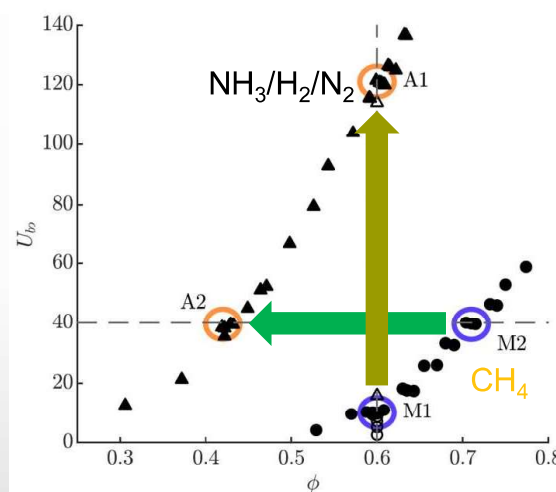
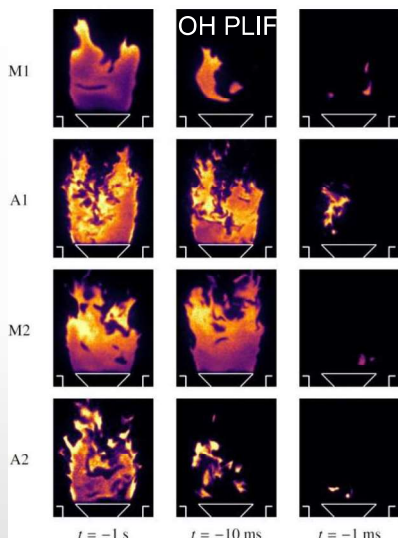


ϕ 0.45
Blow-off velocity 45.0 ms⁻¹
 T_{ad} 1403 K



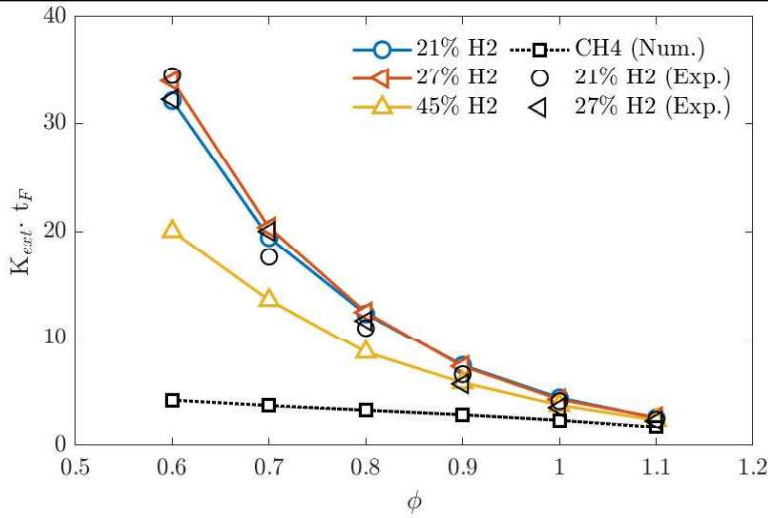
- Select NH₃/H₂/N₂ blend (40%, 45%, 15%) to match S_L and δ_{th} of CH₄
- Similar laminar flame speed BUT very different extinction behavior
- Laminar extinction strain rate, κ_{ext} , is 3.8 times higher for NH₃/H₂/N₂ at $\phi = 0.6$

Lean premixed blowoff – NH₃/H₂/N₂ vs CH₄

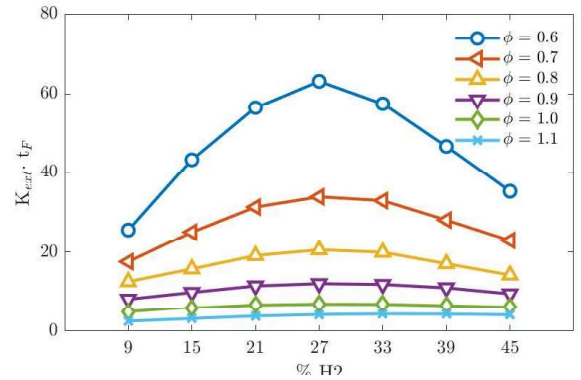
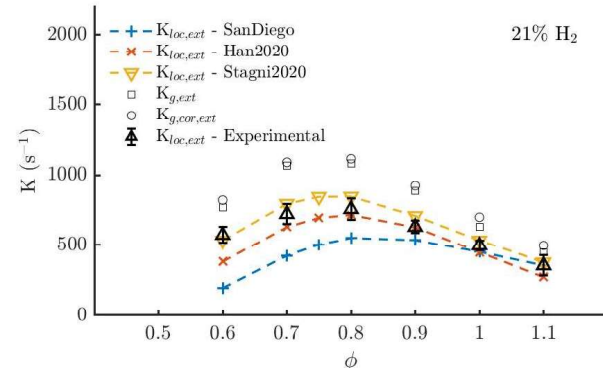


- A1 vs. M1: Turbulent NH₃/H₂/N₂ flame at $\phi = 0.6$ has ~12 times higher U_{bo} than methane
- A2 vs. M2: NH₃/H₂/N₂ blend remains stable to much lower ϕ

Resilience to strain-induced blow-out (RSIB)

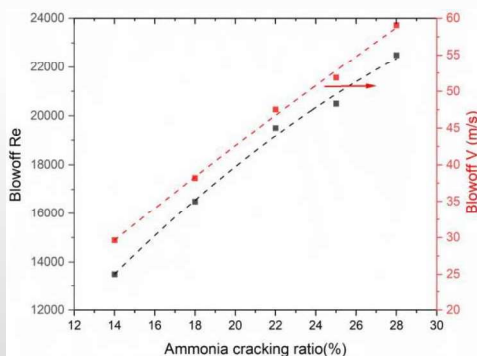


- Resilience to strain-induced blow-out obtained from extinction strain rates multiplied with flame time

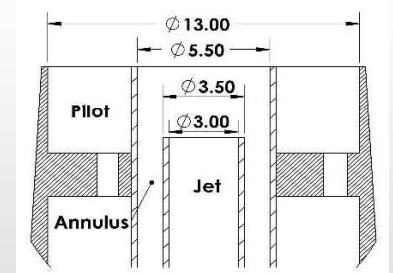
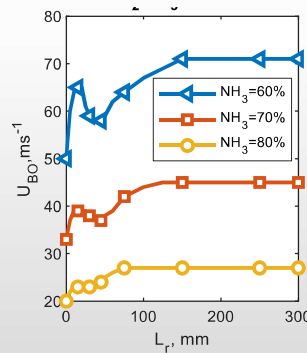


Stability of non-premixed jet-flames

- Simple jet flame, 4.58 mm ID central pipe, 250 mm coflow with 0.3 m/s velocity
- Linear relation between blowoff velocity and cracking ratio



- Sydney inhomogeneous burner
- NH₃/H₂ as fuel
- Global $\phi_{GLBL} = 4.76$
- Local peak in blow-off velocity (U_{BO}) $L_r = 25$ mm
- Peak, U_{BO} is suppressed with NH₃ addition
- Homogenous limit ($L_r = 300$) reduces U_{BO} significantly with NH₃ addition;

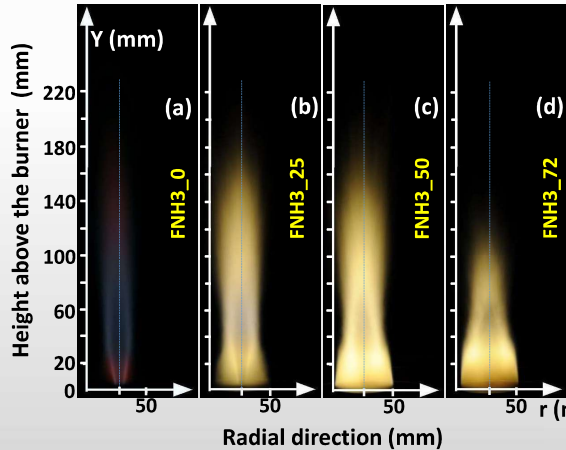


Some additional canonical flames under investigation

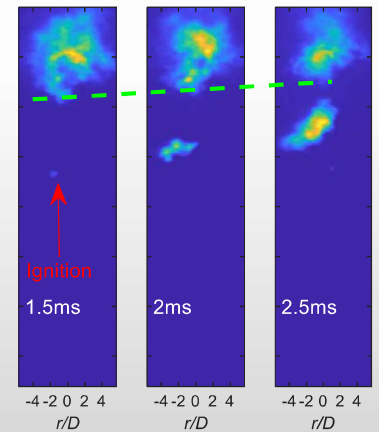
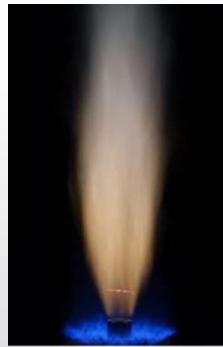
- Bluff-body non-premixed flames
- Constant $Re=5500$
- Variable ammonia cracking ratio
- OH PLIF and emission

- Lund Distributed Reaction Zone (DRZ) burner
- High turbulent Re
- OH+NH, LDA

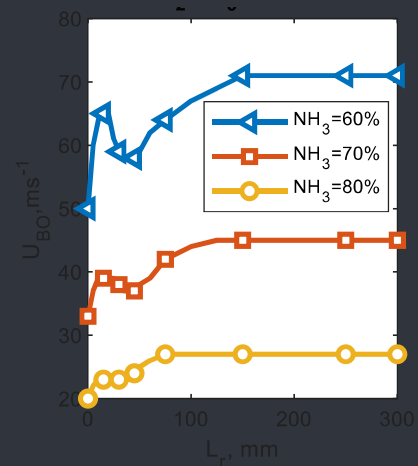
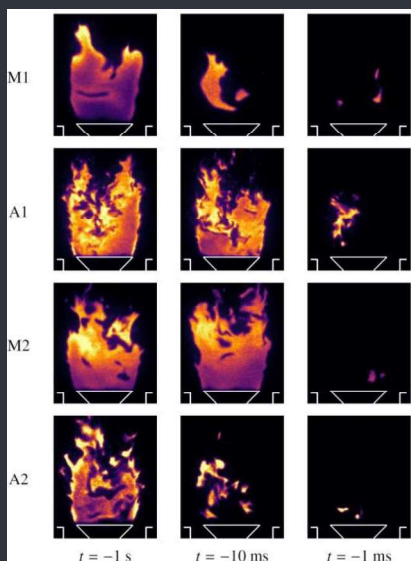
- Sydney auto-ignition burner
- Jet in hot-coflow
- High-speed chemiluminescence



Clean Combustion
Research Center

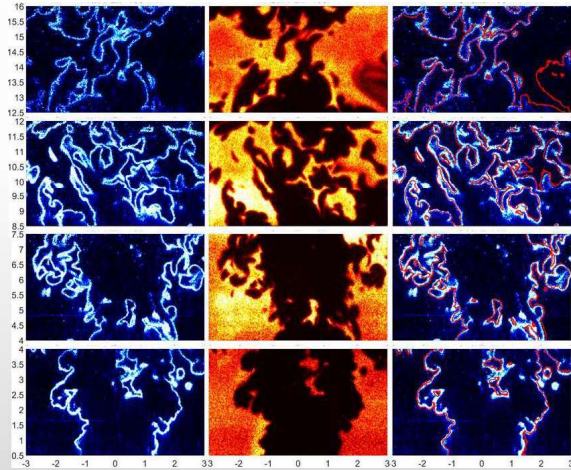


Diagnostics for Ammonia combustion



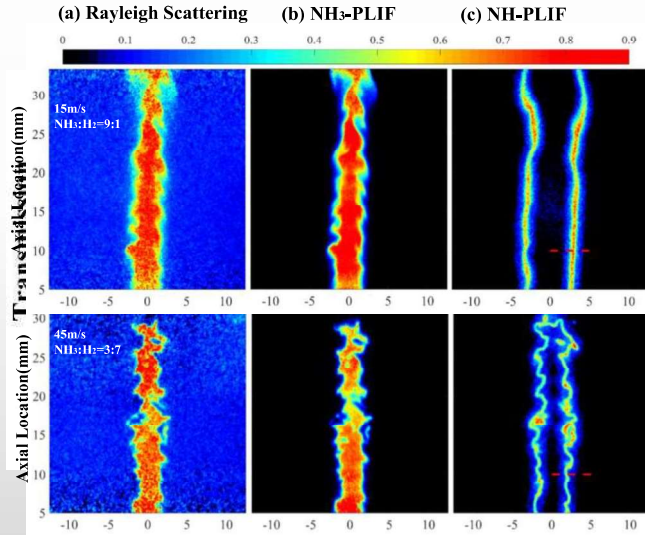
Multi-species PLIF

- Simultaneous OH+NH on Lund DRZ burner
- NH coincident with the edge of the OH layer
- NH remain thin



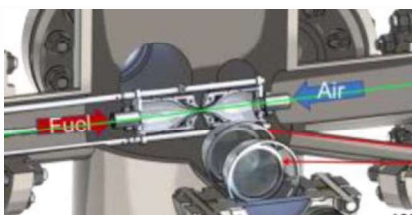
Fan et al. Combustion and Flame 238, 2022

- Simultaneous Rayleigh, NH LIF and NH3 LIF
- Single excitation at 304.8 nm

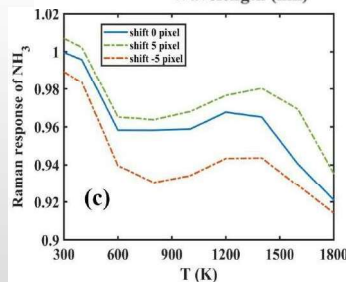
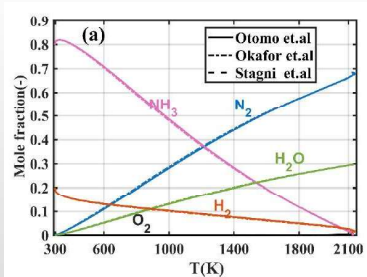
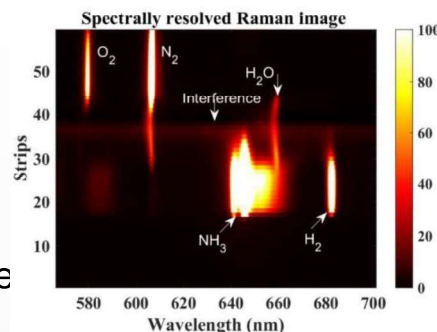


Wang et al. Combustion and Flame 242, 2022

Extending Raman spectroscopy to ammonia flames: response curves



Laminar opposed jet flame



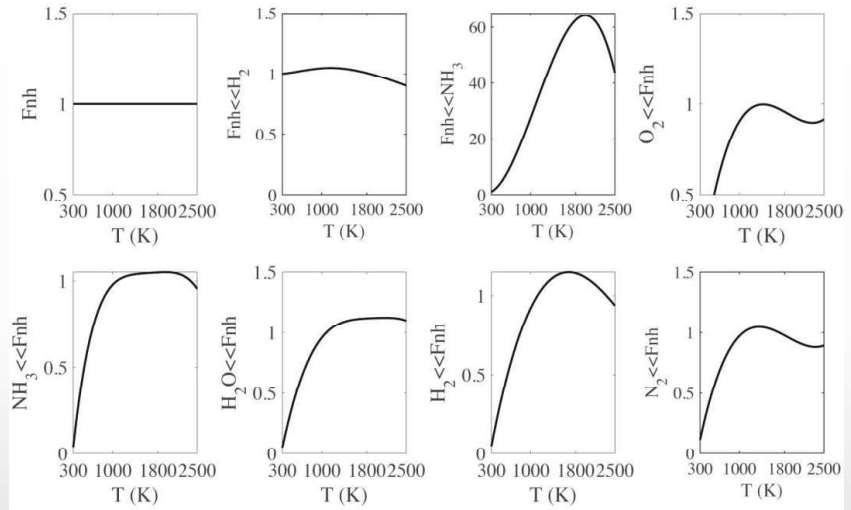
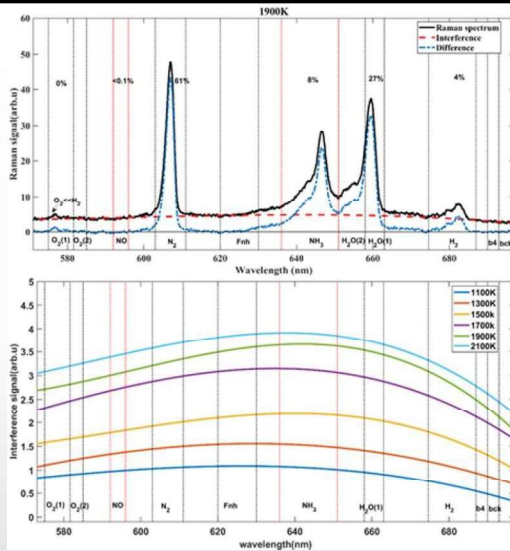
- Calibrate NH₃ Raman response vs. T using laminar flame measurements and simulations
- No significant differences in major species among three mechanisms;
- Only minor effect of strain rate on major species
- **Result: Relatively low T-dependence of NH₃ Raman response**

Tang et al. Combustion and Flame 29, 2021

$$C_{NH_3}(T) = [S_{NH_3}(T) - C_{NH_3 \leftarrow H_2O}(T)N_{H_2O}(T) - C_{NH_3 \leftarrow F_{nh}}(T)S_{F_{nh}}(T)] / N_{NH_3}(T)$$

$$C_{H_2O \leftarrow NH_3}(T) = [S_{H_2O}(T) - C_{H_2O}(T)N_{H_2O}(T) - C_{H_2O \leftarrow F_{nh}}(T)S_{F_{nh}}(T)] / N_{NH_3}(T)$$

Fluorescence interference



- Spectra collected at orthogonal polarizations
- Fluorescence signal approximated to a third order polynomial

- Response curves computed as function of temperature
- Same curves used independently of NH3/H2/N2 ratio



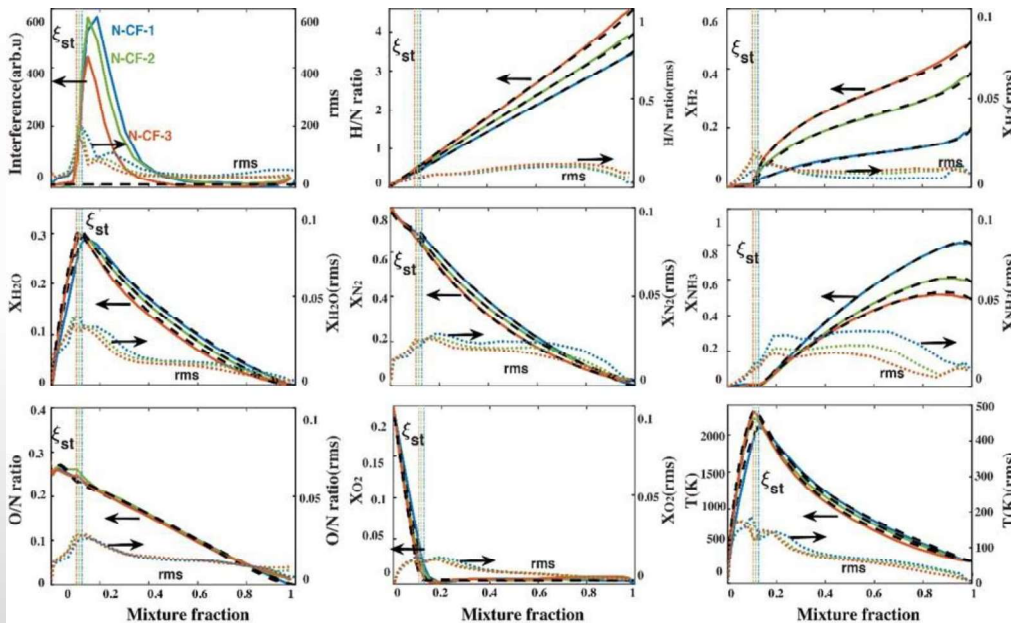
جامعة الملك عبد الله
للعلوم والتقنية
King Abdullah University of
Science and Technology

Clean Combustion
Research Center

Tang et al. Combustion and
Flame 29, 2021

13

Validation in laminar flames



$$F_{bilger} = \frac{\frac{1}{2} \frac{Y_H - Y_{H,2}}{W_H} - \frac{Y_O - Y_{O,2}}{W_O}}{\frac{1}{2} \frac{Y_{H,1} - Y_{H,2}}{W_H} - \frac{Y_{O,1} - Y_{O,2}}{W_O}}$$

- N-CF-1 with 80% NH3
20% H2 used for calibration
- Tested over 10 counterflow
flames with varying
NH3/H2/N2 ratios and
strain rates
- Agreement in mole fraction
within 0.01 for all species
- Temperature within 40 K

Tang et al. Combustion and
Flame 29, 2021



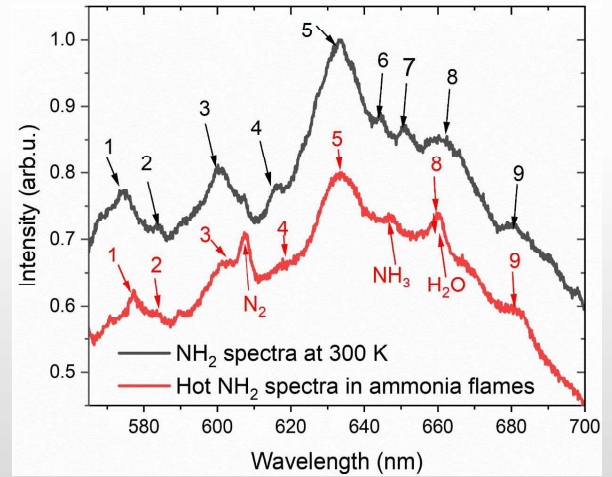
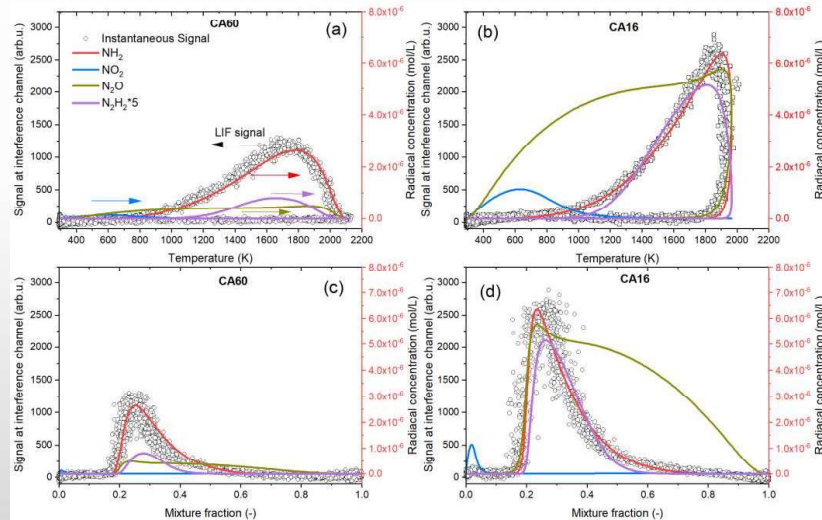
جامعة الملك عبد الله
للعلوم والتقنية
King Abdullah University of
Science and Technology

Clean Combustion
Research Center

14

Interference signal: a measurement of NH₂

- Interference response curve independent of fuel composition
- Experiments in flows seeded with NO, N₂O and NO₂, show negligible contribution from these species
- NH₂ is the main contribution, but not matching a specific excitation line.

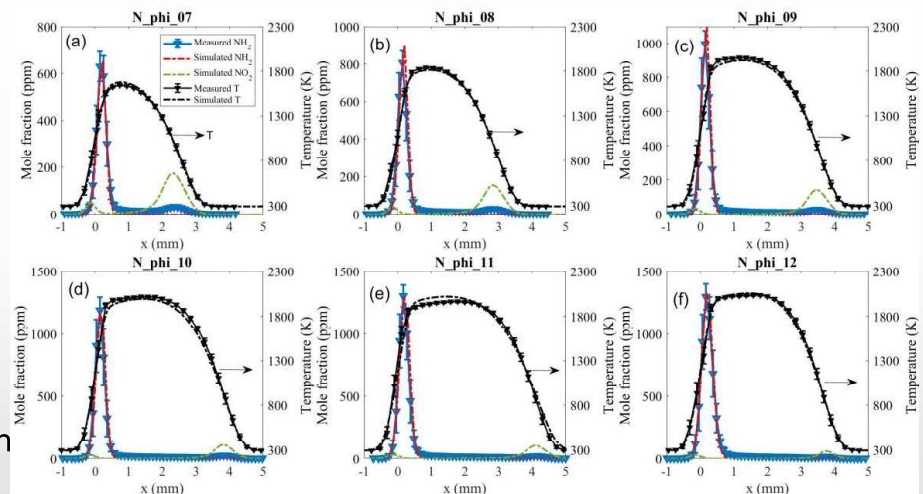


Tang et al. (2P033) to be submitted to Combustion and Flame

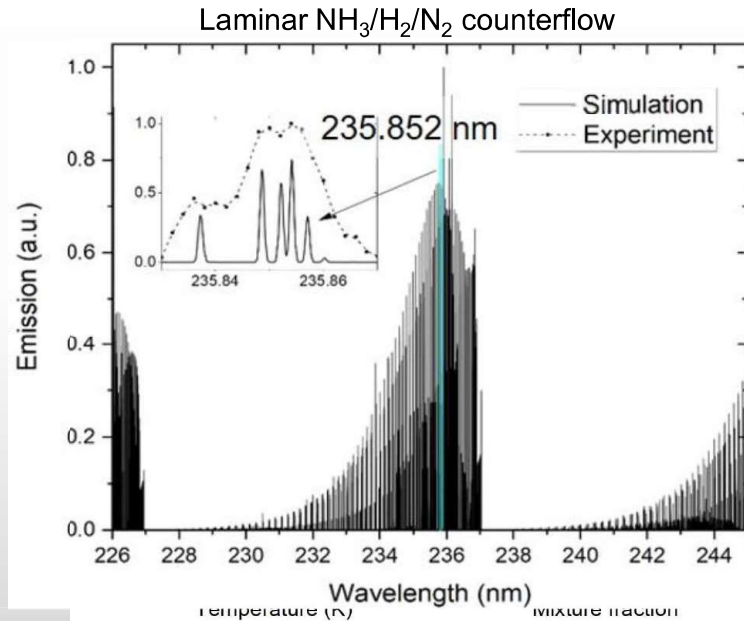
15

Interference signal: a measurement of NH₂: validation

- Linear with number density.
- Calibrated by matching the peak NH₂ concentration from 1-counterflow flame using the Otomo mechanism
- Accuracy < 10% over 23 flames tested, across all range
- ~ 100 ppm standard deviation at peak temperature, ~ 50 ppm elsewhere
- Small crosstalk from NO₂ (<50 ppm)
- Absolute, independent measurements needed (TDLAS?)
- Useful for turbulent-chemistry interaction studies

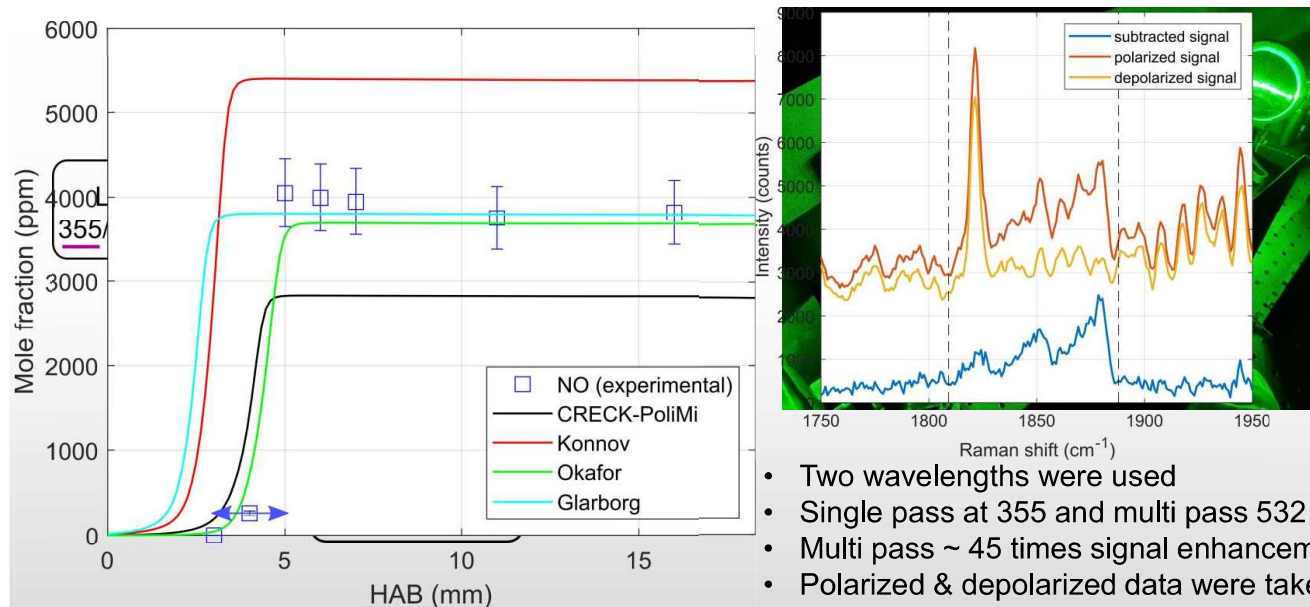


NO LIF in ammonia flames



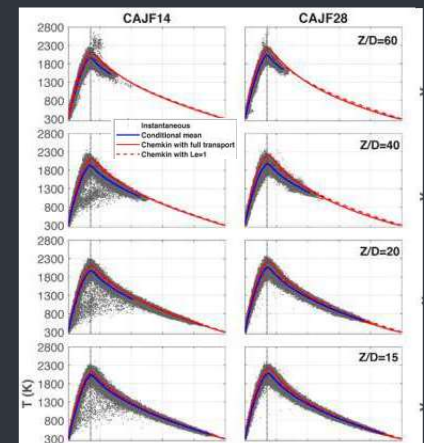
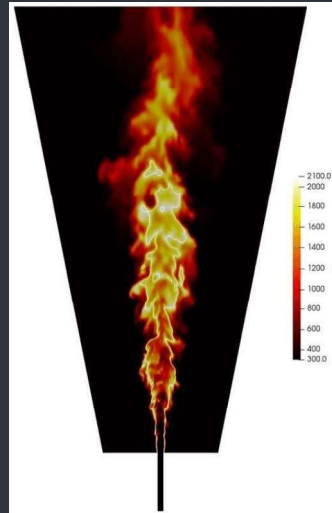
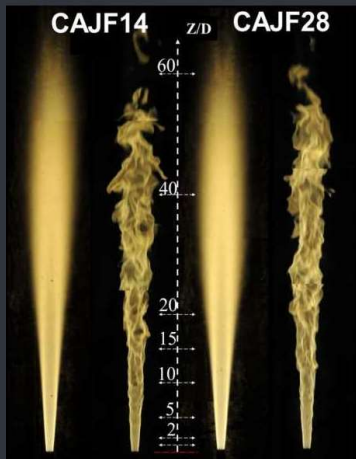
- Excitation of NO in the (0-1) band of the $A^2\Sigma^+ \leftarrow X^2\Pi$ at 235.852 nm to avoid absorption from NH_3
- 4 mJ/pulse, saturated regime
- Contributions from Rayleigh and O_2 LIF signal removed through calibration in laminar flames and simultaneous Raman measurements
- NO-LIF calibration factor from measurements in H_2 flames seeded with NO
- 15%-25% uncertainty in turbulent flames

NO Raman in laminar ammonia flames

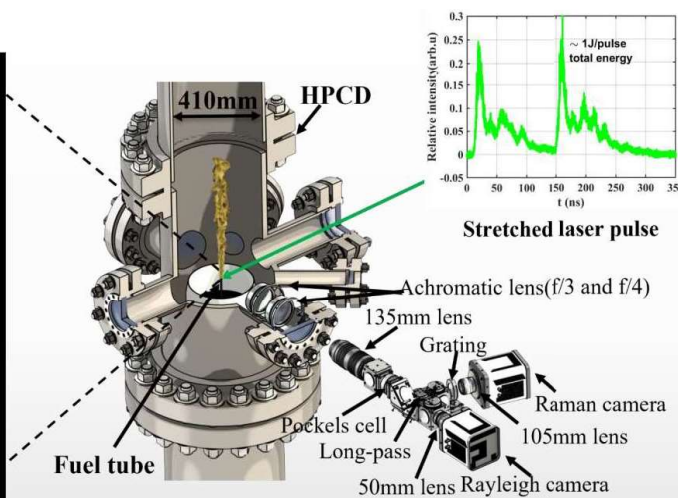
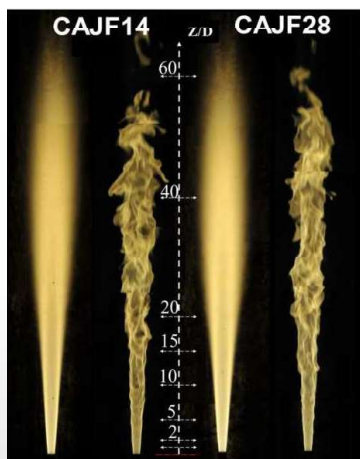


- Two wavelengths were used
- Single pass at 355 and multi pass 532
- Multi pass ~ 45 times signal enhancement
- Polarized & depolarized data were taken
- Reported detection limit of 700 ppm

Simple-jet NH₃/N₂/H₂ flames: Measurements and simulations



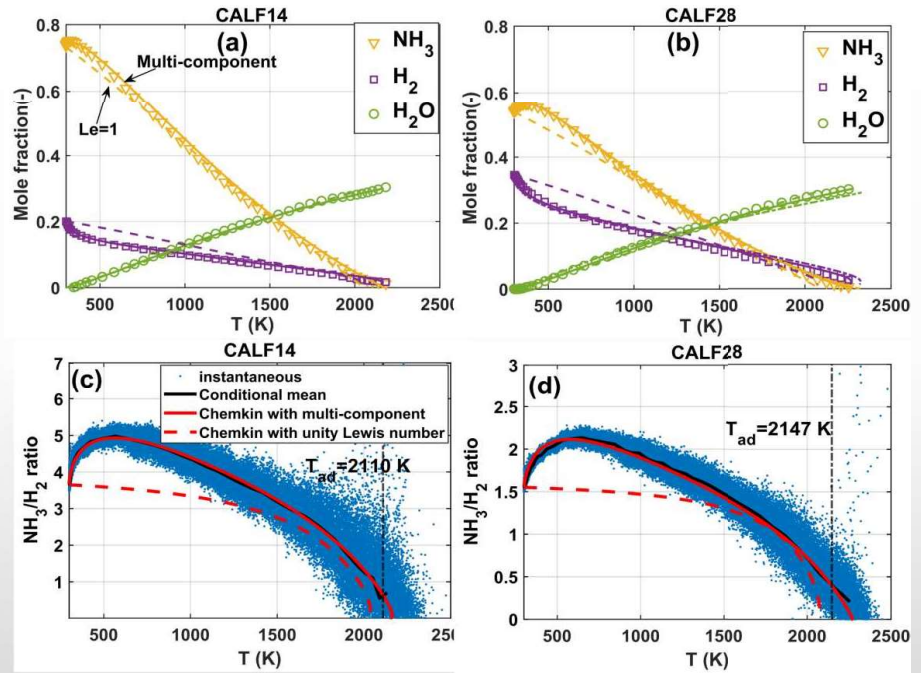
Laminar and turbulent ammonia flames



- Fuel simulating 14% and 28% cracked ammonia
- Non-premixed jet in air co-flow
- 3.35 mm inner diameter
- 5 bar operating pressure**
- Reynolds number of 11000** for the turbulent flames
- Simultaneous Raman and NO LIF
- Velocity measurements (PIV)
- T, major species, NO and velocity data available
- Mean, RMS, PDF...

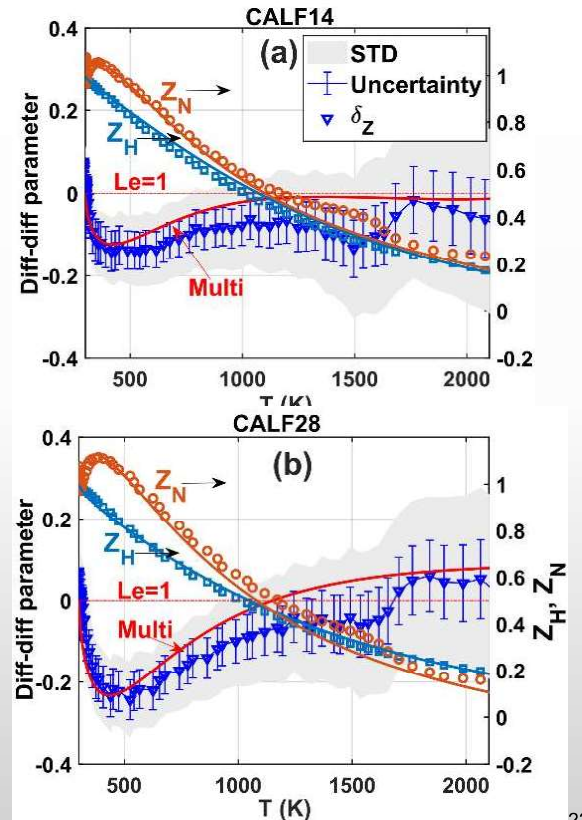
Laminar flames results at $z/D=1$

- Major species in good agreement with the full multi-component transport model
- Non-unity Le effects leading to super-adiabatic peak temperature
- H_2 burns ahead of the ammonia leading to a rapid increase in the NH_3/H_2 ratio



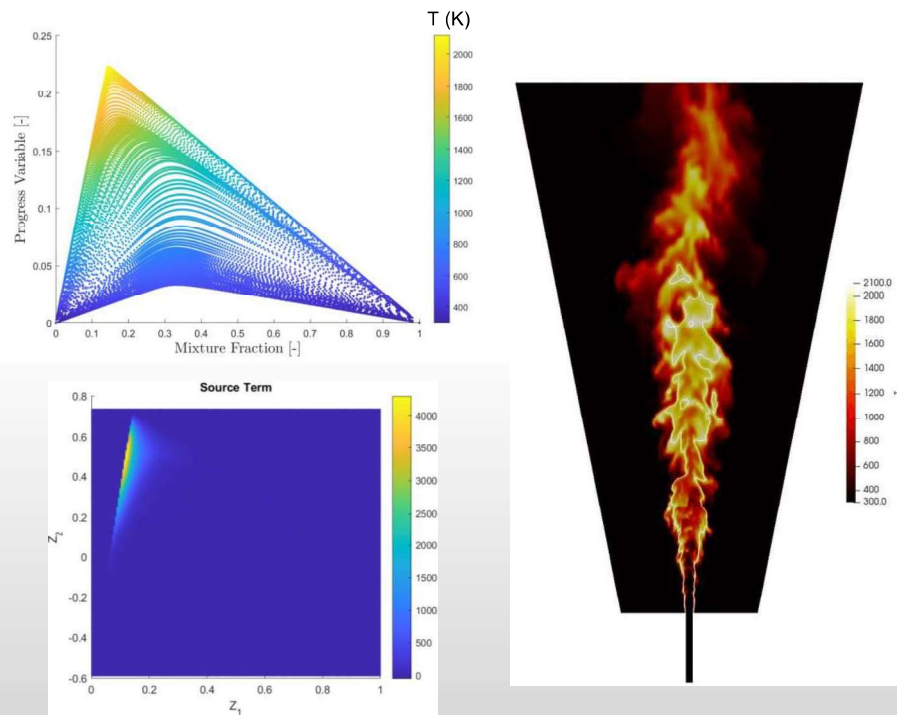
Diff-Diff parameter for ammonia flames

- Diff-Diff parameter based on atom-ratios to better capture diff-diff effects
- N replaces C in the conventional definition
- $\delta_Z = Z_H - Z_N$
- Z_X is the elemental mixture fraction:
- $$Z_H = \frac{Y_H - Y_{H,air}}{Y_{H,fuel} - Y_{H,air}}$$
- $$Z_N = \frac{Y_N - Y_{N,air}}{Y_{N,fuel} - Y_{N,air}}$$
- Correct trend captured in Z_H , some issues in Z_N
- Small denominator in Z_N (0.05) amplifies measurement errors



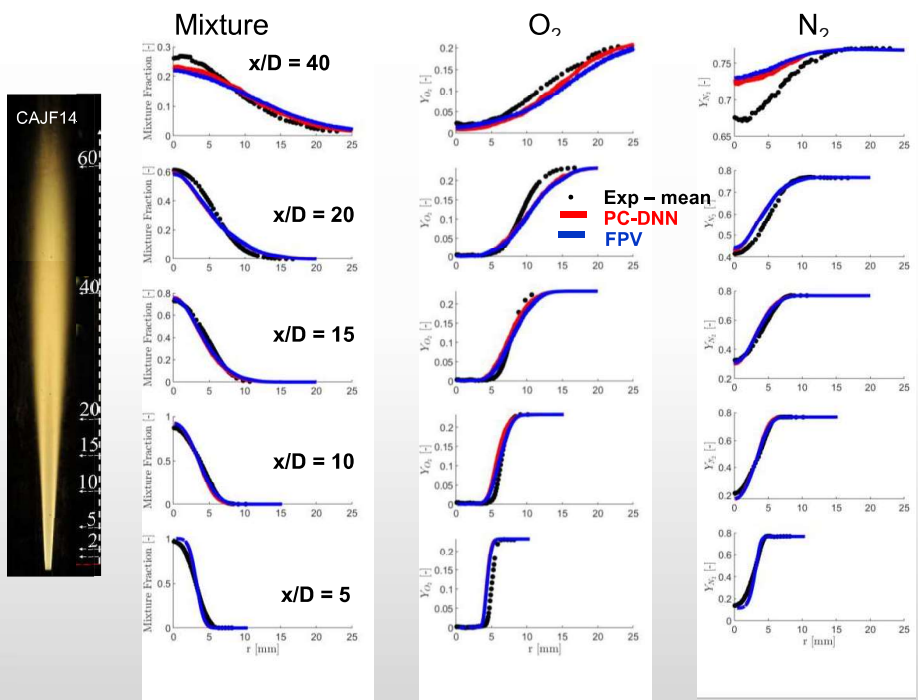
Numerical Simulation

- Flamelet progress variable approach (FPV)
 - H₂O as progress variable
- Principal Component analysis+Deep Neural Network (PC-DNN)
 - Reduced to PC1 and PC2 as input to the DNN to obtain the full thermochemical state
- Unity Lewis number assumed for both approaches

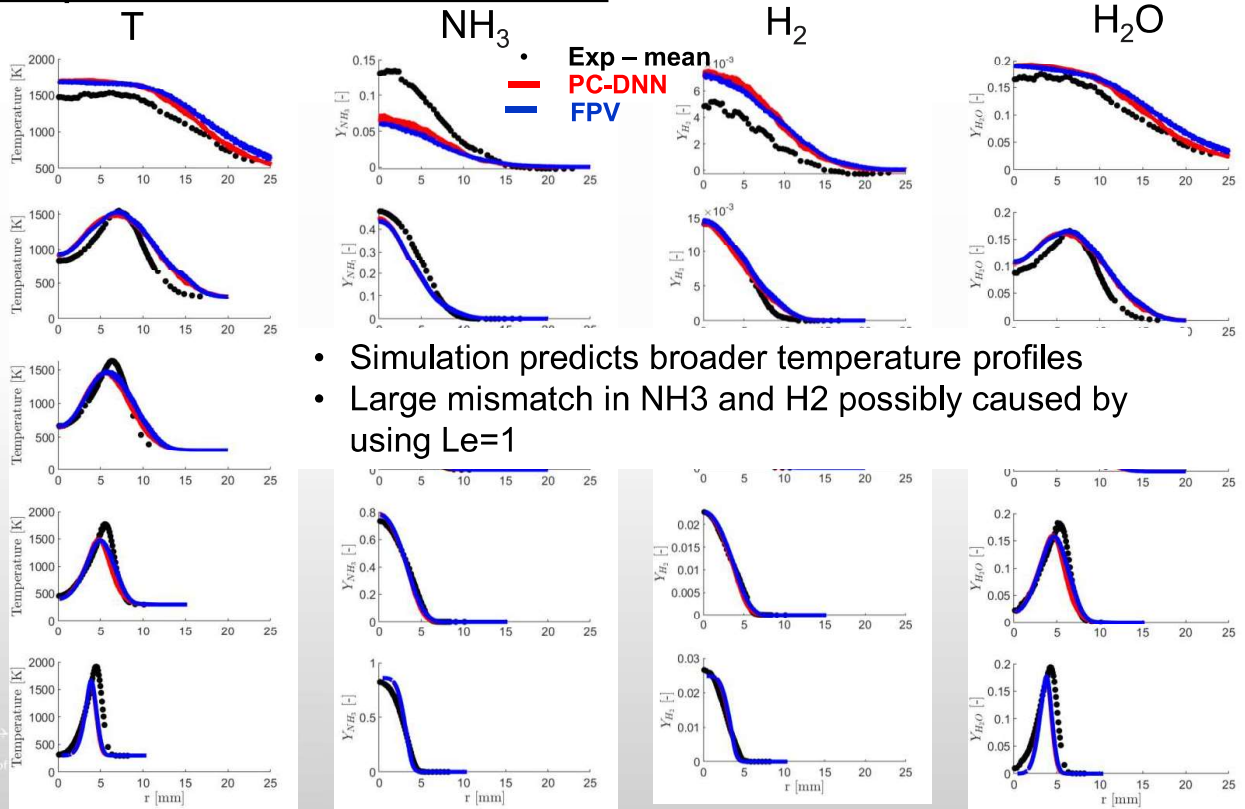


CAJF 14 Experiment vs Simulations

- Small difference between the two models
- Agreement with experiments in the near field but experimental profiles are steeper
- Larger discrepancies downstream

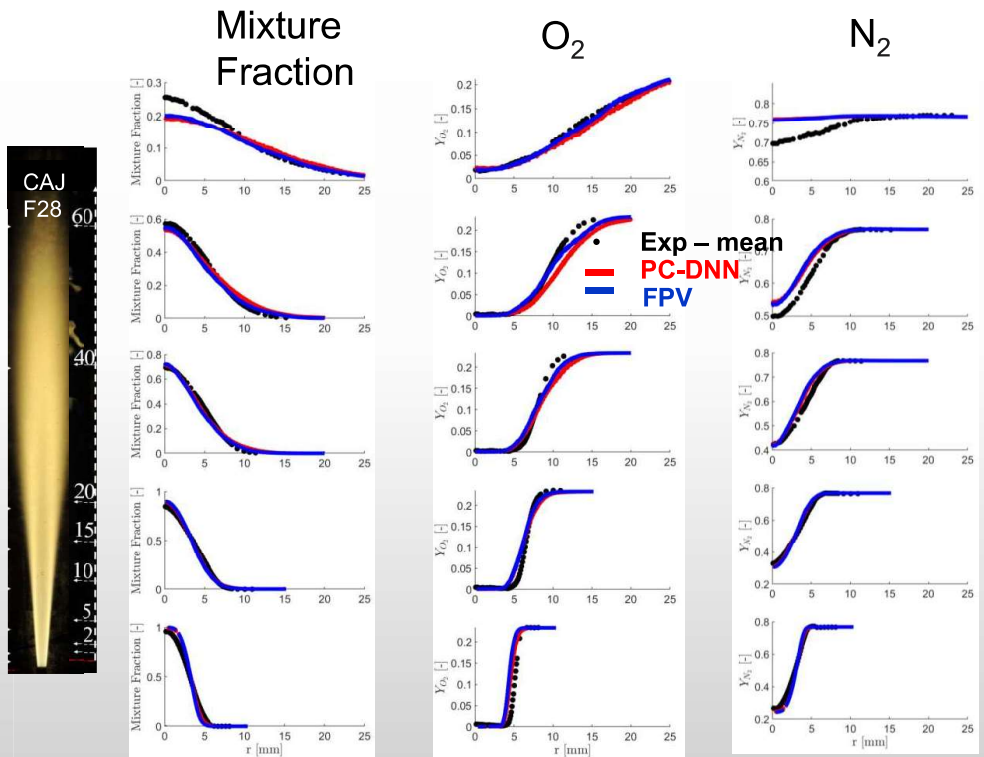


CAJF 14 Experiment vs Simulations

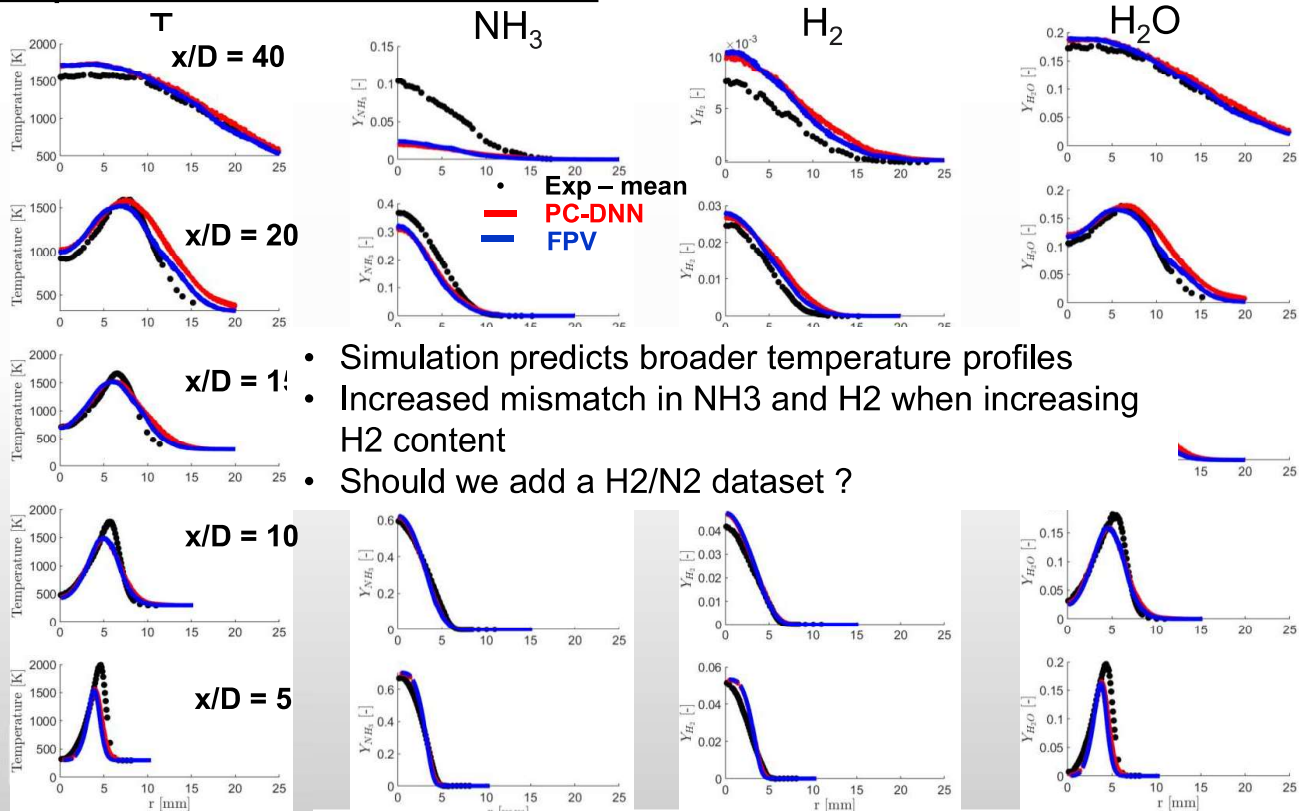


CAJF 28 Experiment vs Simulations

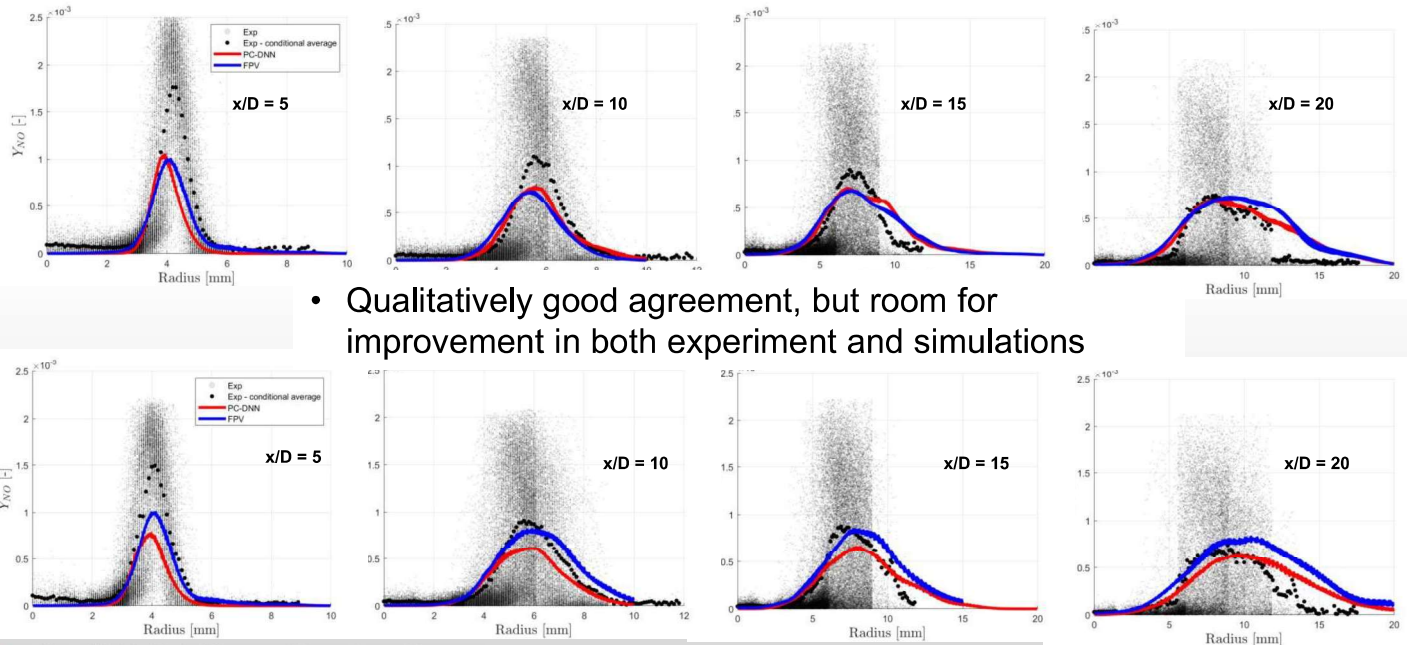
- Higher cracking ratio leads to increased mismatch in mixture fraction and N2



CAJF 28 Experiment vs Simulations

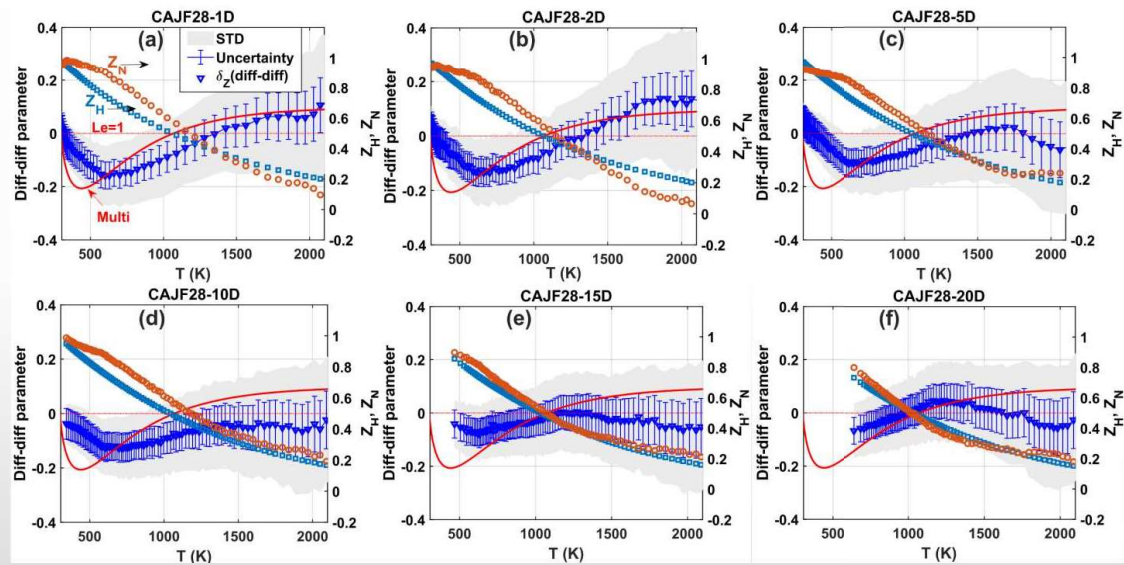


NO Experiment vs Simulations



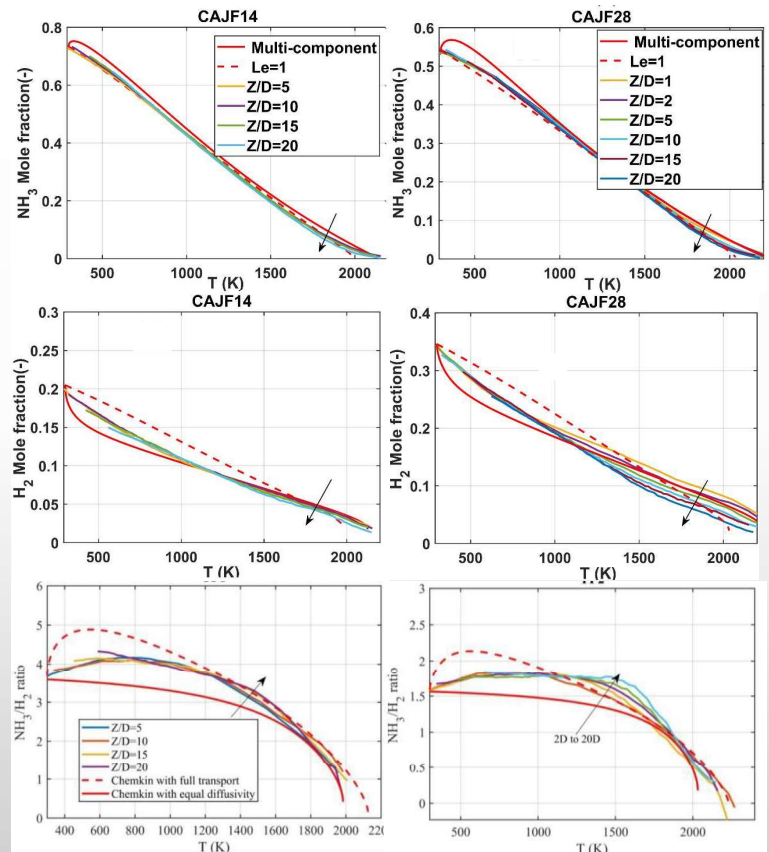
Turbulent flames:diff-diff effects

- Diff-diff parameter indicates that differential diffusion is important up to 15 D
- Improvements needed to obtain lower uncertainties



Turbulent flames:diff-diff effects

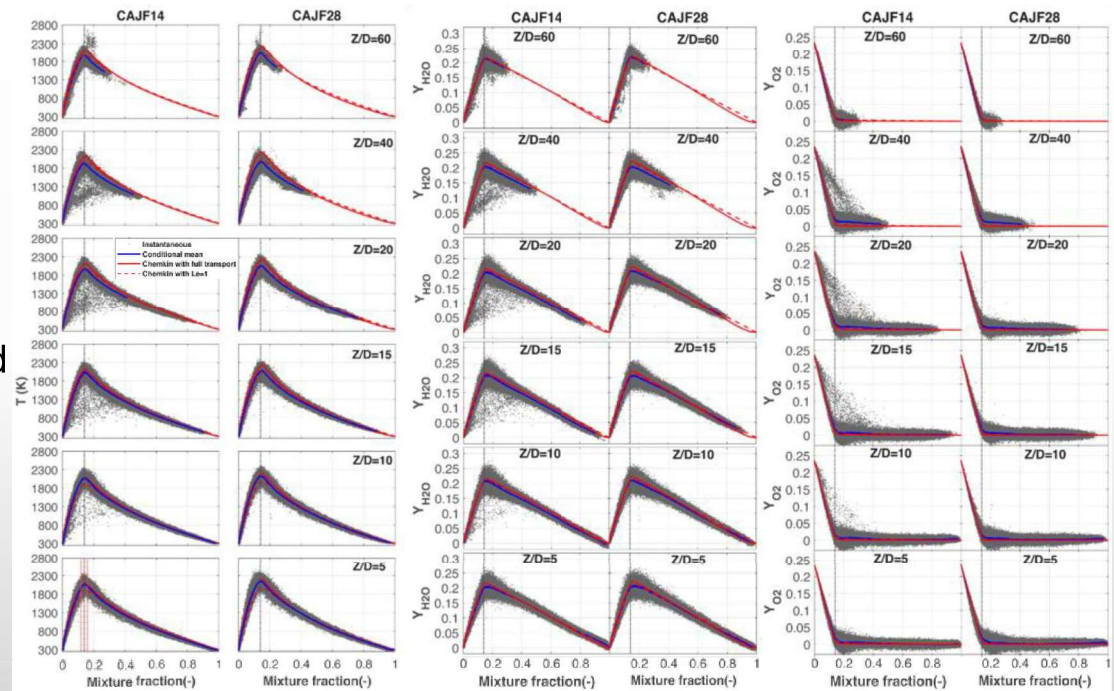
- Ammonia and hydrogen profiles plotted vs temperature
- Profiles intermediate between unity Le and the full multi-component diffusion
- H₂ mole fraction drops below both solutions moving downstream
- Diff-diff effect although stronger near exit is cumulative
- NH₃/H₂ ratios increases with distance from the exit



Turbulent flames: localized extinction

- Temperature profile matches the full multi-diffusion simulation near the exit, and the $Le=1$ downstream
- Evidence of localized extinction for the CAJF14 flame (40% of blowoff velocity)

Tang et al. CNF 2022

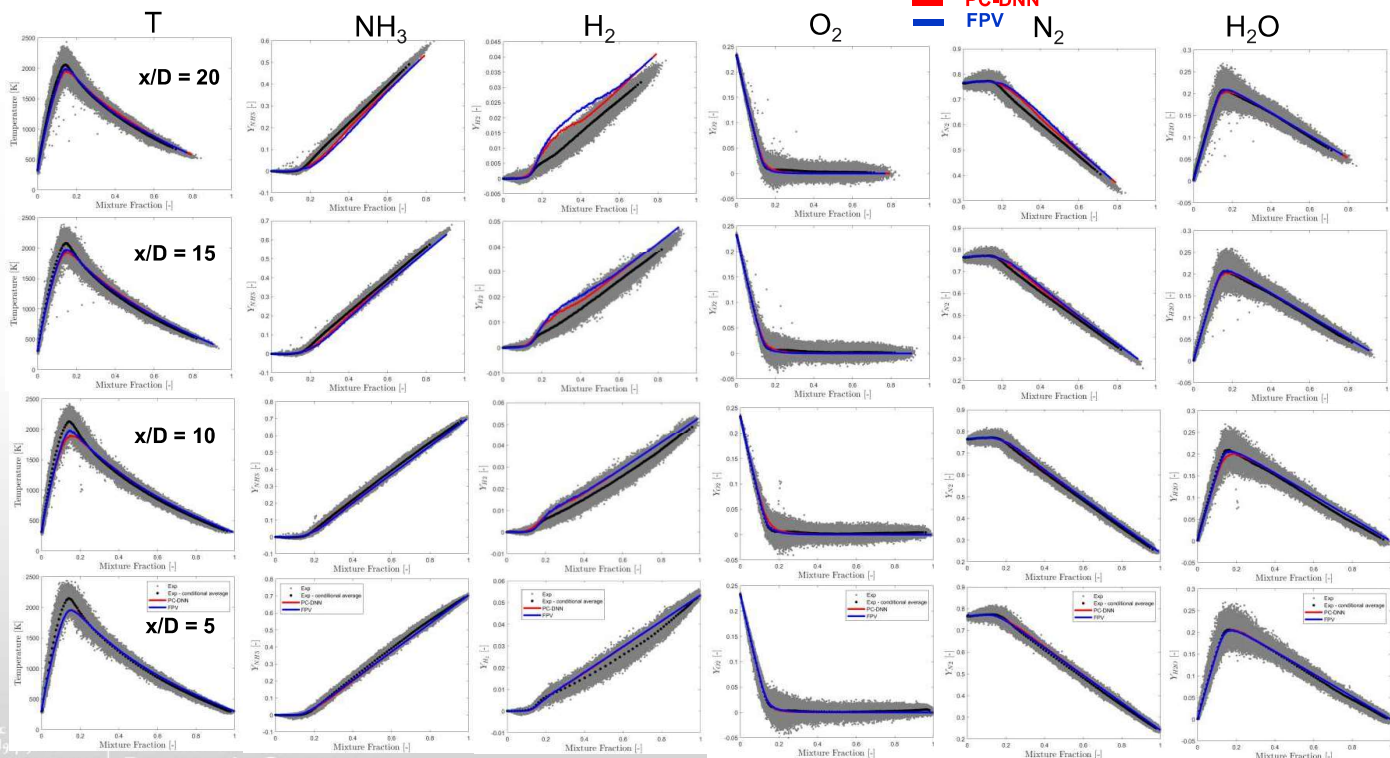


جامعة الملك عبد الله
للعلوم والتقنية
King Abdullah University of
Science and Technology

Clean Combustion
Research Center

31

CAJF 28: Comparison in mixture fraction space



- Exp – instantaneous measurements
- Exp – conditional average
- PC-DNN
- FPV

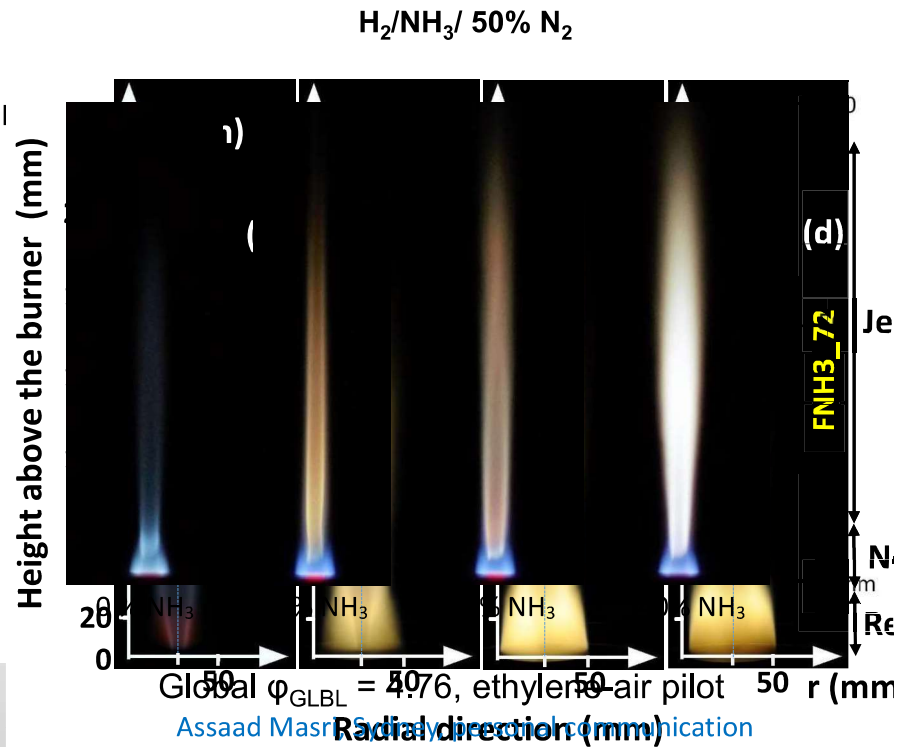


جامعة الملك عبد الله
للعلوم والتقنية
King Abdullah University of
Science and Technology

Research Center

Ongoing work at KAUST

- New polarization/separation Ramai system now operational for measurements at atmospheric conditions
- Effect of Re on 28% cracked an jet flames
- Piloted Sandia/Sydney burner (partially premixed and inhomogeneous)
- Bluff-body stabilized flames
- MILD combustion



Acknowledgements

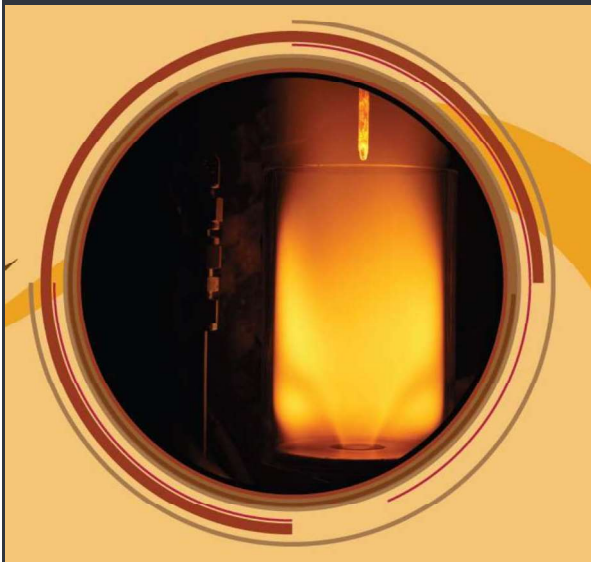
- Thank to contributions from :
- Rob Barlow, Andreas Dreizler, Dirk Geyer
- Assaad Masri and Matt Dunn
- Christian Brackmann
- Bo Zhou
- Bill Roberts Hong Im and Thibault Guiberti
- All the students and postdocs that did the experiments and simulations



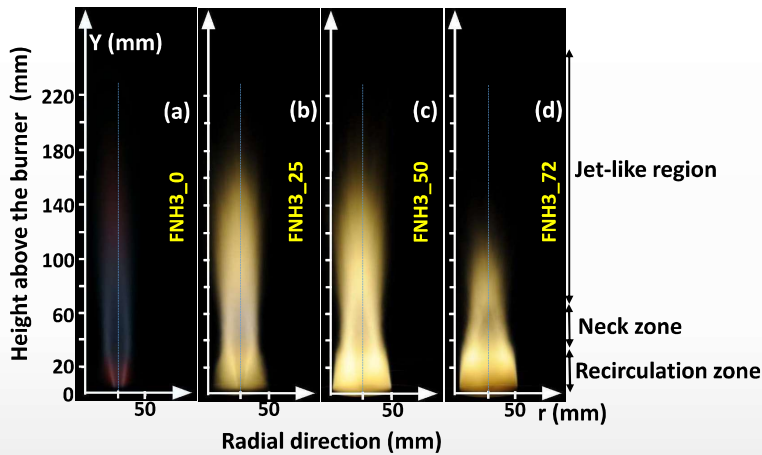
Questions?

Ammonia Combustion Meeting

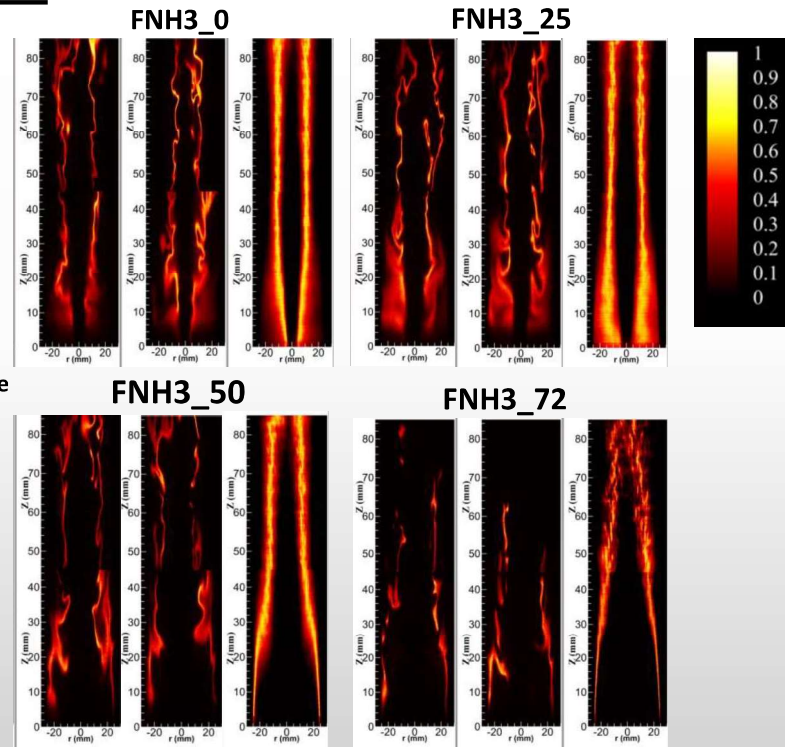
May 12-13 2023



Flames images and OH-PLIF

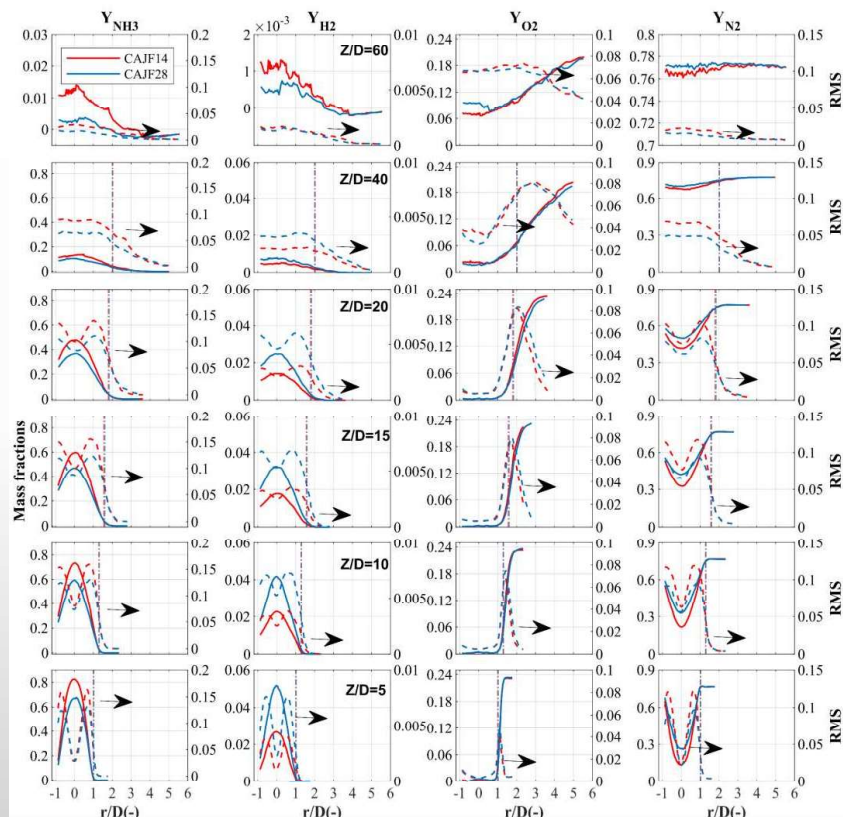


- Flame length increase as H_2 ratio in the blend is increased resulting in a more stable flame with reduce luminosity
- Increase in cracking while keeping Re constant resulted in higher momentum flux (jet/coflow), and shift of the burning region from the outer shear layer to the inner layer next to the jet



Turbulent flames: radial profiles

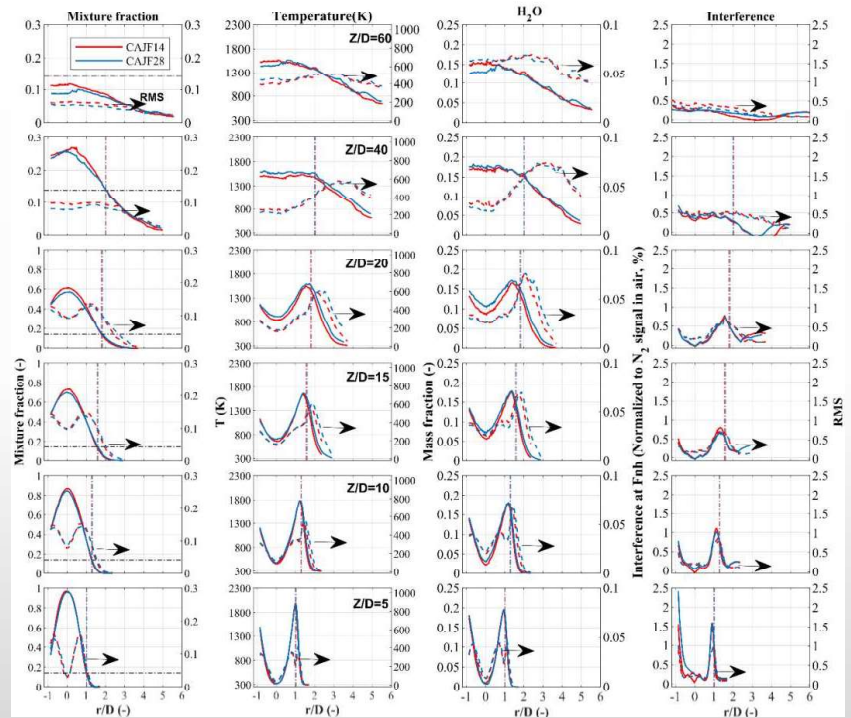
- Mean and RMS data available for Z/D ranging from 1 to 60
- Differences in N_2 , H_2 and NH_3 from the different fuel composition
- Slightly enhanced O_2 decay for the higher cracking ratio



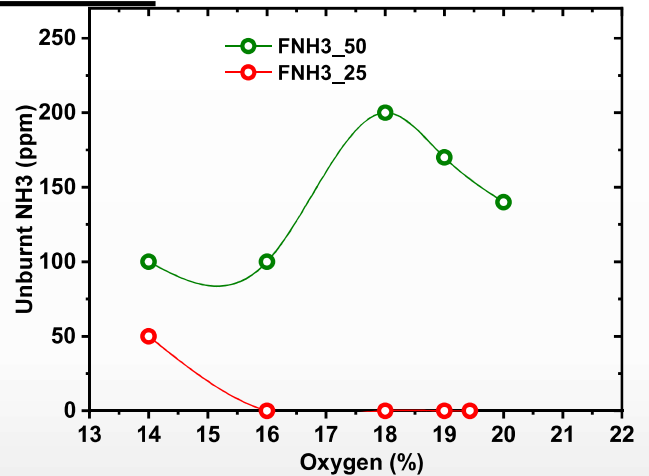
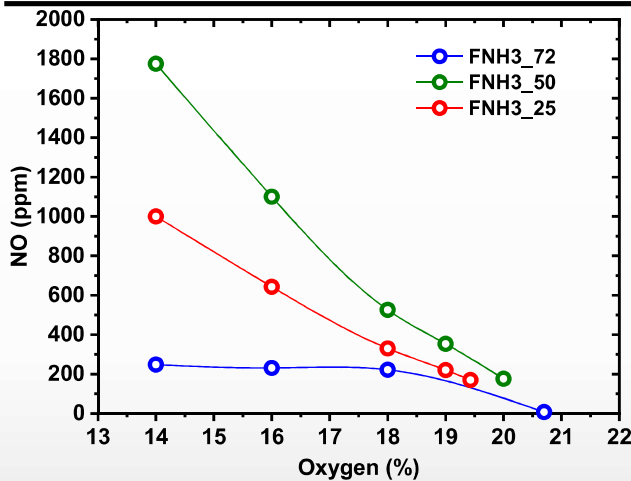
Tang et al. CNF 2022

Turbulent flames: radial profiles

- Slightly higher mean temperature and water concentration for the flame with higher hydrogen content

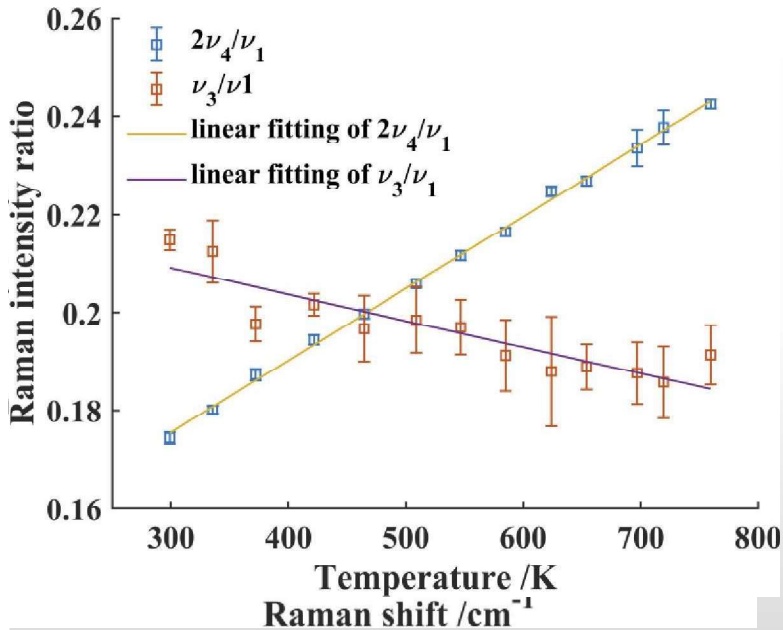


Measured NO and unburnt NH3



- NO is lowest in FNH₃_72 due to lower burning temperatures resulting in delay in NH₃ oxidation
 - In NH₃-rich flames, there is a slip unburnt NH₃ to regions where NO exists thus, promoting the selective non-catalytic reduction reactions to reduce NO
- Unburnt NH₃ in the FNH₃_72 flame exceeds 1000ppm
- FNH₃_0 and FNH₃_25 burns the same way downstream

Extending Raman spectroscopy to ammonia flames: spectra



- High-resolution ammonia spectra taken to temperatures up to 760 K
- Limited by thermal dissociation
- Three major bands identified
- No overlap with other species for $2\nu_4$
- ν_1 and ν_3 partial overlaps with the H_2O channel
- The ratio of $2\nu_4/\nu_1$ is linear with temperature
 - Useful temperature diagnostics for mixing cases in non-isothermal flows



PTF Contributed Talks: Ammonia

- | | |
|-------------|--|
| Dinkelacker | *Flame stability measurements for H ₂ -NH ₃ flames - flashback and liftoff-limits |
| Hayakawa | Combustion characteristics of ammonia/air premixed turbulent flame at high pressure and high temperature |

* Not provided for inclusion in the Proceedings

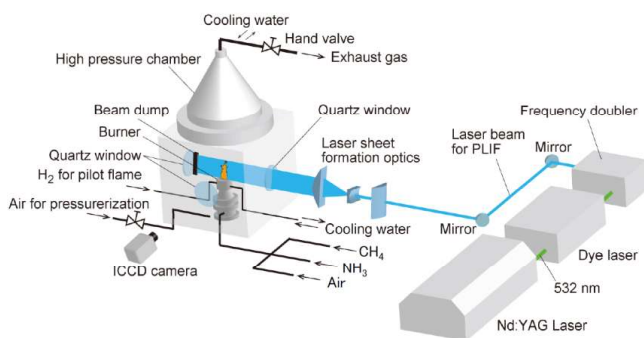
Combustion characteristics of ammonia/air premixed turbulent flame at high pressure and high temperature

OAkihiro Hayakawa, Hideaki Kobayashi

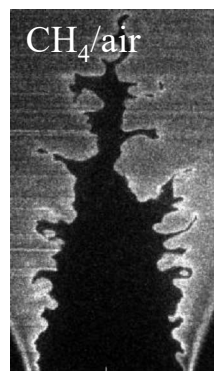
Institute of Fluid Science, Tohoku University, Japan



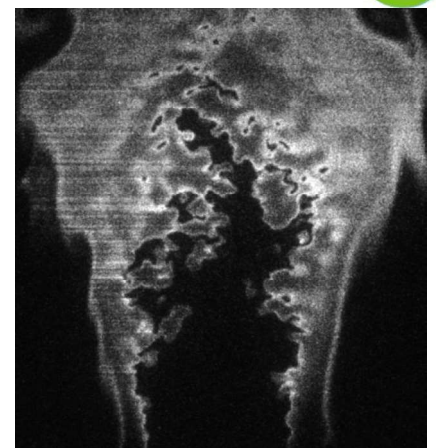
Previous report at Dublin workshop Turbulent combustion of $\text{NH}_3/\text{H}_2/\text{Air}$ flames



Experimental setup for high pressure turbulent combustion



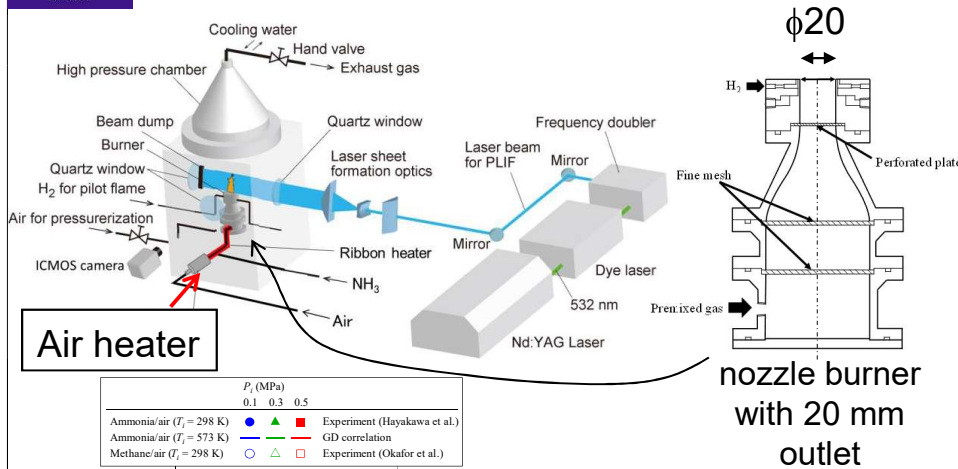
$P=0.5 \text{ MPa}$, $\phi = 1.0$,
 $Le=1.05$



$\text{NH}_3/\text{H}_2/\text{air}$, $Le \ll 1.0$

- ✓ Non-uniformity of OH profiles and OH-PLIF intensity compared to methane/air flames.
- ✓ The difference can be explained from the difference of the role of OH in ammonia and methane flames.
- ✓ We tried NH_3/air flame this time.

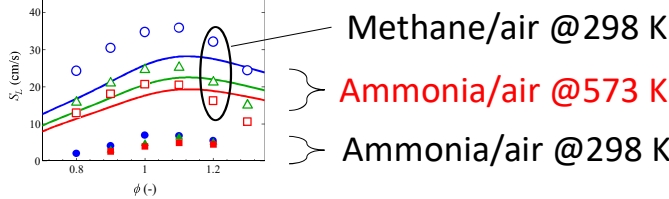
Experimental setup for NH₃/air turbulent combustion



Experimental conditions

Fuel	Ammonia
Oxidizer	Air
Mixture temp., T	573 K (± 8 K)
Pressure, P	0.3, 0.5 MPa
Burner outlet velocity, U_{ave}	1.0~3.0 m/s

LBV, S_L



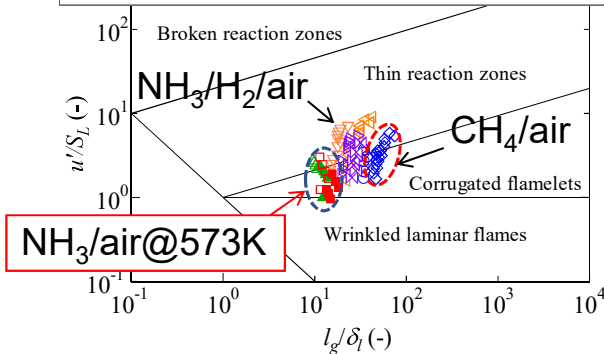
✓ To stabilize ammonia/air flame on the nozzle burner, mixture was pre-heated to 573 K.

Experimental conditions

Experimental condition on Peters diagram

Experimental condition at which S_T can be evaluated

Present study	P (MPa)	ϕ	Ichikawa (2019)	P (MPa)
NH ₃ /air (573 K)	0.3	\triangle	NH ₃ /H ₂ /air ($\phi=0.8$, 298 K)	0.3
	0.5	\square	NH ₃ /H ₂ /air ($\phi=1.0$, 298 K)	0.5
			CH ₄ /air ($\phi=0.9$, 298 K)	



0.3 MPa

0.5 MPa

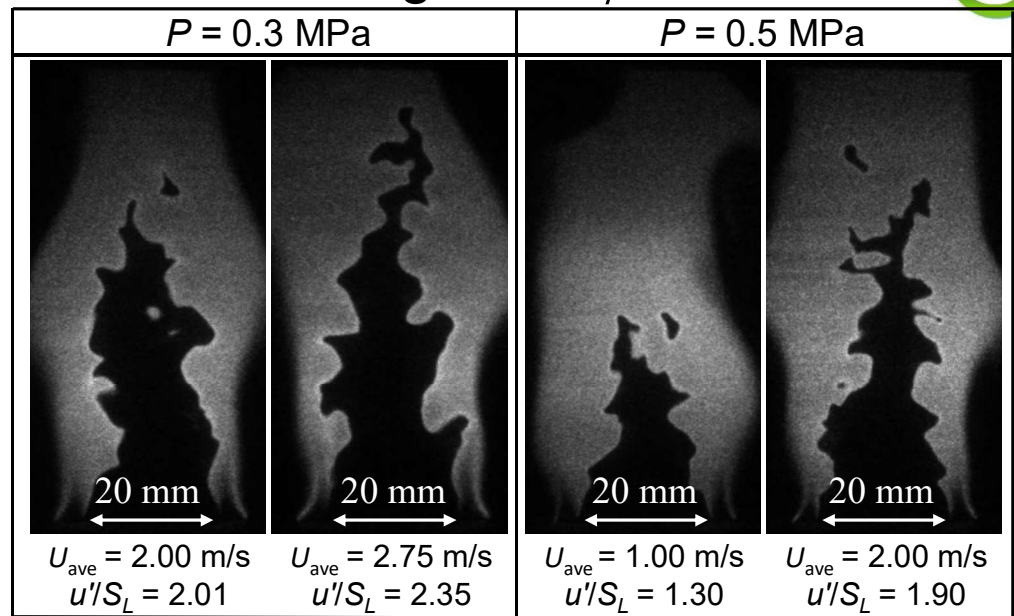
Mixture	x_{H_2} [-]	T [K]	P [MPa]	ϕ [-]	S_L [cm/s]	δ_l [mm]	Le_{eff} [-]
NH ₃ /air	0	573	0.3	0.8	13.32	0.179	0.937
NH ₃ /air	0	573	0.3	0.9	17.04	0.140	0.961
NH ₃ /H ₂ /air	0.4	298	0.3	0.8	13.86	0.0682	0.577
NH ₃ /H ₂ /air	0.4	298	0.3	1.0	18.32	0.0537	0.759
CH ₄ /air	0	298	0.3	0.9	21.02	0.0352	0.952
NH ₃ /air	0	573	0.5	0.8	11.40	0.125	0.937
NH ₃ /air	0	573	0.5	0.9	14.61	0.098	0.961
NH ₃ /H ₂ /air	0.4	298	0.5	0.8	12.56	0.0451	0.577
NH ₃ /H ₂ /air	0.4	298	0.5	1.0	14.50	0.0408	0.759
CH ₄ /air	0	298	0.5	0.9	18.09	0.0246	0.952

- ✓ Most of experimental conditions are in Corrugated flamelets region.
- ✓ Experimental conditions locate slightly left on the Peters diagram because of thicker preheating zone thickness of ammonia/air flames.

NH₃/air turbulent flame images for $\phi = 0.9$

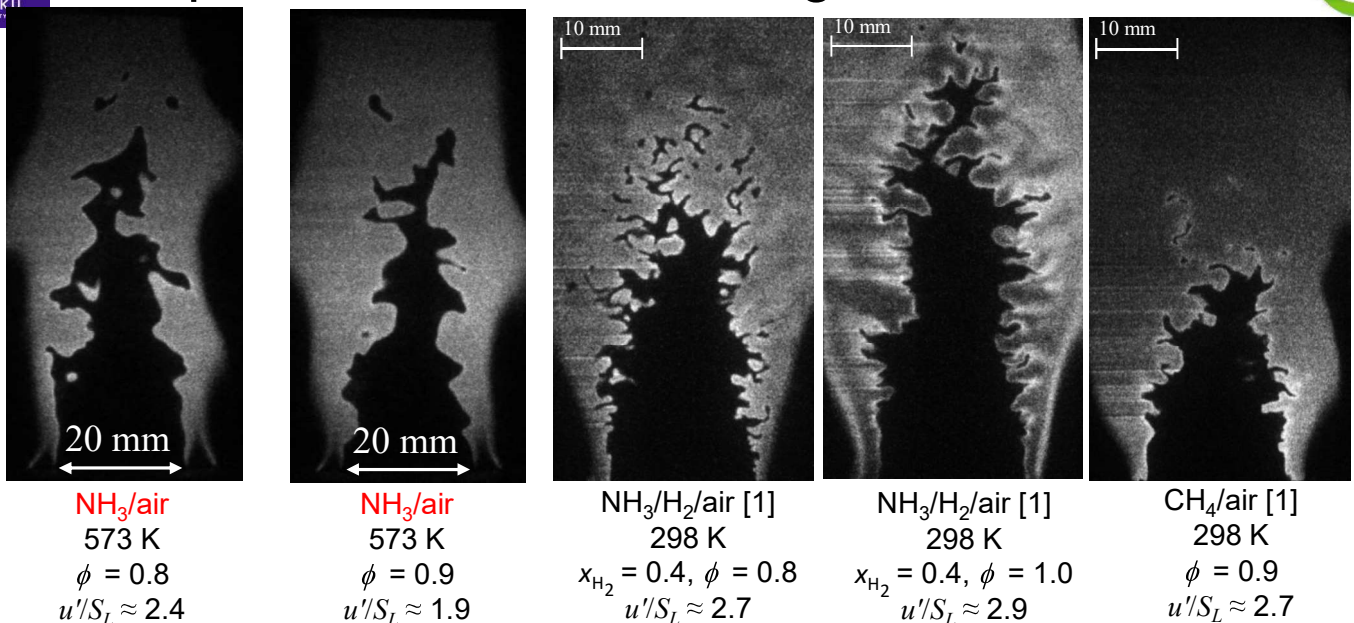


$P = 0.5 \text{ MPa}$, $u'/S_L \approx 2.1$
※ γ value was adjusted



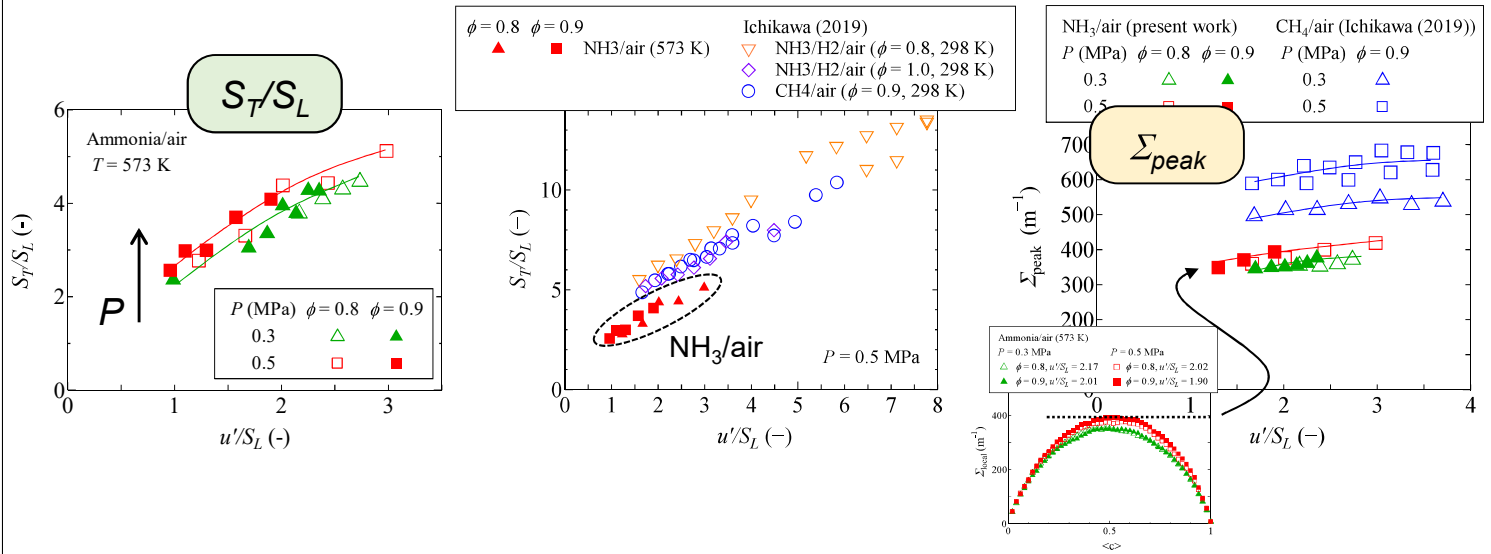
✓ Flame front wrinkling increases with pressure.

Comparison of OH-PLIF images at 0.5 MPa



✓ Flame front of NH₃/air flames are relatively smooth.

S_T/S_L and surface density, Σ_{peak}



- ✓ S_T/S_L and the peak value of flame surface density increase with pressure.
- ✓ The change in these values with equivalence ratio was not observed clearly.

TNF Session: Multi Regime Burner session

Coordinator: Benoit Fiorina

The session consisted of four major parts. First, a brief overview of the burner and available experimental data was presented. Second, the multi-modal flame structure was identified and discussed by applying the Gradient Free Regime Identification (GFRI) on experimental data. Third, the results of the joined numerical study was presented and analyzed. Finally, the session concluded with discussion of future target configurations for challenging H₂ stratified turbulent flames.

The (MRB) configuration consists of three concentric inlet streams, which can be operated independently with different equivalence ratios. A rich premixed flow of methane and air is injected through the center tube (called "jet") at an equivalence ratio of 1.8 or 2.6 for cases MRB18B and MRB26B, respectively. This main injection stream is surrounded by two concentric annular tubes, called "slot 1" and "slot 2". Pure air is injected through "slot 1", while a lean premixed flow of methane/air characterized by an equivalence ratio of 0.8 is injected through "slot 2". The temperature of the conical bluff body separating "slots 1" and "2" is regulated by water at 80 °C. Finally, a second bluff body separates "slot 2" from a low-speed air co-flow.

The objective of the joined numerical study is to give a state-of-the-art of turbulent combustion modeling community. It aims to address the average performance of current simulations and to identify physical phenomena that are not well captured today by most modeling strategies. Ten numerical groups have been involved in the numerical simulation: Technische Universität Darmstadt, University of Cambridge, Université Paris Saclay, KAUST, KTH Royal Institute of Technology, Jiangsu University, Université Libre de Bruxelles, Universität Duisburg Essen, Jiaotong University-Beihang University - the University of Technology and Universität der Bundeswehr München. One non-reacting and two reacting flow simulations (MRB18B and MRB26B) have been considered. Only results obtained on the MRB26B configuration were presented during the workshop.

Simulations were performed on three different LES solvers: OpenFOAM (8 groups), YALES2 (1 group), and PsiPhi (1 group). Chemistry was simplified by using premixed flamelet tabulation (4 groups), non-premixed flamelet tabulation (1 group), and reduced chemical schemes (5 groups). The turbulent combustion models employed, representative of the three main modeling strategies, are the geometrical (4 groups), statistical (2 groups) and mixingbased (3 groups) approaches. One team did account for subgrid scale fluctuation of chemical reaction rates. Different grid resolutions were employed with mesh sizes ranging between 0.93 million and 2.2 billion cells.

As for previous TNF workshops, each group adjusted the inlet velocity (mean + fluctuation) to retrieve the first measurements taken at 3 mm above the burner exit. The comparison of 2-D instantaneous snapshots of heat release along the centerline planes evidenced a high sensitivity of the lift-off height prediction to the mesh resolution. Analysis of mixture fraction fields shows that reaction occurs as soon as the mixture becomes flammable. Increasing the mesh resolution improves the prediction of mixing phenomena and therefore the location of the region where chemical reactions are initiated.

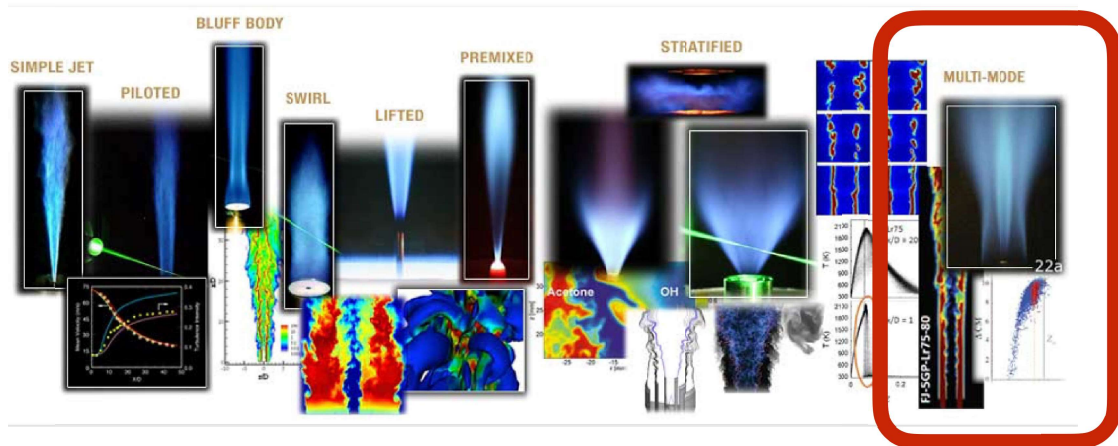
Detailed comparisons between experimental and numerical data along radial profiles taken at

different axial positions showed that the temperature field is fairly captured up to 60 mm from the burner exit. The comparison reveals, however significant discrepancies regarding CO mass fraction prediction. Three causes may explain this phenomenon. The first reason is a higher sensitivity of carbon monoxide to the simplification of detailed chemistry, especially when multiple combustion regimes are encountered. The second one is the bias introduced by artificial thickening, which overestimates the species' mass production rate. This behavior has been illustrated by manufacturing mean thickened turbulent flame brush from a random displacement of 1-D laminar flame solutions. The last one is the influence of the subgrid scale flame wrinkling on the filtered chemical flame structure, which may be challenging to model.

Final discussions raised the need to identify new target stratified or multi-regime turbulent flames for hydrogen combustion. Two interesting configurations that will be experimented with in the future have been identified: an extension of the MRB configuration to hydrogen/air combustion well as to methanol/air respective ethanol/air operated by TU Darmstadt and an H₂-air swirled confined combustor operated by EM2C-CNRS from Université Paris Saclay.

Multi Regime Burner session

Dirk Geyer, Robert Barlow, Christian Hasse and Benoît Fiorina



Vancouver, July 22th 2022 - TNF15

Contents

- 1) Introduction on the burner configuration and overview of the measurements.
Dirk Geyer (10 minutes)
- 2) Brief review on regime identification (GFRI) and application to the MRB.
Applications of GFRI on numerical data.
Rob Barlow and Christian Hasse (15 minutes)
- 3) Joined numerical-experimental comparison and analysis.
Benoît Fiorina (20 minutes)
- 4) Discussion on MRB
(15 minutes)
- 5) Discussion on future H₂ stratified target flames
(10 minutes)

TNF15 Workshop: Darmstadt Multi Regime Burner (MRB)

Experimental setup and flame structure

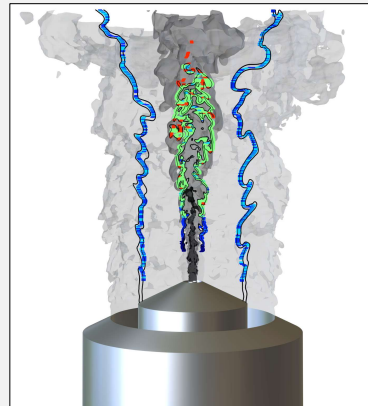
Dirk Geyer, Rob Barlow, Christian Hasse



A. Breicher
S. Walther
S. Hartl
D. Geyer



D. Butz
A. Breicher
A. Dreizler



S. Popp
S. Hartl
C. Hasse

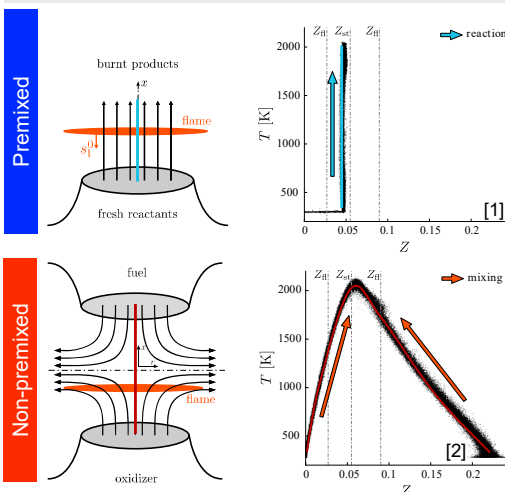


R. Barlow

Motivation



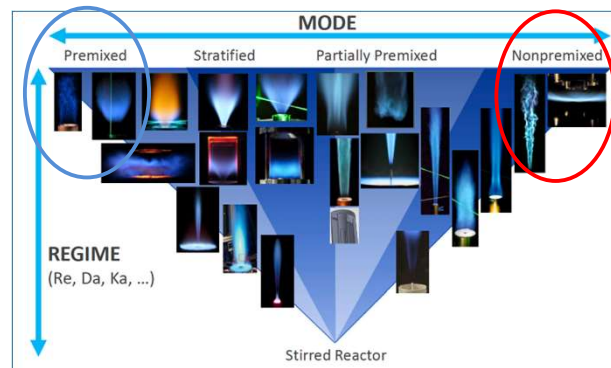
Classification of combustion processes



Turbulent benchmark flames

Workshop on measurement and computation of turbulent flames (TNF)

- A wide range of different benchmark flames
- Multi-regime / multi-mode combustion as topical issue



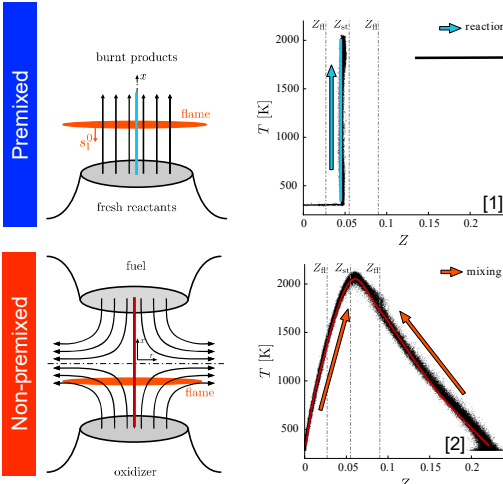
Barlow et al., TNF Workshop

Barlow, 11th Mediterranean Combustion Symposium, 2019

Experimental data: [1] D. Butz et al. Combust. Flame (2019)
[2] R.S. Barlow et al. Combust. Flame (2015)

Motivation

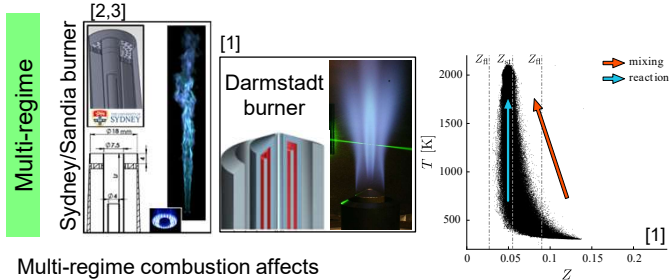
Classification of combustion processes



Turbulent benchmark flames

Workshop on measurement and computation of turbulent flames (TNF)

- wide range of different benchmark flames
- Multi-regime / multi-mode combustion as topical issue
- Two new benchmark flames identified



- Multi-regime combustion affects
 - Flame stability
 - Flame structure, e.g. pollutant emission
- Challenging for combustion modeling, e.g. CO modeling [1,4]

Experimental data: [1] D. Butz et al. Combust. Flame (2019)

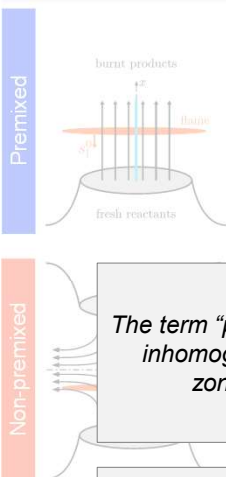
[3] S. Meares and A.R. Masri Combust. Flame (2014)

[2] R.S. Barlow et al. Combust. Flame (2015)

[4] Popp et al., Proc. Comb. Inst. 38 (2021)

Motivation

Classification of



Technical combustion application
More complex flow and mixing patterns – and flame structures

Multi-regime/Multi-mode combustion*
Local reaction zone can combine characteristics of premixed and non-premixed flames

***Different conventions can be found in the literature, e.g.**
The term “partially premixed” refers here to situations where the fluid parcel is compositionally inhomogeneous ... Mixing continues to occur in this parcel so that diffusion-like reaction zones as well as premixed propagating layers may exist within close proximity.
(A. Masri, Proc. Comb. Inst. 35:1115-1136 2015)

→ Darmstadt Multi Regime Burner (MRB)

Experimental data: [1] D. Butz et al. Combust. Flame (2019)

[3] S. Meares and A.R. Masri Combust. Flame (2014)

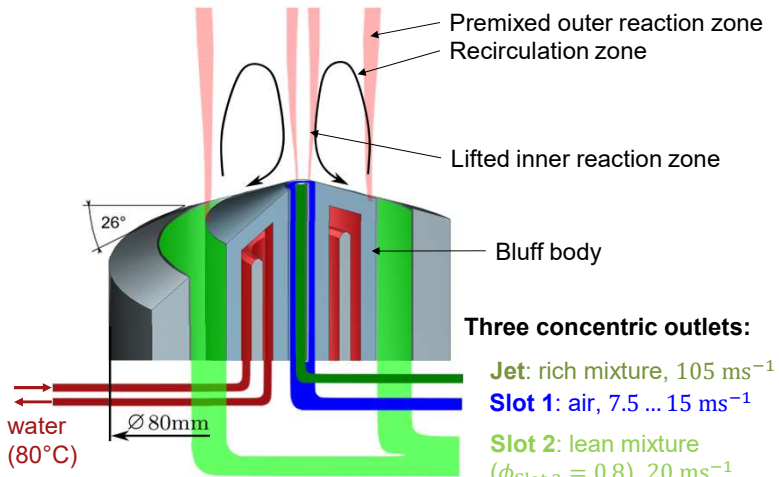
[2] R.S. Barlow et al. Combust. Flame (2015)

[4] Popp et al., Proc. Comb. Inst. 38 (2021)

Darmstadt Multi Regime Burner (MRB): Design

Nozzle diameters:

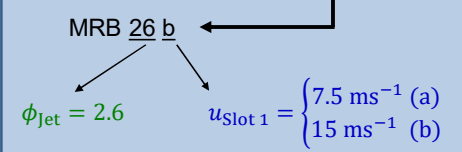
- ▶ Jet: Inner diameter 3 mm, outer diameter 3.3 mm
- ▶ Slot 1: Outer diameter 7 mm
- ▶ Slot 2: Inner diameter 40 mm, outer diameter 60 mm



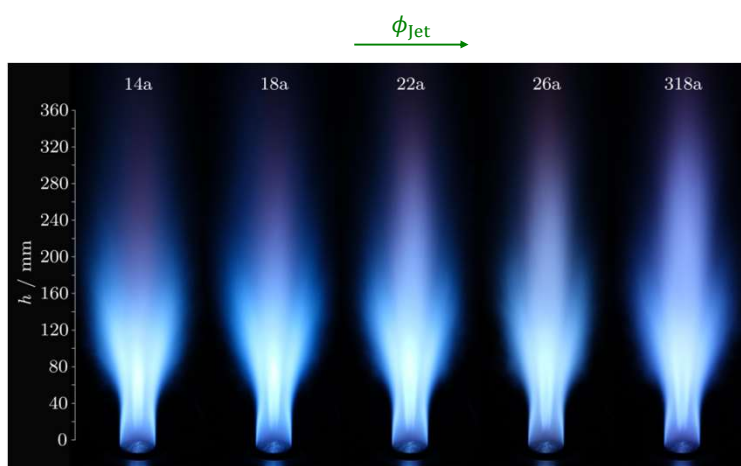
Setpoints:

$u_{\text{Slot 1}}$	ϕ_{Jet}				
	14a	18a	22a	26a	318a
	14b	18b	22b	26b	318b

Denomination scheme:



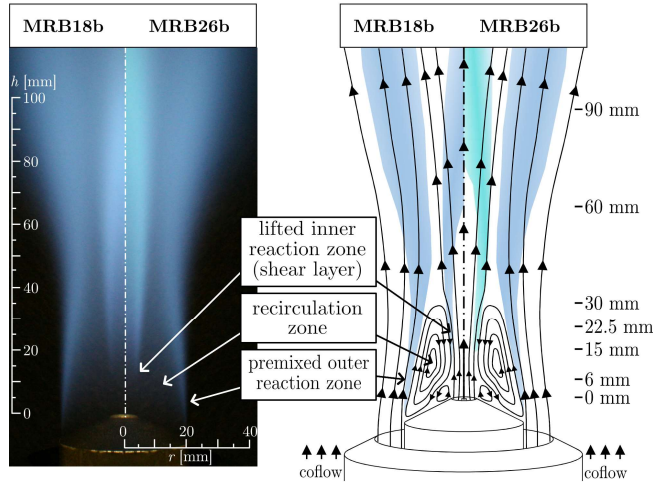
Darmstadt MRB: Configurations



Setpoints:

$u_{\text{Slot 1}}$	ϕ_{Jet}				
	14a	18a	22a	26a	318a
	14b	18b	22b	26b	318b

- ▶ Three inlet streams, operated independently in
 - ▶ **Equivalence ratio**
 - ▶ Exit velocity
- ▶ Fixed equivalence ratios for Slot 1 and Slot 2
- ▶ $\phi_{\text{Jet}} = 1.4 / 1.8 / 2.2 / 2.6 / 3.18$ corresponding to flame configurations 14a, 18a, 22a, 26a, 318a

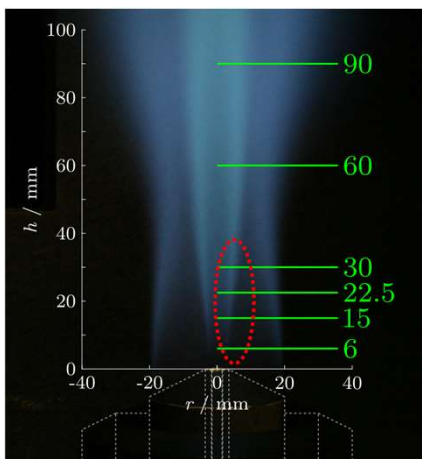


* The heights correspond to the measurement planes of the Raman measurements.

Setpoints:

	ϕ_{Jet}				
	14a	18a	22a	26a	318a
$u_{\text{Slot 1}}$	14b	18b	22b	26b	318b

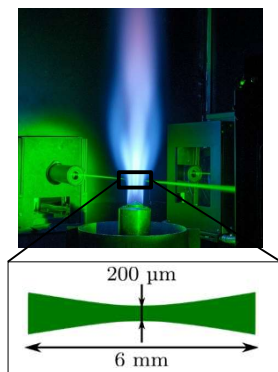
- Recirculation zone between Slot 1 and Slot 2, stabilized by conical bluff body
- Additional air coflow (1 m/s) around the outer body of the burner shields the flame and provides well-defined boundary conditions

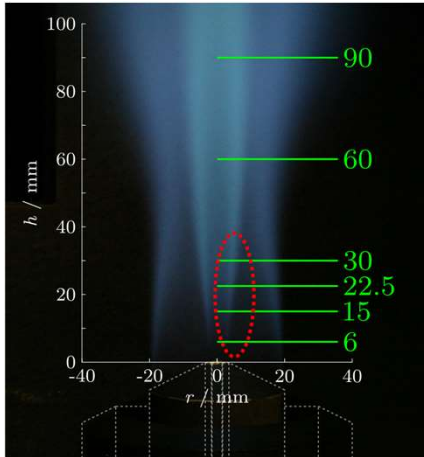


Multi-scalar measurements (Sandia)

Raman/Rayleigh/CO-LIF:

- Main species:
 CH_4 , O_2 , N_2 , CO , H_2 , CO_2 , H_2O
- 1D measurement
- Data spacing 20 μm for all measurements
- 5 Hz
- Radial profiles, 500 samples
- Up to 5000 samples at inner zone
- Optical Resolution of 40 - 60 μm

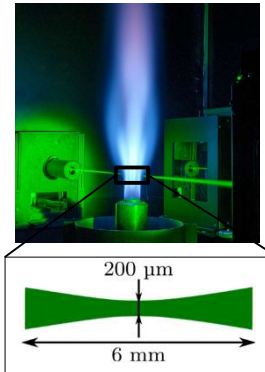




Multi-scalar measurements (Darmstadt)

Raman/Rayleigh:

- ▶ Main species:
 CH_4 , O_2 , N_2 , CO , H_2 , CO_2 , H_2O
- ▶ 1D measurement
- ▶ Data spacing $20\text{ }\mu\text{m}$ for all measurements
- ▶ 5 Hz
- ▶ Radial profiles, 500 samples
- ▶ Up to 5000 samples at inner zone
- ▶ Optical Resolution of $120\text{ }\mu\text{m}$
(10 pixels binning)
- ▶ No denoising necessary due to higher SNR



Darmstadt^[1]

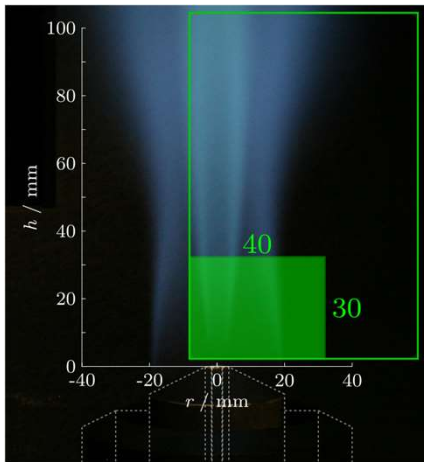
Scalar	Precision (%)	Accuracy (%)	Equivalence ratio ϕ
T	1.2	2	1.0
N_2	2.6	1	1.0
CO_2	5.8	4	1.0
H_2O	4.0	3	1.0
CO	14.4	8	1.3
H_2	16.5	8	1.3

Sandia^[2]

Scalar	Precision (%)	Accuracy (%)	Equivalence ratio ϕ
T	0.8	2	1.0
N_2	0.7	2	1.0
CO_2	3.2	4	1.0
H_2O	2.4	3	1.0
CO	4.5	10	1.3
H_2	7.5	10	1.3

[1] S. Shi, A. Breicher, J. Trabold et al. AECS (submitted)

[2] R. S. Barlow, G.-H. Wang, P. Anselmo-Filho et al. PCI (2009)



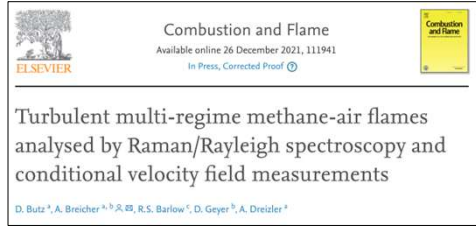
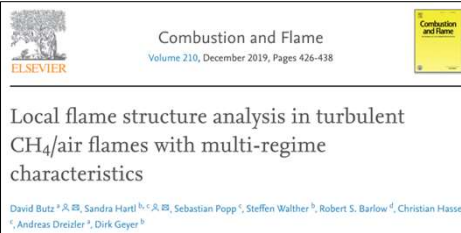
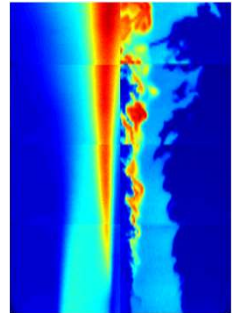
Velocity Measurements (Darmstadt)

Particle Image Velocimetry (PIV):

- ▶ Axial and radial velocity
- ▶ Non-reacting, 500 samples
- ▶ Reacting, 1500 samples
- ▶ 10 Hz
- ▶ Resulting resolution of vector field 300 μm

Simultaneous SO_2 -PLIF:

- ▶ Flame front visualization/temperature field

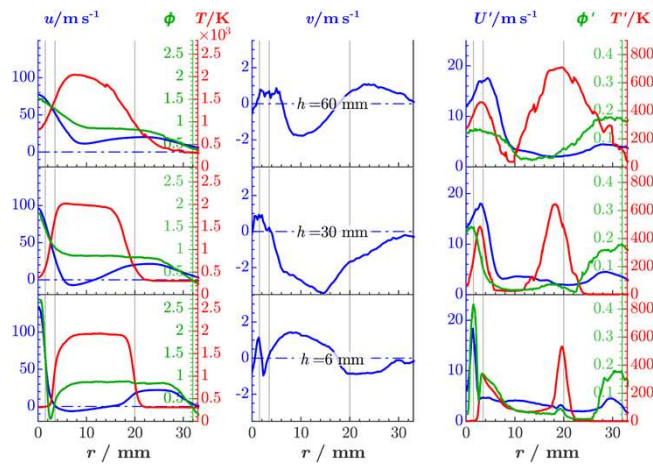
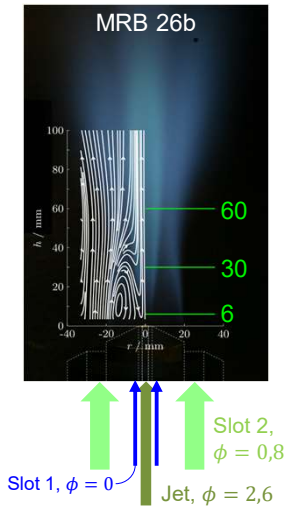


	14		18		22		26		318	
	a	b	a	b	a	b	a	b	a	b
Sandia Ram/Ray/CO-LIF										
Darmstadt PIV/PLIF										
Darmstadt Ram/Ray										

Raman/Rayleigh
Flame regime
analysis

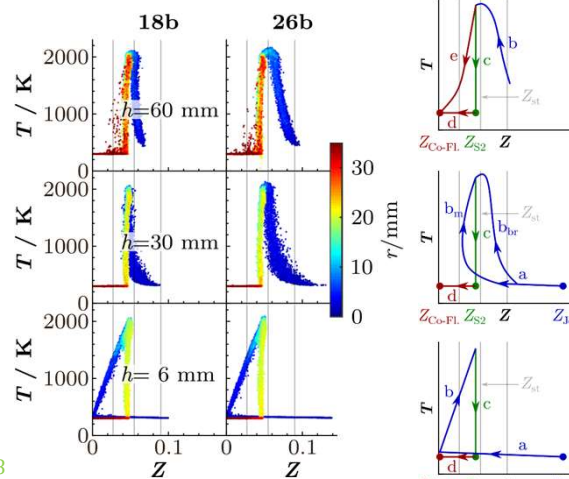
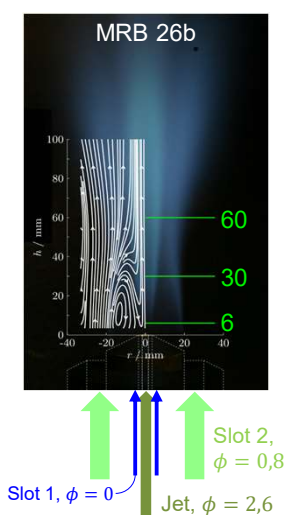
Raman/Rayleigh
PIV

Darmstadt MRB: Experimental results - Radial profiles



13 |

Darmstadt MRB: Experimental results – Scatter plots



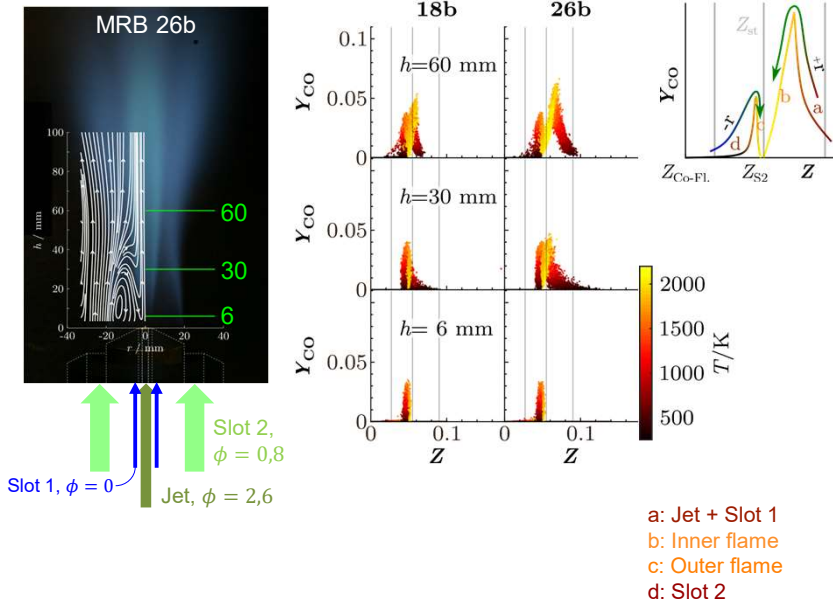
a: Jet + Slot 1
b: Slot 1 + Slot 2
c: Outer flame
d: Slot 2 + coflow

$h = 6\text{ mm}$: Mixing of Jet and Slot 1 and of Slot 1 and lean products from outer premixed zone

Farther downstream:

- ▶ MRB18b: Near-stoichiometric conditions, ranging from unburnt to burnt states
- ▶ MRB26b: Mixing between unburnt fuel-rich and burnt stoichiometric conditions
- ▶ Line c: Transit of outer flame brush (from hot products to cold reactants)
- ▶ Line d: Mixing layer between cold reactants (Slot 2) and coflowing air

14 |



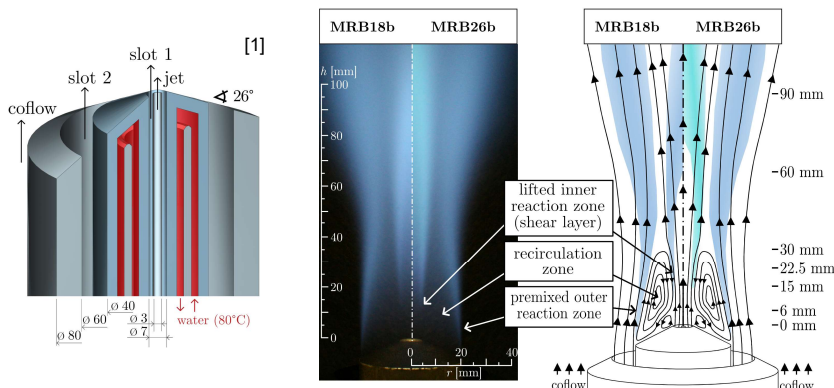
$h = 6$ mm:

- Cold mixing between Jet and Slot 1 and between Slot 1 (air) and Slot 2 → Zero CO values
- Outer premixed reaction at edge of bluffbody

Farther downstream:

- Second region of local reaction, richer than Slot 2, apparent
- Higher levels of CO, due to higher fuel concentrations,
 - close to stoichiometric (MRB18b)
 - fuel-rich (MRB26b)
- Separation between inner and outer reaction zone

Designed to allow for a variety of combustion regimes in single flame configuration with well-defined boundary conditions.



Experimental data:

- Major species and temperature (Raman/Rayleigh and CO-LIF) [1]
- Velocity field (PIV) [2]



- CH_4 /air flame
- Three inlet streams (jet, slot 1, slot 2)
- Varying jet flow conditions
- Pure air issuing from slot 1 and lean mixture ($\phi = 0.8$) from slot 2

TNF15 Workshop: Darmstadt Multi Regime Burner (MRB)

Experimental and numerical flame regime analysis

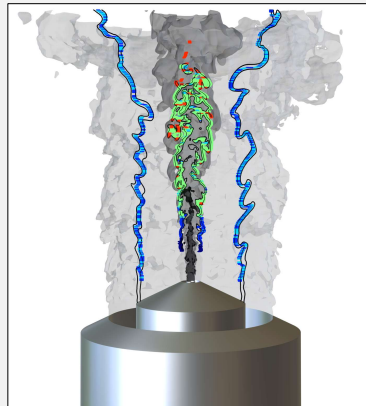
Dirk Geyer, **Rob Barlow**, Christian Hasse



A. Breicher
S. Walther
S. Hartl
D. Geyer



D. Butz
A. Breicher
A. Dreizler



S. Popp
S. Hartl
C. Hasse



L. Vervisch



R. Barlow

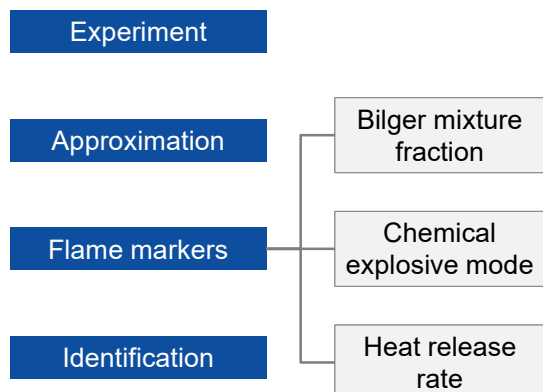
Gradient-Free Regime Identification (GFRI)



Regime identification from Raman/Rayleigh line measurements

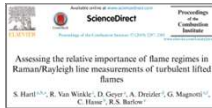
Hypotheses:

1. Major species and temperature from experiment are footprint of thermochemical state/combustion regime
2. Full thermochemical state can be approximated by constrained 0D simulation
3. Relevant flame markers can be calculated from approximated state
4. Combinations of flame markers reliably detect and characterize reaction zones



Validation and applications of GFRI

2018: Introduction of GFRI and application to experimental and numerical data



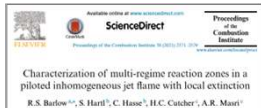
2019: Importance of flame regimes based on correlations among HRR, Z_{CM} and ΔCM

2019: GFRI validation on DNS data of turbulent high Karlovitz flames



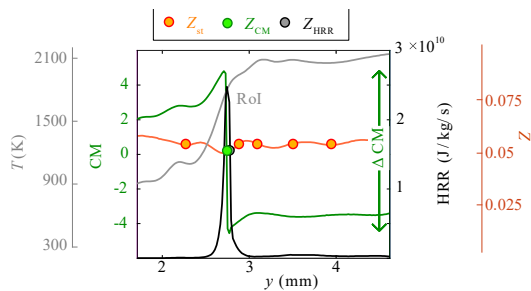
2019: Regime maps of reactions zones in multi regime burner, prior analysis

2020: Training of CNNs for regime detection based on GFRI and Raman/Rayleigh data



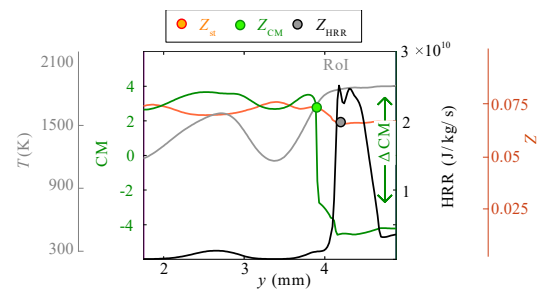
2021: GFRI analysis of piloted inhomogeneous jet flame series with local extinction/re-ignition

GFRI – Assessing relative importance of reaction zones



- ▶ HRR_{max} directly at CM zero-crossing and close to Z_{st}
- ▶ Maximum far greater than HRR in negative CM region
- ▶ High value in ΔCM ($\Delta CM = 8.9$)

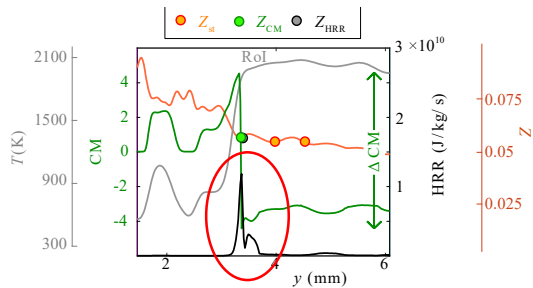
Dominantly premixed structure



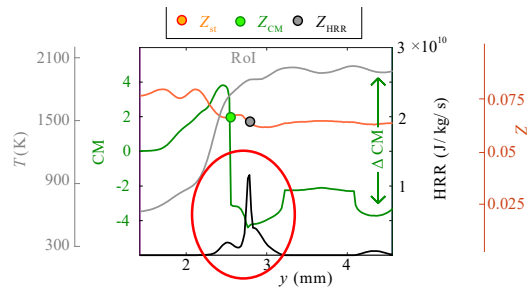
- ▶ HRR in negative CM region exceeds HRR_{CM} by more than a factor of 10
- ▶ Small ΔCM ($\Delta CM = 5$)

Dominantly non-premixed structure

GFRI – Assessing relative importance of reaction zones



$HRR_{CM} > HRR_{NP}$



$HRR_{NP} > HRR_{CM}$

Multi-regime structures

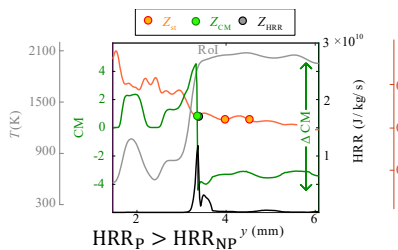
- Premixed and non-premixed structures in close proximity
- Both contribute significantly to overall heat release

ROI – region of interest (0.5 mm in negative CM direction)

Flame regime characterization based on GFRI approach

Multi-regime reaction zones combine premixed and non-premixed characteristics in close proximity

GFRI analysis on single sample line [1]



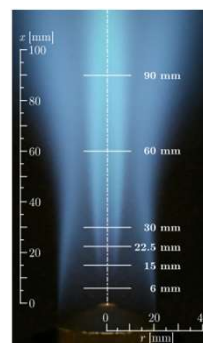
$HRR_P > HRR_{NP}$

Flame regime parameter

$$\eta = \frac{(HRR_P - HRR_{NP})}{HRR_{max}}$$

Premixed	P	$1 \geq \eta > 0.99$ (no detectable NP character in ROI)
Dominantly premixed	DP	$0.99 \geq \eta > 0.8$
Multi-regime	MR	$0.8 \geq \eta > -0.8$
Dominantly non-Premixed	DNP	$-0.8 \geq \eta > -1$
Non-premixed	NP	$-0.99 \geq \eta \geq -1$ (HRR_{max} within $0.055 < Z < 0.07$; no CM zero-crossing)
Lean back-supported	LBS	$Z_{CM} < Z_{max} < Z_{slot 2}$

MRB 26b: overall flame regime distribution



- Large amount of multi-regime characteristics identified within the inner reaction zone ($r < 10\text{mm}$) [1]

TNF15 Workshop: Darmstadt Multi Regime Burner (MRB)

Experimental and numerical flame regime analysis

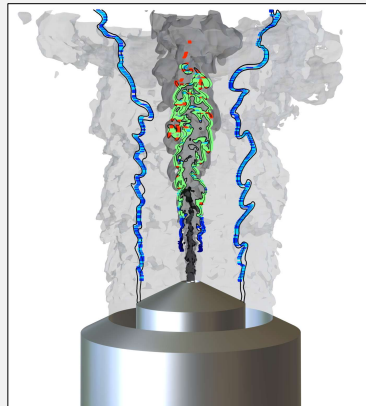
Dirk Geyer, Rob Barlow, **Christian Hasse**



A. Breicher
S. Walther
S. Hartl
D. Geyer



D. Butz
A. Breicher
A. Dreizler



S. Popp
S. Hartl
C. Hasse



L. Vervisch



R. Barlow

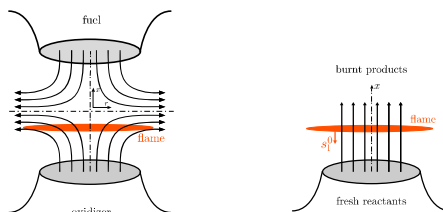
Combustion modeling with tabulated chemistry



Combustion modeling using flamelet-based chemistry tabulation rely on flame structure assumptions, e.g. being either premixed or non-premixed

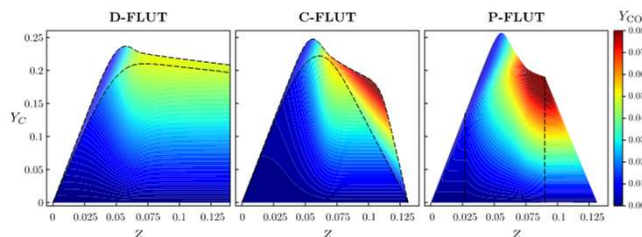
Tabulated manifolds applied for regime identification

Flame configurations



flame regime	abbrev.	fuel BC
non-premixed (NP)	D-FLUT	$Z_f = 1$
	C-FLUT	$Z_f = Z_{jet}$
premixed (P)	P-FLUT	$Z_f = Z_{jet}$

Tabulated manifolds

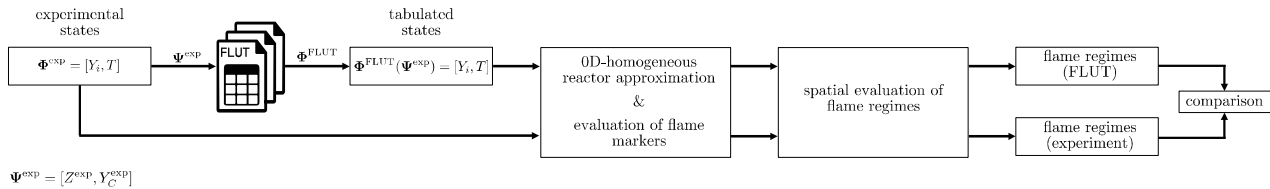


Comparison of tabulated manifolds

- Different flame structures!
- Is a flame regime identification still possible?

GFR using results from tabulated chemistry (*prior* analysis)

Procedure of combined *prior* and GFR analysis

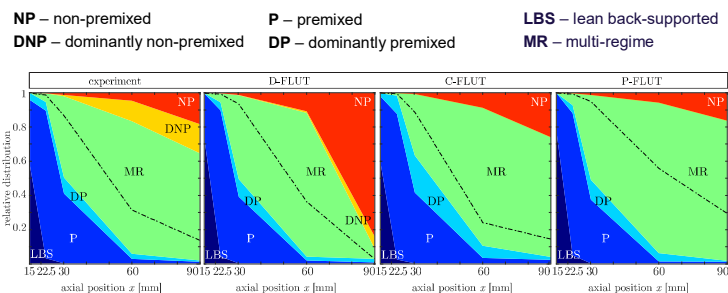


Results of MRB 26b configuration

Applicability of tabulated chemistry to identify multi-regime combustion effects?

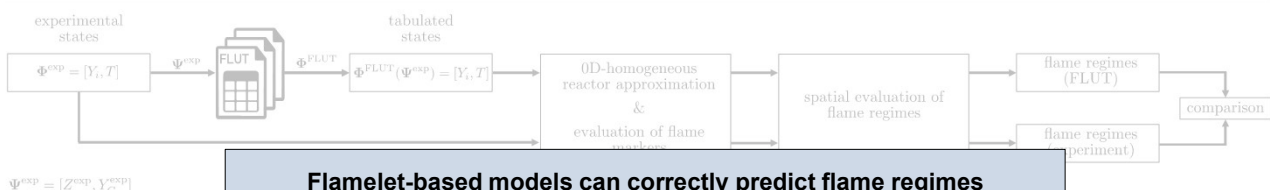
- GFR based on tabulated flame-markers
- Overall trend captured by all tabulation approaches

➡ For correctly predicted local transport, the identification of the correct regime is expected



GFR using results from tabulated chemistry (*prior* analysis)

Procedure of combined *prior* and GFR analysis



Results of MRB 26b configuration

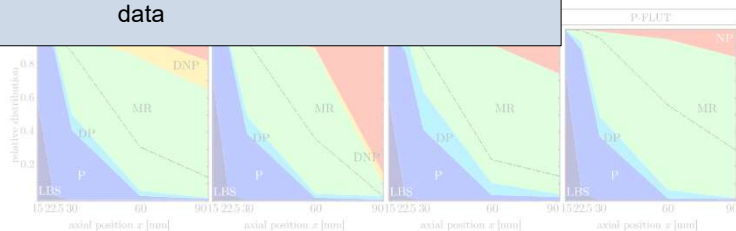
Applicability of tabulated chemistry to identify multi-regime combustion effects?

- GFR based on tabulated flame-markers
- Overall trend captured by all tabulation approaches

➡ For correctly predicted local transport, the identification of the correct regime is expected

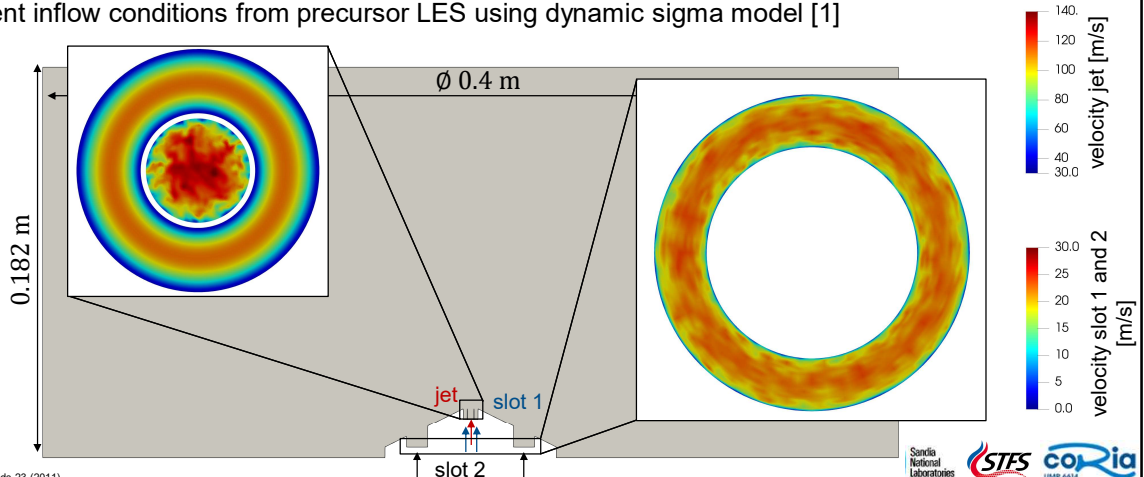
Flamelet-based models can correctly predict flame regimes even multi-regime combustion and despite flame structure assumption

Next: application in combustion LES
general applicability to LES was verified by analysis on filtered experimental data



LES setup – solver, mesh and boundary conditions

- OpenFOAM: 2nd order spatial and temporal discretization
- Mesh: hexahedral O-grid with 31.1 million cells
 - $0.1\text{mm} \leq \Delta_{\text{cell}} \leq 0.2\text{mm}$ in jet core region
 - $0.3\text{mm} \leq \Delta_{\text{cell}} \leq 0.4\text{mm}$ in outer reaction zone
- Turbulent inflow conditions from precursor LES using dynamic sigma model [1]



[1] F. Nicoud et al. Phys. Fluids 23 (2011)

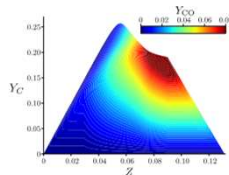
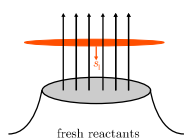
LES setup – combustion model

LES – artificial thickened flame (ATF) with tabulated chemistry

Tabulated chemistry

- Premixed combustion model (FGM)
- Manifold constructed from adiabatic freely-propagating flames

$$\varphi(\tilde{Z}, \tilde{Y}_c) = [\tilde{T}, \tilde{Y}_i]$$



- Progress variable $Y_C = Y_{\text{CO}_2} + Y_{\text{H}_2\text{O}}$

Turbulence-chemistry interaction

- ATF model [1] with grid adaptive thickening factor (F) and efficiency function (E) by Charlette [2]

$$\frac{\partial(\bar{\rho}\tilde{\psi})}{\partial t} + \nabla \cdot (\bar{\rho}\tilde{u}\tilde{\psi}) = \nabla \cdot \left[\left(FE\bar{\rho}D + (1 - \Omega)\frac{\mu_t}{Sc_t} \right) \nabla \tilde{\psi} \right] + \frac{E\bar{\omega}_\psi}{F}$$

- Thickening spatially limited by tabulated flame sensor Ω [3]

$$F = 1 + \Omega(F_{\text{max}} - 1)$$

$$\Omega = \frac{\nabla Y_C}{(\nabla Y_C)_{\text{max}}} + \frac{\dot{\omega}_{Y_C}}{(\dot{\omega}_{Y_C})_{\text{max}}} \left(1 - \frac{\nabla Y_C}{(\nabla Y_C)_{\text{max}}} \right)$$

- Additional CO transport equation, $\psi = Y_{\text{CO}}$, source term treatment following [4,5]

$$\bar{\omega}_{\text{CO}} = \bar{\omega}_{\text{CO}}^+ + \tilde{Y}_{\text{CO}} \frac{\bar{\omega}_{\text{CO}}}{\tilde{Y}_{\text{CO}}^{\text{FLUT}}}$$

[1] O. Colin et al. Phys. Fluids (2000)

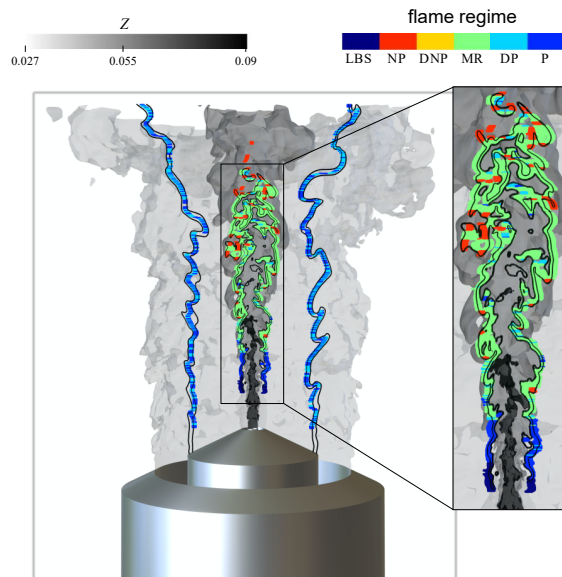
[3] S. Popp et al. Combust. Flame 206 (2019)

[2] F. Charlette et al. Combust. Flame 131 (2002)

[4] M. Ihme and H. Pitsch. Phys. Fluids 20 (2008)

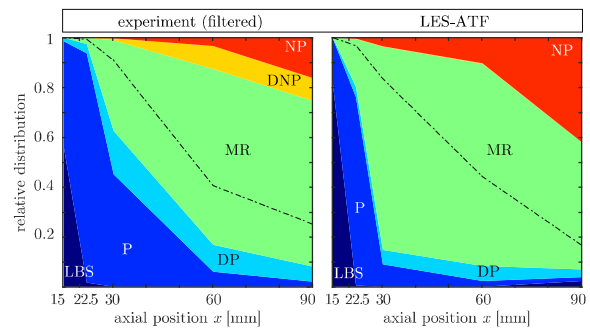
[5] H. Wang et al. Proc. Combust. Inst. 37 (2019)

Gradient-free regime identification in LES



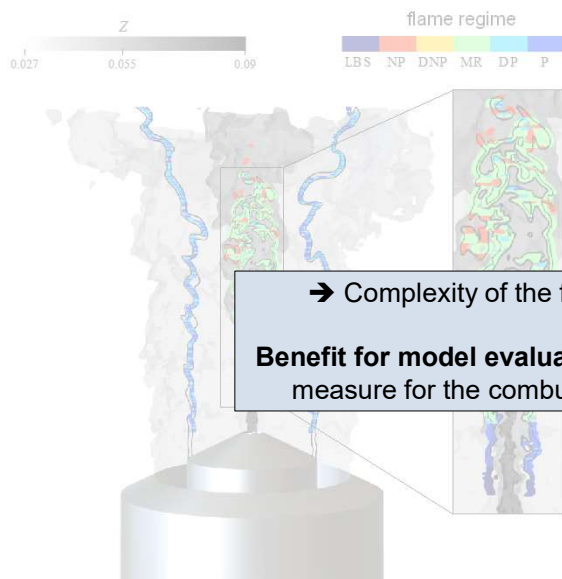
NP – non-premixed
DNP – dominantly non-premixed
LBS – lean back-supported
P – premixed
DP – dominantly premixed
MR – multi-regime

- + Identification of local flame regime possible
- + Overall experimental trend captured by LES
- Differences at 22.5 and 30 mm result from differences in local transport



Hartl et al., 30. Deutscher Flammtag (2021)

Gradient-free regime identification in LES

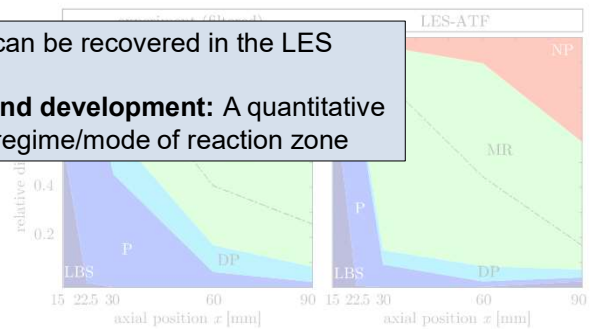


NP – non-premixed
DNP – dominantly non-premixed
LBS – lean back-supported
P – premixed
DP – dominantly premixed
MR – multi-regime

- + Identification of local flame regime possible
- + Overall experimental trend captured by LES
- Differences at 22.5 and 30 mm result from differences in local transport

→ Complexity of the flame can be recovered in the LES

Benefit for model evaluation and development: A quantitative measure for the combustion regime/mode of reaction zone



Hartl et al., 30. Deutscher Flammtag (2021)

Multi Regime Burner

Joined experimental-numerical comparisons

Tan Phong Luu¹, Samuel Dillon^{1,2}, Renaud Mercier², Linus Engelmann³, Andreas Kempf³ and Benoît Fiorina¹

¹Université Paris-Saclay, CNRS, CentraleSupélec, Laboratoire EM2C

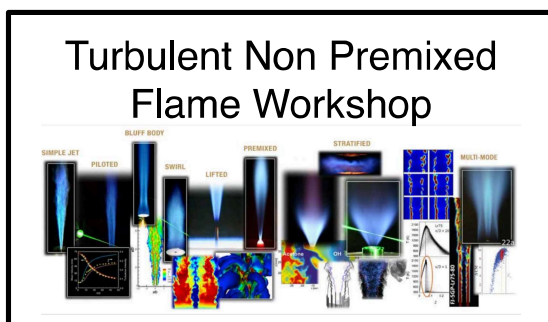
²SafranTECH, Modelling and Simulation

³Universität Duisburg-Essen

3

How multi-regime flames are created ?

During a joined meeting between



&

Premixed Turbulent
Flames Workshops

4

Objectives of this exercise

- Is not to match experiments or to compare models together
- but to give a state of the art of the turbulent combustion modeling community:
 - Address the performances of the current simulations
 - Identify physical phenomena not well captured today by the majority of modeling strategies

5

Participant to TNF 2022



TECHNISCHE
UNIVERSITÄT
DARMSTADT

**Sebastian Popp, David Butz, Dirk
Geyer, Christian Hasse**



Ping Wang



UNIVERSITY OF
CAMBRIDGE

**James Massey, Zhi Chen, Zhiyi Li,
Prof Swaminathan**



Arthur Pequin, Alessandro Parente



CentraleSupélec



**Tan-Phong Luu, Samuel Dillon, Renaud
Mercier, Benoît Fiorina**



Linus Engelmann, Andreas Kempf



KAUST

Lorenzo Angelilli, Hong G. Im



Jiaotong



Beihang



**Weijie Zhang, Wang Han,
Jinhua Wang, Zuohua Huang,
Jeroen van Oijen**



Kai Zhang, Christophe Duwig



**Maximilian Hansinger, Arne Lampmann, Paola
Breda, Micheal Pfitzner**

6

Group	Code type	Grid	Nb of Cells	Spatial scheme	Temporal scheme	Turbulence	Turbulent Combustion Model	Chemistry
CAM	OpenFOAM Compressible	Structured	3.5 M	2nd order	2nd order	Sigma	Presumed PDF	Premixed flamelets
UBM	OpenFOAM Low Mach	Unstructured	5.1 M	2nd order	2nd order	WALE	No-model	19-species ARC (Lu & Law 2008)
EM2C	YALES2 Low Mach	Structured	30.9 M	4th order	4th order	Sigma	D-TFLES + Charlette model	Premixed flamelets
TUD	OpenFOAM Low Mach	Structured	30.9 M	2nd order	2nd order	Sigma	D-TFLES + Charlette model	Premixed flamelets + transported Y_{CO}
JU	OpenFOAM	Structured	4.34 M	2nd order	2nd order	K-equation	D-TFLES	15-species ARC (Toshimitsu et al. 2000)
KAUST	OpenFOAM	Structured	8 M (MRB26b) 64 M (MRB18b)	2nd order	2nd order	WALE	Eddy dissipation concept	15-species ARC
KTH	OpenFOAM Low Mach	Hybrid (hexahedral dominant)	0.93 M	2nd order	2nd order	WALE	PaSR	17-species skeletal (Lu & Law 2009)
UDE	PsiPhi	Structured	2.2 B	4th order	3rd order	Sigma	D-TFLES + Charlette model	Premixed flamelets
XJTU/BUAA	OpenFOAM Low Mach	Structured	30.9 M	2nd order	2nd order	Dynamic Smagorinsky	Presumed PDF	Non-premixed flamelets
ULB	OpenFOAM Compressible	Unstructured	3 M	2nd order	2nd order	K-equation	PaSR	7-species mechanism

Group	Code type	Grid	Nb of Cells	Spatial scheme	Temporal scheme	Turbulence	Turbulent Combustion Model	Chemistry
CAM	OpenFOAM Compressible	Structured	3.5 M	2nd order	2nd order	Sigma	Presumed PDF	Premixed flamelets
UBM	OpenFOAM Low Mach	Unstructured	OpenFOAM = 8			WALE	No-model	19-species ARC (Lu & Law 2008)
EM2C	YALES2 Low Mach	Structured	YALES 2 = 1			Sigma	D-TFLES + Charlette model	Premixed flamelets
TUD	OpenFOAM Low Mach	Structured	30.9 M	2nd order	2nd order	Sigma	D-TFLES + Charlette model	Premixed flamelets + transported Y_{CO}
JU	OpenFOAM	Structured	4.34 M	2nd order	2nd order	K-equation	D-TFLES	15-species ARC (Toshimitsu et al. 2000)
KAUST	OpenFOAM	Structured	8 M (MRB26b) 64 M (MRB18b)	2nd order	2nd order	WALE	Eddy dissipation concept	15-species ARC
KTH	OpenFOAM Low Mach	Hybrid (hexahedral dominant)	0.93 M	2nd order	2nd order	WALE	PaSR	17-species skeletal (Lu & Law 2009)
UDE	PsiPhi	Structured	PsiPhi = 1			Sigma	D-TFLES + Charlette model	Premixed flamelets
XJTU/BUAA	OpenFOAM Low Mach	Structured	30.9 M	2nd order	2nd order	Dynamic Smagorinsky	Presumed PDF	Non-premixed flamelets
ULB	OpenFOAM Compressible	Unstructured	3 M	2nd order	2nd order	K-equation	PaSR	7-species mechanism

Group	Code type	Grid	Nb of Cells	Spatial scheme	Temporal scheme	Turbulence	Turbulent Combustion Model	Chemistry
CAM	OpenFOAM Compressible	Structured	Statistical (presumed PDF)=2				Presumed PDF	Premixed flamelets
UBM	OpenFOAM Low Mach	Unstructured	5.1 M	2nd order	2nd order	WALE	No-model	19-species ARC (Lu & Law 2008)
EM2C	YALES2 Low Mach	Structured	30.9 M	4th order	4th order	Sigma	D-TFLES + Charlette model	Premixed flamelets
TUD	OpenFOAM	Geometrical approach (Dynamic-Thickened Flame for LES)=4					D-TFLES + Charlette model	Premixed flamelets + transported Y_{CO}
JU	OpenFOAM	Structured	4.34 M	2nd order	2nd order	K-equation	D-TFLES	15-species ARC (Toshimitsu et al. 2000)
KAUST	OpenFOAM	Structured	8 M (MRB26b)	2nd order	2nd order	WALE	Eddy dissipation concept	15-species ARC
KTH	OpenFOAM Low Mach	Hybrid (hexahedral dominant)	0.93 M	2nd order	2nd order	WALE	PaSR	17-species skeletal (Lu & Law 2009)
UDE	PsiPhi	Structured	2.2 B	4th order	3rd order	Sigma	D-TFLES + Charlette model	Premixed flamelets
XJTU/BUAA	OpenFOAM Low Mach	Structured	30.9 M	2nd order	2nd order	Dynamic Smagorinsky	Presumed PDF	Non-premixed flamelets
ULB	OpenFOAM Compressible	Unstructured	3 M	2nd order	2nd order	K-equation	PaSR	7-species mechanism

Group	Code type	Grid	Nb of Cells	Spatial scheme	Temporal scheme	Turbulence	Turbulent Combustion Model	Chemistry
CAM	OpenFOAM Compressible	Structured	Statistical (presumed PDF)=2				Presumed PDF	Premixed flamelets
UBM	OpenFOAM Low Mach	Unstructured	No-model = 1		2nd order	WALE	No-model	19-species ARC (Lu & Law 2008)
EM2C	YALES2 Low Mach	Structured	30.9 M	4th order	4th order	Sigma	D-TFLES + Charlette model	Premixed flamelets
TUD	OpenFOAM	Geometrical approach (Dynamic-Thickened Flame for LES)=4					D-TFLES + Charlette model	Premixed flamelets + transported Y_{CO}
JU	OpenFOAM	Structured	4.34 M	2nd order	2nd order	K-equation	D-TFLES	15-species ARC (Toshimitsu et al. 2000)
KAUST	OpenFOAM	Structured	8 M (MRB26b)	2nd order	2nd order	WALE	Eddy dissipation concept	15-species ARC
KTH	OpenFOAM Low Mach	Hybrid (hexahedral dominant)	0.93 M	2nd order	2nd order	WALE	PaSR	17-species skeletal (Lu & Law 2009)
UDE	PsiPhi	Structured	2.2 B	4th order	3rd order	Sigma	D-TFLES + Charlette model	Premixed flamelets
XJTU/BUAA	OpenFOAM Low Mach	Structured	30.9 M	2nd order	2nd order	Dynamic Smagorinsky	Presumed PDF	Non-premixed flamelets
ULB	OpenFOAM Compressible	Unstructured	3 M	2nd order	2nd order	K-equation	PaSR	7-species mechanism

Group	Code type	Grid	Nb of Cells	Spatial scheme	Temporal scheme	Turbulence	Turbulent Combustion Model	Chemistry
CAM	OpenFOAM Compressible	Structured	3.5 M	2nd order	2nd order	Sigma	Presumed PDF	Premixed flamelets
UBM	OpenFOAM Low Mach	Unstructured	5.1 M	2nd order	2nd order	WALE	No-model	19-species ARC (Lu & Law 2008)
EM2C	YALES2 Low Mach	Structured	30.9 M	4th order	4th order	Sigma	D-TFLES + Charlette model	Premixed flamelets
TUD	OpenFOAM Low Mach	Structured	30.9 M	2nd order	2nd order	Sigma	Charlette model	Premixed flamelets + transported Y_{CO}
JU	OpenFOAM	Structured	4.34 M	2nd order	2nd order	K-equation	D-TFLES	15-species ARC (Toshimitsu et al. 2000)
KAUST	OpenFOAM	Structured	8 M (MRB26b) 64 M (MRB18b)	Reduced chemistry = 5			Eddy dissipation concept	15-species ARC
KTH	OpenFOAM Low Mach	Hybrid (hexahedral dominant)	0.93 M	2nd order	2nd order	WALE	PaSR	17-species skeletal (Lu & Law 2009)
UDE	PsiPhi	Structured	2.2 B	4th order	3rd order	Sigma	D-TFLES + Charlette model	Premixed flamelets
XJTU/BUAA	OpenFOAM Low Mach	Structured	3	Non-premixed flamelet tabulation			Presumed PDF	Non-premixed flamelets
ULB	OpenFOAM Compressible	Unstructured	3 M	2nd order	2nd order	K-equation	PaSR	7-species mechanism

Flame configurations

Group	WALL CONDITIONS	COLD (MRB18b)	REACTIVE	
			MRB18b	MRB26b
EXPERIMENTS		U	U, Z, T, Y_{CO}	U, Z, T, Y_{CO}
CAM	ADIABATIC	X	X	X
UBM		X	X	
EM2C	ADIABATIC	X		X
TUD	ADIABATIC			X
JU	IMPOSED T		X	X
KAUST	IMPOSED T	X	X	X
KTH		X	X	X
UDE	ADIABATIC		X	X
XJTU/BUAA	ADIABATIC	X	X	X
ULB	IMPOSED T	X		

Results shown today

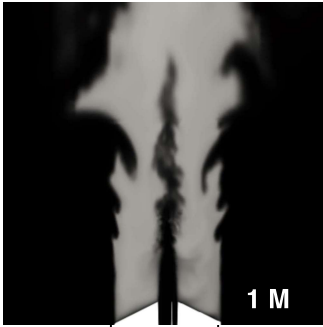
According to Cambridge and TUD data, there is no strong influence of heat losses

Instantaneous snapshots

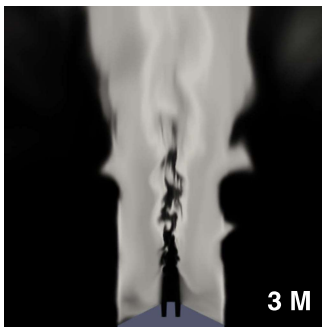
II

Temperature - 26b

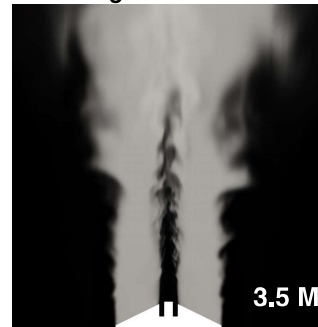
KTH - Stockholm



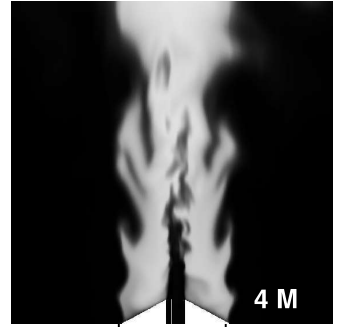
ULB



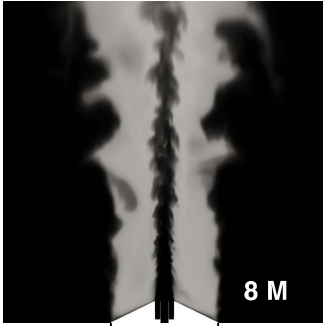
Cambridge



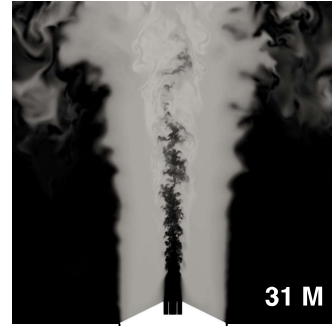
JSU - Zhenjiang



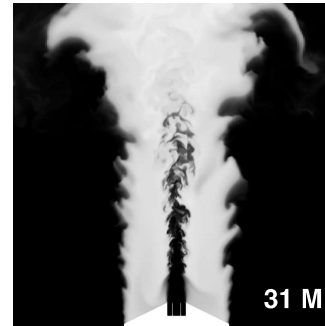
KAUST - Thuwal



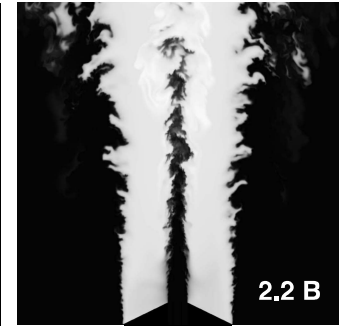
EM2C - Paris



Darmstadt

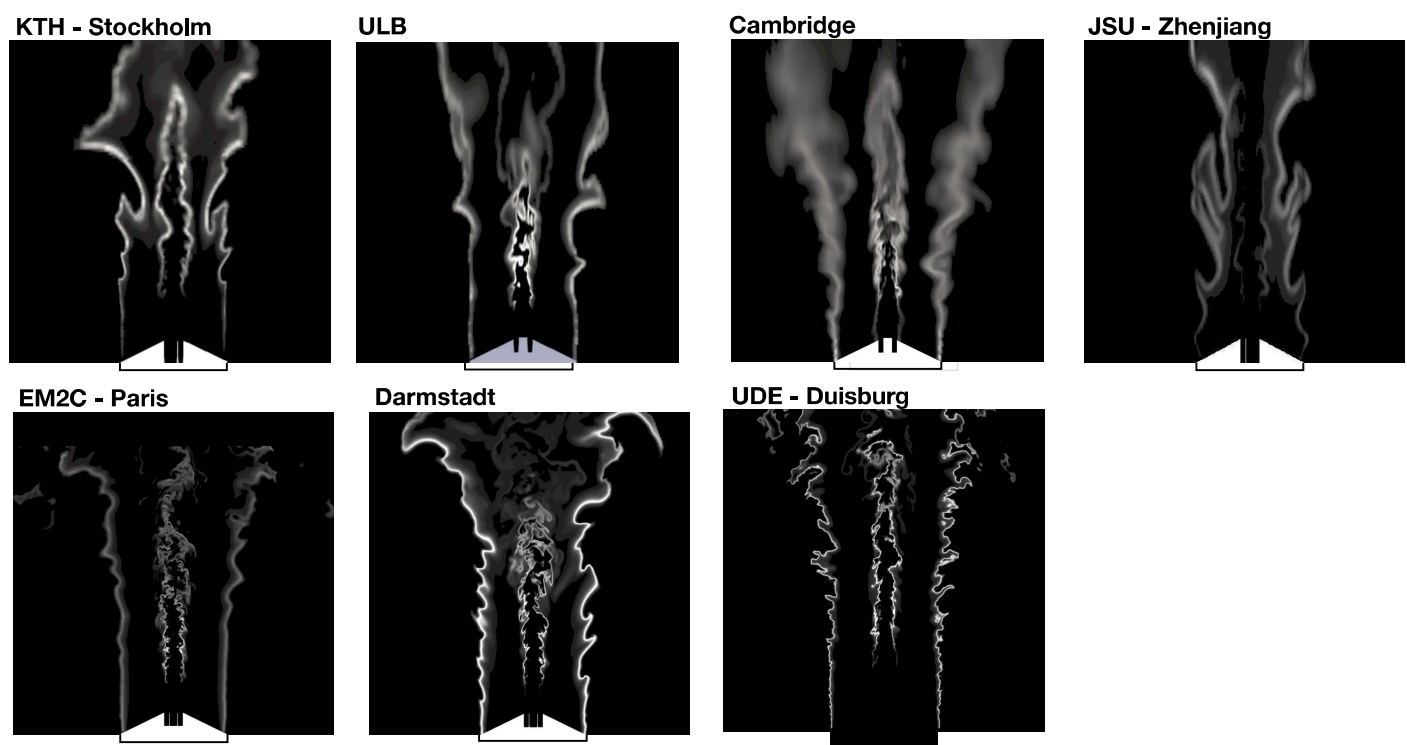


UDE - Duisburg

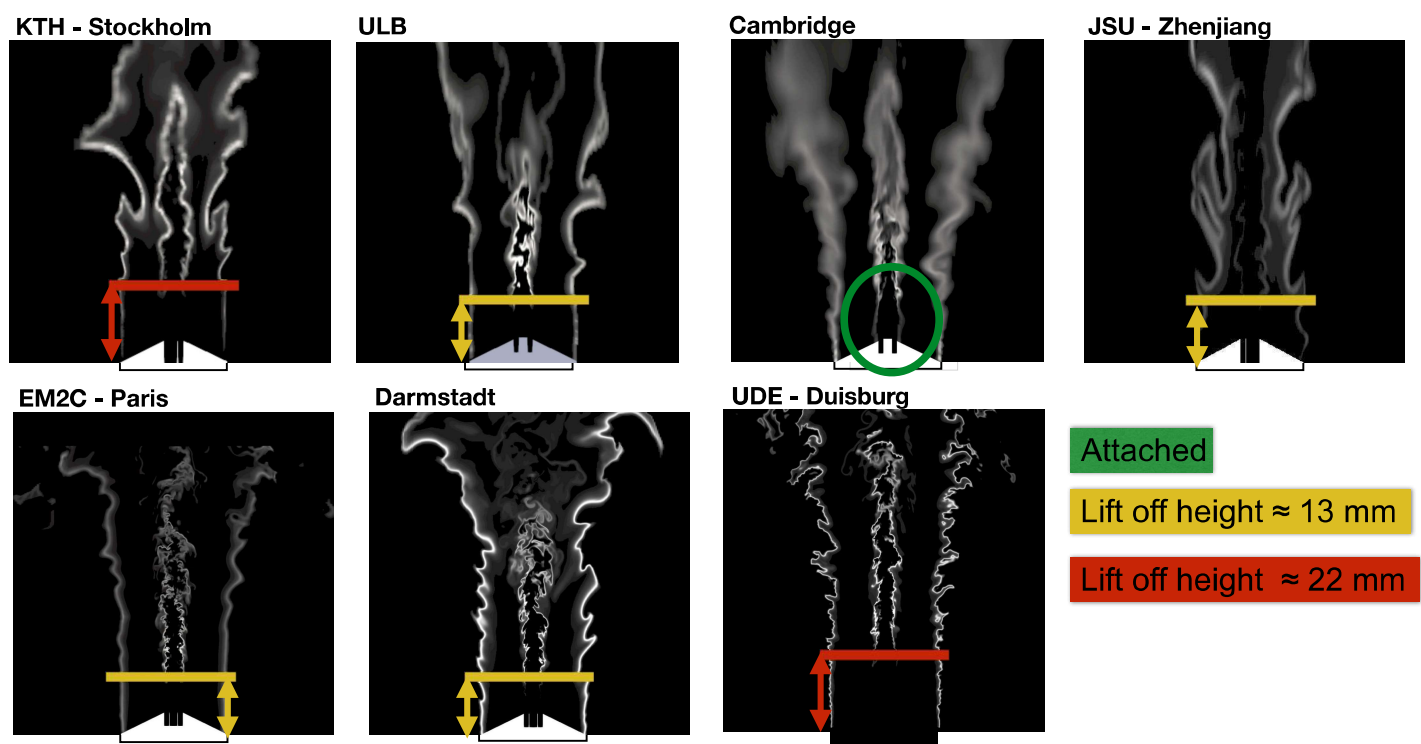


Flame resolution

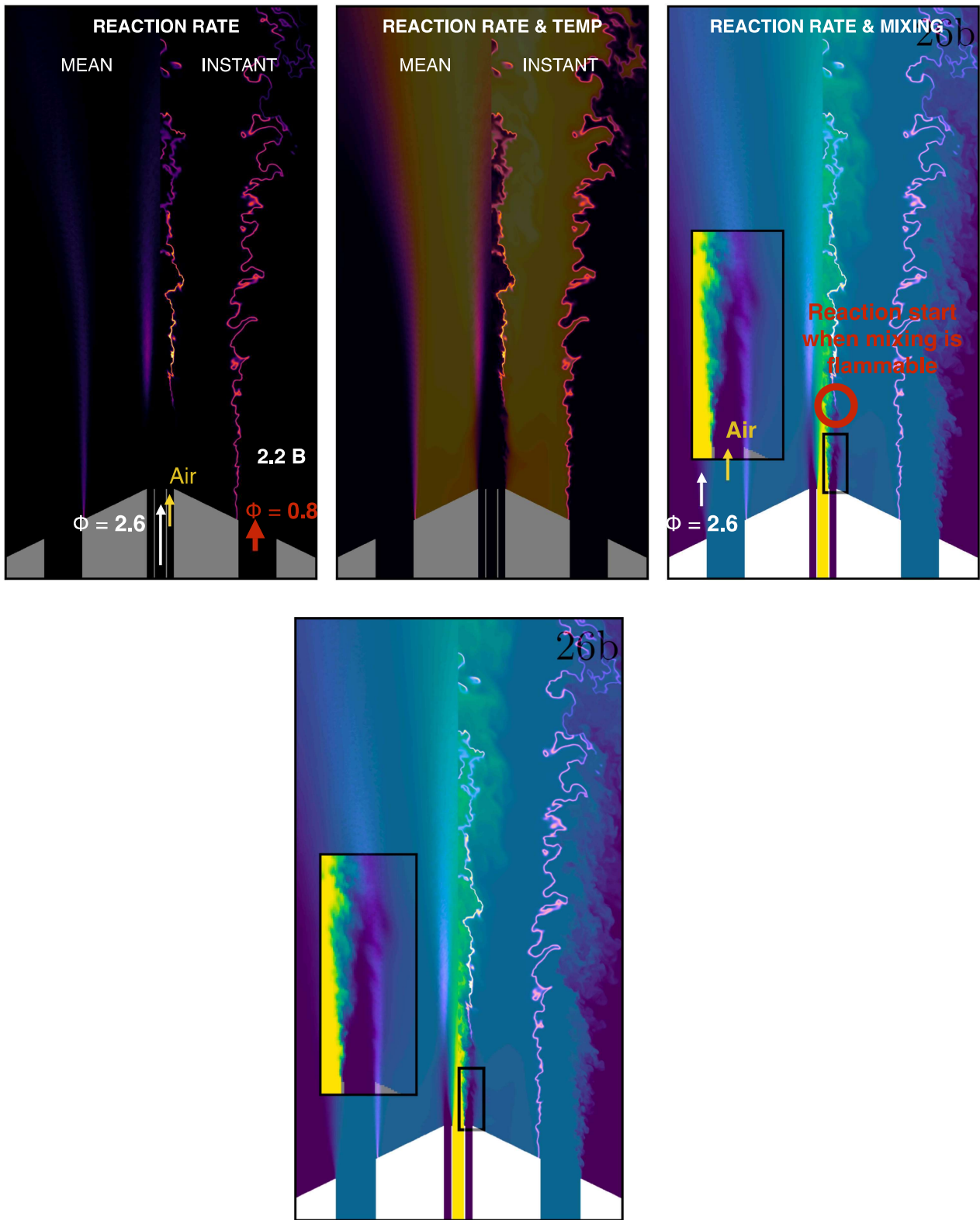
Normalized heat release rate - 26b

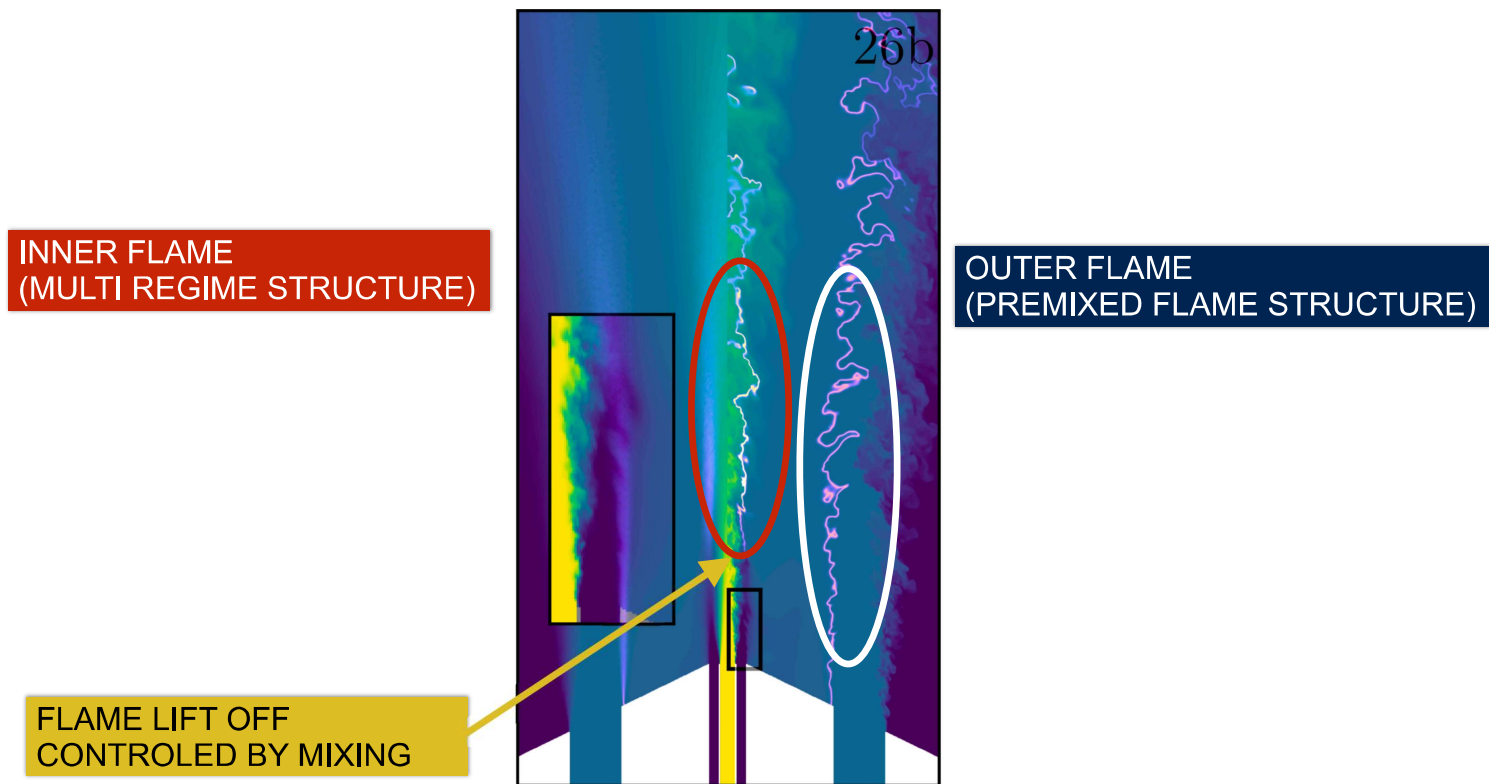


Normalized heat release rate - 26b



Lift-off height given by mixing between main inlet with slot 1





D. Butz, S. Hartl, S. Popp, S. Walther, R.S. Barlow, C. Hasse, A. Dreizler, D. Geyer, Combust. Flame 210 (2019) 426–438

Mean and RMS radial profiles

REACTIVE CASE 26b

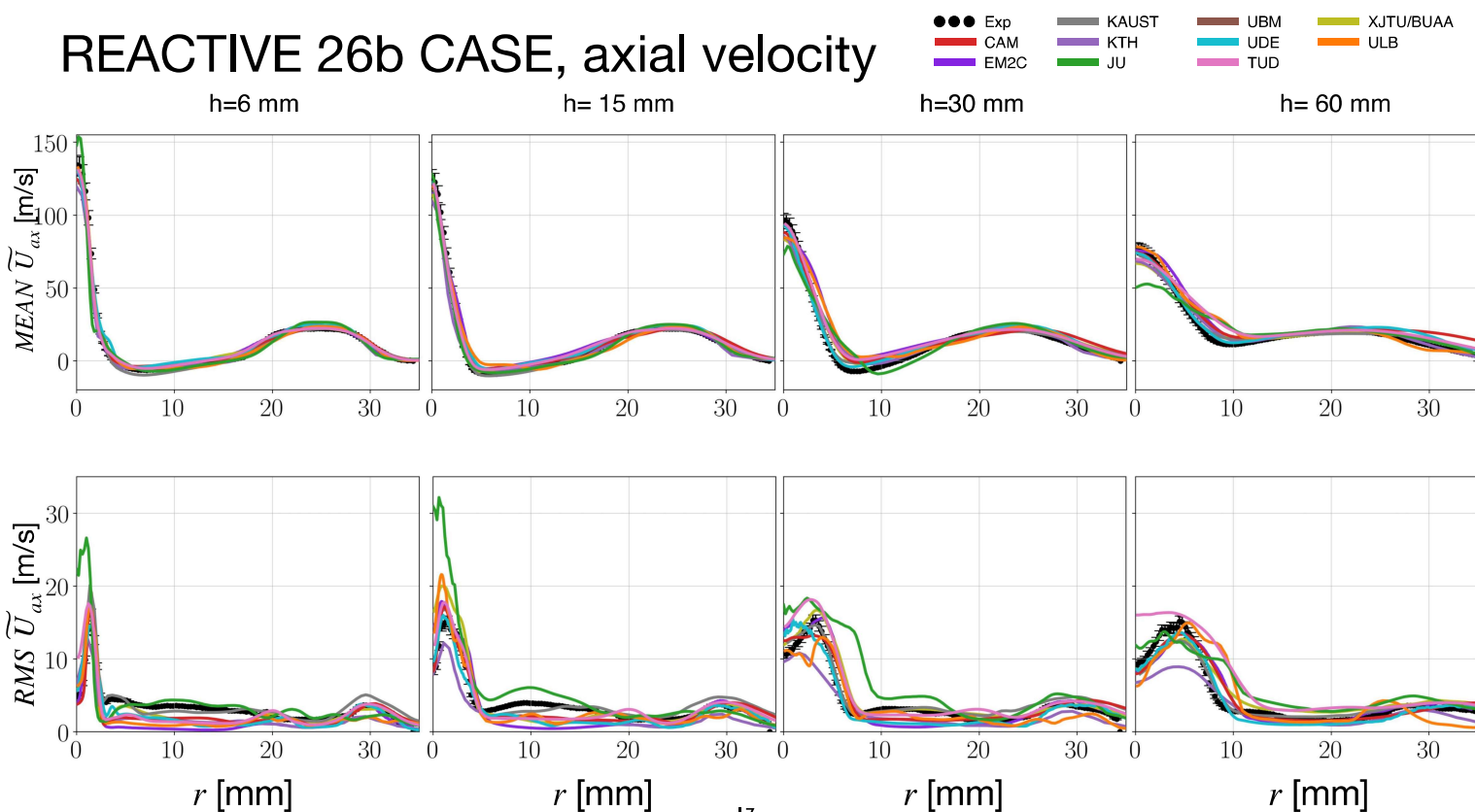
REACTIVE 26b CASE, axial velocity

h=6 mm

h= 15 mm

h=30 mm

h= 60 mm



17

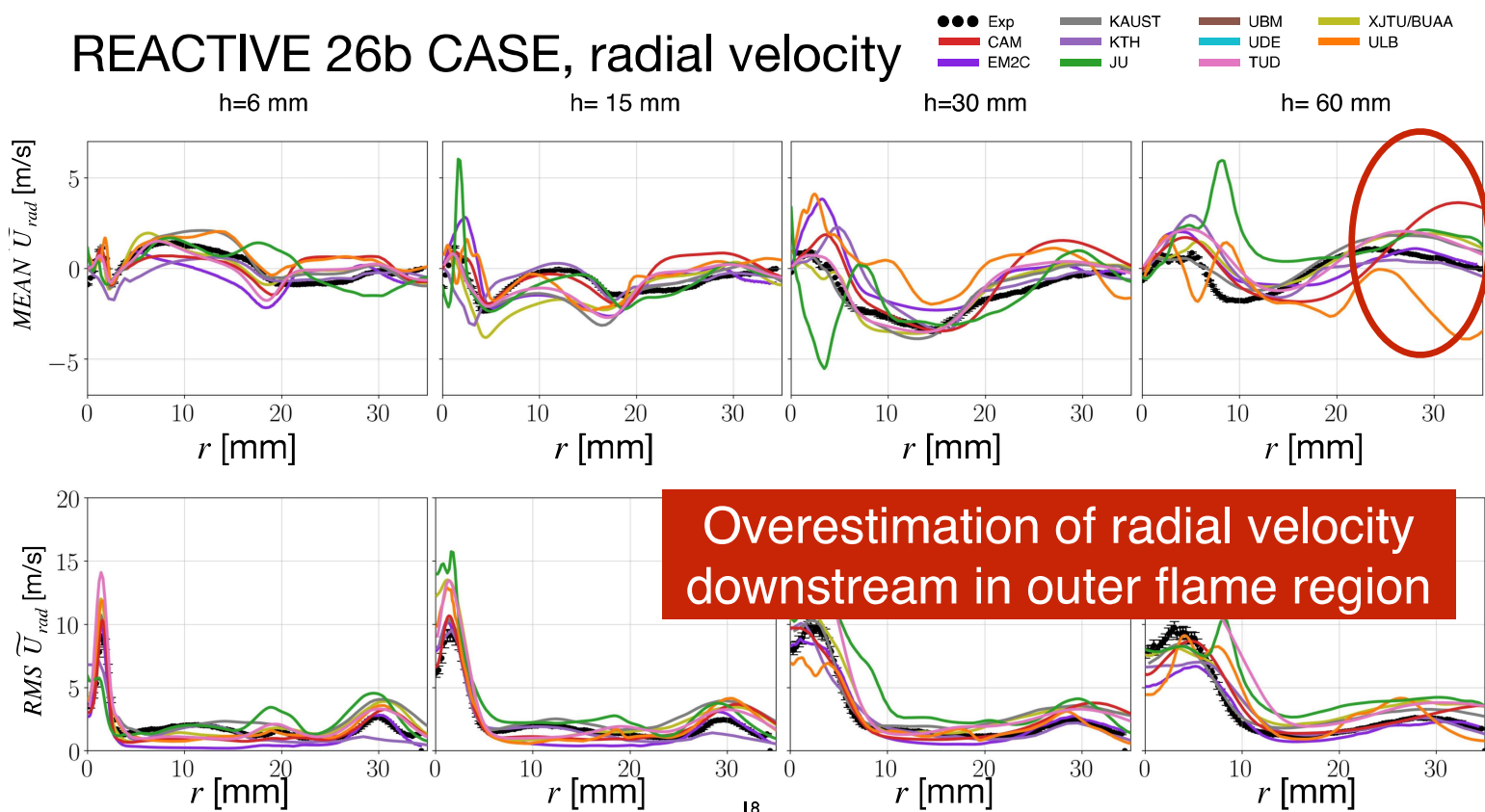
REACTIVE 26b CASE, radial velocity

h=6 mm

h= 15 mm

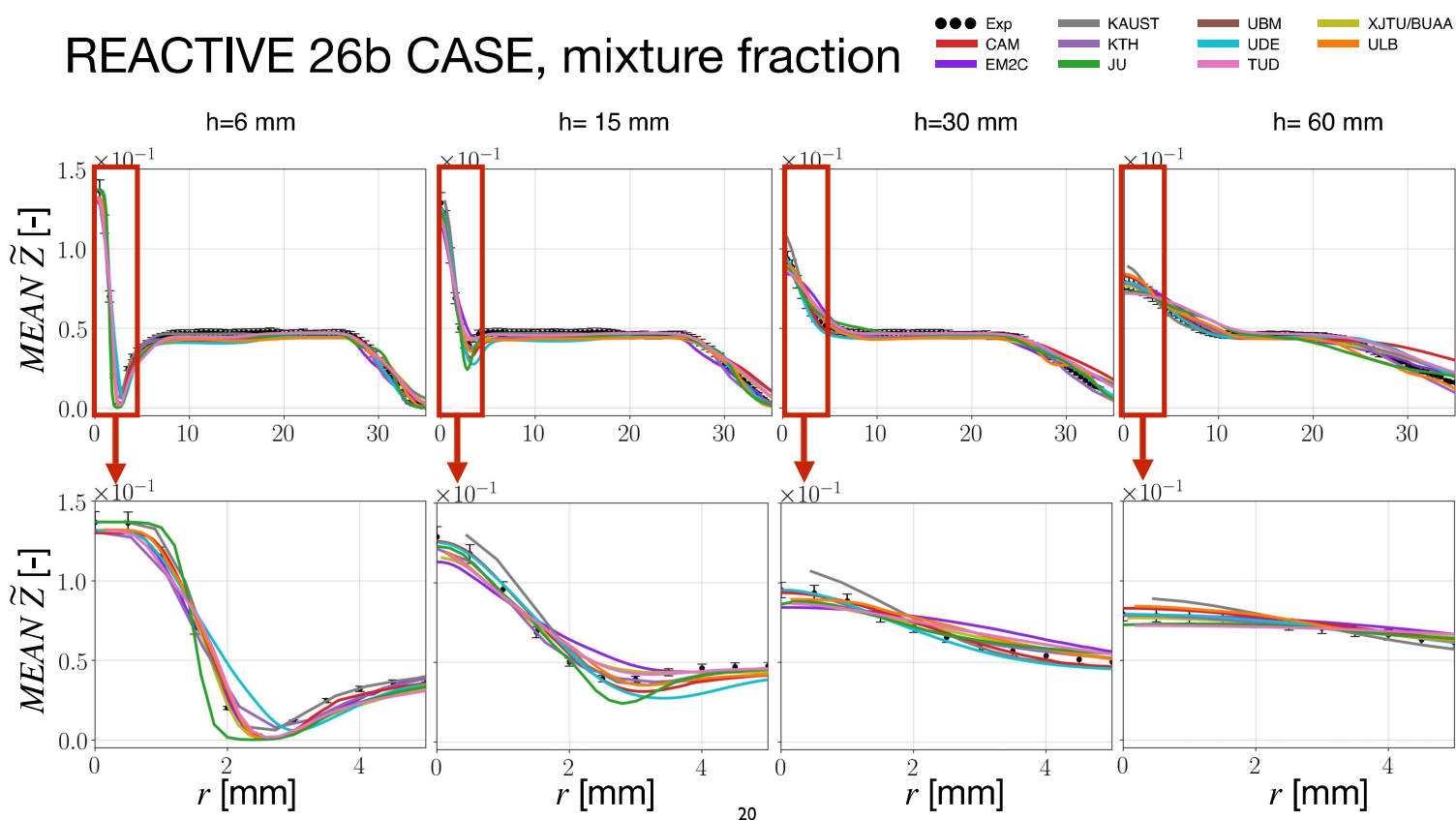
h=30 mm

h= 60 mm

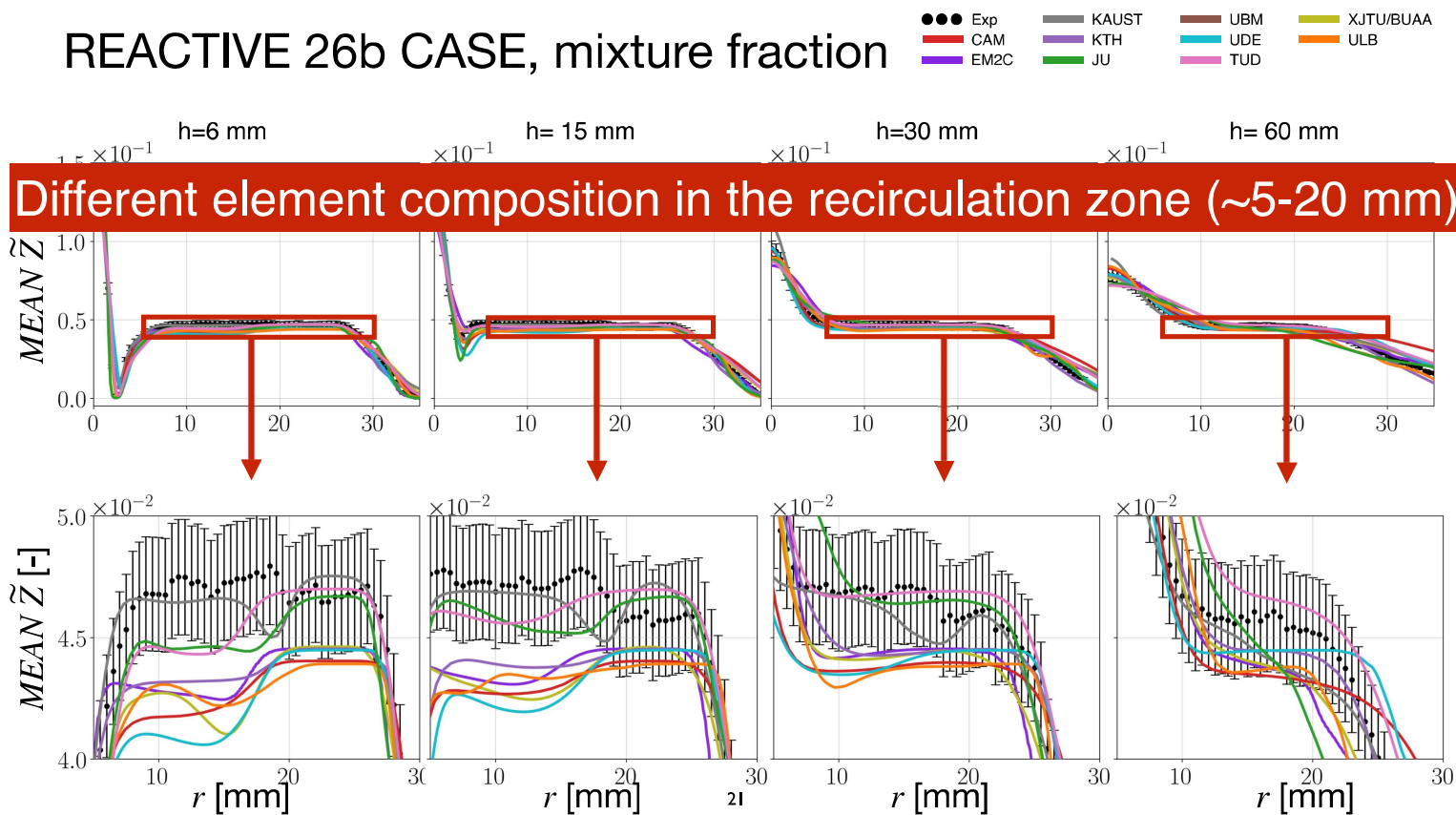


18

REACTIVE 26b CASE, mixture fraction



REACTIVE 26b CASE, mixture fraction



REACTIVE 26b CASE, mixture fraction

●●● Exp — KAUST — UBM — XJTU/BUAA
 — CAM — KTH — UDE — ULB
 — EM2C — JU — TUD

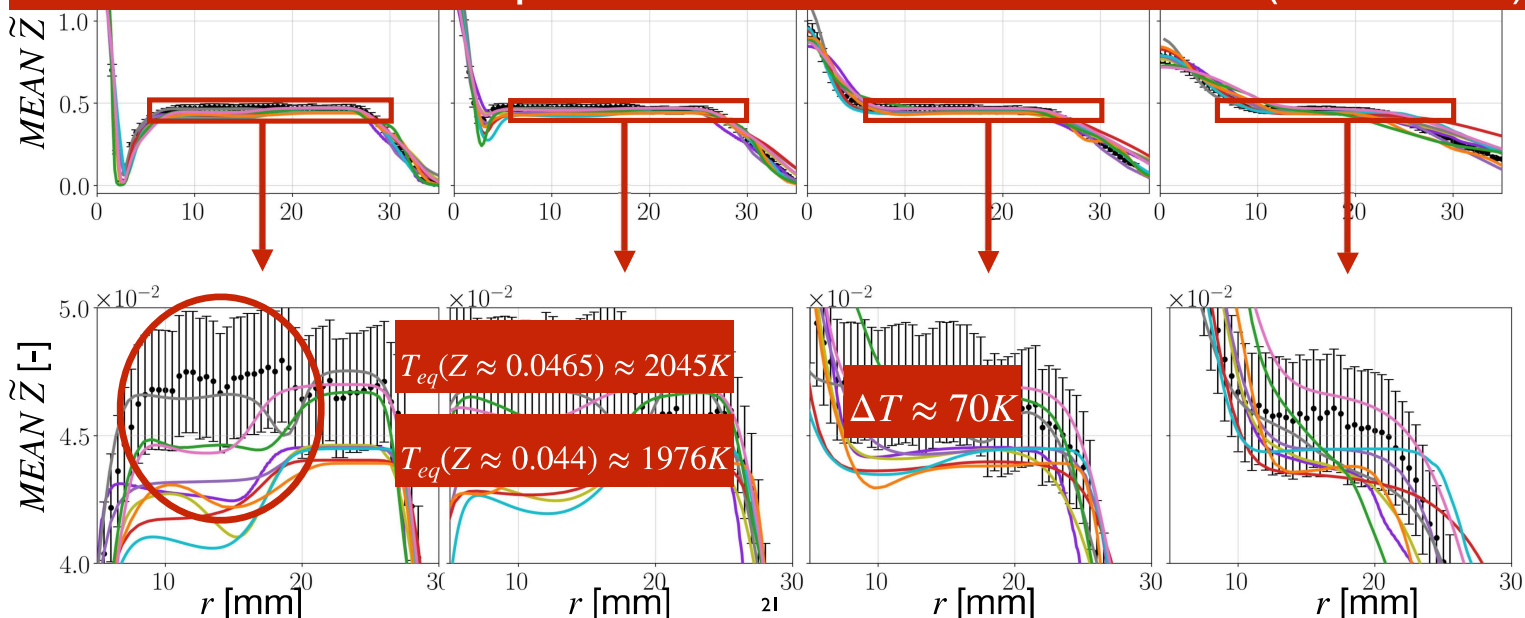
h=6 mm

h= 15 mm

h=30 mm

h= 60 mm

Different element composition in the recirculation zone (~5-20 mm)



REACTIVE 26b CASE, temperature

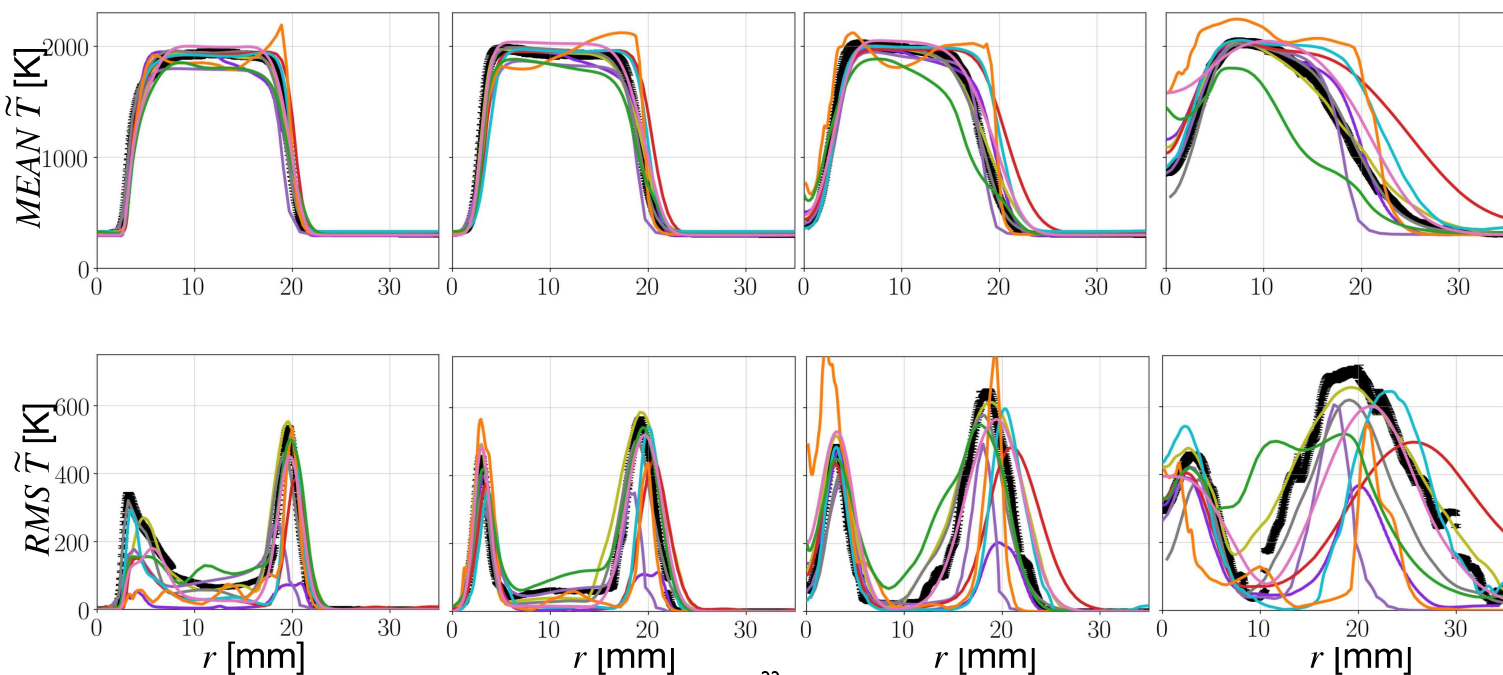
●●● Exp — KAUST — UBM — XJTU/BUAA
 — CAM — KTH — UDE — ULB
 — EM2C — JU — TUD

h=6 mm

h= 15 mm

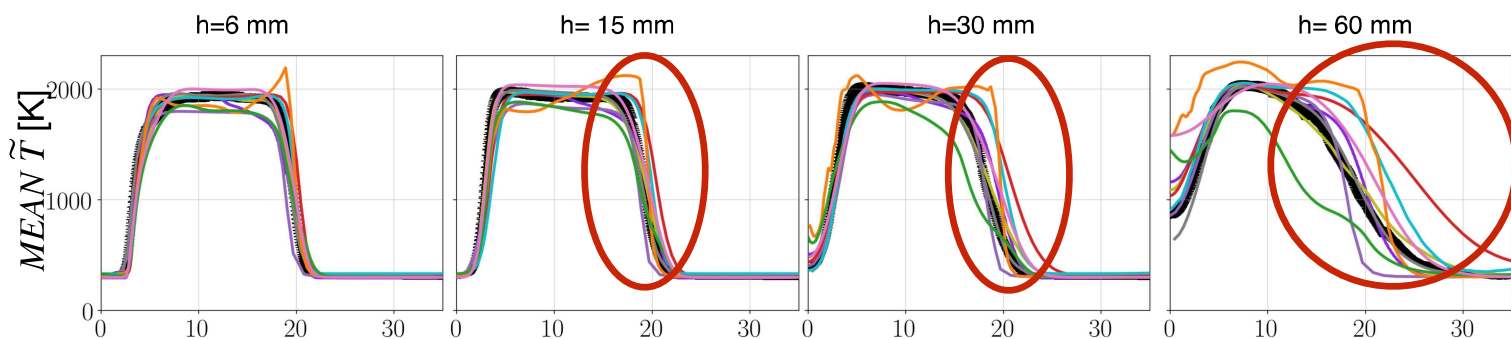
h=30 mm

h= 60 mm

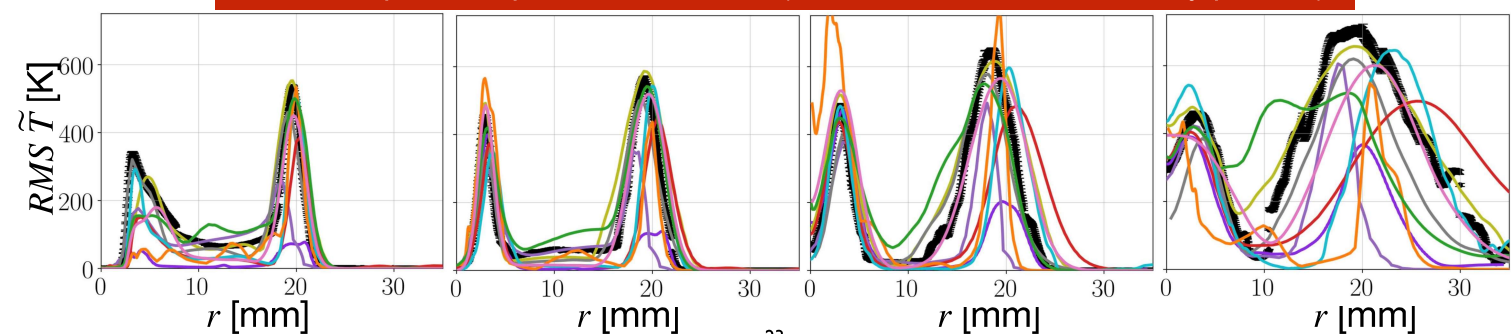


REACTIVE 26b CASE, temperature

●●● Exp KAUST UBM XJTU/BUAA
 CAM KTH UDE ULB
 EM2C JU TUD



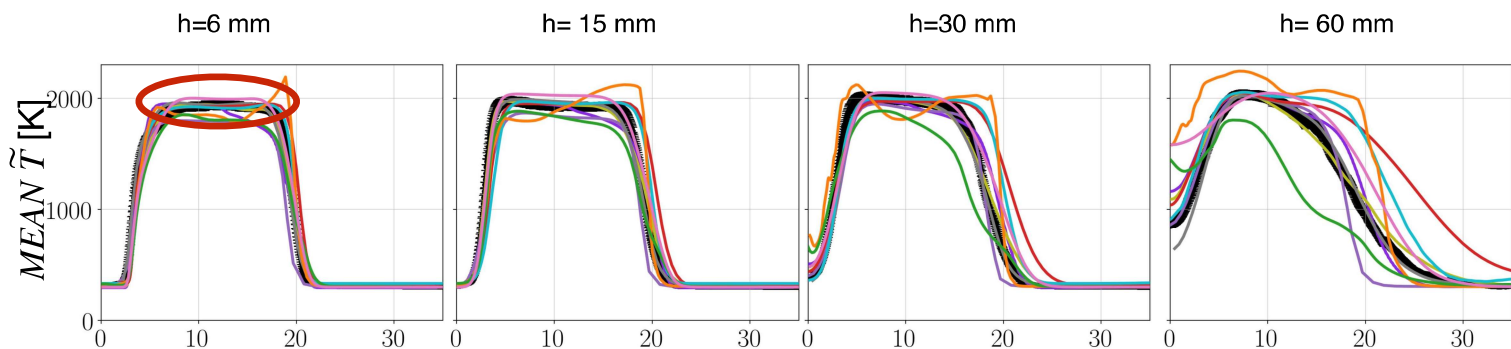
Some temperature profiles are shifted (consistent with radial velocity profiles)



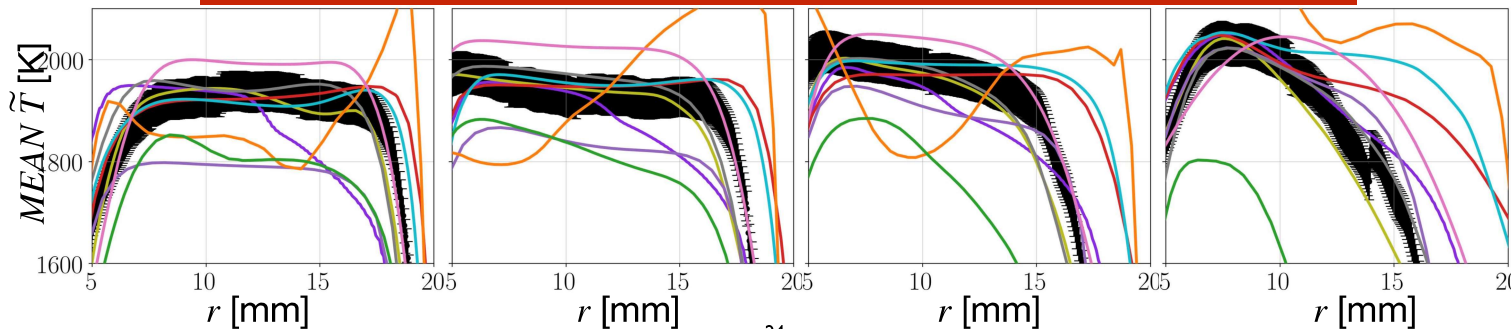
23

REACTIVE 26b CASE, temperature

●●● Exp KAUST UBM XJTU/BUAA
 CAM KTH UDE ULB
 EM2C JU TUD



Discrepancies of temperature profiles in the recirculation zone $\Delta T \approx 200K$



24

REACTIVE 26b CASE, CO mass fraction

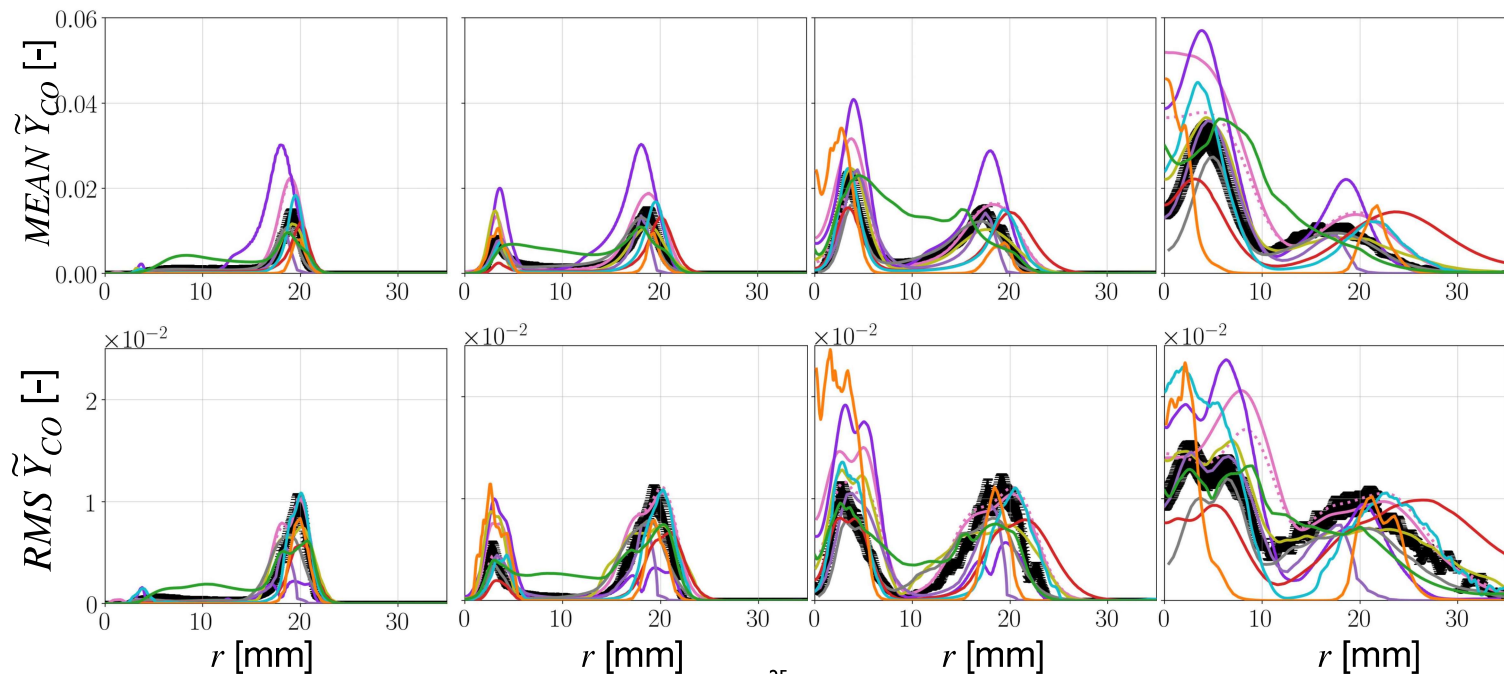
●●● Exp — KAUST — UBM — XJTU/BUAA
 — CAM — KTH — UDE — ULB
 — EM2C — JU — TUD ···· TUD-transCO

h=6 mm

h= 15 mm

h=30 mm

h= 60 mm



25

REACTIVE 26b CASE, CO mass fraction

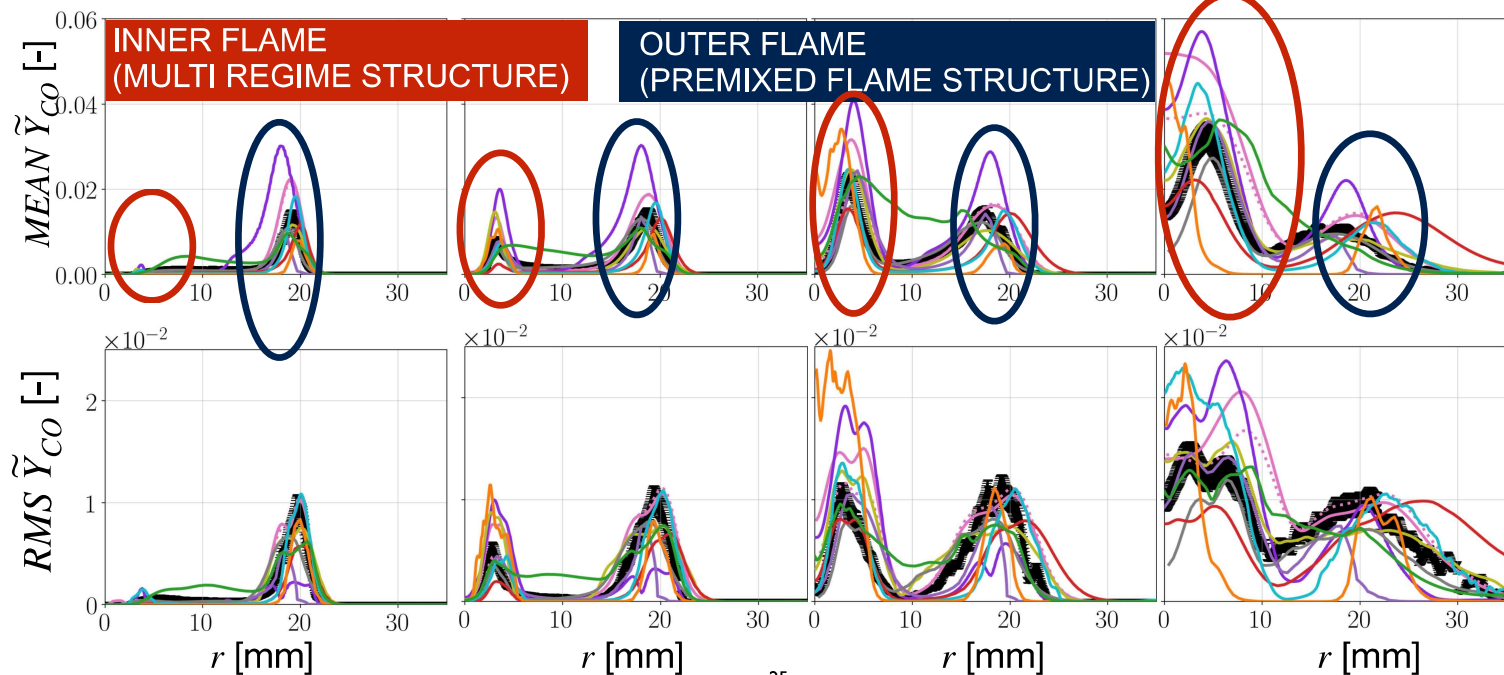
●●● Exp — KAUST — UBM — XJTU/BUAA
 — CAM — KTH — UDE — ULB
 — EM2C — JU — TUD ···· TUD-transCO

h=6 mm

h= 15 mm

h=30 mm

h= 60 mm

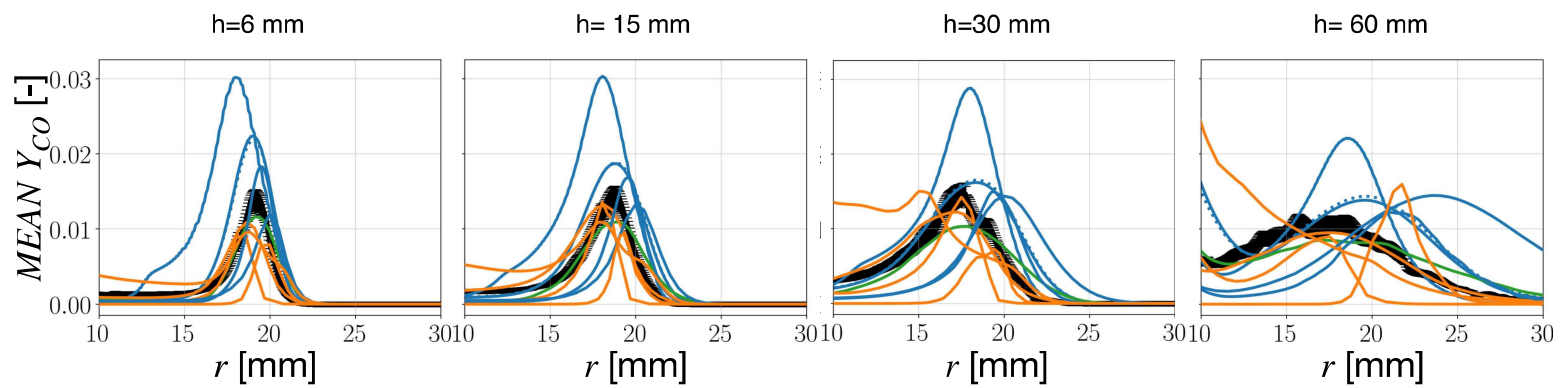


25

OUTER FLAME (PREMIXED FLAME STRUCTURE)

26

Case 26B, mean CO mass fraction



Sorted by chemistry modeling

●●● EXP

— Premixed flamelets

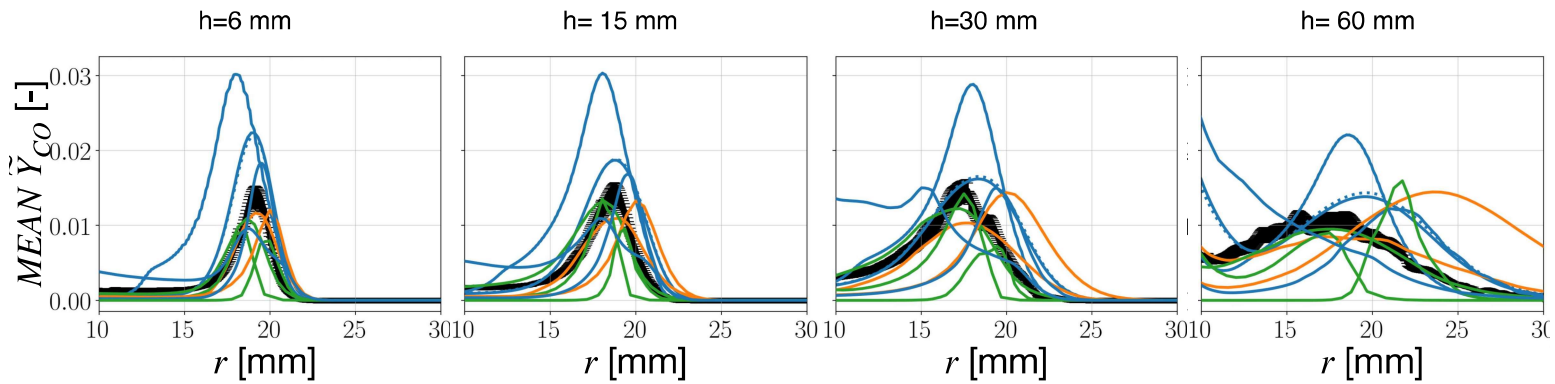
— Non-premixed flamelets

— Reduced chemistry

Surprising !
Premixed flamelet tabulation should work !

27

Case 26B, mean CO mass fraction

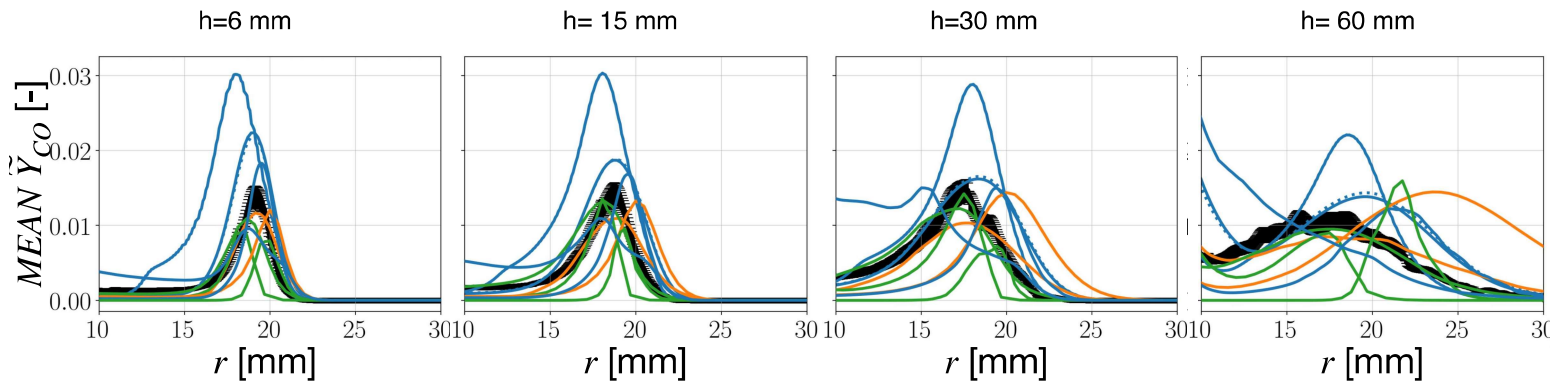


Sorted by turbulent combustion model



28

Case 26B, mean CO mass fraction



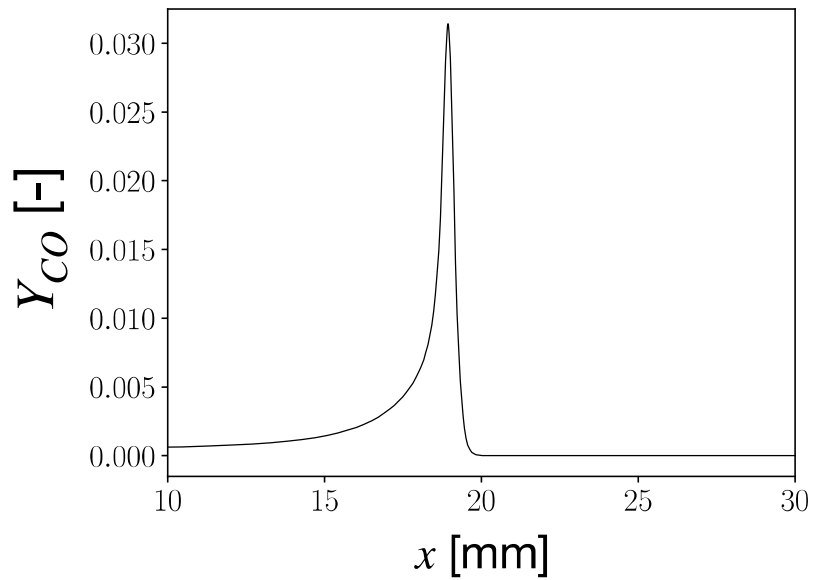
Sorted by turbulent combustion model



28

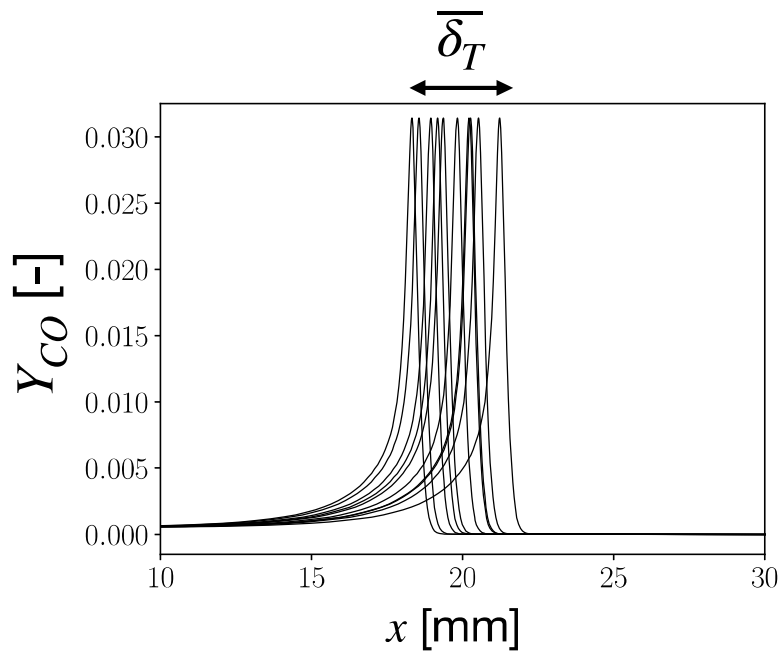
How artificial flame thickening biases the mean turbulent flame structure ?

CO profile from 1-D freely propagating laminar flame computed with detailed chemistry (GRI 3.0)

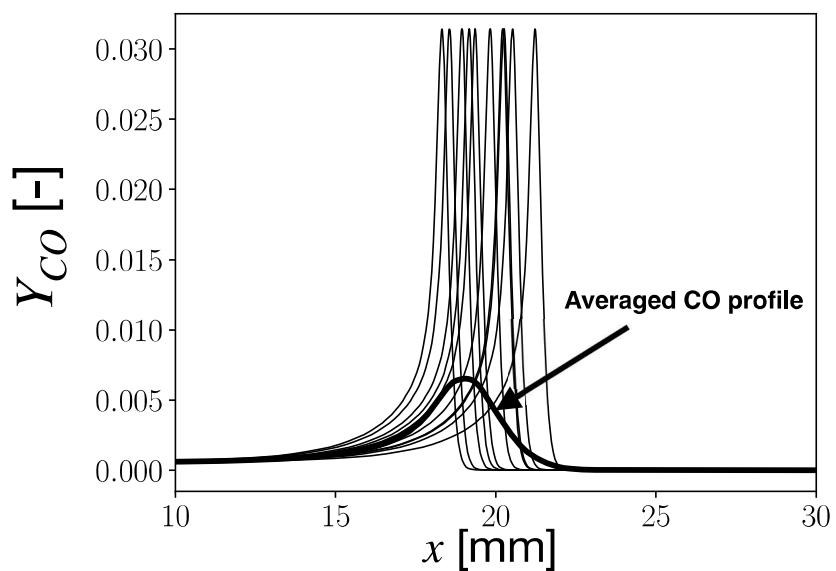


29

Generating of 5 000 randomly displaced 1-D flames to manufacture a mean « turbulent » flame brush



Averaging the ensemble of flame solution gives an estimation of the mean CO profile in the « turbulent » flame brush
(Flamelet regime - flame not wrinkled)

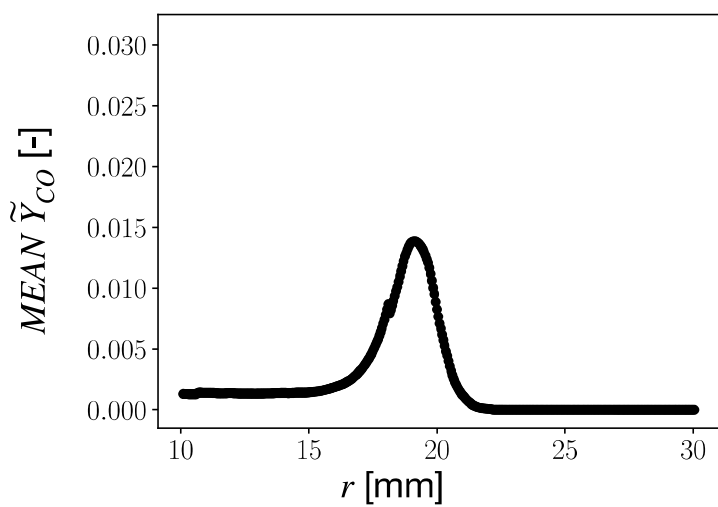


31

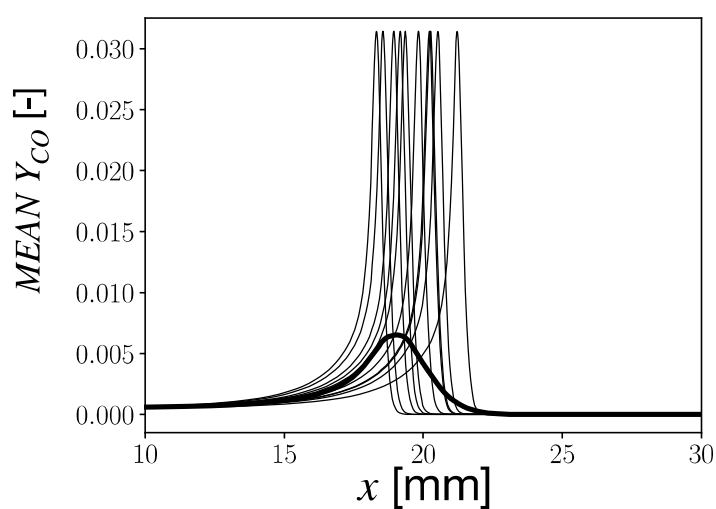
The manufactured flame brush is set to target the experimental turbulent flame brush

$$\overline{\delta_T} = x_{+,FWHM}(Y_{CO}) - x_{-,FWHM}(Y_{CO})$$

Experimental CO mean mass fraction profile



Manufactured CO mean mass fraction profile

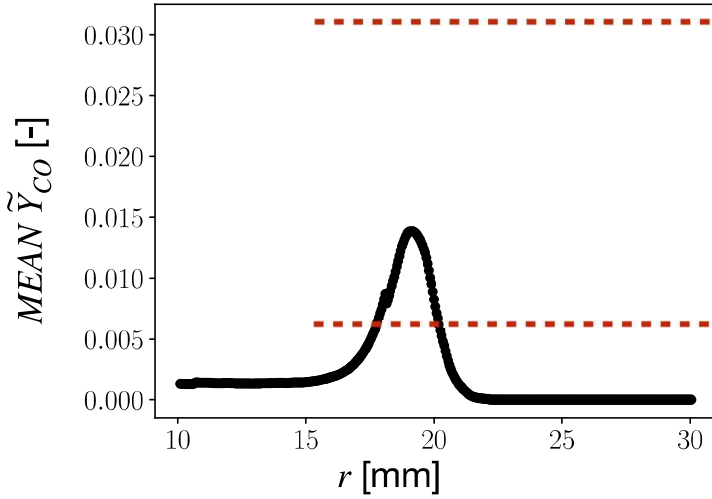


32

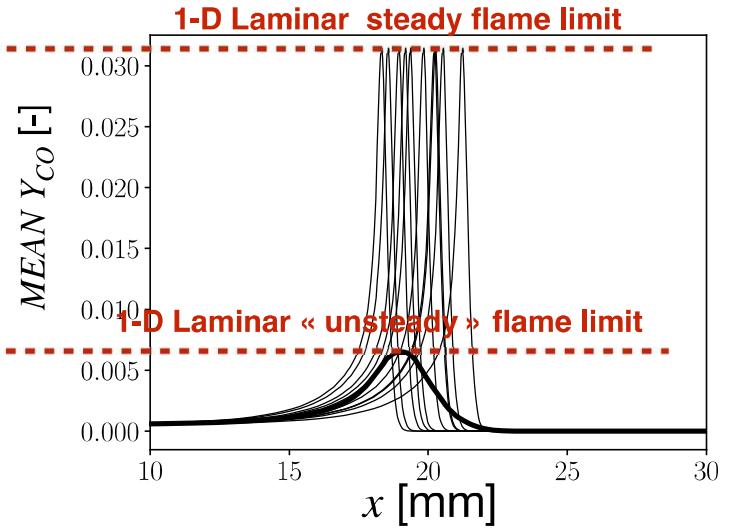
The manufactured flame brush is set to target the experimental turbulent flame brush

$$\overline{\delta_T} = x_{+,FWHM}(Y_{CO}) - x_{-,FWHM}(Y_{CO})$$

Experimental CO mean mass fraction profile



Manufactured CO mean mass fraction profile

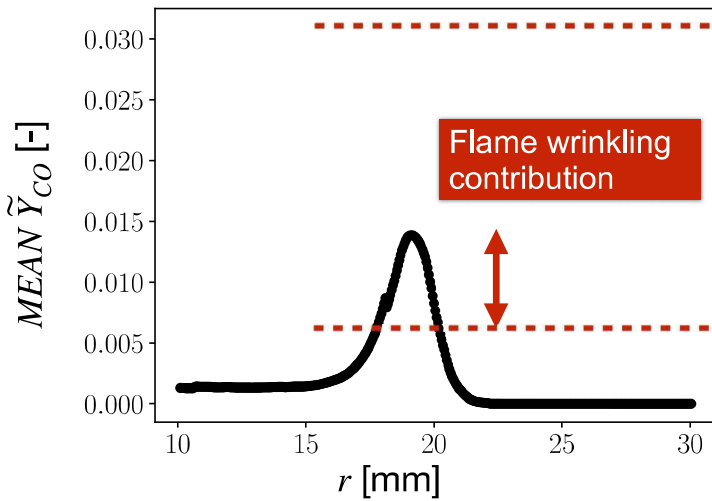


32

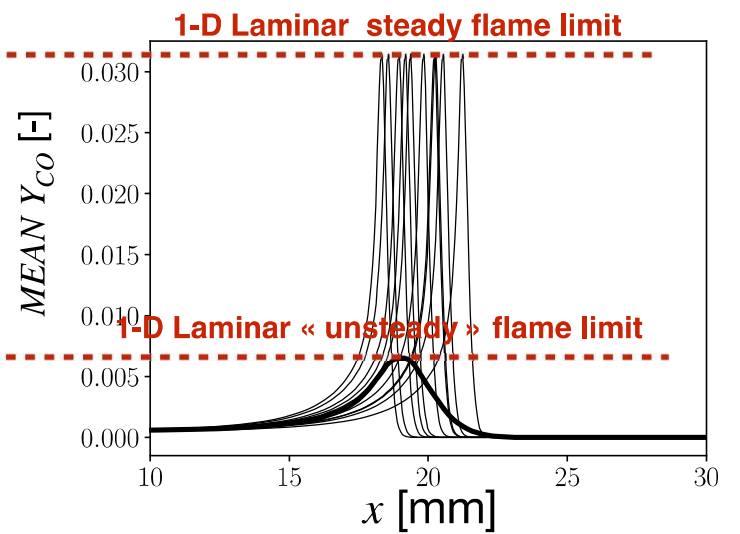
The manufactured flame brush is set to target the experimental turbulent flame brush

$$\overline{\delta_T} = x_{+,FWHM}(Y_{CO}) - x_{-,FWHM}(Y_{CO})$$

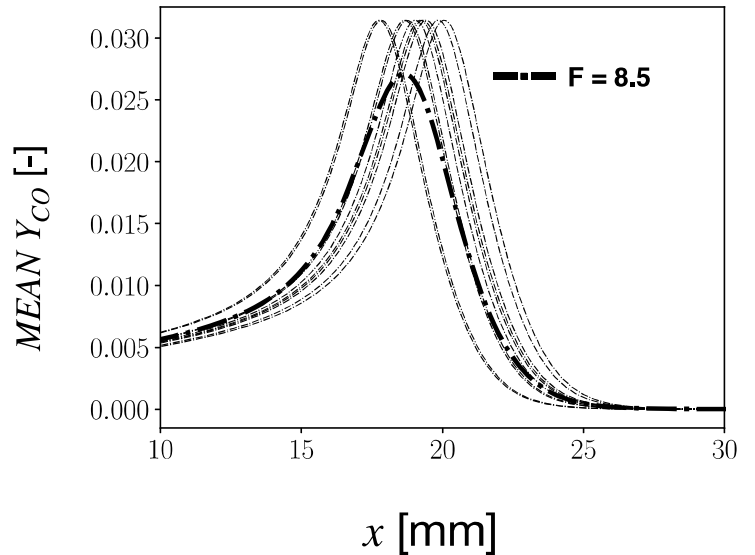
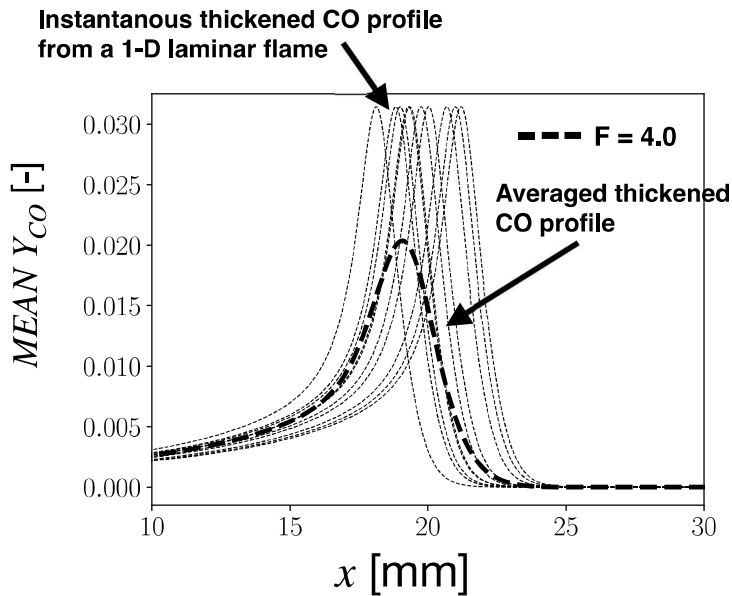
Experimental CO mean mass fraction profile



Manufactured CO mean mass fraction profile



Same exercise ... but for thickened flames



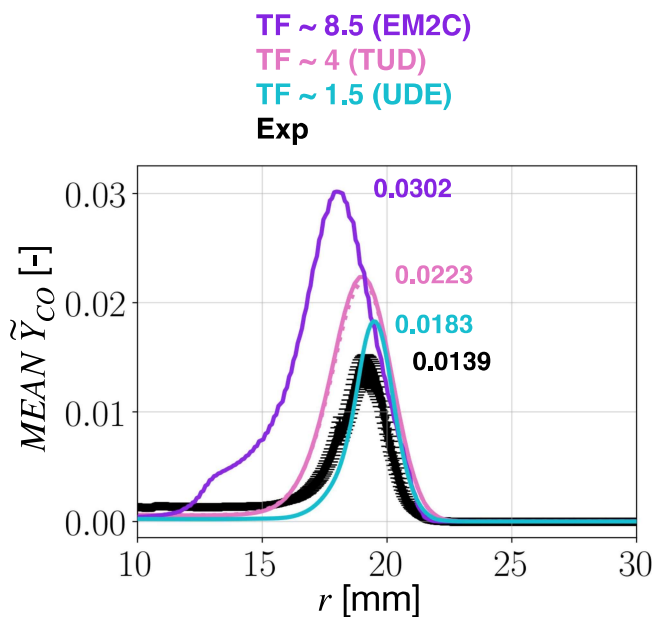
The total mass of the species is overestimated by a factor F

P. Gruhlke, E. Inanc, R. Mercier, B. Fiorina, A. M. Kempf. A Simple Post-Processing Method to Correct Species Predictions in Artificially Thickened Turbulent Flames. Proceedings of the Combustion Institute, (2021)

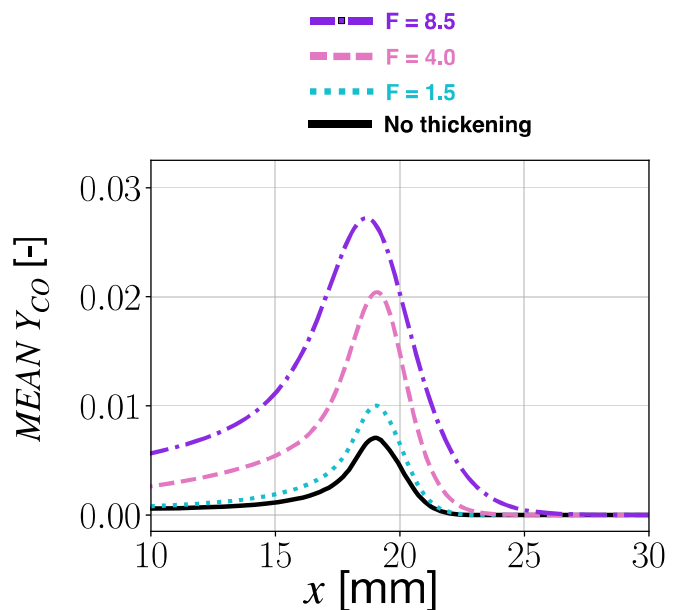
33

Outer flame region, $h = 6$ mm

Mean CO mean mass fraction profile from MRB



Manufactured CO mean mass fraction profile (Planar unsteady flame front assumption)

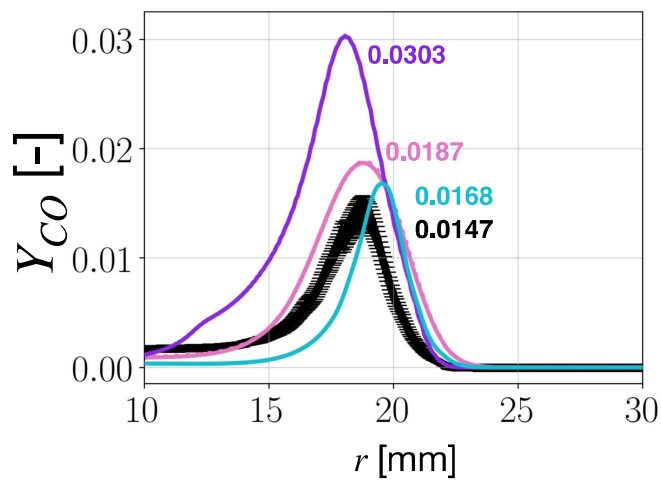


34

Outer flame region, $h = 15$ mm

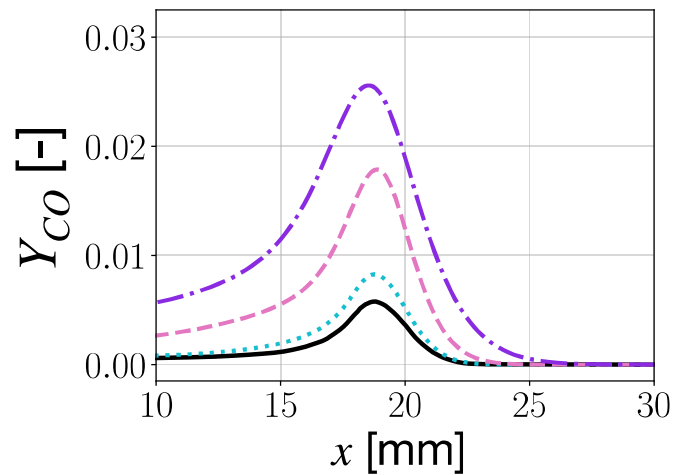
Mean CO mean mass fraction profile from MRB

TF ~ 8.5 (EM2C)
 TF ~ 4 (TUD)
 TF ~ 1.5 (UDE)
 Exp



Manufactured CO mean mass fraction profile (Planar unsteady flame front assumption)

F = 8.5
 F = 4.0
 F = 1.5
 No thickening

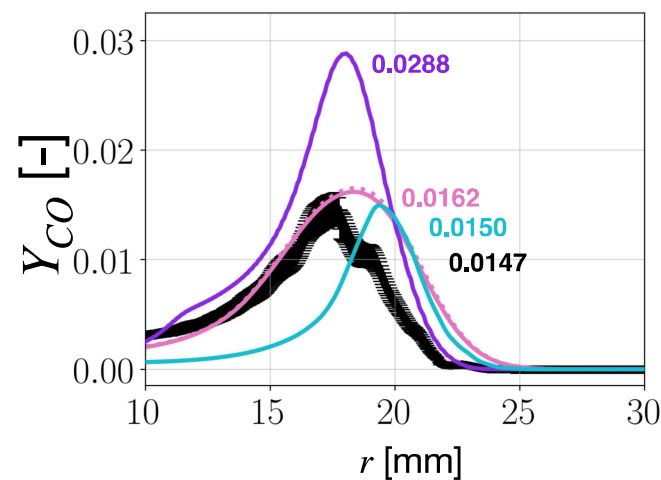


35

Outer flame region, $h = 30$ mm

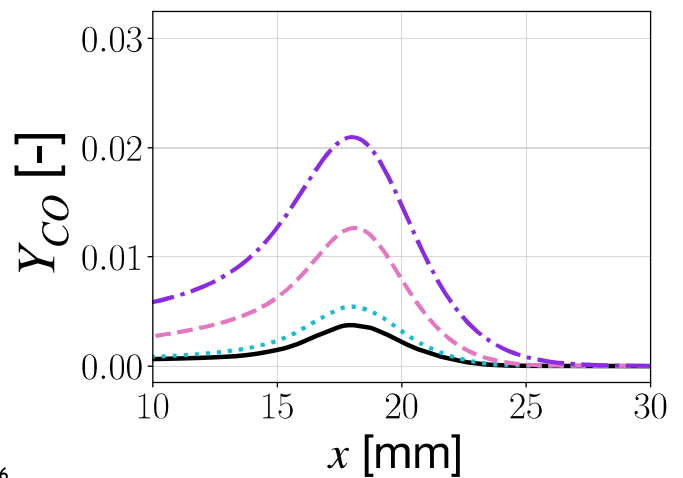
Mean CO mean mass fraction profile from MRB

TF ~ 8.5 (EM2C)
 TF ~ 4 (TUD)
 TF ~ 1.5 (UDE)
 Exp



Manufactured CO mean mass fraction profile (Planar unsteady flame front assumption)

F = 8.5
 F = 4.0
 F = 1.5
 No thickening

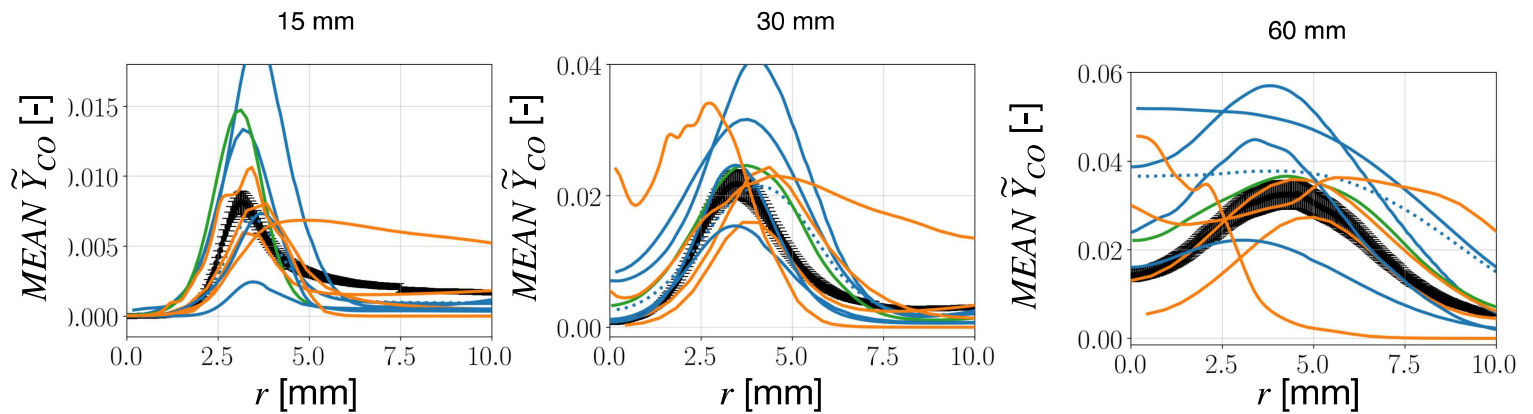


36

INNER FLAME
(MULTI REGIME STRUCTURE)

37

REACTIVE 26b CASE, CO mass fraction



Sorted by chemistry modeling

●●● EXP

— Premixed flamelets

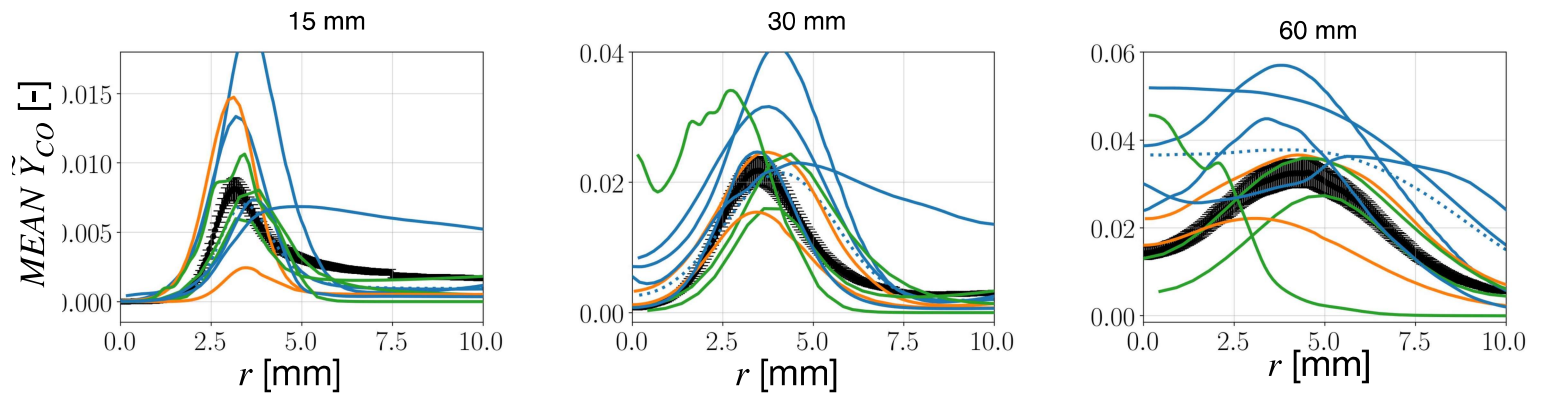
●●● Premixed flamelets + transported CO

— Non-premixed flamelets

— Reduced chemistry

38

REACTIVE 26b CASE, CO mass fraction

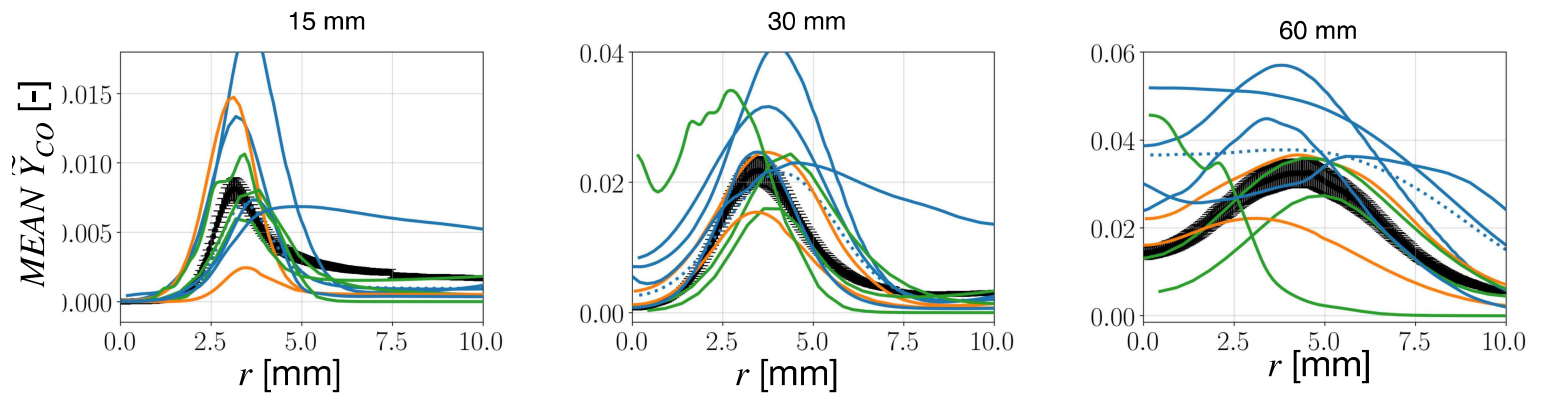


Sorted by turbulent combustion model



39

REACTIVE 26b CASE, CO mass fraction



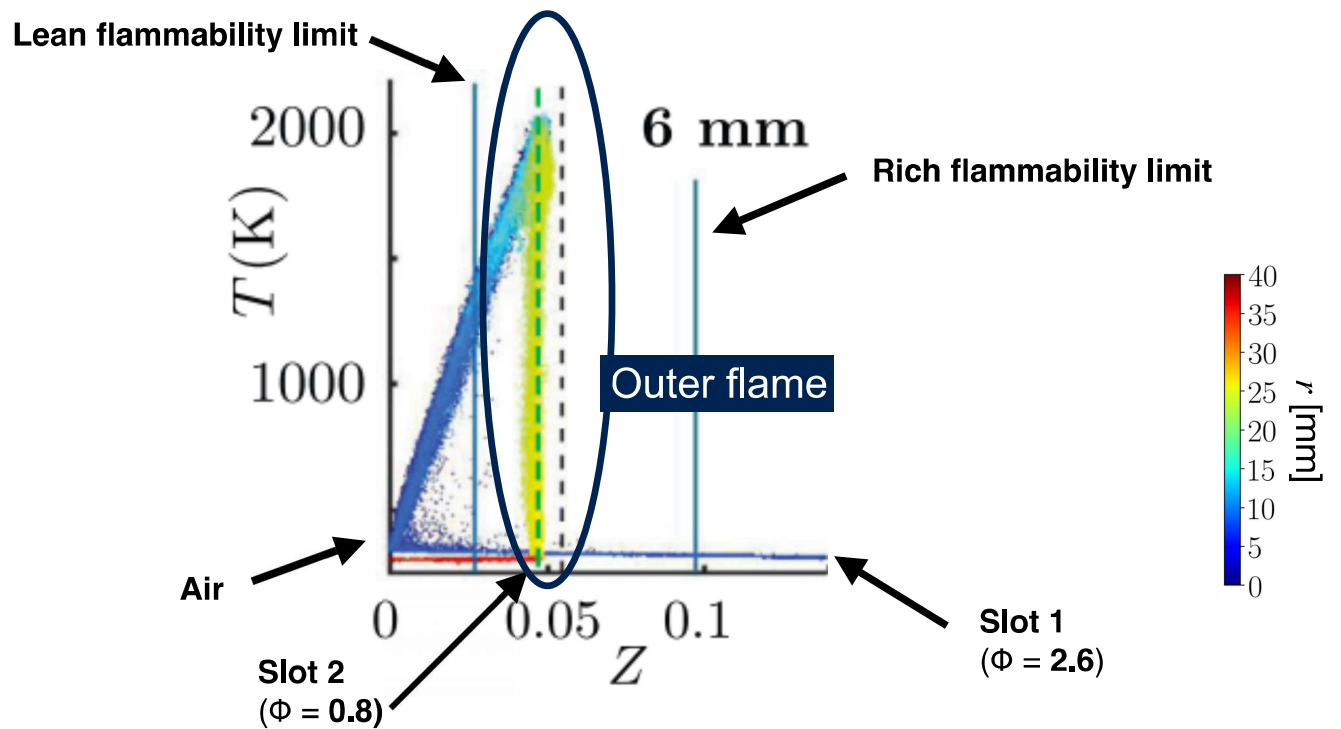
Overestimation of CO mass fraction due to:

- Simplified chemistry assumptions (for FPI/FGM)
- Artificial thickening
- Inaccurate modeling of SGS flame wrinkling on CO chemical rate

SCATTER PLOTS

40

Experimental scatter plot $T = f(Z)$ at $h = 6$ mm



$h = 6 \text{ mm}$

— $Z_{\text{flamLim}} = 0.027 ; 0.09$
 - - - $Z_{\text{slot2}} = 0.045$
 - - - $Z_{\text{st}} = 0.055$

$T = F(Z)$

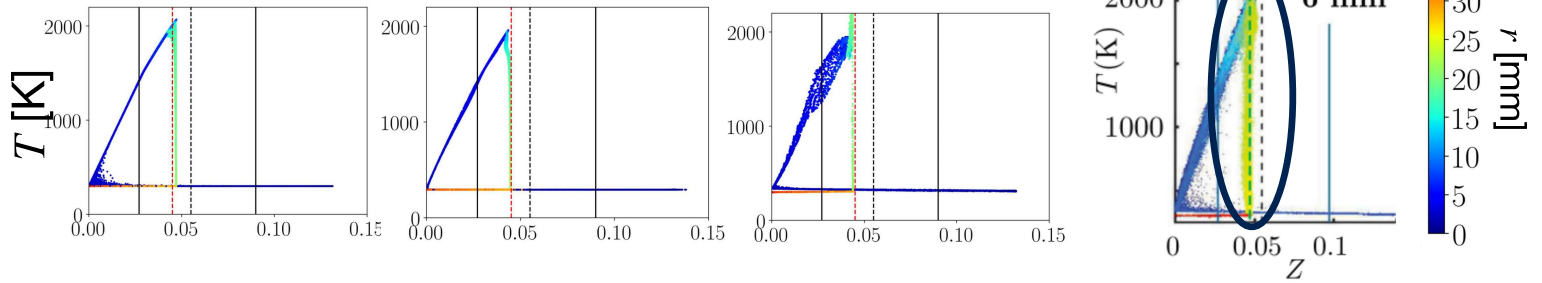
TUD

EM2C

ULB

Outer flame

EXPE
6 mm

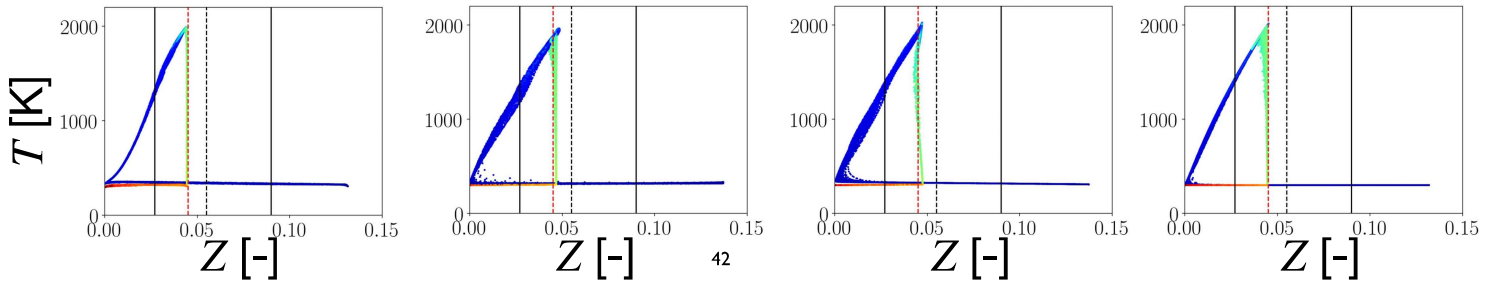


CAM

JU

KAUST

XJTU/BUAA



$h = 15 \text{ mm}$

— $Z_{\text{flamLim}} = 0.027 ; 0.09$
 - - - $Z_{\text{slot2}} = 0.045$
 - - - $Z_{\text{st}} = 0.055$

$T = F(Z)$

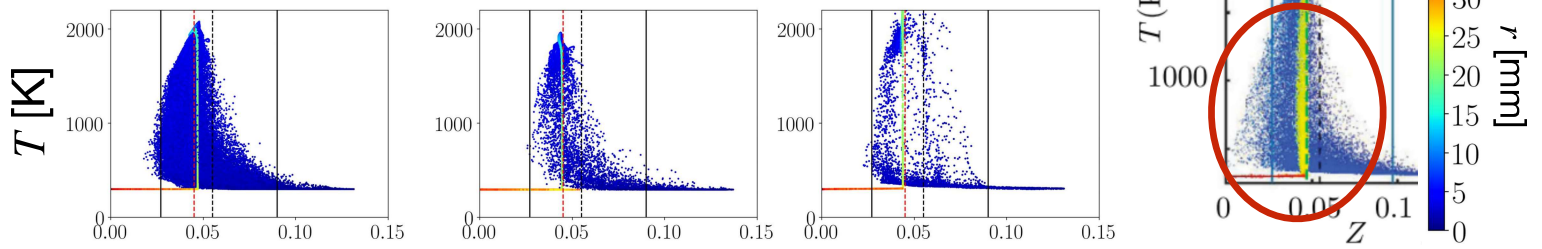
EXPE

TUD

EM2C FPI

ULB

INNER FLAME
(MULTI REGIME STRUCTURE)

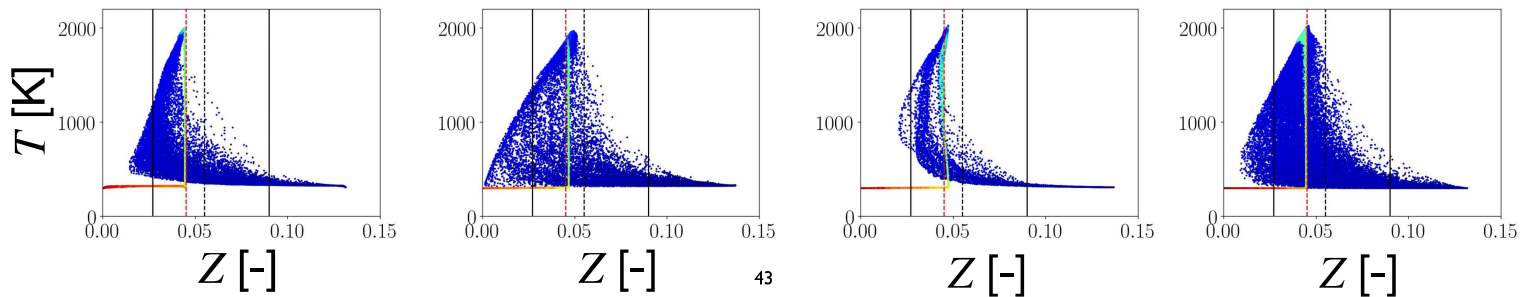


CAM

JU

KAUST

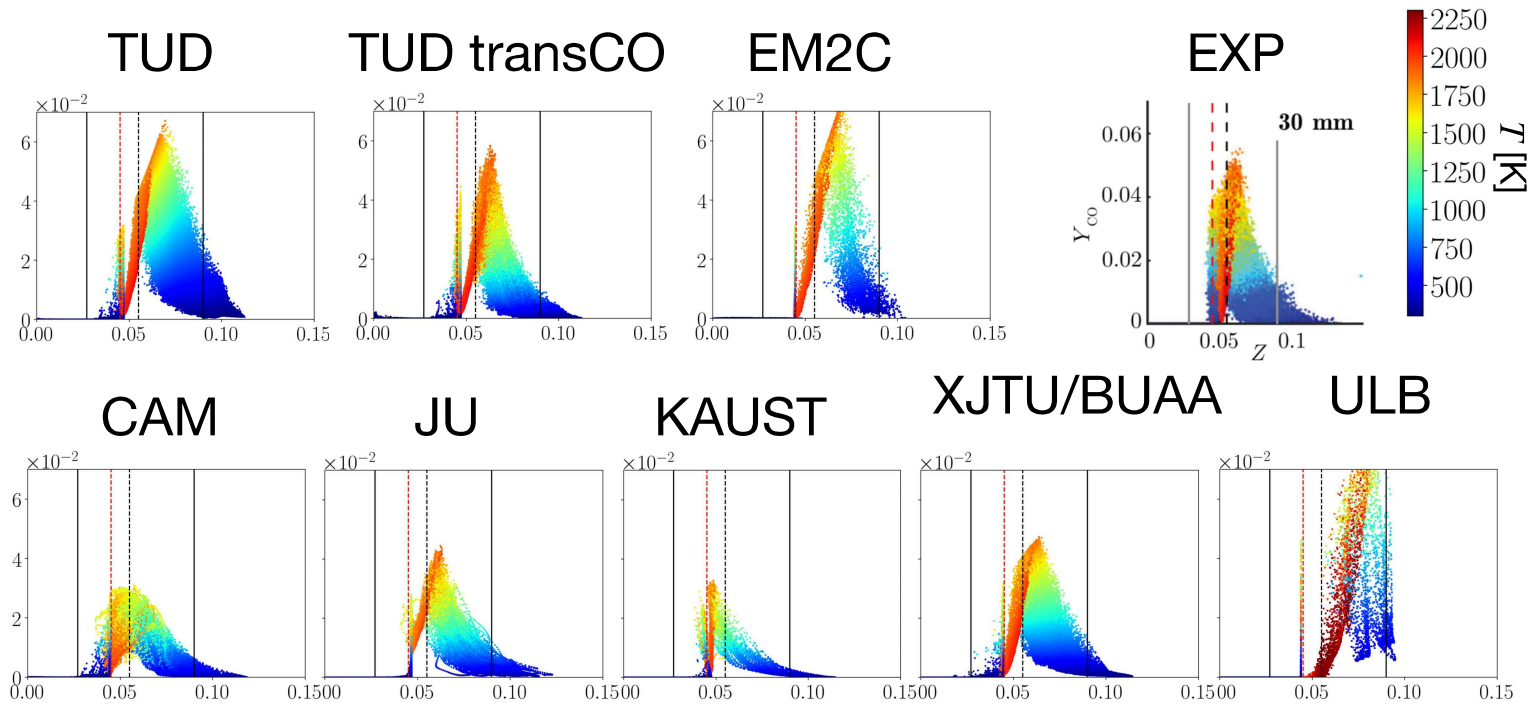
XJTU/BUAA



$h = 30 \text{ mm}$

— $Z_{\text{flamLim}} = 0.027 ; 0.09$
 - - - $Z_{\text{slot2}} = 0.045$
 - - - $Z_{\text{st}} = 0.055$

$$Y_{\text{CO}} = F(Z)$$



44

Conclusion on the MRB joined study

- Flame lift-off is predicted as soon as the mixing is well resolved
- Flow and temperature profiles are rather well captured (at least up to $h=60 \text{ mm}$)
- Flame structure in phase subspace (T, Y_c) or (Y_{CO}, Y_c) is qualitatively well reproduced
- CO mass fraction is more challenging to predict because:
 - More sensitive to the simplification of the chemistry
 - Quickly biased by artificial flame thickening
 - Also influenced by the subgrid scale flame wrinkling

45

Thank you to all contributors !

46

Other results

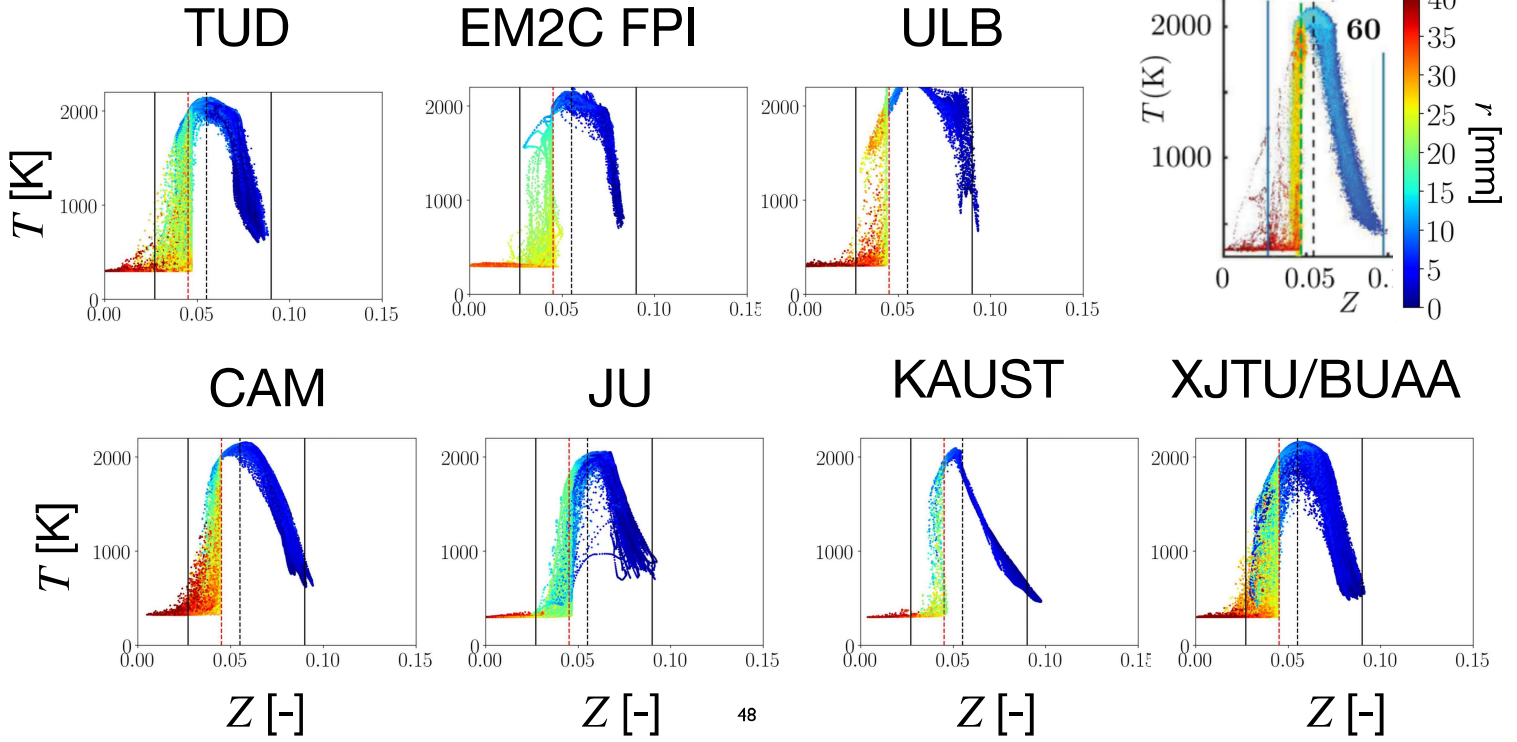
47

X/D = 60

— $Z_{\text{flamLim}} = 0.027 ; 0.09$
 - - - $Z_{\text{slot2}} = 0.045$
 - - - $Z_{\text{st}} = 0.055$

$T = F(Z)$

EXPE

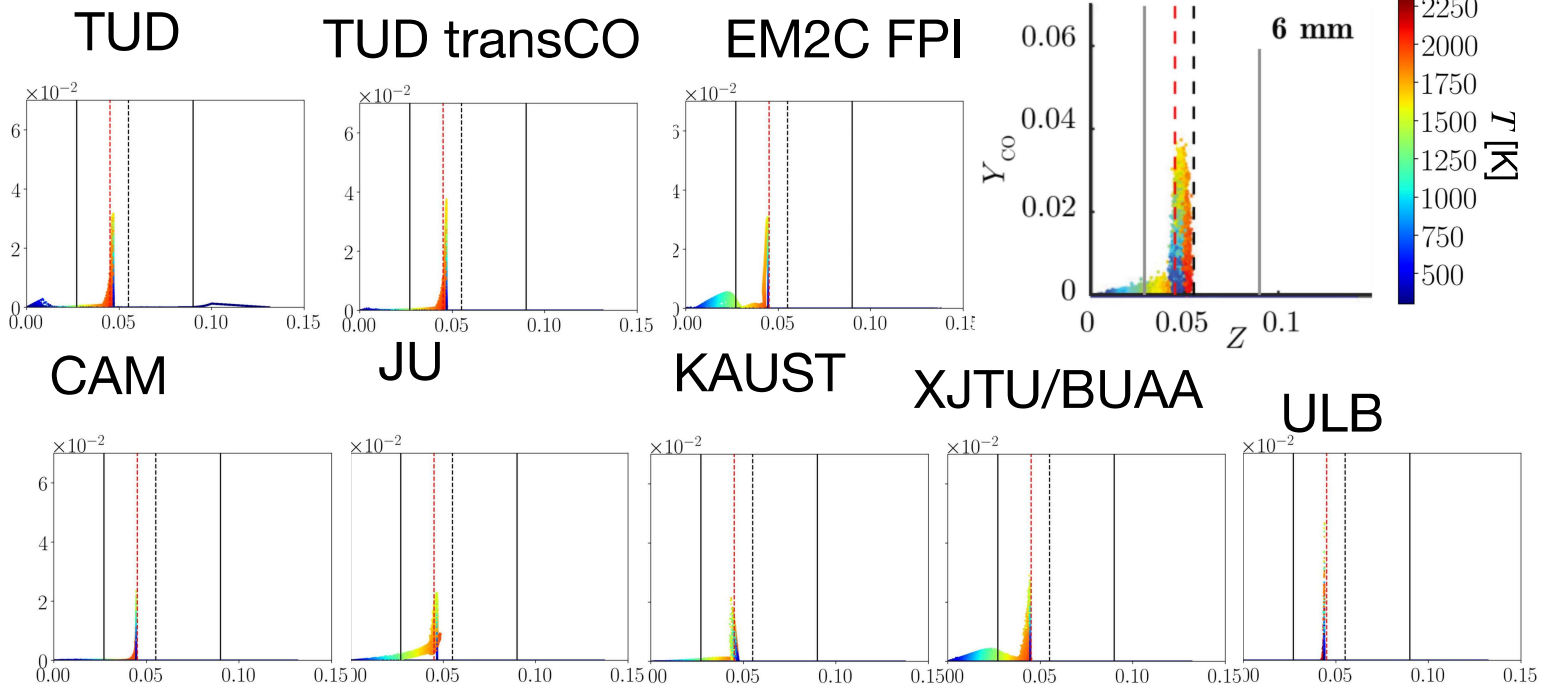


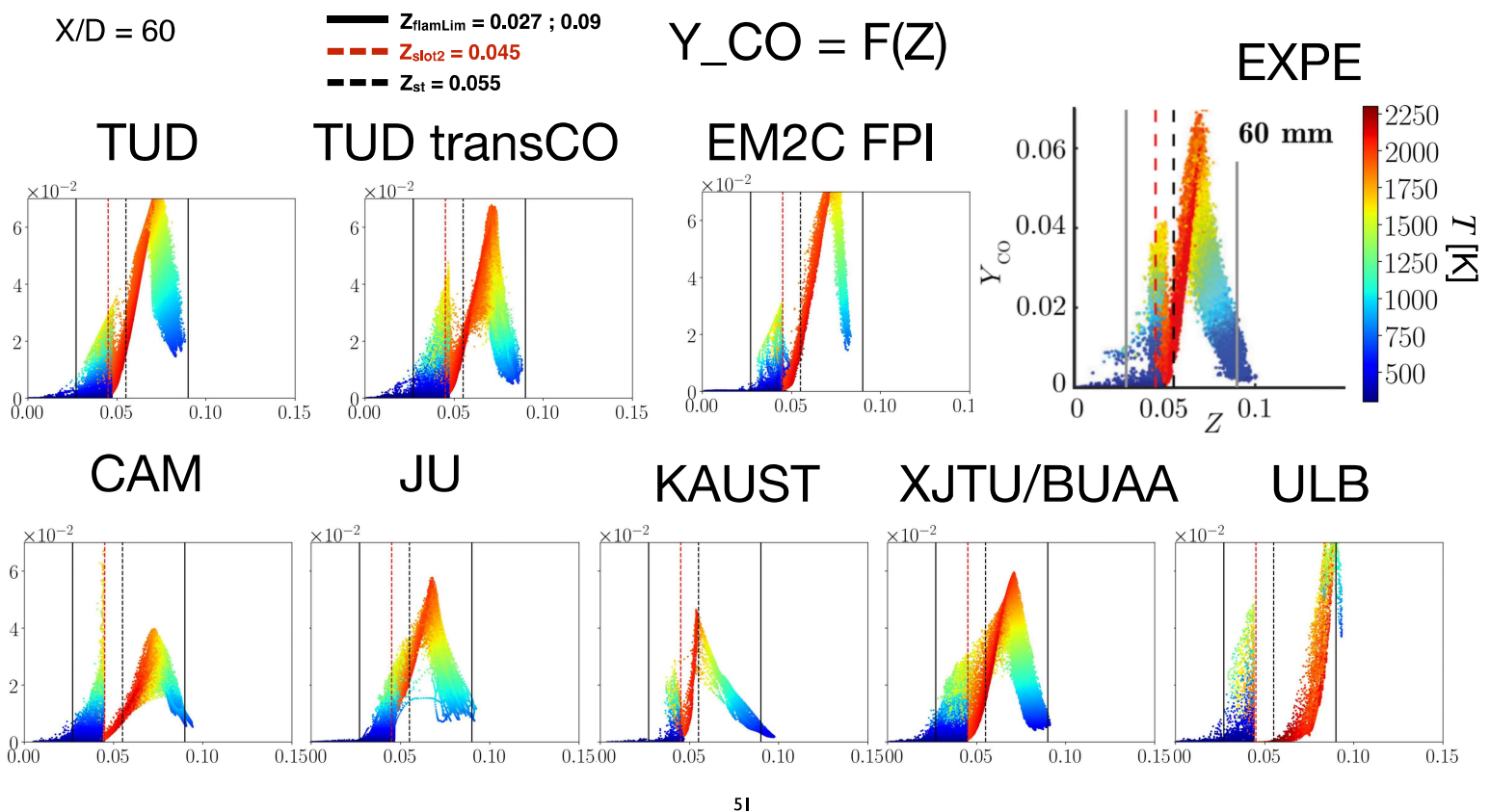
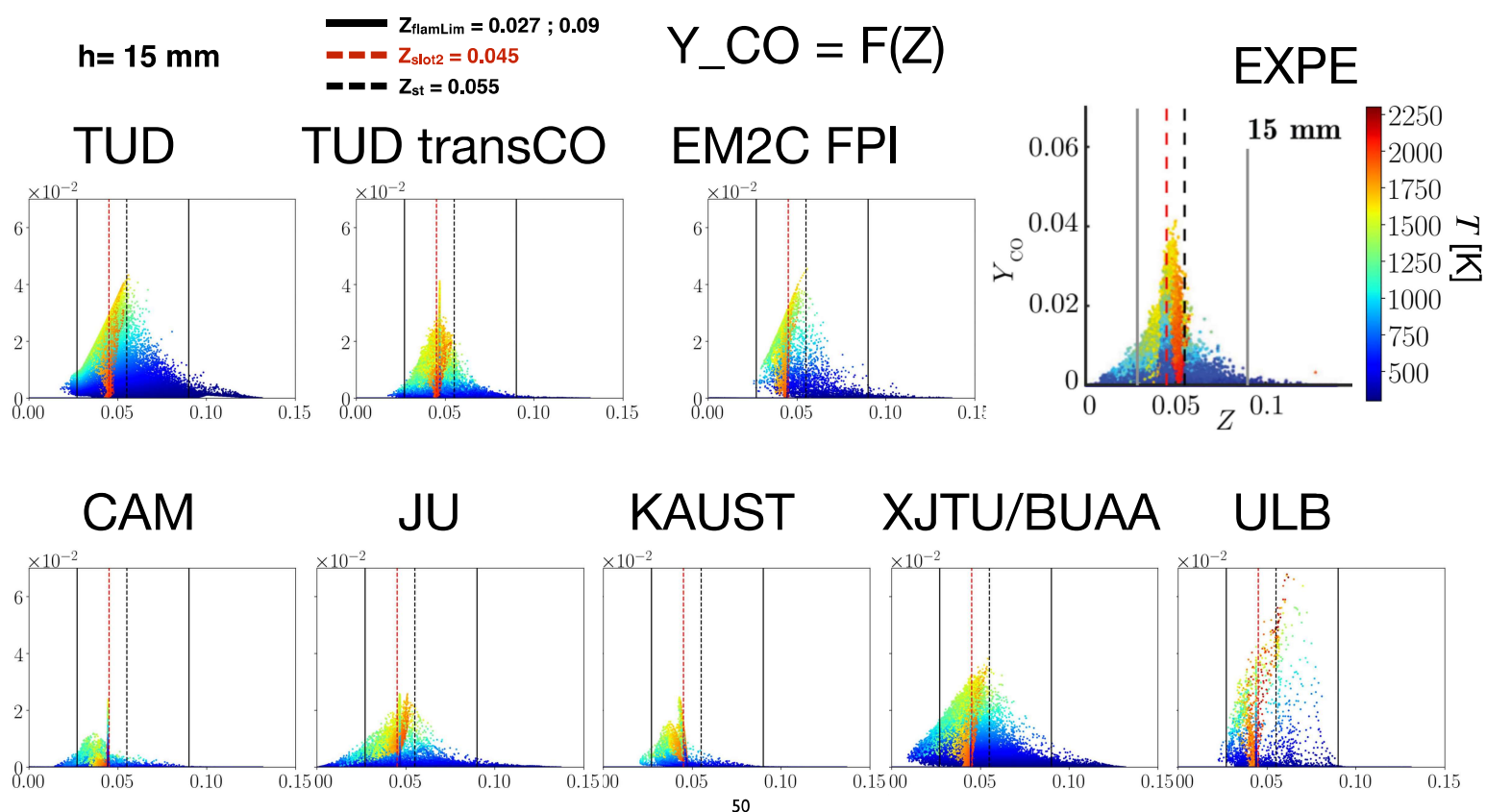
h = 6 mm

— $Z_{\text{flamLim}} = 0.027 ; 0.09$
 - - - $Z_{\text{slot2}} = 0.045$
 - - - $Z_{\text{st}} = 0.055$

$Y_{\text{CO}} = F(Z)$

EXPE





COLD CASE

52

COLD CASE, axial velocity

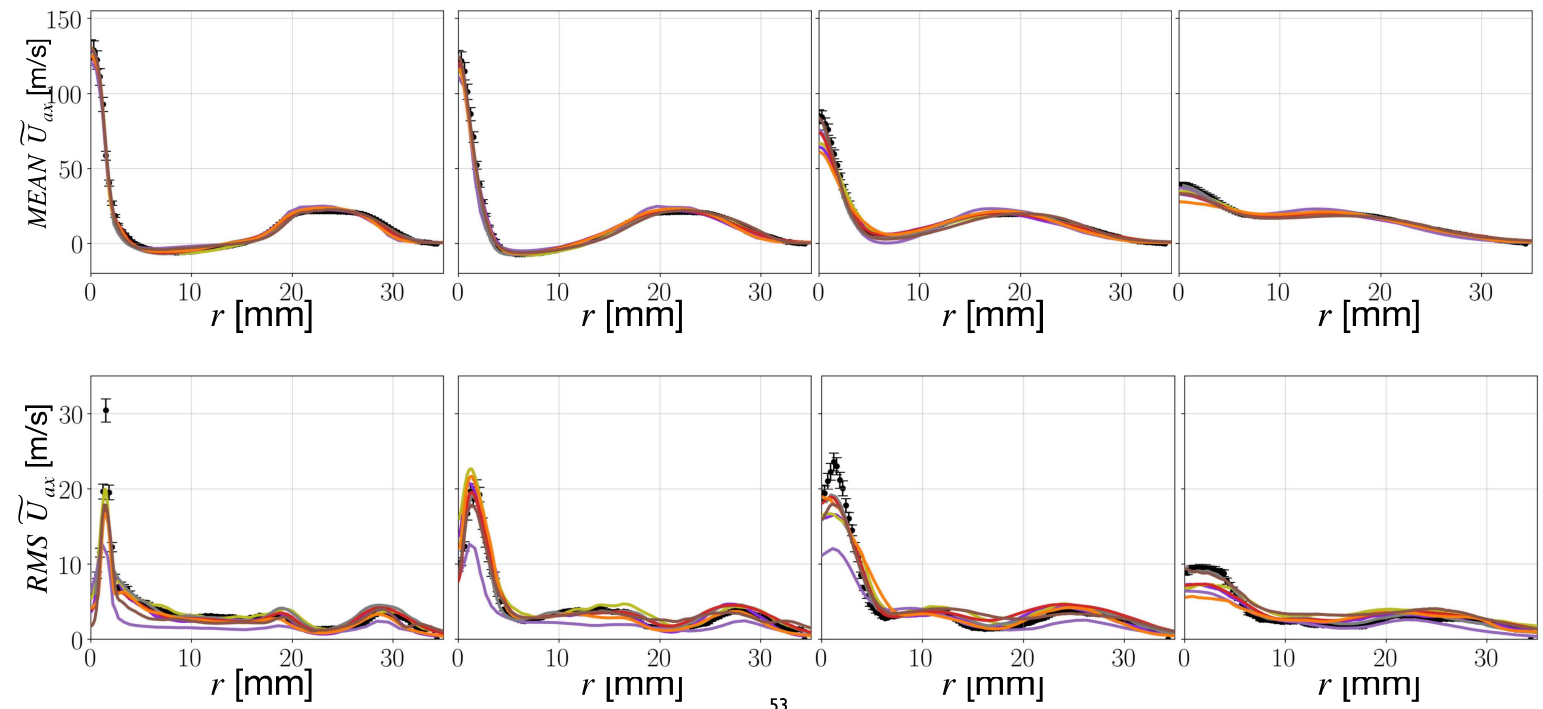
h=6 mm

h= 15 mm

h=30 mm

h= 60 mm

- | | | | |
|---------|---------|-------|-------------|
| ●●● Exp | — KAUST | — UBM | — XJTU/BUAA |
| — CAM | — KTH | — UDE | — ULB |
| — EM2C | — JU | — TUD | |



53

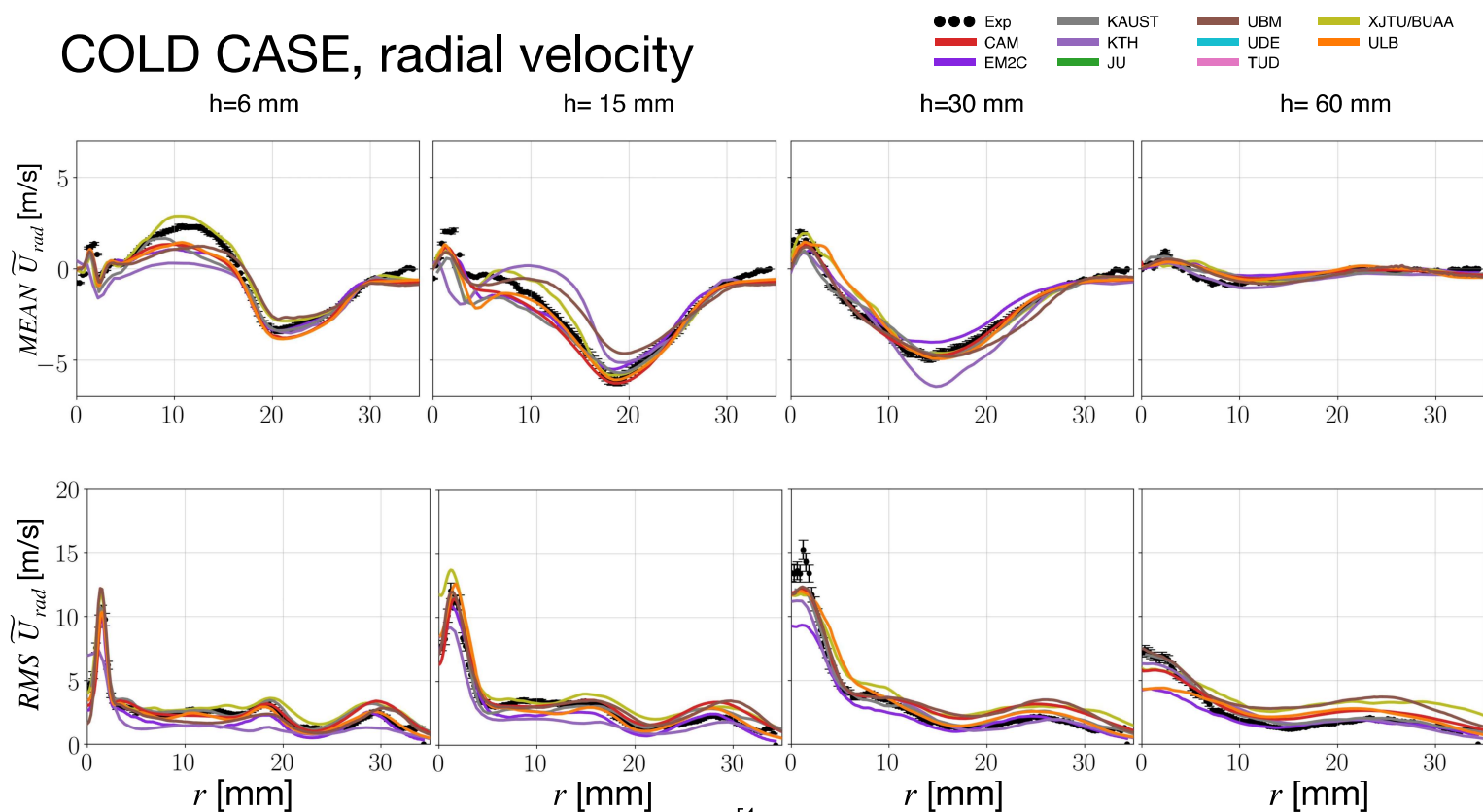
COLD CASE, radial velocity

h=6 mm

h=15 mm

h=30 mm

h=60 mm



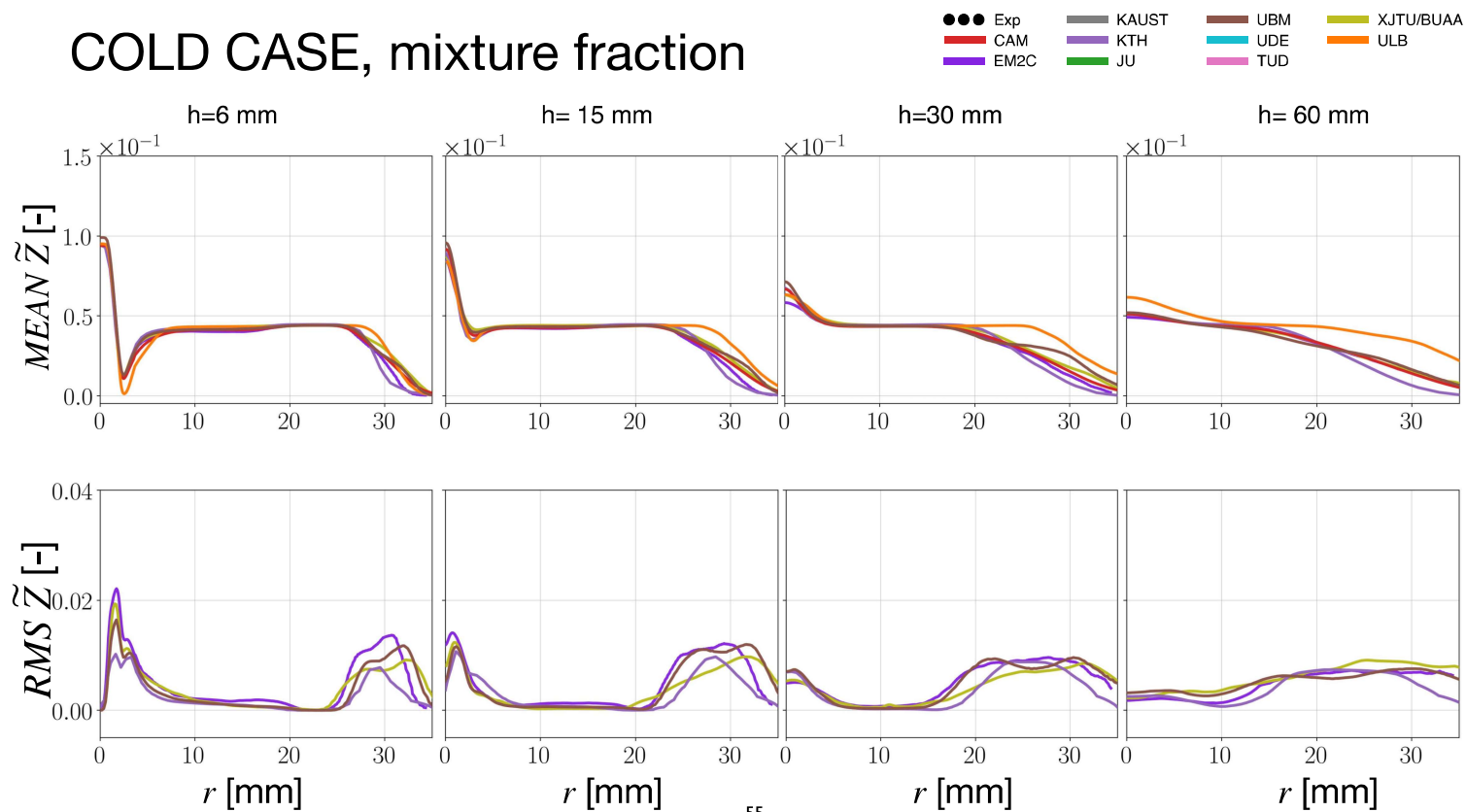
COLD CASE, mixture fraction

h=6 mm

h=15 mm

h=30 mm

h=60 mm



REACTIVE CASE 18b

56

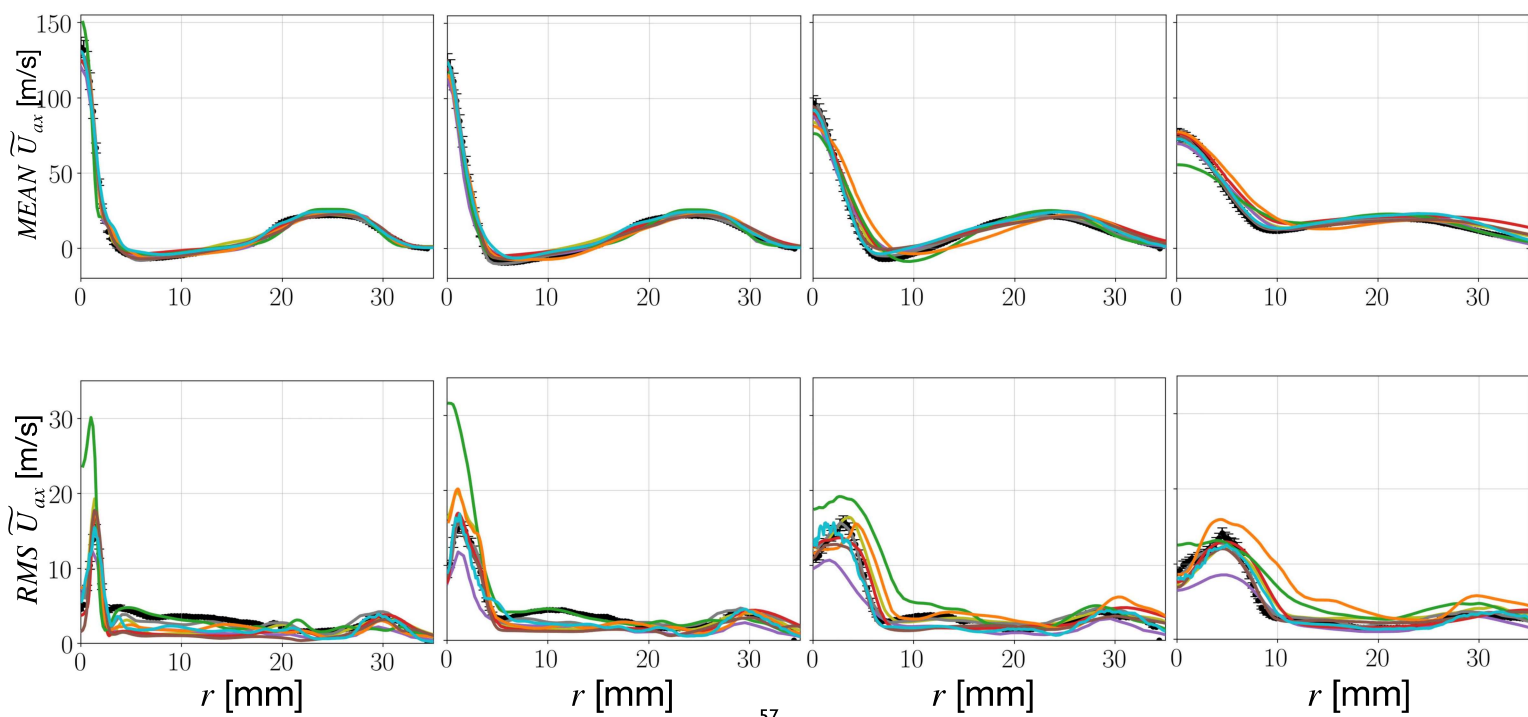
REACTIVE 18b CASE, axial velocity

6 mm

15 mm

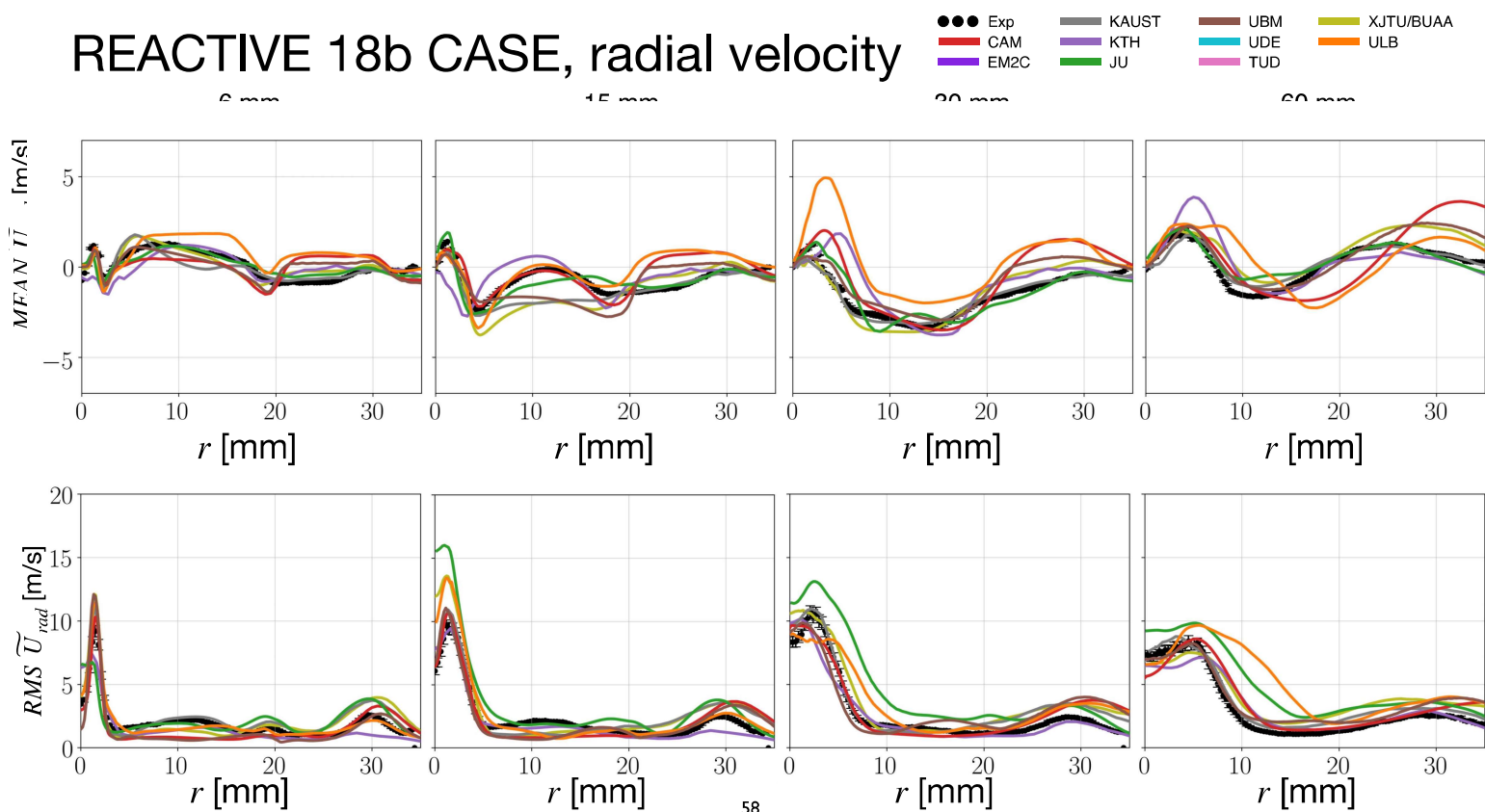
30 mm

60 mm



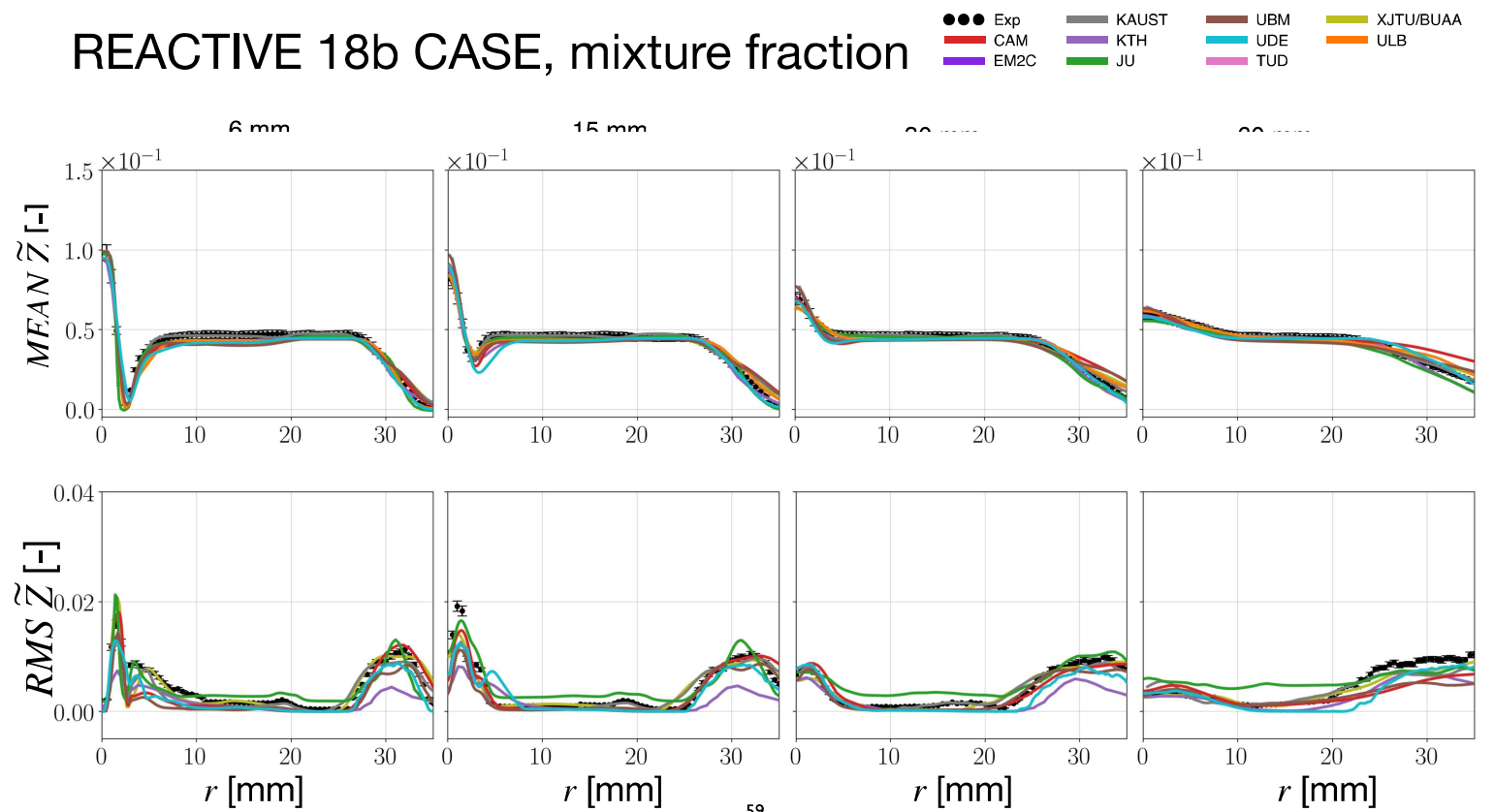
57

REACTIVE 18b CASE, radial velocity



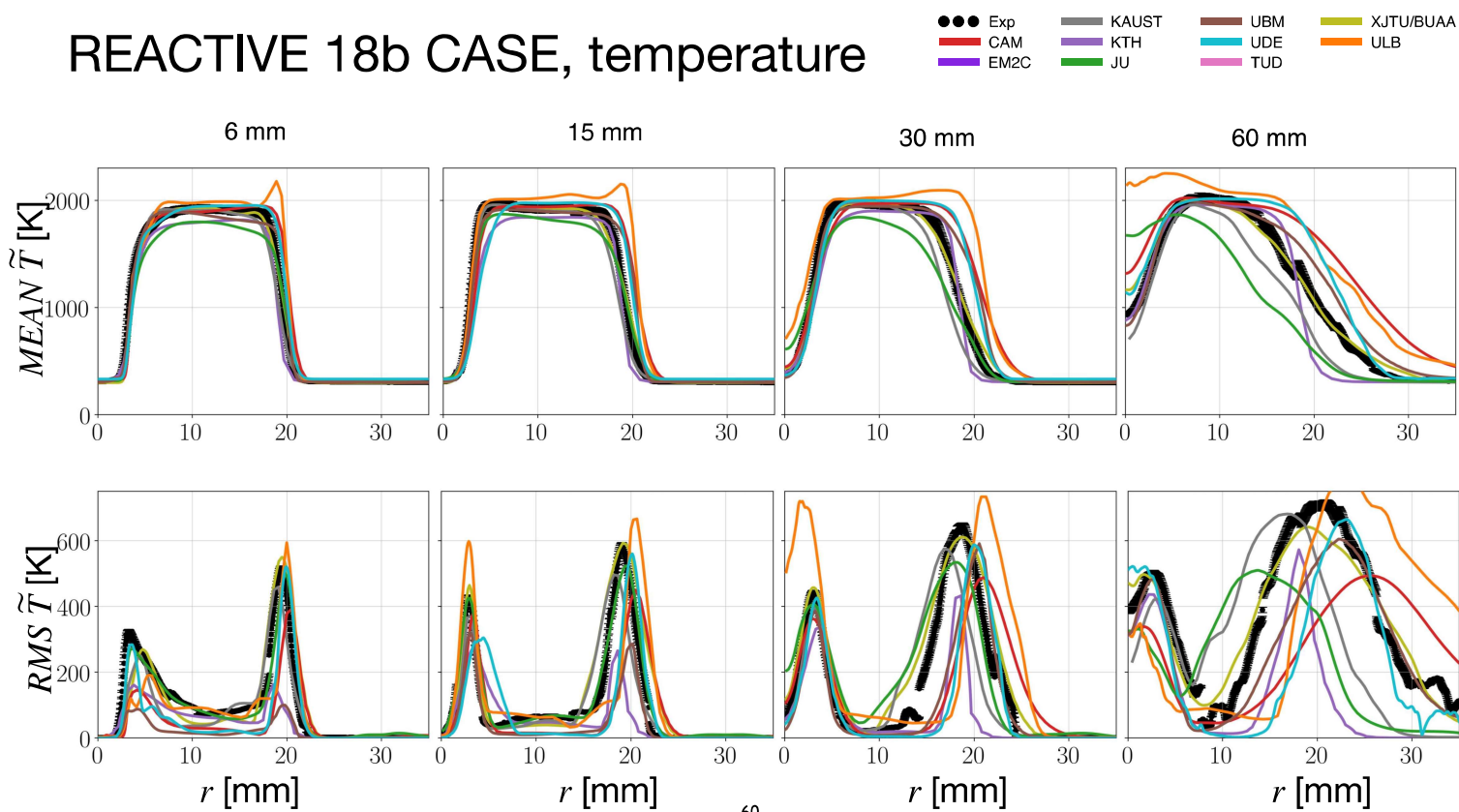
58

REACTIVE 18b CASE, mixture fraction



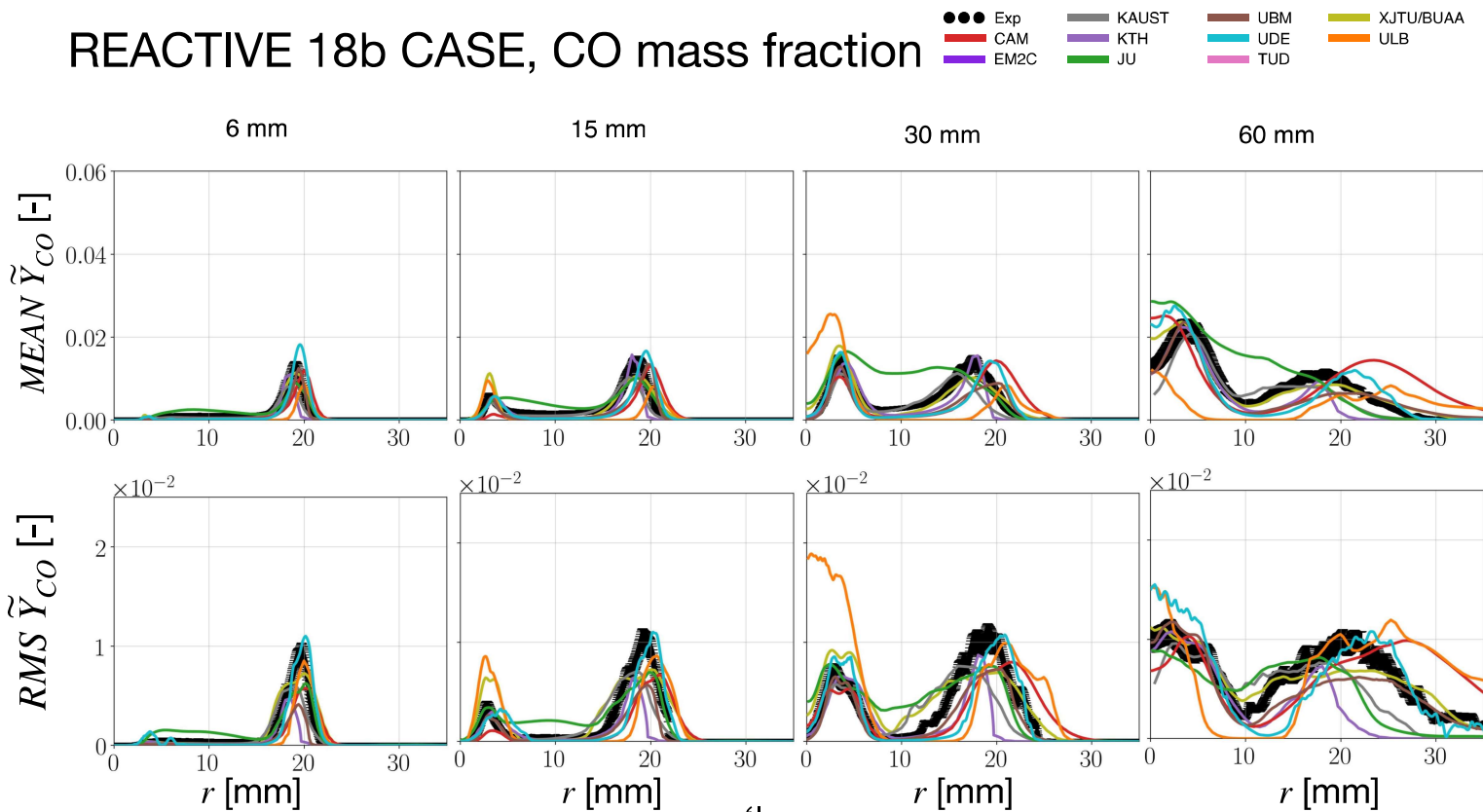
59

REACTIVE 18b CASE, temperature



60

REACTIVE 18b CASE, CO mass fraction



61

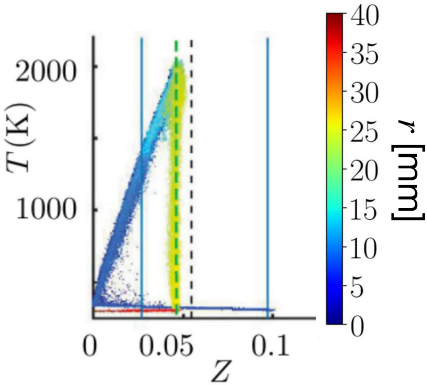
SCATTER PLOTS

62

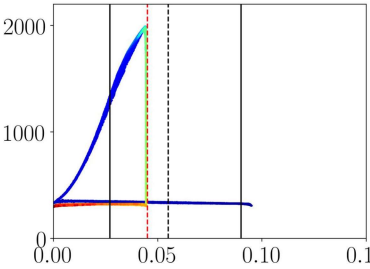
— $Z_{\text{flamLim}} = 0.027 ; 0.09$
- - - $Z_{\text{slot2}} = 0.045$
- - - $Z_{\text{st}} = 0.055$

$T = F(Z)$

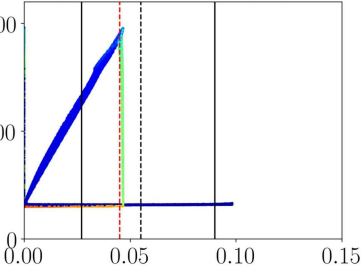
EXPE



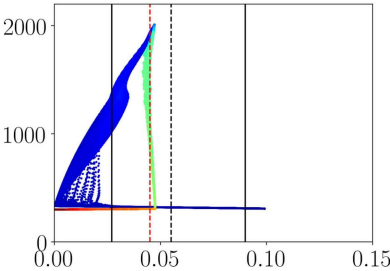
CAM



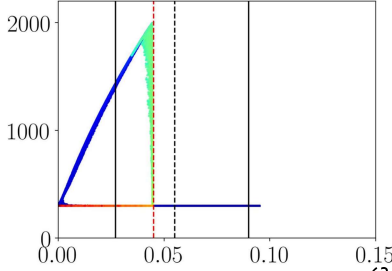
JU



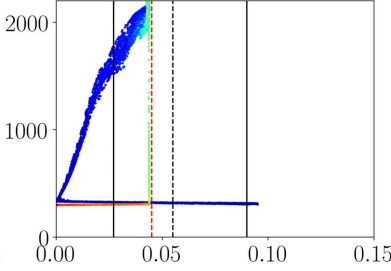
KAUST



XJTU/BUAA



ULB



63

X/D = 15

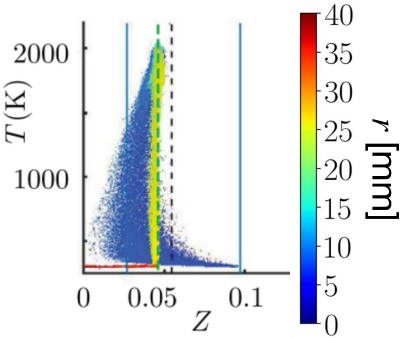
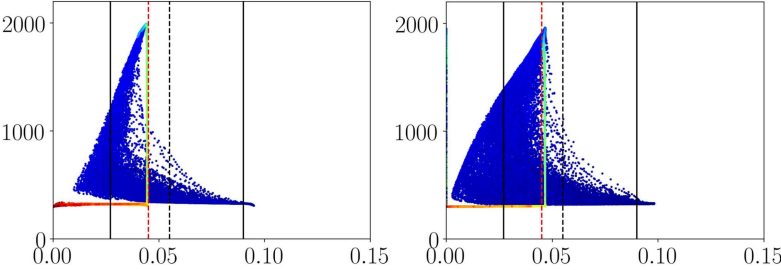
$Z_{\text{flamLim}} = 0.027 ; 0.09$
 $Z_{\text{slot2}} = 0.045$
 $Z_{\text{st}} = 0.055$

$T = F(Z)$

EXPE

CAM

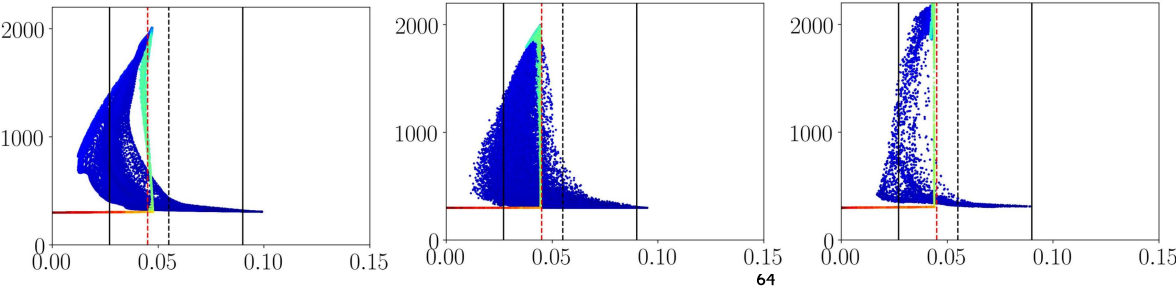
JU



KAUST

XJTU/BUAA

ULB



X/D = 30

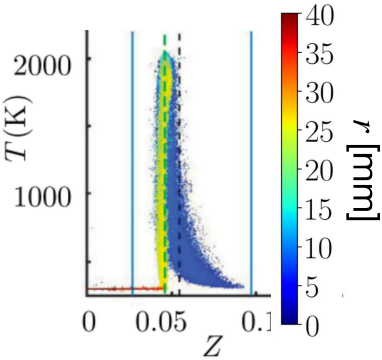
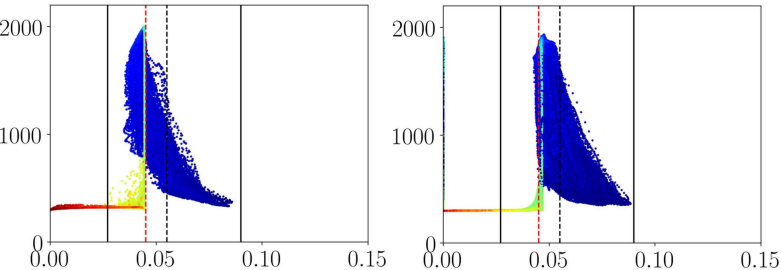
$Z_{\text{flamLim}} = 0.027 ; 0.09$
 $Z_{\text{slot2}} = 0.045$
 $Z_{\text{st}} = 0.055$

$T = F(Z)$

EXPE

CAM

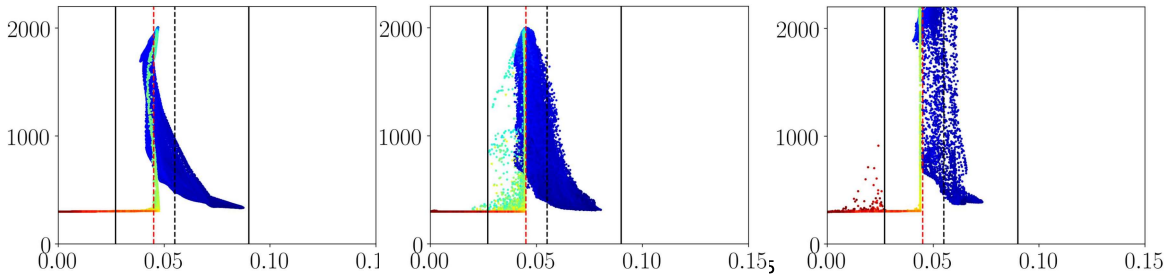
JU



KAUST

XJTU/BUAA

ULB

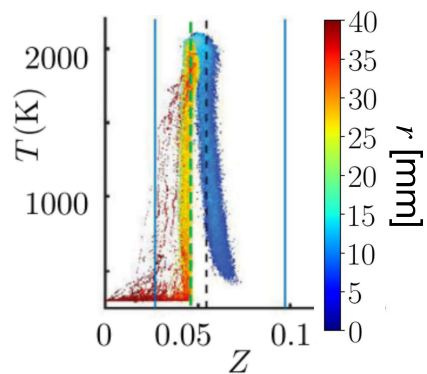
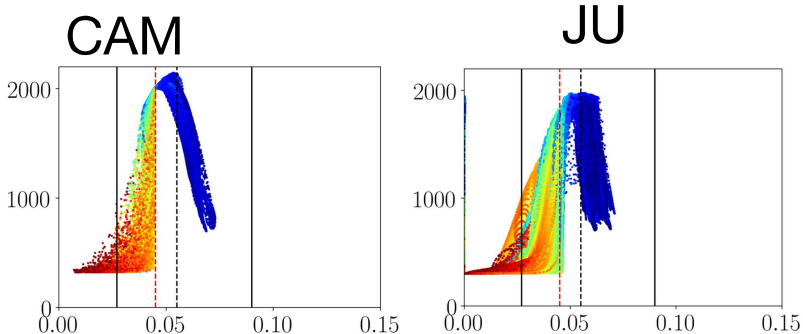


X/D = 60

— $Z_{\text{flamLim}} = 0.027 ; 0.09$
 - - - $Z_{\text{slot2}} = 0.045$
 - - - $Z_{\text{st}} = 0.055$

$T = F(Z)$

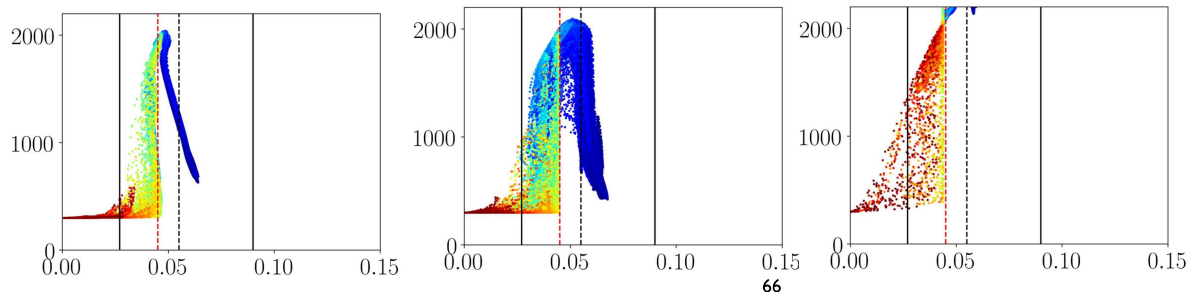
EXPE



KAUST

XJTU/BUAA

ULB

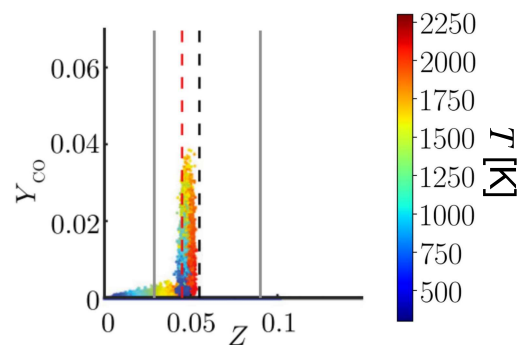
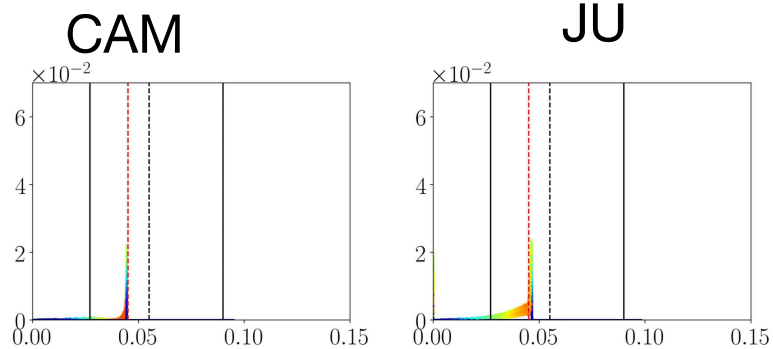


X/D = 6

— $Z_{\text{flamLim}} = 0.027 ; 0.09$
 - - - $Z_{\text{slot2}} = 0.045$
 - - - $Z_{\text{st}} = 0.055$

$Y_{\text{CO}} = F(Z)$

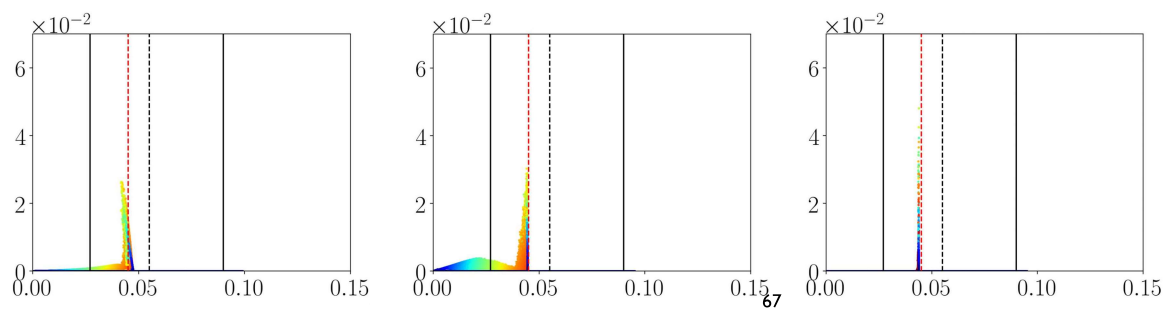
EXPE



KAUST

XJTU/BUAA

ULB

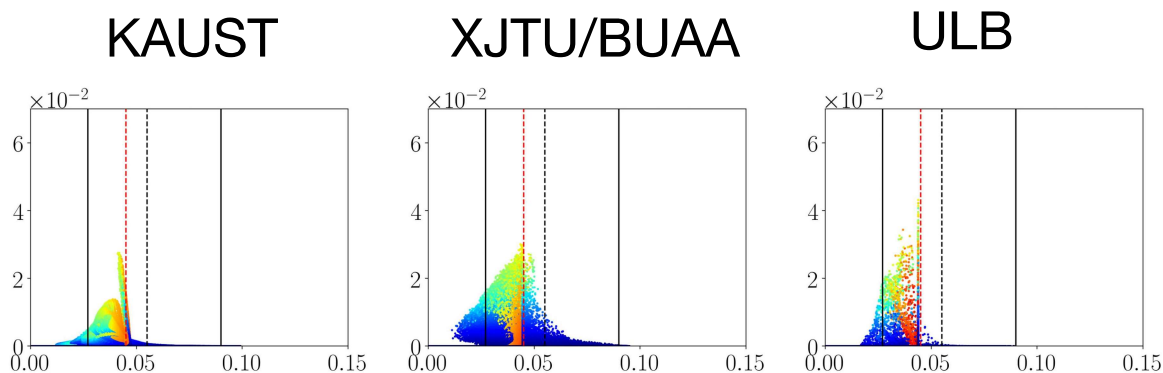
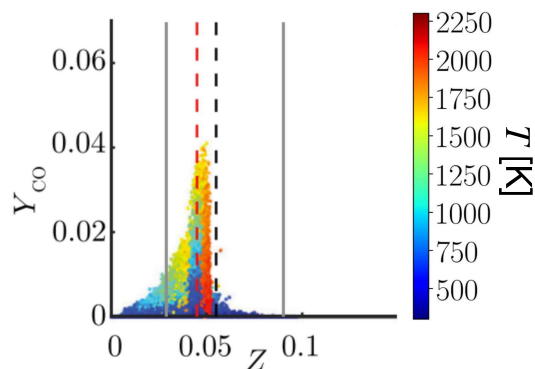
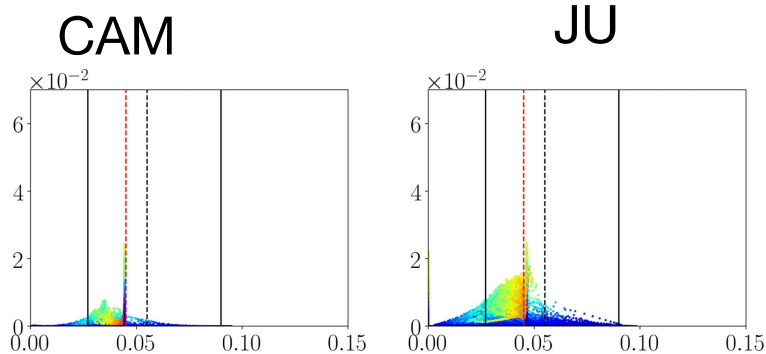


$X/D = 15$

— $Z_{\text{flamLim}} = 0.027 ; 0.09$
 - - - $Z_{\text{slot2}} = 0.045$
 - - - $Z_{\text{st}} = 0.055$

$Y_{\text{CO}} = F(Z)$

EXPE

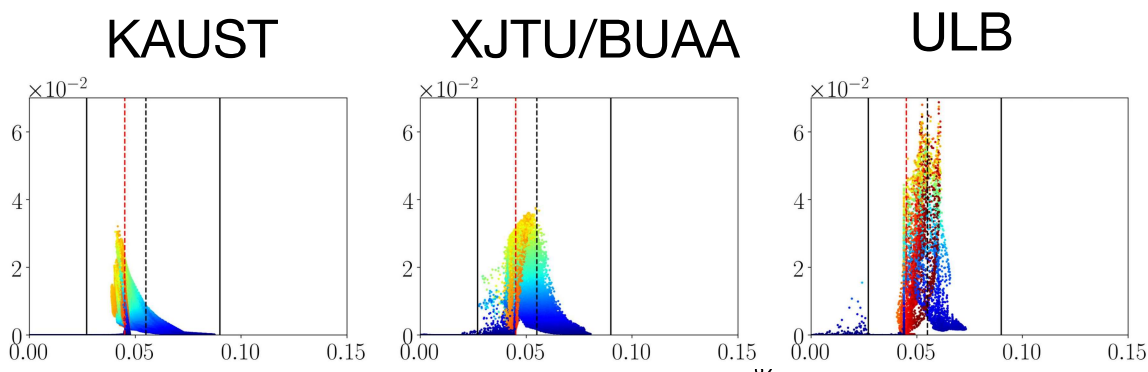
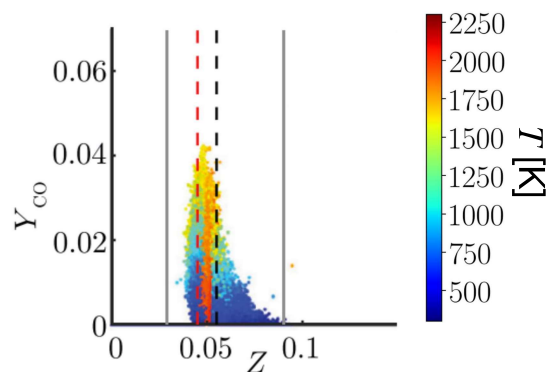
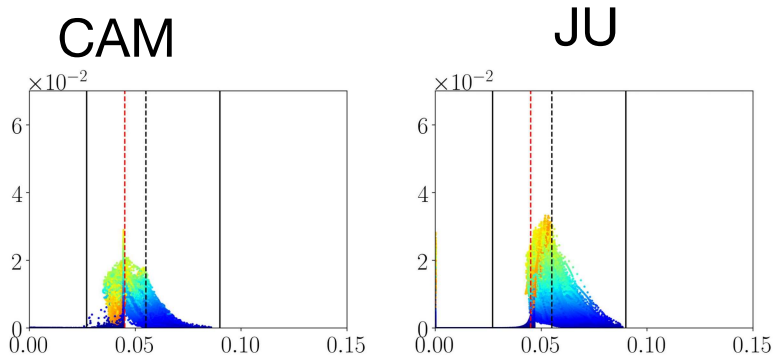


$X/D = 30$

— $Z_{\text{flamLim}} = 0.027 ; 0.09$
 - - - $Z_{\text{slot2}} = 0.045$
 - - - $Z_{\text{st}} = 0.055$

$Y_{\text{CO}} = F(Z)$

EXPE

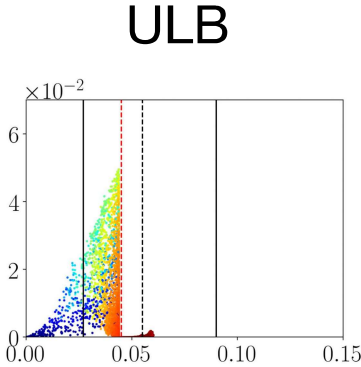
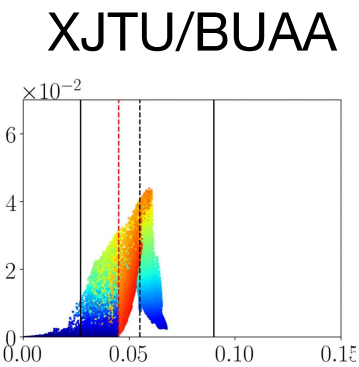
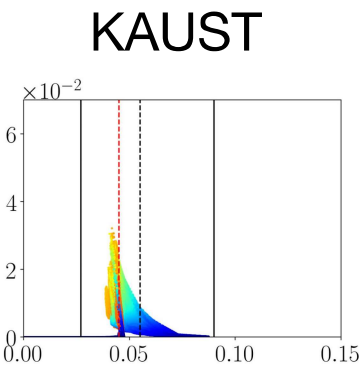
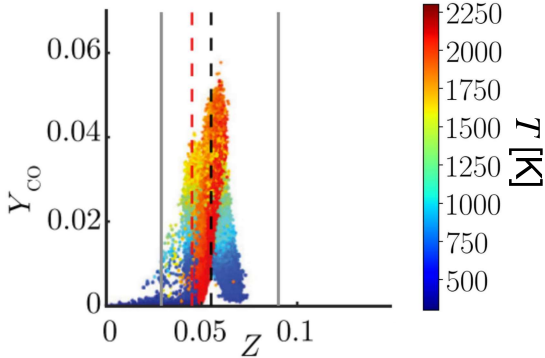
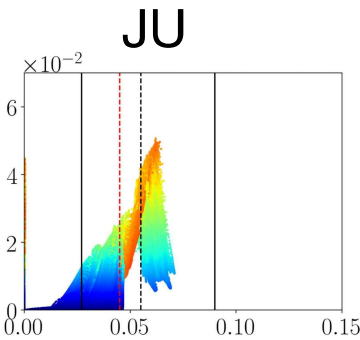
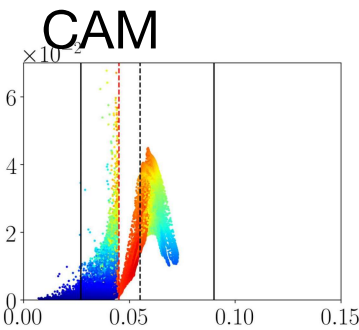


X/D = 60

$Z_{\text{flamLim}} = 0.027 ; 0.09$
 $Z_{\text{slot2}} = 0.045$
 $Z_{\text{st}} = 0.055$

$Y_{\text{CO}} = F(Z)$

EXPE



TNF/PTF Workshops

Blank Page



PTF Contributed Talks: Flame Structure and Speed

Chen	*Spectral Analysis of Premixed Ammonia/Hydrogen/Nitrogen-Air Flames in Sheared Turbulence
Hamlington	What do we get wrong (and right) when we study turbulent premixed flames in a box?
Steinberg	How different is turbulence when burning (and does it matter)?
Kheirkhah	What is the role of non-flamelets in estimating how fast turbulent premixed flames burn?
Chaudhuri	Turbulent flame speed based on mass flow rate of reactants - theory and its validation
Hochgreb	(Difficulties in) closing the balance for progress of reaction in turbulent premixed Bunsen flames

* Not provided for inclusion in the Proceedings

What do we get wrong (and right) when we study turbulent premixed flames in a box?

Peter E. Hamlington

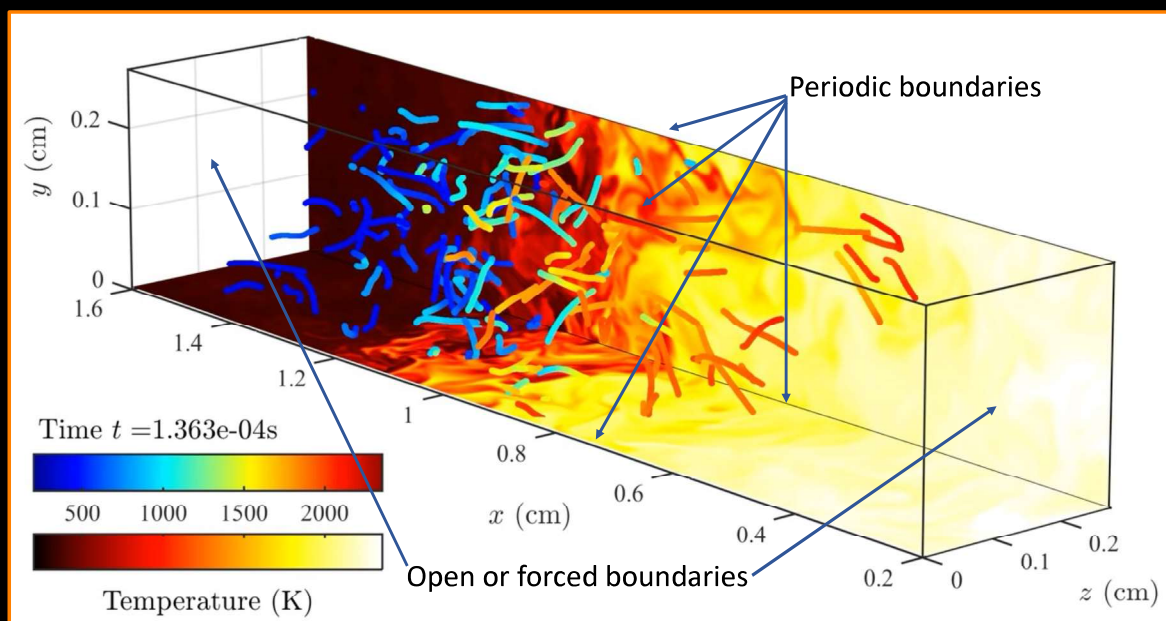
Paul M. Rady Department of Mechanical Engineering, University of Colorado, Boulder, CO



DEPARTMENT OF DEFENSE
HIGH PERFORMANCE COMPUTING
MODERNIZATION PROGRAM



What is a flame in a box?



How do we model flames in boxes?

$$\frac{D\rho}{Dt} = -\rho \frac{\partial u_k}{\partial x_k} \quad \frac{Du_i}{Dt} = -\frac{1}{\rho} \frac{\partial p}{\partial x_i} + \frac{1}{\rho} \frac{\partial \tau_{ij}}{\partial x_j} + \mathcal{F}_i \quad \frac{DY_\beta}{Dt} = \frac{1}{\rho} \frac{\partial}{\partial x_k} \left(\rho \mathcal{D}_\beta \frac{\partial Y_\beta}{\partial x_k} \right) + \dot{\omega}_\beta$$

$$\frac{De_0}{Dt} = -\frac{1}{\rho} \frac{\partial (u_j p)}{\partial x_j} + \frac{1}{\rho} \frac{\partial}{\partial x_j} \left(\kappa \frac{\partial T}{\partial x_j} \right) + \frac{1}{\rho} \frac{\partial (u_i \tau_{ij})}{\partial x_j} + u_i \mathcal{F}_i$$

XXII. *On the Theories of the Internal Friction of Fluids in Motion, and of the Equilibrium and Motion of Elastic Solids.* By G. G. STOKES, M.A., Fellow of Pembroke College.

[Read April 14, 1845.]

5. Having found the pressures about the point P on planes parallel to the co-ordinate planes, it will be easy to form the equations of motion. Let X, Y, Z be the resolved parts, parallel to the axes, of the external force, not including the molecular force; let ρ be the density, t the time. Consider an elementary parallelepiped of the fluid, formed by planes parallel to the

$$\rho \left(\frac{Du}{Dt} - X \right) + \frac{dp}{dx} - \mu \left(\frac{d^2 u}{dx^2} + \frac{d^2 u}{dy^2} + \frac{d^2 u}{dz^2} \right) = 0, \text{ \&c. (13)}$$

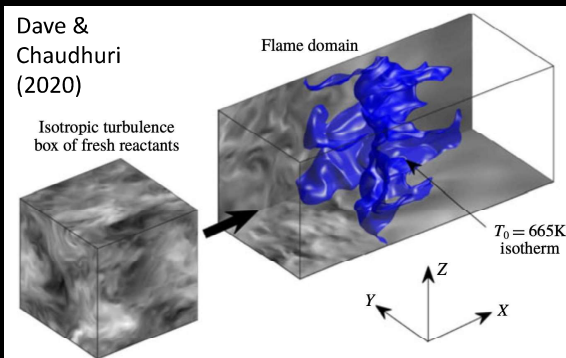
Long history of volumetric forcing in studies of non-reacting turbulence:

- Channel flows (e.g., Kim, Moin, Moser)
- Homogeneous isotropic turbulence (e.g., Yeung, Donzis, Sreenivasan)
- Homogeneous shear turbulence (e.g., Schumacher, Sreenivasan)

How do we model flames in boxes?

$$\frac{D\rho}{Dt} = -\rho \frac{\partial u_k}{\partial x_k} \quad \frac{Du_i}{Dt} = -\frac{1}{\rho} \frac{\partial p}{\partial x_i} + \frac{1}{\rho} \frac{\partial \tau_{ij}}{\partial x_j} \quad \frac{DY_\beta}{Dt} = \frac{1}{\rho} \frac{\partial}{\partial x_k} \left(\rho \mathcal{D}_\beta \frac{\partial Y_\beta}{\partial x_k} \right) + \dot{\omega}_\beta$$

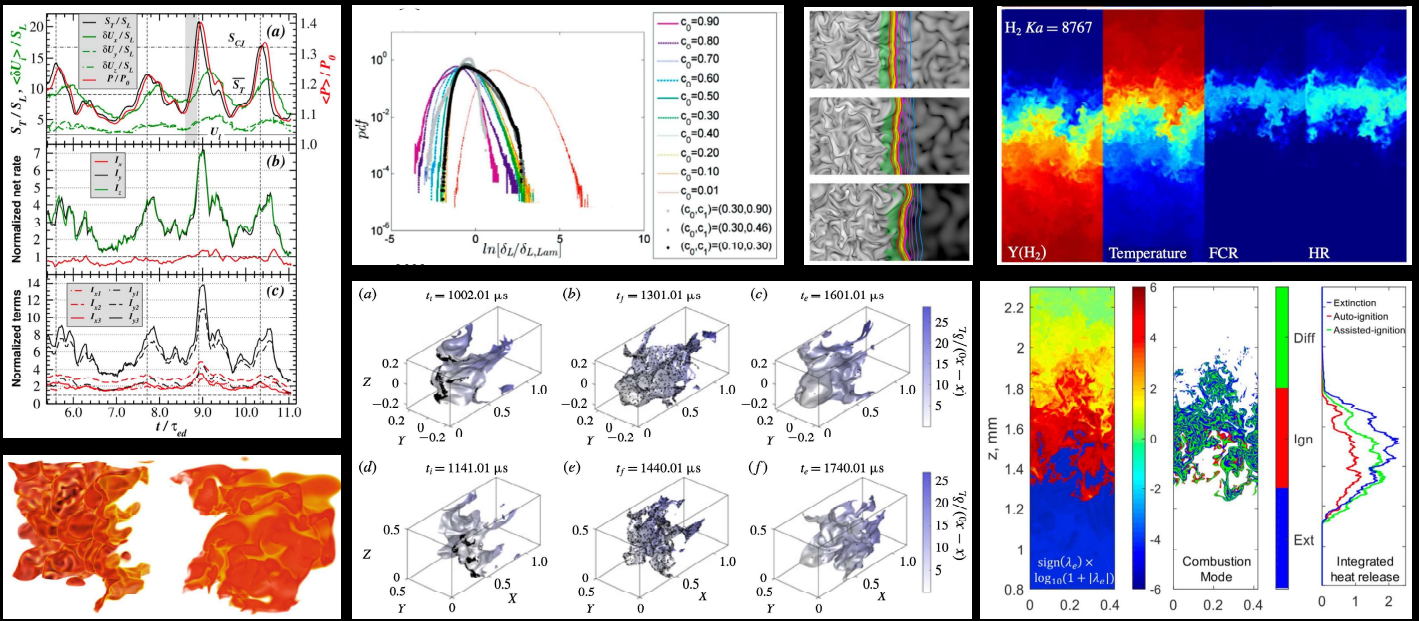
$$\frac{De_0}{Dt} = -\frac{1}{\rho} \frac{\partial (u_j p)}{\partial x_j} + \frac{1}{\rho} \frac{\partial}{\partial x_j} \left(\kappa \frac{\partial T}{\partial x_j} \right) + \frac{1}{\rho} \frac{\partial (u_i \tau_{ij})}{\partial x_j}$$



Comparing premixed flame results from DNS using decaying turbulence, boundary forcing, and linear forcing: "It has been found that there is no method, which is clearly superior to the other two alternative methods."

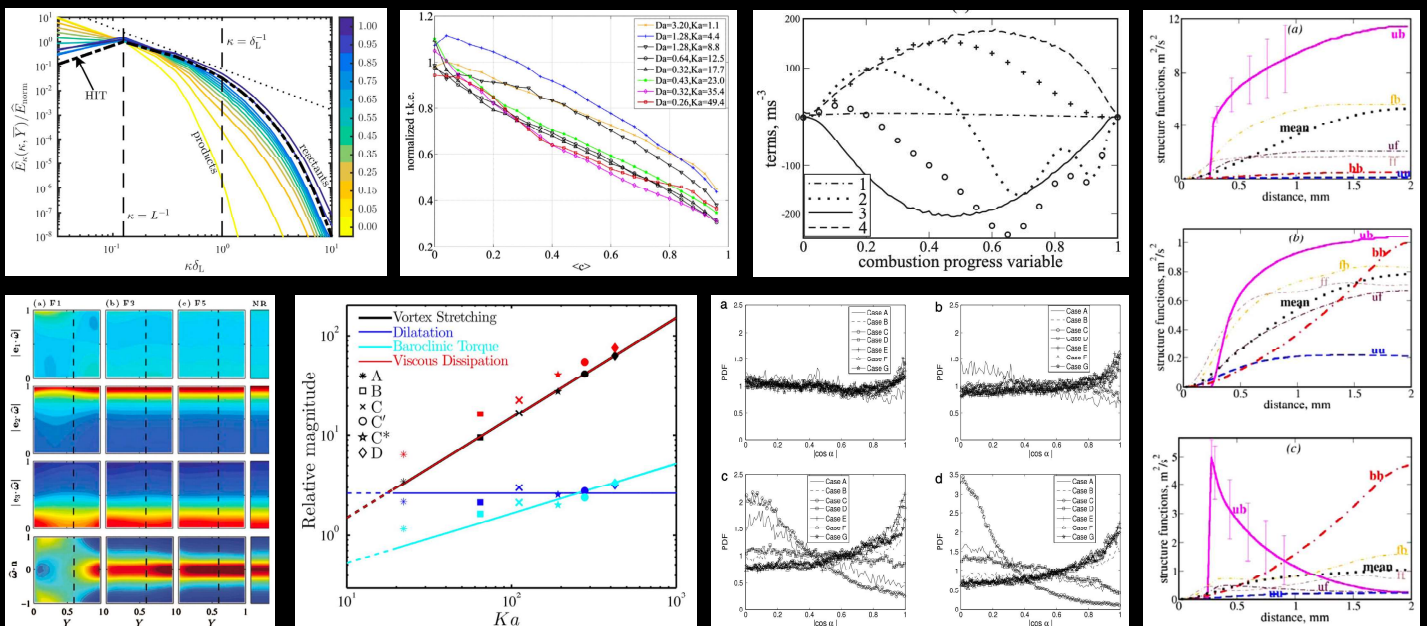
Klein M., Chakraborty N., Ketterl S.. A comparison of strategies for direct numerical simulation of turbulence chemistry interaction in generic planar turbulent premixed flames. Flow Turb Combust 99(3-4), 2017.

What have we learned from flames in boxes?



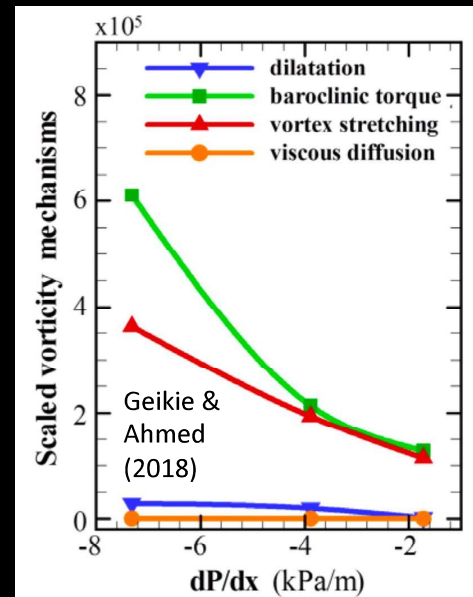
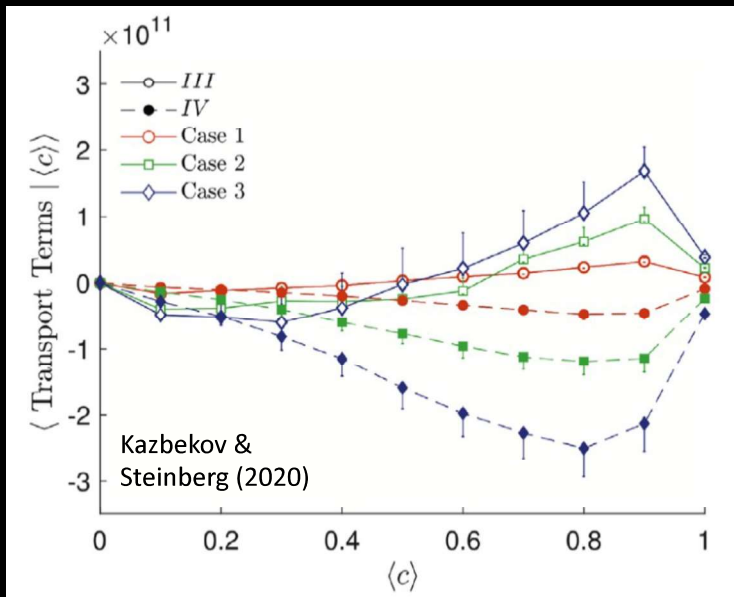
Clockwise from top left: Poludnenko (2015); Chaudhuri et al. (2017); Nilsson et al. (2018); Aspdén et al. (2019); Xu et al. (2019); Dave & Chaudhuri (2020); Im et al. (2016)

What have we learned from flames in boxes?

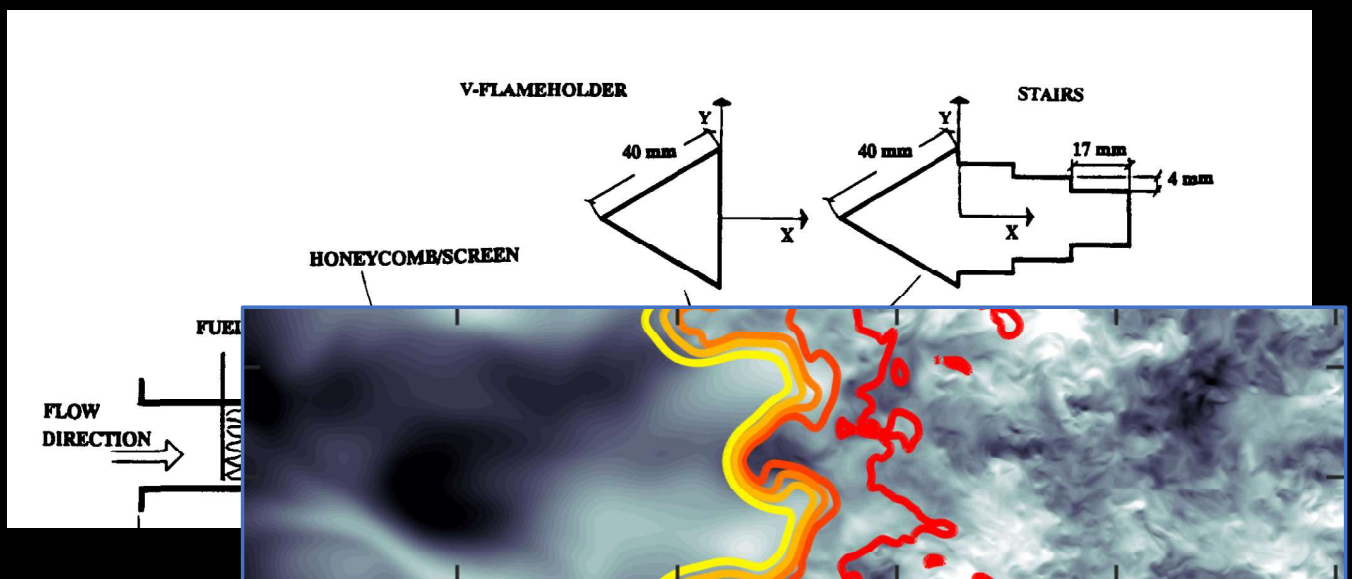


Clockwise from top left: Towery et al. (2017); Wang & Abraham (2017); Lipatnikov et al. (2014); Sabelnikov et al. (2019); Chakraborty (2014); Bobbitt et al. (2016); Hamlington et al. (2011)

Why do we need to “get outside the box”?



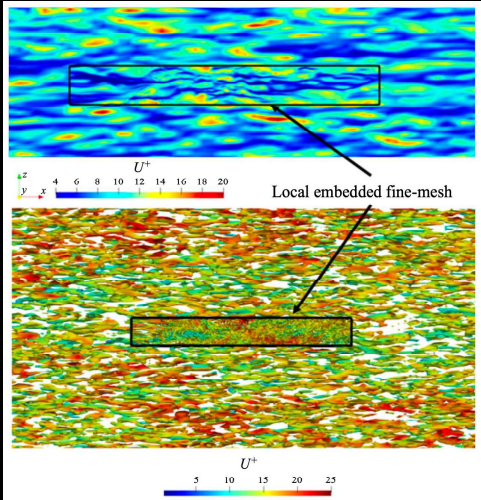
Why do we need to “get outside the box”?



How do we get outside the box?

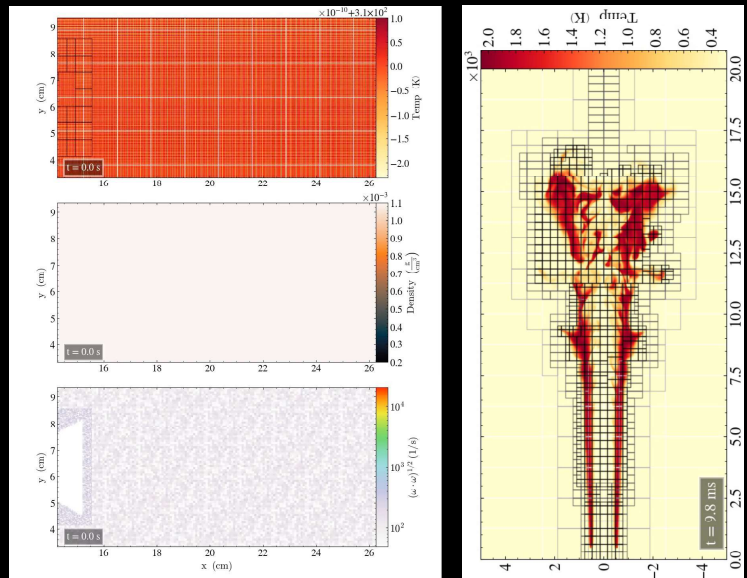
Embedded DNS: Locally and statically refine a region of the simulation

On locally embedded two-scale solution for wall-bounded turbulent flows, C. Chen and L. He, *JFM* (2022), 933, A47



 Turbulence and Energy Systems Laboratory
UNIVERSITY OF COLORADO BOULDER

Adaptive mesh refinement: Dynamically changing grid (PeleC; <https://github.com/AMReX-Combustion/PeleC>)



Acknowledgements

A. M. Steinberg, P. E. Hamlington, and X. Zhao. Structure and dynamics of highly turbulent premixed combustion. *Progress in Energy and Combustion Science*, 85:100900, 2021.



Monday, 12:05pm, Meeting Room 11

1G05: Pressure gradient tailoring effects on vorticity dynamics in the near-wake of bluff-body stabilized flames

S.H.R. Whitman, T.J. Souders, M.A. Meehan, J.G. Brasseur, P.E. Hamlington



Monday, Work in Progress Poster

1P016: Simulated bluff body flames subjected to mean pressure gradient and inlet turbulence

T.J. Souders, S.H.R. Whitman, P.E. Hamlington



 Turbulence and Energy Systems Laboratory
UNIVERSITY OF COLORADO BOULDER

How Different is Burning Turbulence? and Does it Matter?

Askar Kazbekov, Adam M. Steinberg

Daniel Guggenheim School of Aerospace Engineering
Georgia Institute of Technology

PTF/TNF Workshop
Vancouver, Canada
July 22-23, 2022



Effects of Combustion on Turbulence

- Combustion \Rightarrow increased $\nu \Rightarrow$ increased diffusion and dissipation
- Combustion can act as a source or sink of turbulent fluctuations

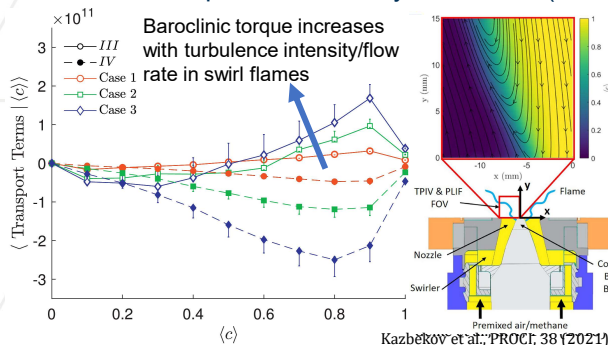
- Flame scale vorticity or kinetic energy
- Part of this depends on pressure and dilatation
 - Baroclinic torque (vorticity)
 - SFS pressure-velocity correlation (kinetic energy)

$$\frac{1}{\rho^2} \omega_i \varepsilon_{ijk} \frac{\partial \rho}{\partial x_j} \frac{\partial p}{\partial x_k}$$

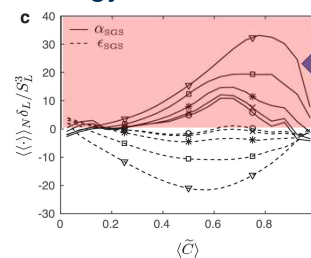
Baroclinic torque

$$\frac{1}{\bar{\rho}} \left(\tilde{u}_i \frac{\partial \bar{p}}{\partial x_i} - \overline{u_i \frac{\partial p}{\partial x_i}} \right)$$

Subfilter $p-\bar{u}$



- Combustion can redistribute kinetic energy across scales



$\alpha_{SGS} > 0 \Rightarrow$ mean backscatter



Effects of Combustion on Turbulence

- C
- C



Contents lists available at ScienceDirect

Progress in Energy and Combustion Science

journal homepage: www.elsevier.com/locate/pecs



Structure and dynamics of highly turbulent premixed combustion

Adam M. Steinberg^{a,*}, Peter E. Hamlington^b, Xinyu Zhao^c

4. Turbulence structure and dynamics	26
4.1. Turbulence kinetic energy, stresses, and fluxes	26
4.1.1. Turbulence kinetic energy	26
4.1.2. Turbulent stresses	29
4.1.3. Turbulent scalar fluxes	29
4.2. Vorticity, strain rate, and scalar gradients	30
4.2.1. Scalar gradients	30
4.2.2. Vorticity and strain rate	33
4.2.3. Coherent structures	36
4.3. Spectral and multi-scale characteristics	37
4.3.1. Spectral and multi-scale structure	39
4.3.2. Spectral and multi-scale dynamics	40
4.4. Summary	42

Transport Terms $\langle c \rangle$

(c)

Premixed air/methane
Kazbekov et al., *PROG. 38 (2021)*

(C)

$$\mu_i \frac{\partial p}{\partial x_i}$$

$$-\bar{u}$$

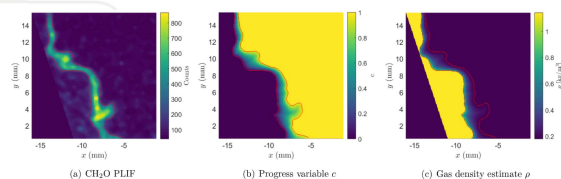
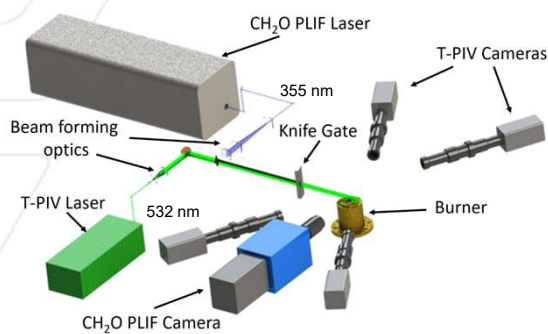
C

mean

(2017)

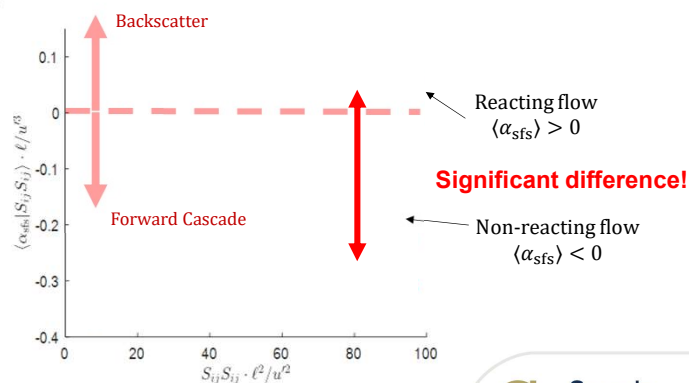
Georgia Tech

Backscatter in Swirl Flames



Kazbekov et al., *CNF*, 229 (2021)

Heat release leads to mean backscatter around the flame scales for the conditions studied

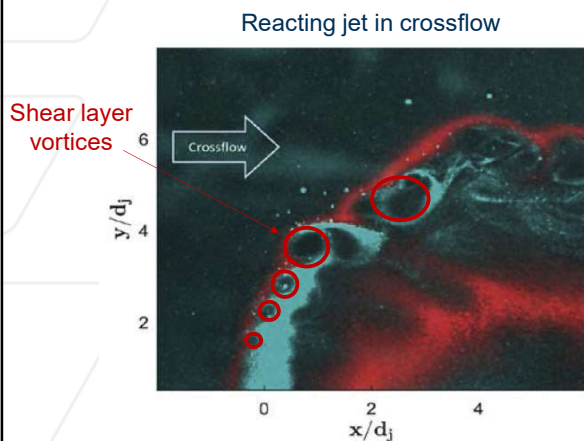


14 m/s bulk velocity flame

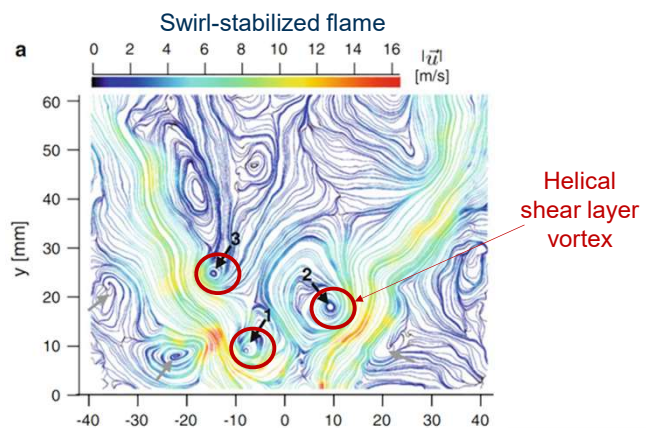
Georgia Tech

Shear Flows And Large-Scale Structures

- Responsible for large-scale mixing and increased reaction rate



Nair et al., PROCI, 36 (2017)



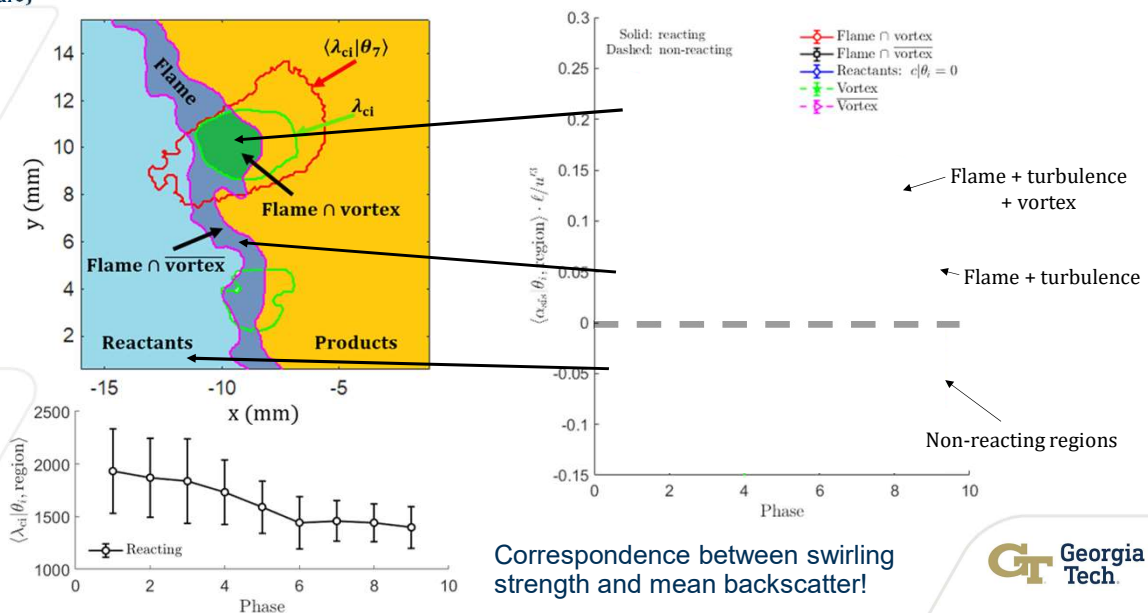
Stöhr et al., Exp. Fluids., 2011

GT Georgia Tech

Phase-Conditioned Analysis

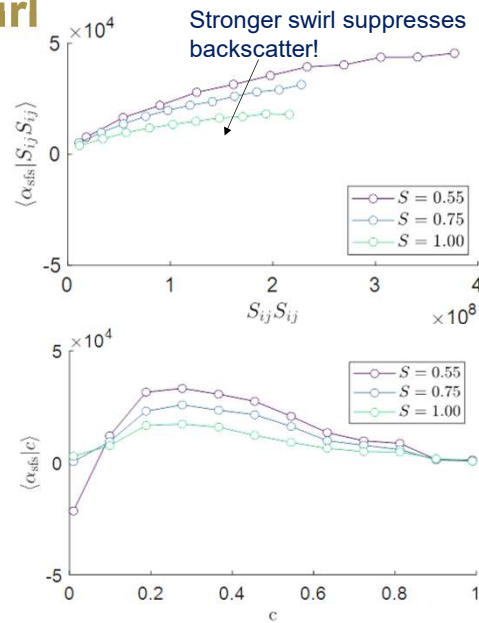
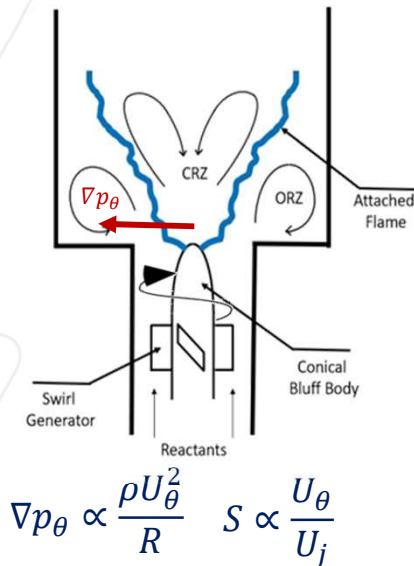
(Kazhekov & Steinberg, 1G01, Monday right after Hottel)

Lecture)



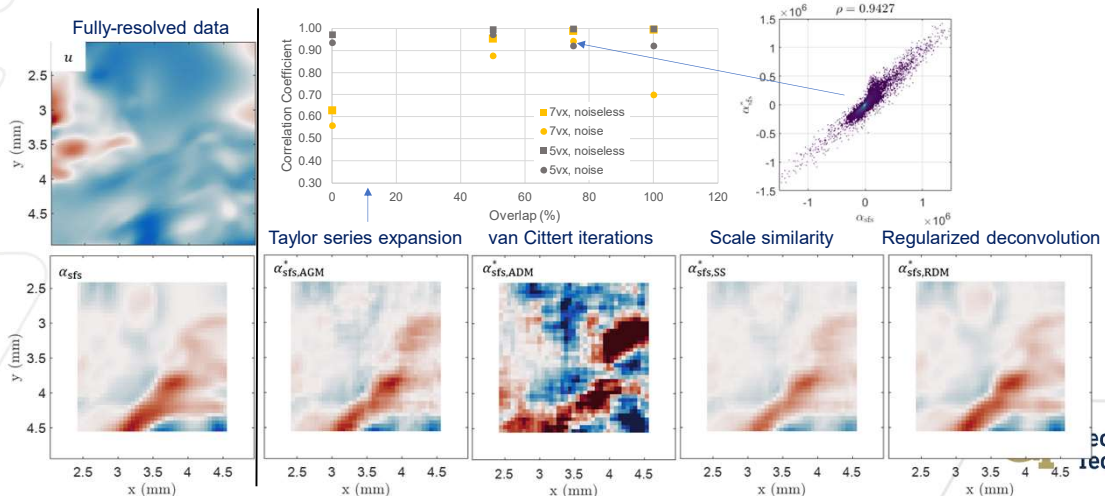
GT Georgia Tech

Next: Influence of Swirl



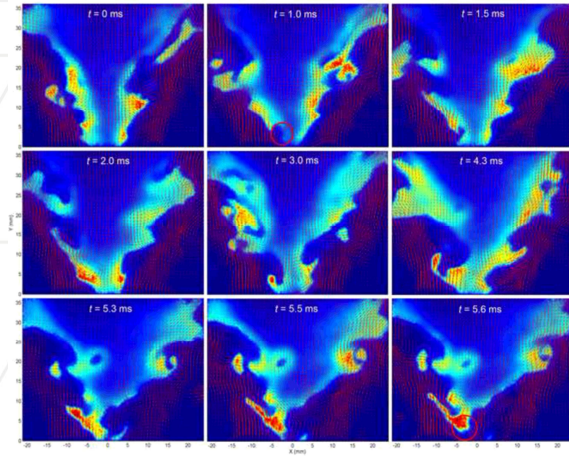
Next: Stronger Turbulence (Thanks to P. Hamlington)

- Fully-resolved velocity measurements are required for α_{sf}
- Unresolved velocity must be first estimated (i.e. deconvolution)

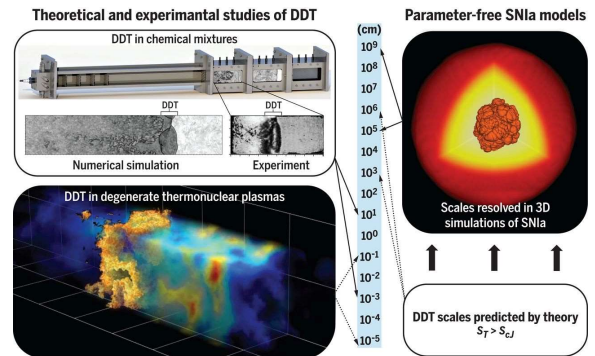


Does It Matter?

- Maybe (capitulation)
 - Depends on configuration, conditions, and what needs to be predicted



An *et al.*, CNF, 168 (2016)



Poludnenko *et al.*, Science, 366 (2019)

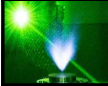
TNF/PTF Workshops

Blank Page

What is the role of non-flamelets in estimating how fast turbulent premixed flames burn?

Sajjad Mohammadnejad and Sina Kheirkhah

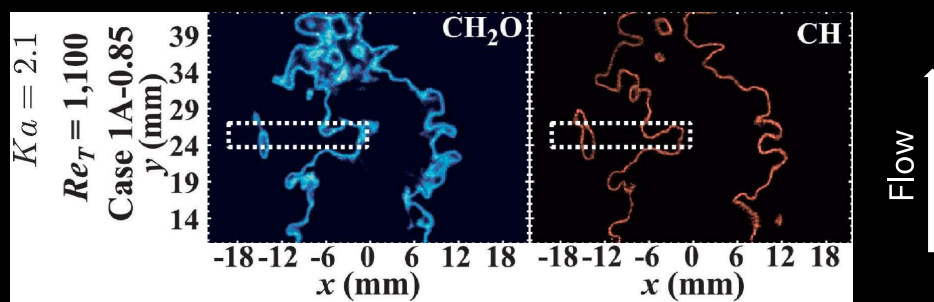
July 22, 2022



Combustion for Propulsion and Power Laboratory



1. Two controversial observations



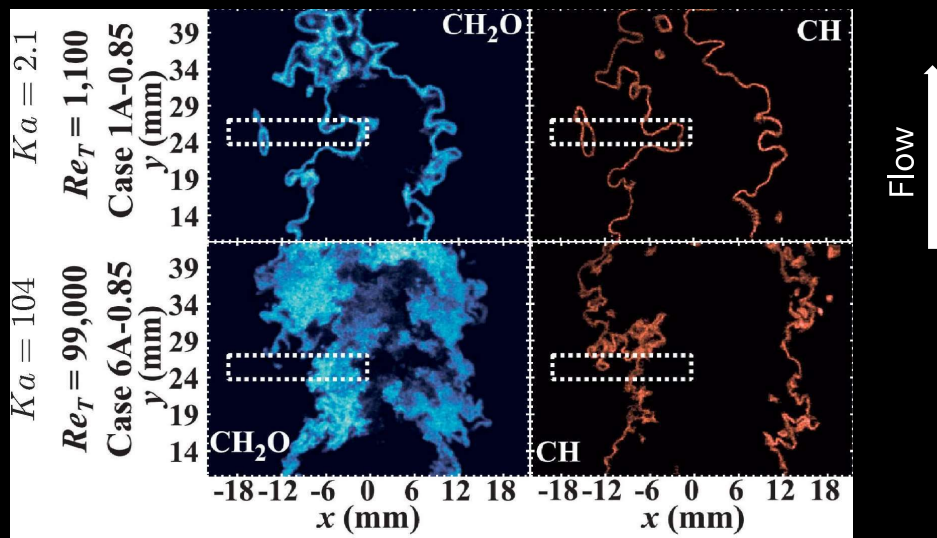
Skiba et al. (PCI, 2021)



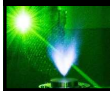
Combustion for Propulsion and Power Laboratory



1. Two controversial observations



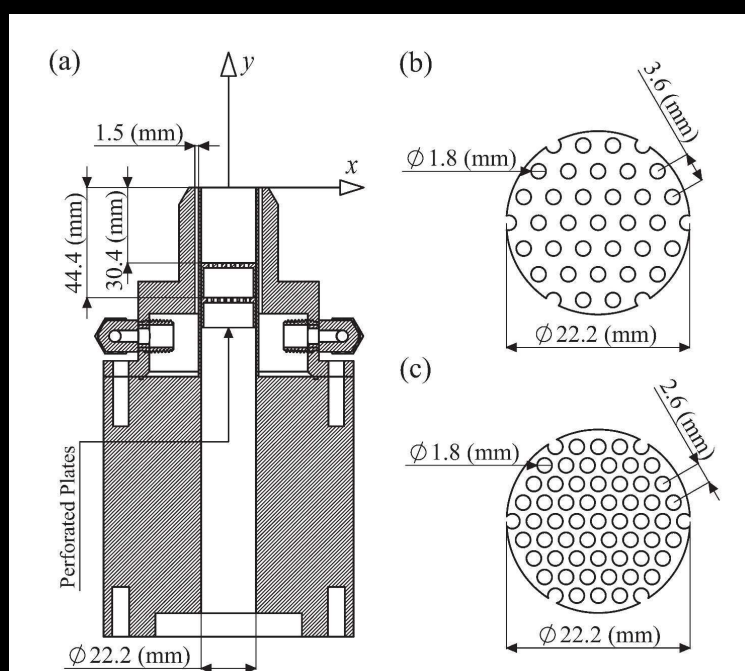
Skiba et al. (PCI, 2021)



Combustion for Propulsion and Power Laboratory



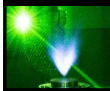
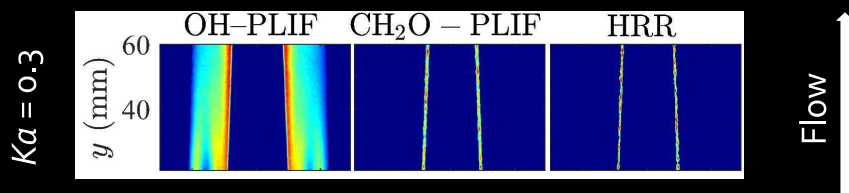
1. Two controversial observations



Combustion for Propulsion and Power Laboratory



1. Two controversial observations

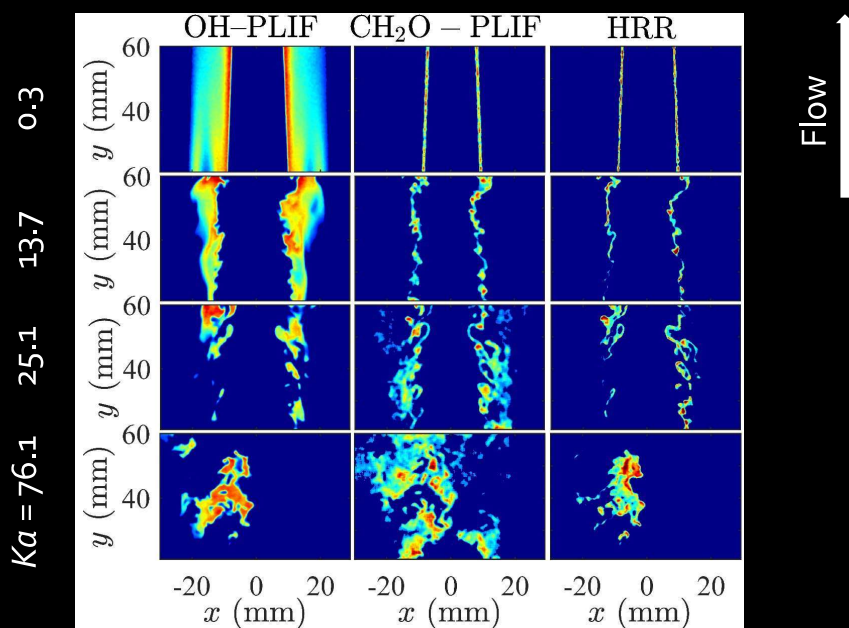


Mohammadnejad et al. (CNF, 2021)

Combustion for Propulsion and Power Laboratory



1. Two controversial observations

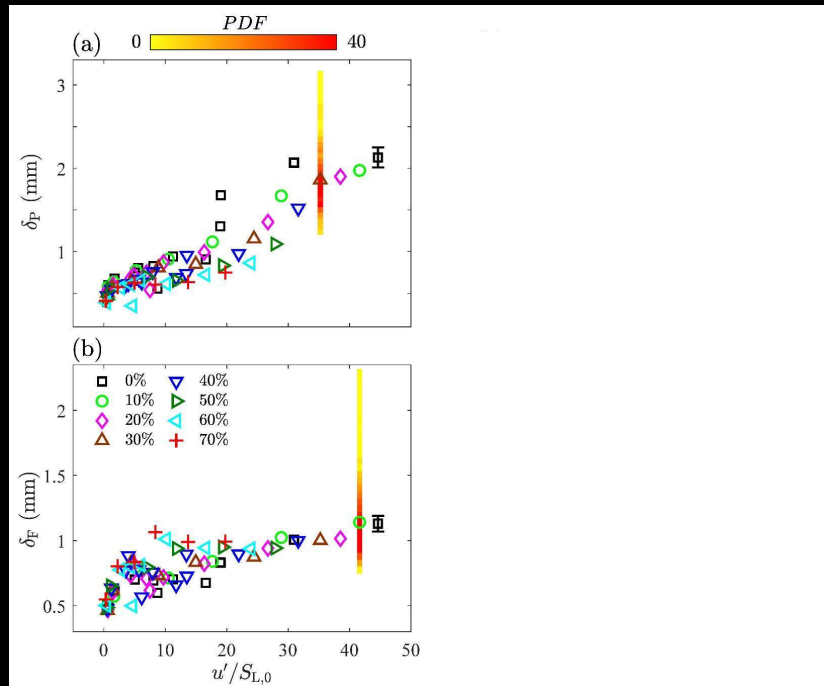


Mohammadnejad et al. (CNF, 2021)

Combustion for Propulsion and Power Laboratory



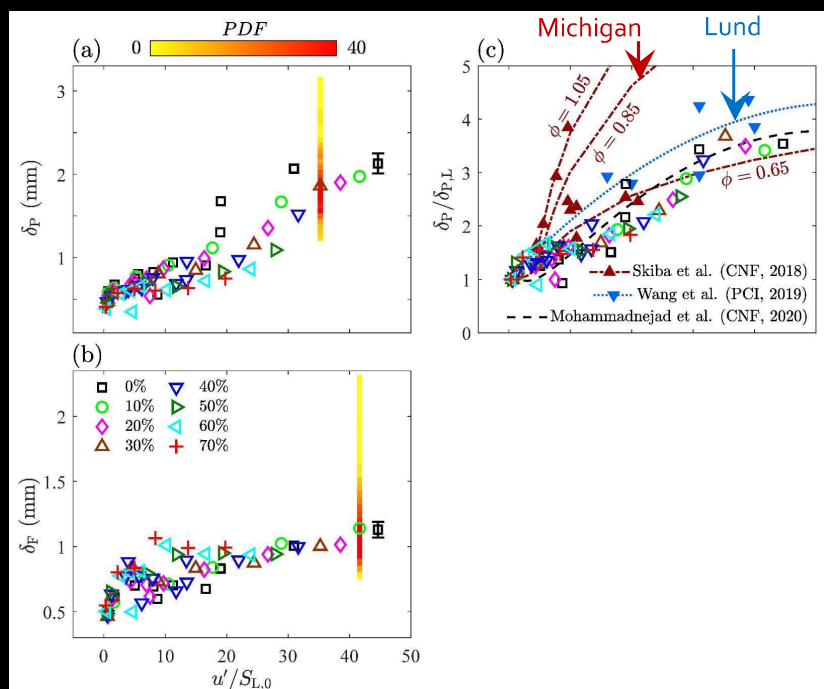
1. Two controversial observations



Combustion for Propulsion and Power Laboratory



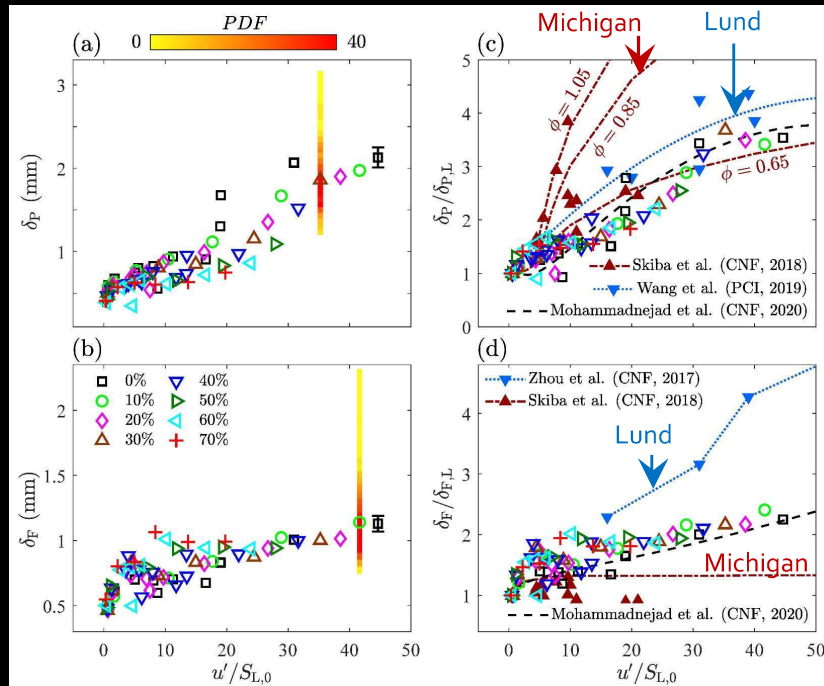
1. Two controversial observations



Combustion for Propulsion and Power Laboratory



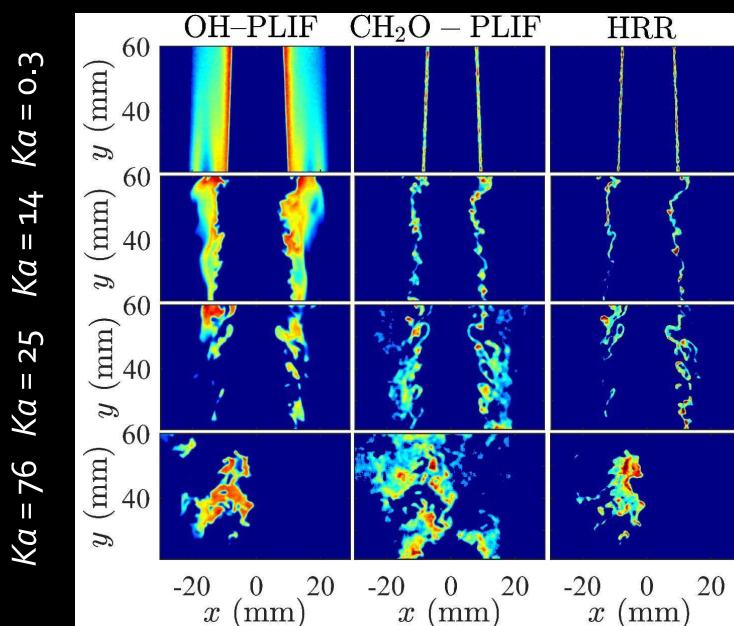
1. Two controversial observations



Combustion for Propulsion and Power Laboratory



1. Two controversial observations: Our hypot.



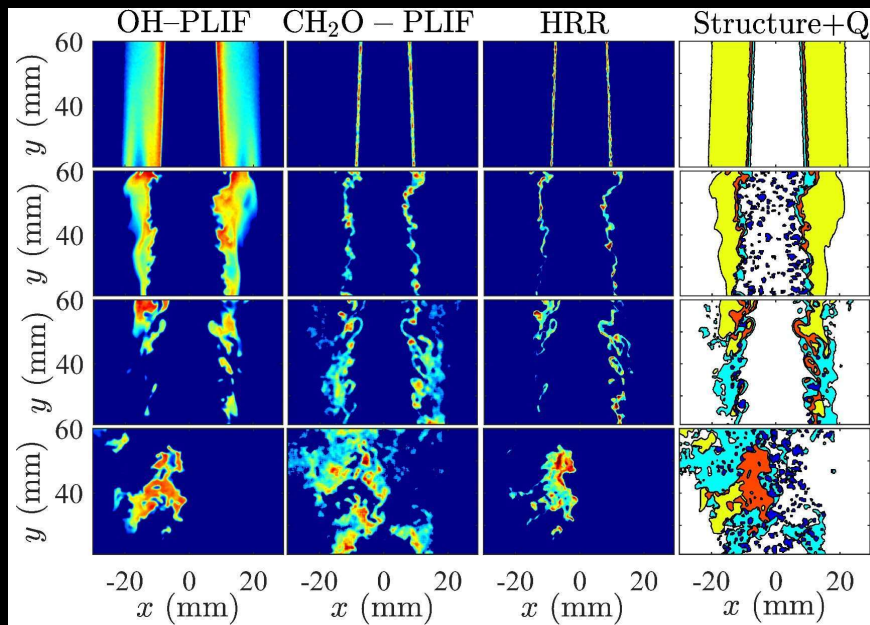
Mohammadnejad et al. (CNF, 2021)

Combustion for Propulsion and Power Laboratory



1. Two controversial observations: Our hypot.

$Ka = 0.3$ $Ka = 14$ $Ka = 25$ $Ka = 76$

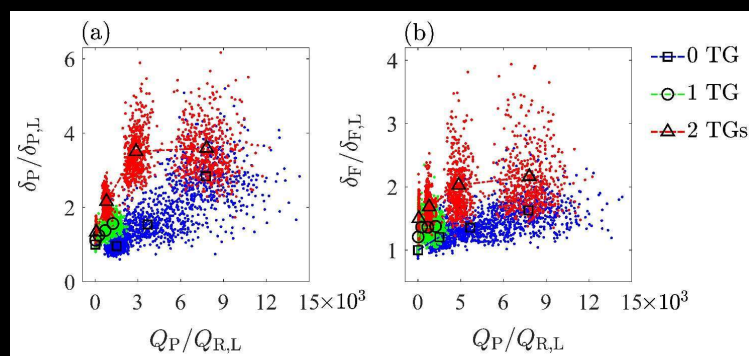


Mohammadnejad et al. (CNF, 2021)

Combustion for Propulsion and Power Laboratory



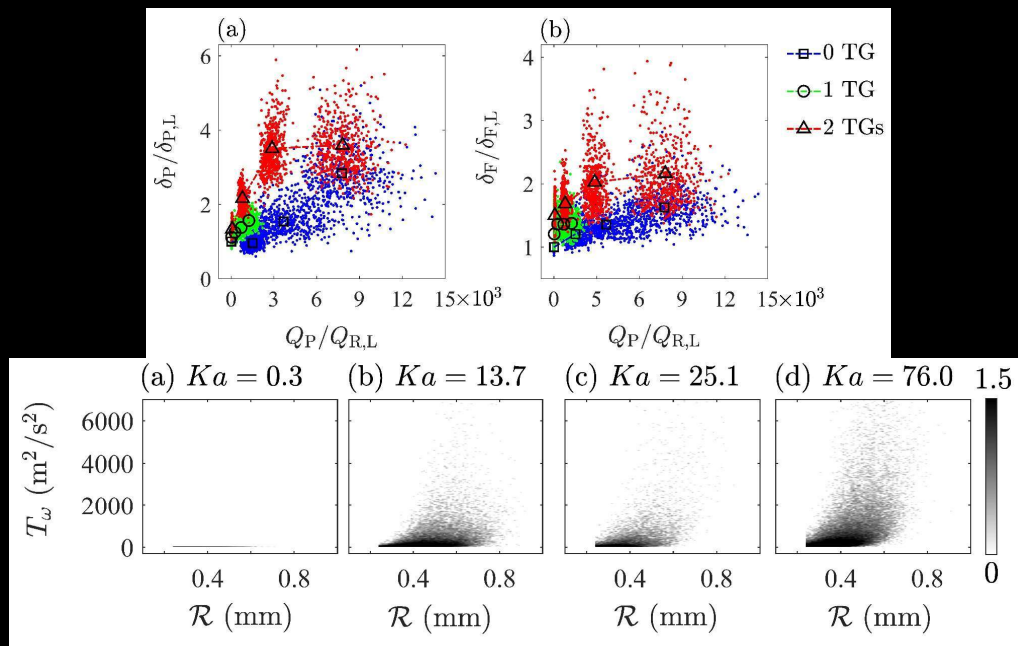
1. Two controversial observations: Our hypot.



Combustion for Propulsion and Power Laboratory



1. Two controversial observations: Our hypot.

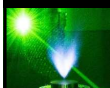
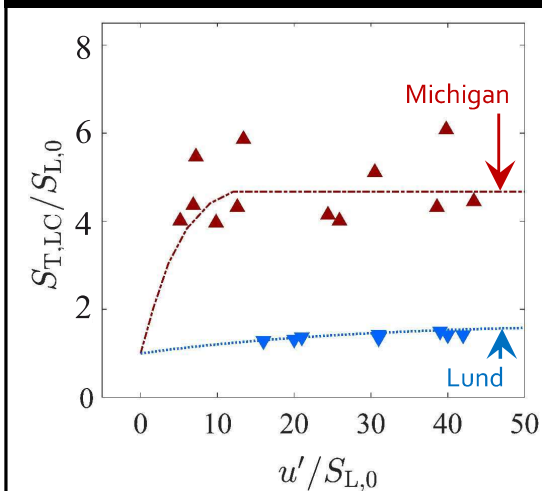


Mohammadnejad et al. (CNF, 2020)

Combustion for Propulsion and Power Laboratory



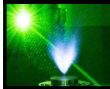
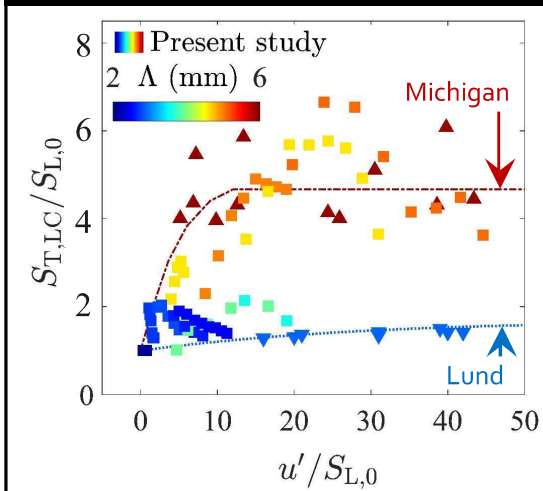
2. Non-flamelets and how fast we burn



Combustion for Propulsion and Power Laboratory



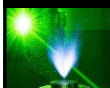
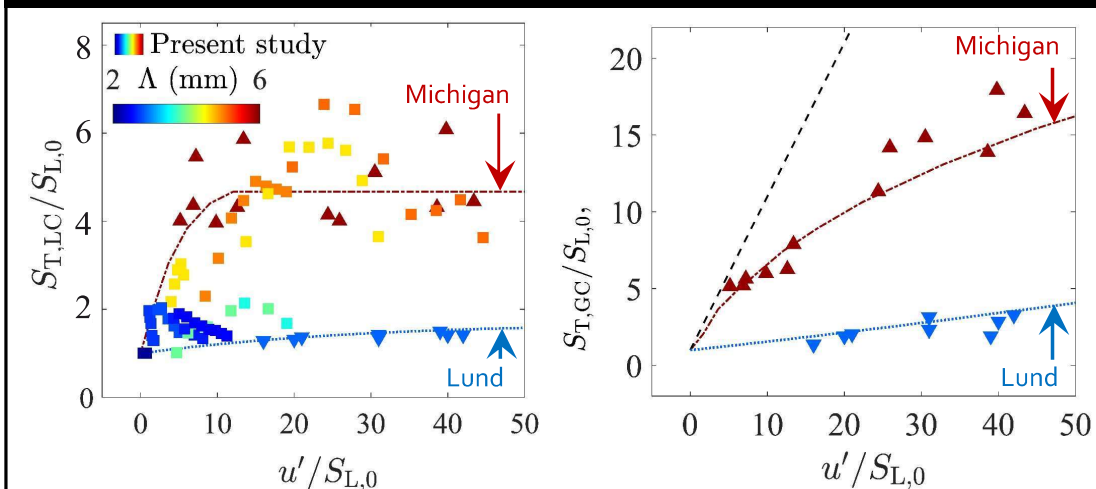
2. Non-flamelets and how fast we burn



Combustion for Propulsion and Power Laboratory



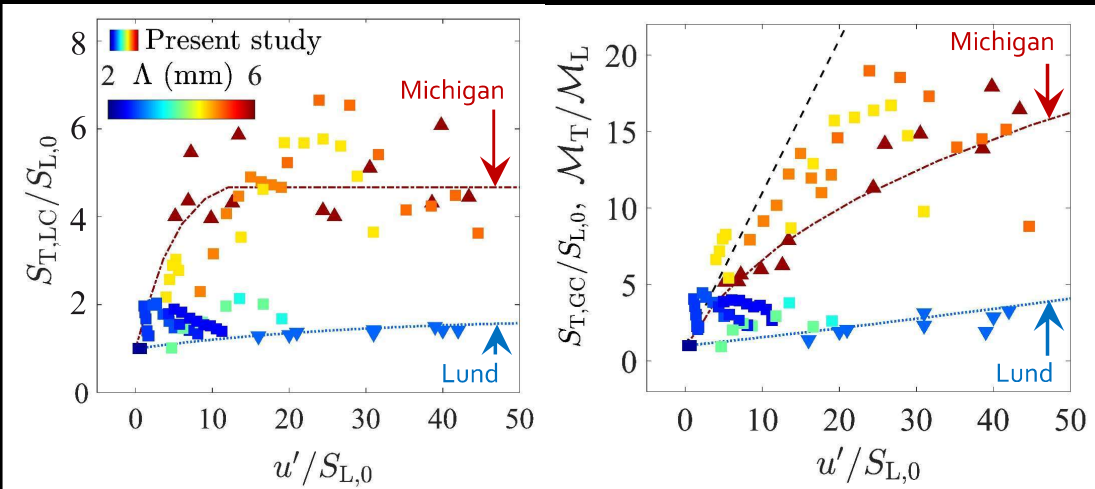
2. Non-flamelets and how fast we burn



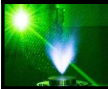
Combustion for Propulsion and Power Laboratory



2. Non-flamelets and how fast we burn



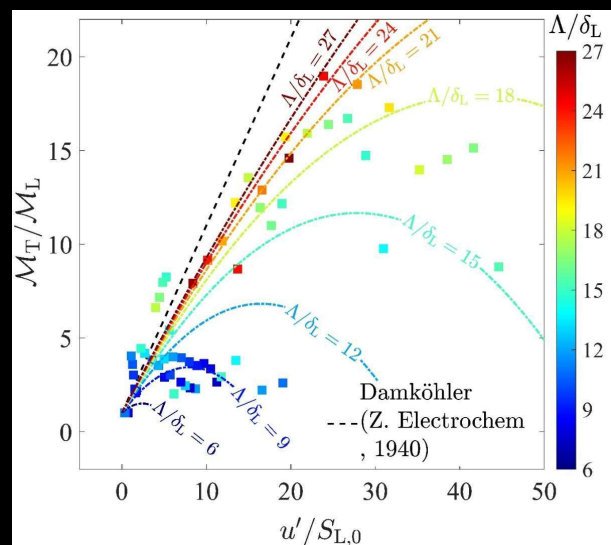
Mohammadnejad et al. (CNF, 2021)



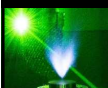
Combustion for Propulsion and Power Laboratory



2. Non-flamelets and how fast we burn



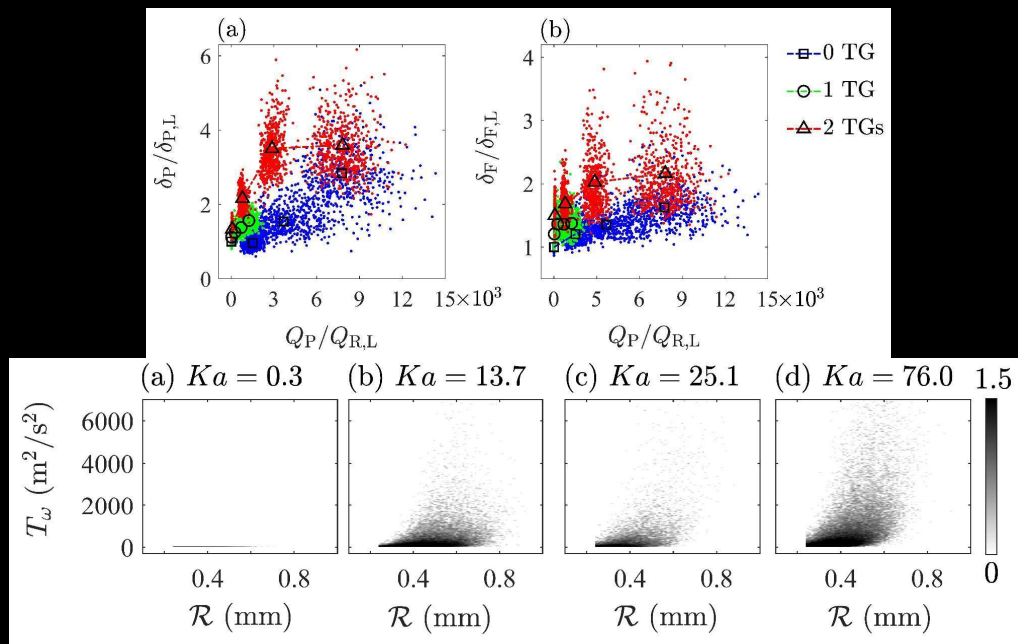
$$\frac{M_T}{M_L} = 1 + \frac{u'}{S_{L0}} - 3.1 Da^{-2} - 3.5 Da^{-1}$$



Combustion for Propulsion and Power Laboratory



3. Turbulent eddy energy distribution matters

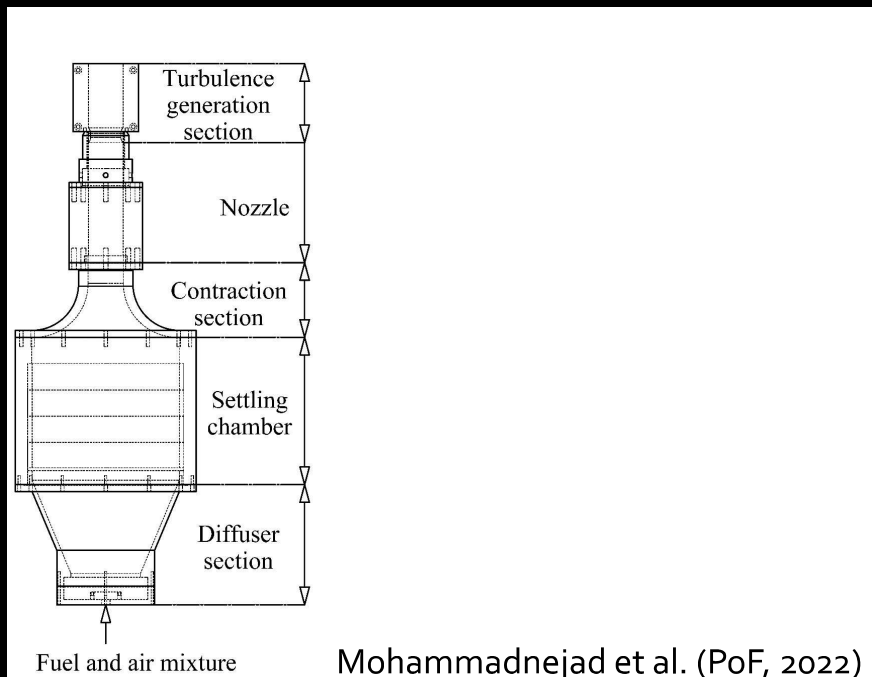


Mohammadnejad et al. (CNF, 2020)

Combustion for Propulsion and Power Laboratory



4. What is next?

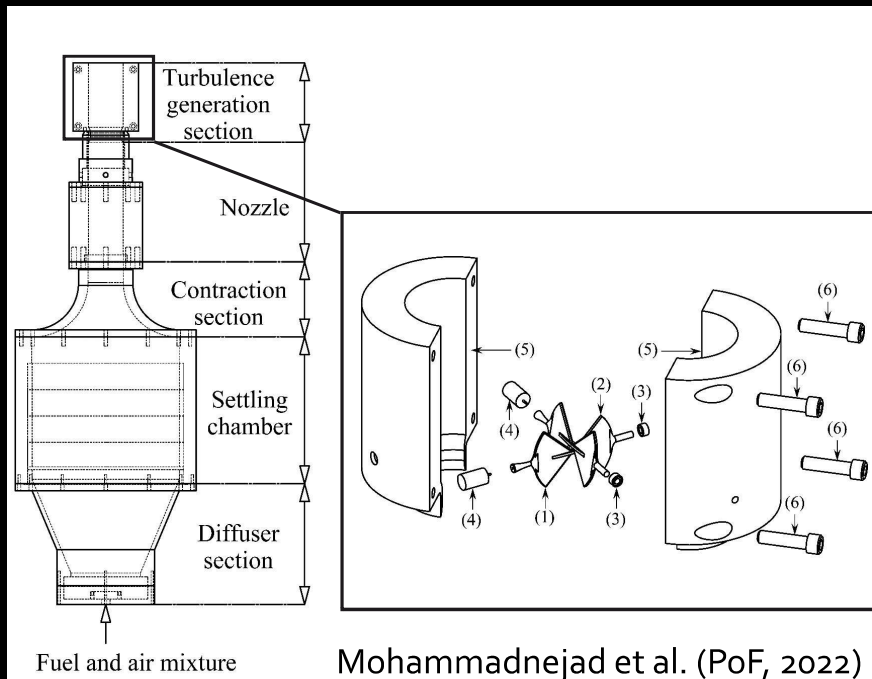


Mohammadnejad et al. (PoF, 2022)

Combustion for Propulsion and Power Laboratory



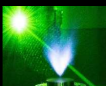
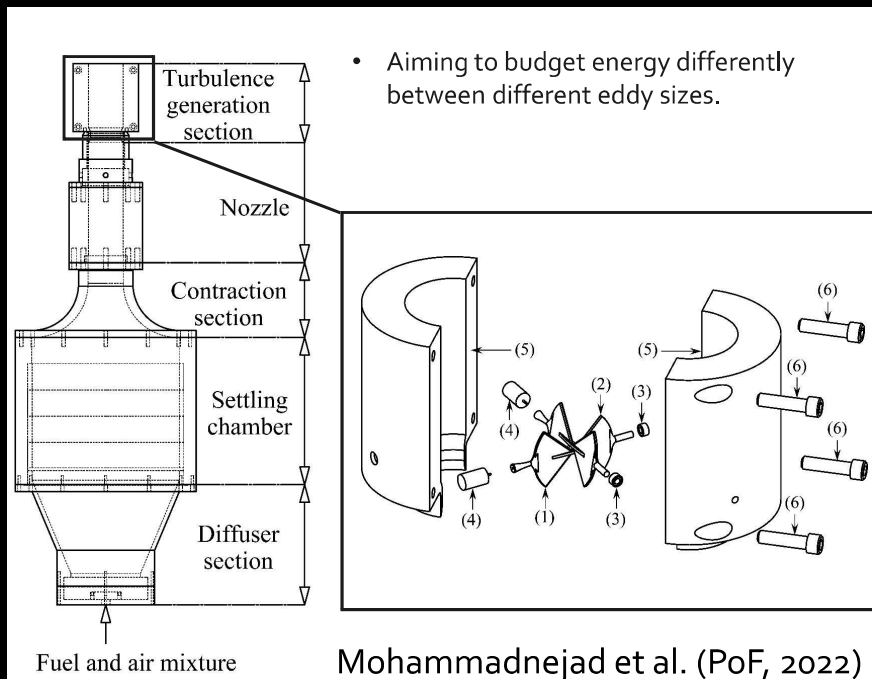
4. What is next?



Combustion for Propulsion and Power Laboratory



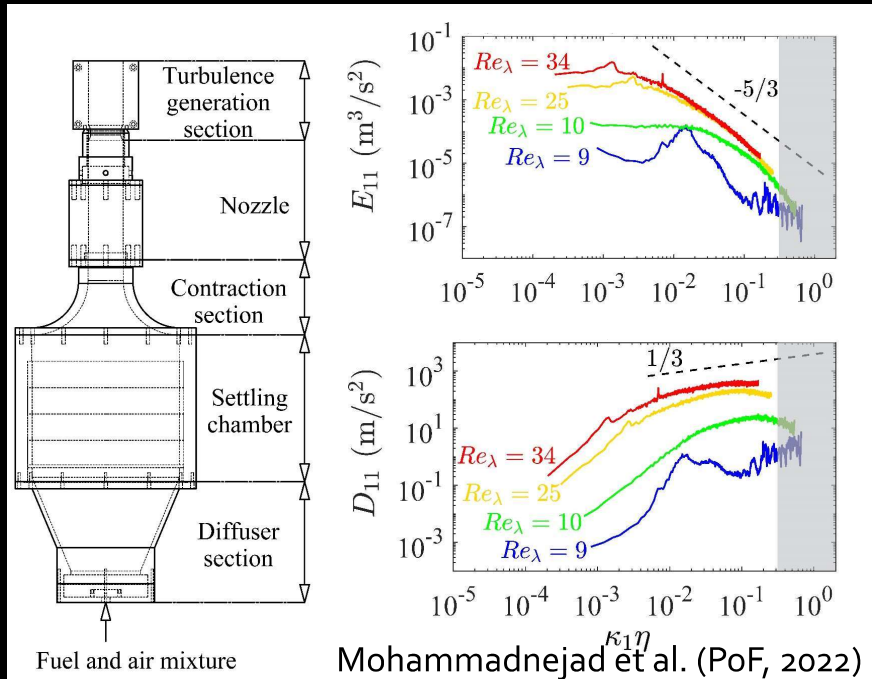
4. What is next?



Combustion for Propulsion and Power Laboratory



4. What is next?



Combustion for Propulsion and Power Laboratory



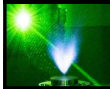
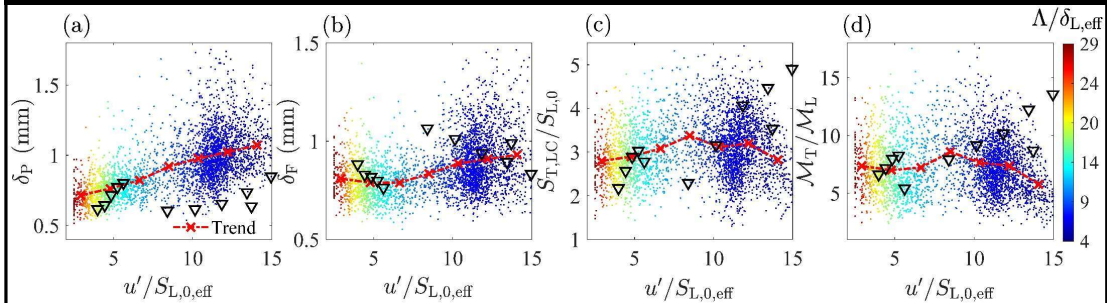
Thank you.

Combustion for Propulsion and Power Laboratory



Some questions/thoughts

- Local extinctions stratify the reactants. How does this influence how fast we burn?



Combustion for Propulsion and Power Laboratory



TNF/PTF Workshops

Blank Page

Turbulent Flame Speed Based on the Mass Flow Rate: Theory and its Validation

PTF and TNF Workshops, Vancouver, July 22-23, 2022

Swetaprovo Chaudhuri and Bruno Savard
University of Toronto and Polytechnique Montréal



1

1

Anatomy of a turbulent flame speed scaling: outline

- Mass flow through an isotherm and average mass flow rate through all isotherms: turbulent flame speed, in a **statistically planar and stationary turbulent premixed flame configuration for unity Le , $Ka > 1$, $Re_t > 100$**
- Closure 1: Density weighted flame displacement speed
- Closure 2: Scalar dissipation rate and scalar variance
- High $Ka=280$, n-heptane/air $\phi=0.9$, unity Le , DNS dataset by Savard et al. PROCI 2015 for validation



2

2

Mass flow rate through an isotherm

$$c = \frac{T - T_u}{T_b - T_u}$$

$$c = c^*$$



$$\dot{m}_{c^*} = - \int_{A_{T_{c^*}}} \rho \vec{v}_r \cdot \hat{n} dA$$

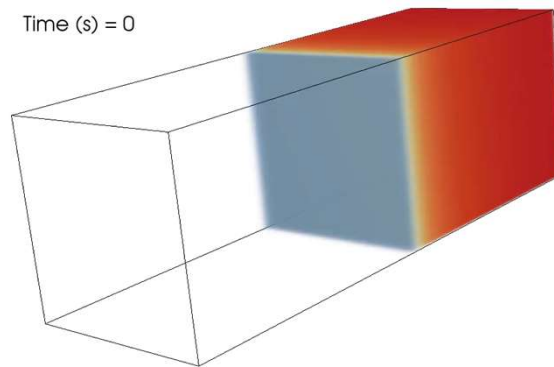
$$\dot{m}_{c^*} = - \int_{A_{T_{c^*}}} \rho (-S_d \hat{n}) \cdot \hat{n} dA$$

flame displacement speed

3

3

Time (s) = 0



T (K) 300 2100

Song et al. CNF 2022

Averaged mass flow rate through all isotherms i.e., entire flame

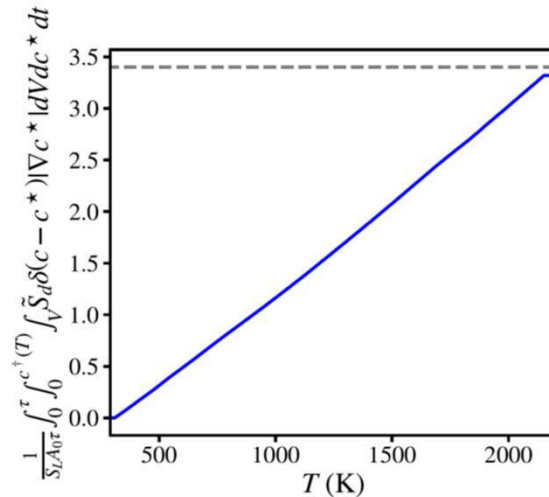
$$\frac{1}{\tau} \int_0^\tau \int_0^1 \int_{A_{T_{c^*}}} S_d dA dc^* dt = \rho_u A_0 S_T$$

$$S_T = \frac{1}{A_0 \tau} \int_0^\tau \int_0^1 \int_V \tilde{S}_d \delta(c - c^*) |\nabla c^*| dV dc^* dt$$

density weighted flame displacement speed

4

$$S_T = \frac{1}{A_0 \tau} \int_0^\tau \int_0^1 \int_V \tilde{S}_d \delta(c - c^*) |\nabla c^*| dV dc^* dt$$



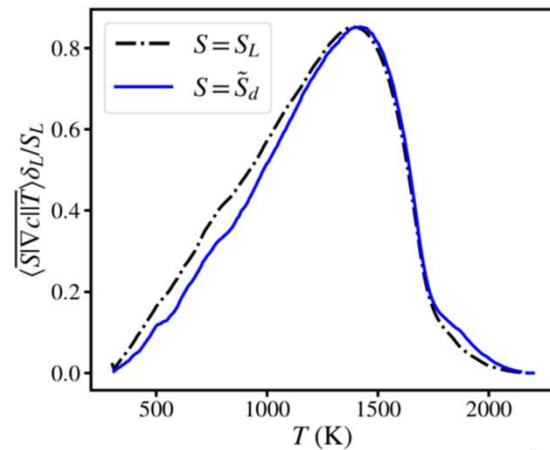
Turbulent flame speed based on average mass flow rate

$$S_T = \frac{1}{A_0 \tau} \int_0^\tau \int_V \tilde{S}_d |\nabla c| dV dt$$

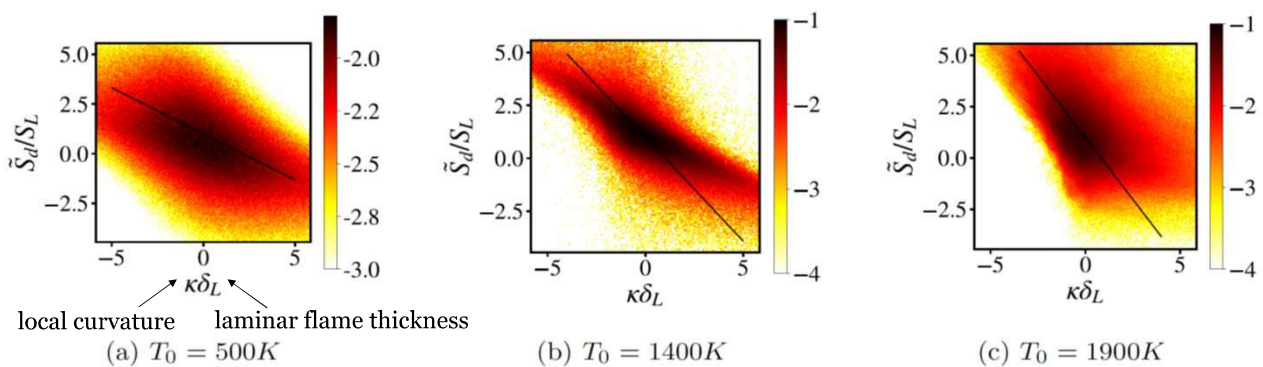
$$S_T = \delta_T \left\langle \overline{\tilde{S}_d |\nabla c|} \right\rangle$$

Closure 1: $\langle \tilde{S}_d |\nabla c| \rangle \approx S_L \langle |\nabla c| \rangle$

↑
unstretched laminar flame speed



Density weighted flame displacement speed

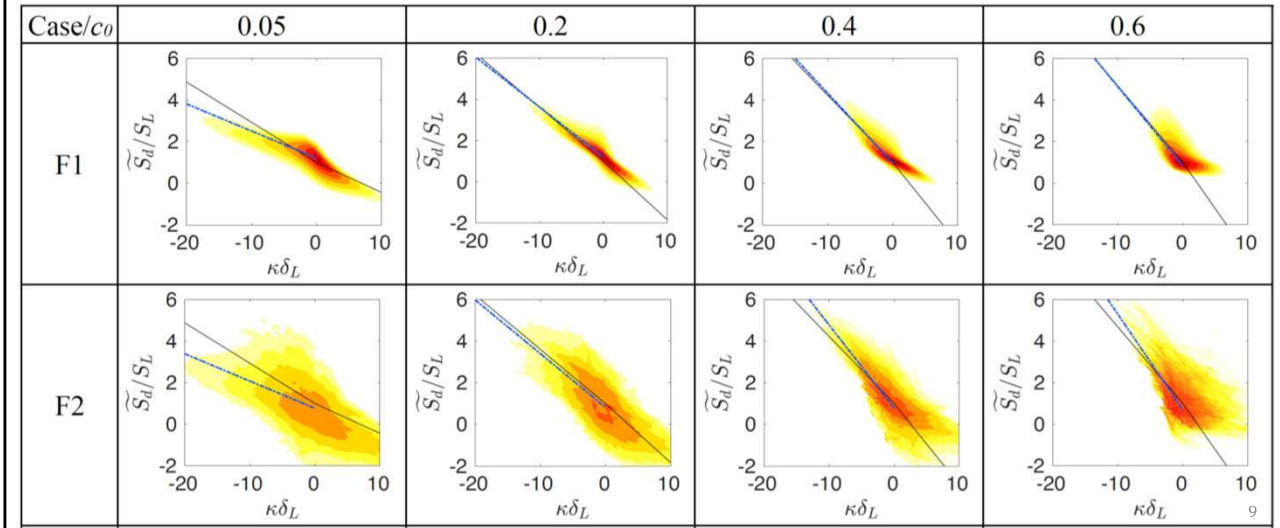


Black line is 1D, transient, flame-flame interaction model: $\tilde{S}_d = S_L - 2\tilde{\alpha}_0 \kappa$

H₂-air ($Re_t \sim 700$; Ka 20-1000)

Black line for $\kappa < 0$ is flame-flame interaction model: $\tilde{S}_d = S_L - 2\tilde{\alpha}_0\kappa$

Yuvraj et al. CNF 2022



9

Why does the closure 1 work ($Le=1$)?

$$S_T = \delta_T \langle \tilde{S}_d |\nabla c| \rangle$$

Overall trends of the JPDF could be modeled as

$$\tilde{S}_d = S_L - \mathcal{A}_1 \kappa \quad \forall \kappa \leq 0$$

$$\tilde{S}_d = S_L - \mathcal{A}_2 \kappa \quad \forall \kappa > 0$$

$$S_T = \delta_T \langle S_L |\nabla c| \rangle - \delta_T \langle \mathcal{A}_1 \kappa |\nabla c| \rangle_{\kappa \leq 0} - \delta_T \langle \mathcal{A}_2 \kappa |\nabla c| \rangle_{\kappa > 0}$$



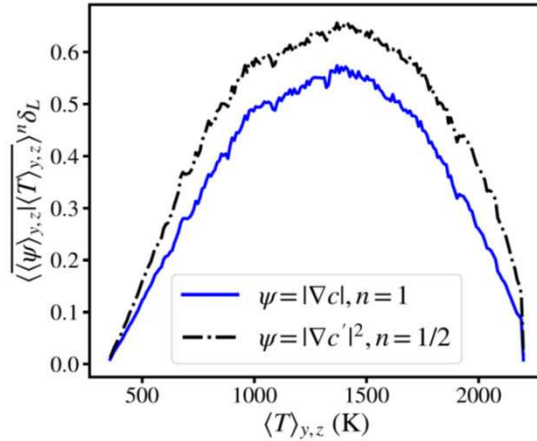
$$\frac{S_T}{S_L} = \delta_T \langle |\nabla c| \rangle + \frac{\delta_T}{S_L} (\mathcal{A}_1 k_1 - \mathcal{A}_2 k_2)$$

10

10

Closure 2:

$$\langle |\nabla c| \rangle \approx \langle |\nabla c'| \rangle = \langle (\nabla c' \cdot \nabla c')^{1/2} \rangle \approx \langle \nabla c' \cdot \nabla c' \rangle^{1/2}$$

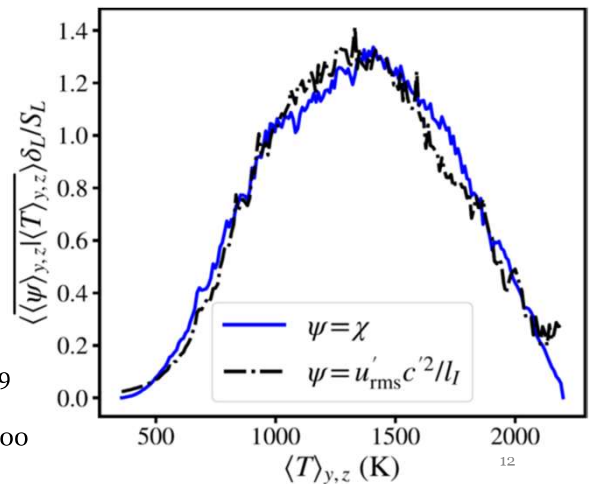


Scalar dissipation rate

$$\langle \bar{\chi} \rangle = 2 \langle \alpha \nabla c' \cdot \nabla c' \rangle \approx 2\alpha_c \langle \nabla c' \cdot \nabla c' \rangle \sim \frac{u'_{rms} \langle \overline{c'^2} \rangle}{l_I} = \frac{u'_r \langle \overline{c'^2} \rangle_r}{r}$$

Using (see paper for derivation and validation)

$$\ell_T = \delta_T \langle \overline{c'^2} \rangle^{1/2} = 1.75 l_I$$



S. Chaudhuri and B. Savard, <https://arxiv.org/abs/2202.06719>

Final scaling

$$\frac{S_T}{S_L} \sim \left[\frac{u'_{rms} l_I}{S_L \delta_L} \right]^{1/2}$$

$$\frac{S_T}{S_L} \sim Re_T^{1/2}$$

Summary:

- Turbulent flame speed based on average mass flow rate through all isotherms constituting a turbulent premixed flame in a cuboid:

$$S_T = \delta_T \left\langle \tilde{S}_d |\nabla c| \right\rangle$$

- Closure 1: $\left\langle \tilde{S}_d |\nabla c| \right\rangle \approx S_L \left\langle |\nabla c| \right\rangle$

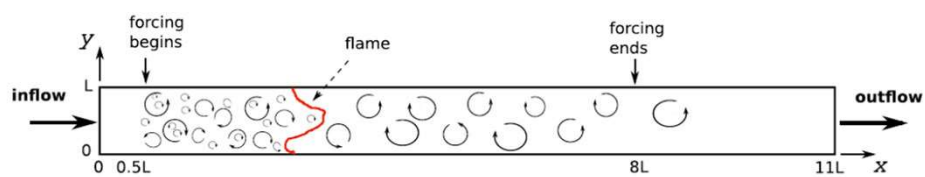
- Closure 2: Dissipation rate anomaly

- For unity Le flames $\frac{S_T}{S_L} \sim Re_T^{1/2}$

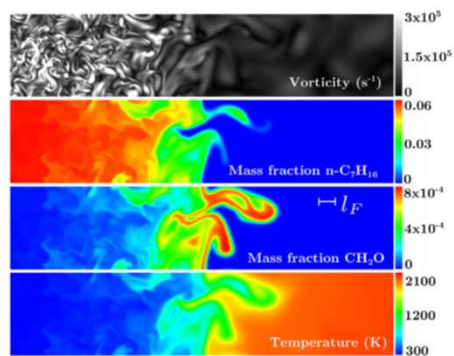
Thank you

15

Validation dataset: n-heptane/air flame DNS, unit Le



	Unity Le
Domain size	$11L \times L \times L$
L (m)	2.3×10^{-3}
Grid	$1408 \times 128 \times 128$
Δx (m)	1.8×10^{-5}
η (m)	9×10^{-6}
n_F	23
Δt (s)	8×10^{-8}
ϕ	0.9
S_L (m/s)	0.29
l_F (mm)	0.43
l/l_F	1.0
u'/s_L	21
$Ka = t_F/t_\eta$	280
$Re_t = (u'l)/\nu$	190



B. Savard et al. PROCI 2015

16

Part 1 – Closing the balance of progress of reaction on a turbulent Bunsen flame: A high-speed Mie scattering system was used to evaluate the closure of the conservation of mean progress variable in a stabilised piloted turbulent Bunsen flame. Velocity distributions were measured by stereo particle image velocimetry techniques by using a 527 nm laser at 3 kHz. Flame edges were detected by the number density method applied to the first frame of Mie scattering images. The conservation equation of the mean progress variable was analyzed along different streamtubes as a balance of velocities, including convective terms for turbulent velocity, turbulent and molecular diffusion fluxes and the mean reaction. Each term was directly measured or estimated using thin flame approximation, and its uncertainty was evaluated based on propagation of experimentally measured statistical correlations. The largest terms as expected were the convective and reaction terms, with smaller roles to turbulent and molecular diffusion across the flame brush. Countergradient diffusion and transition to gradient diffusion were observed. The balance of terms in the conservation equations not consistently observed across the flame brush within the reckoned uncertainties. We offer some observations on the possible reasons for the mismatch, including spatial filtering and 3D effects, and suggest possible future alternatives.

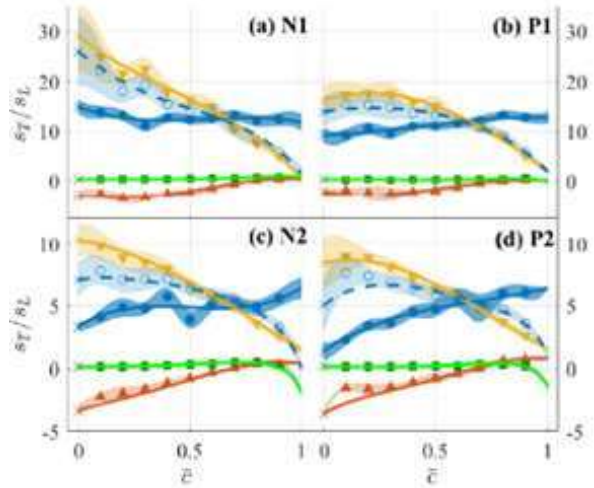


Fig. 1: Conservation of burning velocities considering different terms along streamlines in Case 8 with $\phi=1.2$.

Part 2 – Adaptive PIV interrogation for spherical propagation: The measurement of 3D flame surfaces in turbulent flames remains an ongoing challenge, which is important for the understanding of the behavior of turbulence-flame interactions. We have used a scanning sheet approach, powered by Mie scatter using a Nd:YLF laser at up to 10 kHz to scan half of the same turbulent flame surface, which is reconstructed using conventional methods. We find that the 3D surface density to be significantly higher than the measured 2D surfaces. This difference may contribute to close the discrepancy often found in the literature between the 2D area measurements rotated by symmetry to obtain the 3D area, and the actual 3D measured surface area.

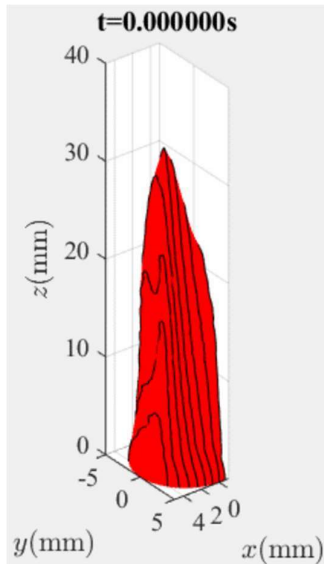


Fig. 2: Sample recon-structed surface using scanning method

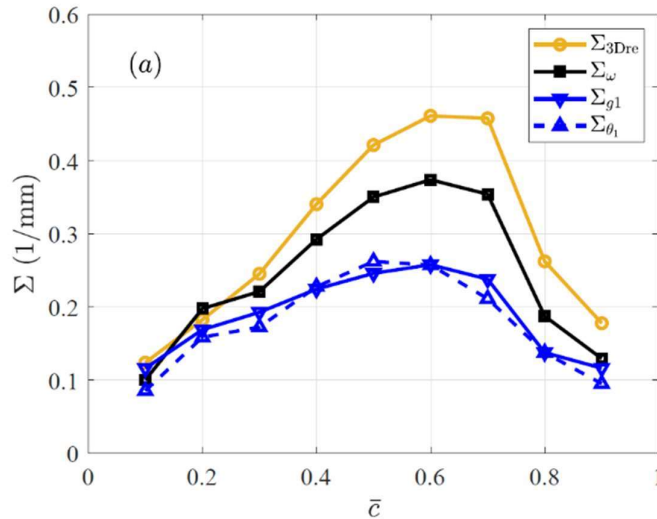


Fig. 3: Measured flame surface density using different methods, as a function of mean surface density: Blue: 2D surface densities using two different reference centreline planes; black: local 3D flame surface density using cross planar technique, yellow: 3D scanning surface measurement.

Closing the balance of progress of reaction on a turbulent Bunsen flame

Yutao Zheng, Lee Weller, Simone Hochgreb

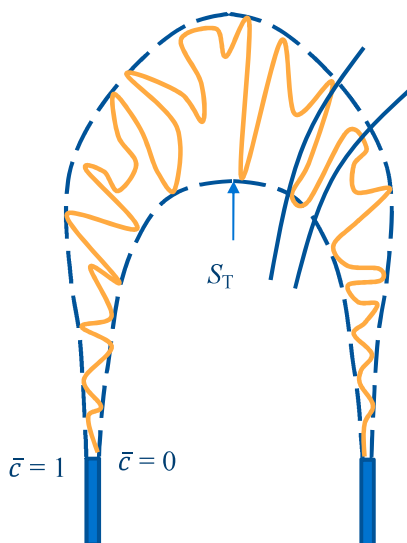
TNF-PTF – July 2022



Yutao Zheng

Lee Weller

Balance of \tilde{c} in statistically steady flames



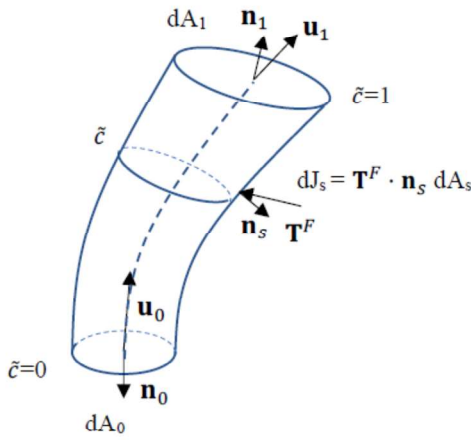
Which turbulent flame speed? What area to choose?

Don't choose. Determine all terms along a streamline.

$$\bar{\rho} \tilde{\mathbf{u}} \cdot \nabla \tilde{c} = -\nabla \cdot \mathbf{T}_c^F + \nabla \cdot \mathbf{T}_c^D + \bar{\omega}_c \quad \div \frac{\bar{\rho}}{|\nabla \tilde{c}|} \quad \begin{aligned} \mathbf{T}_c^F &= \overline{\rho \mathbf{u}'' c''} \\ \mathbf{T}_c^D &= \overline{\rho D_c \nabla c} \end{aligned}$$

$$s_{T,c} = \tilde{\mathbf{u}} \cdot \mathbf{n} = s_F + s_D + s_R$$

Conservation of \tilde{c} in statistically steady flames



$$\bar{\rho} \tilde{\mathbf{u}} \cdot \nabla \tilde{c} = -\nabla \cdot \mathbf{T}_c^F + \nabla \cdot \mathbf{T}_c^D + \bar{\omega}_c \quad \div \frac{\bar{\rho}}{|\nabla \tilde{c}|}$$

$$\mathbf{T}_c^F = \overline{\rho \mathbf{u}'' c''}$$

$$\mathbf{T}_c^D = \overline{\rho D_c \nabla c}$$

$$s_{T,d} = \tilde{\mathbf{u}} \cdot \mathbf{n} = s_F + s_D + s_R$$

$$s_F = -\frac{\nabla \cdot \mathbf{T}_c^F}{\bar{\rho} |\nabla \tilde{c}|}$$

$$s_D = \frac{\nabla \cdot \mathbf{T}_c^D}{\bar{\rho} |\nabla \tilde{c}|}$$

$$s_R = \frac{\bar{\omega}_c}{\bar{\rho} |\nabla \tilde{c}|} = s_L I_0 \frac{\bar{\rho} \Sigma}{\bar{\rho} |\nabla \tilde{c}|}$$

Burner setup: piloted methane flame

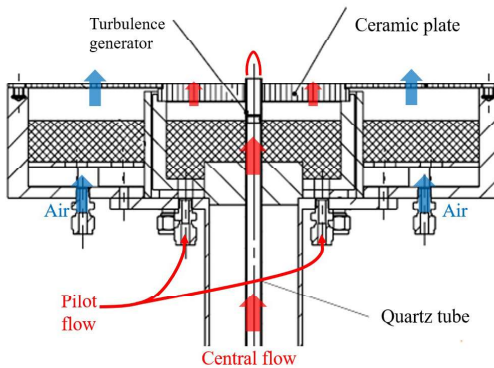


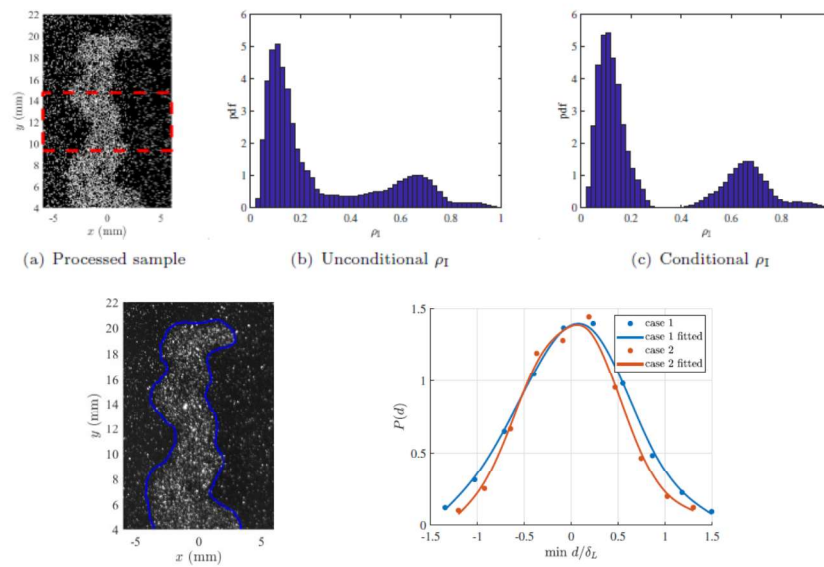
Table 1: Experimental cases for validation of flame brush theory

	Φ	$\bar{U}_0^{(1)}$ (m/s)	$v_{y,rms}$ (m/s)	u' (m/s)	$s_L^{(2)}$ (m/s)	l_0 (mm)	$\delta_L^{(2)}$ (mm)	Re_T	Ka
Case 1	0.9	5.3	0.52	0.81	0.320	1.3	0.479	67.5	4.2
Case 2	0.8	4.8	0.45	0.78	0.257	1.3	0.539	65.0	6.3
Case 3	0.8	4.1	0.47	0.73	0.257	1.3	0.539	60.8	6.1
Case 4	0.9	6.0	0.64	1.01	0.320	1.3	0.479	84.1	4.7
Case 5	1.0	5.6	0.61	1.00	0.361	1.3	0.451	83.3	3.6
Case 6	1.0	5.9	0.63	0.99	0.361	1.3	0.451	82.4	3.6
Case 7	1.1	5.3	0.56	0.93	0.365	1.3	0.440	77.5	3.4
Case 8	1.2	5.5	0.49	0.78	0.319	1.3	0.477	65.0	4.1

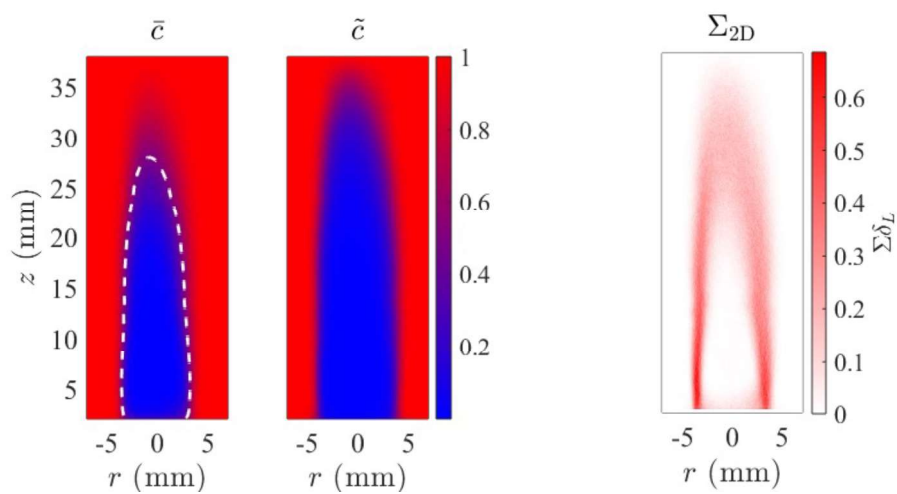
⁽¹⁾ Value for $T_a = 15^\circ C$

⁽²⁾ s_L and δ_L were calculated using Cantera 2.5.1 [32] and GRI Mech 3.0 [33]

Flame edge detection: Number density method

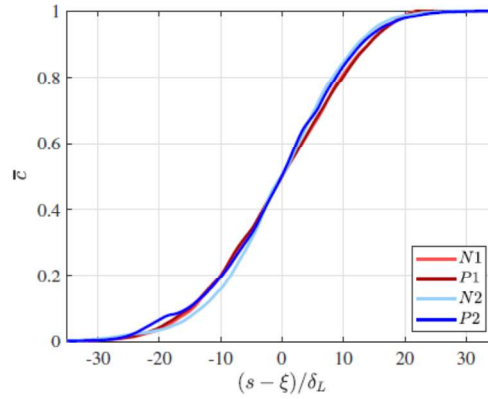
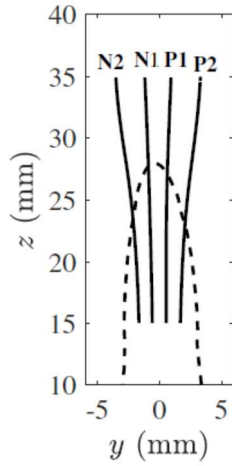


\bar{c} and Σ



$$\Sigma = |\nabla c \delta(c - c^*)|$$

\bar{c} and \tilde{c} along streamlines

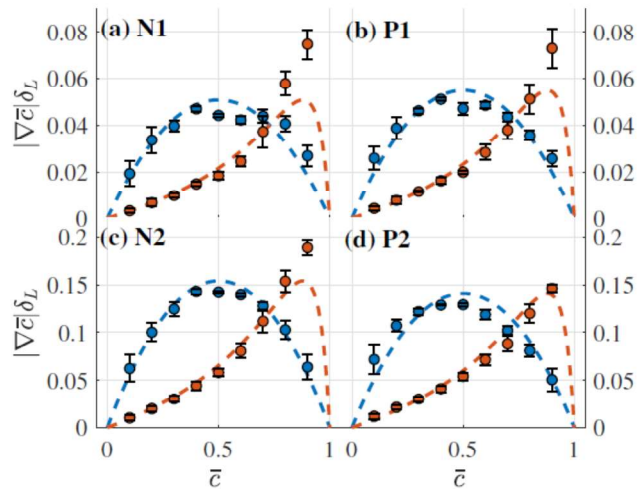


$$\bar{c}_1(s) = \int_{-\infty}^s \frac{1}{\sqrt{2\pi}\sigma} \exp\left(-\frac{(s-\xi)^2}{2\sigma^2}\right) ds$$

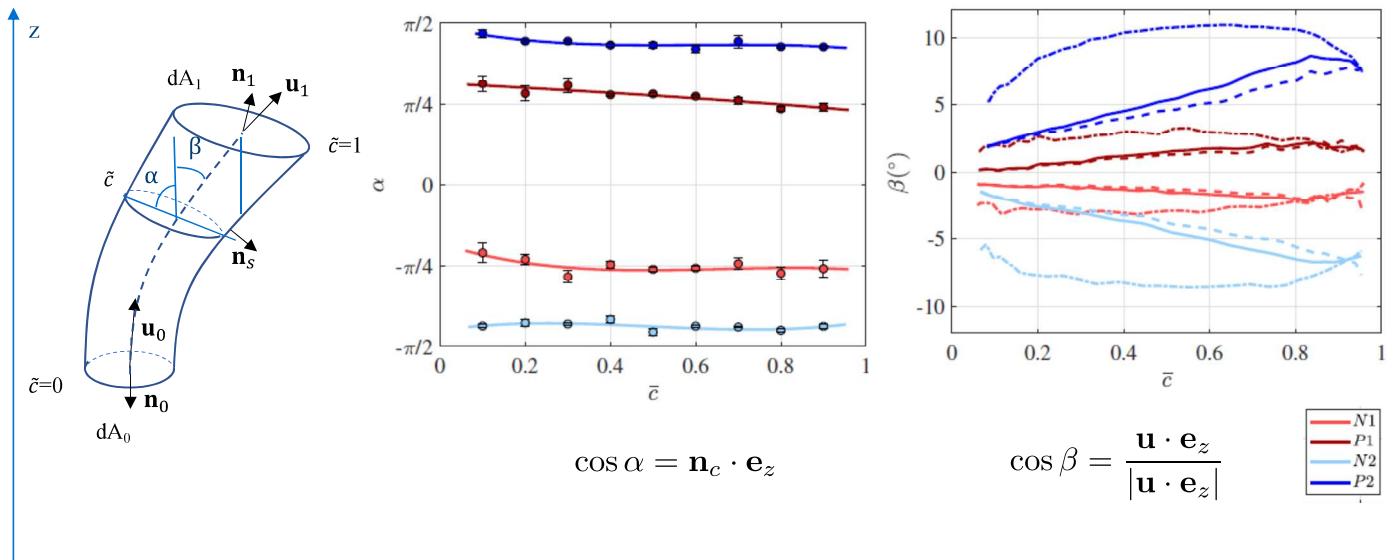
$\nabla \bar{c}$ and $\nabla \tilde{c}$ along streamlines

$$\nabla(\bar{\rho}\tilde{c}) = \bar{\rho}\nabla\tilde{c} + \tilde{c}\nabla\bar{\rho} = \rho_b\nabla\tilde{c}$$

$$\begin{aligned} \nabla\tilde{c} &= \frac{\rho_b}{\bar{\rho}}\nabla\tilde{c} - \frac{\rho_b\tilde{c}}{\bar{\rho}^2}\nabla\bar{\rho} \\ &= \frac{\rho_b}{\bar{\rho}}\nabla\tilde{c} - \frac{\rho_b\tilde{c}}{\bar{\rho}^2}\rho_u\left(\frac{1}{\tau} - 1\right)\nabla\tilde{c} \\ &= \left(1 - \tilde{c}\frac{\rho_b - \rho_u}{\bar{\rho}}\right)\frac{\rho_b}{\bar{\rho}}\nabla\tilde{c} \\ &= (\rho_u + \rho_u\tilde{c}\left(\frac{1}{\tau} - 1\right) - \tilde{c}\rho_b + \tilde{c}\rho_u)\frac{\rho_b}{\bar{\rho}^2}\nabla\tilde{c} \\ &= \frac{\rho_u\rho_b}{\bar{\rho}^2}\nabla\tilde{c} \end{aligned}$$

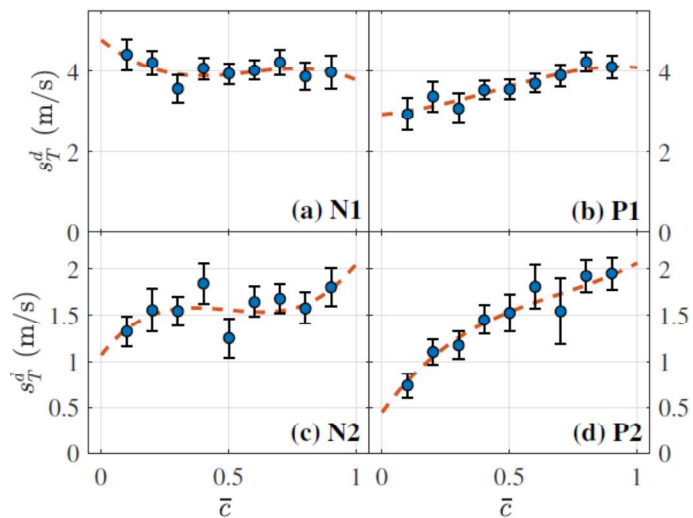


Angles: α and β



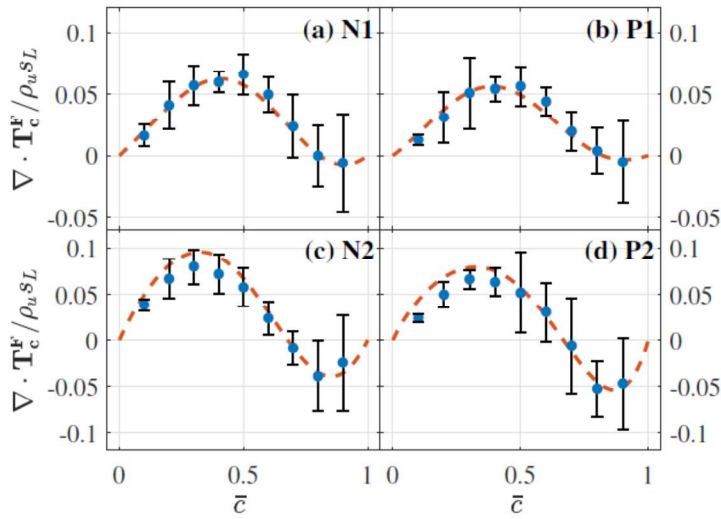
Local displacement speed, $s_{T,d}$

$$s_{T,d} = \tilde{\mathbf{u}} \cdot \hat{\mathbf{n}} = |\tilde{\mathbf{u}}| \cos(\alpha - \beta)$$



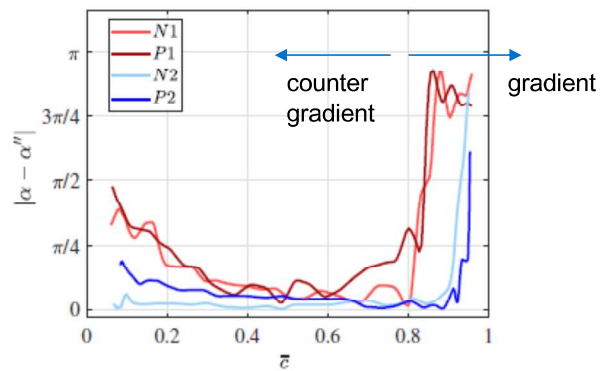
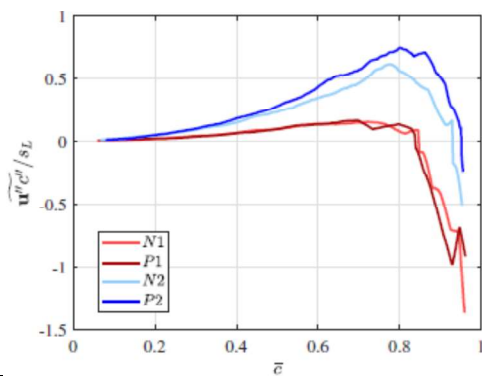
Turbulent flux

$$\mathbf{T}_c^F = \overline{\rho \mathbf{u}'' c''}$$



Turbulent fluxes: gradient and countergradient diffusion

$$\frac{s_F}{s_L}$$

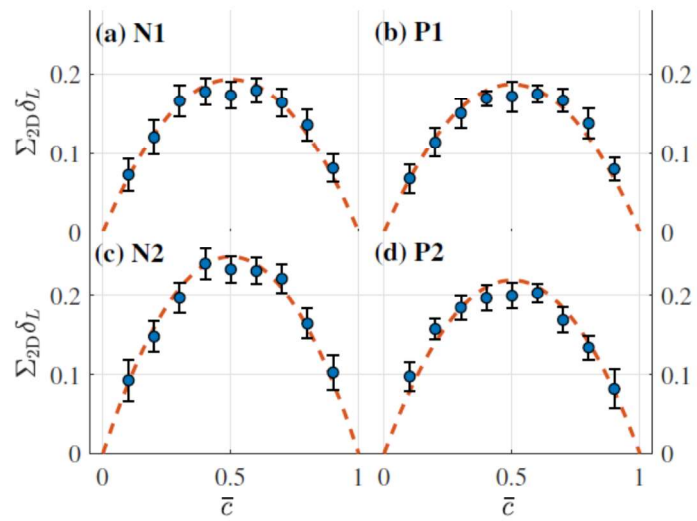


$$\mathbf{T}_c^F = \overline{\rho \mathbf{u}'' c''}$$

$$\begin{aligned} \overline{\rho \mathbf{u}'' c''} &= \overline{\rho(\mathbf{u} - \bar{\mathbf{u}})(c - \bar{c})} \\ &= \rho_b \bar{\mathbf{u}}_b \bar{c} - \bar{\rho} \bar{\mathbf{u}} \bar{c} = \rho_b \bar{c} (\bar{\mathbf{u}}_b - \bar{\mathbf{u}}) \\ &= \bar{\rho} \bar{\mathbf{u}} (1 - \bar{c}) - \rho_u \bar{\mathbf{u}}_u (1 - \bar{c}) = \rho_u (1 - \bar{c}) (\bar{\mathbf{u}} - \bar{\mathbf{u}}_u) \end{aligned}$$

$$\cos \alpha'' = \frac{\tilde{\mathbf{u}}''}{|\tilde{\mathbf{u}}''|} \cdot \mathbf{e}_z$$

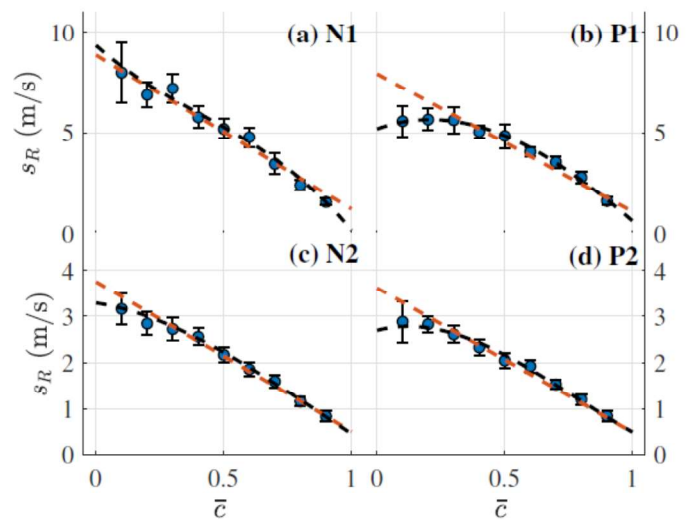
FSD along streamlines



Reaction terms, s_R

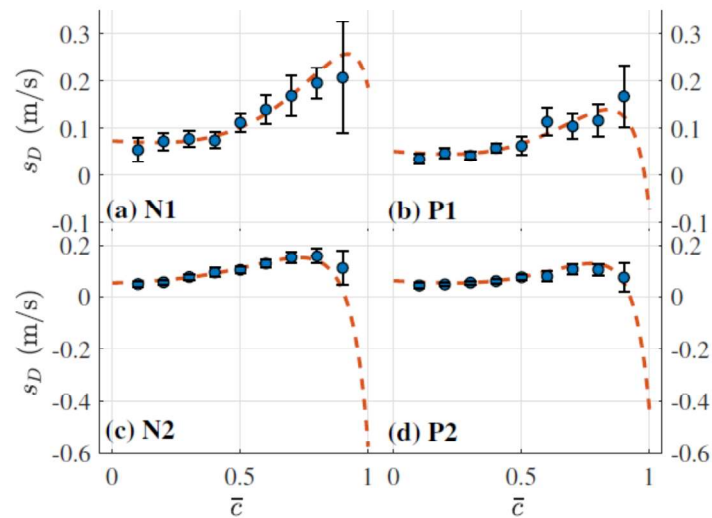
$$s_R = \frac{\bar{\omega}_c}{\bar{\rho} |\nabla \bar{c}|} \sim s_L \frac{\rho_u}{\bar{\rho}} \frac{\Sigma}{|\nabla \bar{c}|} = s_L \frac{\bar{\rho}}{\rho_b} \frac{\Sigma}{|\nabla \bar{c}|}$$

$$= s_L \tau \left(1 + \bar{c} \left(\frac{1}{\tau} - 1 \right) \right) \frac{k_{\Sigma}}{k_{|\nabla \bar{c}|}}$$

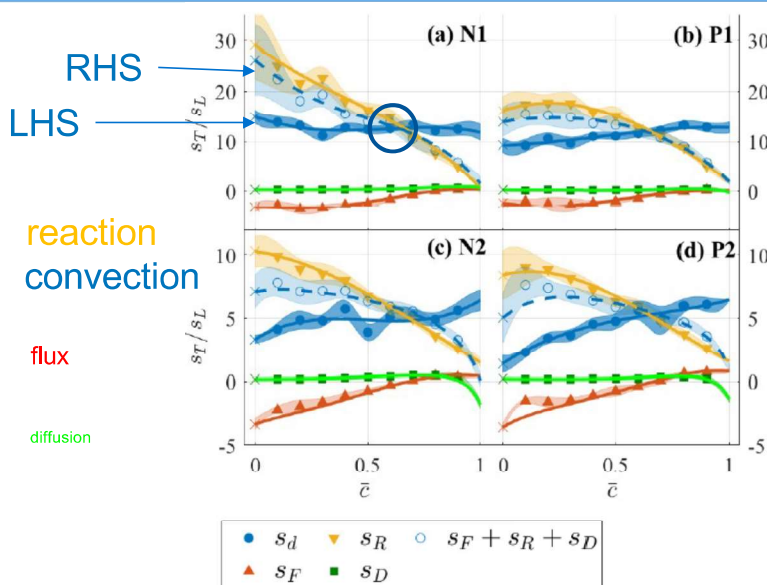


Molecular diffusivity term, s_D

$$s_D = \frac{\nabla \cdot T_c^D}{\bar{\rho} |\nabla \bar{c}|}$$

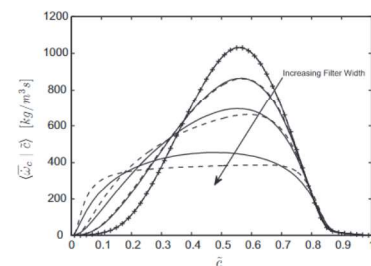


Closure of $s_{T,d} = s_F + s_D + s_R$



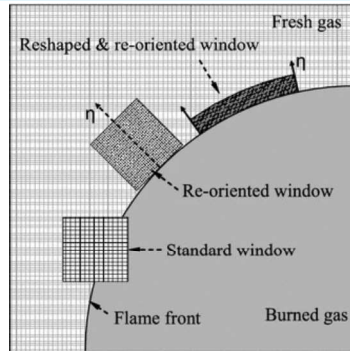
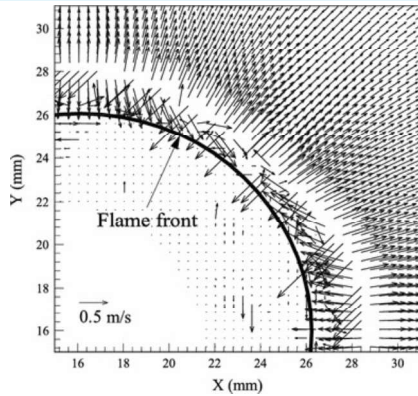
Error sources:

- Spatial filtering
- 3D vs 2D FSD
- Higher order 3D flux diffusion terms across streamlines (use adaptive PIV?)



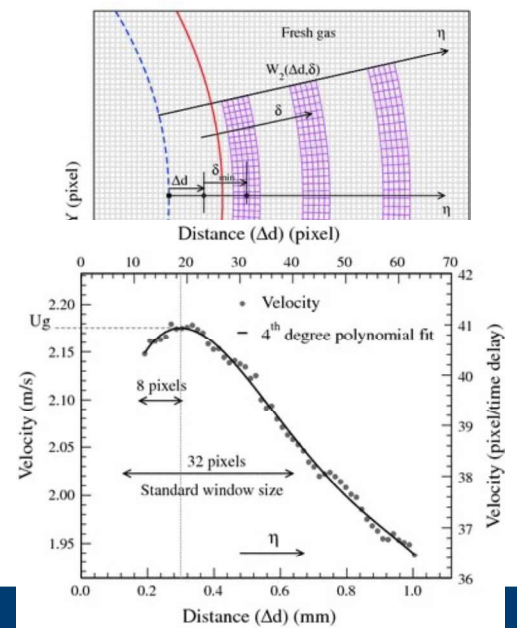
[25] S. Mukhopadhyay, R. Bastiaans, J. van Oijen, L. de Goey, Analysis of a filtered flamelet approach for coarse dns of premixed turbulent combustion, Fuel 144 (2015) 388–399.

Adaptive PIV interrogation for spherical propagation

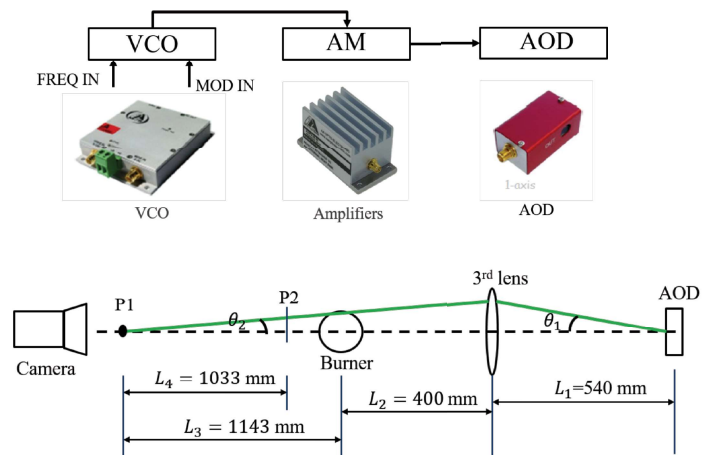
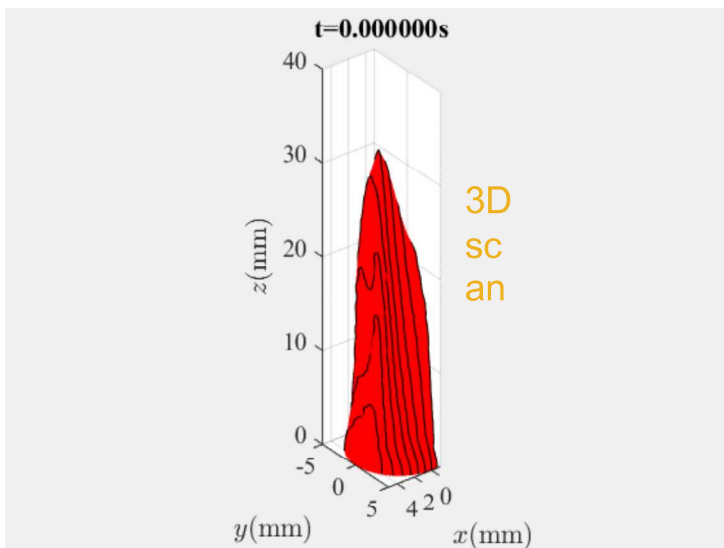


High spatial resolution allows for velocity determination

Balusamy, S., Cessou, A. & Lecordier, B. Exp Fluids 50, 1109 (2011)
 INSA-Rouen

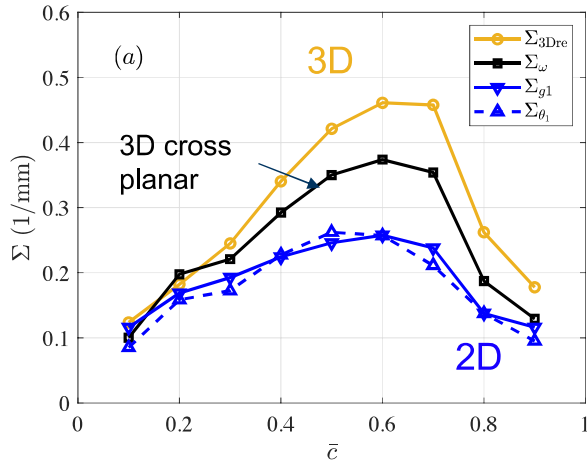


Preview: 3D scanning measurements of FSD at 5 kHz

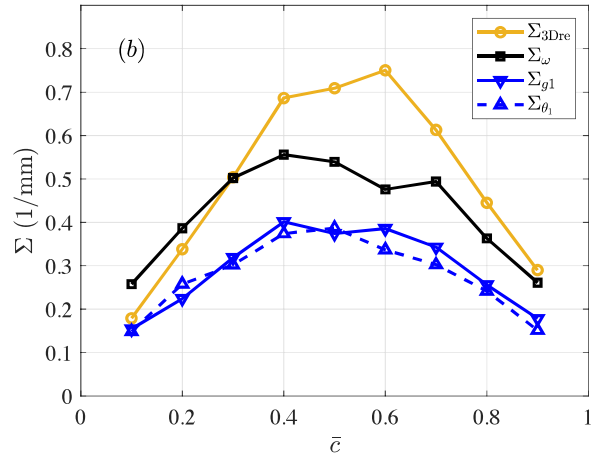


Local FSD: 3D scan vs 2D and 3D cross plane methods

Case 9 $\phi = 0.8$, $Re_T = 75$, $Ka = 9$



Case 10 $\phi = 0.8$, $Re_T = 77$, $Ka = 12$



Summary

- High frequency PIV Mie scatter used to close balance of terms in a flamelet framework
- Agreement is good progress value ~ 0.6 where signal is highest
- Main sources of error likely spatial resolution leading to filtering
- 3D matters! a 3D/stereo balance is underway

TNF/PTF Workshops

Blank Page



Friday Afternoon Panel Discussion:

Topics in Interest

Panelists: Peter Hamlington, Heinz Pitsch, Adam Steinberg, Fabian Hampf

Moderator: Sina Kheirkhah

Prompts (optional) sent prior to the workshop:

1. Some areas of turbulent combustion appear to be of immediate interest. Some of these are listed below:

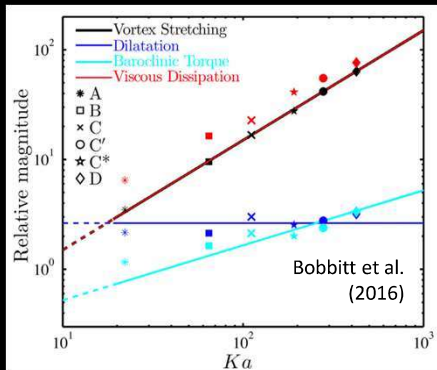
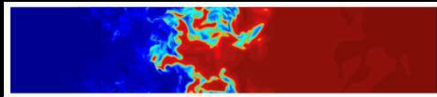
- Premixed and stratified combustion of hydrogen and high-hydrogen content blends
- Ammonia combustion
- High pressure combustion (or effect of pressure on the above)
- Turbulence and chemistry interaction of high Karlovitz number flames

In your opinion, which topics will continue to be of interest (to you)? Discuss what are the important questions or challenges and present your vision of how these should be addressed.

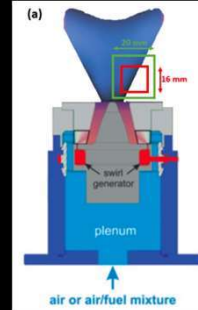
2. There are areas of mutual interest to both PTF and TNF communities. List two topics that you think are of mutual interest for both. Present your vision of how knowledge/experience from each community (PTF and TNF) will help addressing these questions.

Slides used by each panelist to initiate discussion follow in the order listed above.

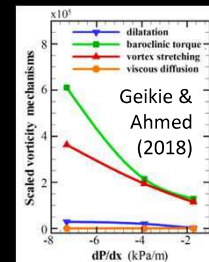
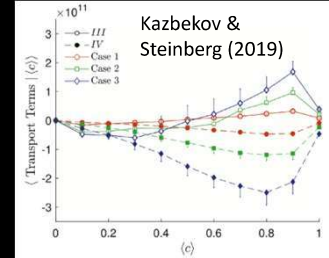
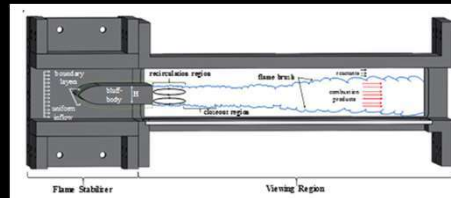
Engineering Relevance



Swirl →
combustor

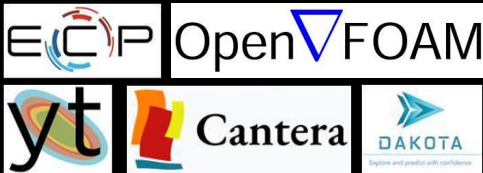


Bluff body
stabilized
flame ↓



Future Priorities

Community-wide code development efforts:
Open-source, freely available software tools
allow the community to build multi-purpose,
multi-physics modeling capabilities



PeleC and PeleLM:

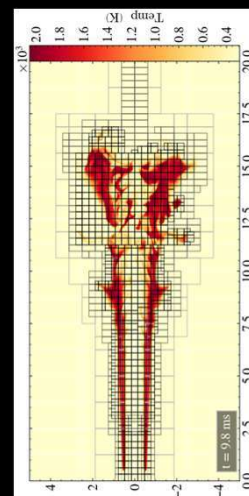
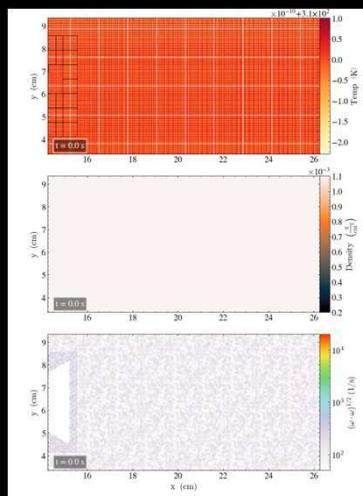
<https://github.com/AMReX-Combustion/PeleC>

<https://github.com/AMReX-Combustion/PeleLM>

A model for us:



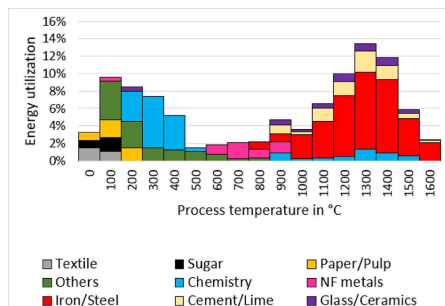
Adaptive mesh refinement: DNS-like resolution in a
computationally efficient approach



Topics of Interest: Application – Physics – Methods

The role of combustion science and technology in low and zero impact energy transformation processes

- Overview and perspectives on
 - Electrical power
 - Mobility
 - Industry



The role of combustion science and technology in low and zero impact energy transformation processes

A. Dreizler^{a,*}, H. Pitsch^b, V. Scherer^c, C. Schulz^d, J. Janicka^e

^a Institute for Reactive Flows and Diagnostics, Technical University of Darmstadt, Otto-Berndt-Str. 3, 64287 Germany

^b Institut für Technische Verbrennung, RWTH Aachen University, Templergraben 64, D-52056 Aachen, Germany

^c Institute for Energy Plant Technology, Ruhr-Universität Bochum, Universitätsstraße 150, D-44780 Bochum, Germany

^d Institute for Combustion and Gas Dynamics, Reactive Flows, University of Duisburg-Essen, 47048 Duisburg, Germany

^e Institute for Energy and Power Plant Technology, Technical University of Darmstadt, Otto-Berndt-Str. 3, 64287 Germany

Fuels

- Biofuels
 - E-fuels
 - Hydrogen
 - Ammonia
- Biohybrid fuels

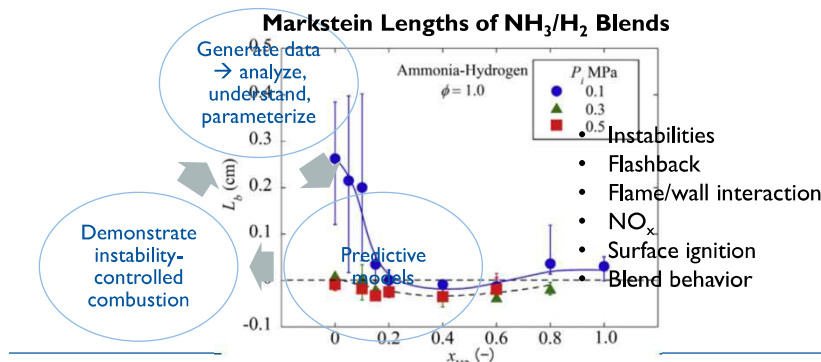
2022, Vancouver



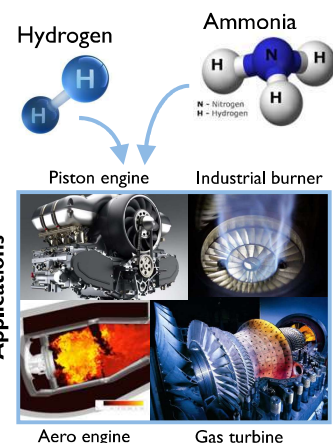
ERC Project Hydrogenate

Hydrogen-Based Intrinsic-Flame-Instability-Controlled Clean and Efficient Combustion

- Understand, model & exploit complexities in hydrogen-based fuel combustion for a sustainable energy future

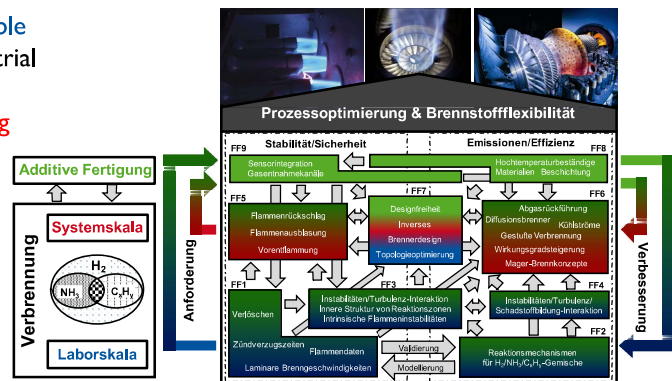


European Research Council



Hydrogen-Based Fuel Combustion using Additive Manufacturing (Pitsch, Dreizler, Kasper, Paschereit, Schleifenbaum)

- Enable **high-efficiency, low-emissions, fuel-flexible** combustion of hydrogen-based fuels for industrial burners and gas turbines by combination of **combustion science** and **additive manufacturing**

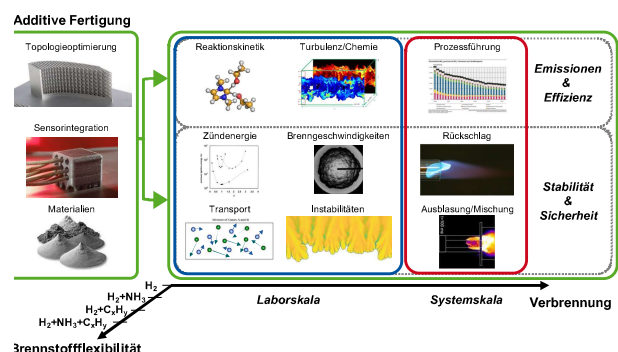


3

Institute for Combustion Technology | TNF Workshop 2022, Vancouver
<https://spp2419.itv.rwth-aachen.de/>

Hydrogen-Based Fuel Combustion using Additive Manufacturing (Pitsch, Dreizler, Kasper, Paschereit, Schleifenbaum)

- Enable **high-efficiency, low-emissions, stable, and fuel-flexible** combustion of hydrogen-based fuels for industrial burners and gas turbines by combination of **combustion science** and **additive manufacturing**
- Computational joint design



4

Institute for Combustion Technology | TNF Workshop 2022, Vancouver
<https://spp2419.itv.rwth-aachen.de/>

Methods

- Data analysis
- Reduced-order models/digital twin
 - e.g. MILD combustion for industrial burners

Topics of Interest for both PTF and TNF

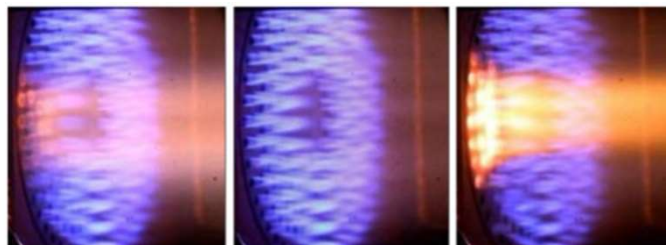
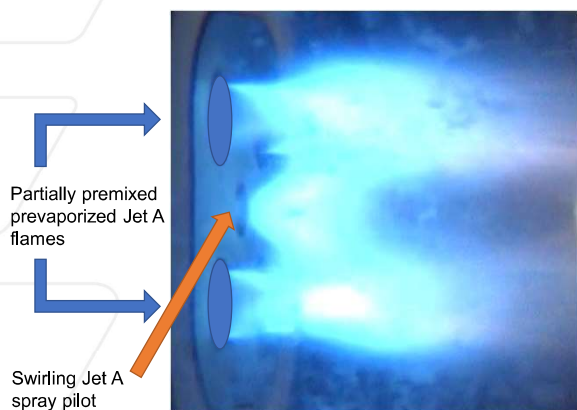
All physics questions are interesting to both and in combination

- Fuels
- High Ka
- High pressure
- FWI
- ...

Data accessibility and process

- Proper research data management → FAIR
- Interactive datasets
- Participation in validation exercises with low activation energy

The Flames Keep Me Awake At Night (and get me up in the morning)



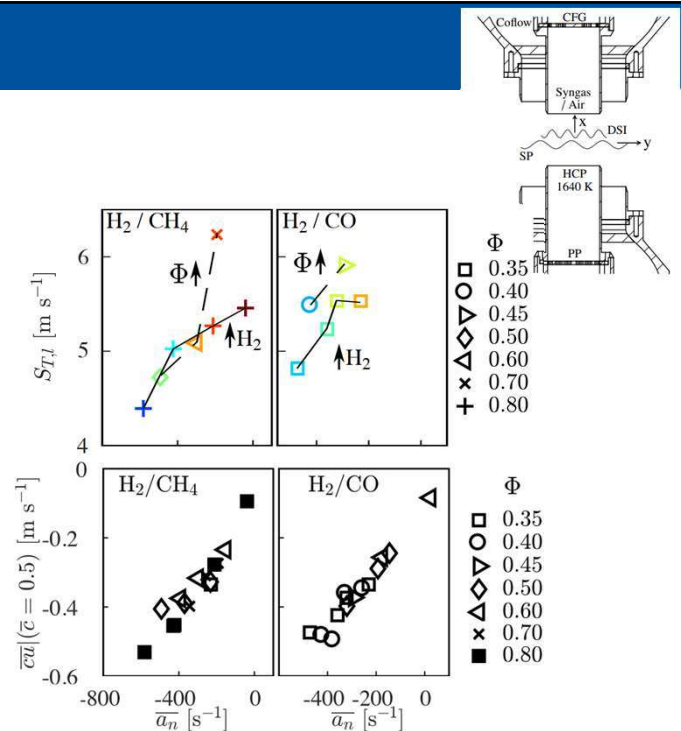
W. York et al. Tech. Rep. DE-FC26-05NT42643,
US Department of Energy (2015)

Fuel flexibility

- $H_2 / CH_4 / CO / N_2 - \text{air}$
- TOJ, Cabra, Shock Tube

Leading edge turbulent flame speed ($S_{T,l}$)

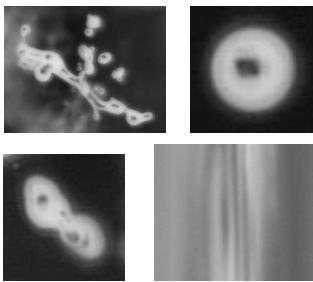
- 100% CH_4 to 100% H_2
- Stronger inhibiting effect of CH_4 compared to CO on H_2
- HyBURN Dataset – Isaac Boxx
- HBK-S to 24 MW industrial S600-GT
- Complex and (pre-vaporised) liquid fuels



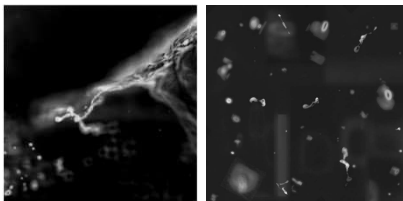
Fabian Hampp - TNF 2022 - University of Stuttgart - IVLR

Open Source Experimental Data Analysis: AI – based models

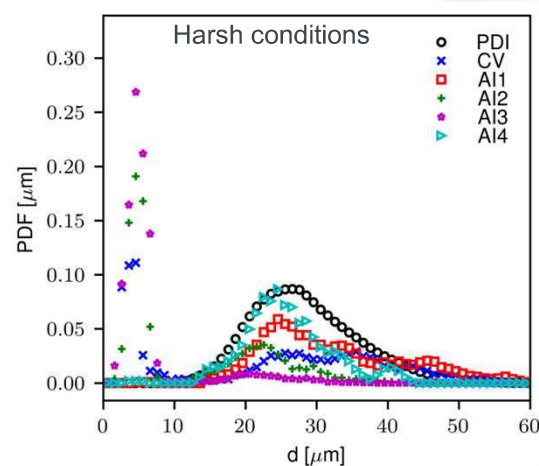
Database



Trainings Data



Trained Models



Fabian Hampp - TNF 2022 - University of Stuttgart - IVLR

TNF/PTF Workshops

Blank Page

Flame-Wall Interaction

Coordinators: Andreas Dreizler and Christian Hasse

Flame-wall interaction (FWI) is a topic since TNF12 in 2014. A side wall quenching (SWQ) geometry has been introduced in TNF13 in 2016 as a first target flame, for which the available experimental data has been continuously expanded for laminar and turbulent flow conditions. A fully premixed flame is anchored at a ceramic rod generating a V-shaped flame brush where one of the two branches is interacting with a temperature-controlled wall. This setup has been investigated in a series of experimental and numerical studies. Based on the SWQ configuration, further, especially numerical, setups for high-resolution simulations were devised.

The primary aim of FWI studies is to gain a deeper understanding of the near-wall dynamics of laminar and turbulent flames. Combustion in enclosed chambers is of great technical relevance, as the walls represent boundary conditions that have a significant impact on the physico-chemical processes and the micro- and macrostructure of the flame. Strong heat losses lead to thermal flame quenching and incomplete combustion results in the formation of primary pollutants such as carbon monoxide (CO) and unburned hydrocarbons (UHC). To understand these processes, the influence of walls on the flame dynamics and in particular turbulence-chemistry interaction as one of the primary fields of interest in the TNF workshop must be studied.

Based on the previous TNF workshops and recent research efforts, the objective of the FWI-session at TNF15 was threefold:

1. Provide an update on recent numerical and experimental efforts
2. Identify common challenges and findings from the different FWI studies
3. Identify the next steps for further studies of FWI

Update on numerical efforts

Results were provided by six groups: University of Melbourne, RWTH Aachen University, Technische Universität Darmstadt (TUD), Newcastle University, SINTEF, University of Edinburgh.

Contributors (in bold contributing PI):

- **M. Talei**, R. Gordon, J. Rivera, R. Palulli, B. Jiang, S. Gupta
- K. Niemietz, L. Berger, M. Huth, A. Attili, **H. Pitsch**
- M. Steinhausen, F. Ferraro, A. Scholtissek, M. Schneider, D. Kaddar, Y. Luo, F. Zentgraf, P. Johe, A. Dreizler, **C. Hasse**
- U. Ahmed, M. Klein, **N. Chakraborty**
- Y. Minamoto, **A. Gruber**
- H. Xia, X. Wei, M. Zhang, J. Wang, Z. Huang, C. Hasse, **W. Han**

In several cases, the work from different groups included collaborations with other universities and industrial partners. Only the affiliation of the main PI is listed here.

An overview of the configurations and the employed models is given in the following table. The groups studied different configurations. Results for the TNF target flame were only

contributed by the TUD group. Unfortunately, this did not allow for a direct “TNF-style” comparison. However, the underlying scientific questions had a lot of overlap, which will be also highlighted below.

Research fields	Research groups					
	Melbourne	RWTH	TUD	Newcastle	SINTEF	Edinburgh
	Turbulence and turbulence chemistry interaction					
DNS	x	x	x	x	x	
LES			x			x
TCI closure			ATF / pPDF			TF-LES
	Chemistry closure					
Chemistry	DC (skeletal) / Flamelet	DC (skeletal) / Flamelet	DC / Flamelet / REDIM	DC (1-step / skeletal)	DC (skeletal)	DC (skeletal)
Fuels	CH ₄	CH ₄	CH ₄ / DME	CH ₄ / H ₂	CH ₄ / H ₂ / NH ₃ -H ₂	CH ₄ -H ₂
Configurations	SWQ (FWI / FCAI)	Jet flame (SWQ like)	HOQ* & SWQ (lam. / turb.)	HOQ & SWQ	Isochoric HOQ	Flashback
Software	NTMIX-CHEMKIN	CIAO	OpenFOAM	SENGA+	S3D	OpenFOAM
HOQ: Head-On Quenching FCAI: Flame-Cooling Air Interaction DC: Detailed (finite rate) chemistry SWQ: Side-Wall Quenching FWI: Flame-Wall Interaction REDIM: Reaction-diffusion Manifold						

The **Melbourne group** performed laminar and turbulent detailed chemistry (DC) simulations of FWI in channel flows. A harmonically perturbed inflow velocity with a range of forcing frequencies was used for the laminar cases. A cooling jet at the wall was considered in another set of cases. The turbulent case included FWI on one side of the channel and flame-cooling air-interaction (FCAI) on the other side. In the case of FCAI, consistent results between laminar and turbulent cases were observed. Head-on and side-wall quenching scenarios can be observed during transient FWI. The dominant role of convection and diffusion for the near-wall CO transport was highlighted. Considering FCAI, a mixture fraction indicating the dilution level with the cooling air is required to capture the T-CO trends. Future work will focus on higher turbulence levels and CO modeling.

The **RWTH Aachen group** performed a turbulent DC simulation of a premixed methane-air turbulent jet flame with FWI. The jet Reynolds number of the simulation is 5,500 and the considered wall temperature 1,000 K. The prediction capability of the near-wall CO formation was validated using different chemistry tables. A 1D chemistry table only considering a progress variable, a 2D (including enthalpy defects) and a 3D table (including enthalpy defects and strain effects) were considered. In addition, a CO transport equation was solved in the calculations. While the more complex models improve the prediction accuracy of the near-wall CO, further research is needed to capture the near-wall CO in sufficient accuracy.

The **TU Darmstadt group** performed laminar and turbulent DC simulations of FWI of a side-wall quenching flame that are validated against experimental data. First, the effect of differential diffusion on the near-wall combustion of DME flames is demonstrated. In a combined experimental and numerical study of a laminar side-wall quenching DME flame, the influence of differential diffusion on the near-wall CO prediction was shown. These findings are extended to turbulent flames based on a flame-resolved simulation of a DME-air flame ignited in a turbulent channel flow. Using the simulation results, the effect of differential diffusion and flame curvature on the local heat-release rate of the turbulent SWQ flame were

investigated. In addition to the DME-air flame, a methane-air flame ignited in a turbulent channel flow was presented. A flame-(tip-)vortex interaction mechanism was investigated (in correspondence with experimental findings) that leads to the entrapment of burnt exhaust gases close to the flame tip, resulting in changes in the thermochemical state that effect pollutant formation and flame dynamics. To capture these effects a new chemistry manifold was derived and validated, showing excellent agreement with the DNS data. Additionally, turbulence-chemistry-interaction closure for near-wall quenching flames was investigated. The results show the complex probability distributions of the unresolved reactive scalars close to the wall. To capture these effects a transported PDF approach is derived and validated using the DNS data. Finally, a partially-premixed SWQ flame was investigated showing the influence of the concentration boundary layer on the flame quenching and additionally the effect of flame retardants on the near-wall thermochemical states.

The **Newcastle group** performed turbulent simulation of HOQ and SWQ flames with single step chemistry. The results focus on the near-wall flame dynamics and the influence of quenching on temperature and velocity fields. A budget analysis of the different terms in the governing equations was performed. The analysis showed that the standard formulations used in RANS and LES models (turbulent kinetic energy, wall functions, and turbulent scalar flux) vary significant for flames undergoing thermal quenching and need to be adapted. The often-assumed balance of production and dissipation in the turbulent kinetic energy equation may not be valid within the turbulent boundary layers during FWI. Further analysis showed that the turbulent burning velocity and the Nusselt number in FWI are linked in the turbulent boundary layer, suggesting the possibility to measure the turbulent burning velocity within turbulent boundary layers using the mean velocity, temperature, and wall heat flux. They also compared head-on quenching between turbulent stoichiometric methane-air and hydrogen-air premixed flames in canonical configuration under identical turbulence intensities using skeletal chemical mechanisms. The wall heat release characteristics for hydrogen-air flames have been found to be considerably different to that in methane-air flames. This makes the FWI modelling for hydrogen-air flames to be more challenging than FWI of hydrocarbon-air flames.

The **SINTEF group** showed first results of the direct numerical simulation of turbulent flame-wall interaction under isochoric conditions. In the simulation, a flame is ignited inside a box with isothermal walls initialized with an isotropic turbulence velocity field. In the study, hydrogen, methane and decomposed ammonia (ammonia-hydrogen-nitrogen) flames were considered. First analyses of the dataset were performed showing the complex nature of the quenching phenomena, due to the overlying pressure increase during quenching in the closed chamber. Further, the analysis showed the importance of the radical recombination reactions at the wall that effect the heat-release rate and pollutant formation at the wall. The analysis of the turbulent dataset is still ongoing.

The **Edinburgh group** performed simulation of experiments conducted in a bluff-body swirl burner that investigates flame-flashback of hydrogen and hydrogen-methane air blends. The simulations were used to predict the flame flashback limit for different equivalence ratios and wall temperatures. Detailed analysis of the flashback phenomena showed two modes during flame flashback: a flame tongue leading flashback that leads to swirling flashback and flame bulges that results in an axial flashback phenomenon. The different flashback modes are

dependent on the wall temperature. While at low temperature the swirling flashback is prominent, at high wall temperatures only the axial flashback was observed. In intermediate conditions, a transition between different flashback modes can be observed.

Update on experimental efforts

Results were provided by four groups (Coria Rouen, France; University of Armed Forces, Munich, Germany; University of Edinburgh, UK; TU Darmstadt, Germany).

The **Coria group** introduced a new test case to study the interaction between premixed flames and cooling air. At atmospheric pressure, a rod-stabilized CH₄/air V-flame interacted with an oil-cooled wall that was shielded by a cooling air film. Blowing ratios between film and main flow were varied between 0.1 and 4. The experimental data base contains wall temperatures, flow velocities and flame visualization. Using measured wall temperatures, the thermal protection was evaluated for different blowing ratios.

The **Munich Group** investigated an inclined jet-in-crossflow. In a confined configuration, five jets of cold fuel (H₂, CH₄ or C₃H₈) were injected into a cross flow composed of hot, oxygen-rich exhaust gases from a CH₄ flame. The wall was water-cooled. Wall temperatures were measured and flames were visualized. Wall heat fluxes were determined and compared for different fuels.

The **Edinburgh Group** studied side-wall quenching in a fixed volume chamber, mimicking a geometry similar to an IC engine. Using 1D CARS, temperature and species profiles have been measured in wall normal direction. In addition, flames were visualized, and wall temperatures and flow fields were measured. For different equivalence ratios, flame dynamics and thermochemical states within the boundary layer have been analyzed in the engine-like combustion chamber and the crevices.

The **Darmstadt Group** studied two configurations. The first one mimics conditions of a gas turbine combustor equipped with effusion cooling at elevated pressure. In the near wall region, the interaction between premixed, swirling flames were studied in their interaction with an effusion cooled wall. The experimental data base contains information on the flow field, gas and wall temperatures, total cooling efficiencies as well as local reaction and heat release rates. The second configuration is a generic setup to investigate flame-wall interaction at laminar and turbulent flow conditions at atmospheric pressure. A large data base for premixed CH₄ and DME flames is available.

Common challenges and findings from the different FWI studies

Recent findings from experimental and numerical studies highlight the **transient aspects of FWI**. These lead to changes in the local propagation mode and the quenching scenario, which can be either head-on-quenching or side-wall-quenching-like. Another phenomenon is flame-vortex-interaction, where combustion products are entrained into the unburnt gas region at the flame tip. This changes the flame propagation, finally leading to substantial variation in the quenching point. How this effect can be considered, e.g., in tabulated manifold methods, is currently unresolved.

Another common challenge in experimental and numerical studies is the quantification and prediction of **near-wall CO**. Several recent studies have shown that the models for freely propagating (laminar or turbulent) flames are not sufficient to describe the transport mechanisms of CO near the wall. First attempts with an equation for transported CO yield an improvement, but the results are not yet fully satisfactory. Especially when considering manifold methods, it has become clear that specific model adaptations are necessary. For flamelet, a new generic configuration based on transient HOQ is required, and for REDIM, the boundary conditions need to be modified accordingly.

Several studies have shown that **the turbulent near-wall statistics of the reactive scalars** are affected by the wall. Suitable closures are required for the PDFs/FDFs or more general TCI.

The interplay between FWI and differential diffusion was also discussed. New fuels such as synthetic hydrocarbons, ammonia, and hydrogen are of particular interest to the community.

Machine learning methods will also become increasingly important in the field of FWI, and initial work from the Rouen group (L. Vervisch) is very promising here.

Summary, next steps and future studies

FWI is a technically relevant field in which there are still many open issues, especially for modeling. Significant progress has been made, but there are still a number of outstanding issues and new challenges, particularly with regard to new fuels.

The above-mentioned knowledge gaps are also evident from the fact that most numerical works are DNS studies. The findings from these studies will lead to improved models for the future simulation of the target flames. In this context, three questions were discussed for future works:

1. How can we ensure a good collaboration and data accessibility for DNS data?
2. What is the interplay of experiments and DNS?
3. How can we deal with uncertainties and model robustness for model derivation using DNS?

DNS data are highly valuable for model development. Availability and sharing of the data will be key for future joint studies and improved models from different groups. This collaboration naturally should also extend to interested experimental groups. DNS data will have idealized or simplified boundary conditions compared to the experiment. Therefore, in the future, in

addition to the direct comparison of the experimental and numerical data, e.g., in the form of (conditioned) statistics, a joint analysis of the observable transient effects should be performed. One example is the flame-vortex-wall interaction of the Darmstadt group.

Another point of discussion was model robustness. Models developed based on DNS data are validated for a limited range of parameters. However, these are used for different inflow boundary conditions, wall temperatures, Reynolds numbers or fuel. This issue has been discussed several times in TNF, but is particularly challenging due to the significantly larger number of parameters in FWI. A promising solution could be a sensitivity analysis in simplified 1D/2D configurations.

For **future studies** on FWI, there is a great need for studies on near-wall hydrogen combustion. Due to the high burning velocities, the quench distances are very small. The high diffusivity of H_2 leads to different flame structures and instabilities. How this affects FWI is still unknown. In most cases, technical combustion processes take place at elevated pressures. This should be considered in future experimental and numerical studies. The pressure does affect the flame thicknesses and the burning velocity of freely propagating flames; the influence on the FWI is still largely unexplored.

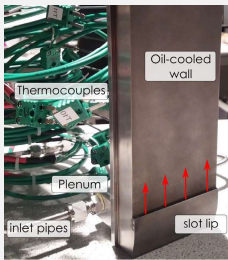
Flame-Wall Interaction (Organizers: C. Hasse & A. Dreizler)

Experiments

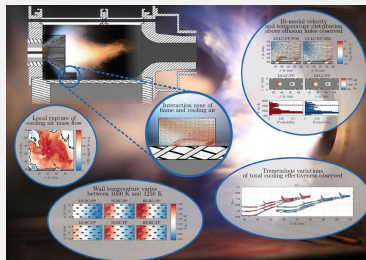
Contributing Institutions: CORIA Rouen, UBW Munich, U Edinburgh, TU Darmstadt

- Energy conversion (GT, ICE, micro combustion, BL-flashback, ...)
- Fire safety

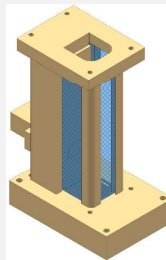
CORIA Rouen



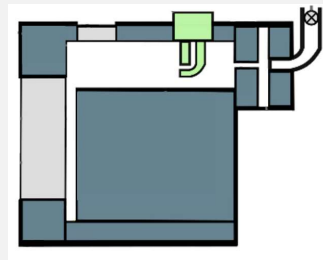
TU Darmstadt



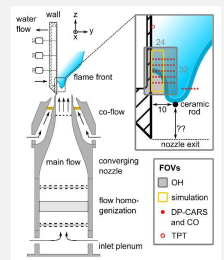
UBW Munich



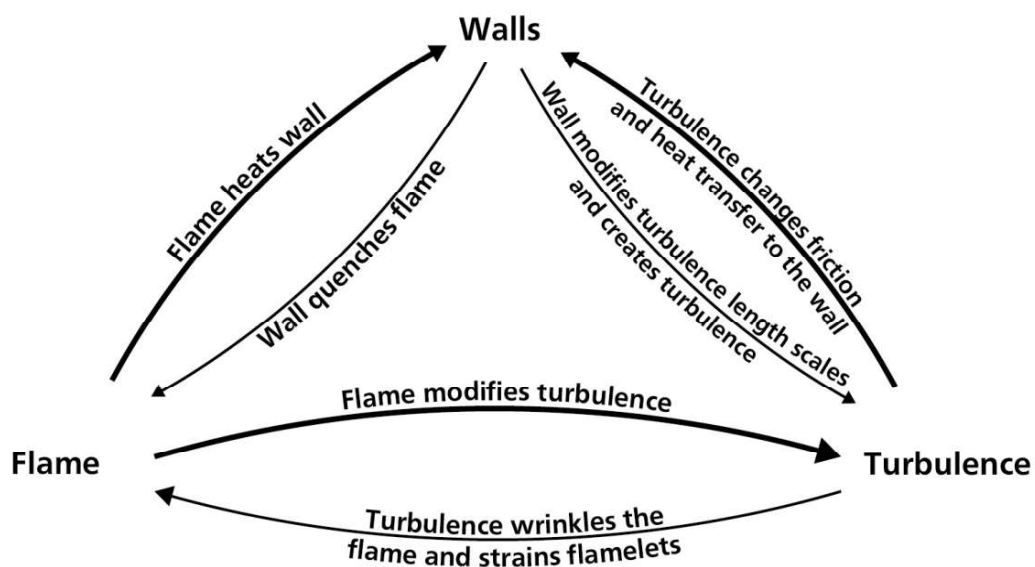
U Edinburgh



TU Darmstadt



Wall-bounded flames | Mutual interaction between Chemistry – Transport – Wall



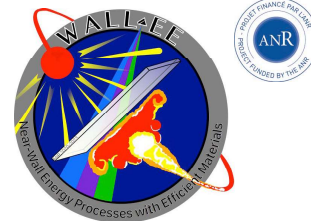
1. Flame-cooling air-wall interaction, contributors:
 - ▶ S. Petit, P. Xavier, F. Grisch et al., CORIA Rouen, France
 - ▶ M. Greifenstein, et int., A. Dreizler, TU Darmstadt, Germany
2. Partially-premixed flame-wall interaction, contributors:
 - ▶ M. Pfitzner, R. Dalshad, UBW Munich, Germany
3. Premixed flame-wall interaction: Contributors
 - ▶ B. Peterson et al., U Edinburgh, Scotland
 - ▶ F. Zentgraf, P. Johe, A. Dreizler et al., TU Darmstadt, Germany

TNF15 Workshop

Near-wall energy processes: 'Flame-cooling air interaction' case in the CENTOR test rig

Dr. Pradip Xavier (PI)

Co-workers: Dr. Sylvain Petit, Dr. Avinash Chaudhary, Antoine Blaise (PhD student) & Prof. Frédéric Grisch
CORIA UMR 6614, Normandy University (CNRS, INSA & University Rouen Normandy), Saint Etienne du Rouvray, France



Publications:

- S. Petit, P. Xavier, G. Godard, F. Grisch, Improving the temperature uncertainty of $\text{Mg}_2\text{FGeO}_6\text{:Mn}^{4+}$ ratio-based phosphor thermometry by using a multi-objective optimization procedure, *Applied Physics B* (2022) 128, 57, <https://doi.org/10.1007/s00340-021-07733-3>
- S. Petit, B. Quevieux, R. Morin, R. Guillot, F. Grisch, P. Xavier, Experimental investigation of flame-film cooling interactions with an academic test rig and optical laser diagnostics, in: *ASME Turbo Expo: Power for Land, Sea, and Air* (2022) (awaiting DOI)
- S. Petit, A. Blaise, G. Godard, B. Mille, T. Muller, P. Toutain, F. Grisch, P. Xavier, Experimental study of the interaction between a turbulent flame and a cooling air film, *20th International Symposium on applications of Laser and Imaging Techniques to Fluid Mechanics (Lisbon)* (2022).

Research objectives



Near-wall energy processes (new activity in the lab):

- Develop a technical and scientific expertise in the understanding of near-wall energy processes (e.g. flame-wall interactions, FWI)
- Topic is part of a long-term process for the aircraft motorists
- Experimental approach by implementing advanced laser diagnostics + physical processes (numerical is considered in the short term)

The literature review indicates a lack of knowledge regarding the Flame-Cooling Air Interaction config (FCAI) [see recent studies from TU Darmstadt and Univ. Melbourne]:

- Flame dynamics (turbulent combustion modelling)
- Pollutant formation (CO, UHC)
- Material aging and cooling strategy (wall thermal loads)
- Advanced laser diagnostics (development, implementation post-processing)
- ...

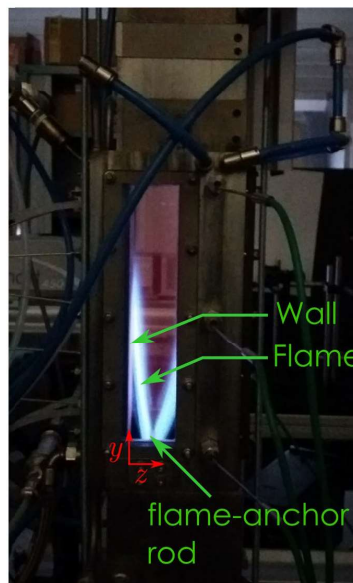
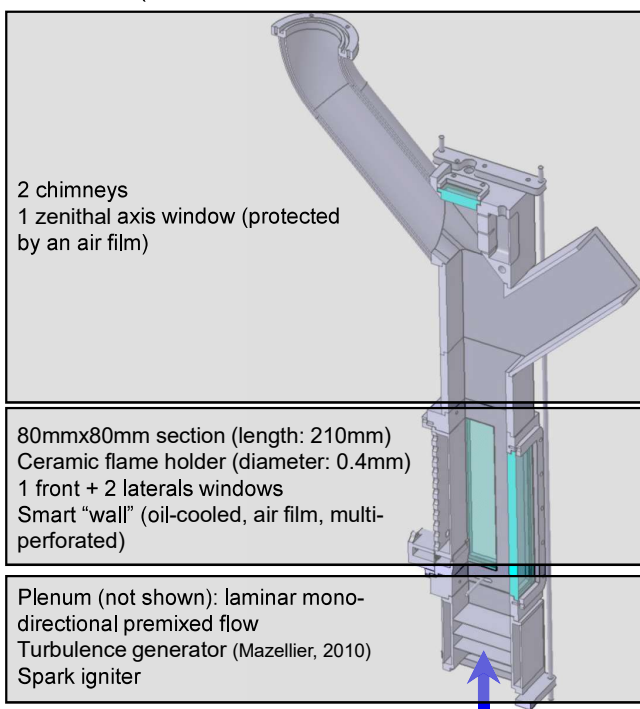
Development of a new test rig mimicking the FCAI + experimental database

5

Experimental setup (1)



CENTOR (Combustion test bench to observe near wall processes)



Parameter	Value
Thermal power (kW)	18 – 75
Wall temperature (K)	320 – 620
Inlet fresh gas temperature (K)	285 – 500
Main flow velocity (m/s)	1.3 – 5.5
Reynolds number (-)	5,000 – 18,000
Isotropic turbulence	8 – 10%
Fuel	CH ₄
Combustion	premixed

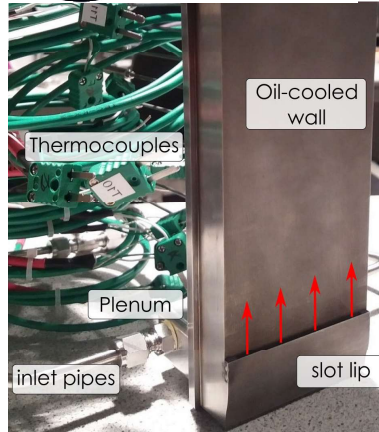
The optical module/chimney casings are water-cooled

6

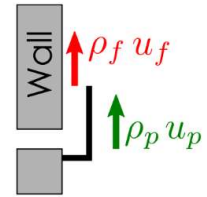
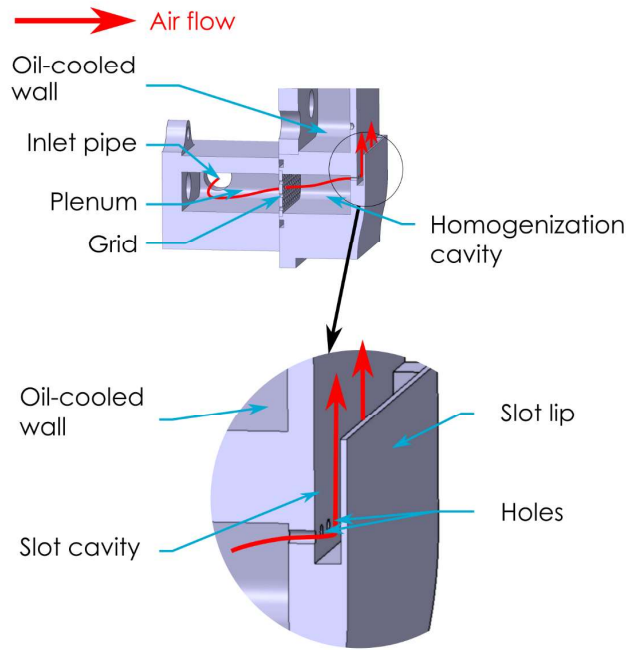
Experimental setup (2)



Air film at the wall: splash cooling system



Bogard, 2006; Gosselin, 1999;
Lefebvre, 2010; Nina, 1971

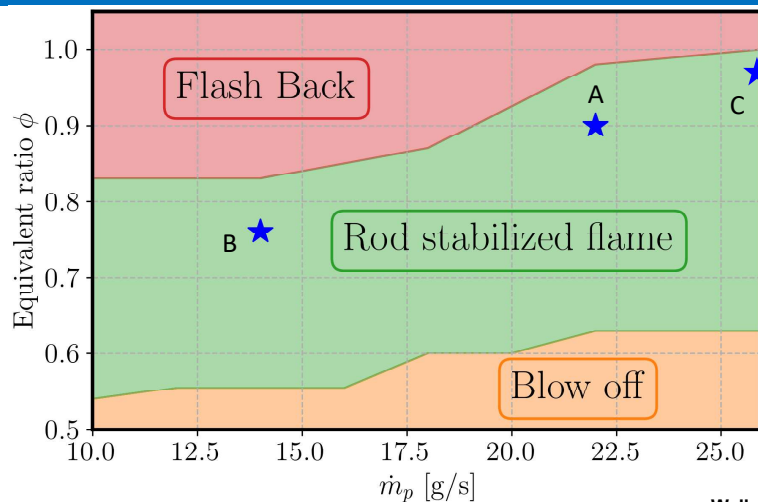


Blowing ratio

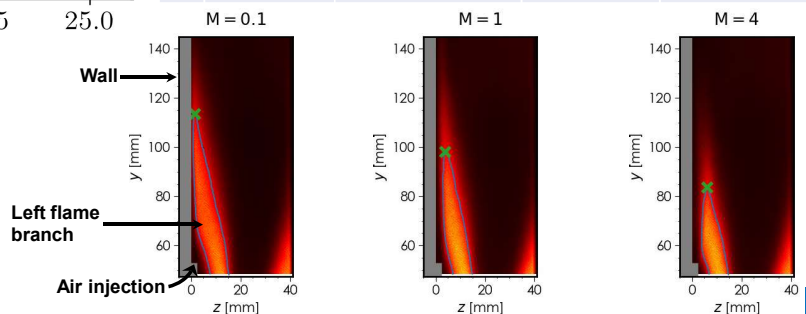
$$M = \frac{\text{film}}{\text{main}} = \frac{(\rho u)_f}{(\rho u)_p}$$

Parameter	Value
Blowing ratio	0.1 – 4
Hole diameter (mm)	1
Slot depth (mm)	2
Lip thickness (mm)	0.5 mm
Inlet air temperature (K)	285 – 600
Air film turbulence	20 – 30%

Stability map

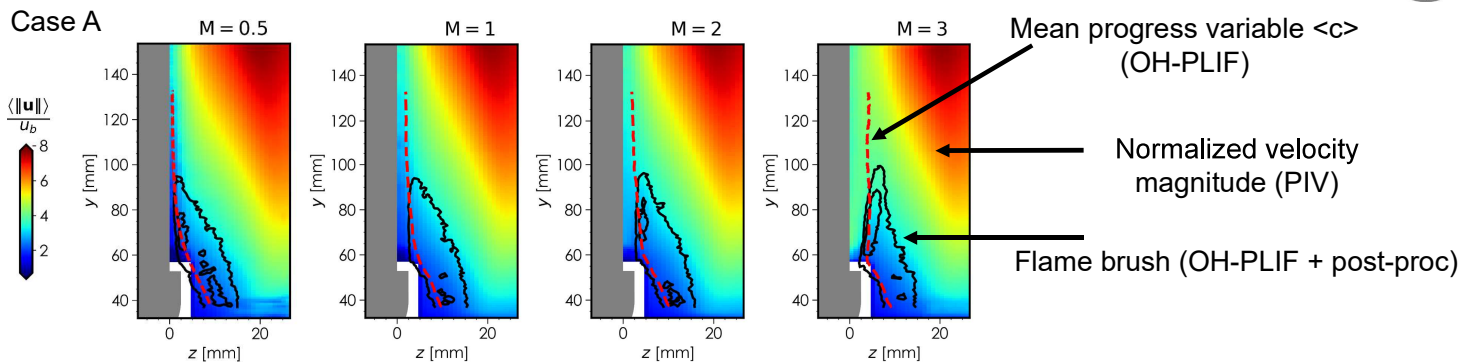


OH* chemiluminescence
Case B



Operating points				
	main air flowrate	equivalence ratio	Blowing ratio	T inlet (main & slot)
A	22 g/s	0.9	0.5; 0.75; 1; 2; 3	298 K
B	14 g/s	0.76	1; 2; 3; 4	298 K
C	26 g/s	0.94	1	298 K

Aerodynamics & flame front



No parietal air film for $M = 0.5$ // Presence of a parietal air film for $M > 1$

Modification of the $\langle c \rangle$ interface for $M=3$, high-deflection into the mainstream

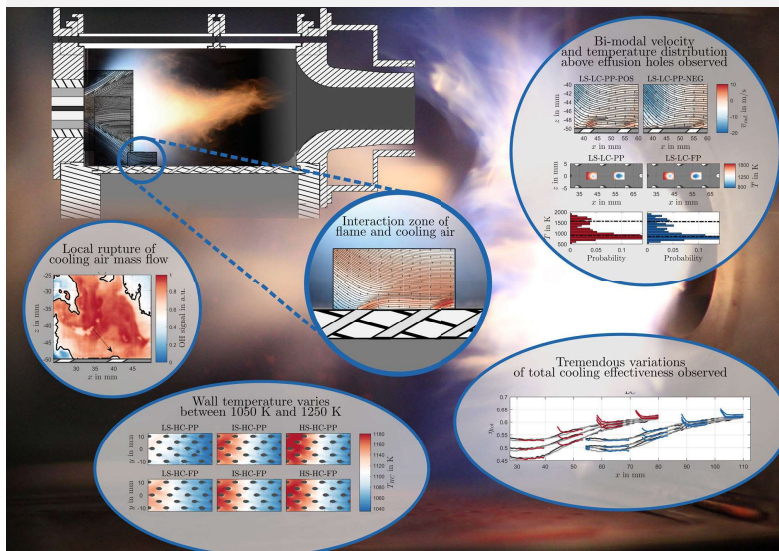
Flame front shape is modification for $M = 3 \rightarrow$ more complex interface (misalignment)

11

Flame-cooling air-wall interaction | Elevated pressures and more realistic cond.



- Swirling flame: premixed or piloted
- Experimental data: Flow field, gas and wall temperature, flame brush, total cooling efficiency, reaction rate imaging, heat release rate imaging



- Greifenstein, Dreizler; Combustion and Flame 226 (2021) 455–466
- Greifenstein et al.; Experiments in Fluids (2019) 60:10
- Hermann et al.; Flow, Turbulence and Combustion (2019) 102: 1025–1052



12

1. Flame-cooling air-wall interaction, contributors:

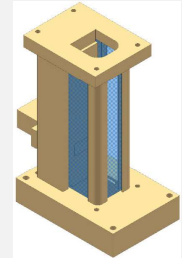
- ▶ S. Petit, P. Xavier, F. Grisch et al., CORIA Rouen, France
- ▶ M. Greifenstein, et int., A. Dreizler, TU Darmstadt, Germany

2. Partially-premixed flame-wall interaction, contributors:

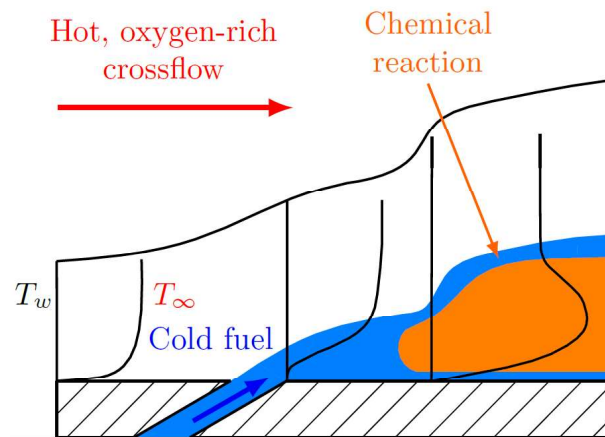
- ▶ M. Pfitzner, R. Dalshad, UBW Munich, Germany

3. Premixed flame-wall interaction: Contributors

- ▶ B. Peterson et al., U Edinburgh, Scotland
- ▶ F. Zentgraf, P. Johe, A. Dreizler et al., TU Darmstadt, Germany



- Jet-in-cross-flow by injecting fuel (H_2 , CH_4 , C_3H_8) into a hot, oxygen-rich crossflow at atmospheric pressure

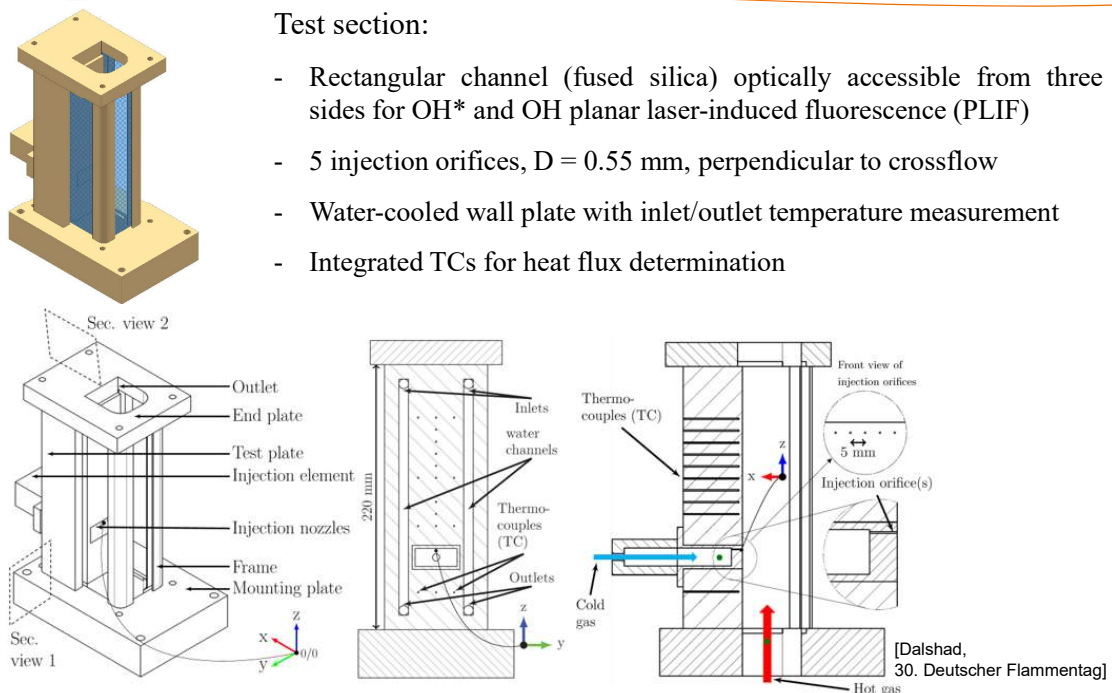


Introduction: Objective

15/10

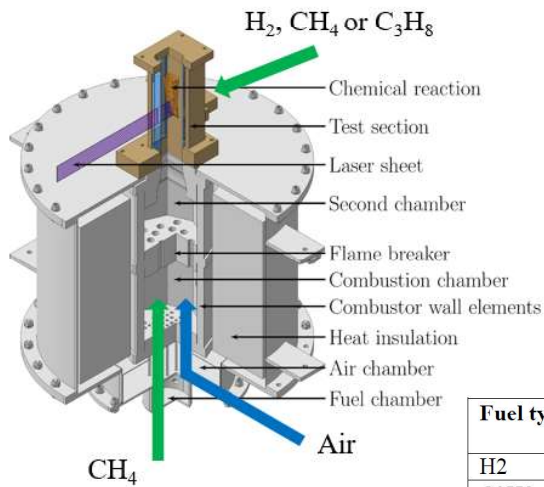
Test section:

- Rectangular channel (fused silica) optically accessible from three sides for OH^* and OH planar laser-induced fluorescence (PLIF)
- 5 injection orifices, $D = 0.55$ mm, perpendicular to crossflow
- Water-cooled wall plate with inlet/outlet temperature measurement
- Integrated TCs for heat flux determination



Experimental Setup: Test Section

16/10



Vitiated crossflow conditions:

- CH₄/air combustion
- $\lambda = 1.6, X_{O_2} = 7.4 \%$
- $u = 27 \text{ m/s}$, turbulent
- $T \approx 1600 \text{ K}$

JICF, injection conditions:

Fuel type	Mass flow rate (g/min)	Temperature (K)	Momentum ratio I	Velocity ratio b	Re _D
H2	0.68	354	8.9	5.2	525
C3H8	4	335	13.3	1.3	3400
CH4	1.94	345	8.83	1.81	1190

Momentum ratio: $I = \frac{\rho_c u_c^2}{\rho_h u_h^2}$

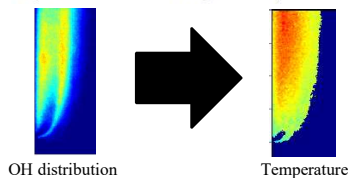
Experimental Setup: Assembly, Conditions

17/10

OH planar laser-induced fluorescence (PLIF):

10 Hz, ~ 300 images each line, 310 nm ± 10 nm
Average reaction zone temperature using two-line method
Excited lines: P₁₁(2), R₂₂(13)

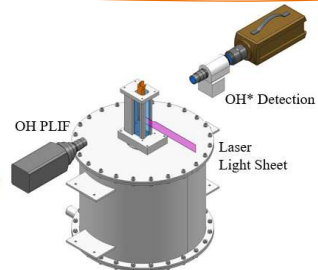
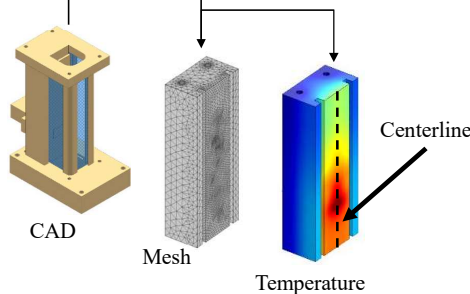
$$\frac{F_2/I_2}{F_1/I_1} = R_{ratio} = \frac{B_2 g_2}{B_1 g_1} \exp\left(-\frac{E_1 - E_2}{kT}\right)$$



Inverse heat conduction:

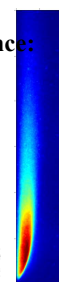
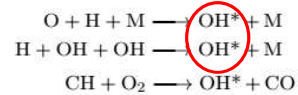
Installed type K thermocouples measure the temperature inside the plate
Calculate the heat flux at the surface numerically

$$T(x,y,z,t) \rightarrow \dot{q}(x=0,y,z,t)$$



OH* chemiluminescence:

7.5 kHz, 300 images, 310 nm ± 10 nm
Qualitative analysis
Line-of-sight method



Measurement Techniques

18/10

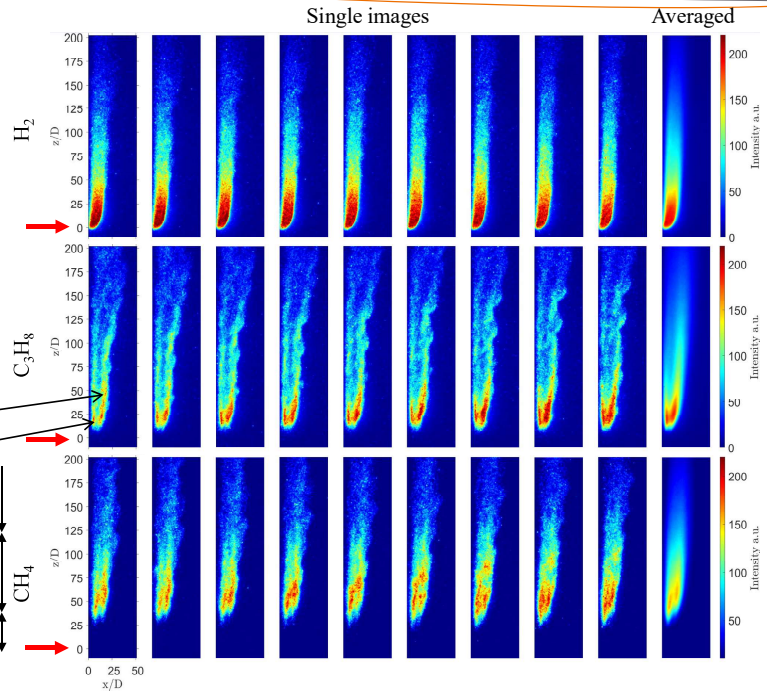
Consecutive images possible due to time-resolved detection

H_2 :

- Direct ignition
- Orifice anchored flame
- Near-wall heat release
- Instantaneous and averaged images are almost identical

C_3H_8/CH_4 :

- Wall-attached lifted flame
- Jet trajectory unavailable
- Significant ignition delay (CH_4)
- Two reaction zones visible as the mainstream gas is transported to near-wall regions
- Instable trailing part
- Lee side reaction
- Windward reaction
- Trail reactions
- Main reaction zone
- Ignition delay length



Results: OH^* Chemiluminescence

19/10

Single images are randomly selected, as the detection is at 10 Hz

H_2 :

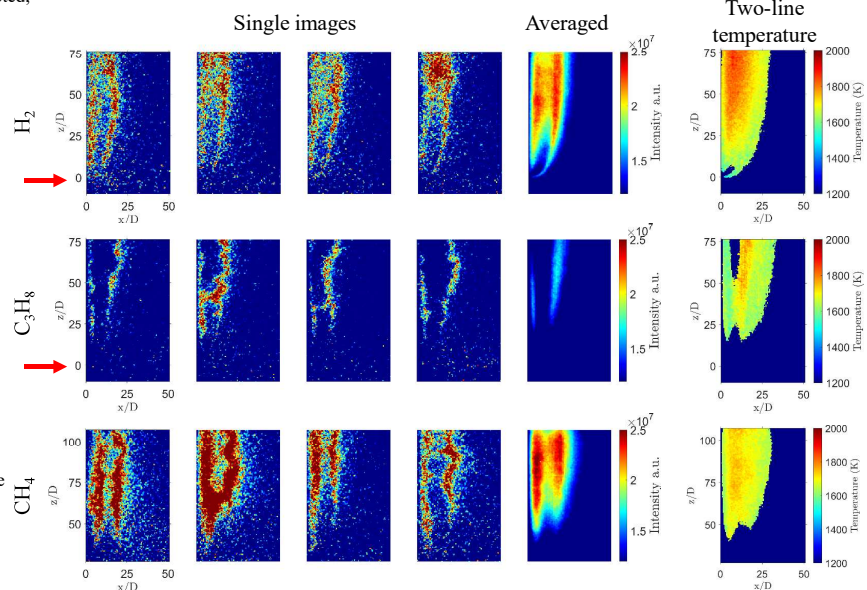
- Double flame structure visible
- Flames follow the jet path
- Stable reaction zones
- Near-wall and windward flames of similar size
- Temperatures around 1800 K

C_3H_8 :

- Double flames visible
- Small near-wall flame
- Mostly 'broken' flames with small 'islands'
- Temperatures around 1600 K, on the level of the crossflow temperature

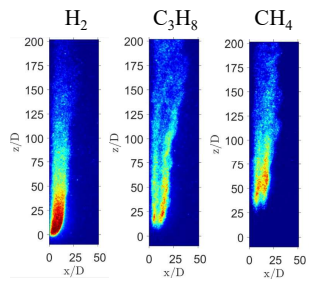
CH_4 :

- Near-wall flame larger than the windward flame
- Similar to C_3H_8 , 'wrinkled' structures visible
- Windward flame located further downstream
- Temperatures around 1700 K



Results: OH PLIF

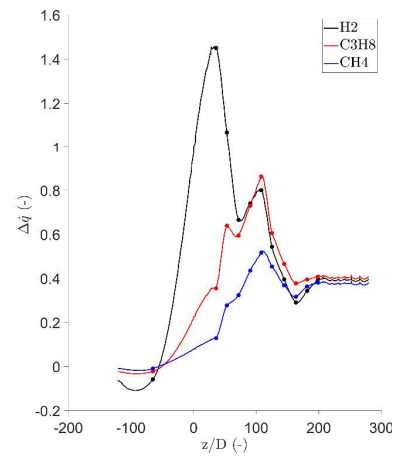
20/10



Heat flux along the test plate centreline:

- Maximum heat flux for H₂ injection, followed by C₃H₈
- CH₄ heat flux increases around 50 %
- C₃H₈ heat flux increases around 90 %
- H₂ heat flux increases around 150 %
- Peak heat flux for H₂ near the injection location, thereafter it decreases rapidly
- Maximum heat flux of the hydrocarbons shifted downstream compared to OH* location

Non-dimensional heat flux estimation



Non-dimensional heat flux along the centerline: $\Delta \dot{q} = \frac{\dot{q}_{\text{reac}} - \dot{q}_0}{\dot{q}_0}$
 \dot{q}_0 : specific heat flux before fuel injection
 \dot{q}_{reac} : specific heat flux during fuel injection and combustion

- Maximum location of H₂ probably not resolved

Results: Wall Heat Transfer

21/10

Content



1. Flame-cooling air-wall interaction, contributors:

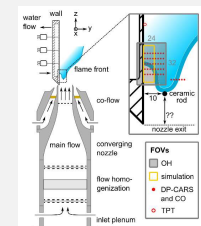
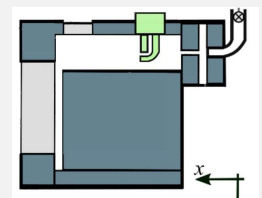
- S. Petit, P. Xavier, F. Grisch et al., CORIA Rouen, France
- M. Greifenstein, et int., A. Dreizler, TU Darmstadt, Germany

2. Partially-premixed flame-wall interaction, contributors:

- M. Pfitzner, R. Dalshad, UBW Munich, Germany

3. Premixed flame-wall interaction: Contributors

- B. Peterson et al., U Edinburgh, Scotland
- F. Zentgraf, P. Johe, A. Dreizler et al., TU Darmstadt, Germany



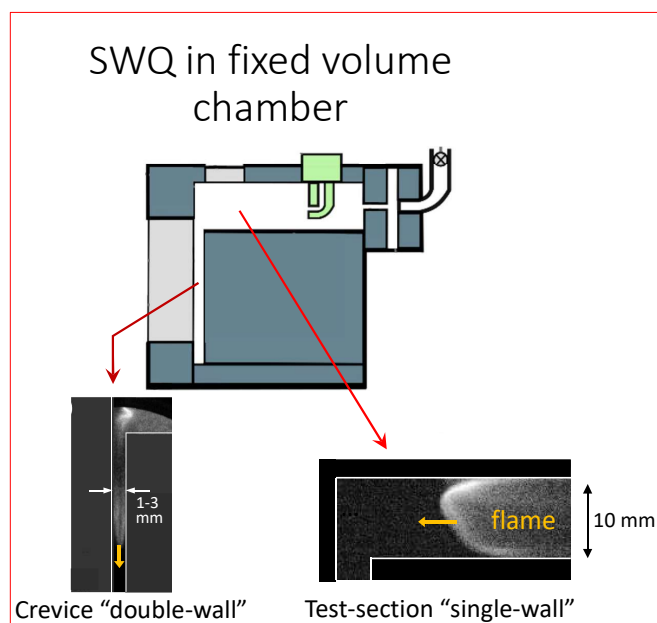
Fundamental FWI and heat-transfer studies

University of Edinburgh

Contributors: David Escofet-Martin, Anthony Ojo, Josh Collins, Mark Linne, Brian Peterson



FWI Contributions



SWQ in V-flame burner



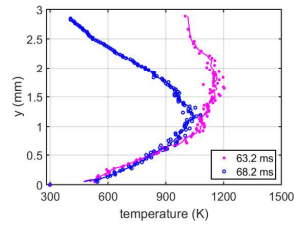
Experimental Measurements



THE UNIVERSITY of EDINBURGH
School of Engineering

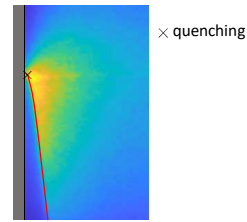
1D temperature & species

Hybrid fs/ps rotational CARS



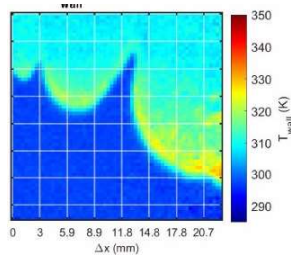
2D Flame distribution

CH*, OH*, OH-LIF



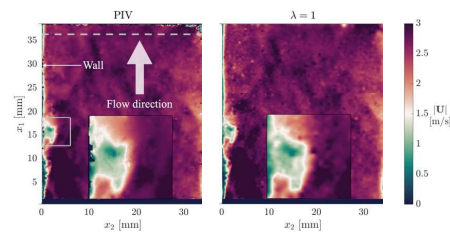
Wall temperature (OD & 2D)

Phosphor thermometry



Flow field

PIV, wavelet-based optical flow



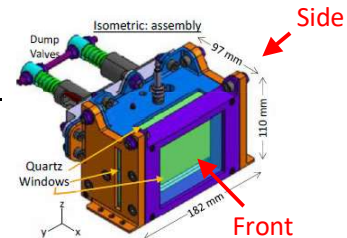
THE UNIVERSITY of EDINBURGH
School of Engineering

Mechanical Engineering

25

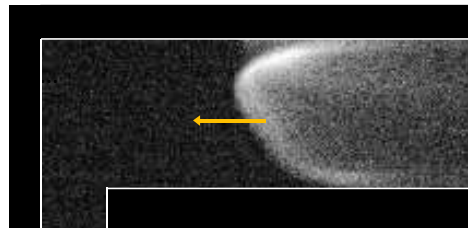
Chamber Operation

- Premixed charge CH_4 -air $\Phi = 0.9$ -1.1; Initial press: 1-2 bar; surface & gas Temp: 298 K
- Volume 150 cm^3 ; Surface/volume = 2.32 cm^{-1}
- Crevice spacing 1-3.5 mm adjustable.



THE UNIVERSITY of EDINBURGH
School of Engineering

Front - crevice



Side - test-section



THE UNIVERSITY of EDINBURGH
School of Engineering

Mechanical Engineering

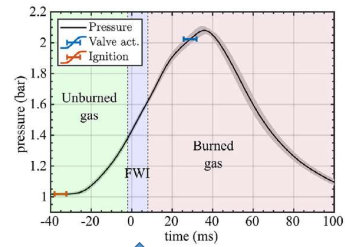
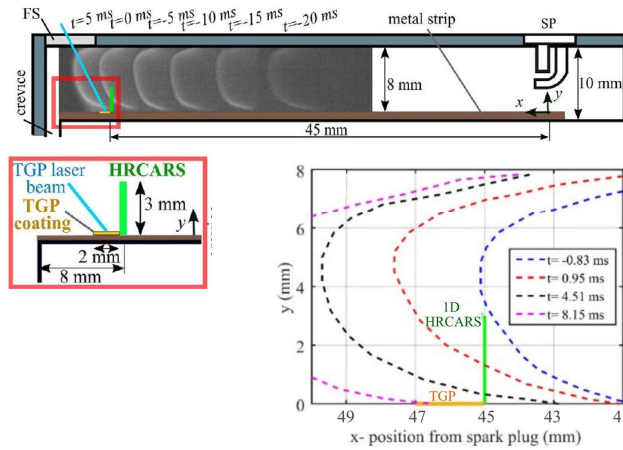
26

Near-wall Energy Transfer



THE UNIVERSITY of EDINBURGH
School of Engineering

- Small “engine-like” chamber for fundamental heat transfer studies
- Thermal boundary layer (HRCARS) + Wall temperature (phosphor thermometry)



Discuss now only FWI regime



THE UNIVERSITY of EDINBURGH
School of Engineering
Mechanical Engineering

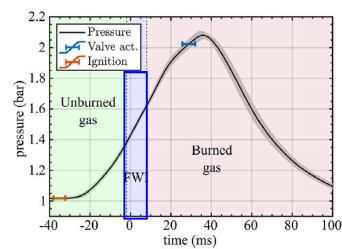
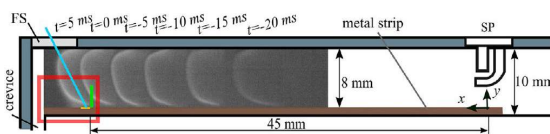
D. Escofet-Martin et al. Proc. Combust. Inst. 38 (2021) 1579-1587
A.O. Ojo et al., Combust. Flame 233 (2021) 11567

27

Measurement Regimes

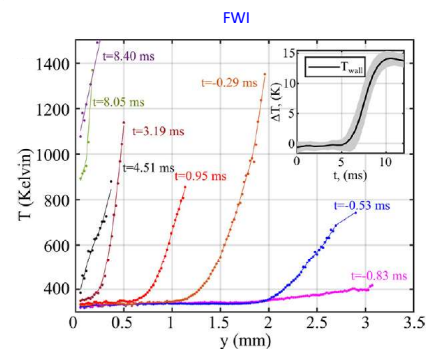
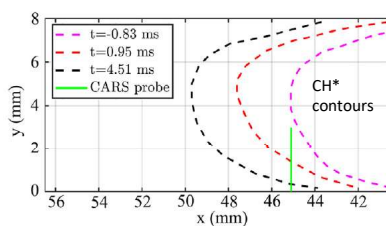


THE UNIVERSITY of EDINBURGH
School of Engineering



FWI

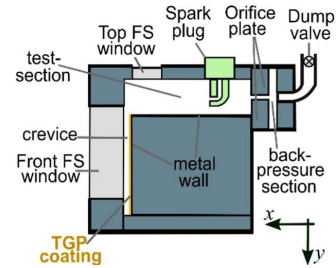
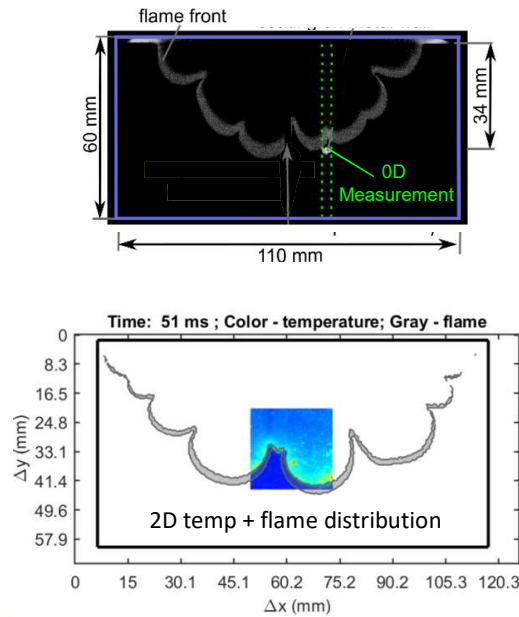
- Thermal gradients up to flame front; signal lost past flame front
- Time $t = 0$ ms, when flame crosses $y = 2$ mm in HRCARS
- $t \leq 0.95$ ms: gases below $y \leq 0.2$ mm follow polytropic compression
 - Near-wall gases do not sense flame until flame 1 mm from wall
- FWI - strong gradients at wall: $T_{wall} = 315$ K; $T_{50\mu m} > 800$ K



THE UNIVERSITY of EDINBURGH
School of Engineering
Mechanical Engineering

28

Focus: Crevice Region



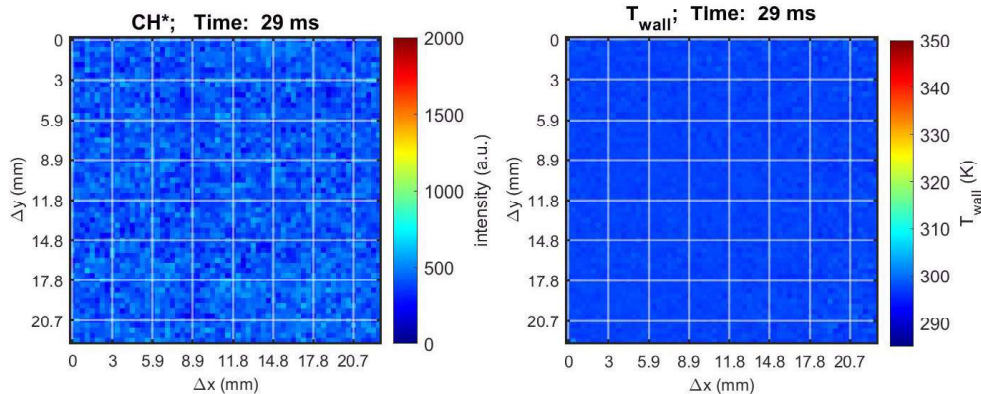
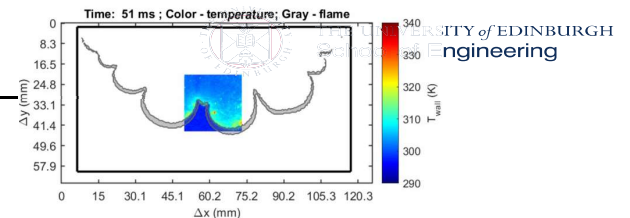
Crevice Region

- Point-wise & 2D wall temperature distributions
- Surface temperature as function of:
 - flame location
 - crevice spacing (1.2 – 3.5 mm)
 - initial pressure (1.0 – 3.0 bar)



2D wall temperature

- Spatiotemporal FWI dynamics



More details given at 1CO4 (Monday 11:45)

CS = 2 mm; $P_{initial} = 2$ bar

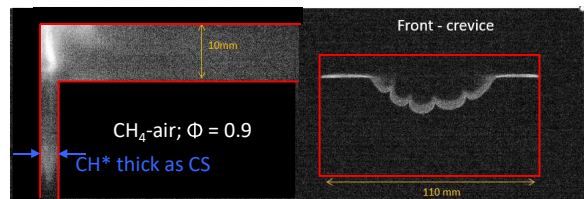
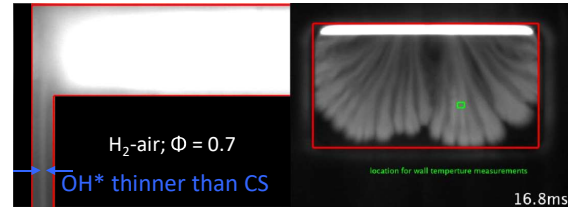
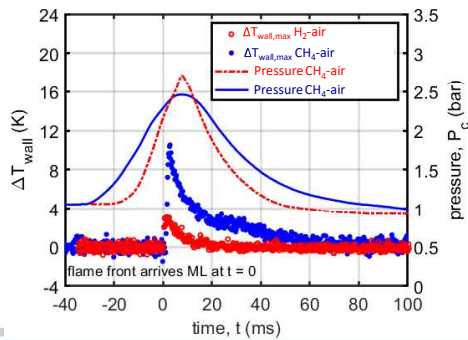


Hydrogen



THE UNIVERSITY of EDINBURGH
School of Engineering

- Preliminary tests
- Distinct hydrogen instability signatures in crevice for hydrogen
- T_{wall} significantly lower for H_2 than CH_4
- H_2 flame in crevice appears further from walls; **hydrogen diffuses away from walls during FWI? Less FWI?**



THE UNIVERSITY of EDINBURGH
School of Engineering
Mechanical Engineering

31

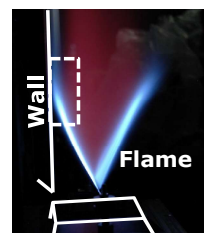
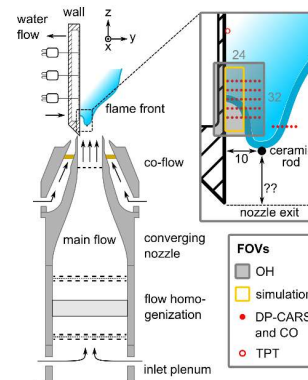
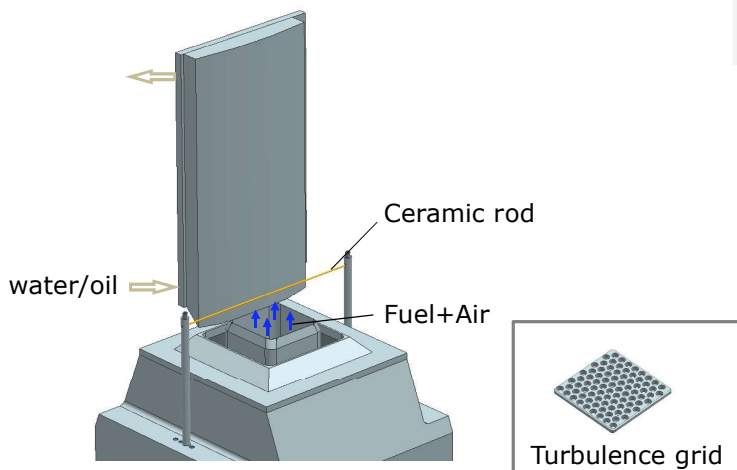
Atmospheric side-wall quenching (SWQ) burner assembly | Parametric variation



- Well-defined boundary conditions
- Optical access to boundary layer
- Focus on premixed flames

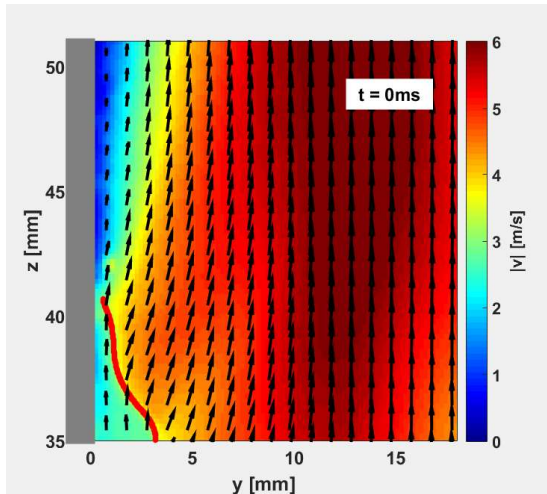
Parametric variation

- Fuel (methane, DME)
- Equivalence ratios
- Wall surface temperatures (330 – 670 K)
- Laminar and **turbulent flows**



32 |

► Turbulent



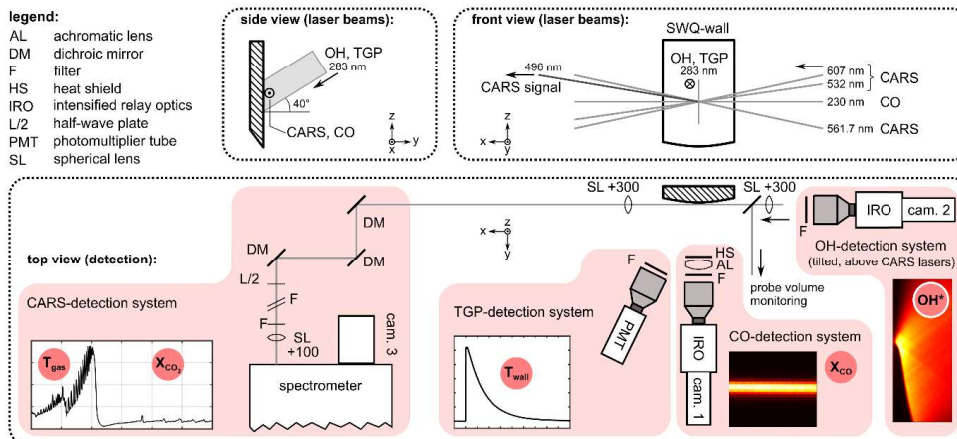
► Data shown are conditioned on location of instantaneous quenching point (measured by OH-PLIF)

Multi-parameter diagnostics

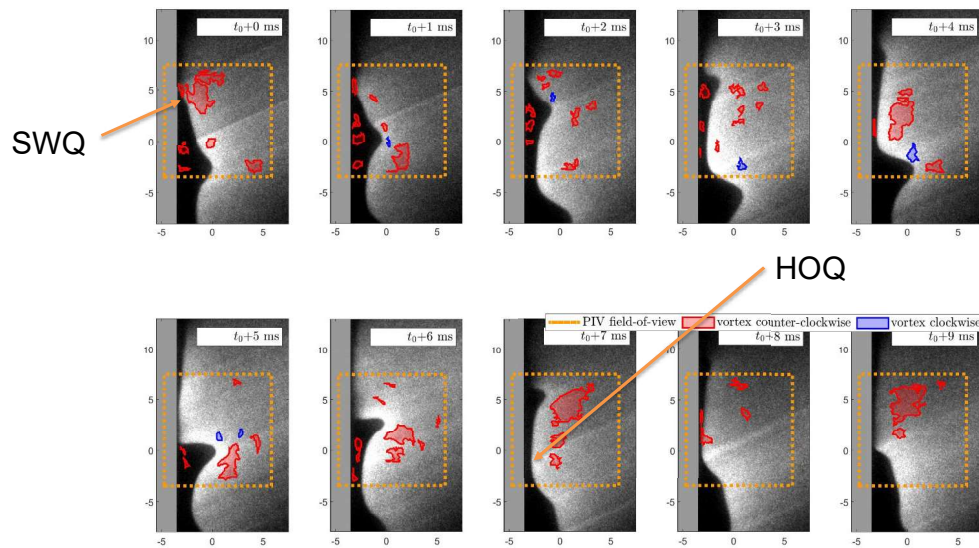
- Gas and wall temperatures, CO₂ and CO mole fractions, flame front tracking, flow field
- Dual-pump-CARS, CO-LIF, LIP, OH-PLIF (low/high-speed), 2C-PIV (low/high-speed)

Zentgraf, et int., Dreizler, Combustion and Flame Volume 239, May 2022, 111681

Zentgraf, et int., Dreizler, Combustion and Flame Volume 235, January 2022, 111707

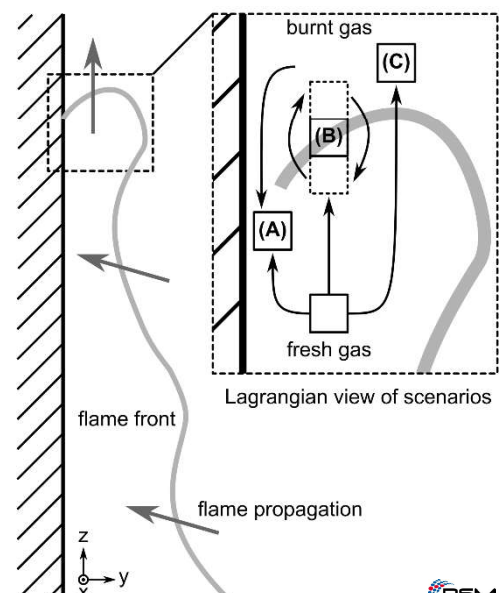
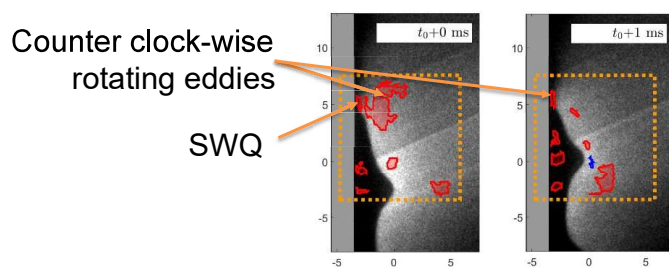


► PIV-OH-PLIF time series show side-wall and head-on quenching like scenarios

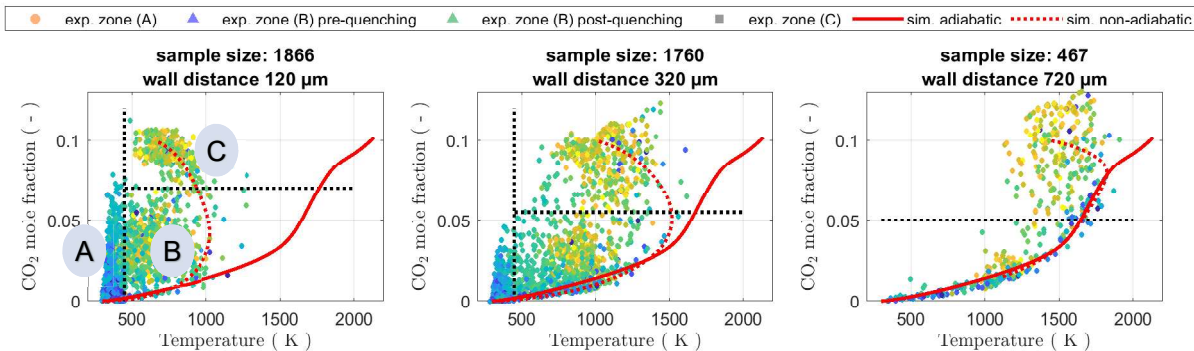


Zentgraf, et int., Dreizler, Combustion and Flame Volume 239, May 2022, 111681

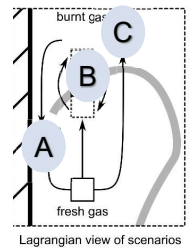
► Focus on side-wall quenching like scenarios (ca. 50%)



- ▶ Completely different scatter plots compared to laminar case
- ▶ Zone A: upstream QP high χ_{CO_2} at $T < 450$ K \rightarrow needs convective transport \rightarrow transport inbetween flame and wall by counter clockwise eddies
- ▶ Zone B: up- and downstream the QP mixing between burnt and unburnt gases
- ▶ Zone C: Reaction without mixing, similar to laminar case, but enhanced heat transfer



The color-coding in the CO₂/T state space shows the wall-axial distance between laser and quenching height (blue: -8 mm (pre-flame) to yellow: +5 mm (post-flame))



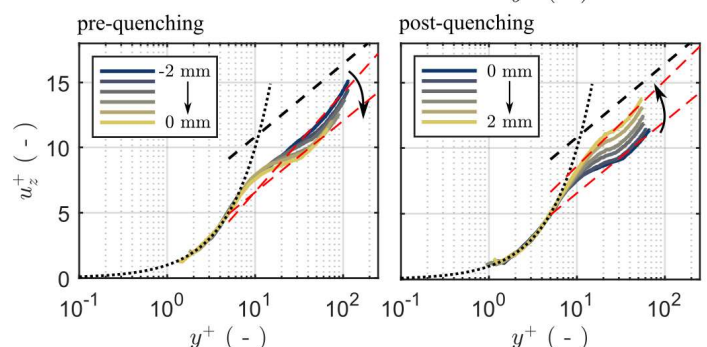
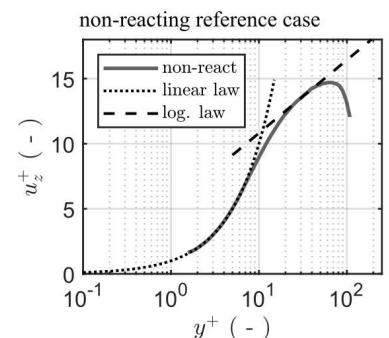
Near-Wall Flame & Flow Dynamics | Boundary Layer Results (1)

Assessing the near-wall turbulent boundary layer (TBL) in the (u^+, y^+) -space:

- Non-react. reference case well-captured by common scaling laws

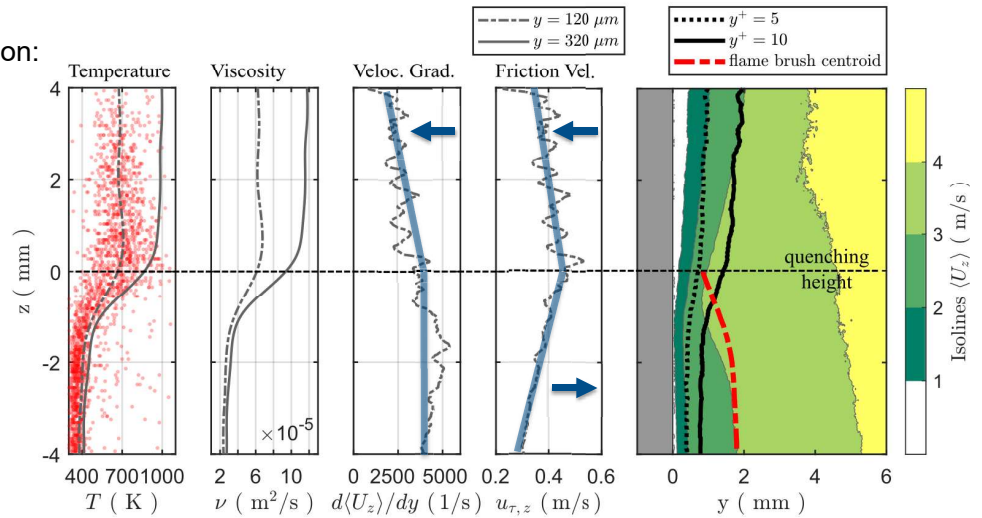
- Reactive case:
 - Linear trend in viscous sublayer preserved for $y^+ \leq 5$
 - Significant deviations from Log-law
 - Trend is increasing when approaching the quenching point (QP) and partially recovers further downstream

Scaling laws for non-reacting TBL no longer valid for near-wall flame (FWI)



Unraveling contributions to TBL evolution:

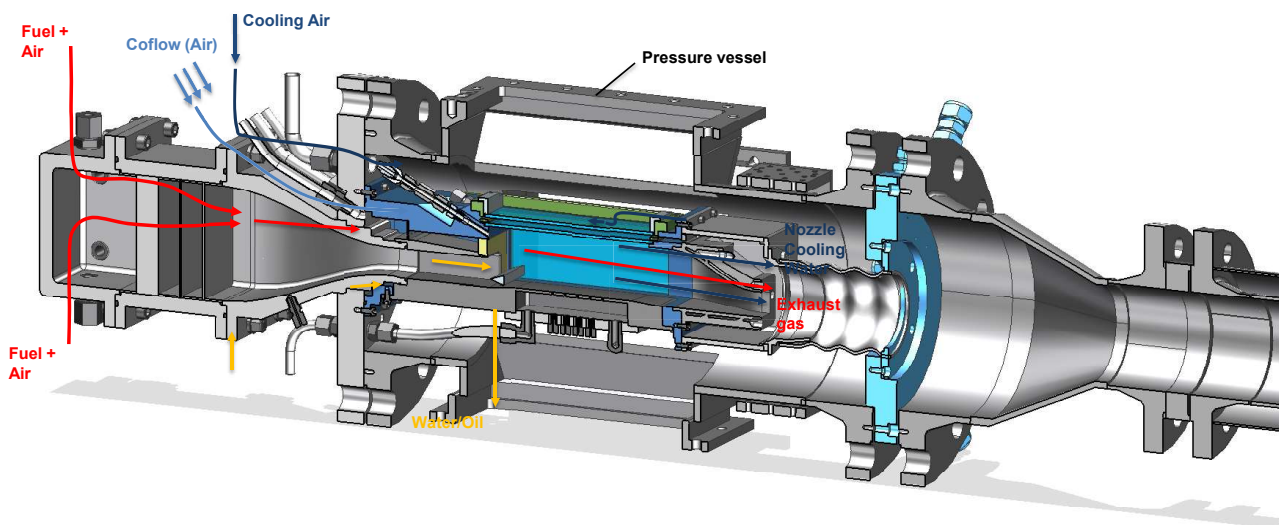
- TBL-thickening across QP
- Temperature-induced viscosity rise across QP
- Velocity gradient drops downstream QP
- Friction Velocity first rises and drops again downstream QP



Temperature-driven viscosity change as major impact, but also the thermal expansion in $\langle U \rangle$

$$u^+ = \frac{\langle U \rangle}{u_\tau} \quad y^+ = \frac{y \cdot u_\tau}{\nu} \quad u_\tau = \sqrt{\nu \cdot \left. \frac{d\langle U \rangle}{dy} \right|_{y=0 \text{ mm}}}$$

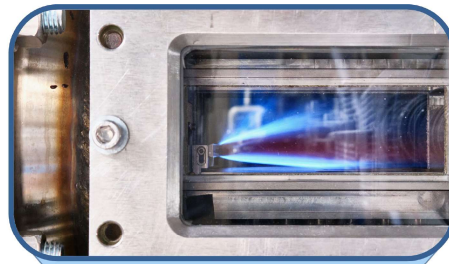
Novel, pressurized side-wall quenching burner



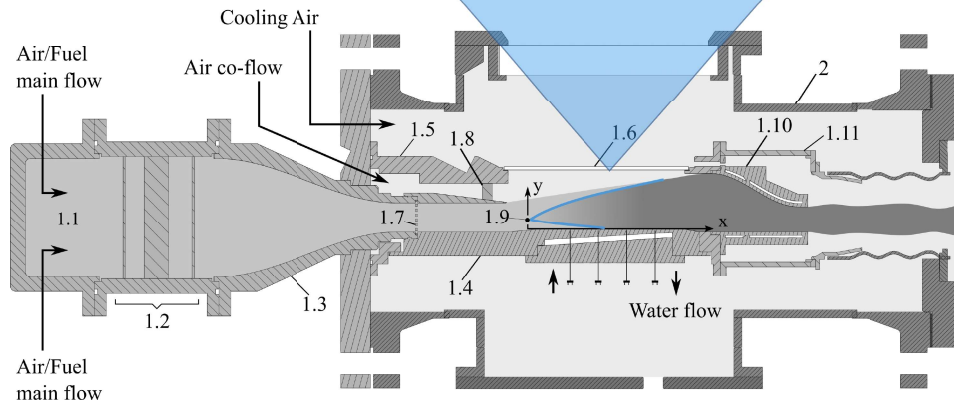
- Johe et al., Dreizler; I. J. Heat Fluid Flow 94, 108921 (2022).
- Johe et al., Dreizler; PCI 2022

Novel, pressurized side-wall quenching burner

- 1.1 Burner plenum
- 1.2 Flow homogenization (grids & meshes)
- 1.3 Morel type nozzle
- 1.4 Quenching wall
- 1.5 Flame tube
- 1.6 Quartz glass windows



- 1.7 Turbulence-generating grid
- 1.8 Co-flow homogenization (sintered bronze structure)
- 1.9 Ceramic rod
- 1.10 Exhaust gas nozzle
- 1.11 Exhaust gas plenum
- 2 Pressure vessel



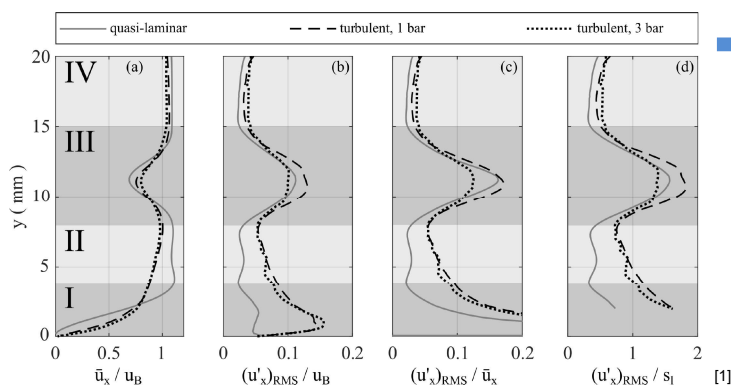
Main design features:

- Pressure vessel for up to 10 bar
- Optical access from 3 sides
- Temperature-controlled quenching wall
- V-shaped flame stabilized at ceramic rod

Novel, pressurized side-wall quenching burner

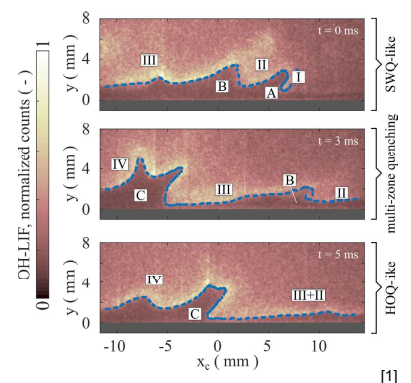
Characterization of inflow boundary conditions and flame front topologies:

- Operating conditions
 - OP1: 1 bar; $Re=8,2000$; $u_{Bulk}=3.8$ m/s; $\Phi=0.8$; $T_{wall}=353$ K; with turbulence-generating grid
 - OP2: 3 bar; $Re=15,000$; $u_{Bulk}=2.3$ m/s; $\Phi=0.8$; $T_{wall}=353$ K; with turbulence-generating grid
 - (OP3: 5 bar; $Re=20,000$; $u_{Bulk}=1.8$ m/s; $\Phi=0.8$; $T_{wall}=353$ K; with turbulence-generating grid
- u_{Bulk} & s_L kept constant → Flame quenching at almost unchanged streamwise (x-direction) position



Good comparability of inflow BC of OP1 & OP3 with regard to normalized velocity (fluctuation)

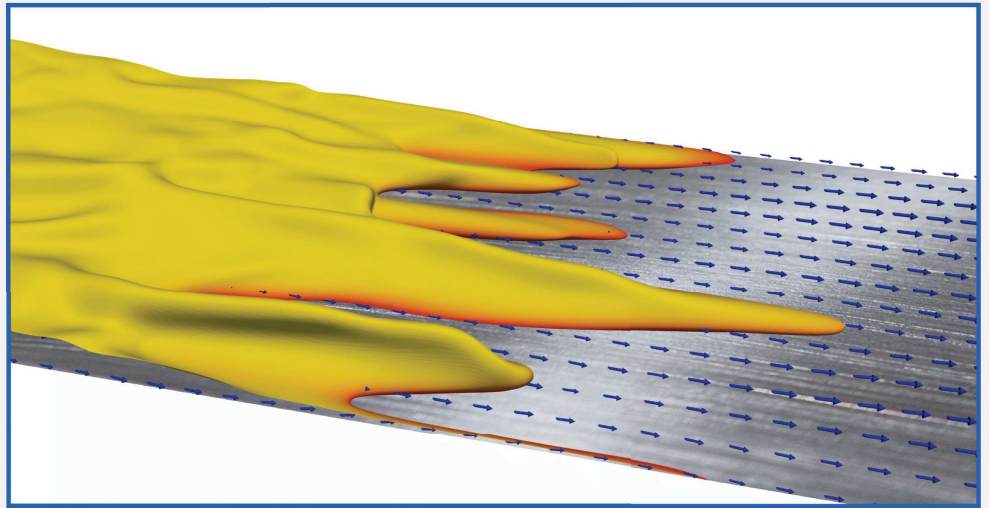
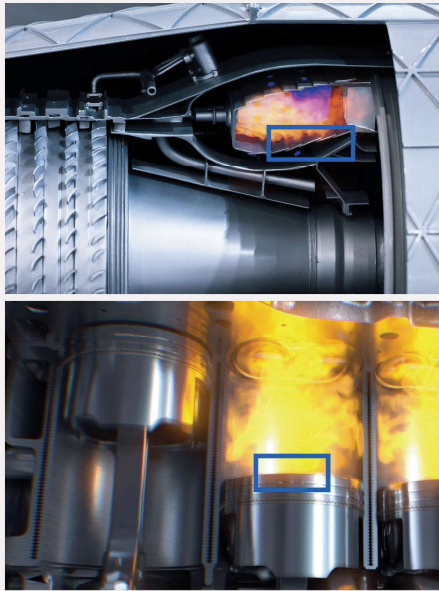
Besides SWQ-like & HOQ-like a multi-zone quenching scenario was identified



Flame-wall interaction (Modeling and Simulation)

TNF Workshop (2022), Vancouver, Canada

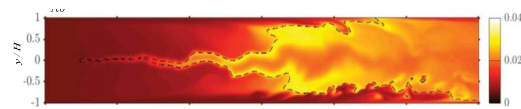
Session coordinators: Andreas Dreizler, Christian Hasse



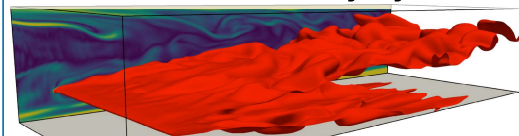
Agenda / Contributors



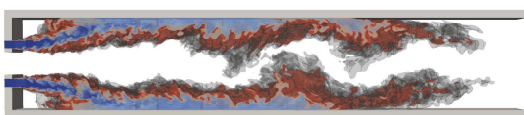
CO modeling in Flame-Wall and Flame-cooling-air Interaction



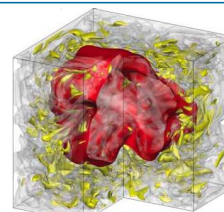
Premixed FWI and heat transfer in turbulent boundary layers



Premixed Turbulent Jet Flames with Flame-Wall Interaction



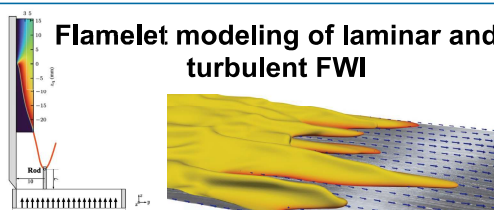
SINTEF



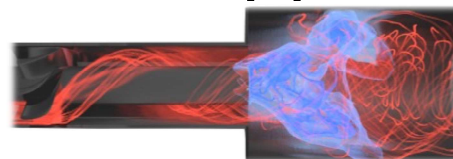
DNS of turbulent FWI in a constant volume vessel



Flamelet modeling of laminar and turbulent FWI



LES of boundary layer flashback



Note: many of the works are collaborations of different universities and Pis. Here, only the main PI is shown.

Overview of modelling of flame-wall interactions

Research fields	Research groups					
	Melbourne	RWTH	TUD	Newcastle	SINTEF	Edinburgh
	Turbulence and turbulence chemistry interaction					
DNS	x	x	x	x	x	
LES			x			x
TCI closure			ATF / pPDF			TF-LES
	Chemistry closure					
Chemistry	DC (skeletal) / <i>Flamelet</i>	DC (skeletal) / <i>Flamelet</i>	DC / Flamelet / REDIM	DC (1-step / skeletal)	DC (skeletal)	DC (skeletal)
Fuels	CH4	CH4	CH4 / DME	CH4 H2	CH4 H2 / NH3-H2	CH4-H2
Configurations	SWQ (FWI / FCAI)	Jet flame (SWQ like)	HOQ* & SWQ (lam. / turb.)	HOQ & SWQ	Isochoric HOQ	Flashback
Software	NTMIX-CHEMKIN	CIAO	OpenFOAM	SENGA+	S3D	OpenFOAM


HOQ: Head-On Quenching
SWQ: Side-Wall Quenching

FCAI: Flame-Cooling Air Interaction
FWI: Flame-Wall Interaction

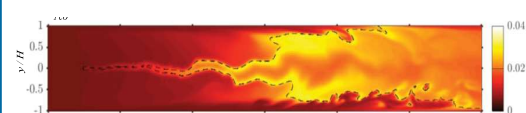
DC: Detailed (finite rate) chemistry
REDIM: Reaction-diffusion Manifold


*HOQ analysis not shown here.

Agenda

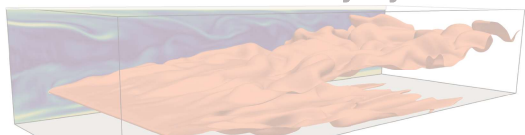



CO modeling in Flame-Wall and Flame-cooling-air Interaction







Premixed FWI and heat transfer in turbulent boundary layers



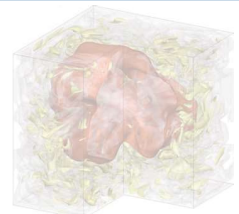



Premixed Turbulent Jet Flames with Flame-Wall Interaction







DNS of turbulent FWI in a constant volume vessel






Flamelet modeling of laminar and turbulent FWI





LES of boundary layer flashback



Note: many of the works are collaborations of different universities and Pis. Here, only the main PI is shown here.



Flame-wall Interaction and Flame-Cooling Air Interaction with a focus on CO emissions*

Project team:

A/Prof Mohsen Talei (Associate Professor, The University of Melbourne),

Dr. Robert Gordon (CTO, MOx Energy Pty Ltd.
Senior Honorary Fellow, University of Melbourne)

Dr. Jacob Rivera (Field Leader, Siemens Energy, Canada)

Dr. Rahul Palulli (PostDoc, KTH Sweden),

Dr. Bin Jiang, (PostDoc, SUSTech China)

Shreshtha Gupta (Ph.D. Candidate, The University of Melbourne),

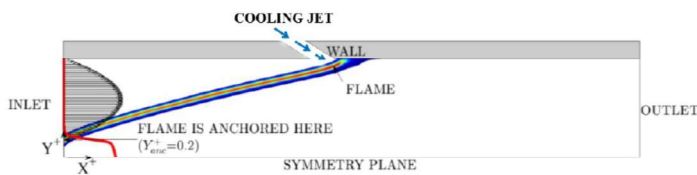
*Slides have been rearranged by STFS.



Flame-wall / Flame-cooling-air interaction

2D forced flame interacting with a cold wall

Palulli et al., Flow Turbul. Combust. (2021), 107(2), 343-365.



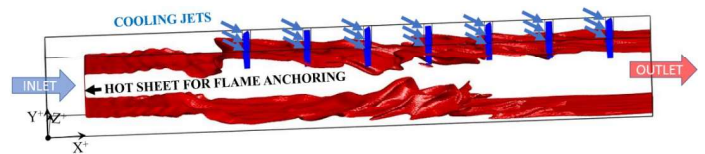
- Stoichiometric, laminar, premixed methane-air flame
- $T_{in} = T_w = 800\text{ K}$, $p = 1\text{ atm}$
- Harmonically perturbed inflow velocity with varying frequency (from 0 to 100 Hz).
- With and without cooling from the wall

Chemistry closure

- Finite rate chemistry
- GRI-3.0 (53 species, 325 reactions)

3D turbulent FWI and FCAI

Palulli et al., Int. J. Heat Fluid Flow (2021), 92, 108888.



- Preheated, premixed methane-air
- 3D channel flow with two flame branches
 - Flame-wall interaction (bottom)
 - Flame-cooling-air interaction (top)

Chemistry closure

- Finite rate chemistry

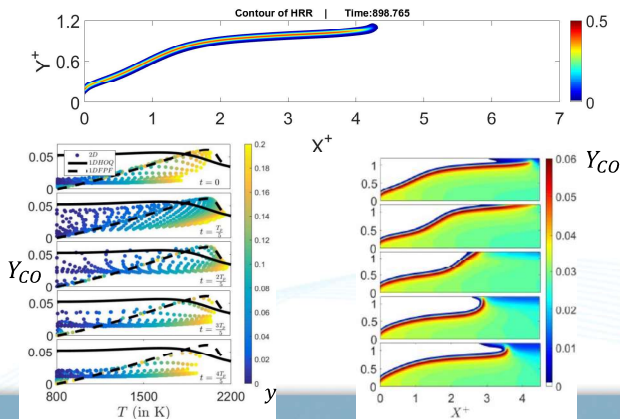
Flame-wall interaction (FWI) Flame-cooling-air interaction (FCAI)

Transient flame-wall interaction

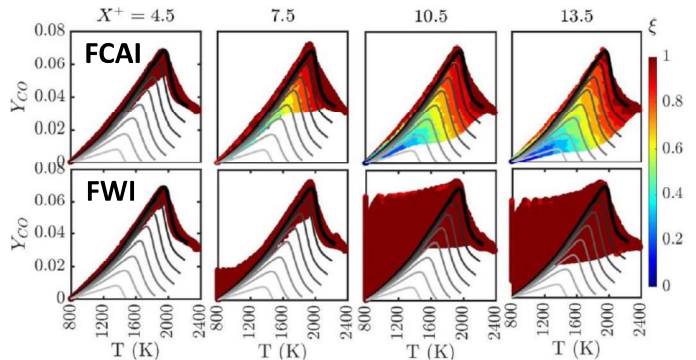
Flame-cooling-air interaction

We observe a consistent thermochemistry between 2D and 3D simulations

- Head-on and side-wall-like quenching events
- Investigation of CO-formation
 - Substantial CO for wall-normal flame tip
 - Comparable T-CO scatter for flame downstream
 - Close to the wall large CO deviations



- Leaner and longer flame tip
- Reduction of CO in the post-combustion zone
- **1D FPF with different mixture fractions (ξ) capture T-CO trends for FCAI**
- **States deteriorate for FWI***



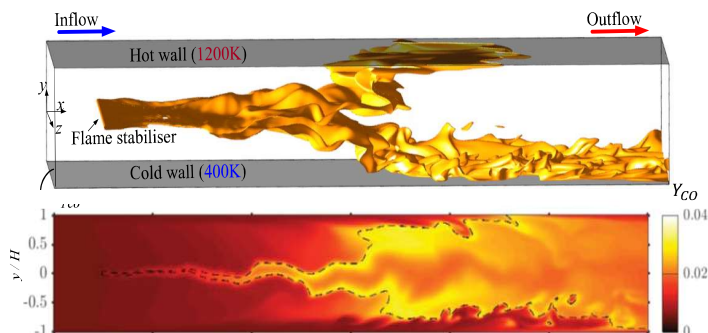
*Hasse: consistent with other experimental and numerical studies (backup)

3D DNS of turbulent FWI

Turbulent FWI for flames diluted by comb. products

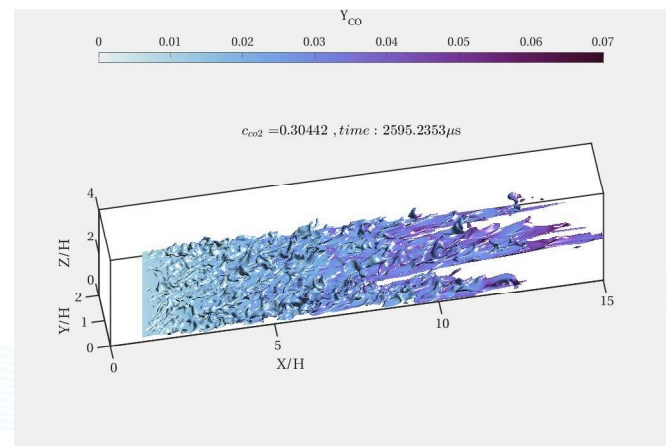
Jiang et al., Comb. Flame (2021), 230, 111432.

- Turbulent ($Re = 3200$) & diluted flames
- $T_w = 400\text{ K} / 1200\text{ K}$
- Diluted flames show larger quenching distances
- Increased CO oxidation times
- Near-wall turbulence-flame interactions create wrinkled and streaky flame surfaces, and localizes the CO.



Intensely Turbulent Flame interacting with a wall

- $Re=10,000, T_w = 800\text{ K}$
- CO modeling based on reaction, turbulence and quenching representative variables
- Work in progress



Agenda



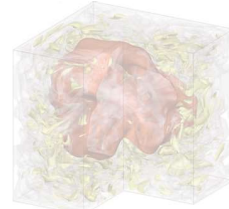
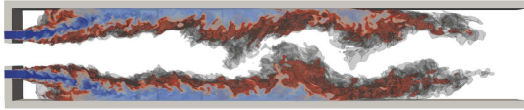
CO modeling in Flame-Wall and Flame-cooling-air Interaction



Premixed FWI and heat transfer in turbulent boundary layers



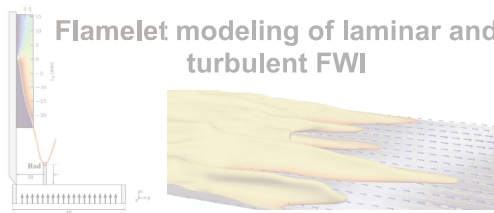
Premixed Turbulent Jet Flames with Flame-Wall Interaction



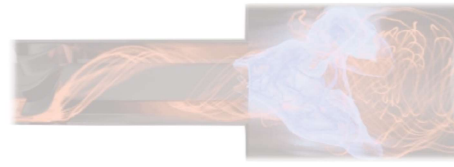
DNS of turbulent FWI in a constant volume vessel



Flamelet modeling of laminar and turbulent FWI

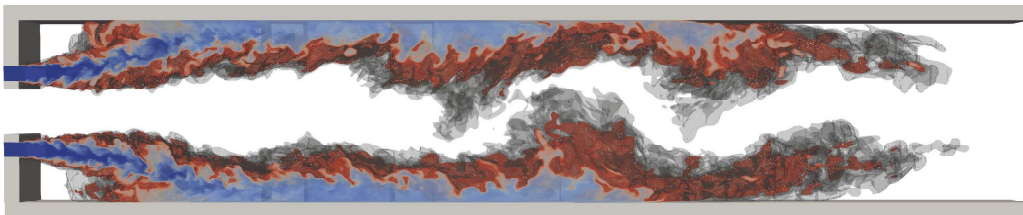


LES of boundary layer flashback



Note: many of the works are collaborations of different universities and Pis. Here, only the main PI is shown here.

Premixed Turbulent Jet Flames with Flame-Wall Interaction



Combustion Symposium 2022

IGII: Direct numerical simulation of flame-wall interaction
at gas turbine relevant conditions
K. Niemietz, L. Berger, M. Huth, A. Attili, H. Pitsch

Institute for Combustion Technology
RWTH Aachen University

- Turbulent Jets

- Jet Reynolds number $Re_j = 5,500$
- Jet velocity $u_j = 73.5$ m/s
- Jet slot height $h_j = 1.2$ mm
- Jet temperature $T_u = 673$ K

- Pilot

- Pilot velocity $u_p = 20$ m/s
- Pilot slot height $h_p = 3 \cdot h_j = 3.6$ mm
- Burnt exhaust gas $T_p = T_b = 1782$ K

- Equivalence ratio $\varphi = 0.5$

- **Pressure** $p = 4$ bar

- **Wall temperature** $T_w = 1000$ K

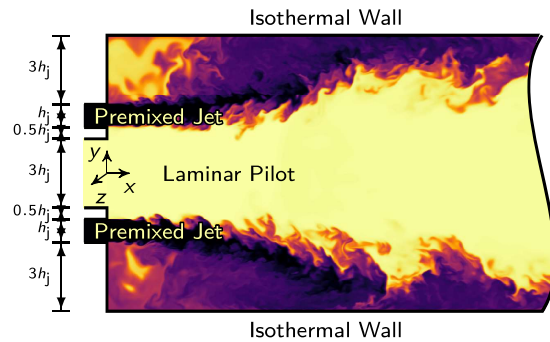
- Fuel ratio $\frac{\dot{m}_{jet}}{\dot{m}_{pilot}} = \frac{9}{1}$

- Domain:

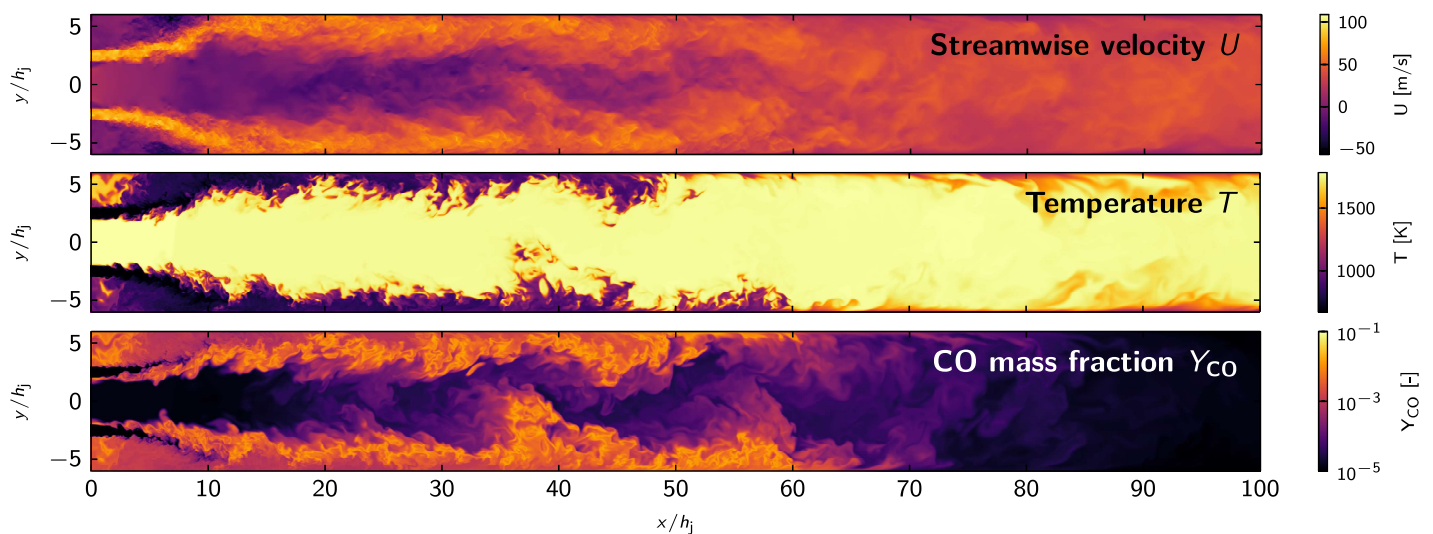
- $120 \times 14.4 \times 7.2$ mm
- $6060 \times 1440 \times 360$ cells
- 3.1 billion cells

- Finite rate chemistry

- Skeletal **methane** mechanism
- 25 Species and 155 Reactions
- Derived from Cai et al.^[1]



DNS Results



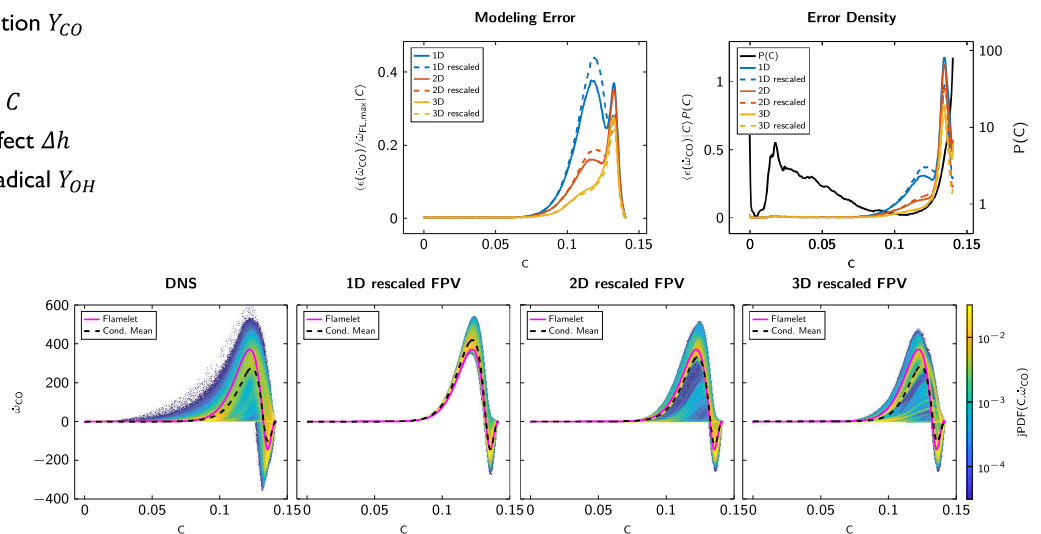
A-priori Investigation of CO Modeling Approaches

Modeling CO Source Term $\dot{\omega}_{CO}$

- Flamelet-Progress Variable (FPV) Model
- Transport equation for CO mass fraction Y_{CO}
- Rescaling of $\dot{\omega}_{CO}$ with local $Y_{CO}^{[1]}$
- 1D chemistry table: Progress Variable C
- 2D chemistry table: C + Enthalpy Defect Δh
- 3D chemistry table: C + Δh + OH Radical Y_{OH}
- The large timescales of CO oxidation are not well captured by the FPV model
 - CO transport equation improves the Y_{CO} prediction downstream
- OH radical very promising for CO model
 - Parameterization of strain^[2]
 - Main reaction partner for CO oxidation
 $CO + OH \rightarrow CO_2 + H$

Model errors for the 3 model versions (with and without source term rescaling)

Error Density is the conditional error multiplied with the PDF of C



13

Institute for Combustion Technology | Heinz Pitsch

[1] Ihme & Pitsch, Phys. Fluids 20 (2008).

[2] Knudsen et al., Combust. Flame 160 (12) (2013) 2911-2927.



Agenda



CO modeling in Flame-Wall and Flame-cooling-air Interaction

Premixed FWI and heat transfer in turbulent boundary layers

Premixed Turbulent Jet Flames with Flame-Wall Interaction

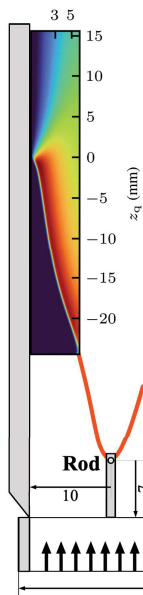
DNS of turbulent FWI in a constant volume vessel

Flamelet modeling of laminar and turbulent FWI

LES of boundary layer flashback

Note: many of the works are collaborations of different universities and Pis. Here, only the main PI is shown here.

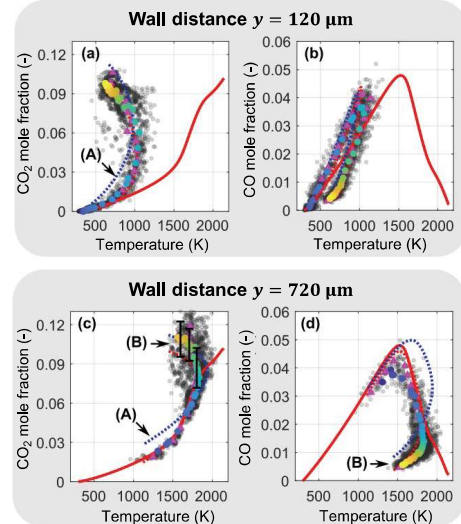
Laminar SWQ: Influence of differential diffusion



Laminar side-wall quenching investigations

- Fully premixed side-wall quenching burner
 - Laminar, dimethyl ether-air flame ($\phi = 0.83$)
 - $Re = 5.900$
 - $T_{in} = 293.15 \text{ K}$; $T_{wall} = 330 \text{ K}$
- Experimental studies [1]
 - Particle image velocimetry
 - Flame visualization (OH-PLIF)
 - Dual-Pump CARS (T & CO₂), CO-LIF
- Numerical simulations [2,3]
 - Reduced two-dimensional simulation domain
 - $(y \times z) = (6 \text{ mm} \times 40 \text{ mm})$; $\Delta_{grid} = 50 \mu\text{m}$
 - Parabolic inflow profile
 - Flame stabilization with hot gases injected in a 0.5mm wide section (right)

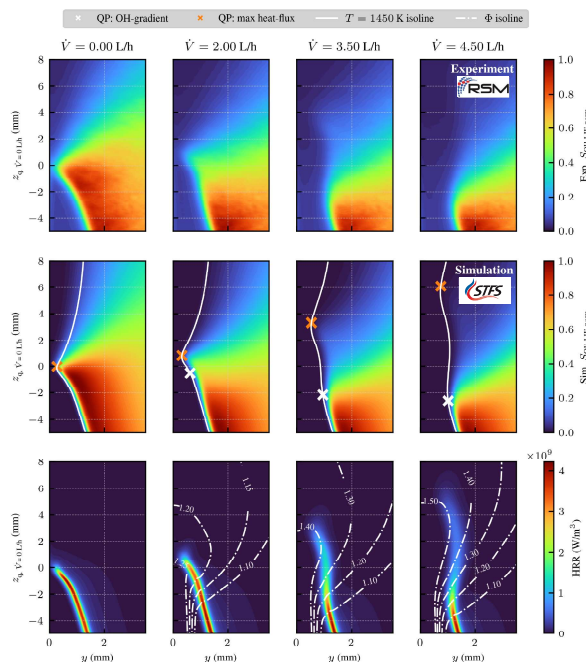
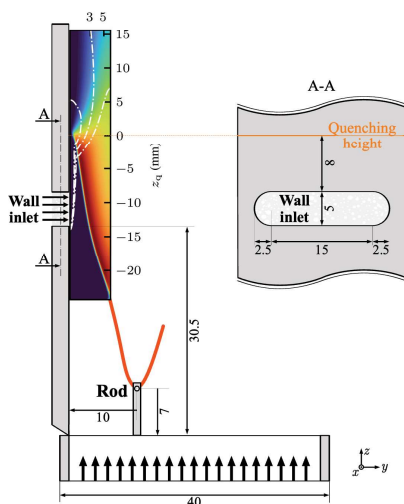
Near-wall differential diffusion important



- [1] Zentgraf et al.; Combust. Flame 235, 111707 (2021)
 [2] Luo et al.; Combust.Theor. Model, 1-26 (2021)
 [3] Stagni et al.; Combust. Flame 232, 111529 (2021)

Laminar SWQ: Combined effect flame retardants and FWI

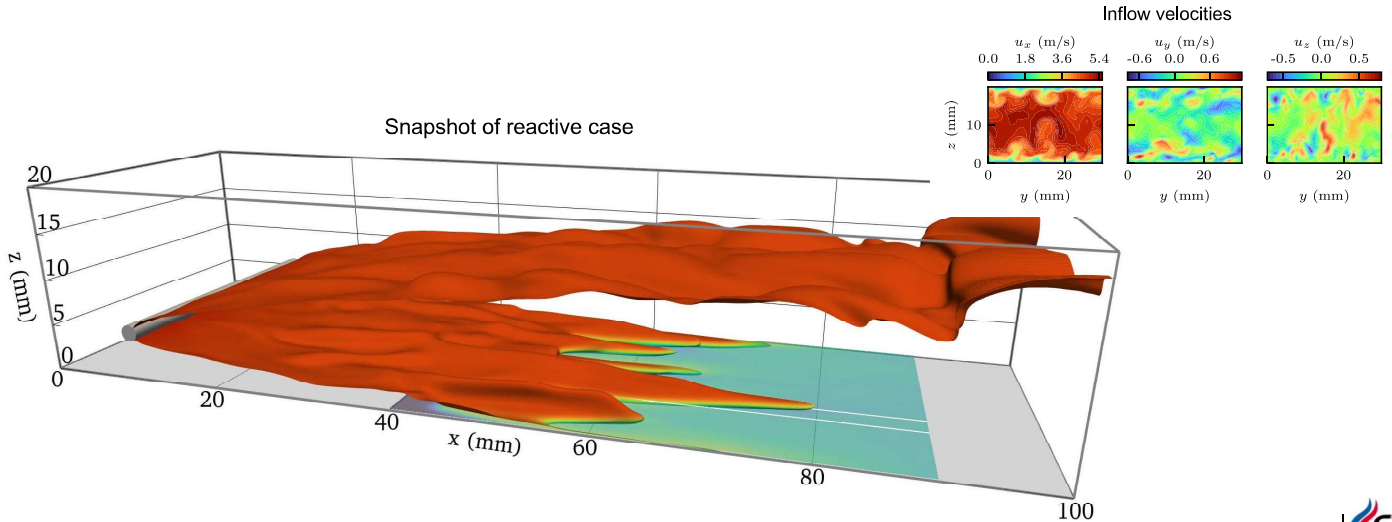
- Wall inlet allows **seeding with additional reactants**
 - Partially-premixed flames
 - Addition of flame retardants
- Wall inlet modeled with Robin-BC



Laminar SWQ methane-air flame with pure methane addition.

- Combined experimental and numerical study
- Laminar, partially-premixed flame structure
- Combined study of heat-loss induced quenching and quenching caused by chemical composition
- Excellent agreement of simulations with experiments

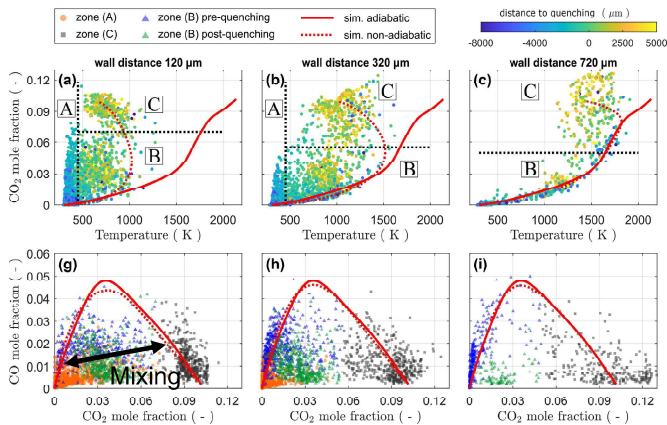
- Fully developed turbulent channel flow
 - $Re_\tau = 180$
 - $p = 1 \text{ atm}$
 - $(x \times y \times z) = (100 \times 30 \times 20) \text{ mm}$
 - > 200 Mio. grid points
- **Case1: Methane-air ($\phi = 1.0$)**
 - $T_{in} = T_{Wall} = 300 \text{ K}$
 - Reduced CRECK-mechanism (24 Species, 165 Reactions)
 - Diffusion modelling: $Le = 1$
- **Case2: DME-air ($\phi = 0.83$)**
 - $T_{in} = T_{Wall} = 300 \text{ K}$
 - Reduced CRECK-mechanism^[1] (20 Species, 93 Reactions)
 - Diffusion modelling: Mixture average



[1] Stagni et al.; Combust. Flame 232, 111529 (2021)

Experiment (A04E) ^[1]

- Turbulent DME-air flame, $p = 1 \text{ atm}$, $\phi = 0.83$
- Exhaust gas recirculation close to the flame quenching point (Flame-vortex-interaction mechanism)

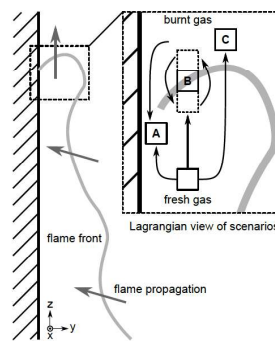


Thermochemical state observed in the experiments. Taken from ^[1]

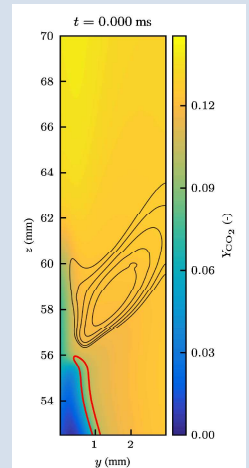
[1] Zentgraf et al.; Combust. Flame, 111681 (2021)

Simulation (Case 1)

- Turbulent methane-air flame $p = 1 \text{ atm}$, $\phi = 1.0$ (Case 1)
- Validation of experimental hypothesis
- Shift in thermochemistry can be accounted for by an additional dimension in the manifold



Flame-vortex interaction mechanism (FVI) ^[1].



Motivation

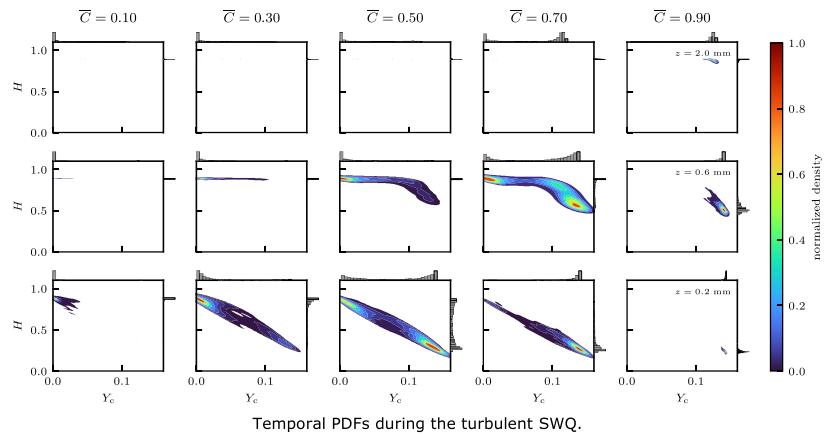
- Analysis of TCI closure models suitable for RANS / LES of turbulent FWI

Setup and Models employed

- Methane-air (Case 1) flame in turbulent channel
- Chemistry manifold: 2D QFM [1]
 - $[T, p, Y_i, \dots, Y_n] = f(Y_c, H)$
 - Joint PDF/FDF $\tilde{P}(Y_c, H)$ is required for TCI

Major findings

- Complex, bivariate temporal PDFs (RANS) and spatial FDFs (LES) close to the wall
- TCI models need to account for this to give correct prediction (validated in an a-priori manner)



$$\tilde{Q} = \int_{Y_c} \int_H \underbrace{\tilde{f}_Q(Y_c, H)}_{\text{Chem. Manifold}} \underbrace{\tilde{P}(Y_c, H)}_{\text{PDF}} dY_c dH$$

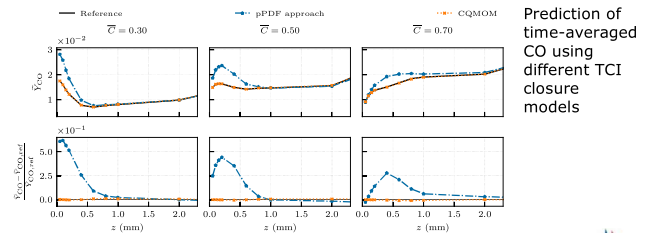
$$\tilde{Q} = \int_{Y_c} \int_H \underbrace{\tilde{f}_Q(Y_c, H)}_{\text{Chem. Manifold}} \underbrace{\tilde{P}(Y_c, H)}_{\text{PDF}} dY_c dH \approx f(\tilde{C}, \tilde{C}^{w2}, \tilde{H}) = \iint \tilde{f}_Q(C, H) \cdot \underbrace{\tilde{P}(C)}_{\beta\text{-PDF}} \underbrace{\tilde{P}(H)}_{\delta\text{-peak}} dC dH$$

$$\tilde{Q} = \int_{Y_c} \int_H \underbrace{\tilde{f}_Q(Y_c, H)}_{\text{Chem. Manifold}} \underbrace{\tilde{P}(Y_c, H)}_{\text{PDF}} dY_c dH \approx f(\tilde{m}_{j,k}) \approx \sum_{\alpha=1}^{N_\alpha} \sum_{\beta=1}^{N_\beta} w_\alpha w_{\alpha\beta} \tilde{f}_Q(\phi_\alpha, \phi_{\alpha\beta})$$

Reference

pPDF

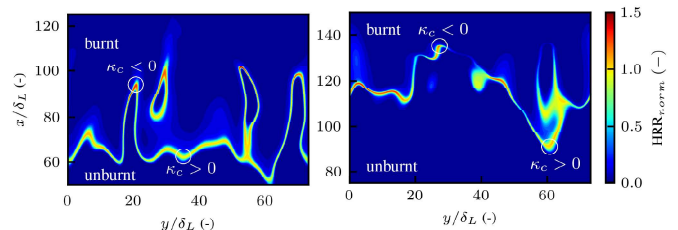
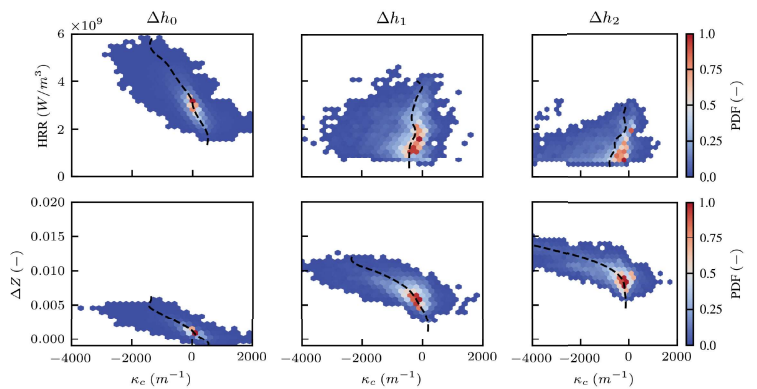
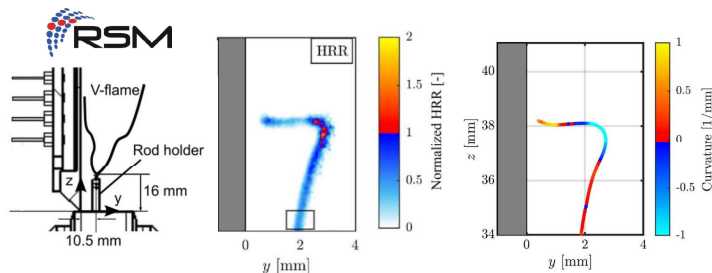
CQMOM



[1] Efimov et al., Comb. Theory and Modelling 24, 72-104 (2020); Results are published in: Steinhausen et al.; Int. J. Heat Fluid Flow, 93(2), 108913 (2022) and data [here](#).

Turbulent SWQ: Combined effects of heat loss and curvature

- **Motivation:** Strong correlation between curvature and heat-loss found in DME-air flames [1]
- DME-air flame under similar conditions to the experiment (**Case 2**)
- High influence of the wall on
 - Local equivalence ratio (differential diffusion)
 - Heat-release \leftrightarrow curvature correlations
- The influence of the wall needs to be accounted for in TCI closure models and manifolds



[1] Kosaka et al., Flow, Turbul. Combust. 104(4), 1029-1046 (2019)

Local HRR in the core flow (left) and near-wall region (right).

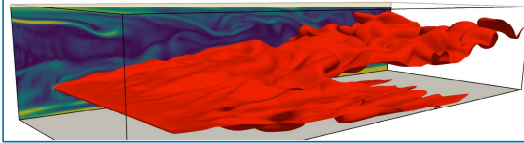
Agenda



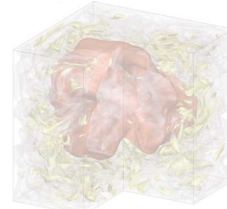
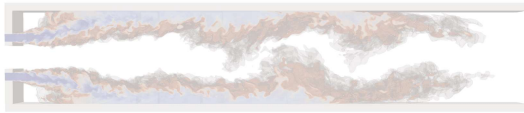
CO modeling in Flame-Wall and Flame-cooling-air Interaction



Premixed FWI and heat transfer in turbulent boundary layers



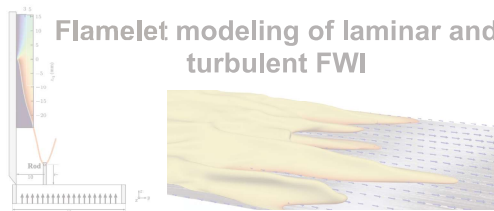
Premixed Turbulent Jet Flames with Flame-Wall Interaction



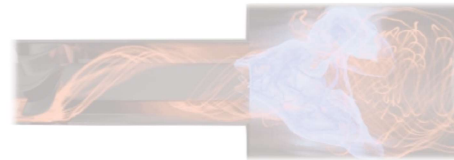
DNS of turbulent FWI in a constant volume vessel



Flamelet modeling of laminar and turbulent FWI



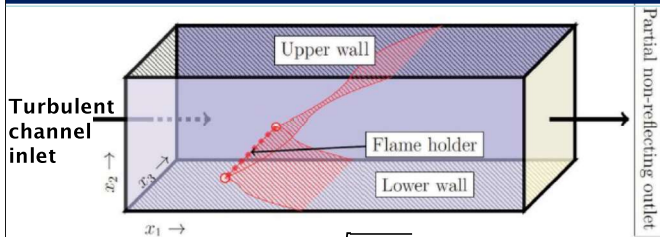
LES of boundary layer flashback



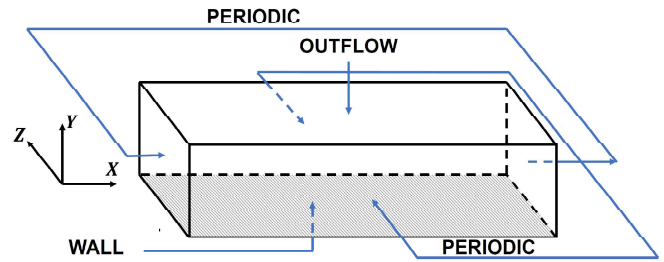
Note: many of the works are collaborations of different universities and Pis. Here, only the main PI is shown here.

Flame-wall Interaction in fully-developed turbulent boundary layers

Simulation set-up



$$\tau_{wall} = \mu \left. \frac{\partial u}{\partial y} \right|_{y=0}, \quad u_{\tau} = \sqrt{\frac{|\tau_{wall}|}{\rho}}, \quad Re_{\tau} = \frac{\rho u_{\tau} h}{\mu} \text{ and } y^+ = \frac{u_{\tau} y}{\nu_{wall}}$$



- ❖ V-flame is investigated in the $Re_{\tau} = 110$ channel flow with inert walls.
- ❖ The flame holder is placed in the log-layer region of the channel flow at $y^+ = 55$.
- ❖ Domain size $10.69h \times 2h \times 4h$ discretised on $1920 \times 360 \times 720$ (approx. 0.5 billion) grid points.
- ❖ The simulation is run for three flow through times after the initial transients have decayed.

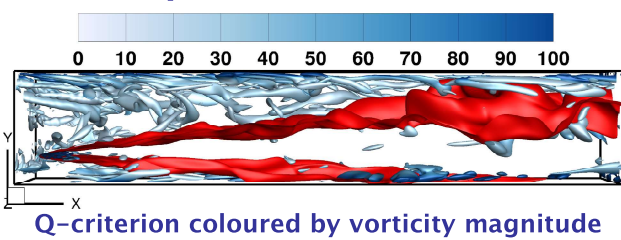
- ❖ HOI is investigated in the $Re_{\tau} = 110$ periodic boundary layer with inert walls.
- ❖ Domain size $10.69h \times 1.33h \times 4h$ discretised on $1920 \times 240 \times 720$ (approx. 0.25 billion) grid points.
- ❖ The simulation is run until the flame has fully quenched.
- ❖ Progress variable is defined in terms of the fuel mass fraction.

U. Ahmed, N. Chakraborty, M. Klein, "Influence of thermal wall boundary condition on scalar statistics during flame-wall interaction of premixed combustion in turbulent boundary layers", *Int. J. Heat and Fluid Flow*, 92, 108881, (2021); U. Ahmed, N. Chakraborty, M. Klein, "Assessment of Bray Moss Libby formulation for premixed flame-wall interaction within turbulent boundary layers: Influence of flow configuration", *Combust. Flame*, 233, 111575 (2021); U. Ahmed, N. Chakraborty, M. Klein, "Scalar gradient and strain rate statistics in oblique premixed flame-wall interaction within turbulent channel flows", *Flow, Turb. Combust.* 106, 701–722, (2021).



Simulation configurations in boundary layers

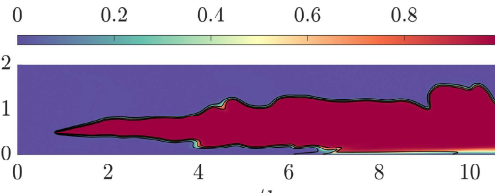
Oblique FWI for V-flames



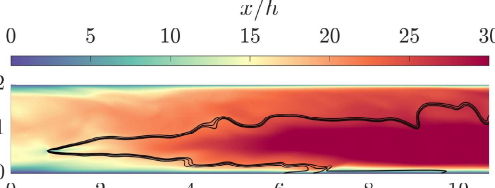
Q-criterion coloured by vorticity magnitude

Non-Dim. Temperature

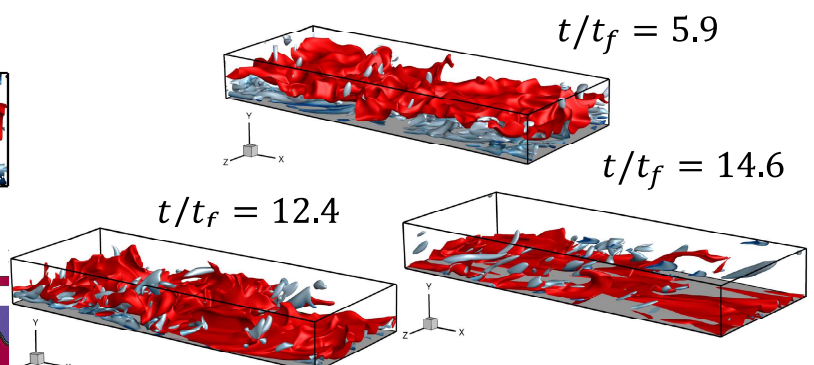
$$T = \frac{\hat{T} - T_R}{T_{ad} - T_R}$$



Non-Dim. Streamwise Velocity

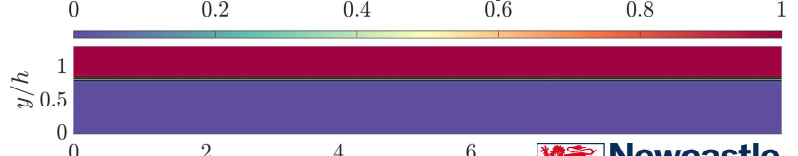


Head-on interaction (HOI)



Q-criterion coloured by vorticity magnitude

Non-Dim. Temperature



U. Ahmed, N. Chakraborty, M. Klein, "Influence of thermal wall boundary condition on scalar statistics during flame-wall interaction of premixed combustion in turbulent boundary layers", *Int. J. Heat and Fluid Flow*, 92, 108881, (2021); U. Ahmed, N. Chakraborty, M. Klein, "Assessment of Bray Moss Libby formulation for premixed flame-wall interaction within turbulent boundary layers: Influence of flow configuration", *Combust. Flame*, 233, 111575 (2021); U. Ahmed, N. Chakraborty, M. Klein, "Scalar gradient and strain rate statistics in oblique premixed flame-wall interaction within turbulent channel flows", *Flow, Turb. Combust.* 106, 701–722, (2021).



Major findings: HOQ and SWQ flames

- ❖ Wall boundary condition, orientation of mean direction of flame propagation with respect to wall normal, and orientation of flame normal to the background flow direction are important factors for FWI
- ❖ **OWI:** Locally counter-gradient behaviour can be observed and the wall boundary condition affects the scalar flux behaviour in this configuration.
- ❖ **HOQ:** Predominantly counter-gradient behaviour can be observed and the wall boundary condition does not affect the scalar flux behaviour in this configuration.

Gradient hypothesis: $\overline{\rho u_i'' q''} = -\frac{\mu_t}{\sigma_t} \frac{\partial \tilde{q}}{\partial x_i}$

Gradient type transport: $\overline{\rho u_i'' q''} \times \frac{\partial \tilde{q}}{\partial x_i} < 0$

Counter-gradient type transport: $\overline{\rho u_i'' q''} \times \frac{\partial \tilde{q}}{\partial x_i} > 0$







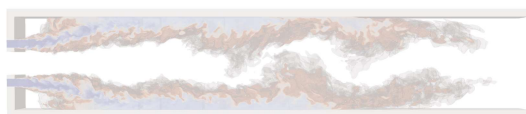




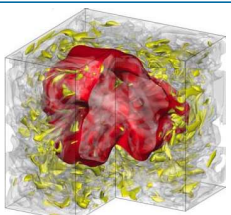


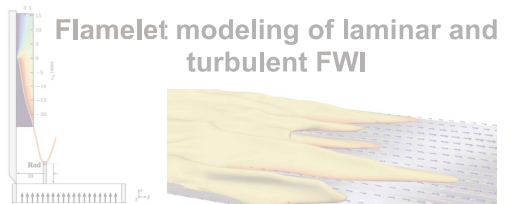
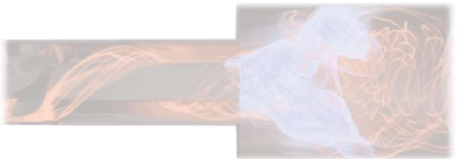


U. Ahmed, N. Chakraborty, M. Klein, "Influence of thermal wall boundary condition on scalar statistics during flame-wall interaction of premixed combustion in turbulent boundary layers", *Int. J. Heat and Fluid Flow*, 92, 108881, (2021); U. Ahmed, N. Chakraborty, M. Klein, "Assessment of Bray Moss Libby formulation for premixed flame-wall interaction within turbulent boundary layers: Influence of flow configuration", *Combust. Flame*, 233, 111575 (2021); U. Ahmed, N. Chakraborty, M. Klein, "Scalar gradient and strain rate statistics in oblique premixed flame-wall interaction within turbulent channel flows", *Flow, Turb. Combust.* 106, 701–733, (2021).

Statistical Behaviour of Turbulent Kinetic Energy Transport in Boundary Layer Flashback of Hydrogen-Rich Premixed Flames

Relations between turbulent burning velocity and wall heat flux using energy integral equation for premixed flame-wall interaction in turbulent boundary layers

see backup slides

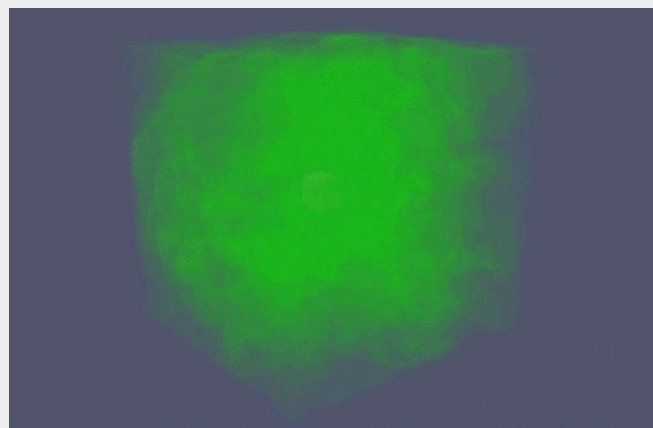
Agenda

 	<h3>CO modeling in Flame-Wall and Flame-cooling-air Interaction</h3> 	<h3>Premixed FWI and heat transfer in turbulent boundary layers</h3> 	 
<h3>Premixed Turbulent Jet Flames with Flame-Wall Interaction</h3> 	 	   <h3>DNS of turbulent FWI in a constant volume vessel</h3>	
 	<h3>Flamelet modeling of laminar and turbulent FWI</h3> 	<h3>LES of boundary layer flashback</h3> 	 

Note: many of the works are collaborations of different universities and Pis. Here, only the main PI is shown here.

Direct Numerical Simulation of turbulent flame-wall interaction for H₂-, CH₄- and NH₃/H₂/N₂-air premixed flames at isochoric conditions

Active collaborations
between
Norway (SINTEF/NTNU)
Japan (Tokyo Tech)
Germany (TU Darmstadt)



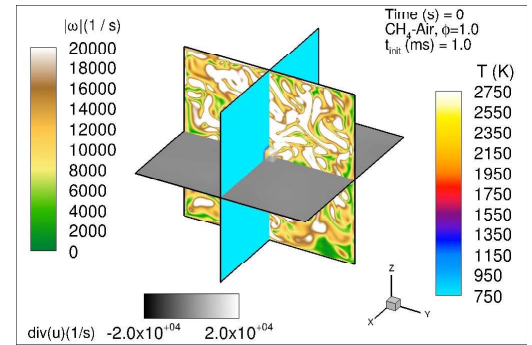
Yuki Minamoto (Tokyo Institute of Technology)
and **Andrea Gruber** (SINTEF/NTNU)



DNS configuration (common features)



- Overall objective is comparative FWI analysis of **partially-decomposed ammonia, methane** and **hydrogen**
- Physical domain is a 1 cm³ cube
- All boundaries are assumed to be no-slip, isothermal walls at $T_w = 750$ K
- Fuel-air mixture at $T_u = 750$ K and $P = 1$ bar is subject to homogeneous isotropic turbulence and allowed a relaxation time 1 ms ($\sim 2.2 \tau_{\text{eddy}}$) before ignition (non-reactive precursor DNS)
- The reactive simulation is initialized by imposing a laminar flame in a 1 mm³ cubical region at the domain geometrical center
- Spatial discretization (mild near-wall refinement):
 - 700³ mesh (initial phase, $P < 2$ bar)
 - 980³ mesh (late phase, $P > 2$ bar)



Overview of DNS cases







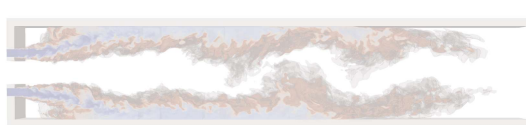




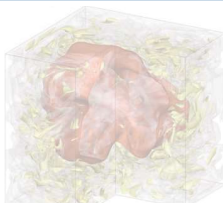



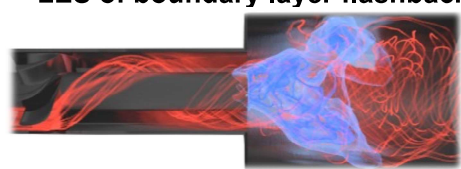




Case	H ₂ lean	H ₂ lean adiabatic	H ₂ stoich	NH ₃ /H ₂ /N ₂ stoich	CH ₄ stoich (Lu)	CH ₄ stoich (S&G)
Boundary Conditions						
Type	Isothermal, no-slip	Periodic	Isothermal, no-slip	Isothermal, no-slip	Isothermal, no-slip	Isothermal, no-slip
Nominal Flame Properties						
ϕ	0.25	0.25	1.0	1.0	1.0	1.0
S_L (m/s)	2.5	2.5	12	2.2	2.1	2.9
T_{ad} (K)	1455	1455	2586	2370	2438	2448
Chemistry						
Kinetics scheme (species/reactions)	Li et al. (9/19)	Li et al. (9/19)	Li et al. (9/19)	Jiang et al. (19/63)	Lu & Law (30/184)	Smooke & Giovangigli (16/35)
Fuel	Hydrogen	Hydrogen	Hydrogen	Ammonia / Hydrogen	Methane	Methane
Initial HIT parameters ($Re_t=715$) & TCI						
u' (m/s) ; l_T (mm)	10.8 ; 5	10.8 ; 5	10.8 ; 5	10.8 ; 5	10.8 ; 5	10.8 ; 5
Ka	11.56	11.56	2.41	10.46	8.33	6
Da	2.31	2.31	11	2.55	3.2	4.61

Summary and outlook

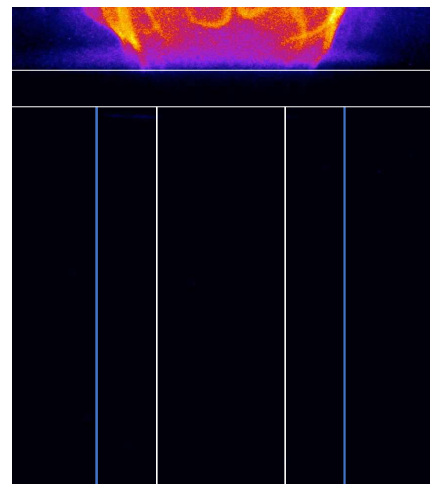
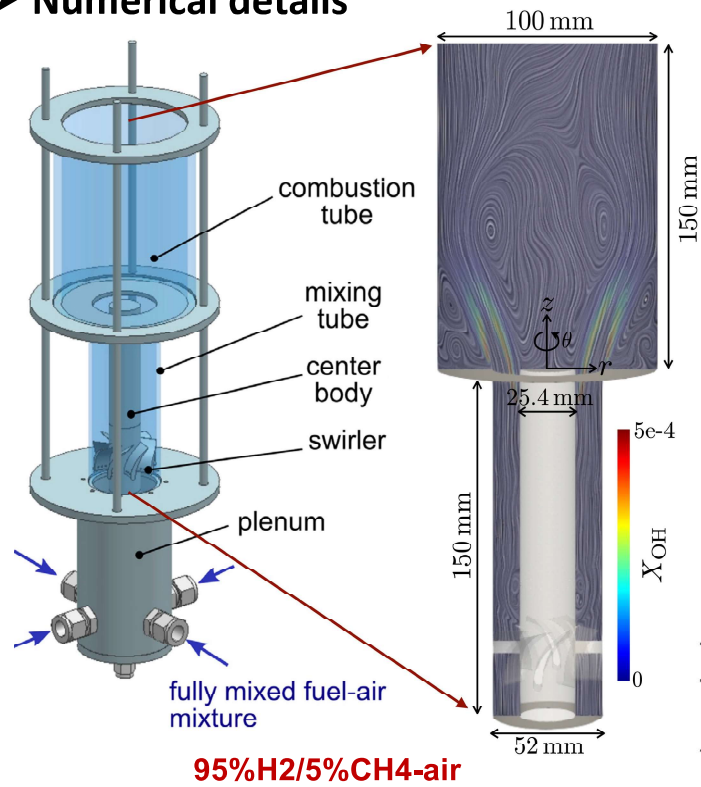
- DNS databases of turbulent FWI at isochoric conditions are built and are being analysed
- The DNS data has revealed to date (for the present condition & fuels):
 - Radical recombination reactions take place at the wall and have a crucial role in the turbulent FWI, affecting heat release rate and pollutants formation
 - For methane-air flames, inclusion of C₂-species (Lu&Law vs Smooke&Giovangigli) is required for correct prediction of FWI process (confirming 1-D HOQ results by Salimath et al.)
- Comparative analysis of the freely-propagating turbulent flames (before FWI) is initiated

Agenda

 	<p>CO modeling in Flame-Wall and Flame-cooling-air Interaction</p> 	<p>Premixed FWI and heat transfer in turbulent boundary layers</p> 	 
<p>Premixed Turbulent Jet Flames with Flame-Wall Interaction</p> 	 	 	<p>DNS of turbulent FWI in a constant volume vessel</p> 
 	<p>Flamelet modeling of laminar and turbulent FWI</p> 	<p>LES of boundary layer flashback</p> 	 

Note: many of the works are collaborations of different universities and Pis. Here, only the main PI is shown here.

➤ Numerical details

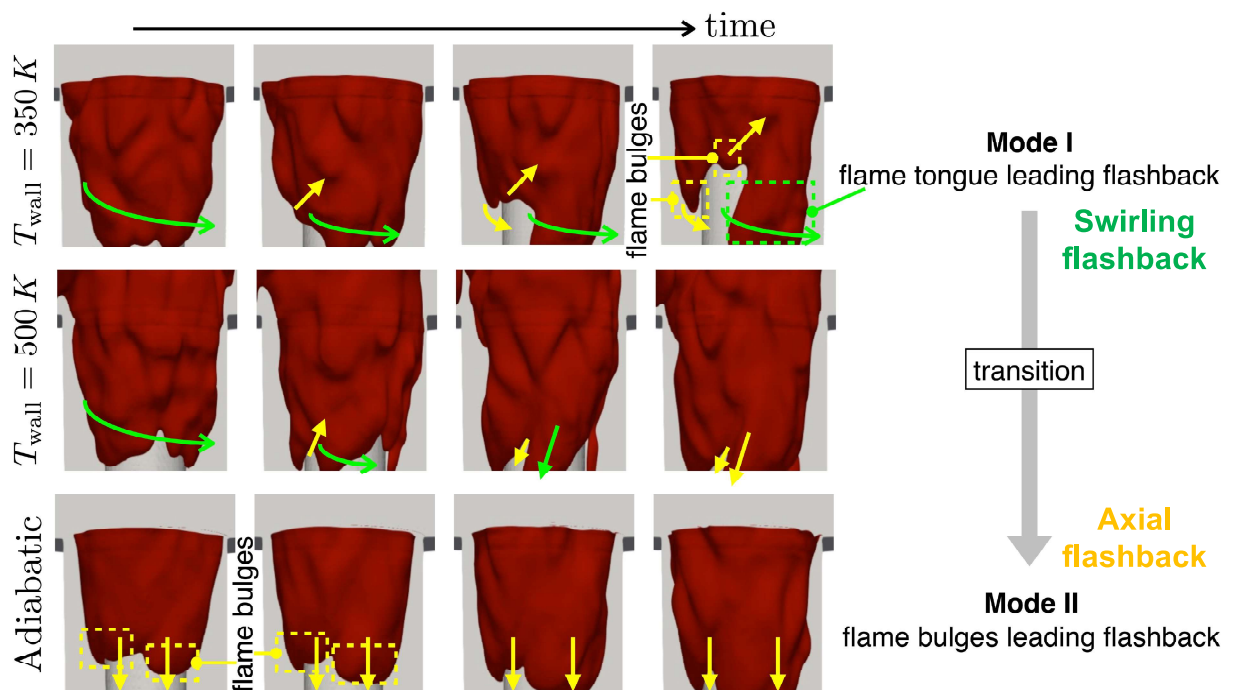


(Ebi et al., CNF2016)

Table 1: Summary of cases simulated in this work.

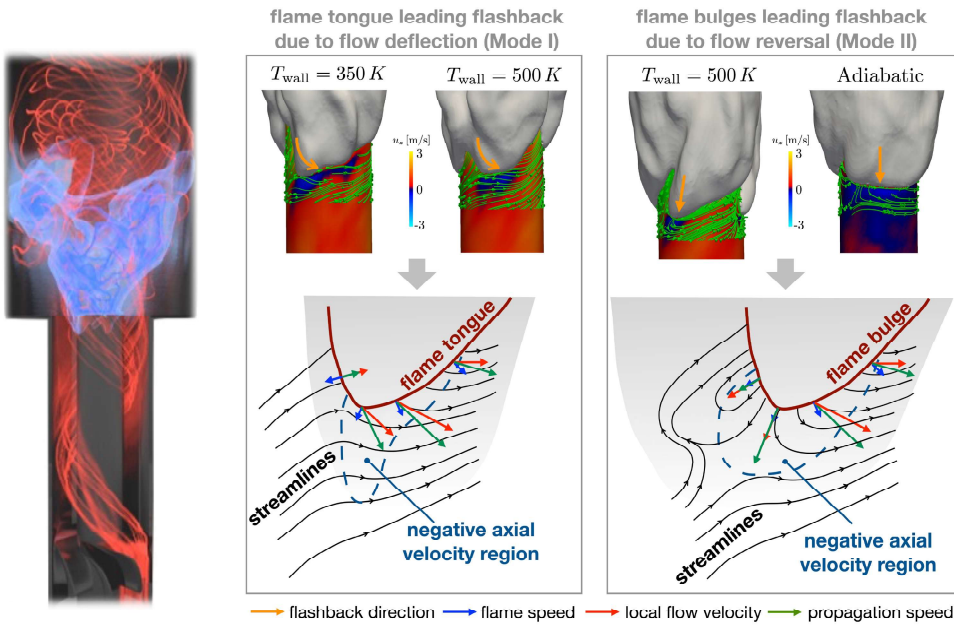
ϕ / Wall BC	350 K	500 K	Adiabatic
Stable flame ($\phi = 0.33$)	✓	-	-
Flashback ($\phi = 0.40$)	✓	✓	✓

➤ Flashback modes



Green box and arrow represents flame tongue. Yellow box and arrow represent flame bulges

➤ Flashback mechanisms

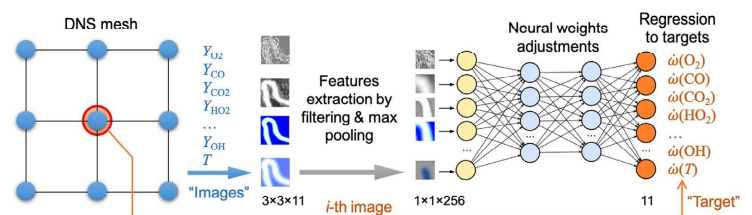


- $T_{wall}=300K$, flame tongue causes the deflection of streamlines and promotes flashback. Small regions of negative axial velocity cannot lead to flashback.
- For adiabatic case, flame bulges cause a large reverse flow pocket, forming a stagnation point, leading to flashback.

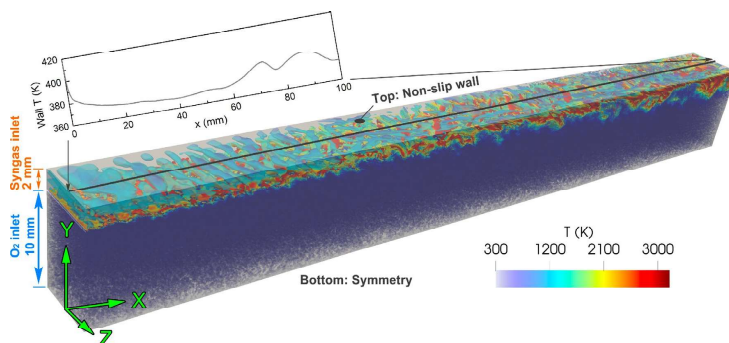
Low-Emission Combustion Technologies, 1D02, 10:35 Monday July 25.

Vervisch: FWI manifolds for non-premixed flames using machine learning

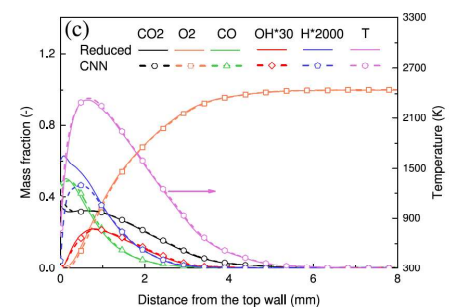
- Tabulation of FWI chemistry manifolds is challenging
 - Influence of heat-losses
 - Differential diffusion
- New approaches for chemistry reduction are promising, e.g. as used in [1, 2] in a non-premixed turbulent methane-air flame



CNN training from 2D Database [1]



Instantaneous iso-surface of Q criterion predicted by CNN-DNS, colored by gas temperature [1].



Averaged distributions of CO_2 , O_2 , CO , OH , H mass fractions and temperature. [1]

- ▶ **Transient aspects of FWI** (laminar or turbulent)
 - ▶ Effects the local propagation (HOQ- / SWQ-like quenching)
 - ▶ FVI is prominent in many turbulent studies
 - ▶ Changes in thermochemistry
 - ▶ Needs to be accounted for in tabulated manifolds
- ▶ **Prediction of near-wall CO**
 - ▶ Freely-propagating flames are not sufficient to capture FWI due to near-wall CO diffusion [1]
 - ▶ Transported CO improves the prediction, but further model development is required
 - ▶ Needs to be accounted for in chemistry manifolds
 - ▶ Dimensions
 - ▶ underlying flamelets (QFM) [2]
 - ▶ boundary conditions (REDIM) [3]
- ▶ **Turbulent FWI changes the statistics of reactive scalars**
 - ▶ PDF / FDFs become very complex close to the wall
 - ▶ Improved TCI models are necessary
- ▶ **Other aspects**
 - ▶ DNS data is very useful for model development
 - ▶ How can we share the data?
(e.g. <https://doi.org/10.48328/tudatalib-673>)
 - ▶ FWI has a crucial effect on
 - ▶ Differential diffusion
 - ▶ curvature statistics and correlations
 - ▶ → next challenges: **Diffusive fuels (like H₂)**
 - ▶ New approaches (e.g. ML) might be needed

[1] Ganter et al., Combust. Flame 186, 299-310 (2017) [2] Efimov et al.; Combust. Theory Model. 24(1), 72-104 (2020)
[3] Strassacker et al.; Combust. Sci. Technol. 191(2), 208-222 (2018)

- ▶ How can we ensure a good collaboration and data accessibility for DNS-data?
 - ▶ DNS are highly valuable for model development.
 - ▶ Detailed insights can answer a multitude of questions raised by different communities.
 - ▶ Availability of DNS data is key for advanced modeling (HPC microscope)
- ▶ What is the interplay of experiments and DNS?
 - ▶ Need to / How to validate DNS results?
 - ▶ Exact reproduction of experimental data always necessary (uncertain boundary conditions)?
 - ▶ Comparison based on physical effects observed?
 - ▶ Are they not rather complementary in terms of high resolution/wealth of resolution vs. possibility to study also higher Re numbers.
- ▶ How can we deal with uncertainties and model robustness for model derivation using DNS?
 - ▶ Problem: DNS are very expensive
→ parameter variations are limited / expensive
 - ▶ Derived models for FWI should be applicable to a variety of inflow conditions
 - ▶ Inflow and wall temperature
 - ▶ Reynolds number / Turbulence
 - ▶ Fuels
 - ▶ Can we perform sensitivity analysis on generic (1D / 2D configurations) for uncertainty quantification / sensitivity analysis of our models?

Flame-wall interactions (SWQ)

- Ahmed, U. et al.: Scalar Gradient and Strain Rate Statistics in Oblique Premixed Flame-Wall Interaction Within Turbulent Channel Flows. *Flow, Turbulence and Combustion*. 2020.
- Ghai et al.: Energy integral equation for premixed flame-wall interaction in turbulent boundary layers and its application to turbulent burning velocity and wall flux evaluations, *Int. J. Heat & Mass Trans.*, 2022.
- Endres, A. & Sattelmayer, T.: Large Eddy simulation of confined turbulent boundary layer flashback of premixed hydrogen-air flames. *International Journal of Heat and Fluid Flow*. 2018.
- Heinrich, A. et al.: 3D Numerical Simulation of a Laminar Experimental SWQ Burner with Tabulated Chemistry. *Flow, Turbul. Combust.* 2018.
- Heinrich, A. et al.: Large Eddy Simulation with tabulated chemistry of an experimental sidewall quenching burner. *Int. J. Heat Fluid Flow*. 2018.
- Kosaka, H., et al.: Effect of Flame-Wall Interaction on Local Heat Release of Methane and DME Combustion in a Side-Wall Quenching Geometry. *Flow Turbul. Combust.* 2020.
- Steinhausen et al.: Numerical Investigation of Local Heat-Release Rates and Thermo-Chemical States in Side-Wall Quenching of Laminar Methane and Dimethyl Ether Flames. *Flow, Turbul. Combust.* 2020.
- Zirwes, T. et al.: Numerical Study of Quenching Distances for Side-Wall Quenching Using Detailed Diffusion and Chemistry. *Flow Turbul. Combust.*, 2021.
- Palulli R. et al.: Unsteady flame-wall interaction: Impact on CO emission and wall heat flux. *Combustion and Flame*, 2019.
- Jiang B. et al.: Turbulent flame-wall interactions for flames diluted by hot combustion products. *Combust. and Flame*, 2021.

Flame-wall interactions (HOQ)

- Luo, Y. et al. Strain Rate Effects on Head-on Quenching of Laminar Premixed Methane-air flames. *Flow, Turbul. Combust.*, 2021.
- Ghai, S.K. et al. Entropy Generation during Head-On Interaction of Premixed Flames with Inert Walls within Turbulent Boundary Layers. *Entropy*, 2022.
- Ghai, S.K. et al.: Enstrophy evolution during head-on wall interaction of premixed flames within turbulent boundary layers, *Phys. Fluids*, 2022
- Lai, J. et al.: A comparison between head-on quenching of stoichiometric methane-air and hydrogen-air premixed flames using Direct Numerical Simulations. *International Journal of Heat and Fluid Flow*, 2022.
- Lai, J. et al.: Heat flux and flow topology statistics in oblique and head-on quenching of turbulent premixed flames by isothermal inert walls. *Combustion Science and Technology*, 2022.
- Gupta S.K. et al.: CO modelling of premixed head-on quenching flame in the context of Large-Eddy Simulation. *International Journal of Heat and Fluid Flow*, 2022.
- Konstantinou, I. et al.: Effects of Fuel Lewis Number on the Near-wall Dynamics for Statistically Planar Turbulent Premixed Flames Impinging on Inert Cold Walls. *Combustion Science and Technology*, 2020.
- Zhao, P. et al.: Vectorial structure of the near-wall premixed flame. *Physical Review Fluids*. 2019.
- Zhao, P. et al.: Effects of the cold wall boundary on the flame structure and flame speed in premixed turbulent combustion. *Proceedings of the Combustion Institute*. 2020.
- Salimath et al.: Computational analysis of premixed methane-air flame interacting with a solid wall or a hydrogen porous wall. *Fuel*. 2020.

Chemistry manifolds for FWI

- Strassacker, C., Bykov, V. & Maas, U.: Reaction-Diffusion-Manifolds for Flame-Wall-Interactions of Stratified Flames, 2019.
- Efimov, D. V. et al.: QFM: quenching flamelet generated manifolds for modelling of flame-wall interactions. *Combustion Theory and modelling*, 2020.
- Ganter, S. et al.: Laminar near-wall combustion: Analysis of tabulated chemistry simulations by means of detailed kinetics. *Int. J. Heat Fluid Flow*. 2018
- Luo, Y., et al: Simulation of side-wall quenching of laminar premixed flames with manifold-based reduced kinetic models implemented in generalised coordinates. *Combust.Theor. Model.*. 2021.
- Wan et al.: Chemistry reduction using machine learning trained from non-premixed micro-mixing modeling: Application to DNS of a syngas turbulent oxy-flame with side-wall effects. *Combust. Flame*, 2020.
- Wan et al.: Machine learning for detailed chemistry reduction in DNS of a syngas turbulent oxy-flame with side-wall effects, *Proc. Combust. Inst.*, 2020

Statistical TCI closure

- Steinhausen, M. et al.: Turbulent flame-wall interaction of premixed flames using Quadrature-based Moment Methods (QbMM) and tabulated chemistry: an a priori analysis. *Int. J. Heat Fluid Flow*. 2022.
- Ahmed, U. et al.: Assessment of Bray Moss Libby formulation for premixed flame-wall interaction within turbulent boundary layers: Influence of flow configuration. *Combustion and Flame*, 2021.
- Ahmed, U. et al: Influence of thermal wall boundary condition on scalar statistics during flame-wall interaction of premixed combustion in turbulent boundary layers. *International Journal of Heat and Fluid Flow*. 2021.

Flame Cooling Air interaction (FCAI)

- Palulli R. et al.: A comparative study of flame-wall interaction and flame-cooling air interaction. *International Journal of Heat and Fluid Flow* (FWI Special Issue), 2021.
- Rivera J.E. et al.: Optimization of CO Turn-down for an Axially Staged Gas Turbine Combustor. *Journal of Engineering for Gas Turbines and Power*, 2021.
- Palulli R. et al.: Analysis of Near-Wall CO due to Unsteady Flame-Cooling Air Interaction. *Flow, Turbulence and Combustion*, 2021.
- Rivera J.E. et al.: Exhaust CO emissions of a laminar premixed propane-air flame interacting with cold gas jets. *Combustion and Flame*. 2019.

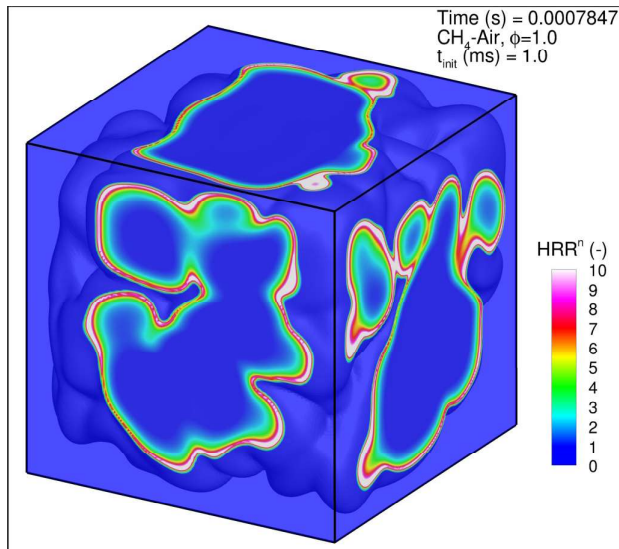
Flashback

- Ahmed, U. et al: Statistical behaviour of turbulent kinetic energy transport in boundary layer flashback of hydrogen-rich premixed combustion. *Physical Review Fluids*. 2019.
- Ahmed, U. et al.: Surface density function evolution and the influence of strain rates during turbulent boundary layer flashback of hydrogen-rich premixed combustion. *Phys. Fluids*. 2022.
- Mao, R. et al.: Effects of flow-flame interactions on the stabilization of ultra-lean swirling CH_4/H_2 /air flames. *Fuel*, 2022.

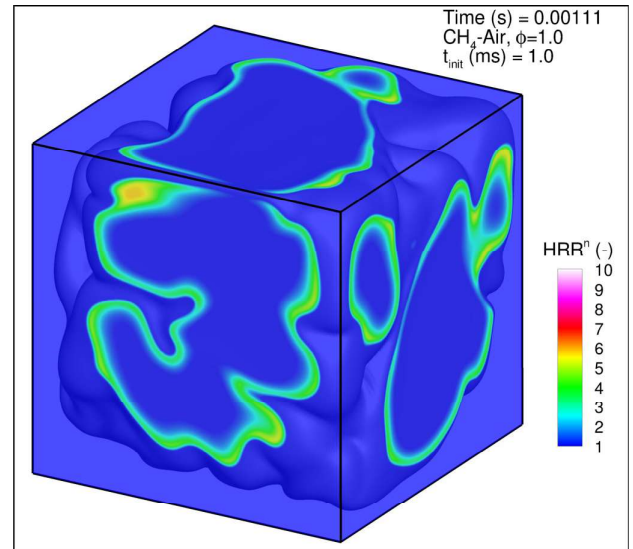
Mechanism development

- Stagni et al.: Chemistry effects in the wall quenching of laminar premixed DME flames. *Combust. Flame*. 2021.
- Jiang et al.: An updated short chemical-kinetic nitrogen mechanism for carbon-free combustion applications. *Int. J. Energy Res*. 2020.
- Lu and Law: A criterion based on computational singular perturbation for the identification of quasi steady state species: A reduced mechanism for methane oxidation with NO chemistry. *Combust. Flame*. 2008.
- Li et al.: An updated comprehensive kinetic model of hydrogen combustion. *Int. J. Chem. Kinet*. 2004.
- Smooke and Giovangigli: Formulation of the premixed and nonpremixed test problems. *Lect. Notes Phys.* vol. 384. Springer Verlag; 1991.

Significant effect of C2-species on thermochemistry of FWI (normalized HRR)

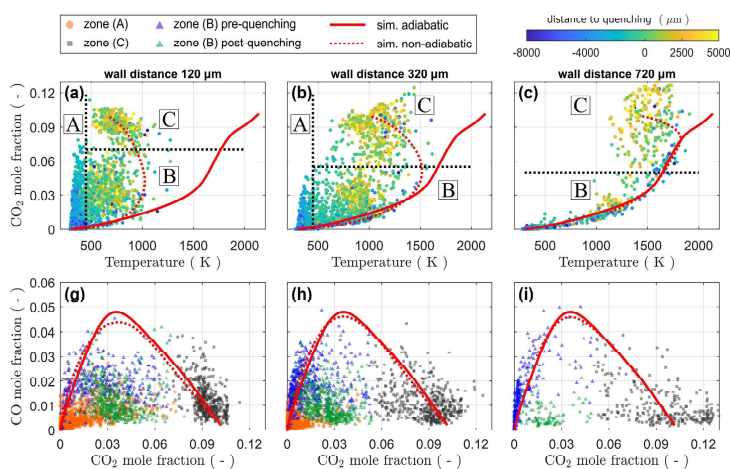


Smooke & Giovangigli (no C2-species)

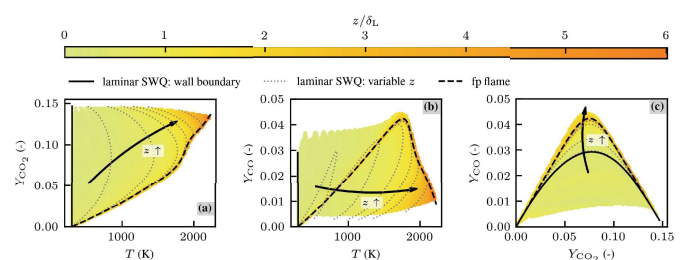


Lu & Law (including C2-species)

Thermochemical state in turbulent side-wall quenching (SWQ)

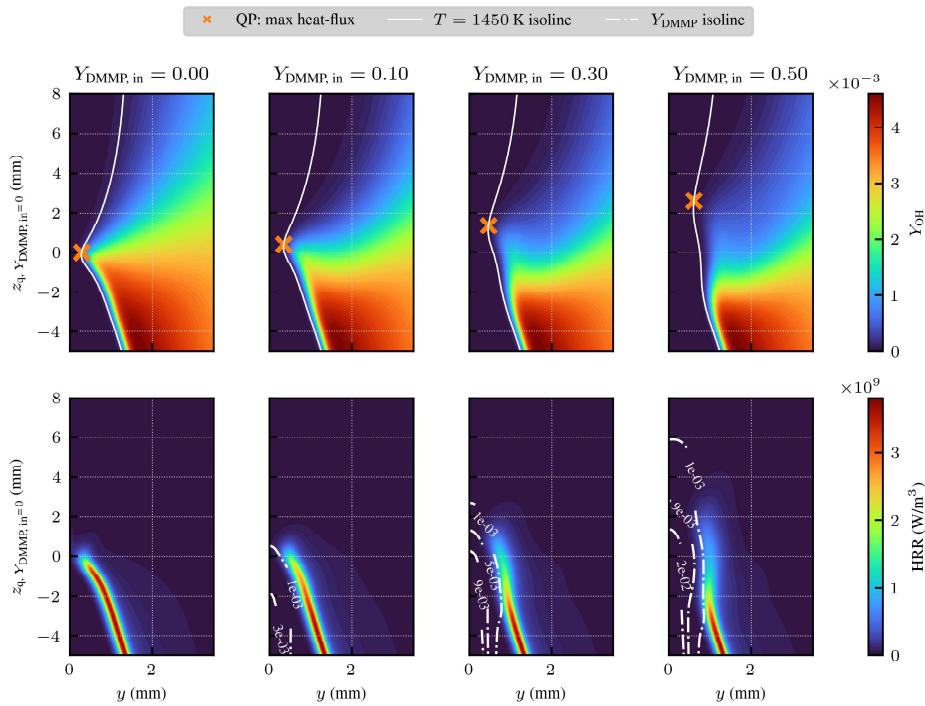


Thermochemical state observed in the experiments. Taken from [1]



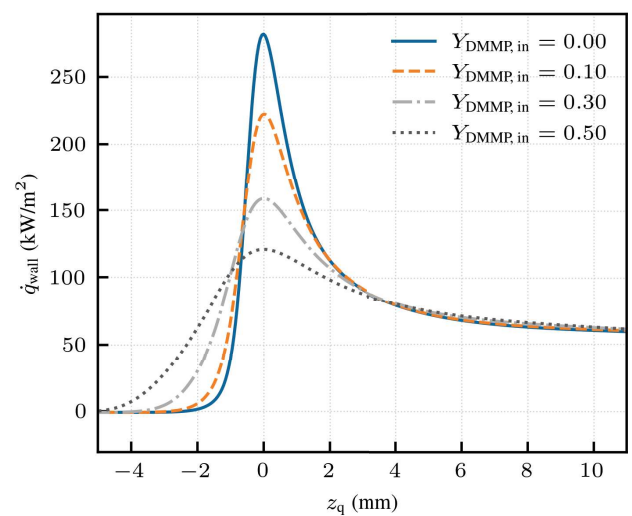
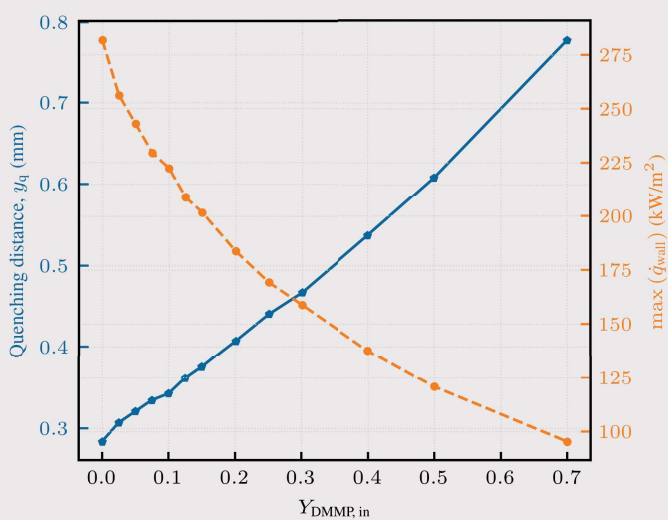
Thermochemical state of the turbulent SWQ methane-air flame colored by the wall distance normalized by the laminar flame thickness z/δ_L . A laminar SWQ with similar conditions is shown as a reference (**Case 1, STFS**)

Laminar SWQ with methane-DMMP seeding from the wall



- ▶ Fixed inflow rate: $\dot{V} = 2$ L/h
- ▶ Injected reactants: methane-DMMP
 - ▶ $Y_{\text{CH}_4,\text{in}} = 1 - Y_{\text{DMMP},\text{in}}$
 - ▶ $T_{\text{in},\text{wall}} = 373$ K

Influence on the global flame characteristics



The **flame retardants** increases the **quenching distance** and reduces the **maximum heat-flux** to the wall. This decreases the thermal load on the wall.

Background and overview



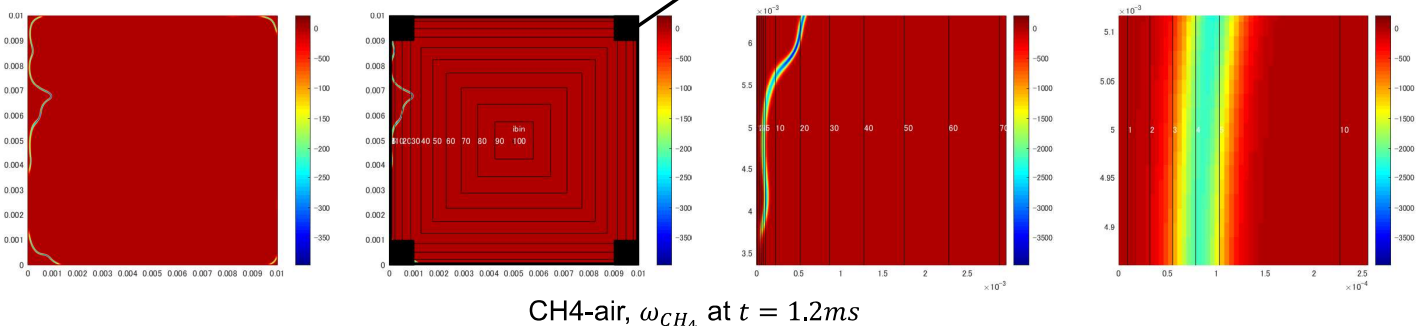
- Ongoing fundamental & applied research projects on NH_3 as fuel in **IC engines**:
 - Overall objective is comparative FWI analysis of **partially-decomposed ammonia**, **methane** and **hydrogen**
- Active collaborations between **Norway (SINTEF/NTNU)**, **Japan (Tokyo Tech)** and **Germany (TU Darmstadt)** on available datasets
- Turbulent FWI datasets created between 2018 (H_2 -air) and 2021 (CH_4 -air & $\text{NH}_3/\text{H}_2/\text{N}_2$ -air) on HPC resources in Norway
- DNS study approx. matches: 1) laminar flame speed and 2) adiabatic flame temperature across the different fuels → analysis ongoing (**work in progress!**)

Binning of data for FWI analysis

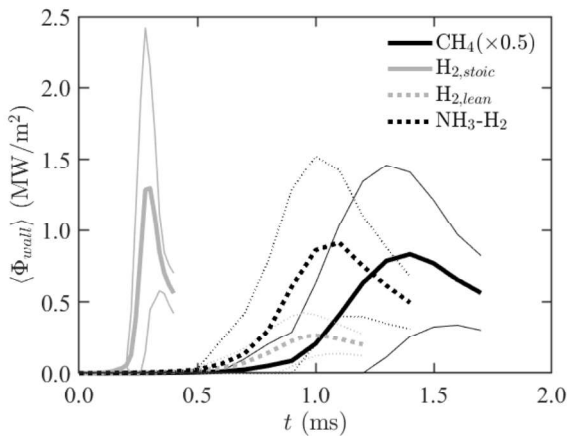


- Computational domain is subdivided in 100 bins in space based on the wall distance d_{wall} (*ibin*).
- A similar subdivision is imposed in time (*its*)
- Corners are excluded

10% of domain is removed from analysis



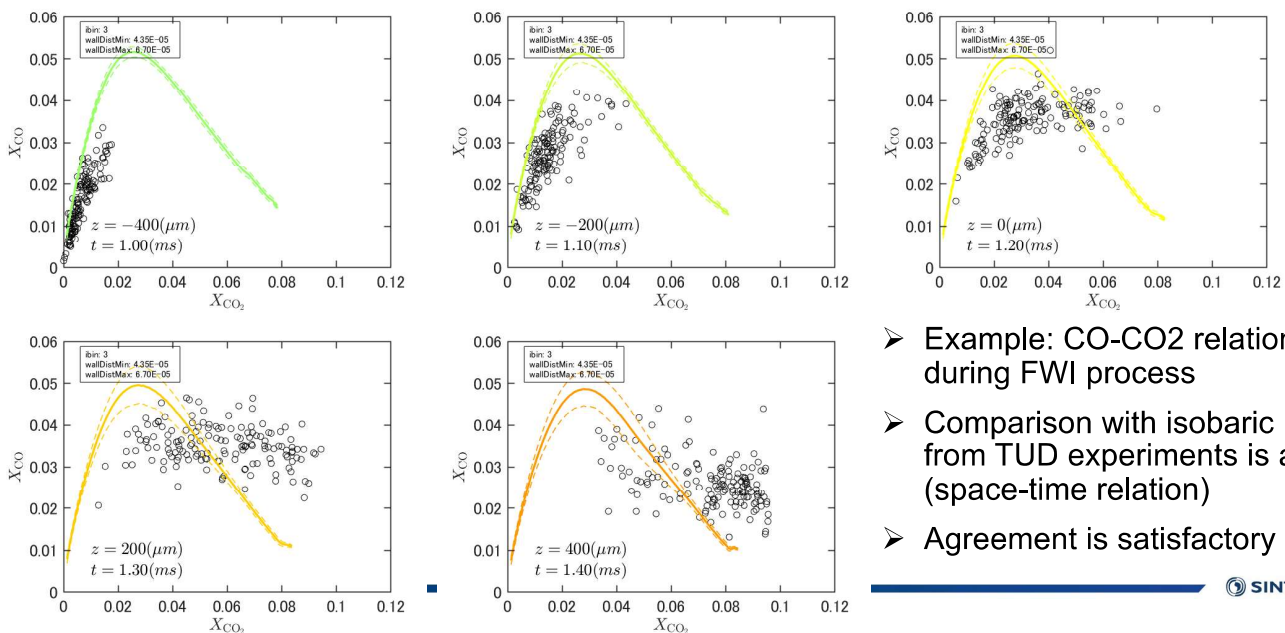
Time history of averaged wall heat flux



- Mean value and standard deviation are shown
- Good agreement between time instant of peak pressure and peak averaged wall heat flux (confirms self-similarity assumption)
- CH₄-air flame has higher T_{ad} (2438 vs 2370 K) and peak pressure (3.2 vs 3.1 bar) compared to NH₃/H₂/N₂-air flame but lower averaged wall heat flux

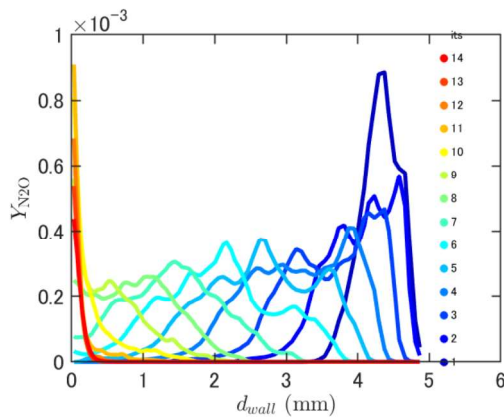
→ Hypothesis: consequence of weaker turbulence at (later) quenching time?

Detailed analysis of species and reactions during FWI is ongoing (1)

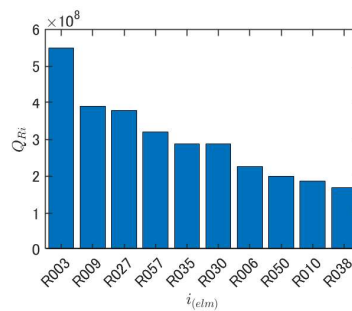


- Example: CO-CO₂ relationship during FWI process
- Comparison with isobaric FWI data from TUD experiments is attempted (space-time relation)
- Agreement is satisfactory

Detailed analysis of species and reactions during FWI is ongoing (2)



$\langle Y_{N_2O} | d_{wall} \rangle$ constructed for different t (its).
its=1 at start and its=14 at end of DNS.



1. R003: $\text{OH} + \text{H}_2 \rightleftharpoons \text{H} + \text{H}_2\text{O}$
2. R009: $\text{O}_2 + \text{H} (+\text{M}) \rightleftharpoons \text{HO}_2 (+\text{M})$
3. R027: $\text{NH}_3 + \text{M} \rightleftharpoons \text{H} + \text{NH}_2 + \text{M}$
4. R057: $\text{H} + \text{HNO} \rightleftharpoons \text{H}_2 + \text{NO}$
5. R035: $\text{NO} + \text{NH}_2 \rightleftharpoons \text{H}_2\text{O} + \text{N}_2$

Reaction-wise heat release rates near the wall.

- A wealth of DNS data is available!
- Active collaboration with TUD for model development
- Detailed near-wall measurements of NH_3 - and $\text{NH}_3/\text{H}_2/\text{N}_2$ -air flames still to be performed...

References



Kinetics schemes:

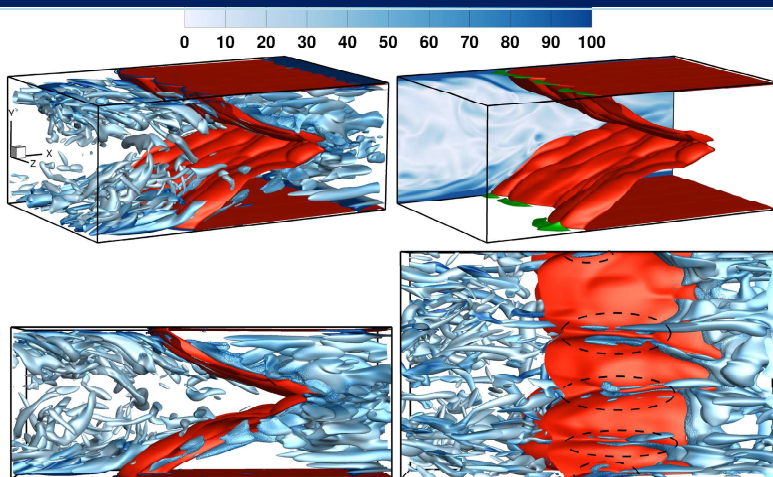
- Smooke and Giovangigli: Formulation of the premixed and nonpremixed test problems. *Lect. Notes Phys.* vol. 384. Springer Verlag; 1991.
- Li et al.: An updated comprehensive kinetic model of hydrogen combustion. *Int. J. Chem. Kinet.* 2004.
- Jiang et al.: An updated short chemical-kinetic nitrogen mechanism for carbon-free combustion applications. *Int. J. Energy Res.* 2020.
- Lu and Law: A criterion based on computational singular perturbation for the identification of quasi steady state species: A reduced mechanism for methane oxidation with NO chemistry. *Combust. Flame.* 2008.

Laminar FWI (1-D HOQ):

- Salimath et al.: Computational analysis of premixed methane-air flame interacting with a solid wall or a hydrogen porous wall. *Fuel.* 2020.

Statistical Behaviour of Turbulent Kinetic Energy Transport in Boundary Layer Flashback of Hydrogen-Rich Premixed Flames

Boundary Layer Flashback for rich H₂-air flames



- ❖ Flame alters the boundary layer structure.
- ❖ Turbulence decays across the flame in the near wall region.
- ❖ Vorticity is generated in the middle of the channel in the wake of the flame.

Findings

- ❖ The wall shear stress increases across the flame due to an increase in the velocity on the product side of the flame.
- ❖ Negative wall shear stress can be seen upstream of the flame in the regions of reverse flow.
- ❖ TKE is zero at the wall and reaches a relatively high value at $y/h = 0.1$ due to shear.
- ❖ Turbulent dissipation is maximum at the wall and decreases towards the centre of the channel.
- ❖ $T_1 = -\frac{\rho \overline{u_i'' u_j''} \partial \tilde{u}_j}{\partial x_j}$ can be negative or positive:
→ **Modelling assumption: $T_1 = \bar{\rho} \tilde{\epsilon}$ may not hold in FWI in turbulent boundary layers.**

Relations between turbulent burning velocity and wall heat flux using energy integral equation for premixed flame-wall interaction in turbulent boundary layers

Steady state energy integral equation

$$\begin{aligned}
 & \underbrace{\frac{\partial}{\partial x} \int_0^{\delta_T} \frac{\bar{\rho} \tilde{u} (\tilde{h} - \tilde{h}_\infty)}{\rho_0 u_{\tau, NR} (h_{ad} - h_0)} dy}_{T_1} + \underbrace{\frac{1}{(h_{ad} - h_0)} \frac{d\tilde{h}_\infty}{dx} \int_0^{\delta_T} \frac{\bar{\rho} \tilde{u}}{\rho_0 u_{\tau, NR}} dy}_{T_2} \\
 &= \underbrace{\frac{\bar{q}_w}{\rho_0 u_{\tau, NR} (h_{ad} - h_0)}}_{T_3} + \underbrace{\frac{1}{\rho_0 u_{\tau, NR}} \int_0^{\delta_T} \bar{\omega}_c dy}_{T_4}
 \end{aligned}$$

Advection Term
Freestream temperature variation term

Wall heat flux term
Mean reaction rate term

After integration in the streamwise direction from $x=L_1$ to $x=L_2$

$$T_{1L} + T_{2L} = -Nu_L / \{Re_\tau Pr\} + A_{proj} S_T / [A_{seg} u_{\tau, NR}]$$

Variation of terms in the wall normal direction

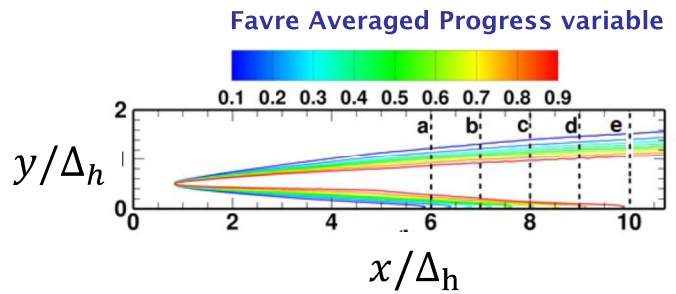
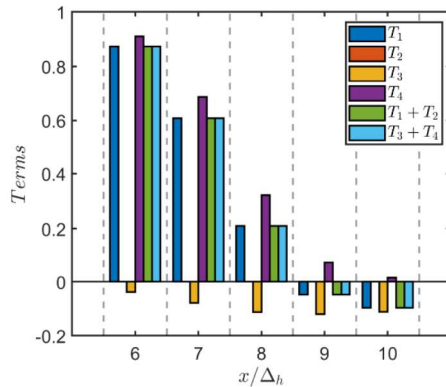
$$\underbrace{\frac{\partial}{\partial x} \int_0^{\delta_T} \frac{\bar{\rho} \tilde{u} (\tilde{h} - \tilde{h}_\infty)}{\rho_0 u_{\tau, NR} (h_{ad} - h_0)} dy}_{T_1} + \underbrace{\frac{1}{(h_{ad} - h_0)} \frac{d\tilde{h}_\infty}{dx} \int_0^{\delta_T} \frac{\bar{\rho} \tilde{u}}{\rho_0 u_{\tau, NR}} dy}_{T_2} = \underbrace{\frac{\bar{q}_w}{\rho_0 u_{\tau, NR} (h_{ad} - h_0)}}_{T_3} + \underbrace{\frac{1}{\rho_0 u_{\tau, NR}} \int_0^{\delta_T} \bar{\omega}_c dy}_{T_4}$$

Advection
Term

Freestream temperature
variation term

Wall heat flux
term

Mean reaction
rate term

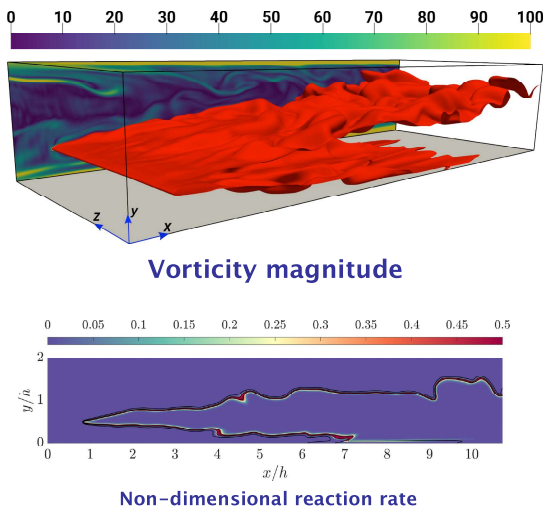


Variations of $T_1, T_2, T_3, T_4, T_1 + T_2$ and $T_3 + T_4$ at $x/\Delta_h = 6.0, 7.0, 8.0, 9.0$ and 10.0 .

**Flame-wall Interaction in fully-developed
turbulent boundary layers**

Flow behaviour

V-flame with isothermal walls



HOQ with an isothermal wall

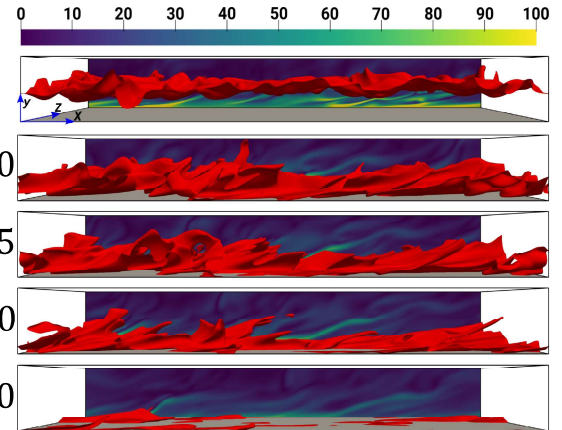
$$t/t_f = 4.20$$

$$t/t_f = 10.50$$

$$t/t_f = 11.55$$

$$t/t_f = 12.60$$

$$t/t_f = 14.70$$



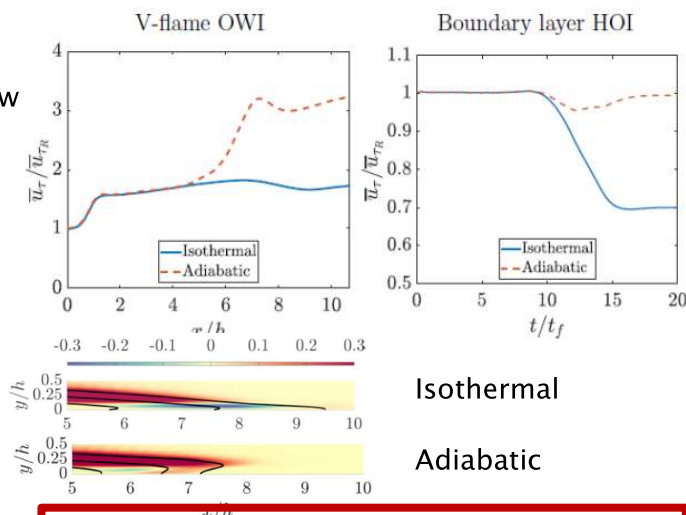
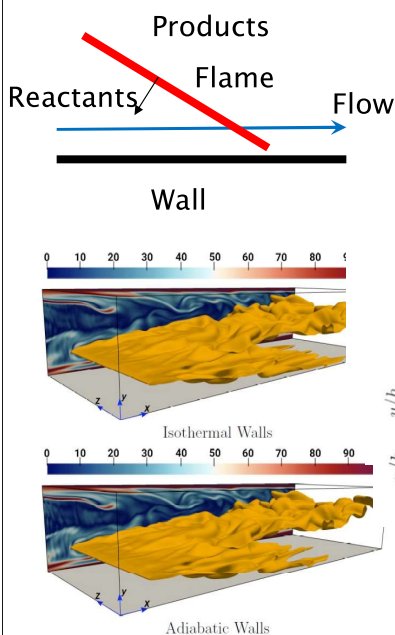
Vorticity magnitude



U. Ahmed, N. Chakraborty, M. Klein, "Assessment of Bray Moss Libby formulation for premixed flame-wall interaction within turbulent boundary layers: Influence of flow configuration", *Combust. Flame*, 233, 111575 (2021)

U. Ahmed, N. Chakraborty, M. Klein, "Scalar gradient and strain rate statistics in oblique premixed flame-wall interaction within turbulent channel flows", *Flow, Turb. Combust.*

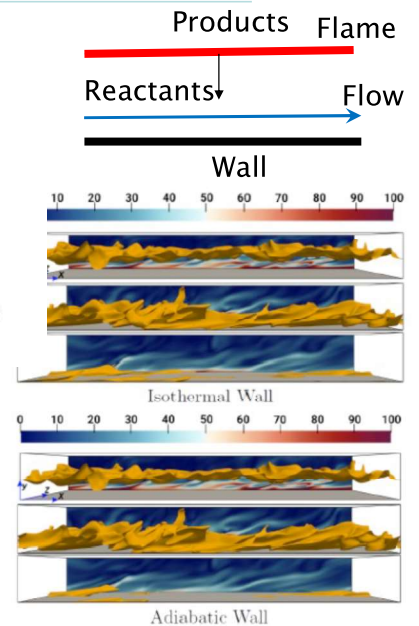
Mean shear stress at the wall for different boundary conditions



Isothermal

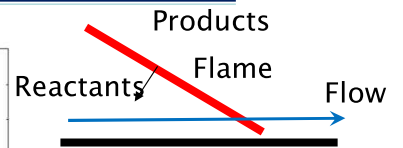
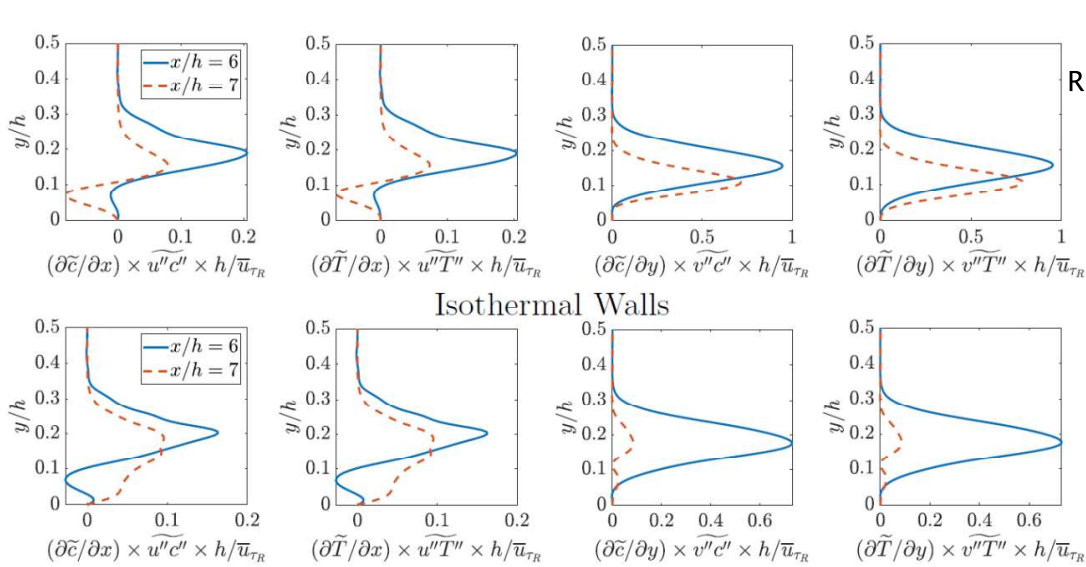
Adiabatic

Wall boundary condition, orientation of mean direction of flame propagation with respect to wall normal, and orientation of flame normal to the background flow direction are important factors for FWI



U. Ahmed, N. Chakraborty, M. Klein, "Influence of thermal wall boundary condition on scalar statistics during flame-wall interaction of premixed combustion in turbulent boundary layers", *Int. J. Heat and Fluid Flow*, 92, 108881, (2021)

Nature of turbulent transport for V flame OWI



Wall

Gradient hypothesis:

$$\overline{\rho u_i'' q''} = - \frac{\mu_t}{\sigma_t} \frac{\partial \tilde{q}}{\partial x_i}$$

Gradient type transport:

$$\overline{\rho u_i'' q''} \times \frac{\partial \tilde{q}}{\partial x_i} < 0$$

Counter-gradient type transport:

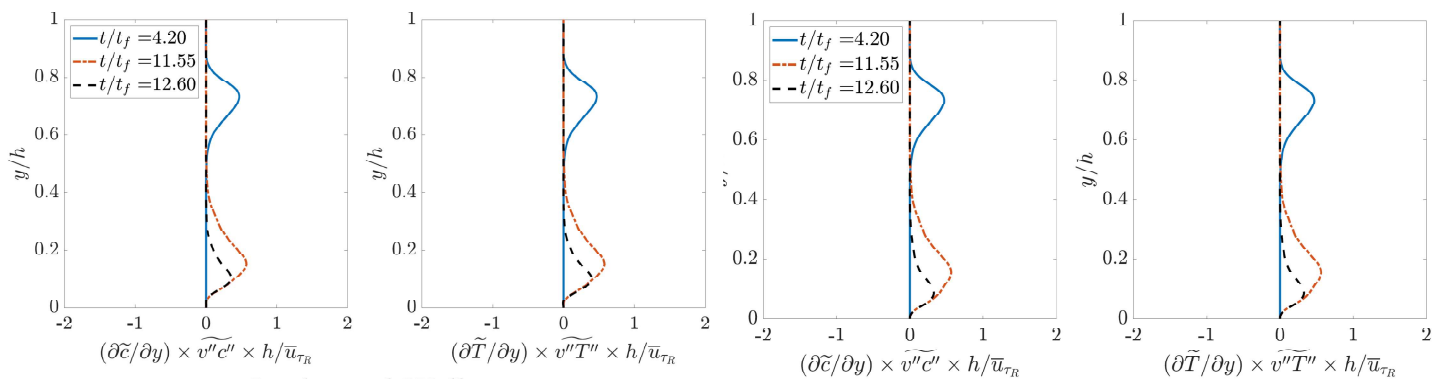
$$\overline{\rho u_i'' q''} \times \frac{\partial \tilde{q}}{\partial x_i} > 0$$

Locally counter-gradient behaviour can be observed and the wall boundary condition affects the scalar flux behaviour in this configuration.

U. Ahmed, N. Chakraborty, M. Klein, "Influence of thermal wall boundary condition on scalar statistics during flame-wall interaction of premixed combustion in turbulent boundary layers", *Int. J. Heat and Fluid Flow*, 92, 108881, (2021)



Nature of turbulent transport for HOI

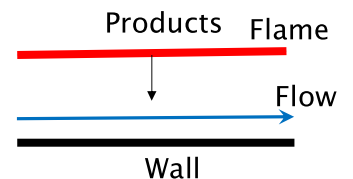


Gradient hypothesis: $\overline{\rho u_i'' q''} = - \frac{\mu_t}{\sigma_t} \frac{\partial \tilde{q}}{\partial x_i}$

Gradient type transport: $\overline{\rho u_i'' q''} \times \frac{\partial \tilde{q}}{\partial x_i} < 0$

Counter-gradient type transport:

$$\overline{\rho u_i'' q''} \times \frac{\partial \tilde{q}}{\partial x_i} > 0$$

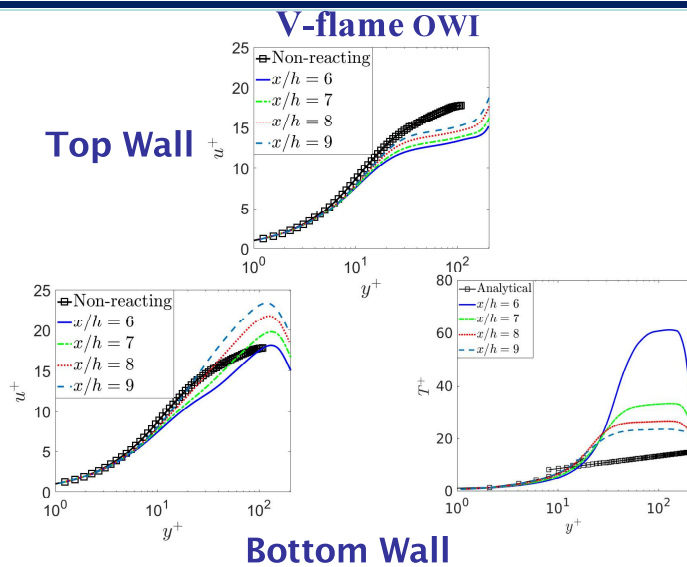


Predominantly counter-gradient behaviour can be observed and the wall boundary condition does not affect the scalar flux behaviour in this configuration.

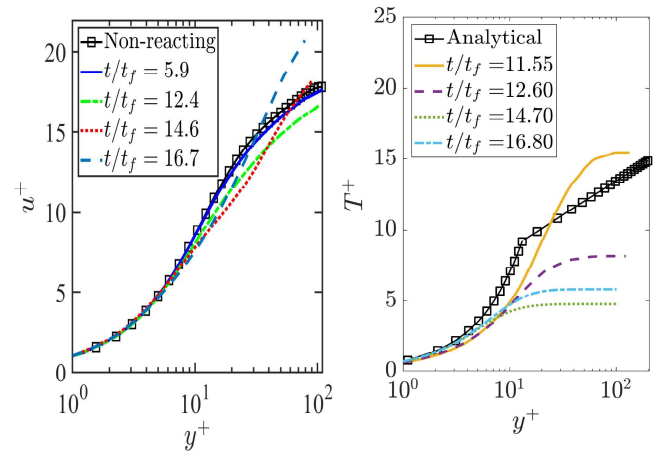
U. Ahmed, N. Chakraborty, M. Klein, "Influence of thermal wall boundary condition on scalar statistics during flame-wall interaction of premixed combustion in turbulent boundary layers", *Int. J. Heat and Fluid Flow*, 92, 108881, (2021)



Mean variation of velocity and temperature



Statistically planar flame HOI



- ❖ The trend $y^+ = u^+$ is obeyed in the viscous sub-layer.
- ❖ $T^+ = (\tilde{T}/\bar{\Phi}_{wall}) \times u_\tau / S_L$
- ❖ The analytical function by Kays & Crawford¹ for T^+ is not able to predict the correct behaviour

Statistical Behaviour of Turbulent Kinetic Energy Transport in Boundary Layer Flashback of Hydrogen-Rich Premixed Flames

Turbulent kinetic energy transport equation

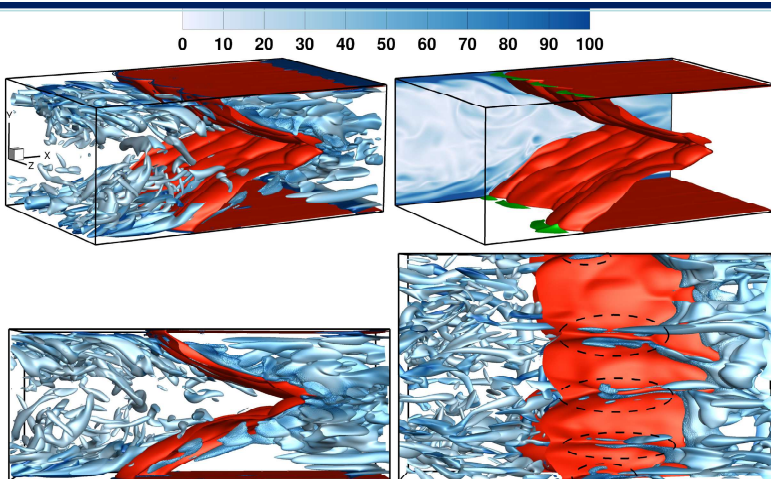
❖ The transport equation for the Favre averaged turbulent kinetic energy (TKE) is given by:

$$\frac{\partial \bar{\rho} \tilde{k}}{\partial t} + \frac{\partial \bar{\rho} \tilde{u}_j \tilde{k}}{\partial x_j} = \underbrace{-\overline{\rho u_i'' u_j''} \frac{\partial \tilde{u}_i}{\partial x_j}}_{T_1} \underbrace{- \tilde{u}_i'' \frac{\partial \bar{p}}{\partial x_i}}_{T_2} + \underbrace{\overline{p'} \frac{\partial u_k''}{\partial x_k}}_{T_3} + \underbrace{\overline{u_i''} \frac{\partial \tau_{ij}}{\partial x_j}}_{T_4} \underbrace{- \frac{\partial \overline{p' u_i''}}{\partial x_i}}_{T_5} \underbrace{- \frac{\partial}{\partial x_i} \left(\frac{1}{2} \overline{\rho u_i'' u_k'' u_k''} \right)}_{T_6}$$

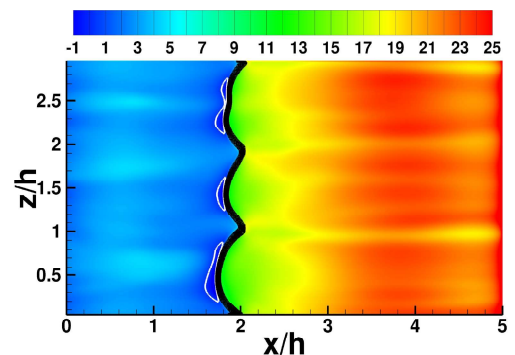
- T_1 is the production of TKE by mean velocity gradients.
- T_2 represents production by the mean pressure gradient.
- T_3 is the pressure dilatation term.
- T_4 describes the combined effects of molecular diffusion and viscous dissipation.
- T_5 represents the transport of TKE by pressure fluctuations.
- T_6 represents the transport of TKE by velocity fluctuations.



Boundary Layer Flashback for rich H₂-air flames



- ❖ Flame alters the boundary layer structure.
- ❖ Turbulence decays across the flame in the near wall region.
- ❖ Vorticity is generated in the middle of the channel in the wake of the flame.

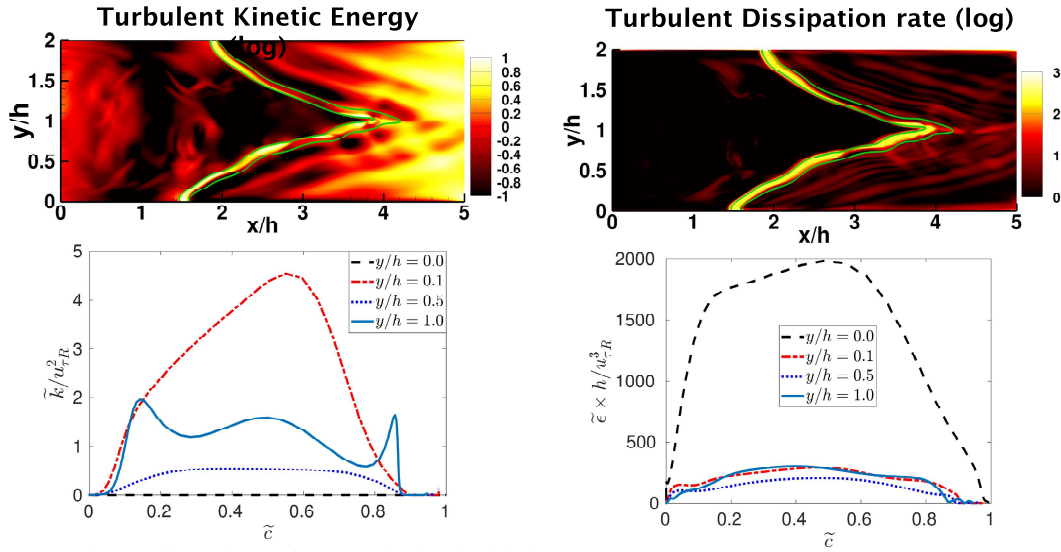


Wall shear stress on the top wall

- ❖ TKE is zero at the wall and reaches a relatively high value at $y/h = 0.1$ due to shear.
- ❖ Turbulent dissipation is maximum at the wall and decreases towards the centre of the channel.



Turbulence statistics



❖ TKE is zero at the wall and reaches a relatively high value at $y/h = 0.1$ due to shear.

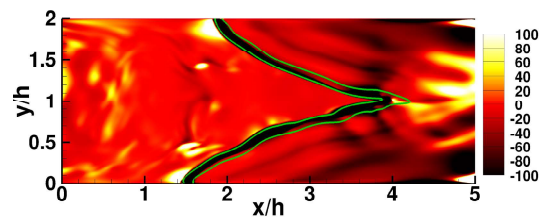
❖ Turbulent dissipation is maximum at the wall and decreases towards the centre of the channel.



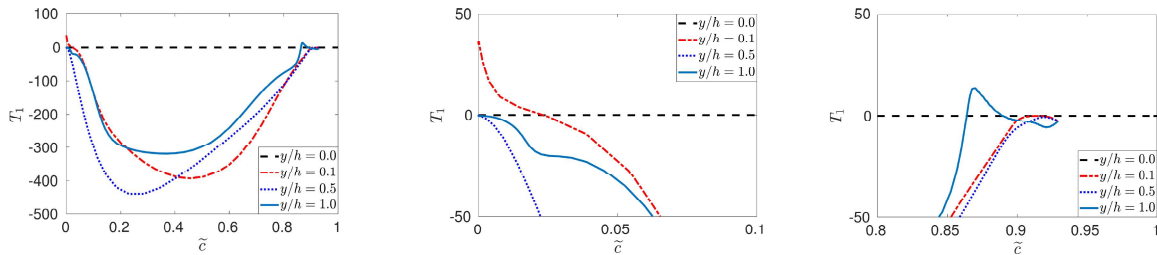
U. Ahmed, A. Pillai, N. Chakraborty, R. Kurose, "Statistical behaviour of turbulent kinetic energy transport in boundary layer flashback of hydrogen-rich premixed combustion", *Phys. Rev. F*, 4, 103201, 2019.

Mean velocity gradient term T_1

$$T_1 = -\overline{\rho u_i'' u_j''} \frac{\partial \tilde{u}_i}{\partial x_j}$$



U. Ahmed, A. Pillai, N. Chakraborty, R. Kurose, "Statistical behaviour of turbulent kinetic energy transport in boundary layer flashback of hydrogen-rich premixed combustion", *Phys. Rev. F*, 4, 103201, 2019.



❖ T_1 can be negative or positive depending on the alignment of eigensystems for $-u_i'' u_j''$ and $\partial \tilde{u}_i / \partial x_j$.¹ Therefore, $T_1 = \bar{\rho} \tilde{\epsilon}$ may not hold in FWI in turbulent boundary layers.



¹ U. Ahmed, N. Chakraborty, M. Klein, *Scientific Reports* (2019) 9(1): 5092

Relations between turbulent burning velocity and wall heat flux using energy integral equation for premixed flame-wall interaction in turbulent boundary layers

Steady state energy integral equation

$$\begin{aligned}
 & \underbrace{\frac{\partial}{\partial x} \int_0^{\delta_T} \frac{\bar{\rho} \tilde{u} (\tilde{h} - \tilde{h}_\infty)}{\rho_0 u_{\tau, NR} (h_{ad} - h_0)} dy}_{T_1} + \underbrace{\frac{1}{(h_{ad} - h_0)} \frac{d\tilde{h}_\infty}{dx} \int_0^{\delta_T} \frac{\bar{\rho} \tilde{u}}{\rho_0 u_{\tau, NR}} dy}_{T_2} \\
 &= \underbrace{\frac{\bar{q}_w}{\rho_0 u_{\tau, NR} (h_{ad} - h_0)}}_{T_3} + \underbrace{\frac{1}{\rho_0 u_{\tau, NR}} \int_0^{\delta_T} \bar{\omega}_c dy}_{T_4}
 \end{aligned}$$

Advection Term
Freestream temperature variation term

Wall heat flux term
Mean reaction rate term

After integration in the streamwise direction from $x=L_1$ to $x=L_2$

$$T_{1L} + T_{2L} = -Nu_L / \{Re_\tau Pr\} + A_{proj} S_T / [A_{seg} u_{\tau, NR}]$$

Energy integral equation: Premixed FWI in Boundary Layers

$$T_{1L} + T_{2L} = -Nu_L / \{Re_\tau Pr\} + A_{proj} S_T / [A_{seg} u_{\tau, NR}]$$

$$T_{1L} = (L_2 - L_1)^{-1} \int_{L_1}^{L_2} T_1 dx ,$$

$$T_{2L} = (L_2 - L_1)^{-1} \int_{L_1}^{L_2} T_2 dx ,$$

$Nu_L = (L_2 - L_1)^{-1} \int_{L_1}^{L_2} Nu_x dx$ is the mean Nusselt number

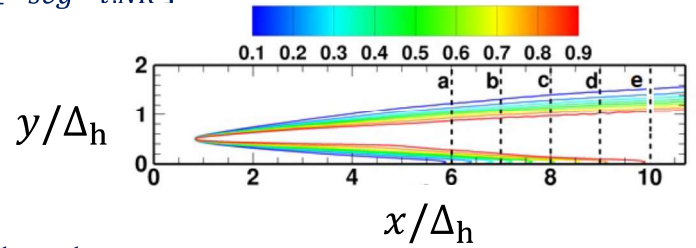
A_{proj} is the projected flame surface area

$A_{proj} = W(L_2 - L_1) / \cos \phi$ with $\phi = 3.07^\circ$ with $\tilde{c} = 0.94$ with the x -axis.

The iso-contours of smaller values of \tilde{c} make an angle in the range of $\phi = 4^\circ - 5^\circ$ with the x -axis.

$A_{seg} = (L_2 - L_1)W$ is the area of the segment

$S_T = (\rho_0 A_{proj})^{-1} \int_{L_1}^{L_2} \int_0^{\delta_T} \bar{\omega}_c W dx dy$ is the turbulent burning velocity



Favre Averaged Progress variable

- Location $a = x/h = 6$
- Location $b = x/h = 7$
- Location $c = x/h = 8$
- Location $d = x/h = 9$
- Location $e = x/h = 10$



Variation of terms in the wall normal direction

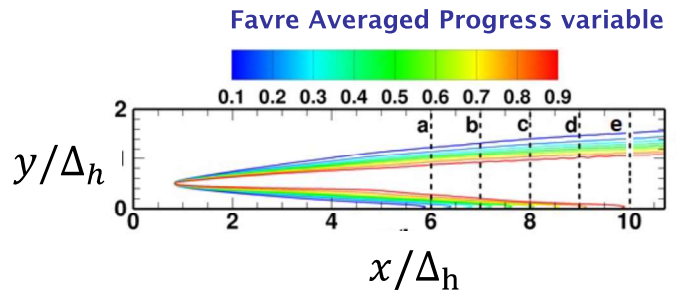
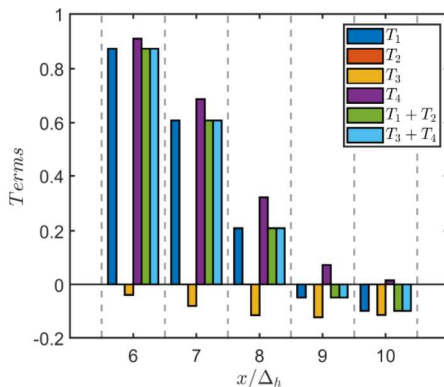
$$\underbrace{\frac{\partial}{\partial x} \int_0^{\delta_T} \frac{\bar{\rho} \tilde{u} (\tilde{h} - \tilde{h}_\infty)}{\rho_0 u_{\tau, NR} (h_{ad} - h_0)} dy}_{T_1} + \underbrace{\frac{1}{(h_{ad} - h_0)} \frac{d\tilde{h}_\infty}{dx} \int_0^{\delta_T} \frac{\bar{\rho} \tilde{u}}{\rho_0 u_{\tau, NR}} dy}_{T_2} = \underbrace{\frac{\bar{q}_w}{\rho_0 u_{\tau, NR} (h_{ad} - h_0)}}_{T_3} + \underbrace{\frac{1}{\rho_0 u_{\tau, NR}} \int_0^{\delta_T} \bar{\omega}_c dy}_{T_4}$$

Advection Term

Freestream temperature variation term

Wall heat flux term

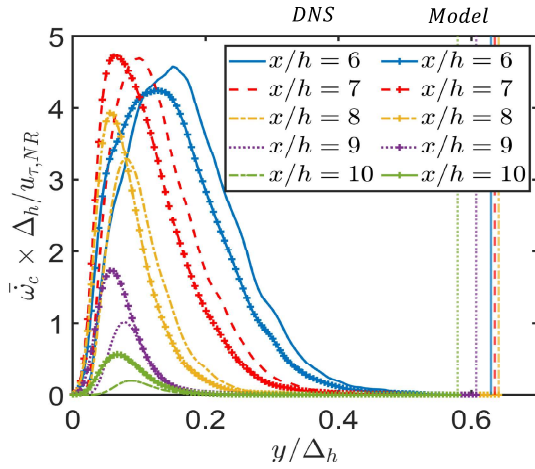
Mean reaction rate term



Variations of $T_1, T_2, T_3, T_4, T_1 + T_2$ and $T_3 + T_4$ at $x/\Delta_h = 6.0, 7.0, 8.0, 9.0$ and 10.0 .



Mean reaction rate closure



$$\bar{\omega}_c = I_0 \rho_0 S_L \Sigma_{gen} \text{ (lines with symbols)}$$

$$\text{where } I_0 = 0.5 [\text{erf}(y/\delta_z - Pe_Q) + 1]^{1,2}$$

where $\delta_z = \alpha_{T0}/S_L$ is the Zel'dovich flame thickness,

$Pe_Q = \delta_Q/\delta_z$ is the wall Peclet number for the laminar head-on quenching configuration (=2.19 for the present thermochemistry)

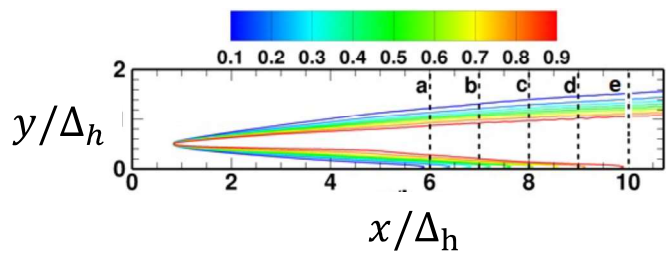
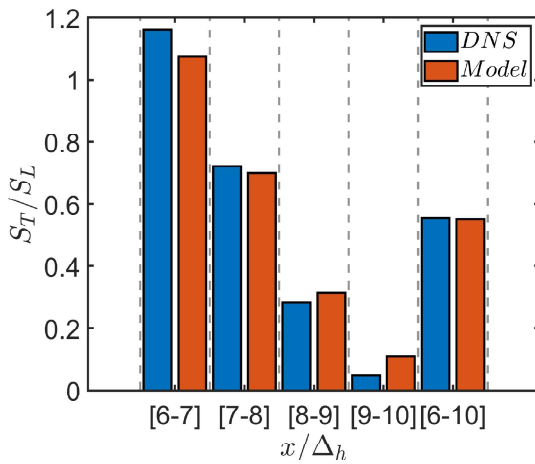
¹J. Sellmann, J. Lai, A. M. Kempf, N. Chakraborty, Flame surface density based modelling of head-on quenching of turbulent premixed flames, Proc. Combust. Inst. 36 (2017).

²U. Ahmed, N. Chakraborty, M. Klein, Assessment of bray moss libby formulation for premixed flame-wall interaction within turbulent boundary layers: Influence of flow configuration, Combust. Flame 233 (2021).

Variations of $\bar{\omega}_c \times \Delta_h / \rho_0 u_{\tau, NR}$ (lines) with y/Δ_h for the bottom wall along with the predictions of $I_0 \rho_0 S_L \Sigma_{gen} \times \Delta_h / \rho_0 u_{\tau, NR}$ (lines with symbols) where $I_0 = 0.5 [\text{erf}(y/\delta_z - Pe_Q) + 1]$ for $x/\Delta_h = 6.0, 7.0, 8.0, 9.0$ and 10.0 . Vertical lines represents the cut-off limits of the thermal boundary layer thickness δ_t .



Implications of reaction rate closure on S_T



Favre Averaged Progress variable

- Location a = $x/h = 6$
- Location b = $x/h = 7$
- Location c = $x/h = 8$
- Location d = $x/h = 9$
- Location e = $x/h = 10$

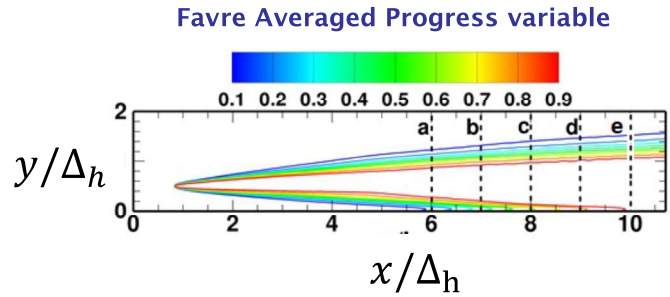
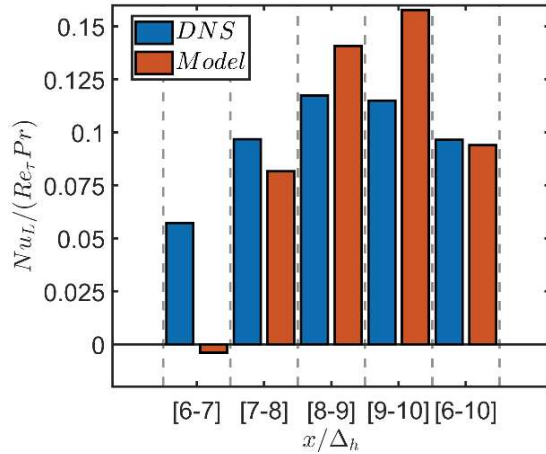
$$\text{DNS: } S_T = (\rho_0 A_{proj})^{-1} \int_{L_1}^{L_2} \int_0^{\delta_T} \bar{\omega}_c W dx dy$$

$$\text{Model: } S_T^{model} = (\rho_0 A_{proj})^{-1} \int_{L_1}^{L_2} \int_0^{\delta_T} I_0 \rho_0 S_L \Sigma_{gen} W dx dy$$



Nusselt number prediction using modelled S_T

$$T_{1L} + T_{2L} = - \left[\frac{Nu_L}{\{Re_\tau Pr\}} \right] + A_{proj} S_T / [A_{seg} u_{\tau, NR}]$$



Predictions of $Nu_L / \{Re_\tau Pr\}$ by using S_T^{model} to $Nu_L / \{Re_\tau Pr\}$ extracted from DNS data.



Conclusions

- ❖ Mean behaviour of velocity and temperature is significantly affected by the flame/flow configuration.
- ❖ The standard formulations in RANS and LES used for non-reacting flows have to be modified to account for flame-wall interaction in fully developed turbulent boundary layers. These variations should be included in the turbulence (e.g. turbulent kinetic energy, wall function and turbulent scalar flux) and combustion modelling
- ❖ Production and dissipation balance in the TKE equation may not be maintained within turbulent boundary layers under FWI.
- ❖ Turbulent burning velocity and Nusselt number are linked in FWI in turbulent boundary layers. This suggests that the measurements of mean velocity, temperature and wall heat flux can be utilised to estimate the turbulent burning velocity within turbulent boundary layers.
- ❖ Modelling of the mean reaction rate of major species is not sufficient for the prediction of heat release rate for H_2 -flames.





PTF Contributed Talks: Low Swirl, Instability, Modeling, Liquid Fuels, MI for FGM

Savard	DNS of a laboratory lean CH ₄ /H ₂ low-swirl flame impinging on an inclined wall
Acharya	Nonlinear Heat Release Characteristics for Triggering of Combustion Instabilities
Cleary	Probability density function modelling in the flamelet regime using multiple mapping conditioning
Salehi	Conditional Expansion Methods for Turbulence-Chemistry Interaction Modelling in Highly-Turbulent Premixed Flames
Yao	*Using tabulated chemistry and LES to capture non-unity Lewis number effects in turbulent premixed flames
Zimmermann	*Search for sustainable liquid fuels for clean aviation
Allison	Turbulent Liquid Fuel Flame Topologies via CH and OH PLIF: Two Truths and One Lie
Yellapantula	Co-Optimized Machine Learned Manifolds: Relearn FGM or FGM with major improvements

* Not provided for inclusion in the Proceedings

(Towards) DNS of a laboratory lean CH₄/H₂ low-swirl flame impinging on an inclined wall

**Mohammadreza Nozari¹, Martin Vabre¹, Luming Fan^{1,2}, Lucas Esclapez³,
Patrizio Vena², Marc Day³, Bruno Savard¹**

¹Department of Mechanical Engineering, Polytechnique Montréal, Montréal, Canada

²Aerospace Research Centre, National Research Council, Ottawa, Canada

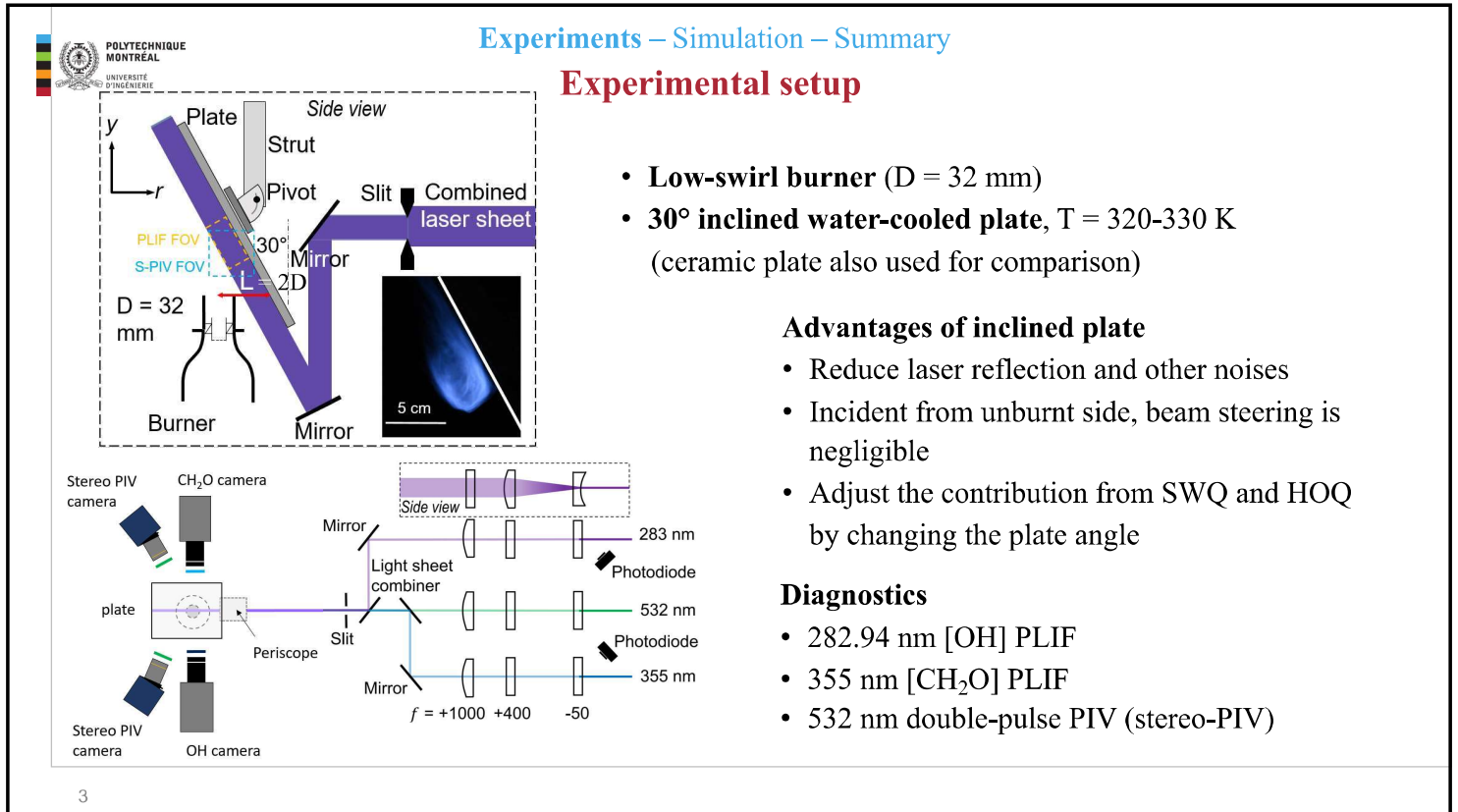
³National Renewable Energy Laboratory, Golden, Colorado, United States

TNF/PTF Workshop 2022, Vancouver, Canada

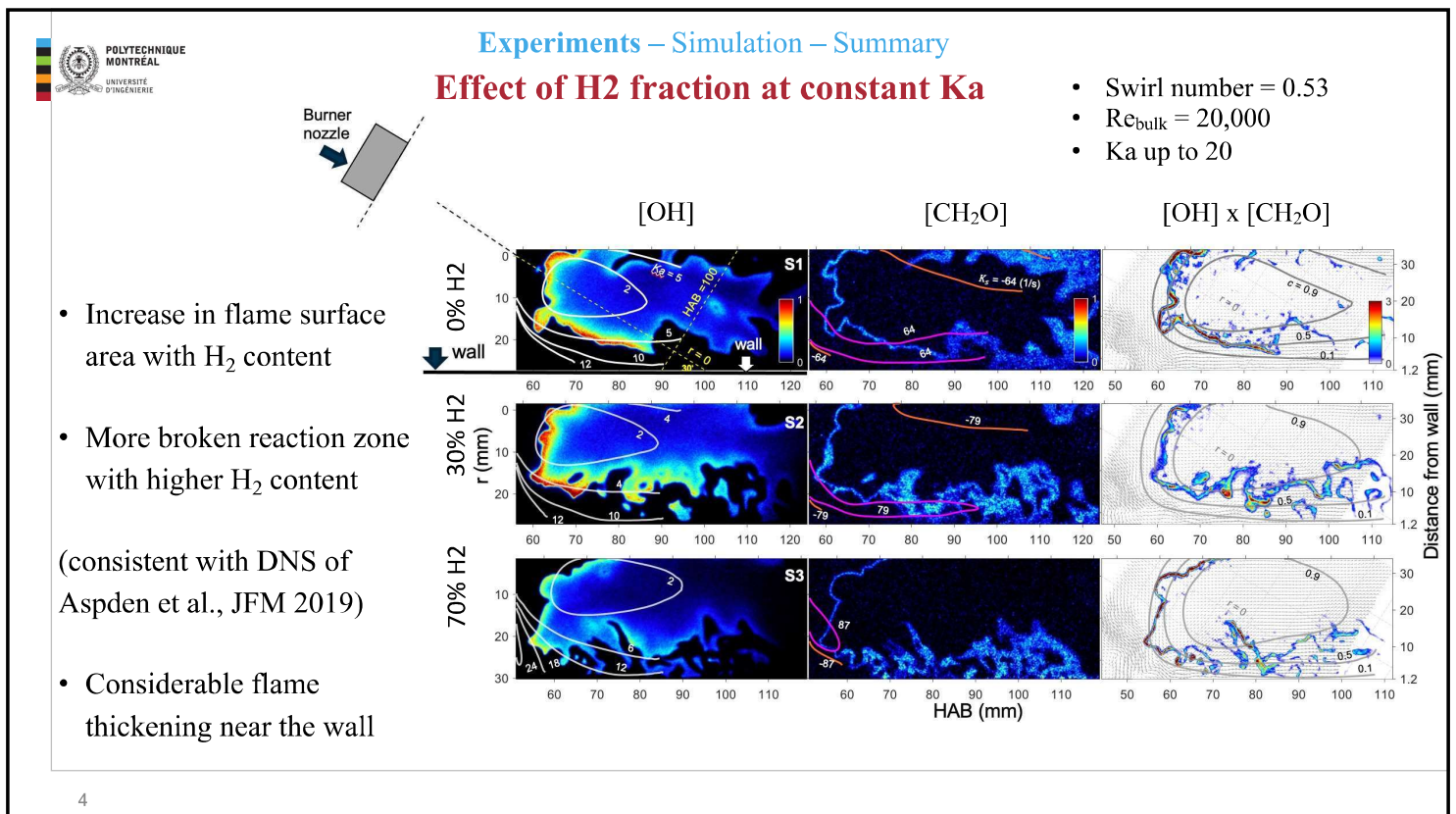


Outline

1. Experiments (more details during the Symposium)
2. Simulation (work in progress)
3. Summary



3



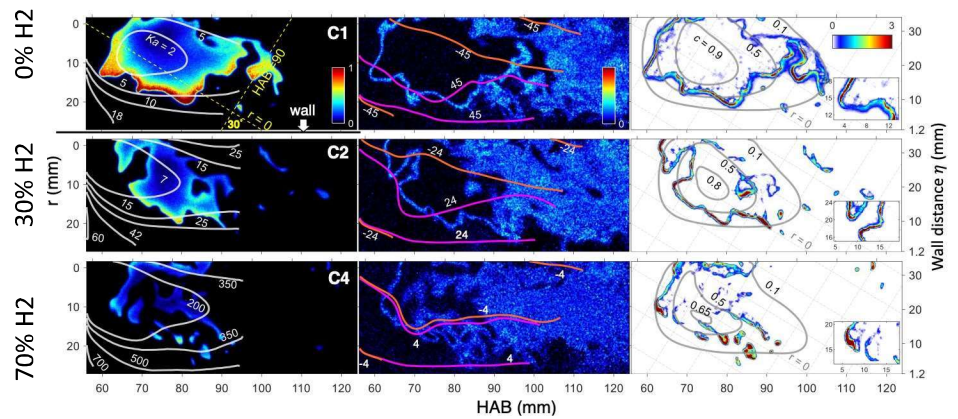
4

Experiments – Simulation – Summary

At blow-off limit

- Swirl number = 0.53
- $Re_{bulk} = 20,000$
- Ka up to 500

- Large cloud of formaldehyde formed behind the flame



5

5

Experiments – Simulation – Summary

Objectives for the simulation

1. Identify the cause of formaldehyde cloud formation
2. Quantify and model the respective roles of turbulence, mean strain rate, air entrainment, and wall heat loss on flame structure

6

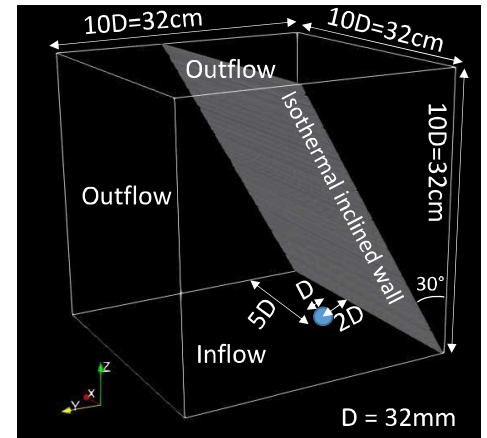
6

Flow and thermochemical conditions

- Fuel: 30% CH₄, 70% H₂
 - Equivalence ratio: 0.41
 - Ambient T and P for fuel and air
 - $U_{\text{bulk}} = 10 \text{ m/s}$
 - $Re_{\text{bulk}} \approx 20,000$
 - $Re_t \approx 400$
 - $Ka \approx 200$
- $S_L = 4 \text{ cm/s}$
 $l_F = 2.3 \text{ mm}$

Computational setup

- 10D x 10D x 10D box, with D=32mm (same as experiment)
- Isothermal (330K) inclined plate as embedded boundary
- Inflow matches (to some extent) PIV measurements at burner exit plane



7

7

Low-Mach assumption

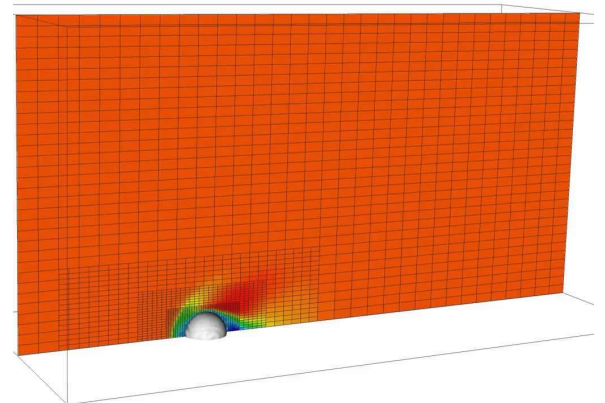
Transport model: mixture-averaged

Chemical kinetics: reduced Aramco mechanism with 25 species and 105 reactions [1]

Solver: PeleLMex



- Adaptive mesh refinement (AMR) capability
- Sub-cycling removed w.r.t. PeleLM
- More robust embedded boundary features w.r.t. PeleLM



<https://github.com/AMReX-Combustion/PeleLM>

8

Cost estimate

Resolution requirements

Flame (10 pts/species layer) → 80 microns
 Turbulence ($dx=2\eta$) → 110 microns
 Viscous sub-layer ($y^+_{min}=1$) → 60 microns

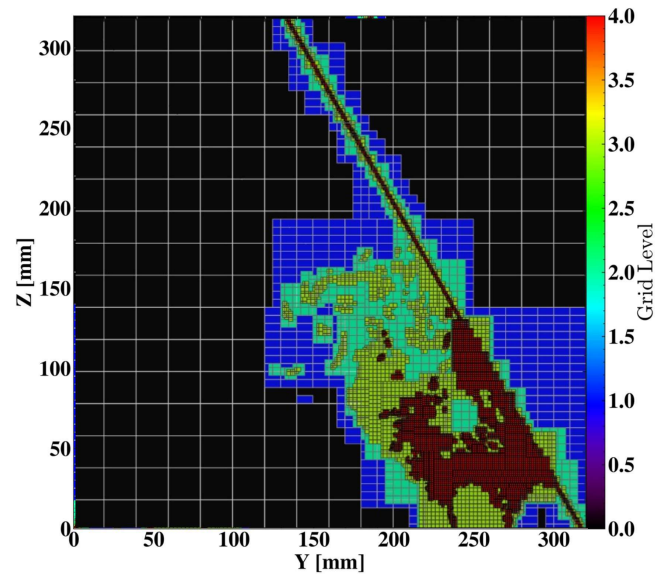
AMR level	Grid spacing (microns)	Number of cells (million)	Total cost per flow through (MCPU-hrs*)
0	1,266	17	-
1	633	60	-
2	316 (8pts/l _F)	240	0.1
3	158	460	1.3
4	79	2,300	11.2

* On Niagara at University of Toronto (Intel Skylake and CascadeLake)



Digital Research
Alliance of Canada

Alliance de recherche
numérique du Canada



Cost estimate

Resolution requirements

Flame (10 pts/species layer) → 80 microns
 Turbulence ($dx=2\eta$) → 110 microns
 Viscous sub-layer ($y^+_{min}=1$) → 60 microns

AMR level	Grid spacing (microns)	Number of cells (million)	Total cost per flow through (MCPU-hrs*)
0	1,266	17	-
1	633	60	-
2	316 (8pts/l _F)	240	0.1

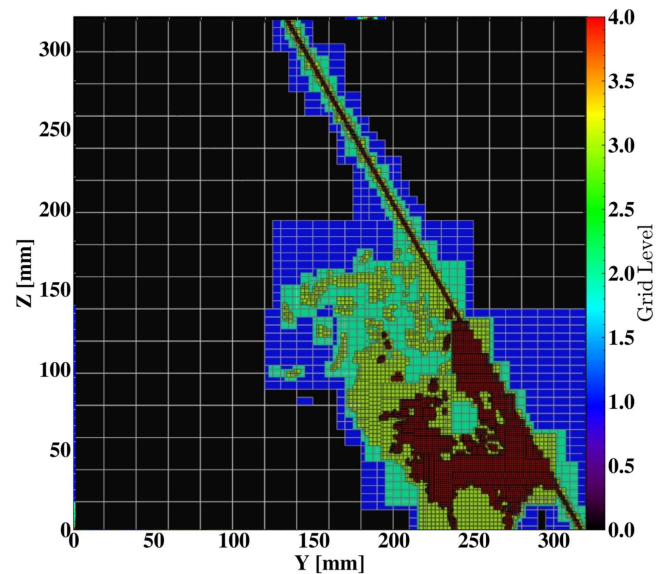
Only preliminary results with 2 AMR levels presented today

* On Niagara at University of Toronto (Intel Skylake and CascadeLake)



Digital Research
Alliance of Canada

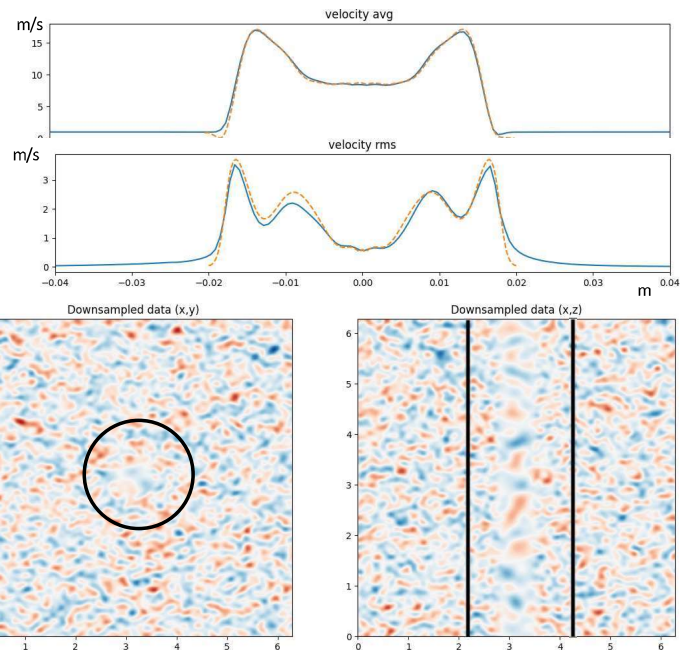
Alliance de recherche
numérique du Canada



Inflow

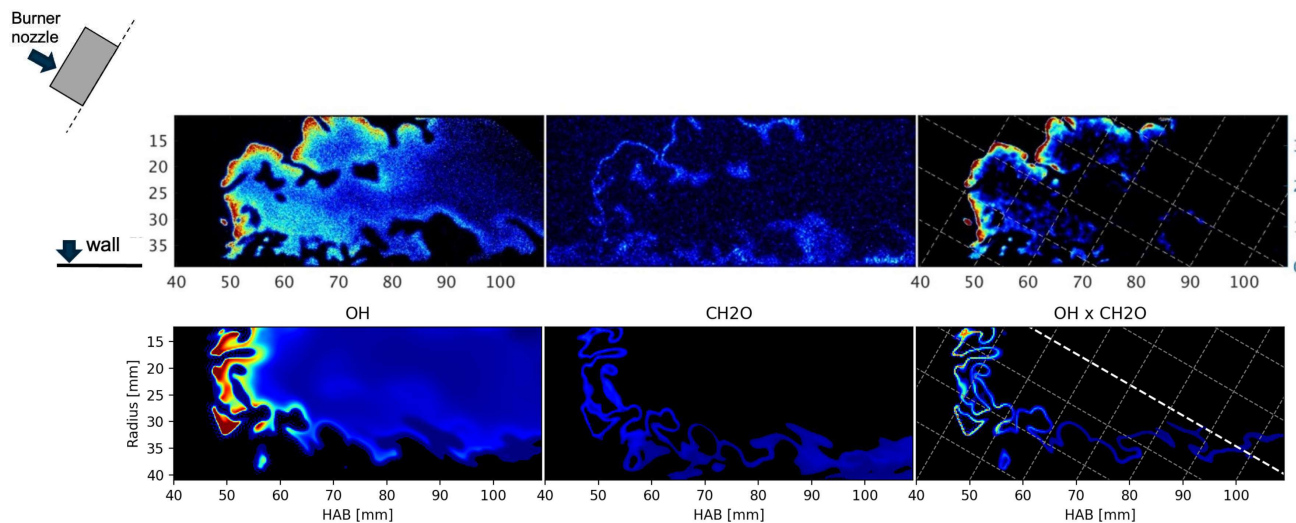
Approach used

- Match experimentally measured mean and rms velocity profiles (each of 3 components)
- Superimpose turbulent velocity field generated from model spectrum
 - Merge two fields with different integral length scales to match radial dependency experimentally measured



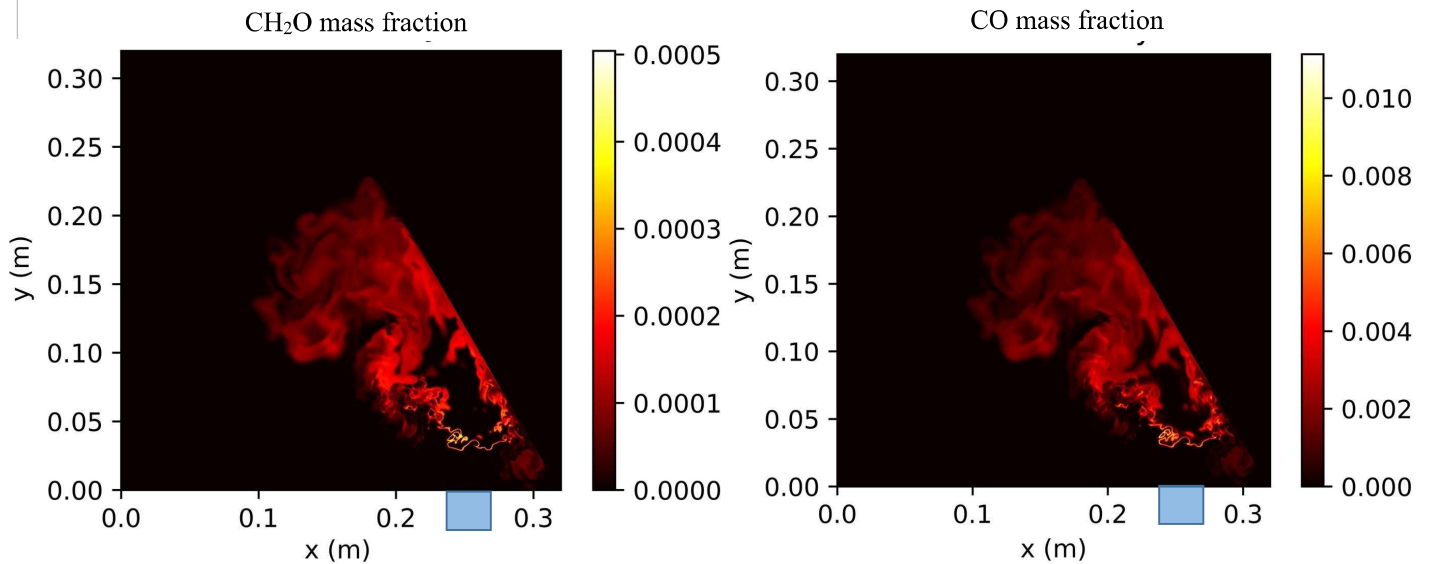
11

Comparison with experiment – instantaneous field



12

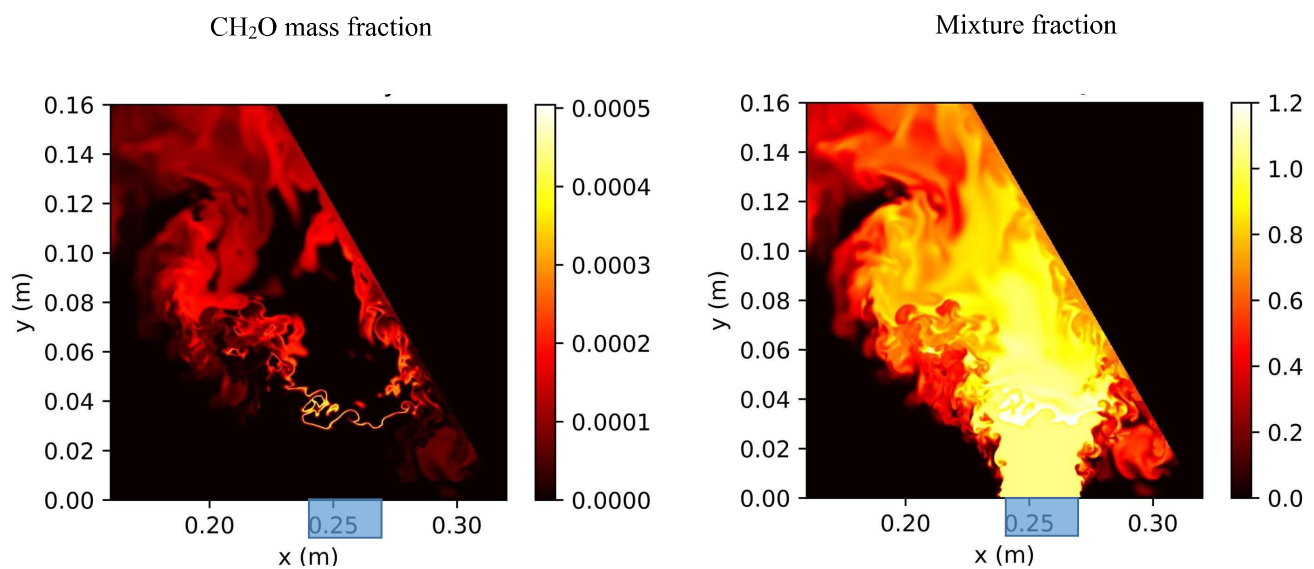
Incomplete combustion



13

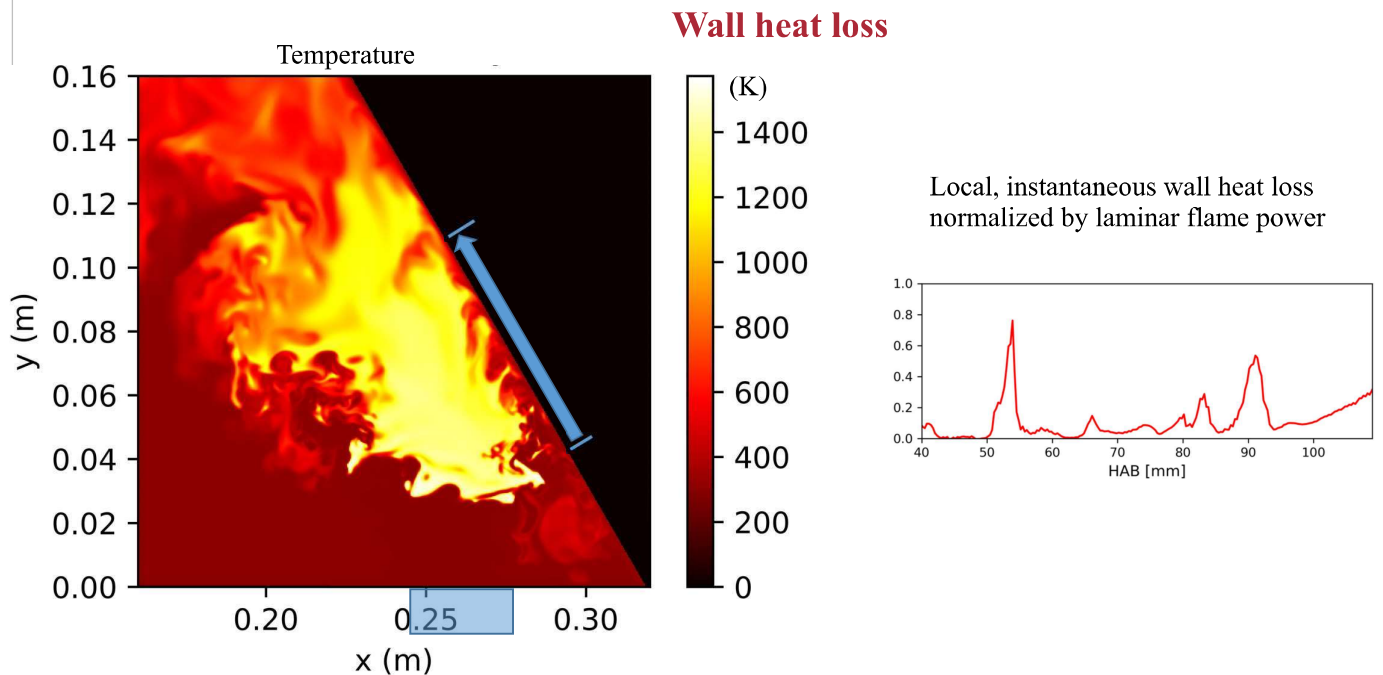
13

Incomplete combustion



14

14



Summary

- Experimental database with OH x CH₂O PLIF and stereo-PIV:
Ka = 10 – 1000, Re = 20k – 30k, 100% CH₄ to 100% H₂
- Some lean conditions targetable with DNS (O(1-10) M CPU-hrs)
- Preliminary simulation results indicate incomplete combustion near and away from the wall, consistent with experiments.
- Yet significant local wall heat loss identified
- Challenge remains to get the right inflow feed (DNS or LES of the burner needed?)

Acknowledgments



Digital Research
Alliance of Canada

Alliance de recherche
numérique du Canada



PTF Workshop 2022 (July 22-23, 2022)

Nonlinear Heat Release Characteristics for Triggering of Combustion Instabilities

Dr. Vishal Acharya

*Aerospace Combustion Lab, School of Aerospace Engineering,
Georgia Institute of Technology, Atlanta, Georgia, 30332*

Combustion instabilities manifest themselves as large amplitude acoustic oscillations over a range of frequencies depending upon the nature of the combustor geometry, combustor-combustor interactions, and heat release distribution in the combustor volume. The temporal growth/decay of the acoustic energy for a given natural acoustic mode is determined by the Rayleigh Integral which is the product of the acoustic pressure and unsteady heat release rate fluctuations integrated over the combustor volume. For low frequencies, flames are acoustically compact resulting in the global heat release oscillations determining stability through the flame transfer function.

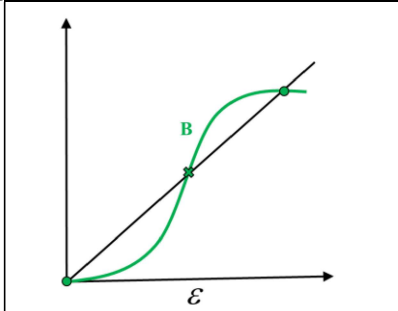


Figure 1 – Flame response amplitude for triggering.

To understand limit-cycles in the acoustically compact case, it is important to understand non-linearities in the flame response function: $\hat{F}(\varepsilon, \omega_0) = \hat{Q}(\varepsilon, \omega_0) / \bar{Q}(\varepsilon, \omega_0)$. These limit-cycles or fixed points of the system determined when driving equals damping. Previous studies have correlated the amplitude dependent heat release response directly with the fixed points, specifically with the occurrence of triggering, shown in **Figure 1**. The flame response exhibits inflection points – three intersection points exist, and both the zero amplitude and finite amplitude cases are stable with an intermediate unstable point.

When the system is triggered beyond this point, it reaches the higher amplitude limit-cycle. Also, note that in non-normal systems with strong transient amplification, the external disturbance amplitude required for the system to cross the unstable fixed point (denoted by green X) may be much smaller than the amplitude at this fixed point. For example, studies have shown even as low as 0.25% amplitude leading to triggering – making for a strong motivation for this work.

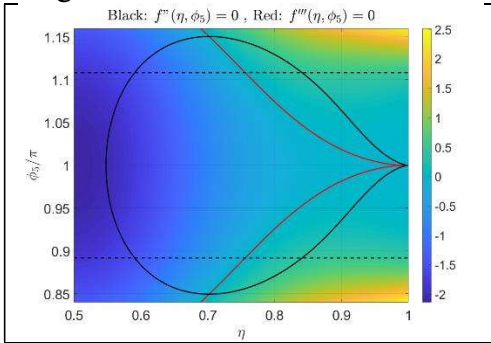


Figure 2 – Locus of points for triggering.

The goal of this work is two-fold: First, to establish the relationship between the different heat release orders (linear, third, fifth order terms) that lead to such behaviors/variations in the heat release. Second, determine the parametric regions where the above relationship is satisfied for non-linear premixed flame response. An example of the parametric space where triggering is possible is shown in Figure 2. This figure shows the variation of the relative phasing of the 5th order flame response with respect to the 3rd order flame response for the case where there is no linear flame response (i.e., $FTF = 0$). The region of the solid black

curve between the dashed curves, to the left of the red curves is the locus of points where triggering is possible. For the non-linear response of premixed flames, the G -equation is used which helps determine the heat release at different orders from which the parametric regions lying on the above locus of points is determined. However, accurate simulations of the flame position require the turbulent flame speed as input. Several models of the turbulent flame speed have been established in the literature; however, this motivates work for current fuel blends of interest such as ammonia/hydrogen blends for which turbulent flame speed scaling are not yet established.



Nonlinear Heat Release Characteristics for Triggering of Combustion Instabilities

PTF Workshop 2022, Vancouver, BC, Canada
July 23, 2022

Dr. Vishal Acharya

*Senior Research Engineer
Aerospace Combustion Lab*



What are the questions here?

- Nonlinear heat release studies
 - Forced flame with increasing amplitude levels
 - Single frequency
- Can we determine nonlinear heat release characteristics that lead to certain variations in flame response with forcing amplitude?
 - Non-monotonic variations
 - Variations that can lead to triggering
- Why do we need this?
 - Each of the above relationships result in specific limit-cycle behaviors
 - Having mathematical conditions/constraints illustrate when such behaviors occur and help determine them from data



Nonlinear Flame Response: Modeling

- Nonlinear Heat release
 - Expand heat release in terms of the disturbance amplitude ε

$$Q(t) = Q_0 + \varepsilon Q_1(t) + \varepsilon^2 Q_2(t) + \varepsilon^3 Q_3(t) + O(\varepsilon^4)$$

- Focus on single-frequency (i.e., no inter-frequency interactions)

$$\overline{Q} = Q_0 + \varepsilon^2 \overline{Q_2} + \varepsilon^4 \overline{Q_4}$$

$$\hat{Q}'(\omega) = \varepsilon \hat{Q}'_1(\omega) + \varepsilon^3 \hat{Q}'_3(\omega) + \varepsilon^5 \hat{Q}'_5(\omega)$$

- Flame Response Function

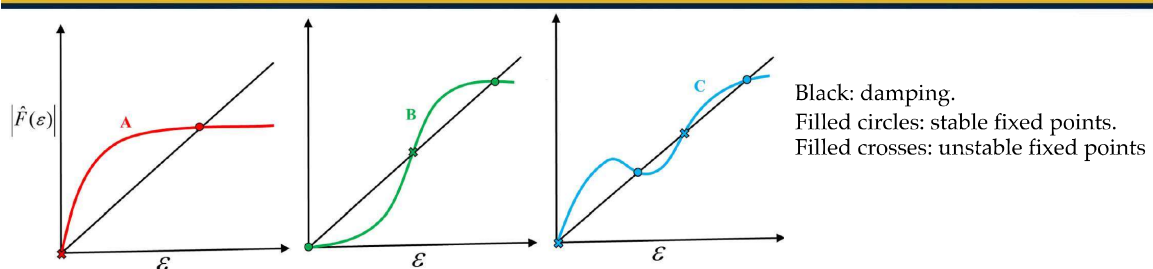
$$\hat{F}(\varepsilon, \omega) = \frac{\varepsilon \hat{Q}'_1(\omega) + \varepsilon^3 \hat{Q}'_3(\omega) + \varepsilon^5 \hat{Q}'_5(\omega)}{Q_0 + \varepsilon^2 \overline{Q_2} + \varepsilon^4 \overline{Q_4}}$$

- Focus on flame response amplitude

$$F(\varepsilon, \omega_0) = |\hat{F}(\varepsilon, \omega_0)|$$

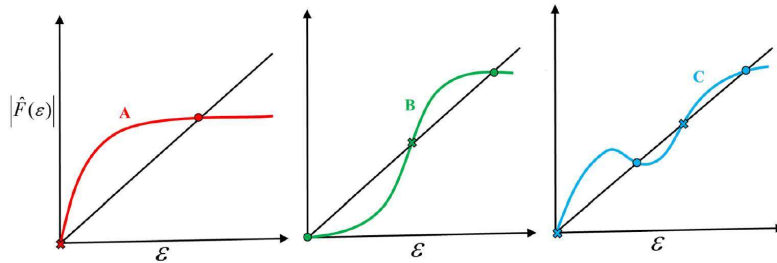


Nonlinear Flame Response: Damping vs Driving



- **A:** linear increase (non-zero FTF) followed by saturation
 - Stable fixed point of non-zero amplitude
- **C:** linear increase followed by non-monotonic trend
 - Multiple stable fixed points; possible to trigger
- **B:** low or zero FTF followed by purely non-linear increase and saturation
 - Stable system at zero amplitude
 - Sufficient triggering pushes to a stable non-zero limit cycle
- Not exhaustive but covers what's predominantly observed

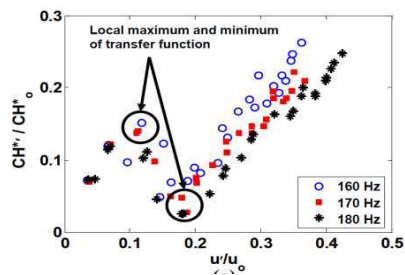




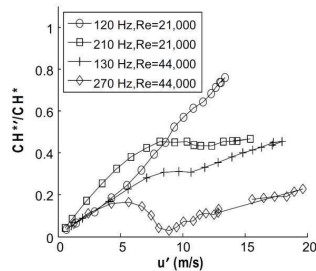
CASE C – NON-MONOTONIC BEHAVIORS

Data from Literature

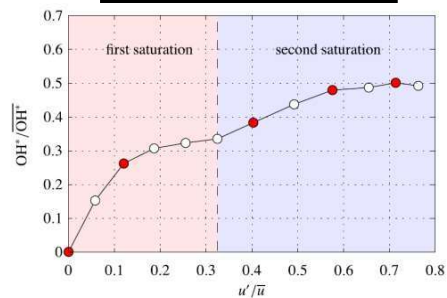
Bellows et al., JEGTP 2007



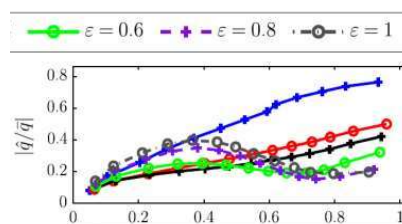
Thumuluru et al., PROCI 2009



Oberleithner et al., C&F 2015



Ćosić et al., C&F 2015

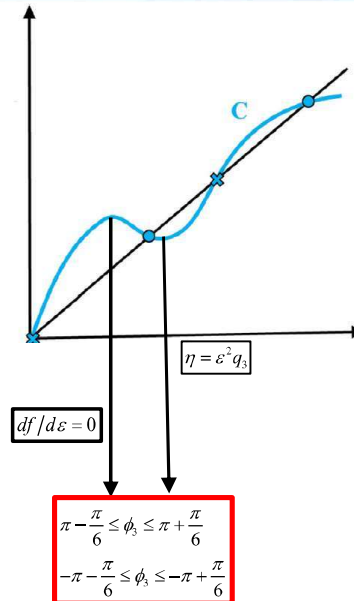


How do we model this behavior?

$$F(\varepsilon, \omega_0) = |\hat{F}(\varepsilon, \omega_0)| = \varepsilon \frac{|\hat{Q}'_1(\omega_0) + \varepsilon^2 \hat{Q}'_3(\omega_0)|}{Q_0 + \varepsilon^2 \bar{Q}_2}$$

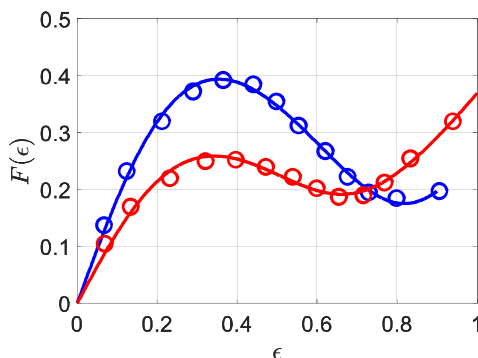
$$\begin{aligned} \hat{q}_i &= \hat{Q}_i / Q_0 & q_i &= |\hat{q}_i / q_1| \\ \bar{q}_i &= \bar{Q}_i / Q_0 & q_i &= |\hat{q}_i| \\ \hat{q}_i / q_1 &= q_i e^{i\phi_i} & f &= (\sqrt{q_3} / q_1) F \\ \eta &= \varepsilon^2 q_3 & \mu &= \bar{q}_2 / q_3 \\ \phi_i &= \angle \hat{q}_i & \phi_i &= 0 \end{aligned}$$

$$f(\eta) = \sqrt{\eta} \left| \frac{1 + \eta e^{i\phi_3}}{1 + \eta \mu} \right| = \sqrt{\eta} \sqrt{\frac{1 + 2\eta \cos \phi_3 + \eta^2}{(1 + \eta \mu)^2}}$$



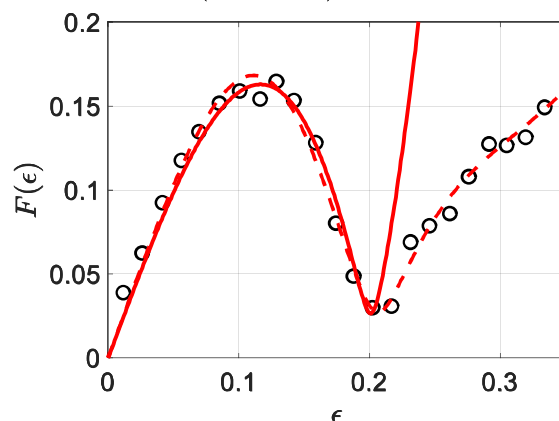
Model vs Data

- Data from Ćosić *et al.*, C&F 2015
 - Third order model captures all points
 - No time average shift



Red – fuel-split between injection at burner and far upstream
Blue – fuel injected only at burner.
Circles: Measured data, Solid curve: Model.

- Data from Bellows *et al.*, JEGTP 2007
 - Third order model works until second characteristic point (solid red)
 - Time-average shift
 - Fifth order model captures high amplitude behavior (dashed red)

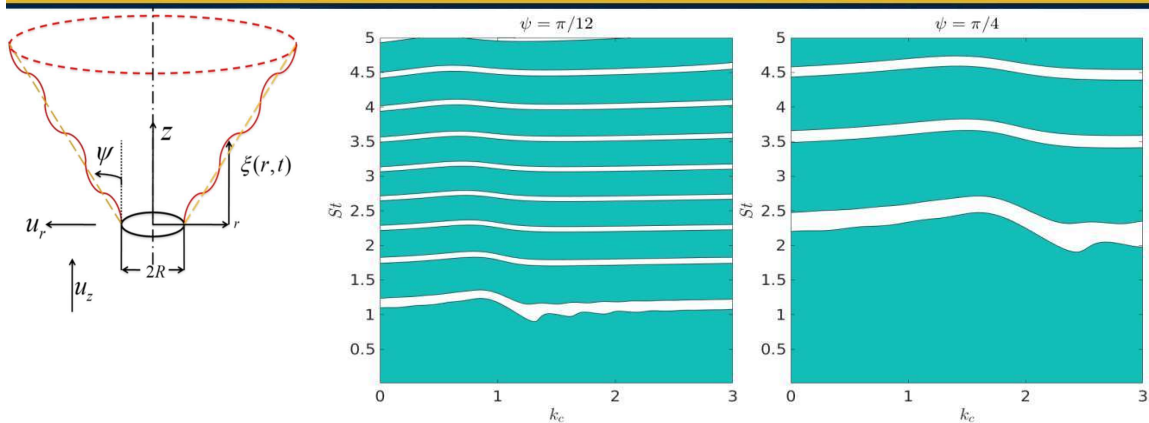


Solid Red – Third order model
Dashed Red – Fifth order model
Circles: Measured data



Model Premixed Flame

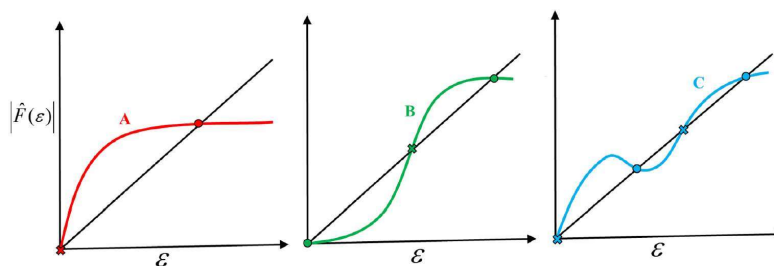
(Acharya & Lieuwen, Proc. Comb. Inst., 2021)



- Model Premixed Flame using G-equation
 - Parameters set same as measured data cases
- LES using G-equation + sub-grid models (on-going)
 - Results sensitive to turbulent flame speed
 - Less sensitive to turbulent flow parameters



White region: parameter combinations where the flame response shows the non-monotonic behavior



CASE B – TRIGGERING



Modeling – Zero linear response

- Zero linear flame response case
 - Linearly stable system but non-linearly unstable

$$\hat{F}(\epsilon, \omega) = \epsilon \frac{\hat{Q}'_1(\omega) + \epsilon^2 \hat{Q}'_3(\omega) + \epsilon^4 \hat{Q}'_5(\omega)}{Q_0 + \epsilon^2 Q_2 + \epsilon^4 Q_4}$$

$$\hat{q}_j = \hat{Q}_j / Q_0 = q_j e^{i\phi_j} \text{ for } j = 1, 3, 5$$

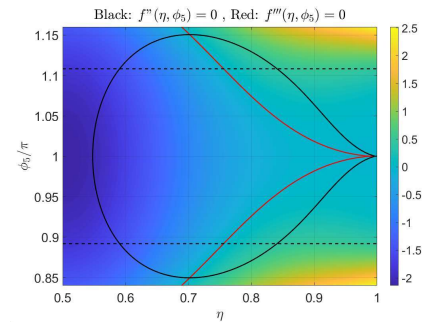
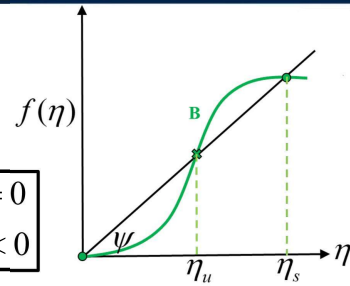
$$\beta = q_5 / q_3$$

$$\eta^2 = \epsilon^2 \beta$$

$$f(\eta) = \eta^3 \sqrt{1 + 2\eta^2 \cos \phi_5 + \eta^4}$$

$$-1 \leq \cos \phi_5 \leq -\frac{2\sqrt{2}}{3}$$

$$\begin{aligned} f''(\eta) &= 0 \\ f'''(\eta) &< 0 \end{aligned}$$



Modeling – Non-zero linear response

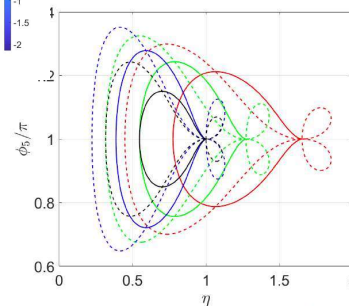
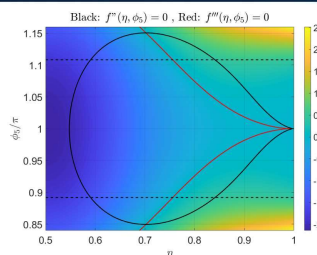
- Non-zero linear heat release

$$\hat{F}(\epsilon, \omega) = \epsilon \frac{\hat{Q}'_1(\omega) + \epsilon^2 \hat{Q}'_3(\omega) + \epsilon^4 \hat{Q}'_5(\omega)}{Q_0 + \epsilon^2 Q_2 + \epsilon^4 Q_4}$$

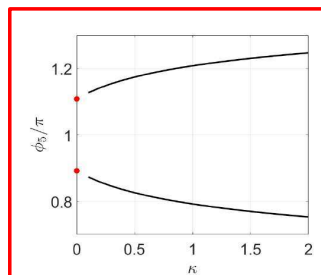
$$\hat{q}_j = \hat{Q}_j / Q_0 = q_j e^{i\phi_j} \text{ for } j = 1, 3, 5$$

$$\kappa = q_5 q_1 / q_3^2$$

$$\eta^2 = \epsilon^2 q_3 / q_1 \quad f(\eta, \kappa, \phi_5) = |\hat{F}| \sqrt{q_3 / q_1^3} = \eta \left| 1 + \eta^2 + \eta^4 \kappa e^{i\phi_5} \right|$$



$$-1 \leq \cos \phi_5 \leq -\frac{2\sqrt{2}}{3}$$



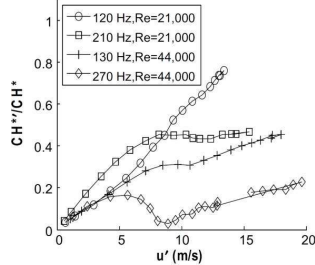
Effect of κ on the locus of points for $\partial f / \partial \eta = 0$ (solid) and the $\partial f / \partial \phi_5 = 0$ (dashed)
Black: baseline case where $q_1 \equiv 0$. Red: $\kappa = 0.5$, Blue: $\kappa = 1$, Green: $\kappa = 2$.



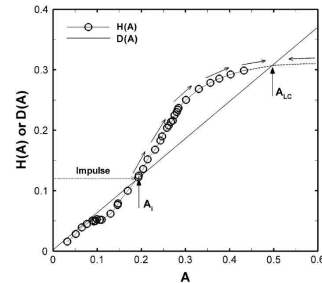
Data from Literature, Simulations

- Not a whole lot of data out there that can aid in this study

Thummuluru *et al.*, PROCI 2009



Kim & Hochgreb, C&F 20012



- We need more data from experiments and simulations with potential triggering tendencies
 - How do we design for this across a range of parameters?
- Model Premixed Flames – on-going



Takeaways and Additional considerations

- Methodology presents a physics-based deduction on how high order non-linear components are related to each other to enable triggering of instabilities
 - Constraints on phasing
- Application to Data: physics-based fitting to data can illustrate how non-linearities behave and relate them back to control parameters
 - Need data for this effort
- Premixed Flame Model
 - G-Equation model for turbulent premixed flame to capture parameter spaces where triggering occurs
 - Captures data regions with great accuracy
 - Need validated inputs to model (turbulent flame speed, flow etc)



Probability density function modelling in the flamelet regimes of premixed combustion

Matthew Cleary

The University of Sydney, School of Aerospace, Mechanical and Mechatronic Engineering

Thanks to:

Sydney – Y. Shoraka, S. Aldawsari, S. Galindo Lopez, A.R. Masri

Queensland – A.Y. Klimenko

Stuttgart – N. Iaroslavtceva, A. Kronenburg, O. Stein



Joint TNF and PTF Workshops
Vancouver, 22 – 23 July 2022

Motivation

- Broadly, there are PDF-type models and flamelet-type models
- PDF methods inherent advantage, source terms exact
- Distributed regimes – inner structure is broken. PDF methods expected to perform better than flamelet methods
- Flamelet and thin reaction zone regimes – inner structure is intact. Standard PDF models cannot capture this
- Option 1 – tune mixing constant for specific conditions but this is not predictive
- Option 2 – conditioning, imposing flamelet-like properties

High level introduction to PDF conditioning

- Transported joint PDF equation

$$\frac{\partial \bar{\rho} f_\phi}{\partial t} + \frac{\partial}{\partial x_i} \left(\bar{\rho} \tilde{u}_i f_\phi - \bar{\rho} \mathcal{D}_e \frac{\partial f_\phi}{\partial x_i} \right) + \frac{\partial \bar{\rho} W_\alpha f_\phi}{\partial \psi_\alpha} = - \frac{\partial}{\partial \psi_\alpha \partial \psi_\beta} \left(\bar{\rho} \mathcal{D} \frac{\partial \phi_\alpha}{\partial x_i} \frac{\partial \phi_\beta}{\partial x_i} | \psi \right) f_\phi$$

↑ reaction term closed ↑ conditional dissipation term unclosed

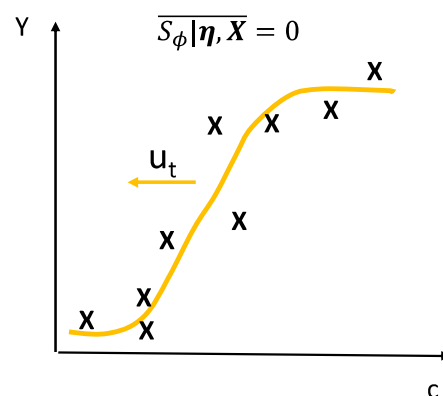
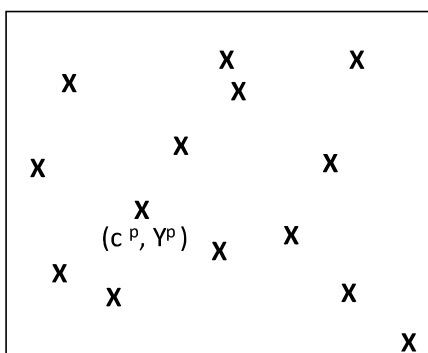
$$dx_i^p = \left[\tilde{u}_i + \frac{1}{\bar{\rho}} \frac{\partial}{\partial x_i} (\bar{\rho} \mathcal{D}_e) \right]^p dt + [\sqrt{2\mathcal{D}_e}]^p d\omega_i^p$$

$$d\phi^p = [W_\phi + S_\phi]^p dt$$

- The mixing is conditioned

$$\overline{S_\phi | \bar{X}} = 0 \xrightarrow{\text{conditioning}} \overline{S_\phi | \boldsymbol{\eta}, \bar{X}} = 0 \quad \text{where } \boldsymbol{\eta} \text{ is low dimensional manifold for } \psi$$

High level introduction to PDF conditioning



Non-premixed flames – conditioning on mixture fraction

Premixed flames – need to distinguish fresh reactants from burnt gas

High level introduction to PDF conditioning

- Conservation of conditional moments during mixing is always desirable
- With good selections, can improve quality/accuracy of mixing model and reduce computational cost
- MMC uses independent reference variables $\eta^p \neq \phi^p$, so mixing is also linear with respect to all scalars

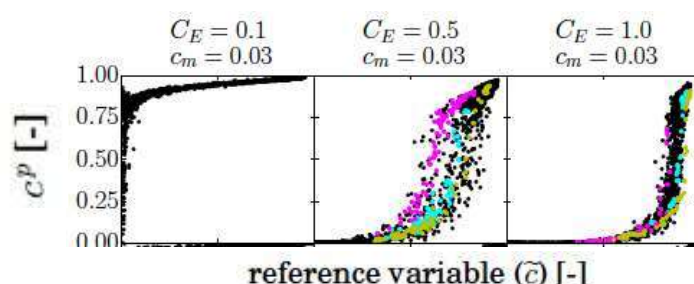
For example:

RANS: $d\eta^p = -\frac{C_\phi}{\tau}(\eta^p - \tilde{\eta}(x^p, t))dt + b_0\sqrt{\frac{2C_\phi\tilde{\eta}^2(x^p, t)}{\tau}}d\omega^p$

LES: $\eta^p = \tilde{\eta}(x^p, t)$ (sparse particle methods)

MMC for premixed combustion

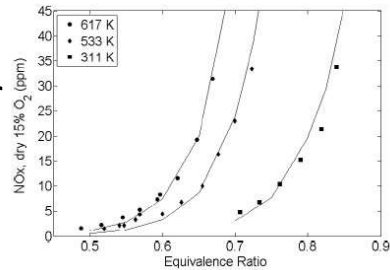
1. Conditioning on progress variable from artificially thickened flame model (Stuttgart)
 - flamelet structures are preserved
 - good match with data (Darmstadt stratified flame)
 - uses sparse particle method, very efficient
 - unless mixing rate is tuned, PDF flame propagates too fast relative to the reference flame



MMC for premixed combustion

2. Conditioning on distance to the flame front (University of Queensland)

- simple and practical, successfully applied in PaSR for combustor NOx prediction
- level set approach suggested for general flame simulations
- impractical due to ambiguity of flame speed scaling in the inertial interval



MMC for premixed combustion

3. Conditioning on shadow position (Sydney, Queensland)

- stochastic particles have a shadow position $\eta^p = \xi^p$

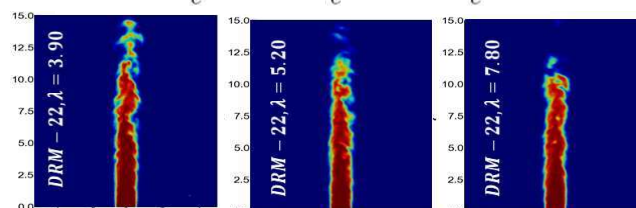
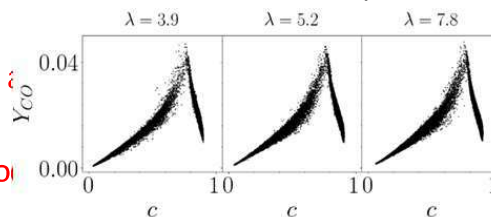
$$d\xi^p = \bar{U}dt + \frac{x^p - \xi^p}{\tau_\xi} + \left(\sqrt{2\mathcal{D}_\xi} \right) d\mathbf{w}_\xi^p$$

$$\mathcal{D}_\xi = \mathcal{D}\lambda^2; \quad \lambda = u_t/s_l$$

- flame speed and inner structure are independent, no mixing rate tuning required

- λ implemented as u_t and s_l are variables

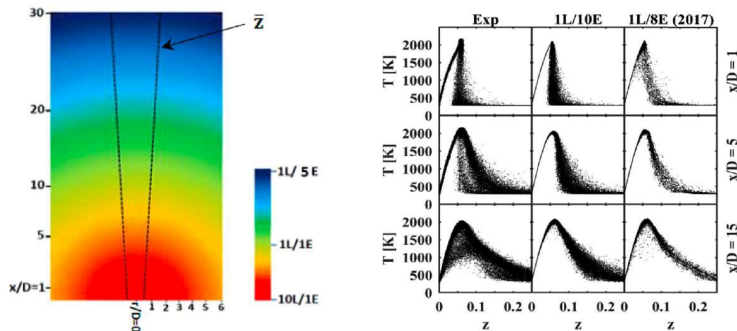
- intensive method



MMC for premixed combustion

4. Hybrid sparse/intense method (Sydney)

- conditioning via increased resolution
- suitable for mixed mode flames
- only suitable for distributed premixed regions
- requires regime sensor for dynamically changing between sparse in the non-premixed regions and intensive in the premixed regions



Current directions and outlook

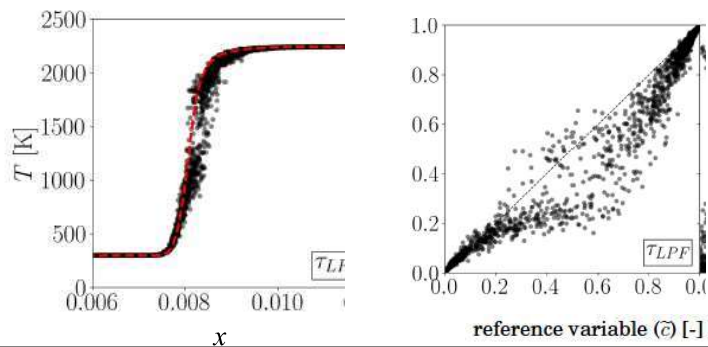
- To be useful, PDF models for premixed combustion should:
 - (A) be applicable to different premixed regimes
 - (B) have few (hopefully no) tunable parameters and low sensitivity to those parameters
 - (C) be computationally affordable

		property			
model		A	B	C	Viable
	1	yes	?	yes	?
	2	yes	no	no	no
	3	yes	?	?	?
	4	no	yes	no	no

Current directions and outlook

- Model 1 with conditioning on progress variable (Stuttgart)
- The problems are:
 1. decorrelation of the flame that is predicted by the particles and by the artificially thickened flame model
 2. sensitivity to the mixing constant
- Advances have been made in both areas through analysis of the laminar (unthickened) limit

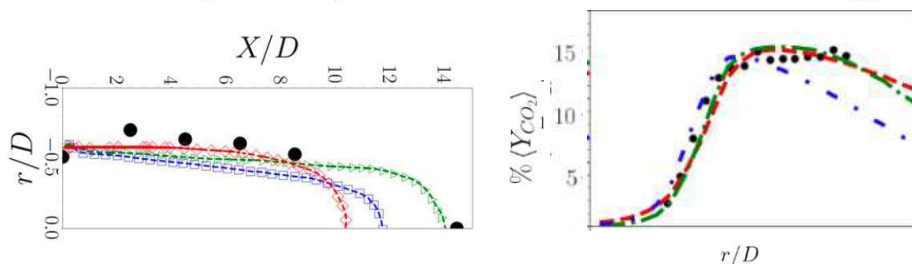
2G08: PDF mixing time scales for premixed combustion in the laminar flame limit
N. Iaroslavtceva, A. Kronenburg, O.T. Stein



Current directions and outlook

- Model 3 with conditioning on shadow position (Sydney)
- The problems are:
 1. the parameter $\lambda = u_t/s_l$ was global
 2. formulated as an intensive PDF method, so expensive
- The first problem has been addressed through locally modelled wrinkling factor (Charlette et al. 2002)

$$\lambda = \frac{S_{T,\Delta E}}{s_L} = \left[1 + \min \left(\max \left(\frac{\Delta E}{\delta_c} - 1, 0 \right), \Gamma_{\Delta E, C} \left(u'_{\Delta E}, \frac{\Delta E}{\delta_L}, Re_{\Delta} \right) \left(\frac{u'_{\Delta E}}{s_L} \right) \right) \right]^\beta$$



Acknowledgements

Australian Research Council funding

Compute time on the National Computing Infrastructure under the merit allocation scheme, NCMAS

Sydney Informatics Hub and the University of Sydney's high-performance computing cluster, Artemis

TNF/PTF Workshops

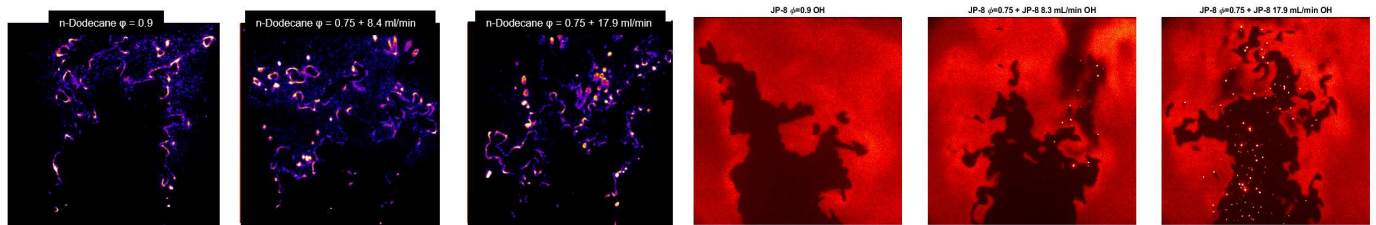
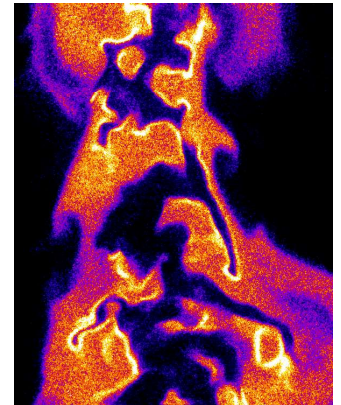
Blank Page

Turbulent Liquid Fuel Flame Topologies via CH and OH PLIF: “Two Positives and One Warning”

Patton M. Allison, Amirreza Gandomkar, and John Schihl
Michigan State University

Campbell Carter, Thomas McManus, and Aaron Skiba
US Air Force Research Lab, WPAFB

Savvas Gkantonas
University of Cambridge, UK



Motivations

A. Liquid Fuel Extinction Physics: Prevaporized and Spray

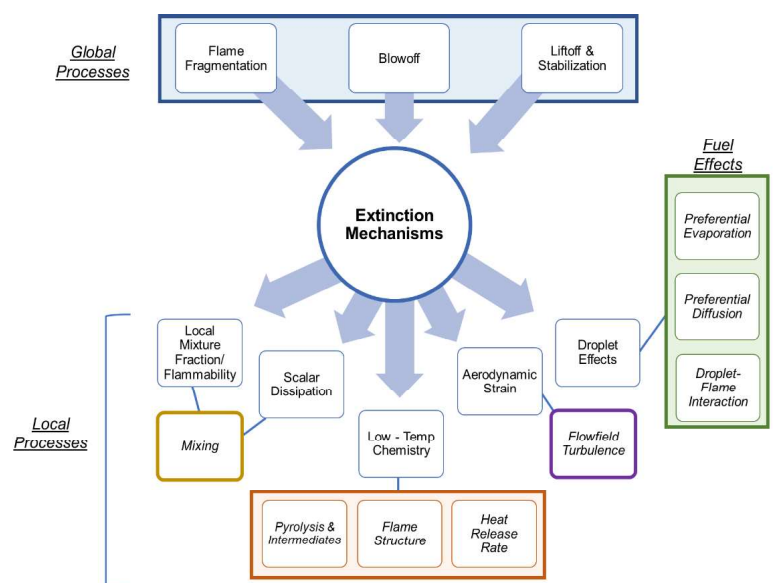
1. How are finite-rate chemistry for low-temperature processes represented in changes to the local flame structure and heat release?
2. How is extinction in spray flames different than in prevaporized/gaseous fuel flames?

B. Real Fuel Effects of Kerosenes

1. How is extinction altered by multicomponent fuel effects? How are the preheat/pyrolysis regions of the flame affected?
2. What is the comparison between computational predictions of kerosene/surrogates compared to real fuel experiments?

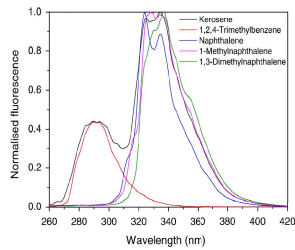
C. Diagnostic Needs

1. Is our standard toolbox for gaseous flames adequate for liquid fuels?
2. If not, then what?

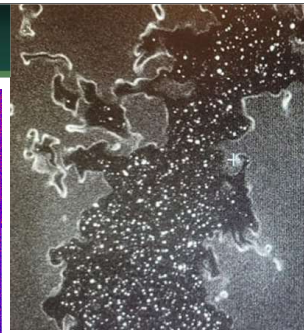
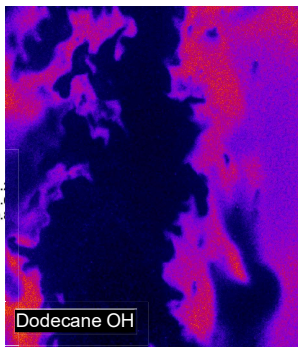
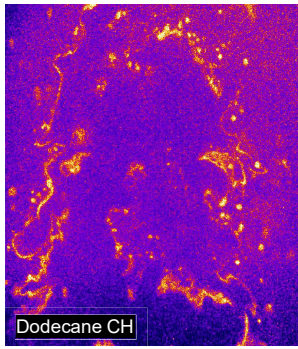
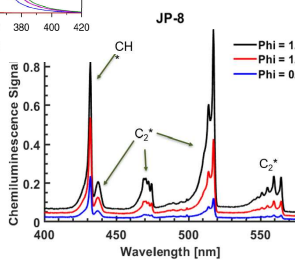


"Two Positives and One Warning"

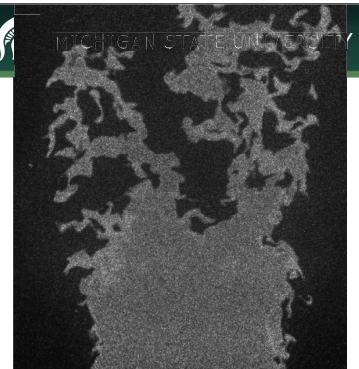
1. Is interference-free imaging is feasible?
2. Can flame structure is accurately captured and measured?
3. Can flame structure be affected by Le effects?



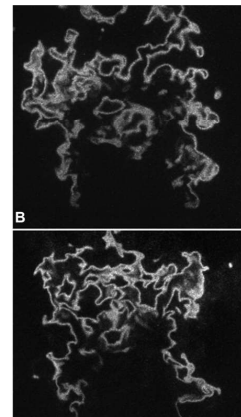
Ortiz, M., Baranger, P., Leder, C., Apeloig, J., and Grisch, F., Fluorescence Spectroscopy of Kerosene Vapor at High Temperatures and Pressures: Potential for Gas Turbine Measurements, *Applied Physics B: Lasers and Optics*, 2014, Volume 116, 729-745.



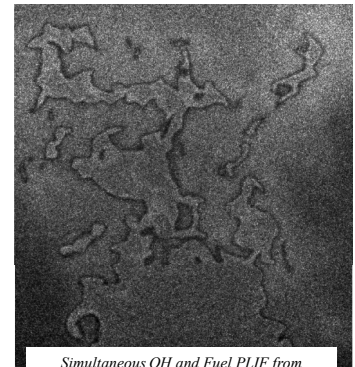
CH and Fuel PLIF from JP-8 kerosene spray



Fuel PLIF from prevaporized JP-8 kerosene



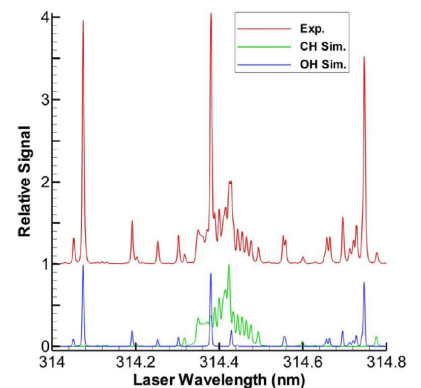
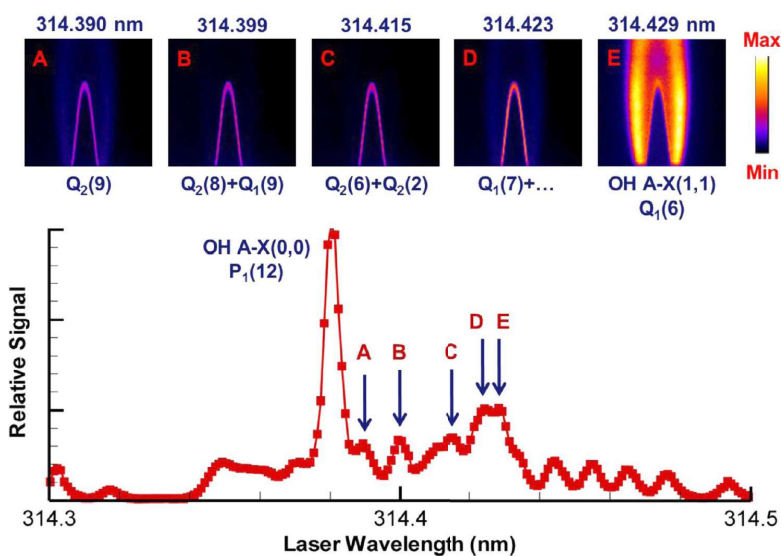
Formaldehyde PLIF from JP-8



Simultaneous OH and Fuel PLIF from prevaporized JP-8 kerosene

**CH C_2^+ -X² Π PLIF, Q-branch**

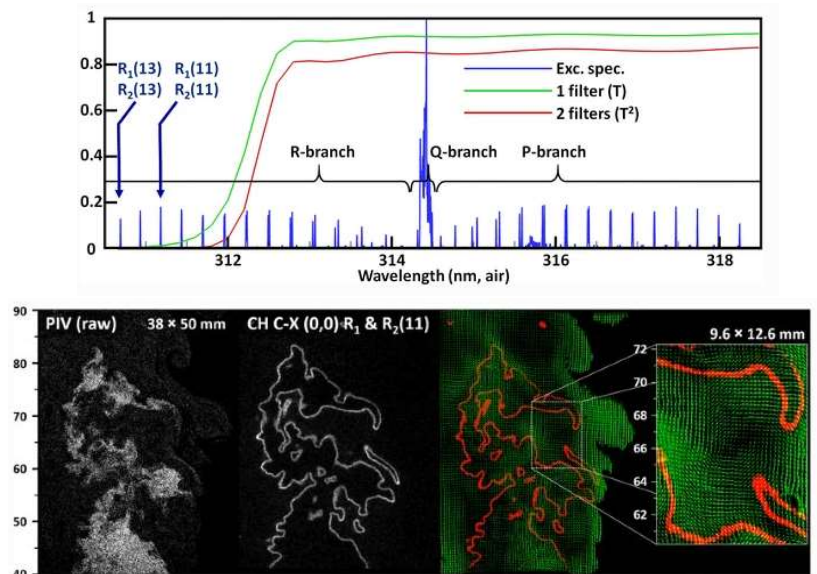
Carter et al. have shown the capability to simultaneously capture CH C-X band PLIF and OH A-X band PLIF with single laser excitation in the overlapping bands occurring between 314.390 and 314.429 that excite either the OH A-X (1,1)-band $Q_1(6)$ transition or the A-X (0,0)band $P_1(12)$ transition.



Carter, C.D., Hammack, S., and Lee, T., High-Speed Flamefront Imaging in Premixed Turbulent Flames Using Planar Laser-Induced Fluorescence of the CH C-X Band, *Combustion and Flame*, 2016, Volume 168, 66-74.

CH $C^2\Sigma^+-X^2\Pi$ PLIF, R-branch

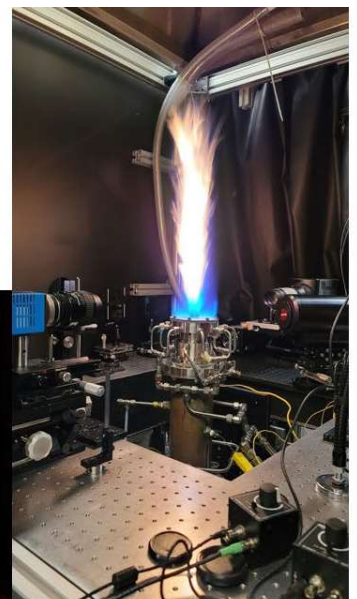
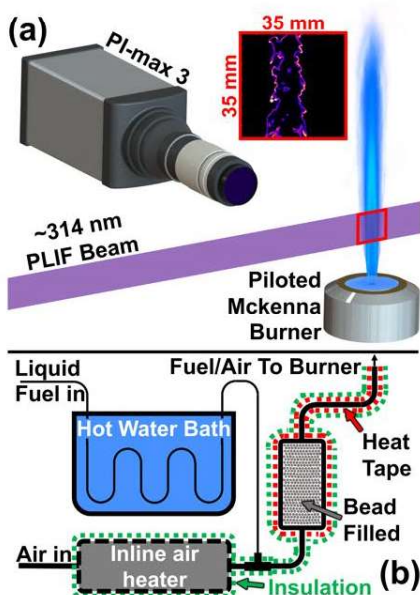
- Carter et al. have shown the capability to capture CH C-X band PLIF and OH A-X band PLIF with single laser excitation
- Overlapping bands occurring near 311 nm that excite either the CH (0,0) or the OH A-X (0,0) transition. Fluorescence occurs near 314 nm.
- Custom Semrock (AFRL-0002) and UG-5 filters remove Mie scattering and incandescence.
- Goal 1: Apply R-branch excitation to liquid fuel sprays to examine alteration of flame topology
- Goal 2: Compare topological structures captured with CH vs OH PLIF



Hammack, S.D., Skiba, A.W., Lee, T., and Carter, C.D., CH PLIF and PIV Implementation Using C-X (0,0) and Intra-Vibrational Band Filtered Detection, *Applied Physics B: Lasers and Optics*, 2018

5

McKenna Jet Burner + Prevaporizer

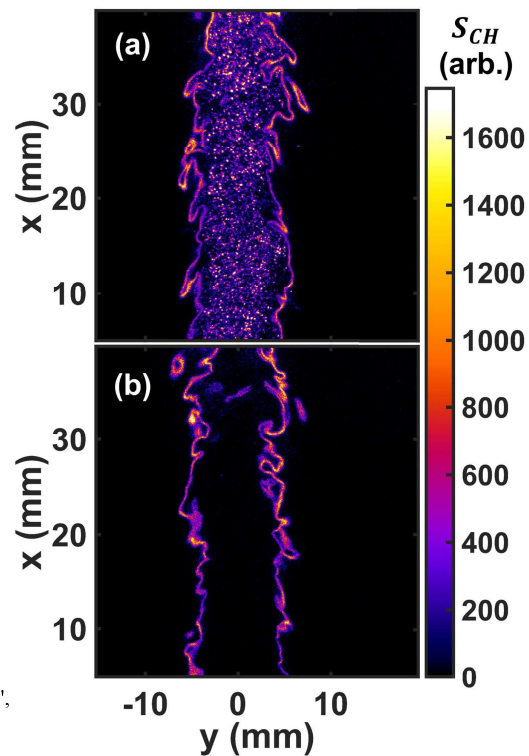


6

Premixed CH Imaging: Q-branch

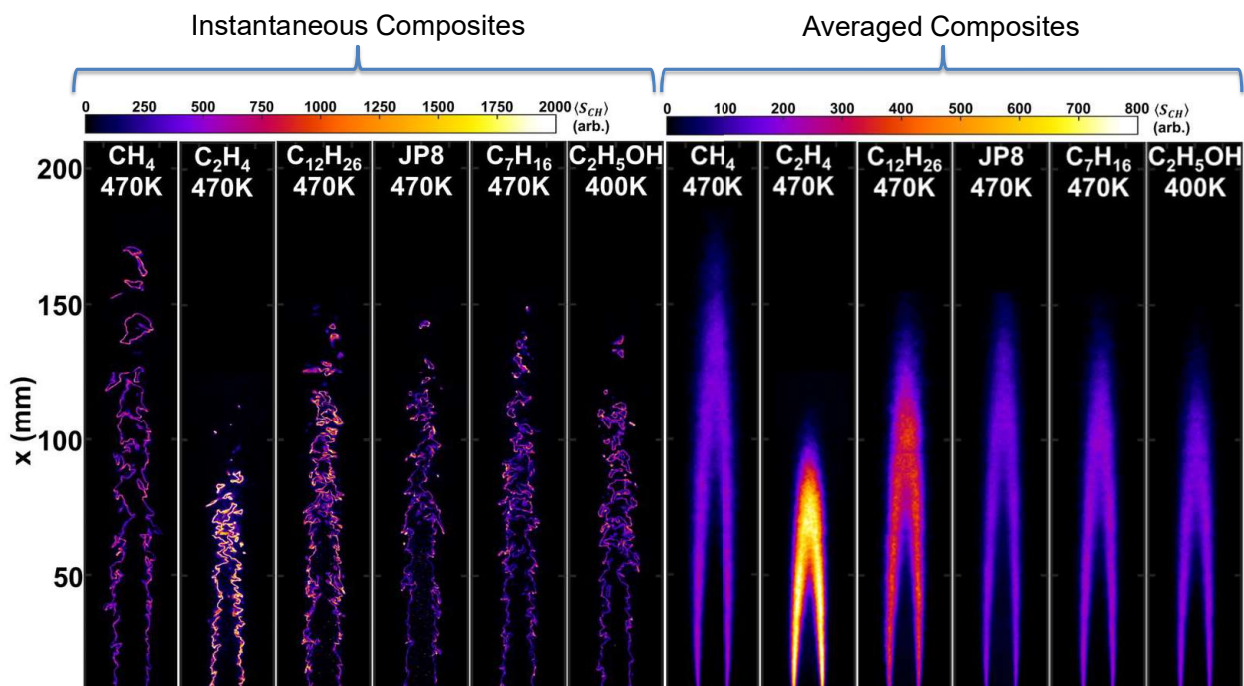
- C-X band excitation method is a resonant technique.
- Mie scattering from fuel droplets can be a source of interference.
- With the low pulse energies of this technique, the Mie scattering is on the same order of magnitude as the fluorescence.
- Compared to other resonant methods, such as Rayleigh or Raman scattering, that require higher pulse energies where particles would result in saturation of the signal, this method is resilient to dilute droplet-laden two-phase flows.
- Thus imaging is capable in a fully-prevaporized flow or even in the presence of a dilute-droplet field

T. McManus, [A. Gandomkar](#), C. Carter, and **P.M Allison**, "Topological imaging of turbulent premixed, prevaporized liquid fuel jet flames using CH (C-X) band PLIF", *Proceedings of the Combustion Institute*. Vol. 38 (2), 2021.



7

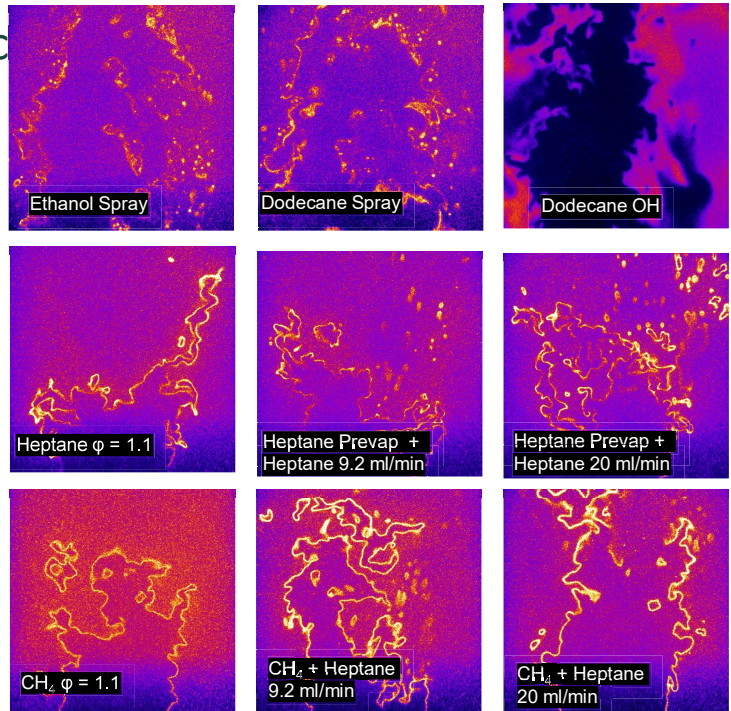
Premixed Jet Flame Structure



8

Spray Imaging – CH PLIF R-bran

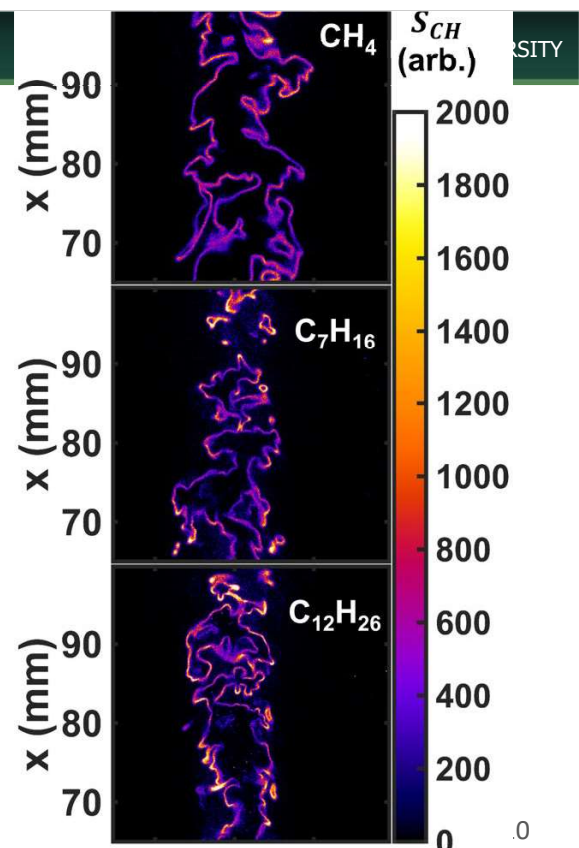
- Initial efforts with pure fuel sprays show sparsely connected CH structures and burning droplets. OH imaging also captures fuel pockets and possible local extinctions.
- Prevaporized, premixed heptane air flames are operated with increasing heptane spray injection. A consistent flame structure is captured with increasing structural complexity and droplet burning in the product stream.
- Premixed methane-air flames are operated with increasing heptane spray injection. The overall flame height is lengthened, droplet penetration is captured, and more local extinctions are observed at the highest injection flow rates.
- Interference-free imaging is capable in a fully-prevaporized flow or even in the presence of a droplet field.



9

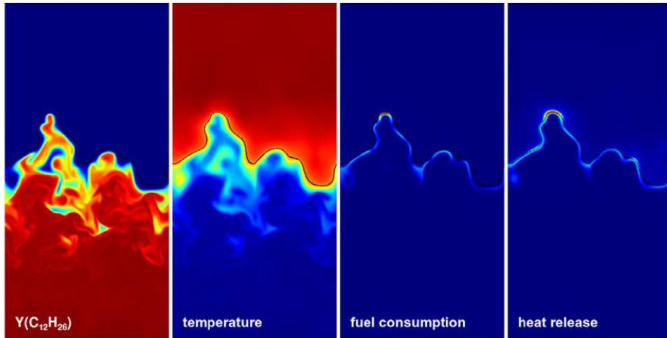
Le & Curvature Effects in Prevap/Premix

- In methane, where *Le* is slightly greater than 1, in rich flames, there is little variation of signal along the imaged reaction layer.
- In rich n-heptane and n-dodecane flames, where *Le* is ~2-4, large signal variation (~20-30%) is observed.**
- Increased signal is seen in regions of high negative curvature, which form pockets/fingers concave to the reactants.
- Decreased signal and local extinction occur in regions of high positive curvature, which are convex into the reactants.



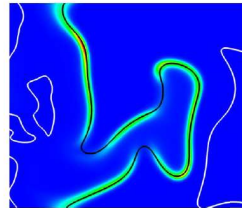
Le & Curvature Effects seen in DNS

- These results have been seen in DNS studies of turbulent, high Ka, n-heptane and n-dodecane flames, where in regions of negative curvature the fuel consumption and heat release rate is significantly elevated.
- Looking into the relation between CH PLIF signal and HRR

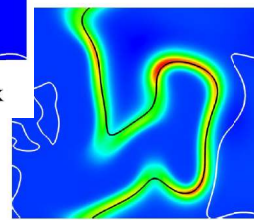


A.J. Aspden, J.B. Bell, M.S. Day, and F.N. Egolfopoulos, Turbulence-flame interactions in lean premixed dodecane flames, Proc. Combust. Inst. 36 (2017) 2005–2016.

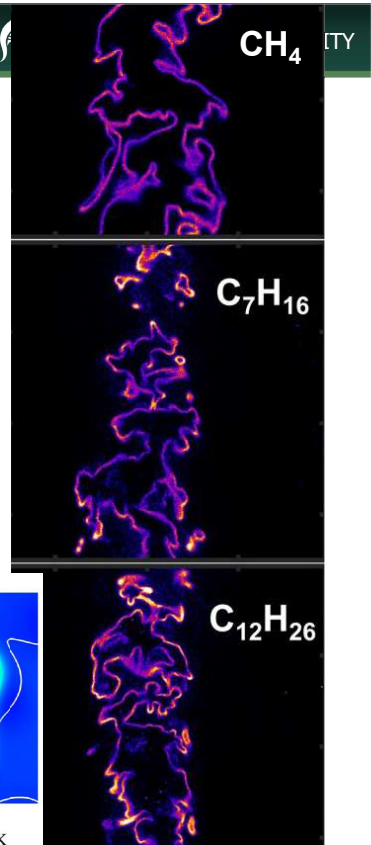
B. Savard, B. Bobbitt, and G. Blanquart, Structure of a high Karlovitz n-C7H16 premixed turbulent flame, Proc. Combust. Inst. 35 (2015) 1377–1384



(d) $\dot{\omega}_{C7H16}$; $T_{peak} = 1240$ K

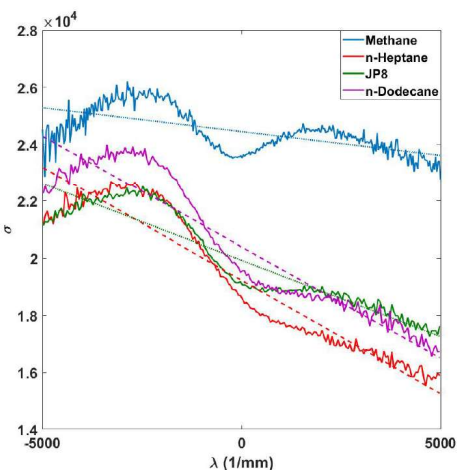


(e) $\dot{\omega}_{H2O}$; $T_{peak} = 1592$ K

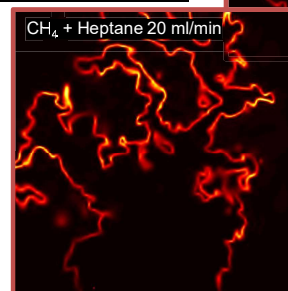
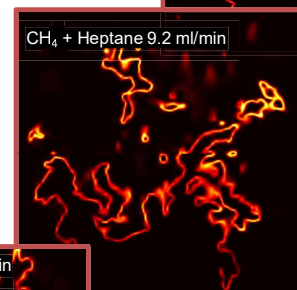
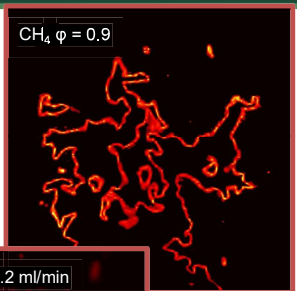


Curvature PDF Results – Signal-Curvature Correlation

- Linear correlation Coefficient and strong R^2 values obtained for liquid case;
- Larger negative slope of linear correlation for n-Dodecane and n-Heptane

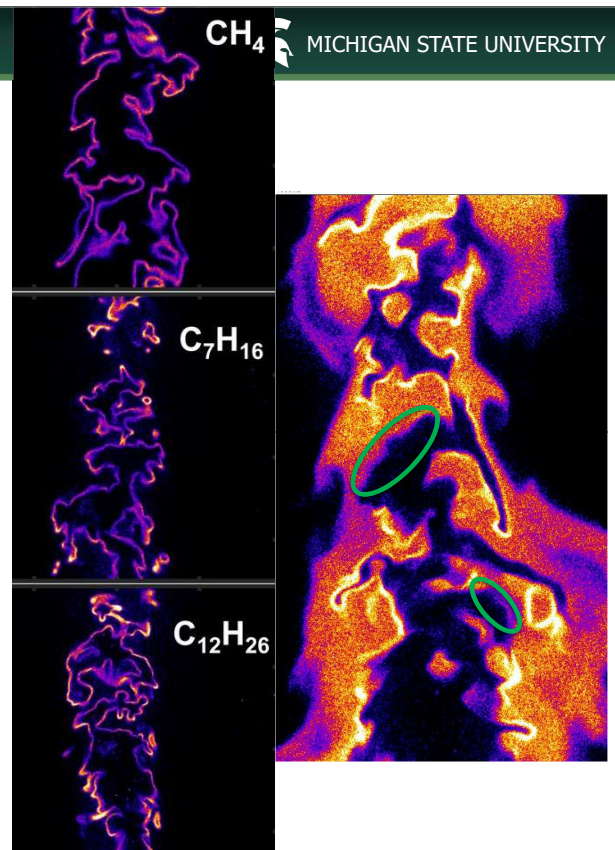


ϕ	Fuel	Coef	R2
0.8	Methane	-0.563	0.317
	n-Heptane	-0.965	0.931
	n-Dodecane	-0.96	0.922
1	Methane	-0.706	0.498
	n-Heptane	-0.935	0.875
	n-Dodecane	-0.95	0.903
1.2	Methane	-0.691	0.478
	n-Heptane	-0.904	0.817
	n-Dodecane	-0.965	0.932



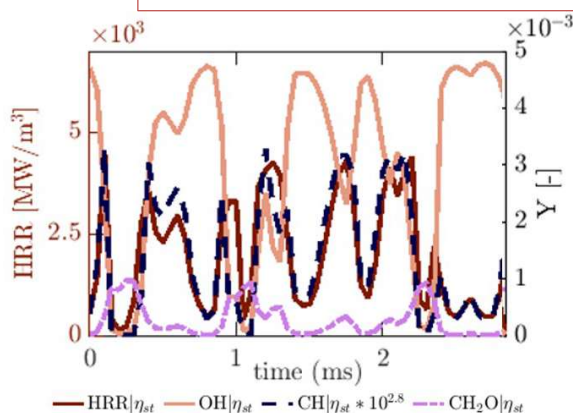
Existential Challenges

- Issues determining sign of curvature: With only the CH layer, there is no orientation provided towards the reactant or product stream
- Edge detection of OH PLIF yields a single sided structure, whereas CH PLIF edge detection yields reactant and product side
- However, OH PLIF alone may provide false “edges” where a local extinction has occurred.
- Non-unity Le effects in the liquid fuels result in what appear to be local extinctions or low signal at positive curvatures. This was not seen in methane or ethylene flames.
- Orientation and edge tracking complicated by severe wrinkling, fragmentation, and local extinction

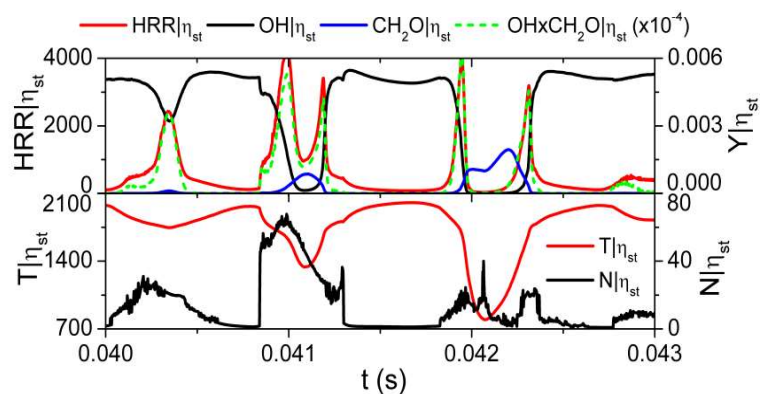


Local Extinction Dynamics

At a local extinction point, there is a temporal lag between the decrease in HRR and OH concentration, but CH concentration tracks



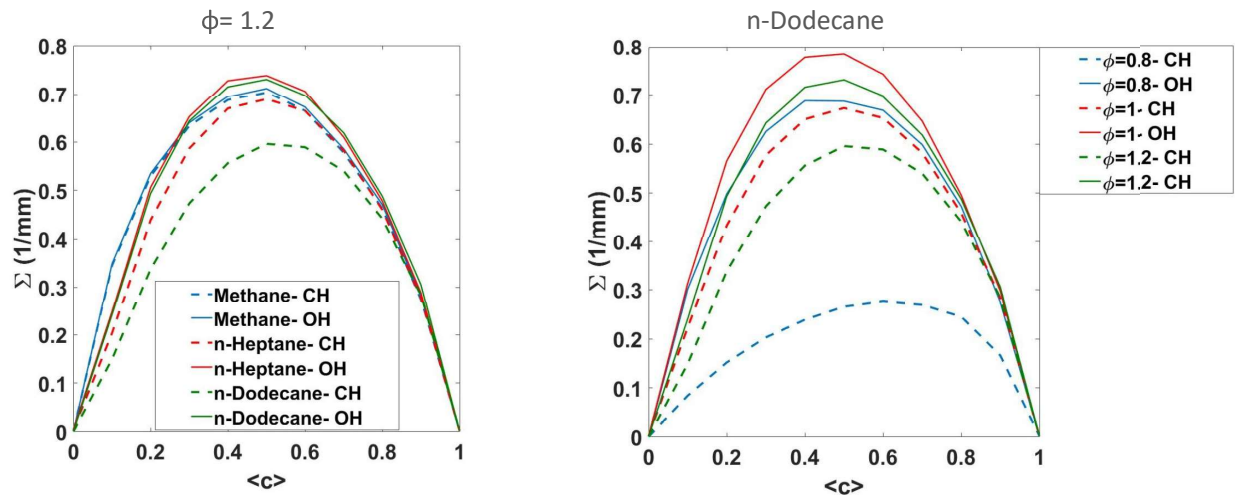
Time evolution of conditional quantities along the stoichiometric mixture fraction indication extinction in Jet-A occur at decreased CH and heat release, and formaldehyde accumulation. Foale, Jenna; Mastorakos, E., Personal Communication, 2021.



Giusti, A., and Mastorakos, E., Detailed Chemistry LES/CMC Simulation of a Swirling Ethanol Spray Flame Approaching Blow-Off, *Proceedings of the Combustion Institute*, 2017, Volume 36, 2625–2632. doi:10.1016/J.PROCI.2016.06.035.

CH and Pseudo-OH FSD comparison: Premix/Prevap

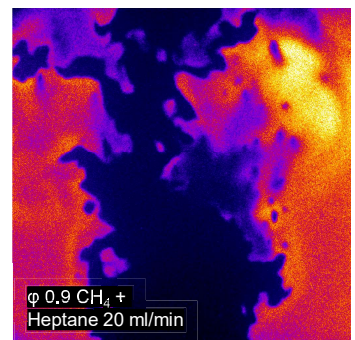
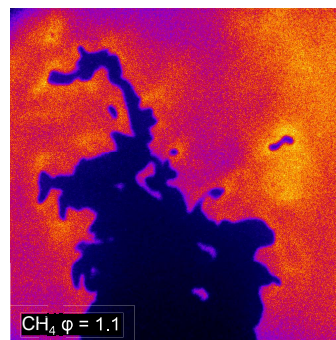
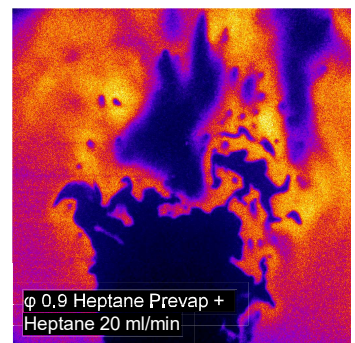
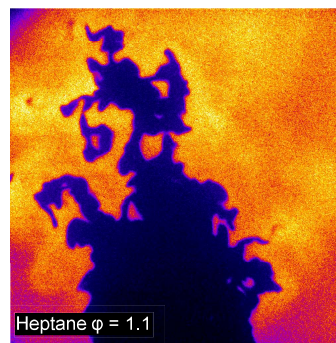
- The results indicate the effect of extinction on FSD reduction at $\Phi = 1.2$ where the PLIF signal and SNR is highest.
- For methane, the difference between CH and pseudo-OH is low which indicates fewer extinctions. While n-dodecane has the largest differences.
- For n-dodecane, there is a significant difference between the CH-based FSD profiles. It may be due to the low CH signal at lean conditions that leads to under-capture of detected edges.



15

Spray Imaging – OH PLIF

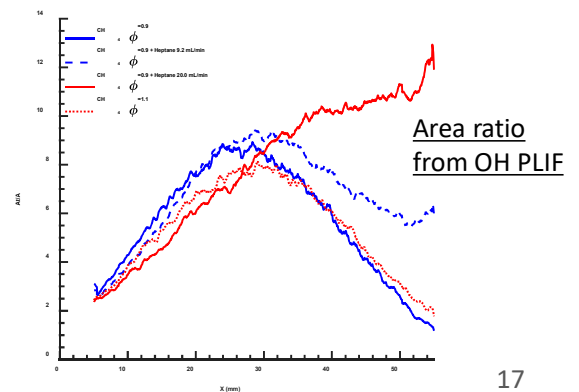
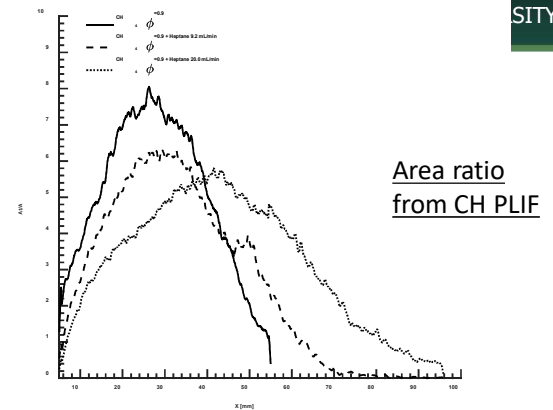
- Spray injection into prevaporized heptane or premixed methane flames results in severe alterations to the observed OH field.
- Large pockets and droplets are captured in the pilot stream with spray injection. This is never observed in single fuel operation and suggests pockets of fuel vapor are the cause.
- The penetration of fuel droplets resulting in local vapor pockets can also lead to local extinction of the flame surface.
- Note that the OH structures of the pure sprays and dual fuel mixtures appear similar despite clear differences in the CH imaging.
- Given that OH PLIF is commonly used for topological studies, accurate flame edge detection is critical. However, edge detection via gradients or thresholding is complicated given vapor pockets.



Turbulent Flame Area Ratio - Spray

- Enhancement of the turbulent flame surface area is observed when spray injection is increased in addition to lengthening of the flame
- While Damköhler hypothesized that the increase in flame surface area is correlated with the increase in turbulent flame speed. It is not clear this explanation is the primary cause attributed here.
- Increased FSD observed with liquid fuel must be tied to fuel effects impacting turbulence-chemistry interactions or droplet interactions.
- However, there are strong differences presented depending on the imaging technique used. Formation of fuel pockets captured by the OH PLIF may be incorrectly identified as flame surface due to difficulty in discernment.
- CH PLIF may provide a more accurate methodology for topological observations in sprays.

$$\left(\frac{A_T}{A_L}\right)_L = \int_{-\infty}^{\infty} \Sigma d\eta$$



17

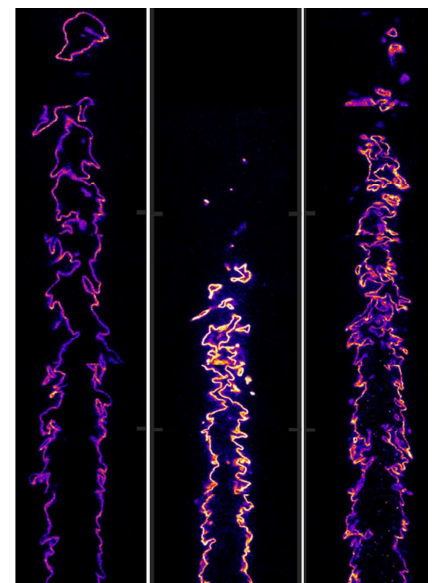


Conclusions

Two “Truths” and One “Lie” -- Two Positives and a Warning

- Interference-free imaging is feasible
- ~~Flame structure is accurately captured and measured~~ with exceptions
- Flame structure can be affected by Le effects

- CH PLIF imaging is possible in prevaporized and dilute fuel sprays with little interference from droplets or PAHs
- Conclusions regarding flame topology may vary depending on the imaging strategy used.
- It appears that local extinction, droplet penetration, and vaporization in the product stream may “trick” OH PLIF analysis; suggesting CH edge tracking is more accurate.
- Non-unity Le effects in the liquid fuels result in what appear to be local extinctions or low signal at positive curvatures. This is not seen in methane or ethylene flames.

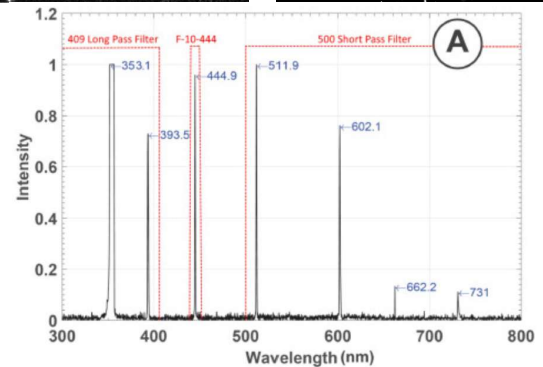
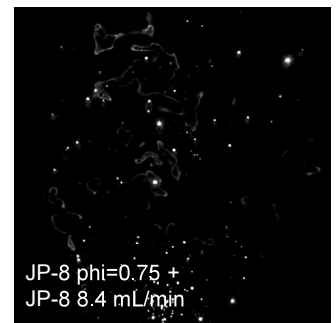
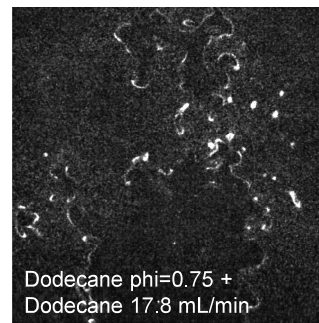


Questions: Patton Allison alliso63@egr.msu.edu

18

CH PLIF Challenges

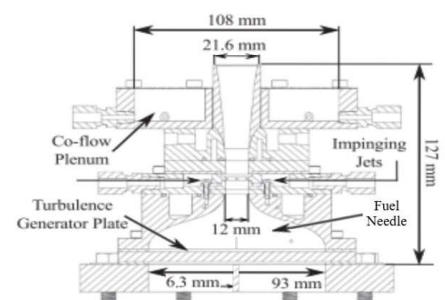
- Strong Lewis number effects alter signal levels depending curvature. Can also lead to flame quenching in negative curvature.
- Strong Raman scattering observed from larger droplets (similar to previous Masri work).
- Low PLIF signal for $\phi < 0.8$ and > 1.5 due to low CH number density
- Pure sprays generate sparse/distributed burning around droplets. No coherent CH layer.



Singh, G. Juddoo, M., Dunn, M.J., Masri, A.R., "Heat release zones in turbulent, moderately dense spray flames of ethanol and biodiesel," *Combust. Flame*, Vol 220, pg 298-311, 2020.

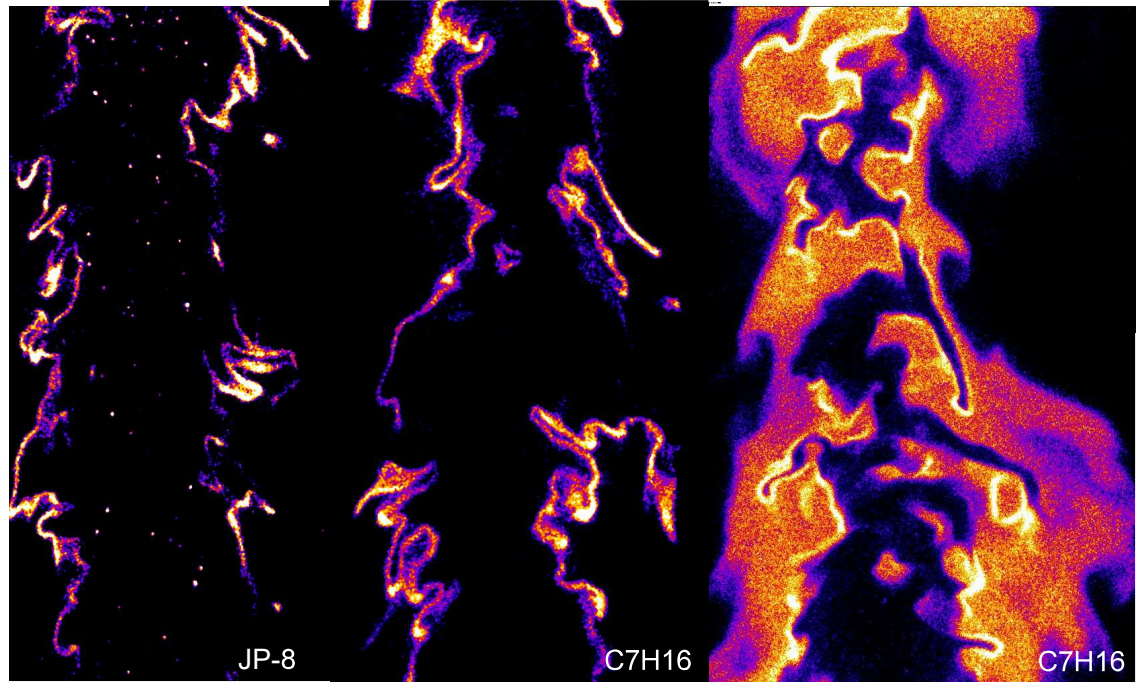
Operating Conditions

- Hi-Pilot burner modified for spray injection: 108 mm methane-air pilot ($\phi = 1$), Hypodermic needle (ID: 260 microns) + syringe pump, 3.2 kW inline heater for pre-vaporized fuel-air mixtures.
- 10 Hz imaging of CH and OH fluorescence emission near 311 nm, Semrock AFRL-0002 and UG-5 filter. CH PLIF 1-2mJ/pulse; OH 3-4mJ/pulse
- Imaging resolution 49 microns/pixel. 50 x 50 mm FOV
- Hi-Pilot Case 2 conditions – 212 slpm air, $Re_T \sim 1400$, $Re \sim 25,000$, $T = 385K$
- Premixed, prevaporized n-heptane, n-dodecane, or JP-8, $\phi = 0.9$ or 1.1
- Premixed, prevaporized fuel-air ($\phi = 0.75$) + liquid fuel injection (8-20 ml/min) into premixed flame; Global $\phi = 1.1-1.5$



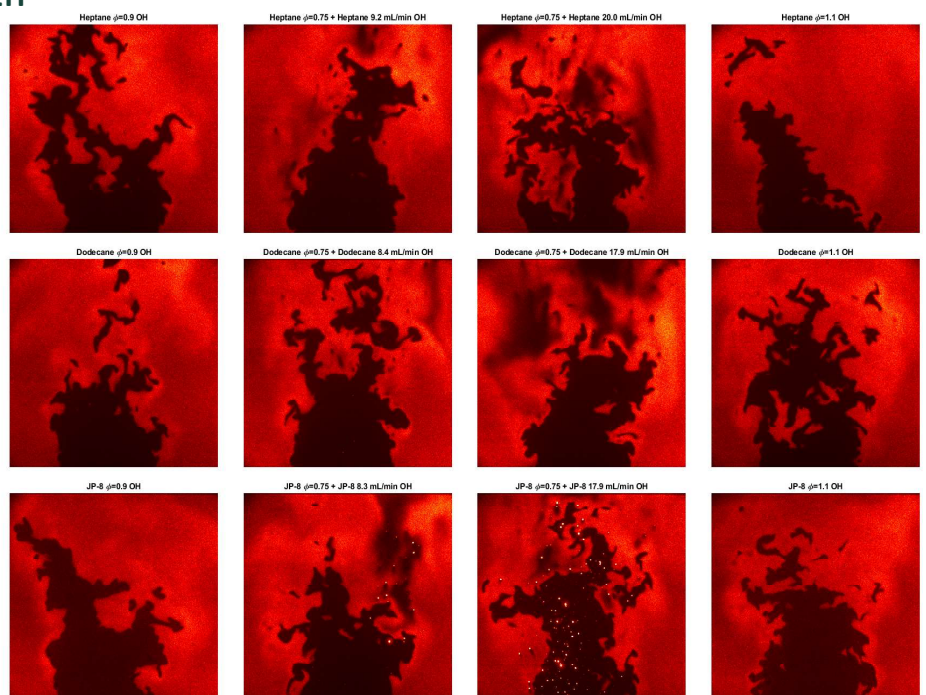
Extinction Samples - Extrema

- In simultaneous CH and OH PLIF images in heptane flames, it is possible to visualize regions of local CH extinction where OH is still present.
- If only OH PLIF imaging is performed, clear evidence of local extinction would not be possible.



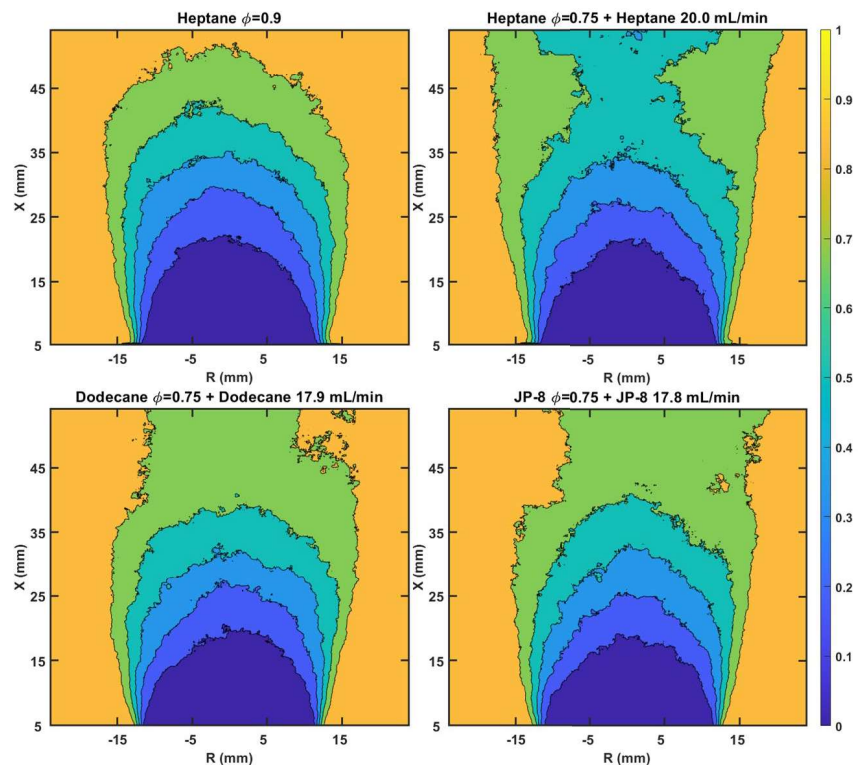
Imaging Examples – OH PLIF

- Flame surface processing requires detailed handling of edge detection.
- Droplets and fuel vapor pockets observed in cases with spray.
 - It is likely that this causes OH to overestimate flame surface density.



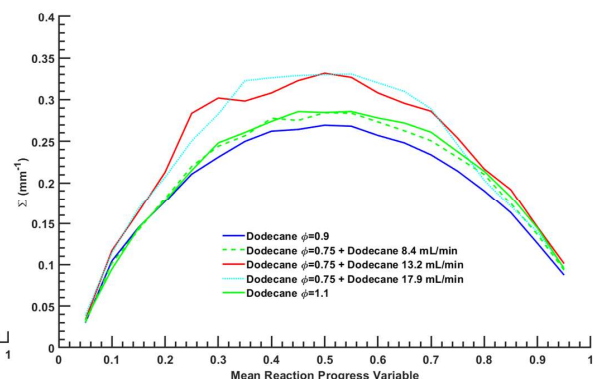
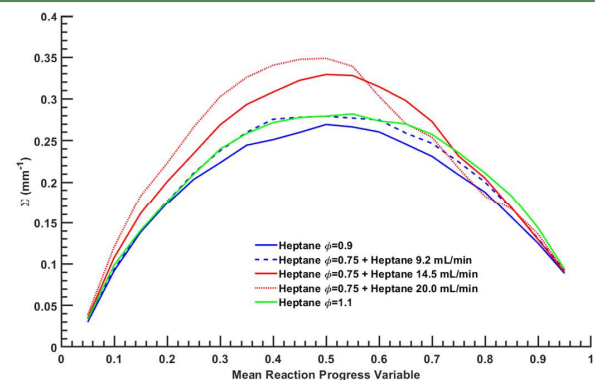
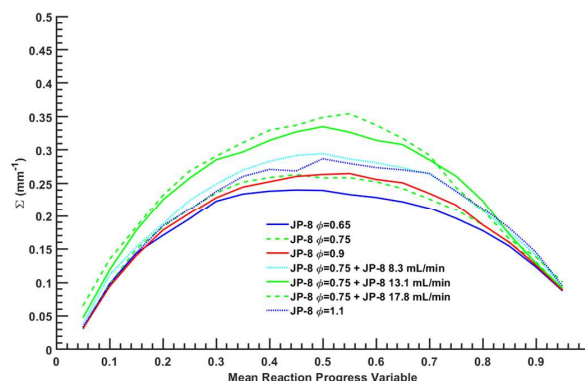
Reaction Progress Variable

- In flames with high spray loadings, local extinction occurs with droplet interaction causing flame tip to open
- This is observed more frequently in flames with lower C-number pre-vaporized/gaseous fuels.
- Flame brush size is comparable.



Flame Surface Density vs. Reaction Progress Variable

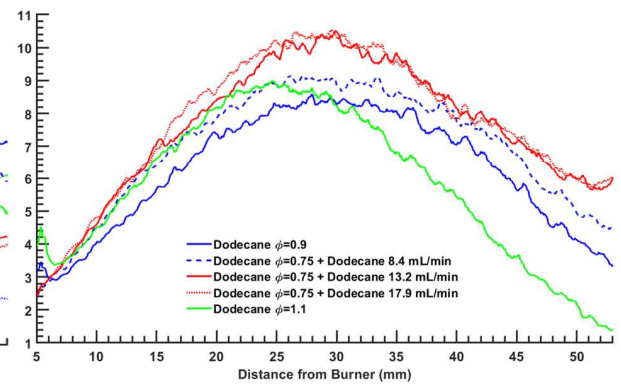
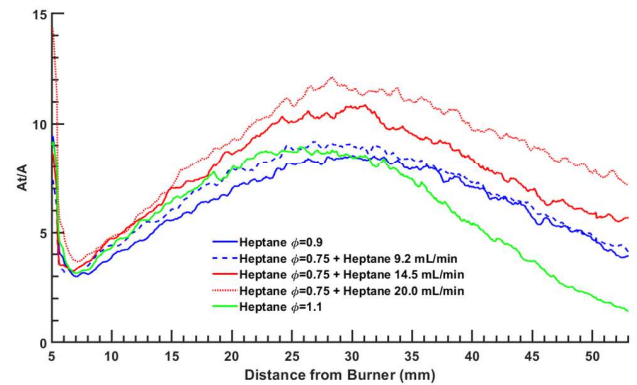
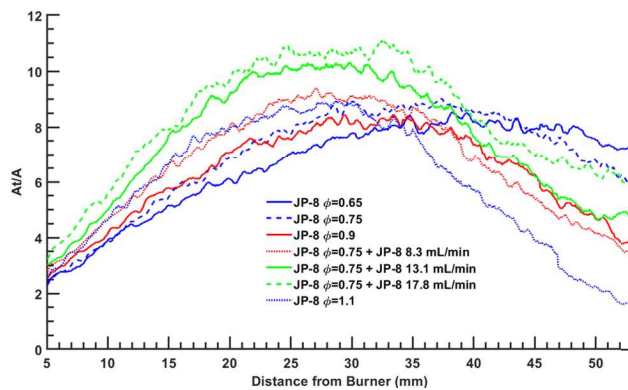
- Higher spray loading leads to increased surface wrinkling across progress variable space.
- Fuel vapor pockets may lead to overestimation of FSD



Turbulent Area Ratio

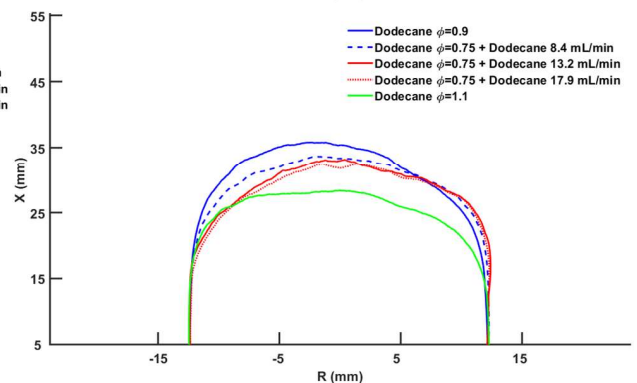
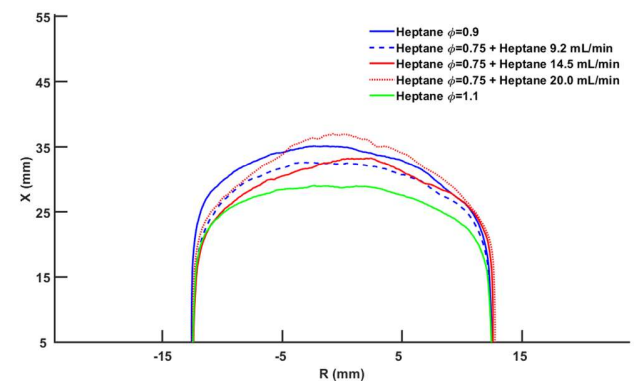
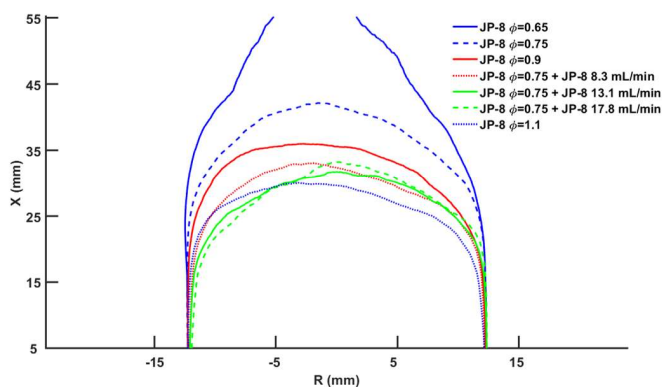
- Higher spray loading leads to increased surface wrinkling along flame axis

$$\left(\frac{A_T}{A_L}\right)_L = \int_{-\infty}^{\infty} \Sigma d\eta$$



Flame Height

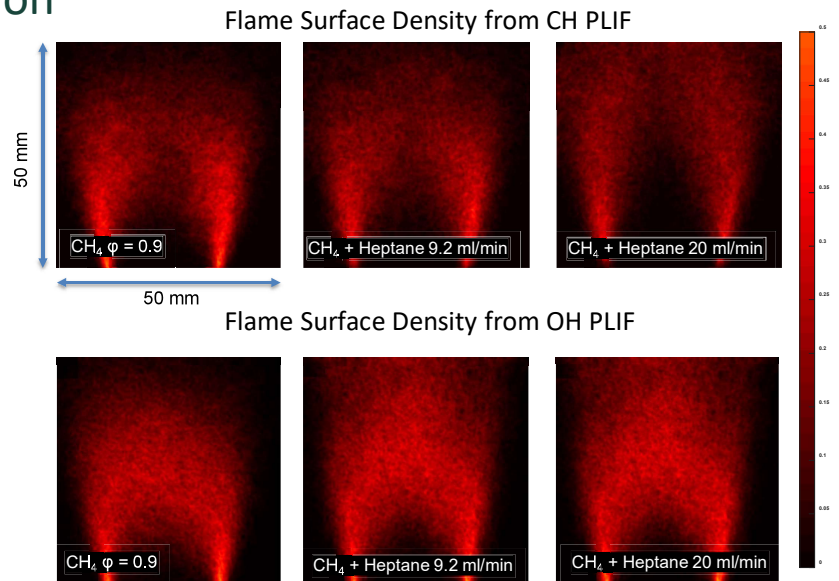
- Premixed prevaporized flame heights bracket spray data, indicating partially-premixed mixture ratios between 0.9-1.1



Flame Surface Density Variation

- Flame surface densities are calculated from flame edge detection algorithms applied to CH and OH imaging
- Similar FSD values are locally calculated given both imaging techniques.
- The flame brush increases in length, moving out of the FOV as the spray injection increases
- However, higher FSD is observed along the centerline at lower axial locations in the OH imaging

$$\Sigma = \lim_{\Delta x \rightarrow 0} \frac{\bar{L}_f}{\Delta x^2}$$



27

Conclusions and Next Steps

- Conclusions
 - CH PLIF can be performed with minimal droplet/fuel PLIF interference, but is limited by sparse droplet burning and lean equivalence ratios
 - CH postprocessing techniques need further refinement to identify flame surfaces and statistics.
 - OH PLIF may overestimate flame surface statistics due to droplets and fuel vapor pockets.
- Next Steps
 - Perform similar measurements on flames at and near global extinction to investigate the relationship of sprays and extinctions.
 - Further develop CH PLIF post processing in order to evaluate heavy fuel surface statistics, such as dodecane and JP-8.

Machine Learning Techniques for Manifold-based Models

Bruce A. Perry, Malik Hassanaly, Nicholas Wimer, Marc T. Henry de Frahan, Michael E. Mueller & Shashank Yellapantula

National Renewable Energy Laboratory (NREL), Golden, CO, USA

Photo from iStock-627281636

1

LES Modeling Challenges

For LES (or RANS), model filtered/averaged thermochemical quantities $\tilde{\phi}$ using a subfilter PDF \tilde{P} :

Any quantity needed for closure: $\dot{\omega}_j, \rho, \tilde{D}, \tilde{\mu}, \tilde{Y}_j, \tilde{T}, \dots$ $\longrightarrow \tilde{\phi}(x_k, t) = \int \underbrace{\phi(Y_j, T, p)}_{\text{Detailed chemical mechanisms: "Easy" to model, but high-dimensional and expensive to evaluate}} \underbrace{\tilde{P}(Y_j, T, p)}_{\text{Subfilter PDF: High-dimensional, hard to model, expensive to solve for}} dY_j dT dp$

Reduce computational cost by projecting the thermochemical state onto a low-dimensional manifold $(Y_k, T, p) \rightarrow \xi_i$ with $N_\xi \ll N_S$:

$\tilde{\phi}(x_k, t) = \int \underbrace{\phi(\xi_i)}_{\text{Manifold model: Harder to model, regime sensitive (Modeling Challenge 2)}} \underbrace{\tilde{P}(\xi_i; \tilde{\xi}_i, \tilde{\xi}_{i,var})}_{\text{Subfilter PDF: Low-dimensional so model development is tractable (Modeling Challenge 3)}} d\xi_i$ \longleftarrow Parameters for low-dimensional manifold: e.g., $\xi_i^* = W_{ij} Y_j = (Z, C, \dots), p, \tilde{\chi}_c$

Which parameters to use? How to provide closure (if needed)? **(Modeling Challenge 1)**

NREL | 2

2

Targeted Regression-based Closures

One approach: use ML models to *fill in the gaps* of ad hoc or poorly performing physical models

Progress Variable Dissipation Rate Model

$$\tilde{\chi}_{C,sgs} = 2D_C|\nabla\tilde{C}|^2 - 2\tilde{D}_C|\nabla\tilde{C}|^2$$

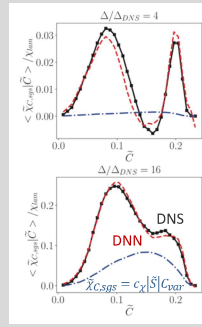
- Sink term in C_{var} equation

Approach [1]: use a deep neural network to regress $\tilde{\chi}_{C,sgs}$ against known physically important inputs:

$$\tilde{\chi}_{C,sgs} = \text{DNN}(\tilde{C}, C_{var}, \tilde{D}_C, 2D_C|\nabla\tilde{C}|^2, |\nabla\tilde{C}|^2, \alpha, \beta, \gamma, \dots)$$

- Data from filtered DNS [2,3] of planar premixed flames at varied Ka

DNN provides robust predictions across conditions/fuels

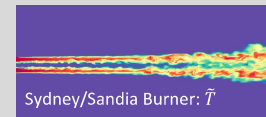


Subfilter PDF Models

$$\tilde{P}(Z_1, Z_2; \tilde{Z}_1, \tilde{Z}_2, \dots)$$

Approach [4]: use a deep neural network or other method to regress \tilde{P} based on scalar mixing DNS [5]

Application: three-stream mixing closure



Sydney/Sandia Burner: \tilde{T}

$$\tilde{\phi}(x_k, t) = \int \phi(\xi_i) \tilde{P}(\xi_i; \tilde{\xi}_i, \tilde{\xi}_{i,var}) d\xi_i$$

Manifold model:
Harder to model, regime sensitive
(Modeling Challenge 2)

Subfilter PDF:
Low-dimensional so model
development is tractable
(Modeling Challenge 3)

Parameters for low-dimensional manifold:
e.g., $\xi_i^* = W_{ij}Y_j = (Z, C, \dots), p, \tilde{\chi}_C$

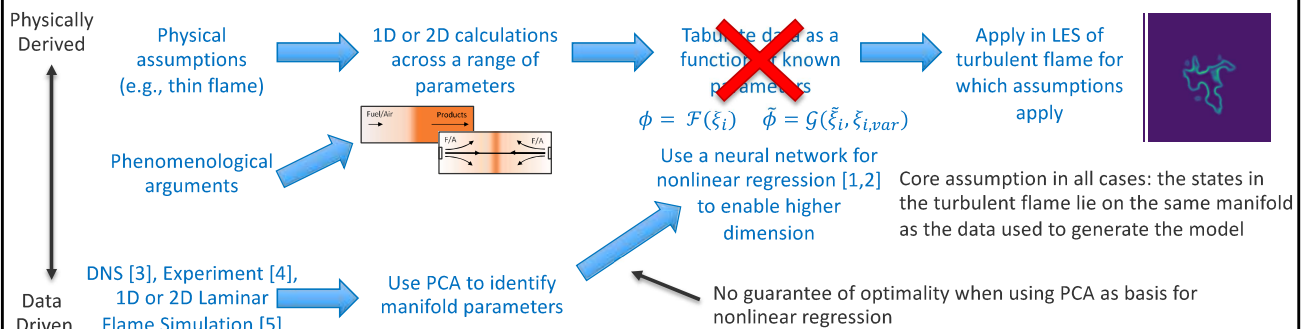
Which parameters to use?
How to provide closure (if
needed)?
(Modeling Challenge 1)

NREL | 3

3

Machine Learning for Manifold Model Definition

Physically-derived manifold models (FPV, FGM, FPI, etc.): use **data** from computations determined by applying assumptions to the governing equations



Co-optimized Machine Learned Manifolds Approach: Expand neural network used for nonlinear mapping to span entire process, range of different input data/assumptions

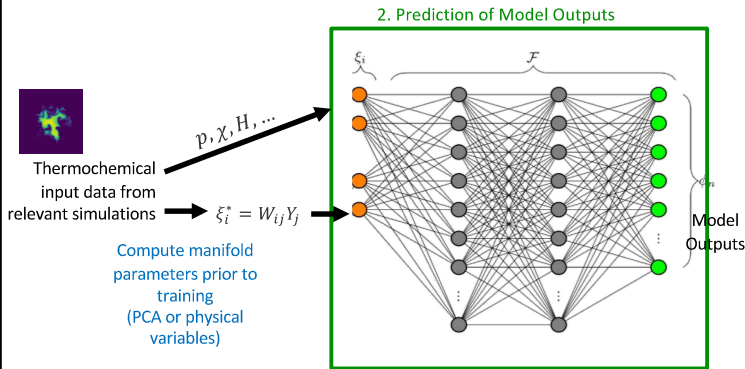
[1] A. Kempf, F. Flemming, J. Janicka. Proc. Combust. Inst. 30 (2005) 557–565.
[2] M. Ihme, C. Schmitt, H. Pitsch. Proc. Combust. Inst. 32 (2009) 1527–1535.
[3] J. C. Sutherland, A. Parente. Proc. Combust. Inst. 32 (2009) 1563–1570.

[4] D. K. Dalakoti, A. Wehrfritz, B. Savard, M. S. Day, J. B. Bell, E. R. Hawkes. Proc. Combust. Inst. 38 (2021) 2701–2709.
[5] H. Mirgolbabaei, T. Echekki. Combust. Flame 162 (2015) 1650–1652.

NREL | 4

4

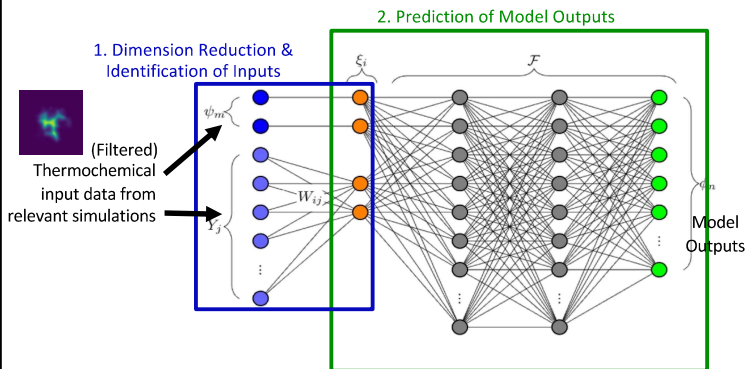
Combining Steps: Start with Manifold + NN



Single neural network structure optimizes model functional form

5

Combining Steps: Manifold Co-optimization



Single neural network structure optimizes functional form, model inputs

Key Features:

- Auto-encoder-like structure, building on prior works [1]
- ● nodes correspond to manifold parameters
- Linear manifold definitions, $\xi_i = W_{ij} Y_j$

$$\rho \frac{\partial Y_j}{\partial t} + \rho u_k \frac{\partial Y_j}{\partial x_k} = \frac{\partial}{\partial x_k} \left(\rho D \frac{\partial Y_j}{\partial x_k} \right) + \dot{\omega}_j$$

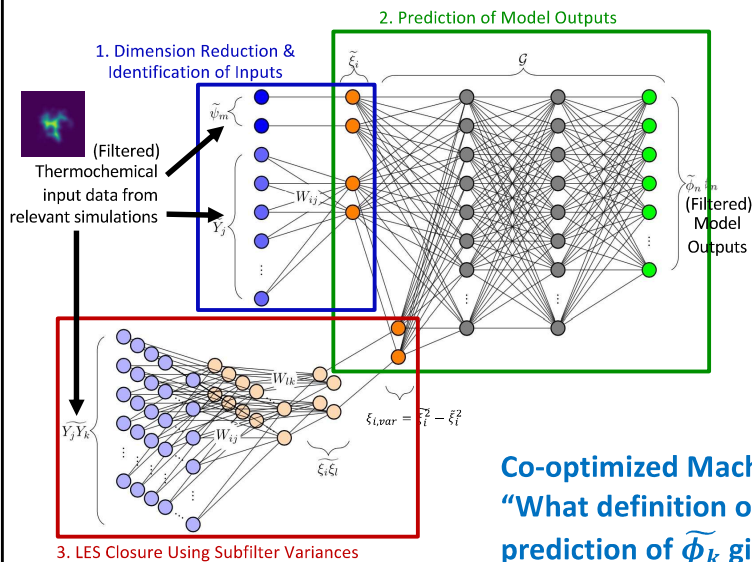
$$\rho \frac{\partial \xi_i}{\partial t} + \rho u_k \frac{\partial \xi_i}{\partial x_k} = \frac{\partial}{\partial x_k} \left(\rho D \frac{\partial \xi_i}{\partial x_k} \right) + \dot{\omega}_i$$

- Sparsity in manifold definition

$$Loss = \|\phi_{true} - \phi_{pred}\|_2^2 + \alpha \frac{\|W_{ij}\|_1}{\|W_{ij}\|_2}$$

6

Combining Steps: Manifold Co-optimization w/Closure



Single neural network structure optimizes functional form, model inputs, and subfilter closure

For LES closure, train using filtered data with additional inputs:

$$\tilde{\phi}_k = \int \phi_k(\xi_i) \tilde{P}(\xi_i, \tilde{\xi}_i, \xi_{i,var}) d\xi_i \rightarrow \tilde{\phi}_k = \mathcal{G}(\tilde{\xi}_i, \xi_{i,var})$$

Directly model this function rather than using PDF "middleman"

Similar in spirit to approaches like F-TACLES and Multi-Filtered FGM.

Co-optimized Machine Learned Manifolds [1]:
"What definition of ξ_i allows for the optimal prediction of $\tilde{\phi}_k$ given $\tilde{\xi}_i, \xi_{i,var}$?"

[1] B.A. Perry, M.T. Henry de Frahan, S. Yellapantula. Combustion and Flame 244C (2022) 112286

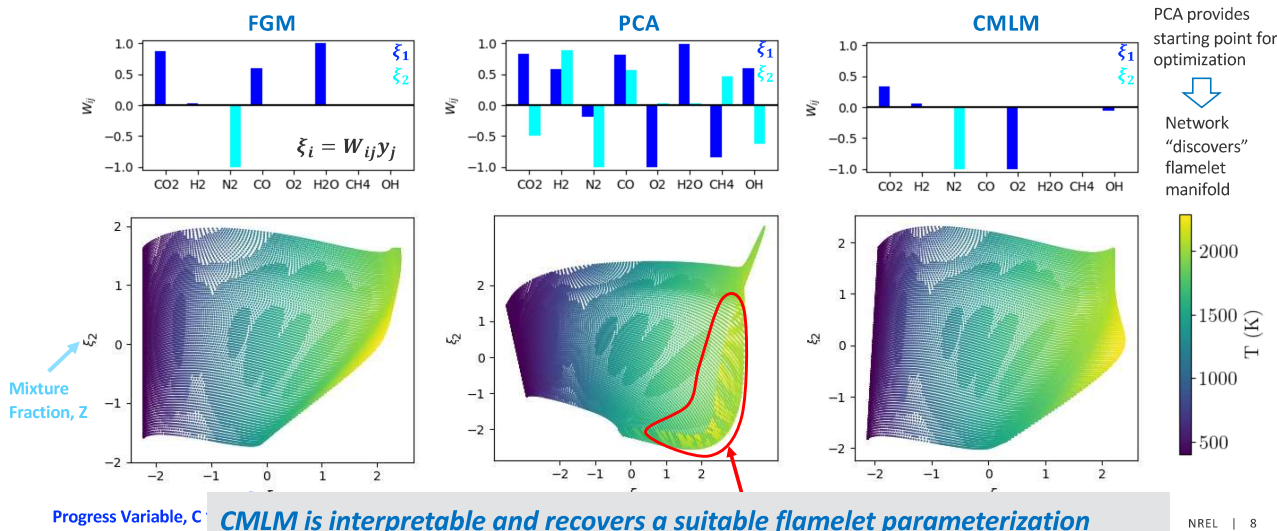
NREL | 7

7

CMLM Interpretation: Exploratory Tool



1D Premixed Flames, CH₄ (DRM19 mech.), $\phi = 0.5-1.5$, 1 atm, $T_0 = 400$ K



NREL | 8

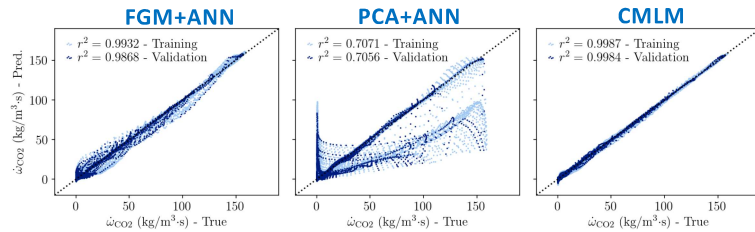
8

CMLM Interpretation: Enhanced Physical Model



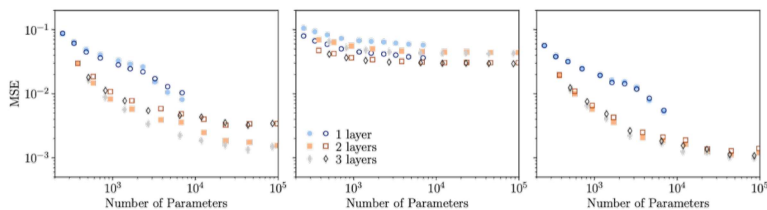
1D Premixed Flames, CH₄ (DRM19 mech.), $\phi = 0.5-1.5$, 1 atm, $T_0 = 400-1100$ K

Comparison of true and predicted values across all data points



Effect of network structure:

- CMLM has lowest error for any network structure (important for forward evaluation efficiency)
- Error plateaus for PCA due to non-uniqueness

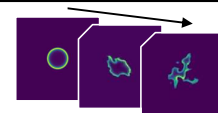


CMLM can improve accuracy of physics-based models using the same data/assumptions
Obtain insight from opening neural network "black box"

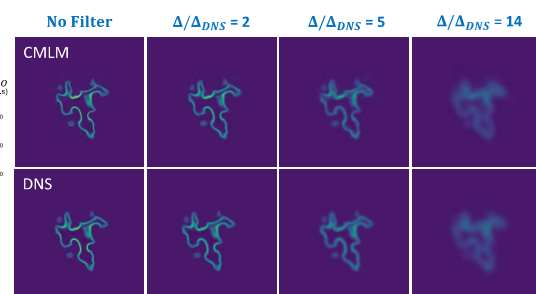
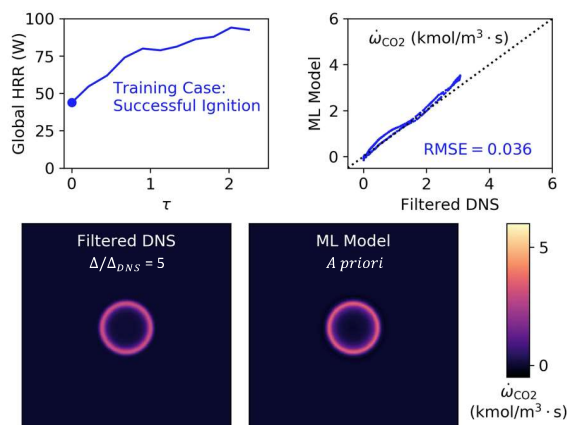
NREL | 9

9

CMLM Interpretation: Data-Driven Model

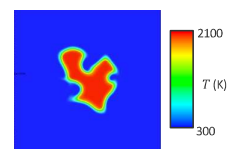


Jet-A hot spot in isotropic turbulence DNS [1] (Case D, $\phi = 1.0$) \rightarrow (Case B, $\phi = 1.0$)



In progress: A posteriori model testing for 2D pseudoturbulent version of this case [2]

Goal: train model entirely on 2D data but apply to 3D case

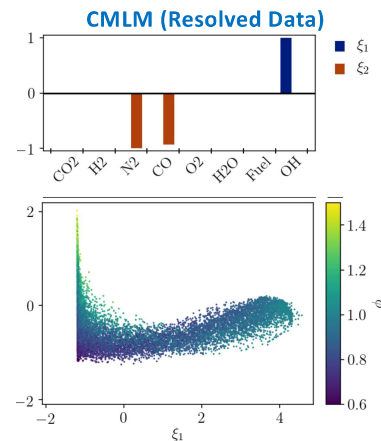
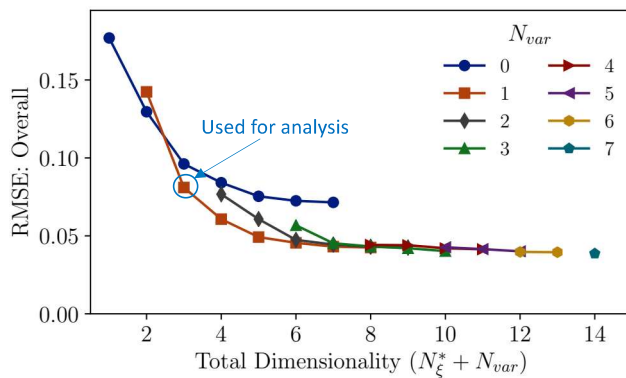
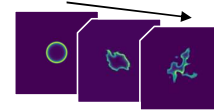


[1] A. Krisman, P. Meagher, X. Zhao, J.-W. Park, T. Lu, J. H. Chen. Combustion and Flame, 225 (2021) 349–363.
[2] B.A. Perry, K. Eiden, M.T. Henry de Frahan, S. Yellpantula, M. Day, Poster #1P014

NREL | 10

10

CMLM Interpretation: Exploratory Tool

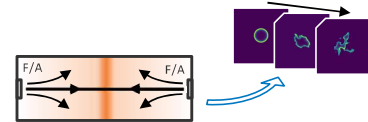


- Only one variance required for filtered closure (analogous to many flamelet-like models)
- Manifold parameters encode reaction progress and differential diffusion effects

NREL | 11

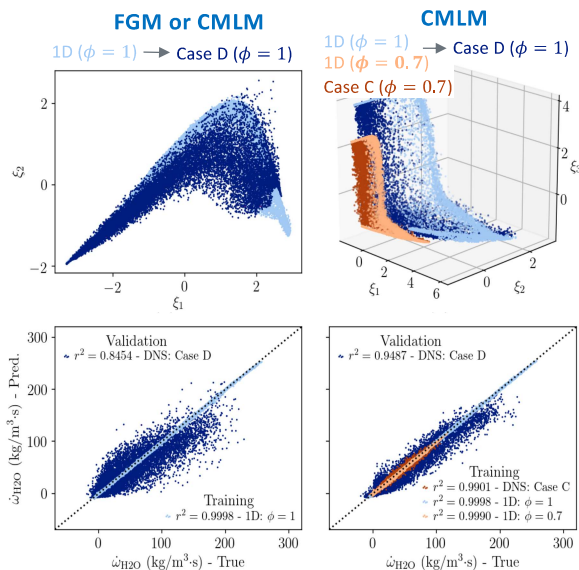
11

CMLM Interpretation: Hybrid Model



- In practice, DNS data is available for very limited conditions
- FGM: Apply data from 1D flames to model turbulent flame
- Challenge: thermochemical states in turbulent flame don't match 1D flames
- CMLM: Combine 1D flame data with DNS data at different conditions (equivalence ratio)

CMLM can combine multi-fidelity data, essentially resulting in "data-augmented" FGM



NREL | 12

12

ML for Manifold Models: Conclusions

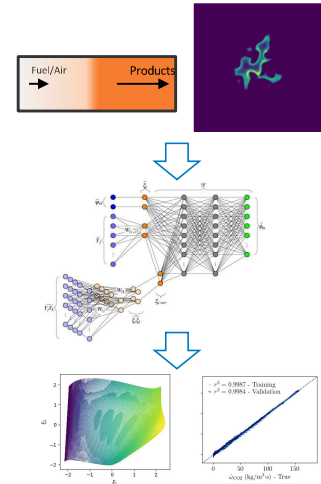
Manifold-based models lie on a continuum between being physically-derived and being based entirely on data

The proposed CMLM approach integrates three aspects of manifold-based modeling (manifold definition, functional form, and subfilter closure) into a single neural network. Depending on the data supplied, it can span the continuum between physics and data:

- Recovers and improves upon flamelet manifold parameterization
- Can improve efficiency of models generated from DNS data relative to PCA
- Allows for integration of different data types for “data-augmented” modeling
- Can serve as an exploratory tool to learn about potential model inputs

Other thoughts on applying ML in manifold models for combustion

- Tailor method to problem, not the other way around: encode desired physics in the model structure
- Can gain insight by opening the “black box” for neural networks
- **There is such a thing as too much data!**

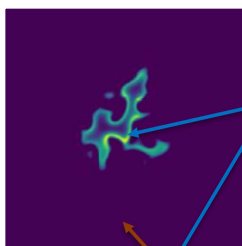


NREL | 13

13

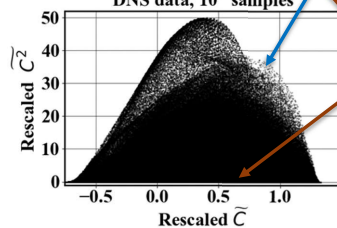
Data Down Sampling

Jet-A Ignition
Kernel DNS [1]
4 Case
28 species
832³ Grid
100 Snapshots
~20 TB



Rare points are not discarded

Planar Premixed Flame [2]
DNS data, 10⁷ samples



Prune redundant data points

Big Data challenges:

- Difficult to store, share, and analyze
- Desire to maintain control over data
- Very large N ($\sim 10^{12}$), moderately large D (~ 100)
- Rare data points re the most important (reaction zones, ignition kernels, etc); many data points are redundant

Especially important for combustion

Objective:

- Create small “summary” data sets that represent the diversity of the full data set without fully replicating it
- Reduce N (data selection) rather than D (compression/dimension reduction): avoid information loss

Strategy:

- Efficient and accurate representation of data by uniformly covering I/O feature space (phase space)
- To achieve this, sample with probability inversely related to density of data in feature space

[1] A. Krisman, P. Meagher, X. Zhao, J.-W. Park, T. Lu, J. H. Chen. Combustion and Flame, 225 (2021) 349–363.
[2] S. Lapointe, B. Savard, G. Blanguant. Combustion and Flame 162 (2015) 3341–3355.

14

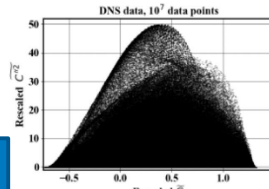
Phase Space Sampling: Approach



<https://github.com/NREL/Phase-space-sampling>

Normalizing flows: Neural Network-based method for estimating $p(x)$

- Suitable for high-dimensional data
- Train using small fraction of data



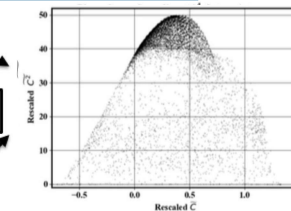
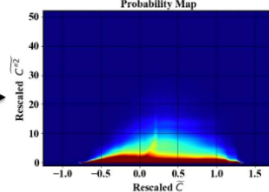
Accept each datapoint with a sampling probability

$$s(x) = \min\left(\frac{c}{p(x)}, 1\right)$$

Step 1

Step 2

Step 1 correction



Very computationally efficient:
Only 2 forward evaluations needed on entire data set

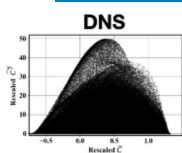
Hassanally, M., Perry, B. A., Mueller, M. E., & Yellapantula, S. (2021). Uniform-in-Phase-Space Data Selection with Iterative Normalizing Flows. *arXiv preprint arXiv:2112.15446*.

15

Phase Space Sampling: Performance



<https://github.com/NREL/Phase-space-sampling>

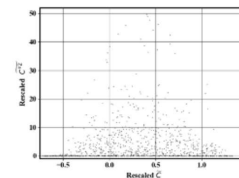
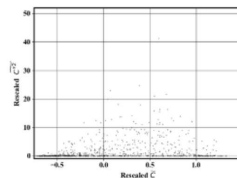
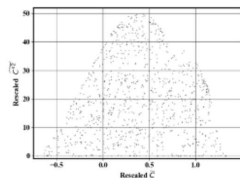


Phase Space Sampling

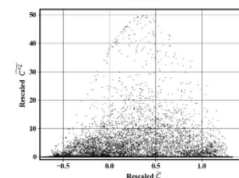
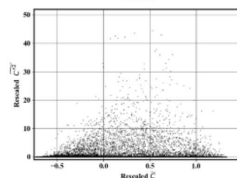
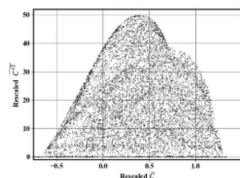
Random Sampling

K-means Stratified Sampling [1,2]

$n=10^3$



$n=10^4$



[1] S. Yellapantula, B. A. Perry, R. W. Grout. *Proceedings of the Combustion Institute* 38 (2020) 2929-2938.
[2] H.-T. Nguyen, P. Domingo, L. Vervisch, P.-D. Nguyen. *Energy and AI* 5 2021 100082

16

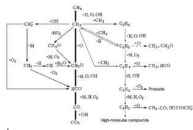
Phase Space Sampling: Mechanism Reduction

“Flame Chemistry People”

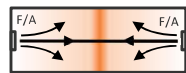
Molecular scale calculations

DFT

Experimental rate measurements



Chemical mechanism
Thermodynamic properties
Rate parameters



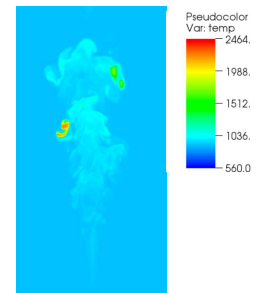
Validation & Reduction:
Data-driven
Limited Conditions
0D and 1D Configurations

Chemical Mechanism



State information
from CFD for
validation

“TNF/PTF People”



Apply mechanisms in complex turbulent configurations that may lead to significantly different conditions than 0D/1D validation

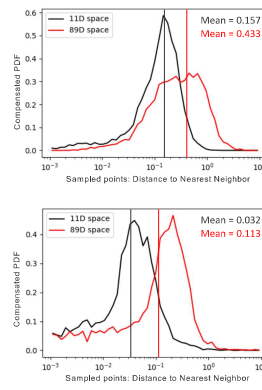
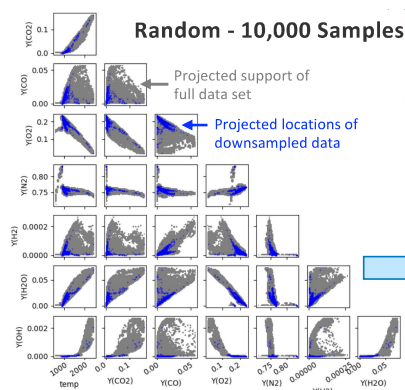
- Collaboration w/ W. Green (MIT) [1]: Assess validity of an 89-species *n*-heptane skeletal mechanism in a turbulent flame
- **Challenge:** Mechanism analysis can only be run for a limited number of points. Need to extract $O(10^3)$ states out of $O(10^8)$ in turbulent flame, focused on the small reacting regions.

[1] H.-W. Pang, M. Hassanali, B.A. Perry, M. Day, W.H. Green. Poster #3P032

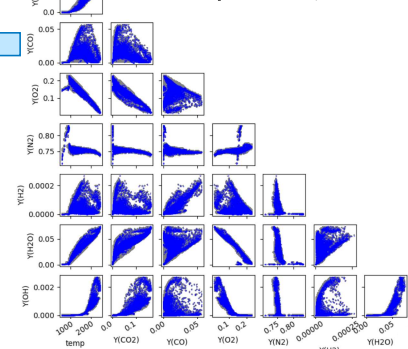
NREL | 17

17

Phase Space Sampling: Mechanism Reduction



Phase-Space – 10,000 Samples



Solution: use Uniform-in-Phase-Space sampling tool [1] developed for training ML models

- Points are sampled w/likelihood inversely proportional to density map estimated using iterative normalizing flows
- Sampled points represent diversity of states in full data set, eliminate redundancy
- 1,000 representative points provided to chemistry modeling group for further analysis

NREL | 18

18



Thank You

www.nrel.gov

This work was authored by the National Renewable Energy Laboratory, operated by Alliance for Sustainable Energy, LLC, for the U.S. Department of Energy (DOE) under Contract No. DE-AC36-08GO28308. Funding provided by Department of Energy Office of Science and Office of Energy Efficiency and Renewable Energy Vehicle Technologies Office. The views expressed in the article do not necessarily represent the views of the DOE or the U.S. Government. The U.S. Government retains and the publisher, by accepting the article for publication, acknowledges that the U.S. Government retains a nonexclusive, paid-up, irrevocable, worldwide license to publish or reproduce the published form of this work, or allow others to do so, for U.S. Government purposes.

Photo from iStock-627281636



Summary: Combustion Machine Learning: Principles, Progress, Perspective

Matthias Ihme, Stanford University, mihme@stanford.edu

With the increasing interest in machine learning (ML), this session was organized to provide the TNF community with an overview of ML techniques and their application to combustion. While ML has had a presence in various areas related to combustion, recent advances in ML methods, computational resources, and data have contributed to a substantial resurgence in expanding the application of ML method to combustion (CombML). This session reviewed these advances with the specific goal of connecting the broad field of ML to TNF/PTF-related problems. To this end, this session solicited and reviewed contributions from the TNF research community, resulting in a total of eleven contributions.

The session started with providing background on CombML, identified opportunities for utilizing data generated within the combustion community (from measurements, simulations, and sensors) for applications to data-driven learning methods, and identified challenges in adopting ML methods for combustion. These challenges are primarily related to well-established foundational knowledge, physical principles, as well as dealing with spatio-temporal scales, physical coupling, and the chemical complexity of turbulent combustion. Another issue of equal importance is the need for data, which is limited to specific operating conditions, fuels, and simple geometries, and the accessibility of data to the broader combustion community. Hybrid and physics-informed ML was identified as approaches to address some of these limitations.

Following a short review on different ML methods (supervised, unsupervised, and semi-supervised/generative learning methods), the second part of this session focused on the application of CombML in the context of experimental analysis and turbulent combustion modeling. These topics are of direct relevance to the overarching focus of the TNF/PTF workshop, and several of these applications considered data from the TNF/PTF flame database. Discussed applications of CombML for experimental analysis were primarily geared towards physical understanding, the characterization of combustion regimes, the identification of coherent features and structures, data reduction, and the construction of low-order models for control-oriented applications. Perhaps one of the most prominent examples for the successful application of unsupervised learning techniques is the principal component analysis (PCA), which has been used for feature extraction and structural invariance analyses for the Sandia piloted flame and the Jet-in-hot-coflow flame series. Other supervised learning techniques utilized various forms of neural networks to map species onto velocity fields, for the reconstruction of tomographic imaging from laser absorption and Schlieren measurements.

ML application for combustion modeling has largely been concerned with the parameterization of combustion manifolds, the data augmentation, and development of combustion closures and subgrid-scale models, and the physical embedding to reduce computational cost. Contributions from different groups, discussed in this session, involved the construction of data-assisted combustion modeling in which supervised learning methods were used as classifiers for the local combustion-submodel selection based on local flow-field information; the parameterization of combustion manifolds using neural network architectures to represent high-dimensional thermochemical state-spaces, as well as the optimization of virtual chemistry models using data from simulations. An area of significant interest and discussion was the consideration of physical principles and physics-informed

CombML. To this end, progress has already been made by constructing turbulent subgrid-models and the discovery of closure models using gene-expression programming and sparse regression. While these methods demonstrated the ability of identifying SGS-models that have features similar to models that were derived previously using mathematical principles, these approaches showed the potential for application to a broader range of conditions, which become increasingly more important for combustion applications, such as complex fuel mixtures, high-pressure conditions, and multiphase flows. Another interesting area for CombML is generative models for constructing high-resolution data from filtered LES results as an alternative to deconvolution methods.

The discussion session evolved around four main topics, namely (i) data and how TNF/PTF's existing database can be leveraged for CombML applications, (ii) the integration of ML into TNF and PTF workshop, and (iii) pathways for establishing ML-models, best practice, and benchmarks for ML training and ML evaluation, and (iv) the integration of domain knowledge into CombML. Some recent attempts of community-based database were discussed, such as the community-driven BLASTNet database (<https://blastnet.github.io>). Discussions on CombML-specific challenges were concerned with the interpretability of CombML models, the need for uncertainty quantification, and the generalization of CombML models.

It was agreed that the TNF/PTF workshop provides a viable forum to support various CombML effects. By targeting specific flame configurations, immediate next steps for CombML applications could involve TNF/PTF community efforts around benchmark comparisons of CombML models on combustion regime classifications or manifold parameterization from experimental data. Such ML-tasks are affordable to accomplish using existing TNF/PTF data and could initiate a forum for benchmark comparisons and further discussion within the TNF/PTF workshop. With direct benefits to the broader combustion community, a direct benefit would involve the sharing of CombML models, establishing best practice for CombML-model training and testing, and pathways for integrating CombML-models in applications beyond *a priori* tests.

References:

Ihme, Chung, Mishra, "Combustion machine learning: Principles, progress and prospects." Progress in Energy and Combustion Science, 91:101010, 2022.

Combustion Machine Learning: Principles, Progress, Perspective

MATTHIAS IHME

In coordination with Tarek Echekki and Luc Vervisch

Stanford University

2

Contributions

- Tarek Echekki (NC State)
- Chuyu Wei, Mitch Spearrin (UCLA)
- Anthony Carreon, Shivam Barwey, Venkat Raman (UM)
- Wai Tong Chung (Stanford)
- Sam Grauer (PSU)
- Luc Vervisch (CORIA)
- Benoit Fiorina (CentralSupelec)
- Markus Klein (UBM)
- Mathis Bode, Ludovico Nista, Heinz Pitsch (RWTH Aachen)

Stanford University

Overview

CombML @ TN/PF (60')

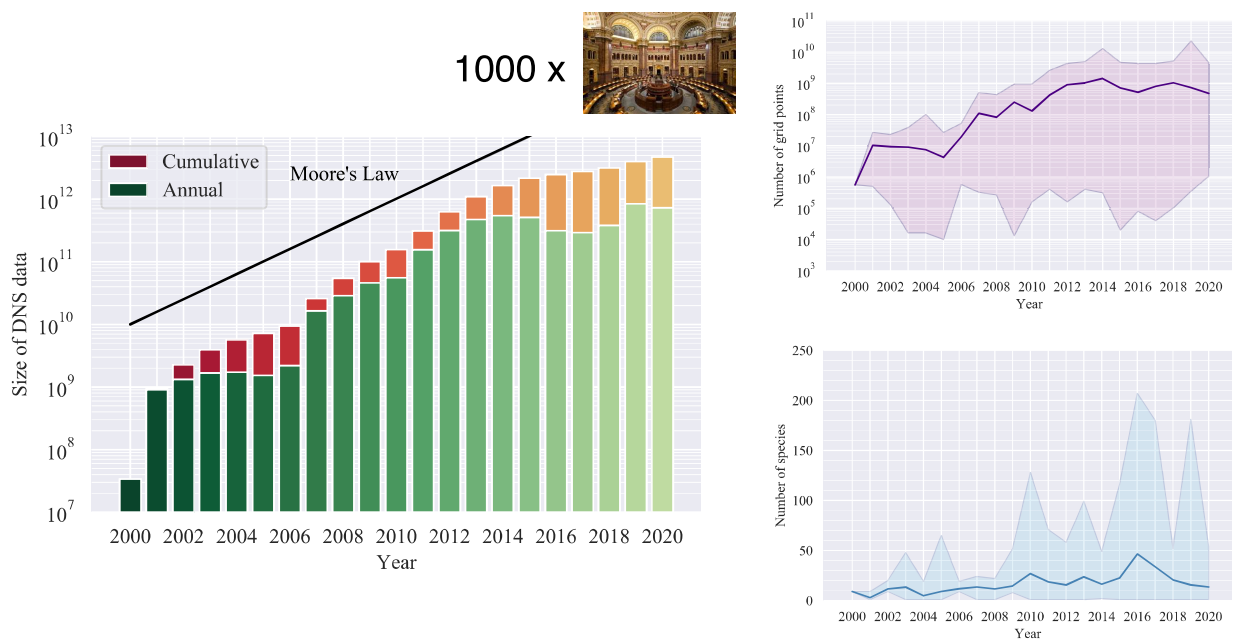
- Background on CombML
- CombML for experimental analysis
- CombML for turbulent combustion modeling

ML-related research at NREL (Bruce Perry, Shashank Yellapantula) (15')

Discussion and CombML@TN/FP (15')

Stanford University

Data in combustion science and engineering

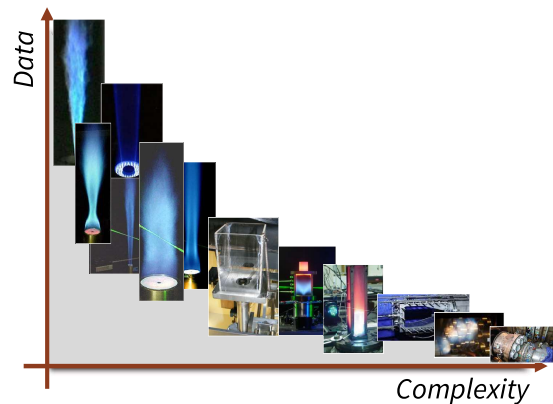


Stanford University

Data in combustion science and engineering

Challenges

- Data limited to specific operating conditions, fuels, and geometries
- Lack of data for complex combustion conditions
- Data accessibility



Stanford University

Data in combustion science and engineering

Challenges

- Well-established theoretical foundation of chemically reacting flows
 - › Thermodynamic principles
 - › Conservation relations
 - › Law of mass action
- Solution limited by
 - › Wide range of scales
 - › Chemical complexity
 - › Incomplete knowledge of constitutive relations

Conservation equations (momentum, species, energy)

$$\underbrace{\partial_t U} + \underbrace{\nabla \cdot F(U)} - \underbrace{\nabla \cdot Q(U, \nabla U)} = \underbrace{S(U)}$$

$$\begin{pmatrix} \rho u \\ C \\ \rho e_t \end{pmatrix} \quad \begin{pmatrix} \rho u \otimes u + pI \\ C \otimes u \\ u(\rho e_t + p) \end{pmatrix} \quad \begin{pmatrix} \tau \\ -j \\ \tau \cdot u - q \end{pmatrix} \quad \begin{pmatrix} 0 \\ \dot{\omega} \\ 0 \end{pmatrix}$$

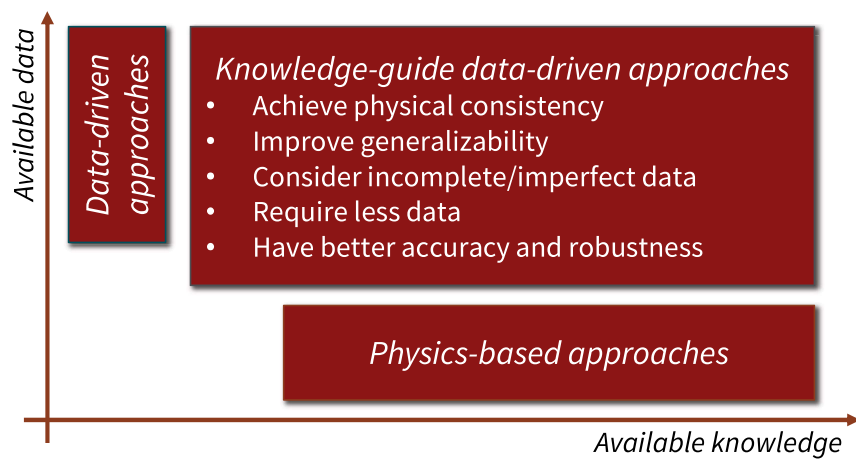
State relation $g(p, e, C) = 0$

Conservation and coupling functions

$$W^T C = \rho, \quad W^T \dot{\omega} = 0, \quad W^T j = 0$$

Stanford University

Knowledge discovery paradigms



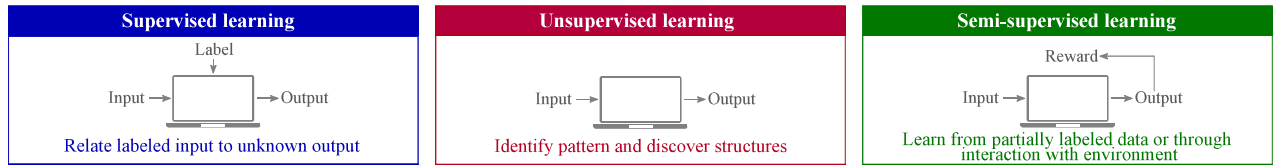
Stanford University

ML Methods



Stanford University

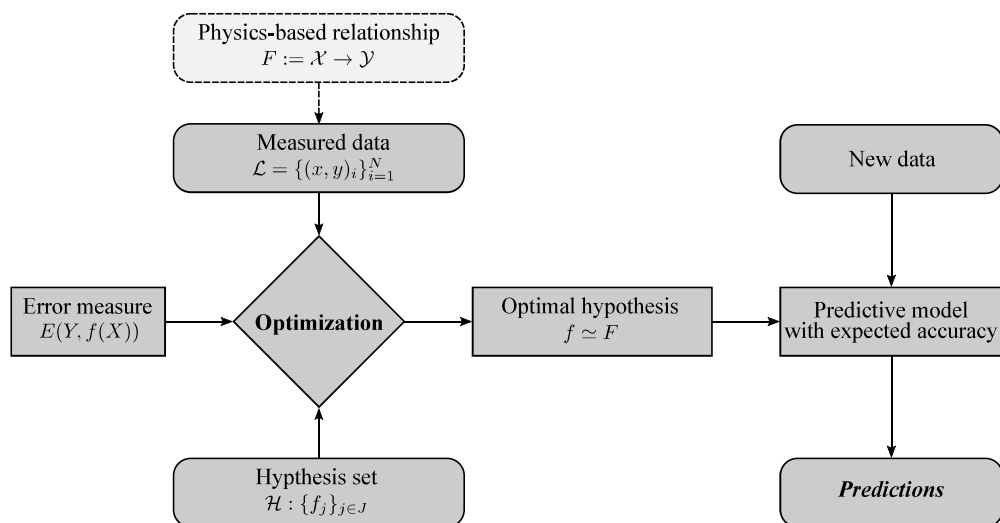
Machine learning methods for combustion



Stanford University

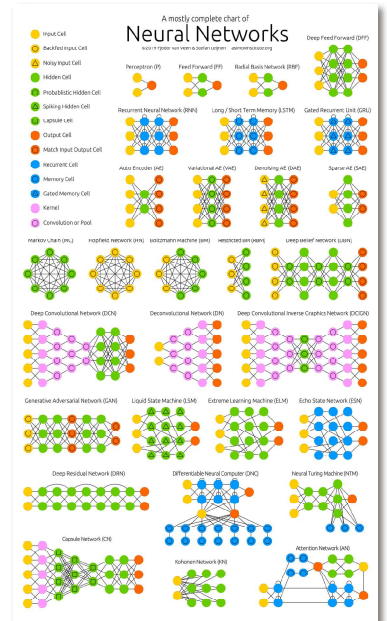
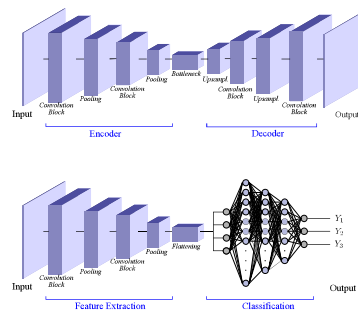
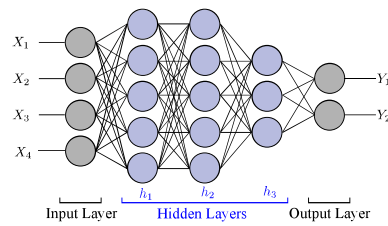
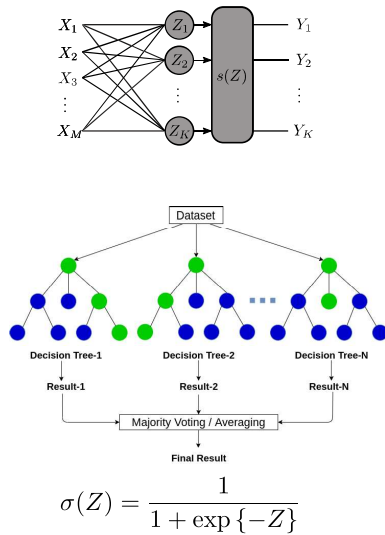
What is ML?

A generic supervised learning algorithm



Stanford University

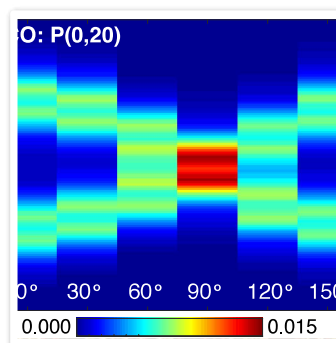
Learning methods



Stanford University

CombML for experimental analysis

CONTRIBUTIONS: ECKEKKI,
PARENTE, RAMAN,
SPEARRIN, GRAUER



Stanford University

CombML for experimental analysis

- Physical understanding and discovery
- Discovery of structures, combustion-regime, and coherent feature
- Construction of low-order models for control-oriented applications
- Data-generation

CombML for combustion modeling

- Parameterization of combustion manifolds
- Data augmentation and data generation
- Combustion-closure models
- Physical embedding to reduce computational cost

Stanford University

Machine Learning with Multiscalar Point/Line Measurements

Tarek Echekki

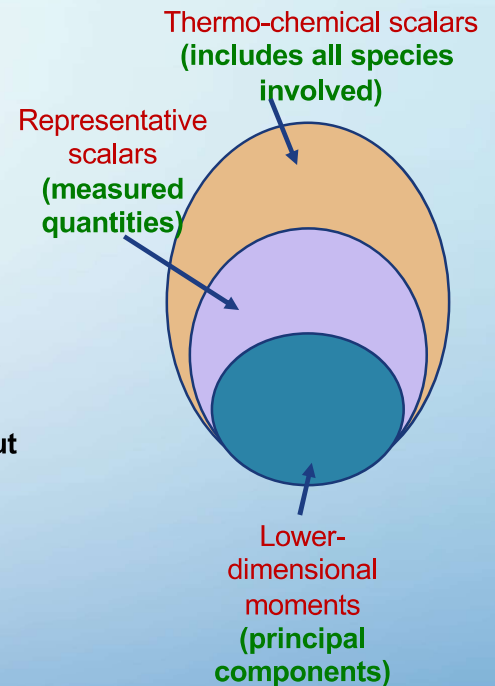
Machine Learning with Multiscalar Point/Line Measurements

Inherent hierarchy in composition space.

- **Full thermo-chemical scalars** (all species, temperature, pressure) needed for a full chemistry description.
- **Representative scalars**: Adequate subset of the thermo-chemical scalars to describe the composition space.
- **Low-dimensional moments** (such as mixture fraction, progress variables) define a low-dimensional description of the composition space.

Use ML to determine moments from data without assumptions about combustion mode or regime

- **Principal component analysis (PCA)** applied on the representative scalars (the measured quantities) is one such ML technique.
- PCA used for denoising (surrogate composition space) or modeling. (experimental based closure models).

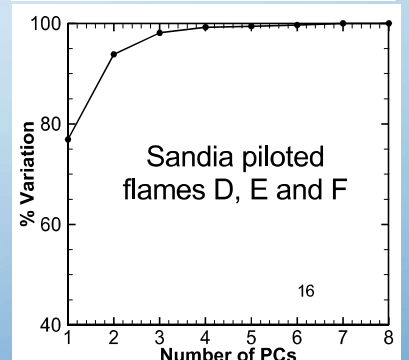
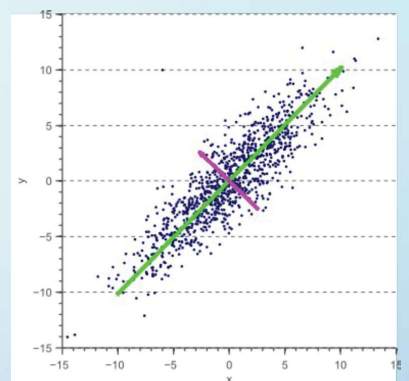


Principal Component Analysis (PCA)

- PCA: converts set of correlated variables (species and temperature) to weakly correlated ones (principal components, PCs): $\phi = Q^T \theta$
 - ϕ : PCs vector (size N)
 - θ : representative scalars (size N)
 - Q : matrix of eigenvectors of the **covariance matrix** of θ (size $N \times N$)
- **Benefit of PCA: Interpretability**
 - PCs are linear combinations of measured quantities
 - Coefficients of Q^T tells us the important contributions
- Dimensionality Reduction: Retain subset ($N_{PC} \ll N$) of PCs that represent bulk of data variance: $\phi^{\text{red}} = A^T \theta$, with A the leading N_{PC} vectors of Q
- Instantaneous transport equations for PCs (Sutherland and Parente, 2009) similar to scalars' equations in combustion

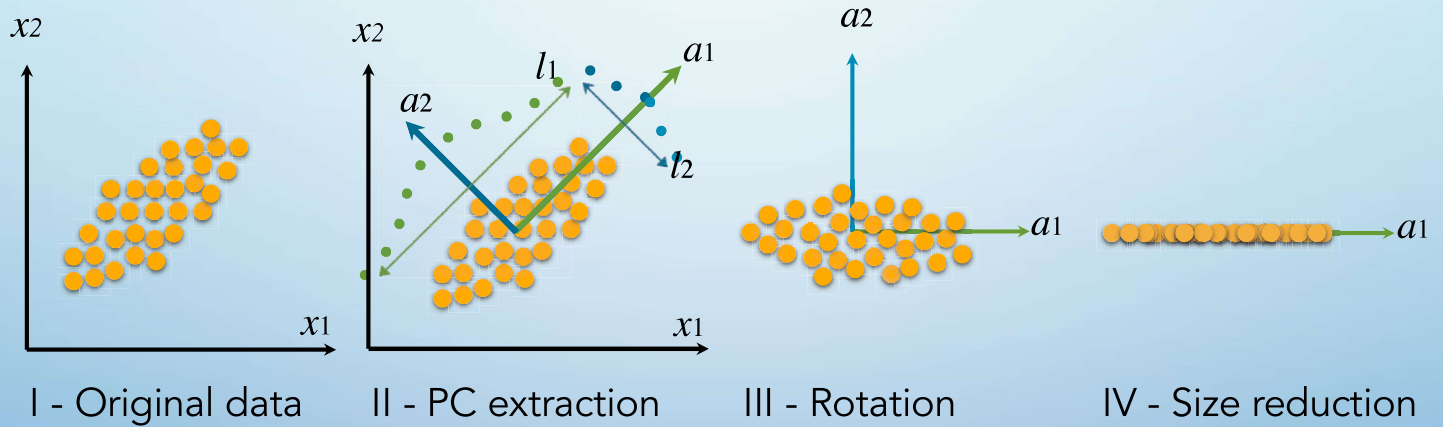
$$\frac{\partial \rho \phi_k}{\partial t} + \frac{\partial \rho u_j \phi_k}{\partial x_j} = \frac{\partial}{\partial x_j} \left[\rho D_k \frac{\partial \phi_k}{\partial x_j} \right] + s_{\phi_k}, \quad k = 1, \dots, N, \quad \text{where } s_{\phi} = A^T s_{\theta}$$

From V. Spruyt (Computer Vision for Dummies)



Scree Plot

PCA allows to identify direction of maximum variance in data (Parente)



Many tools for feature extract (Parente)

Principal Component Analysis

Non-linear Principal Component Analysis

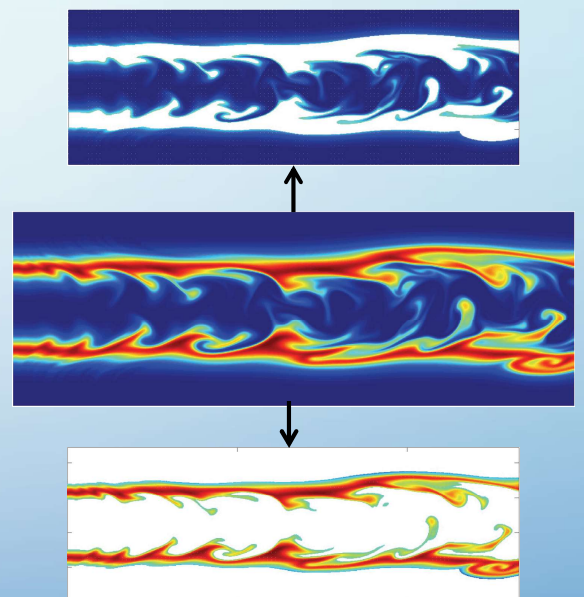
Isometric Mapping

T-distributed Stochastic Neighbor Embedding (t-SNE)

Autoencoders

Local Principal Component Analysis

... and many others



Experimental-Data Based Modeling: Constructing Turbulent Combustion Models Using Experimental Data

- **Premise:**

- Measured quantities are **representative scalars** that define low-dimensional manifold of composition space.
- PCA is evaluated on measured data in composition space.
- Data defines the low-dimensional manifold of the composition space.

- **Practical Relevance:**

- No need for prior assumptions about combustion mode/regime

- **Challenges - Experimental Data is:**

- **Partial:** Only measure a subset of the thermo-chemical scalars, no reaction rates.
- **"Noisy":** Small uncertainty in measurements can translate into larger uncertainties in derived scalars, such as reaction rates.



Sandia flames
(Barlow & Frank, 1998)

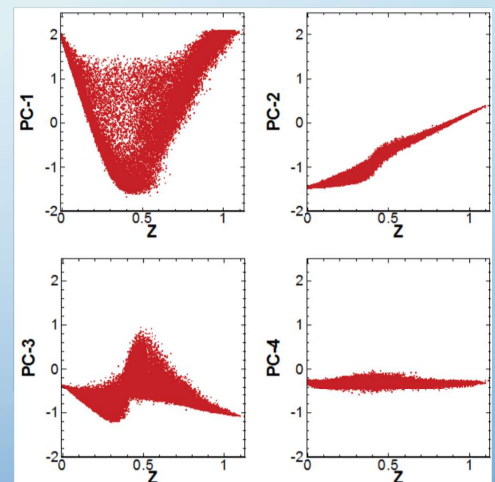
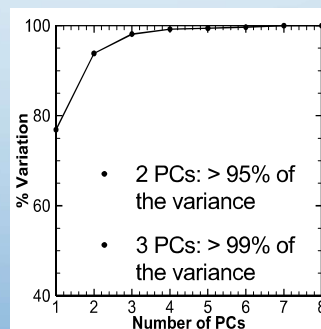
PC feature extraction: Sandia Flames D, E and F (Barlow & Frank, 1998)

- A single set of PCs and closure are evaluated with 3 flames' data

- Flame D: $Re = 22,400$
- Flame E: $Re = 33,600$
- Flame F: $Re = 44,800$

- The measured scalars are $T, Y_{H_2}, Y_{O_2}, Y_{OH}, Y_{H_2O}, Y_{CH_4}, Y_{CO}, Y_{CO_2}$.

- PCs vs. Mixture Fraction
- PC_1 mimics a progress variable
 - PC_2 mimics a mixture fraction
 - PC_3 main contribution is OH



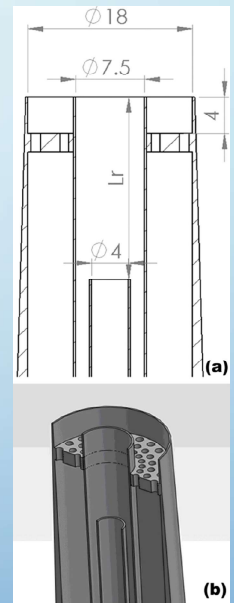
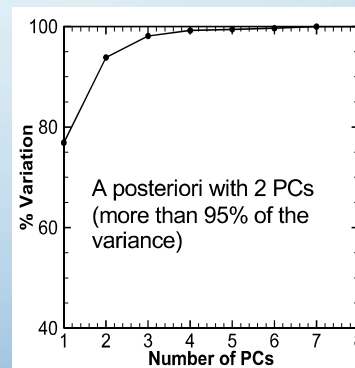
A Posteriori Validation: The Sydney Inhomogeneous Inlet Flames (Ranade, Echekki, Masri, FTC 2022)

A single set of PCs and closure are evaluated with 3 flames' data

- Flame **FJ200-5GP-Lr300-59**: $Re = 27,600$, $L_r = 300$ mm
- Flame **FJ200-5GP-Lr75-57**: $Re = 26,800$, $L_r = 75$ mm
- Flame **FJ200-5GP-Lr75-80**: $Re = 37,500$, $L_r = 75$ mm
- Blind testing with a posteriori simulations also includes
 - Flame **FJ200-5GP-Lr75-103**: $Re = 48,300$
- Measured scalars are $T, Y_{H_2}, Y_{O_2}, Y_{H_2O}, Y_{CH_4}, Y_{CO}, Y_{CO_2}$

Special features of these flames

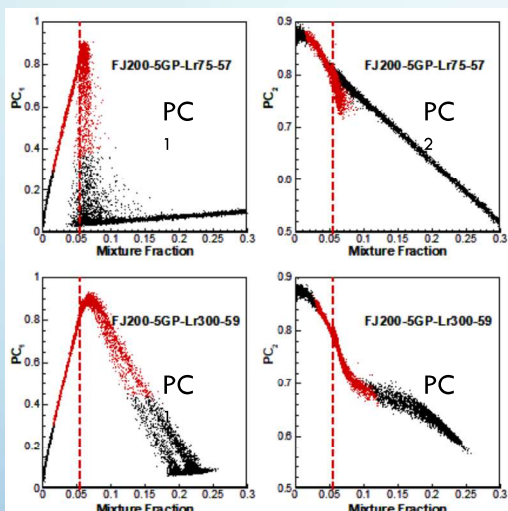
- Presence of **extinction and reignition** as Re increases.
- Presence of **multiple modes of combustion**



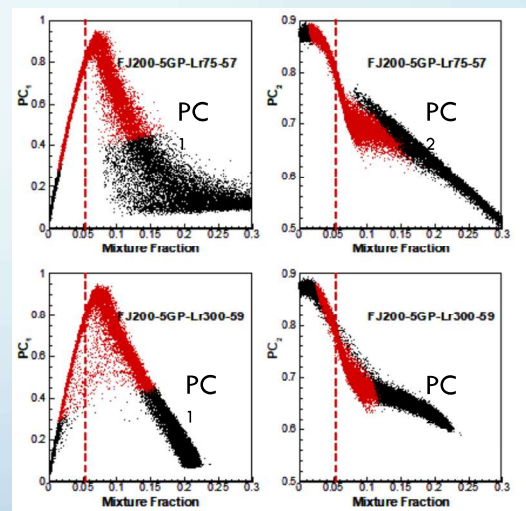
Sydney burner (S. Meares & A.R. Masri, C&F 161, pp. 484-495, 2014)

What are the PCs Telling Us for these Flames?

Inhomogeneous



Nearly-homogeneous



near inlet: $x/d = 1$ transition to non-premixed $x/d = 10$
 PC_1 and PC_2 vs. the Mixture Fraction for 2 flames. Red: $T > 1000$ K, black: $T < 1000$.

- Near the inlet ($x/d = 1$): Inhomogeneous inlet – dominance of pilot
- Further downstream ($x/d = 10$): both cases exhibit similar patterns of non-premixed combustion with PC_1 closer to a progress variable and PC_2 closer to a mixture fraction.

Data-driven method for feature extraction from experimental data

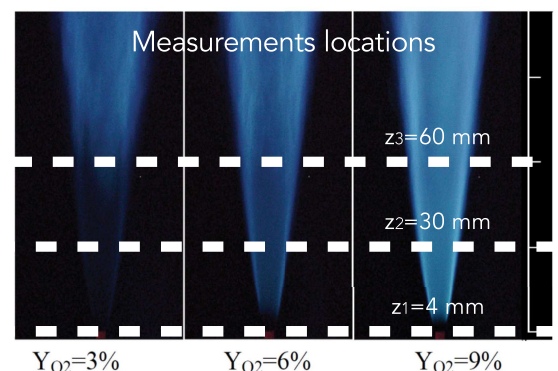
Alessandro Parente

PCA for feature extraction from experimental data: Jet in Hot Co-flow

Transition from conventional to MILD combustion

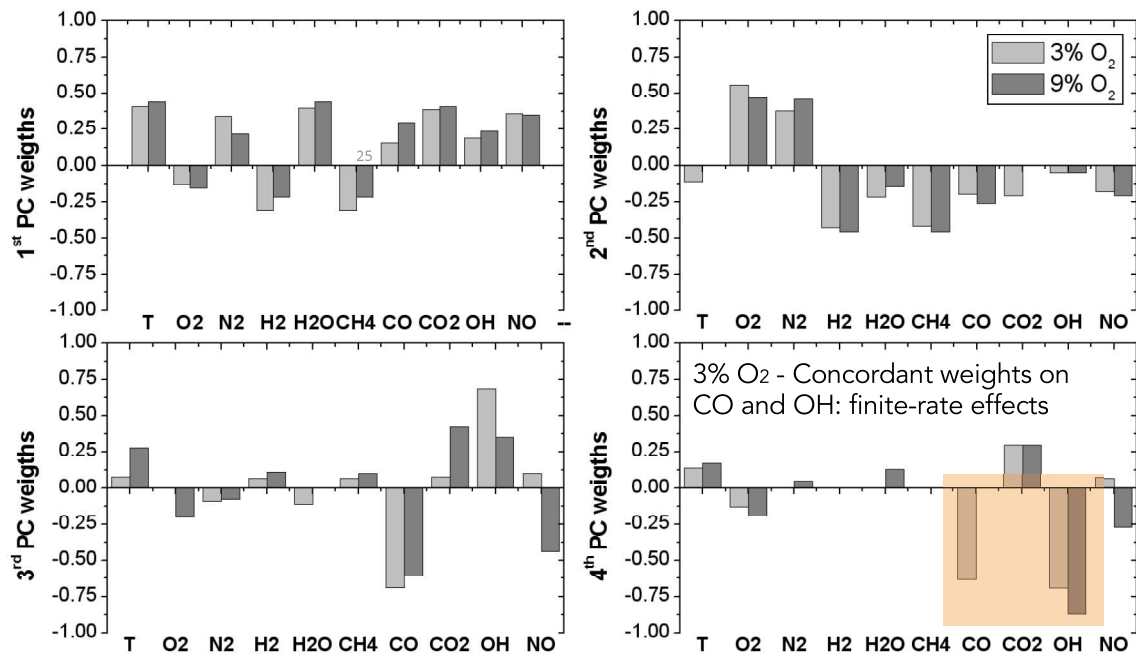
- Can PCA provide physical insight on the change of flame structure?
- How is the change in structure reflected on the PCs definition?
- What are optimal progress variables in MILD regime?

Number of realizations		
HM1 - 3% O ₂	HM2 - 6% O ₂	HM3 - 9% O ₂
56000	55000	61000

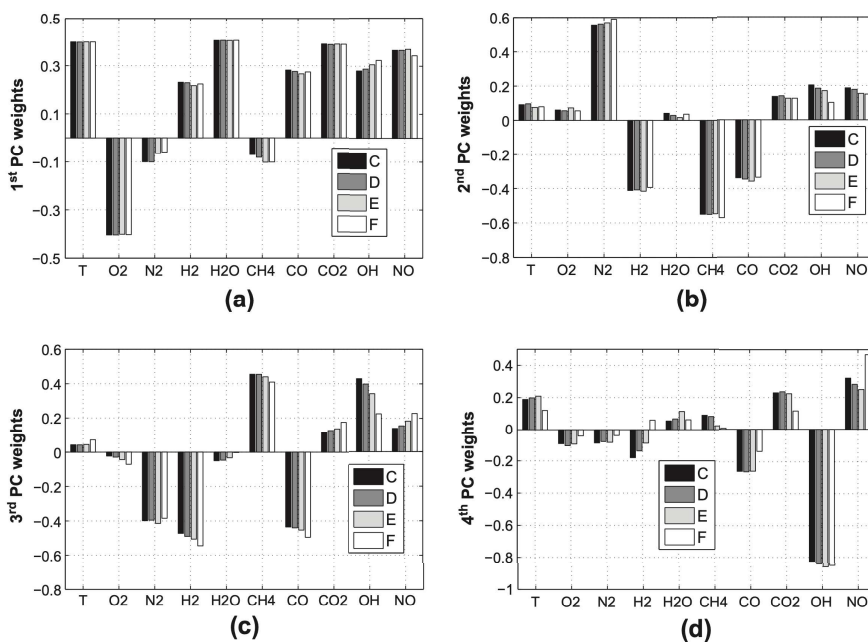


B.B. Dally, A.N. Karpetis, R.S. Barlow, Proceedings of the Combustion Institute 29 (2002) 1147-1154

The PC structure is modified going from conventional to MILD regime



PCA-based models have shown relative invariance to turbulence parameters



Barlow and Frank, 1998.

The PCA structure remains nearly invariant with Re across the range from Sandia flame C (Re=13,400) to flame F (Re=44,800)

Machine Learning Applications in Combustion

Anthony Carreon, Shivam Barwey, Venkat Raman

 University of Michigan, Ann Arbor
Department of Aerospace Engineering



Constructing PIV Fields from OH-PLIF Data Using CNNs



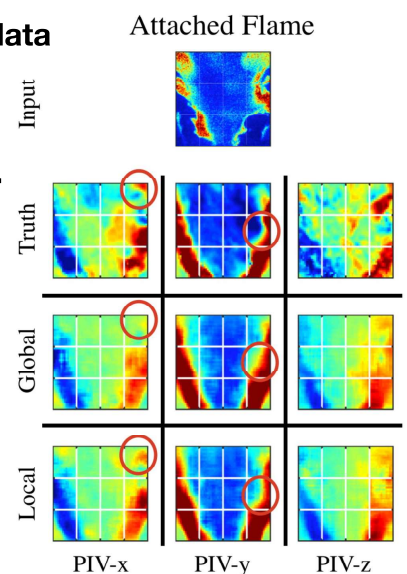
Motivation; Use data to directly obtain models for control-oriented applications; Understand physics; learn to generate experimental data

Convolutional neural networks (CNNs) are trained to map from OH concentration fields to x/y/z-velocity fields using simultaneously measured OH-PLIF and PIV images of a premixed swirl combustor.

Two CNN models:

1. A global CNN that maps entire image domain.
2. A set of local CNNs that map different image subdomains

- ✓ Including time history showed negligible improvement, implying the importance of spatial correlations over temporal correlations
- ✓ Local CNNs were tested on unseen subdomains and were able to use symmetry/anti-symmetry in PIV reconstruction



[Barwey, S., Hassanaly, M., Raman, V., & Steinberg, A. \(2022\). Using machine learning to construct velocity fields from OH-PLIF images. Combustion Science and Technology, 194\(1\), 93-116.](#)

PIV information is extracted from OH-PLIF fields using artificial neural networks (ANNs).

Two viewpoints:

Macroscopic viewpoint:

What lengthscale is required for ANNs to accurately decode PIV fields from OH-PLIF fields?

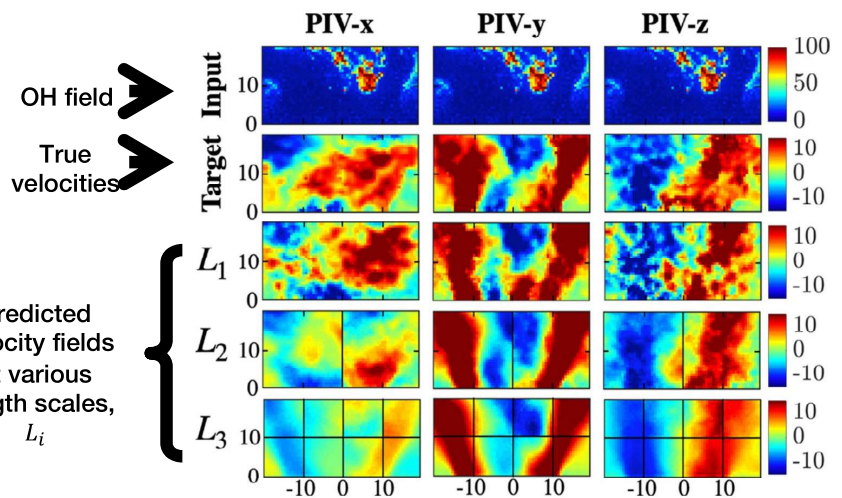
Microscopic viewpoint:

How can the ANN weights be interpreted to gain physical insight on the spatial distribution of information overlap?

✓ OH-PLIF fields must span at least two integral lengthscales

✓ Weights are viewed as multi-field coherent structures.

✓ Local OH interactions are added to global OH structures, consistent with the macroscopic viewpoint.



[Barwey, S., Raman, V., & Steinberg, A. M. \(2021\). Extracting information overlap in simultaneous OH-PLIF and PIV fields with neural networks. *Proceedings of the Combustion Institute*, 38\(4\), 6241-6249.](#)

6

Deep learning inversion for tomographic laser absorption imaging of species and temperature in reacting flows

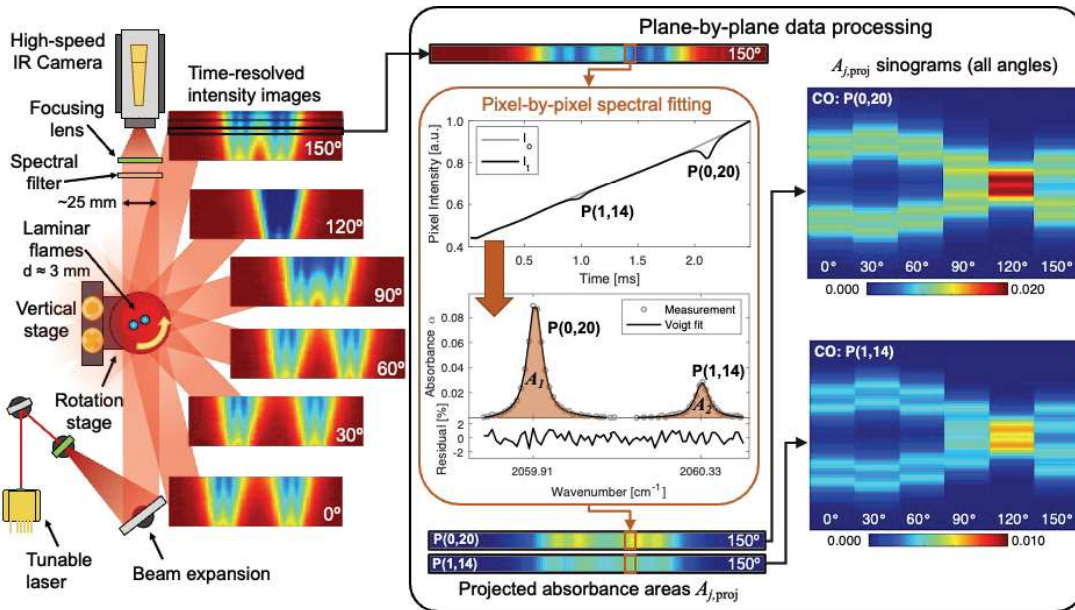
Chuyu Wei, Ph.D.

PI: Prof. R. Mitchell Spearrin

University of California, Los Angeles
Laser Spectroscopy and Gas Dynamics Laboratory
Mechanical & Aerospace Engineering Dept.

Tomographic Laser Absorption imaging

3D/Volumetric imaging needs measurements from multiple projections



$$A_{proj} = \int S(T) X_i P dL = \int K dl$$

Projection sinograms A_{proj} need to be inverted to reconstruct local absorption field K inside the flame

Two-line thermometry for species and temperature

$$\frac{K_2}{K_1} = \frac{S_2}{S_1} = f(T)$$

Mole Fraction

$$X_i = \frac{K_1}{S_1(T)P} = \frac{K_2}{S_2(T)P}$$

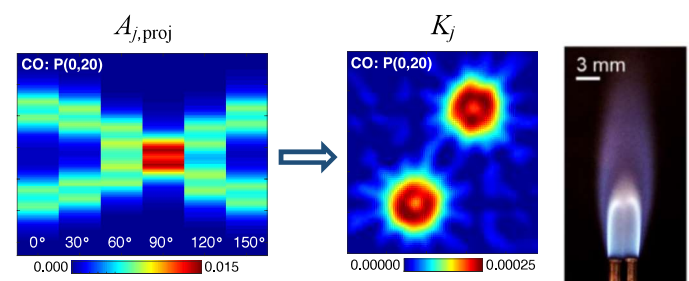
32

Introduction

- Often result in sparse-view inverse problem (measurement << unknowns) due to limitations in available cameras/optical access
- Typically addressed by introducing analytical priors (smoothness, total variation, etc.) using regularization methods

Challenges in sparse-view LAI:

- Blurring effects
 - more angles/cameras needed to resolve steep gradients
- Non-physical artifacts
 - Results outside flame region
 - Non-circular shape/streaking
- High computational cost
 - Deep learning inversion



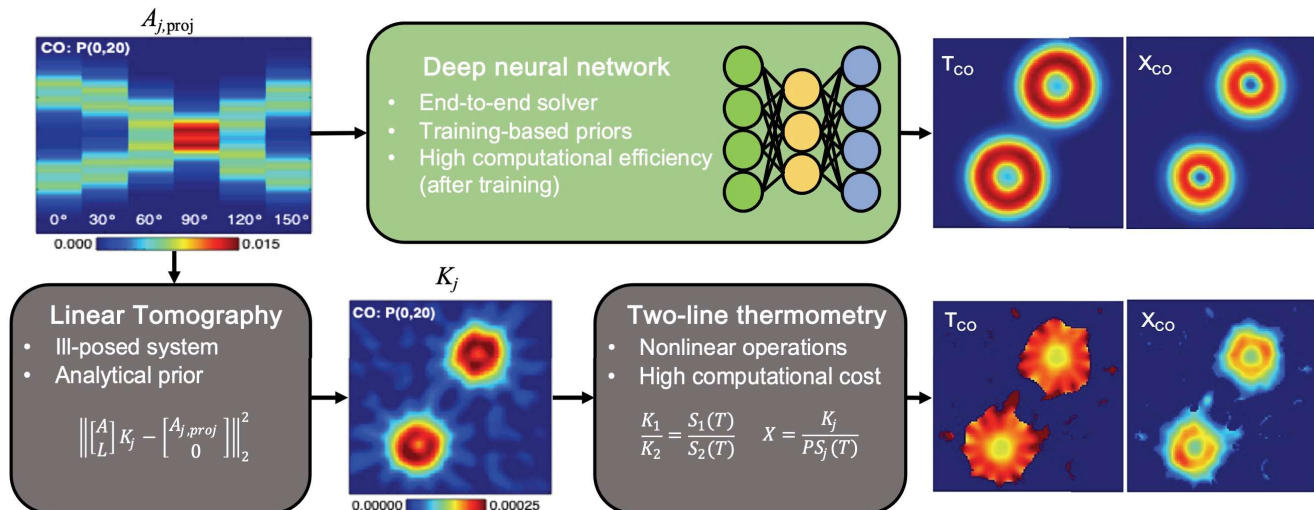
Tikhonov regularization (smoothness prior)

$$K_{j,3D,\lambda} = \arg \min \left\| \begin{bmatrix} W_{3D} \\ \lambda L_{3D} \end{bmatrix} K_{j,3D} - \begin{bmatrix} A_{j,proj,3D} \\ 0 \end{bmatrix} \right\|$$

33

Deep learning inversion

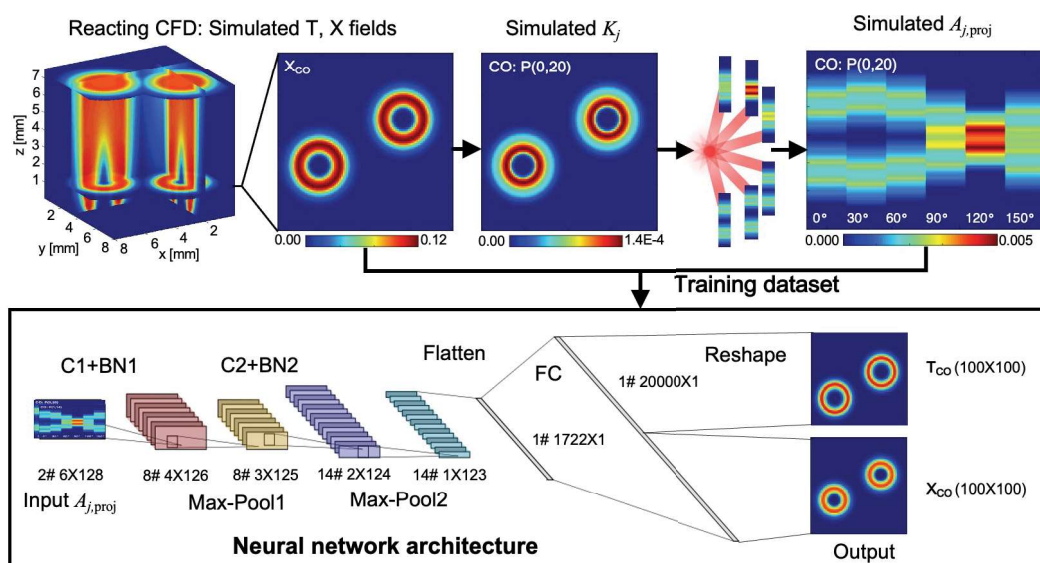
- Sparse-view LAI inversion: linear tomography v.s. deep learning



34

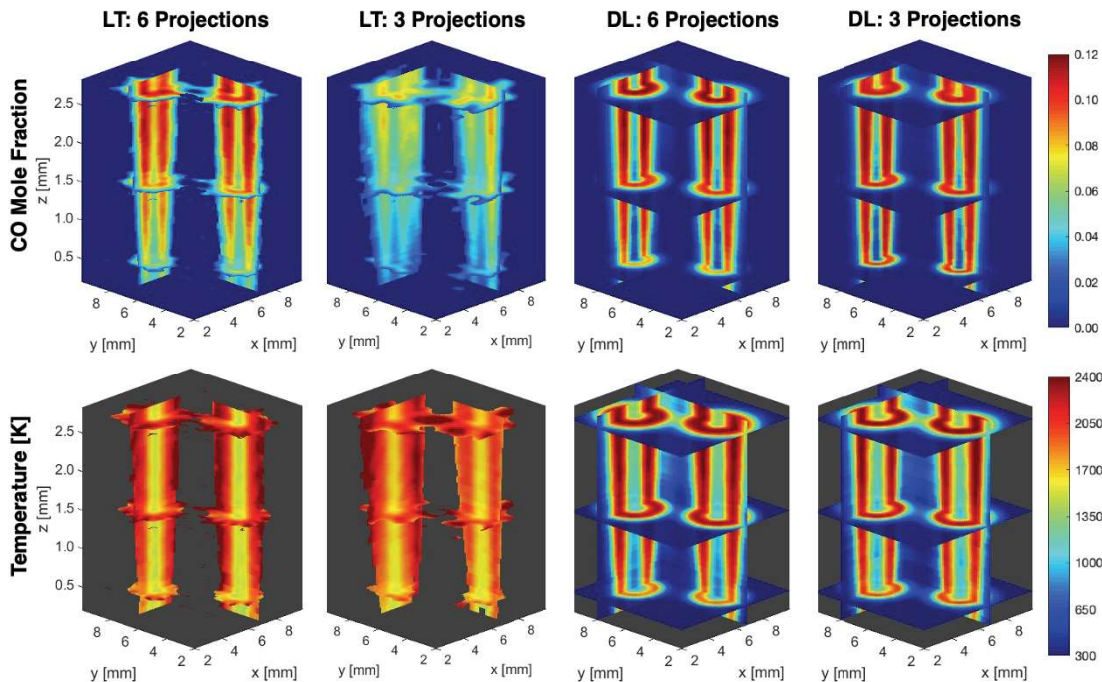
Deep learning inversion

- Our approach: introduce physical priors (flow-field geometry/thermodynamics/scalar correlations) via simulations as training dataset to assist experimental measurements



35

Experimental results: 3D/volumetric imaging



36

Summary

Benefits of DL inversion

- Easy leverage of non-analytical priors (physics/flow geometry)
- Resolution of steep gradients in flames
- Reduced requirement for # of projection angles
- High computational efficiency (after training)
 - Large dataset processing/ Real-time monitoring

Challenges of DL inversion

- Limited dataset available for training
- Generalization to other flow

Bayesian inference for volumetric combustion tomography and future physics-informed methods

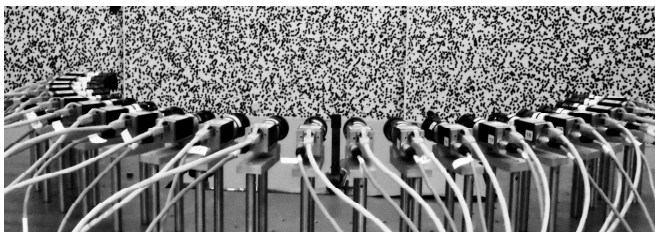
Samuel J Grauer

Department of Mechanical Engineering, Pennsylvania State University

39th International Symposium on Combustion, Vancouver, Canada, Jul. 24–29, 2022

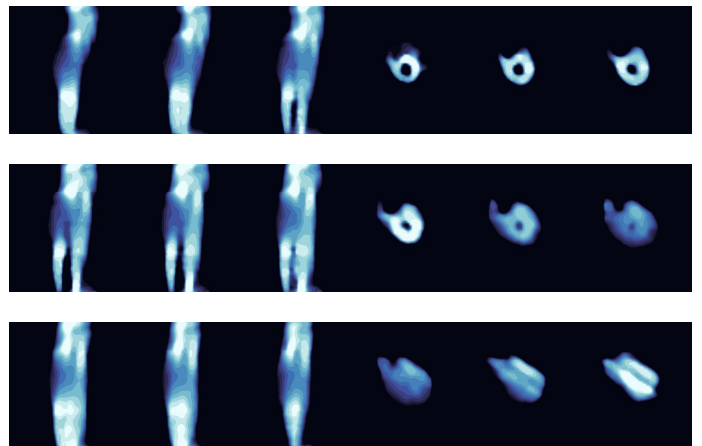


BOS Tomography of a Bunsen Flame



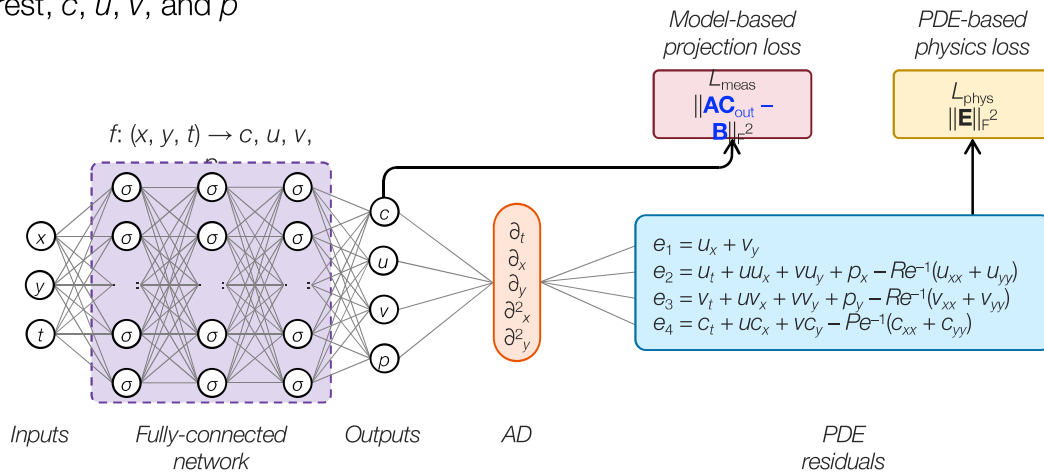
Experimental Conditions

- 23x Bassler acA645-100gm cameras
- 694×494 px sensor with $9.9 \times 9.9 \mu\text{m}$ pixels
- F-stop of f/16
- Unsteady premixed methane-air flame from a Bunsen burner



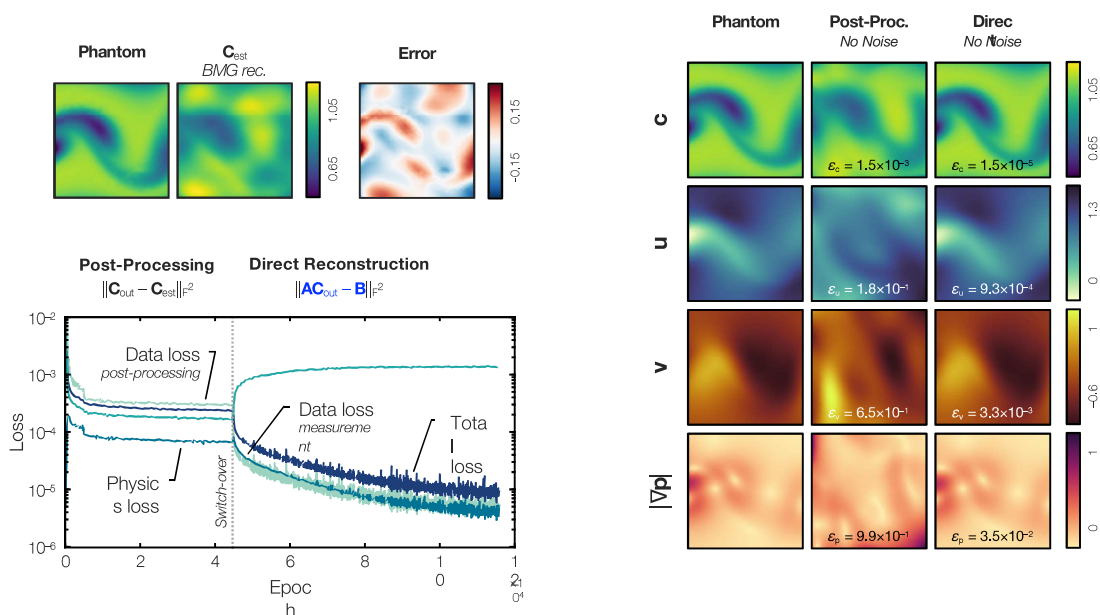
Physics-Informed Reconstruction

- Physics-informed neural networks (*PINNs*) map spatiotemporal inputs, (x, y, t) , to the fields of interest, c, u, v , and p



40

Physics-Informed Reconstruction



41

CombML for experimental analysis

- Physical understanding and discovery
- Discovery of structures, combustion-regime, and coherent feature
- Construction of low-order models for control-oriented applications
- Data-generation

CombML for combustion modeling

- Parameterization of combustion manifolds
- Data augmentation and data generation
- Combustion-closure models
- Physical embedding to reduce computational cost

Stanford University

ML for combustion modeling

CONTRIBUTIONS: CHUNG,
VERVISCH,



Stanford University

Motivation

- Large-eddy simulations enable predictions of complex combustion processes through solution of filtered conservation equations:

$$\begin{aligned}\partial_t \bar{\rho} + \nabla \cdot (\bar{\rho} \tilde{\mathbf{u}}) &= 0 \\ \partial_t (\bar{\rho} \tilde{\mathbf{u}}) + \nabla \cdot (\bar{\rho} \tilde{\mathbf{u}} \tilde{\mathbf{u}}) &= -\nabla \cdot (\bar{p} \mathbf{I}) + \nabla \cdot (\bar{\boldsymbol{\tau}}_v + \boldsymbol{\tau}^{sgs}) \\ \partial_t (\bar{\rho} \tilde{e}_t) + \nabla \cdot [\tilde{\mathbf{u}} (\bar{\rho} \tilde{e}_t + \bar{p})] &= -\nabla \cdot (\bar{\mathbf{q}}_v + \mathbf{q}^{sgs}) + \nabla \cdot [(\bar{\boldsymbol{\tau}}_v + \boldsymbol{\tau}^{sgs}) \cdot \tilde{\mathbf{u}}] \\ \partial_t (\bar{\rho} \tilde{Y}_k) + \nabla \cdot (\bar{\rho} \tilde{\mathbf{u}} \tilde{Y}_k) &= -\nabla \cdot (\bar{\mathbf{j}}_v + \mathbf{j}^{sgs}) + \bar{\omega}_k \quad \text{where } k = 1, 2, \dots, N_s - 1\end{aligned}$$

- High computational costs arises from:
 - Many species
 - Multiple scales and chemical stiffness
 - Closure models for turbulence chemistry interaction and turbulent transport

Stanford University

CombML for dynamic combustion model assignment

Topology-based combustion models

- ✓ Lower computational cost
- ✗ Strong dependency on combustion regime and flame structure
- ✗ Require pre-computation and tabulation
- Examples: flamelet-type models (FPV, FPI, FGM, etc.)

Topology-free combustion models

- ✓ Weak dependency on combustion regime and flame structure
- ✓ On-the-fly evaluation of modeled species
- ✗ Higher computational cost
- Examples: DRG, PFA, QSS, PE, RCCE

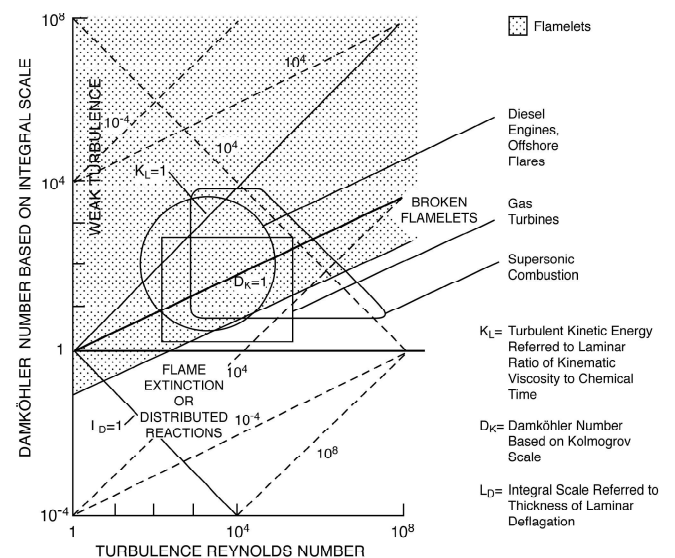


Fig. 2 Regimes of turbulent combustion in a diagram of a turbulence Reynolds number Re_t and a Damköhler number D_t , both based on the integral scale of the turbulence.

Stanford University

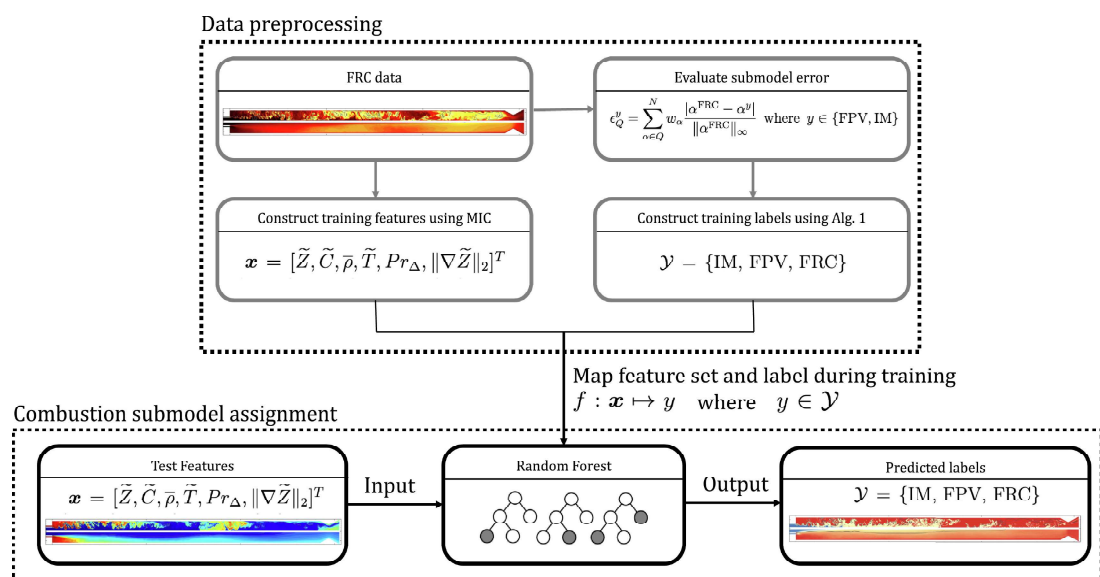
CombML for dynamic combustion model assignment

- **Physical models** versus **data-driven models**: **conservation laws** versus **complex cross-correlations**
- Data-driven models may violate physics during extrapolation tasks
- Data driven models are prone to numerical instability

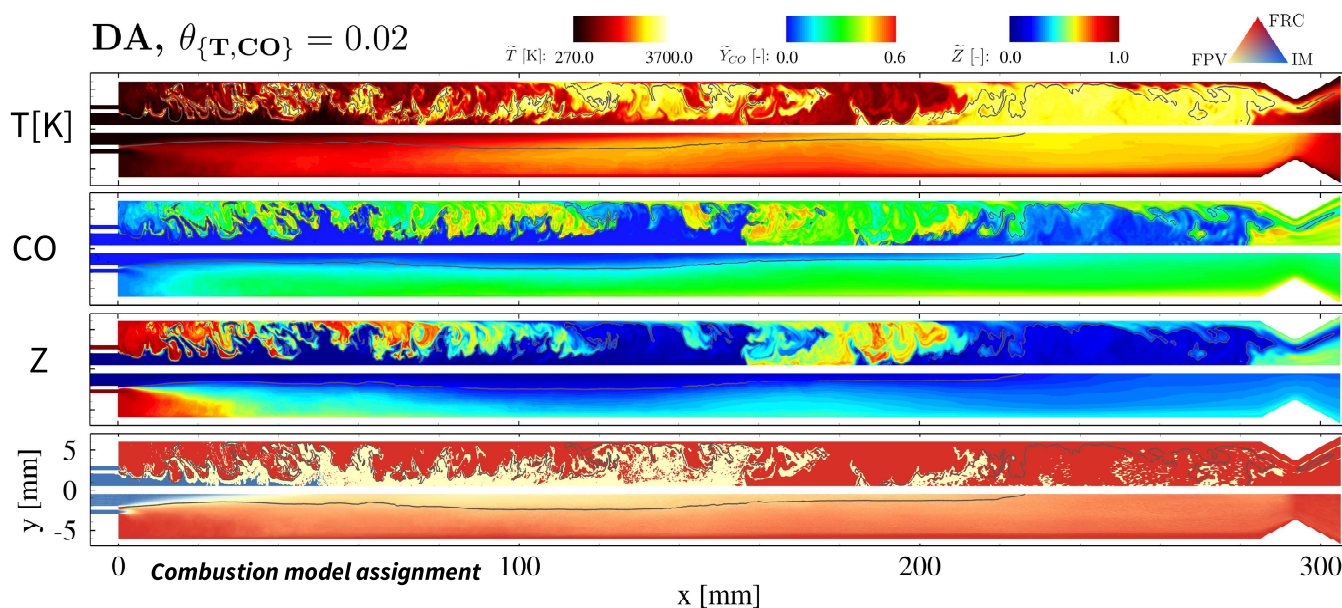
Solution?

- Use **data-driven method** to **assist** the selection of low-fidelity **physics-based model** through classification → supervised classification
- Dynamic combustion-model assignment

CombML for dynamic combustion model assignment



A posteriori results

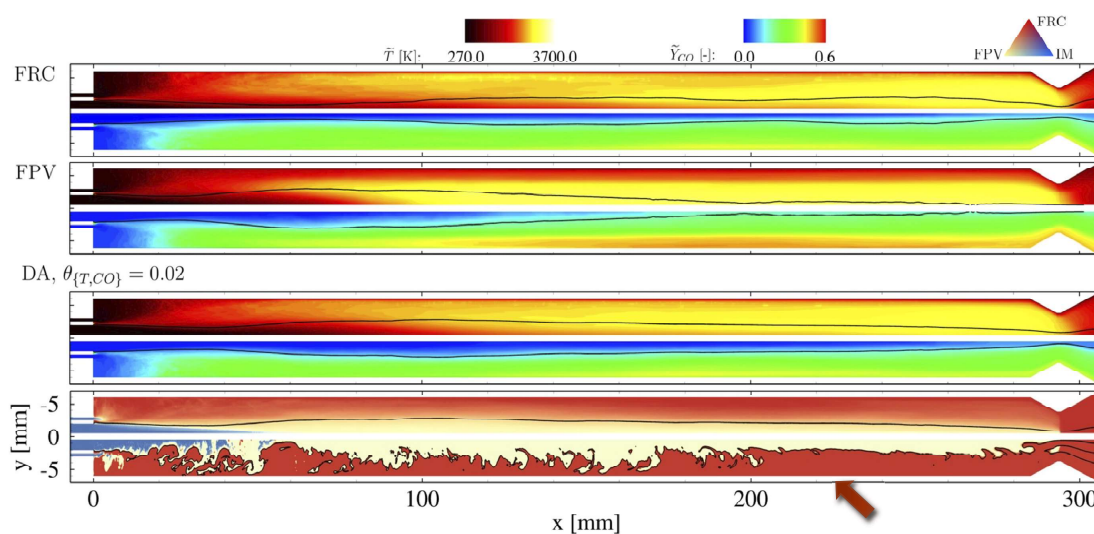


Chung, Mishra, Perakis, Ihme, CF, 227, 172-185

Stanford University

A posteriori results: Extrapolation task?

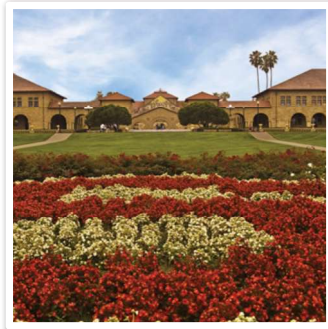
- Method demonstrates ability to generalize for different configurations (3x higher inlet velocity)



Chung, Mishra, Perakis, Ihme, CF, 227, 172-185

Stanford University

Manifold parameterization



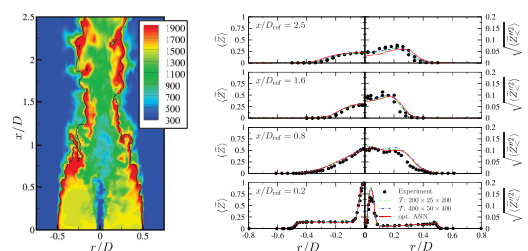
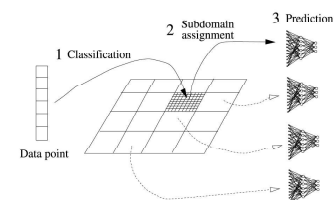
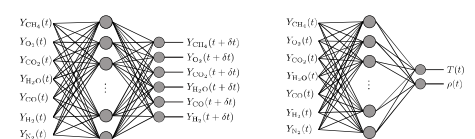
Stanford University

51

Before there was ML

MLP-ANNs for manifold parameterization

- Christo, Masri, Nebot, An integrated PDF/neural network approach for simulating turbulent reacting systems, PCI, 26, 1996
- Blasco, Fueyo, Dopazo, Ballester, Modelling the temporal evolution of a reduced combustion chemical system with an artificial neural network, CF, 113, 1998.
- Blasco, Fueyo, Dopazo, Chen, A self organizing-map approach to chemistry representation in combustion applications, CTM, 4 2000
- Kempf, Flemming, Janicka, Investigation of lengthscales, scalar dissipation, and flame orientation in a piloted diffusion flame by LES, PCI, 30 (2005)
- Ihme, Marsden, Pitsch, Generation of optimal artificial neural networks using a pattern search algorithm: Application to approximation of chemical systems, Neural Comput. 20 (2008)
- Ihme, Schmitt, Pitsch, Optimal artificial neural networks and tabulation methods for chemistry representation in LES of a bluff-body swirl-stabilized flame, PCI, 32 (2009).
- Sen, Menon, Linear eddy mixing based tabulation and artificial neural networks for large eddy simulations of turbulent flames, CF 157 (2010)



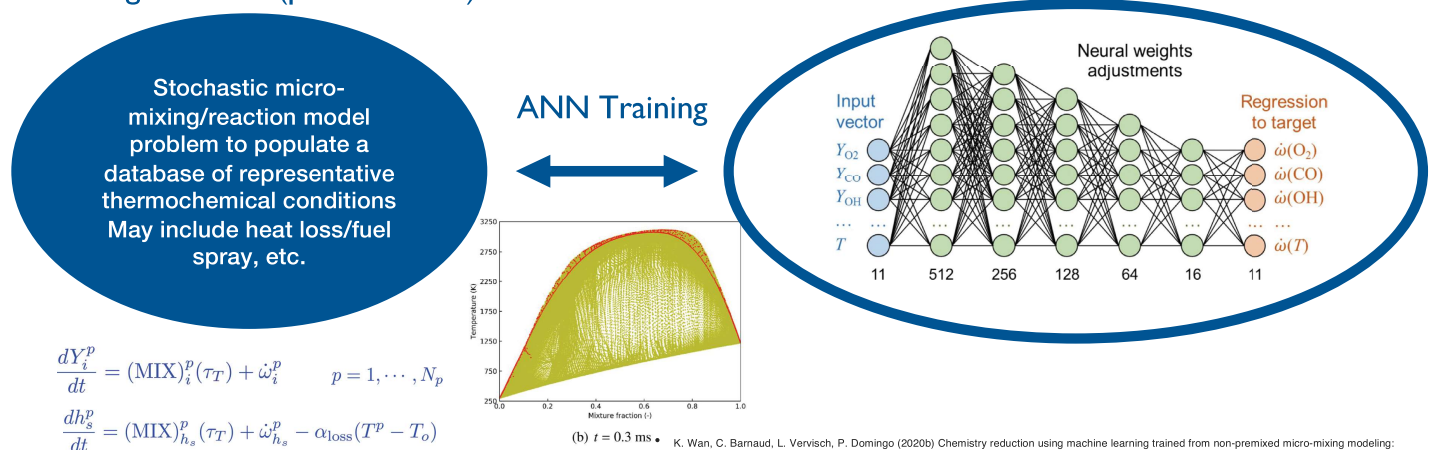
Stanford University

Luc Vervisch

Machine learning for speeding up computational combustion:

- ✓ Starting from detailed chemistry and a model problem, generate through ANN the non-linear relations between a limited set of thermochemical parameters and their increment
- ✓ ANN training replaces chemistry-reduction step
- ✓ ANN usage replaces stiff-chemistry integration

Database generation (prior to CFD)



K. Wan, C. Barnaud, L. Vervisch, P. Domingo (2020b) Chemistry reduction using machine learning trained from non-premixed micro-mixing modeling: Application to DNS of a syngas turbulent oxy-flame with side-wall effects, *Combust. Flame* 220: 119-129.
 H.-T. Nguyen, P. Domingo, L. Vervisch, P.-D. Nguyen (2021) Machine learning for integrating combustion chemistry in numerical simulations, *Energy & AI* 5:100082.

Machine learning for speeding up computational combustion:

Direct numerical simulation (DNS) of a non-premixed flame syngas turbulent oxy-flame with side-wall effects:

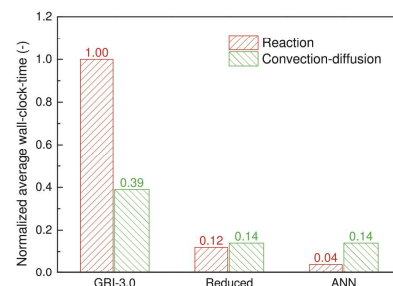
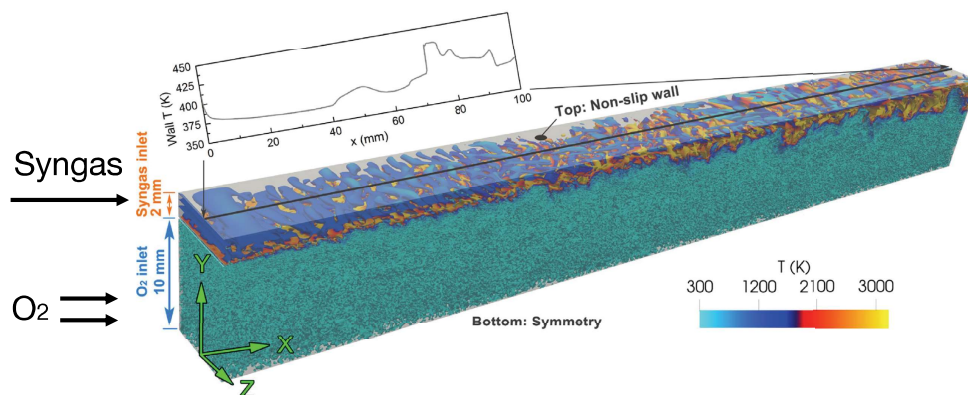


Fig. 11. Normalized average wall-clock-time per time step for solving reaction sources and the convective-diffusive part of the equations in 2D DNS coupled with GRI-3.0, 11-species reduced mechanism (Table 2), and ANN. (Normalization by GRI-3.0.)

- 25 faster than detailed chemistry.
- 3 times faster than a reduced scheme for the same number of transported species.

• K. Wan, C. Barnaud, L. Vervisch, P. Domingo (2020b) Chemistry reduction using machine learning trained from non-premixed micro-mixing modeling: Application to DNS of a syngas turbulent oxy-flame with side-wall effects, *Combust. Flame* 220: 119-129.
 • H.-T. Nguyen, P. Domingo, L. Vervisch, P.-D. Nguyen (2021) Machine learning for integrating combustion chemistry in numerical simulations, *Energy & AI* 5:100082.

Machine learning for speeding up computational combustion:

ANN-chemistry validation against detailed and reduced chemistry :

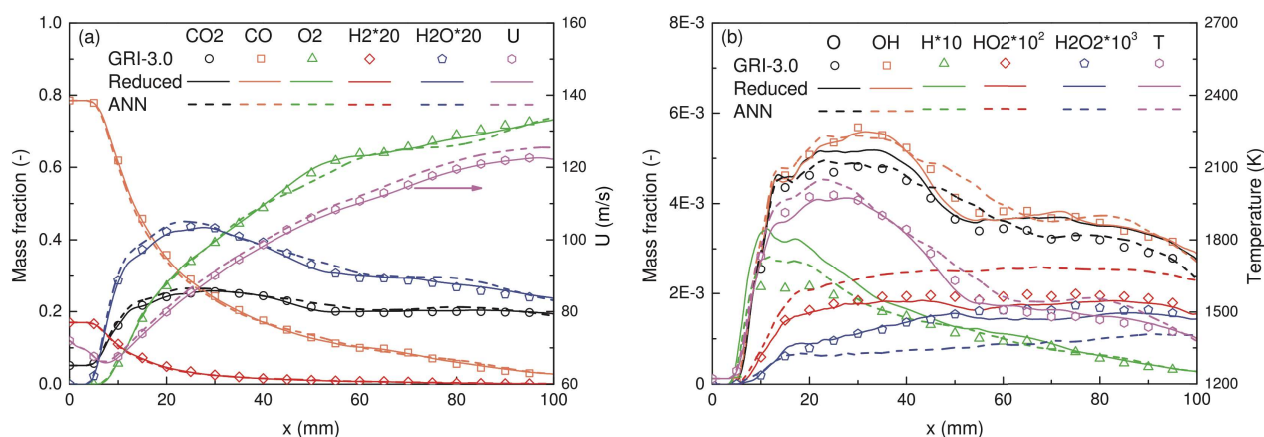
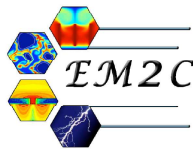


Fig. 5. Averaged distributions along the planar fuel-jet centerline ($y = 11$ mm). Symbols: GRI-3.0. Solid line: Reduced mechanism (Table 2). Dashed line: ANN chemistry. (a) Streamwise velocity and major species mass fractions: CO_2 , CO , O_2 , H_2 and H_2O . (b) Temperature and radicals and minor species mass fractions: O , OH , H , HO_2 , and H_2O_2 . 2D case.

• K. Wan, C. Barnaud, L. Vervisch, P. Domingo (2020b) Chemistry reduction using machine learning trained from non-premixed micro-mixing modeling: Application to DNS of a syngas turbulent oxy-flame with side-wall effects, *Combust. Flame* 220: 119-129.
 • H.-T. Nguyen, P. Domingo, L. Vervisch, P.-D. Nguyen (2021) Machine learning for integrating combustion chemistry in numerical simulations, *Energy & AI* 5:100082.

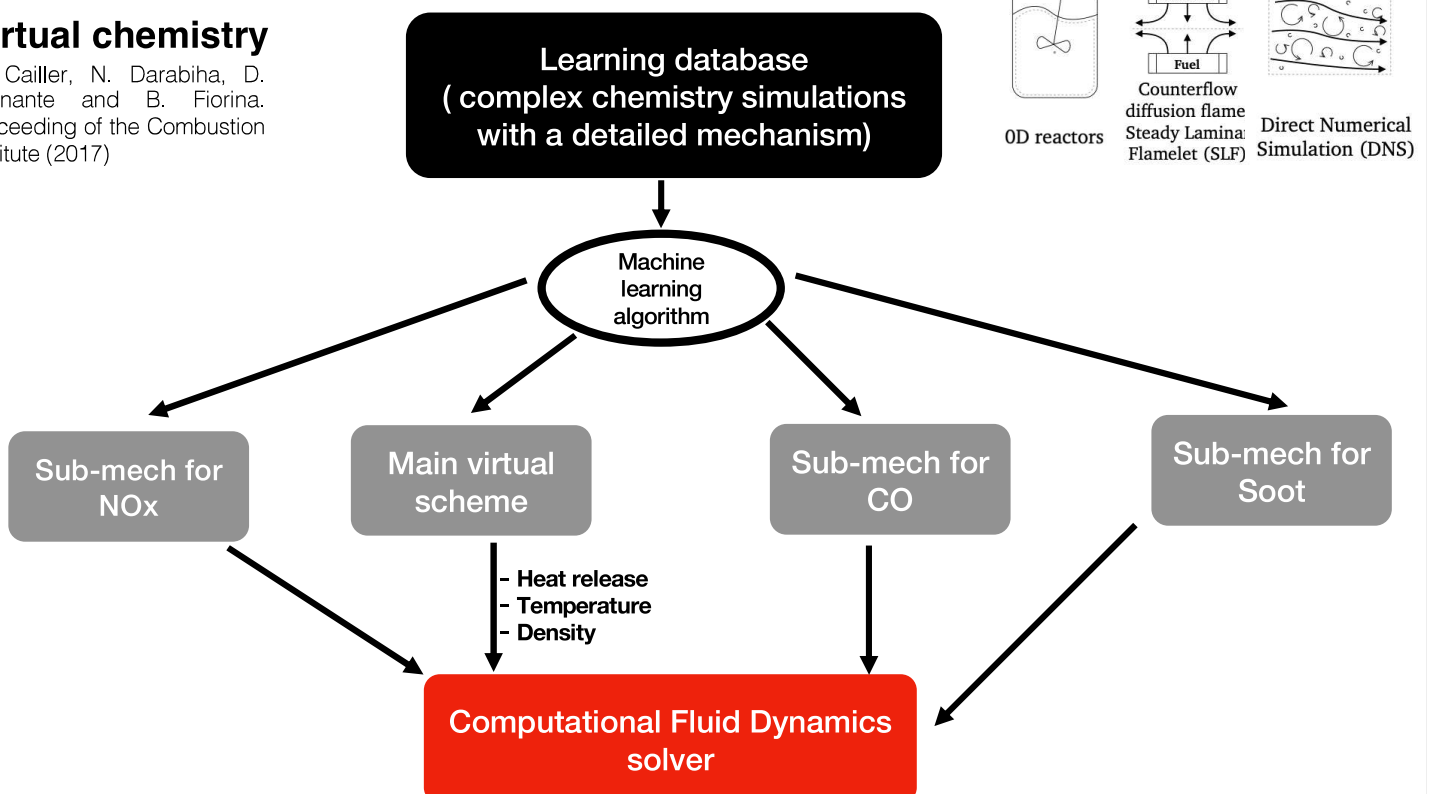
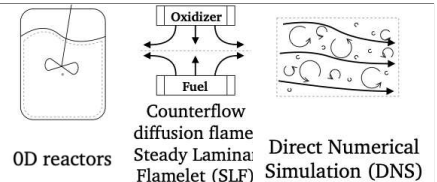
Optimized chemistry for Large Eddy Simulations of wrinkled flames

C. Mehl, M. Cailler, R. Mercier, V. Moureau, B. Fiorina

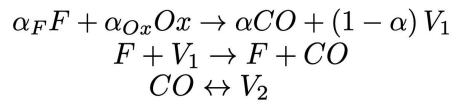


Virtual chemistry

M. Cailler, N. Darabiha, D. Veynante and B. Fiorina.
Proceeding of the Combustion
Institute (2017)



Carbon monoxide (CO)



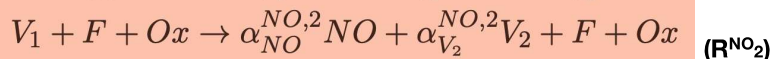
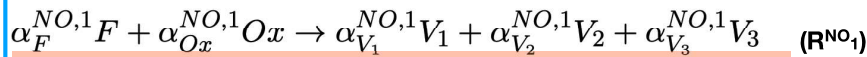
$$q_3 = A_3 f_3 (Y_D^v) \exp\left(\frac{-E_{a,3}}{RT}\right) [F]^{F_F^3} [Ox]^{F_{Ox}^3}$$

$$q_4 = A_4 f_4 (Y_D^v) \exp\left(\frac{-E_{a,4}}{RT}\right) [F]^{F_F^4} [V_1]^{F_{V_1}^4}$$

$$q_5 = A_5 f_5 (Y_D^v) \exp\left(\frac{-E_{a,5}}{RT}\right) \left([CO]^{F_{CO}^5} [V_1]^{F_{V_1}^5} - \frac{[CO]^{R_{CO}^5} [V_1]^{R_{V_1}^5}}{\exp\left(\frac{-\Delta G_5^0(Y_D^v)}{RT}\right)} \right)$$

A_i , $E_{a,i}$, $F_{k,i}$, f_4 and f_5 are optimized through an in-house genetic algorithm

Nitrogen oxide (NOx)



Slow chemistry:
Thermal and
reburning pathways

G. Maio, M. Cailler, A. Cuoci and B. Fiorina. A virtual chemical mechanism for prediction of NO emissions from flames. Comb. Theory and Modeling, pp1-31 (2020)

M. Cailler, N. Darabiha and B. Fiorina. Development of a virtual optimized chemistry method. Application to hydrocarbon/air combustion. Comb. Flame. Vol. 211. pp 281-302 (2020)

58

Optimizing the chemistry for turbulent flames

Issue:

$$\overline{\text{RHS}(\Phi)} \neq \text{RHS}(\overline{\Phi})$$

Transport equation of filtered species mass fraction:

$$\frac{\partial \bar{\rho} \tilde{Y}_k}{\partial t} + \nabla \cdot (\bar{\rho} \tilde{u} \tilde{Y}_k) = \bar{\tau}_k + \nabla \cdot (\bar{\rho} D_k \nabla \tilde{Y}_k) + \bar{\rho} \tilde{\omega}_k^A(\Phi) = \boxed{\text{RHS}(\Phi)}$$

Retained formulation:

$$\text{RHS}^* = \nabla \cdot (\bar{\rho} \alpha^* \tilde{D} \nabla \tilde{Y}_k) + \boxed{\bar{\rho} \tilde{\omega}_k^{A^*}}$$

Constant in space and
identical for each species

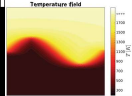
$$A^* = (A_j^*, E_{a,j}^*, n_{ij}^*)$$

$$\bar{\rho} \tilde{\omega}_k^{A^*} = W_i \sum_{j=1}^{N_R} A_j^* (\nu_{kj}^b - \nu_{kj}^f) \times \prod_{i \in S_j} \left(\frac{\bar{\rho} \tilde{Y}_i}{W_i} \right)^{n_{ij}^*} \exp\left(\frac{-E_{a,j}^*}{\bar{R} \tilde{T}}\right)$$

ISSUE: how do we compute A^* and α^* ?

SGS wrinkling also impact species mass fraction

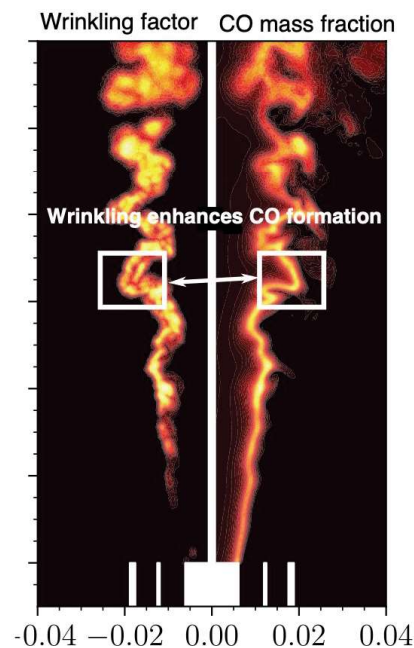
Learning database made of filtered wrinkled flamelets



Machine learning algorithm

Subgrid scale wrinkling model

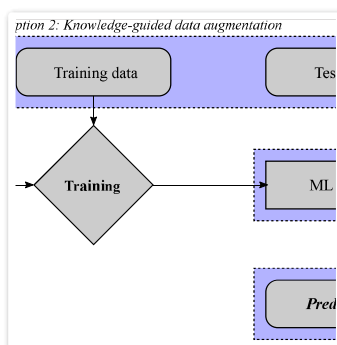
Filtered virtual mechanism for CO



C. Mehl, R. Mercier, V. Moureau and B. Fiorina. Optimized chemistry for Large Eddy Simulations of wrinkled flames. Proceedings of the Combustion Institute, Vol 38, (2021)

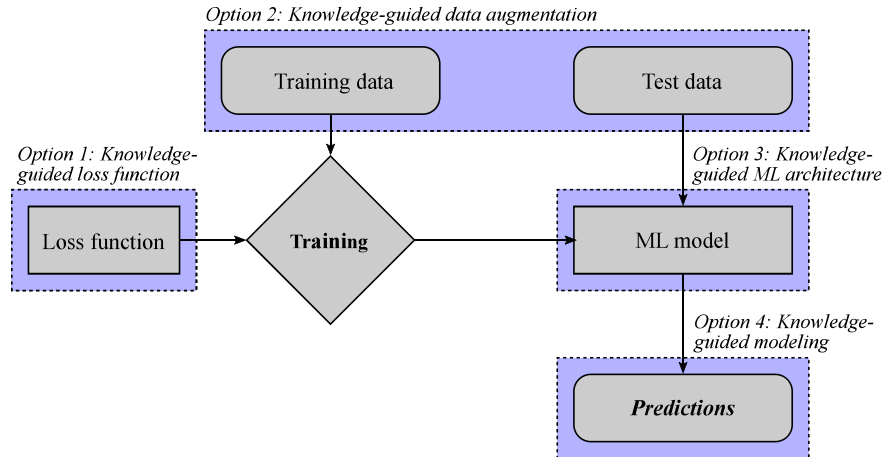
60

Knowledge-Guided data-Driven Methods



Physics-informed CombML

Leverage domain knowledge to reduce dependence on data



Stanford University

Physics-informed CombML

- Large-eddy simulations enable predictions of complex combustion processes through solution of filtered conservation equations:

$$\begin{aligned}
 \partial_t \bar{\rho} + \nabla \cdot (\bar{\rho} \tilde{\mathbf{u}}) &= 0 \\
 \partial_t (\bar{\rho} \tilde{\mathbf{u}}) + \nabla \cdot (\bar{\rho} \tilde{\mathbf{u}} \tilde{\mathbf{u}}) &= -\nabla \cdot (\bar{p} \mathbf{I}) + \nabla \cdot (\bar{\boldsymbol{\tau}}_v + \boldsymbol{\tau}^{sgs}) \\
 \partial_t (\bar{\rho} \tilde{e}_t) + \nabla \cdot [\tilde{\mathbf{u}} (\bar{\rho} \tilde{e}_t + \bar{p})] &= -\nabla \cdot (\bar{\mathbf{q}}_v + \mathbf{q}^{sgs}) + \nabla \cdot [(\bar{\boldsymbol{\tau}}_v + \boldsymbol{\tau}^{sgs}) \cdot \tilde{\mathbf{u}}] \\
 \partial_t (\bar{\rho} \tilde{Y}_k) + \nabla \cdot (\bar{\rho} \tilde{\mathbf{u}} \tilde{Y}_k) &= -\nabla \cdot (\bar{\mathbf{j}}_v + \mathbf{j}^{sgs}) + \bar{\omega}_k \quad \text{where } k = 1, 2, \dots, N_s - 1
 \end{aligned}$$

- High computational costs arises from:
 - Many species
 - Multiple scales and chemical stiffness
 - Closure models for turbulence chemistry interaction and turbulent transport

Stanford University

Machine learning for turbulent combustion modelling

M. Klein, M. Pfitzner, R. Sandberg, N. Chakraborty,
J. Shin, C. Kasten, ...

¹Department of Aerospace Engineering
University of the Bundeswehr Munich, Germany
Email: markus.klein@unibw.de

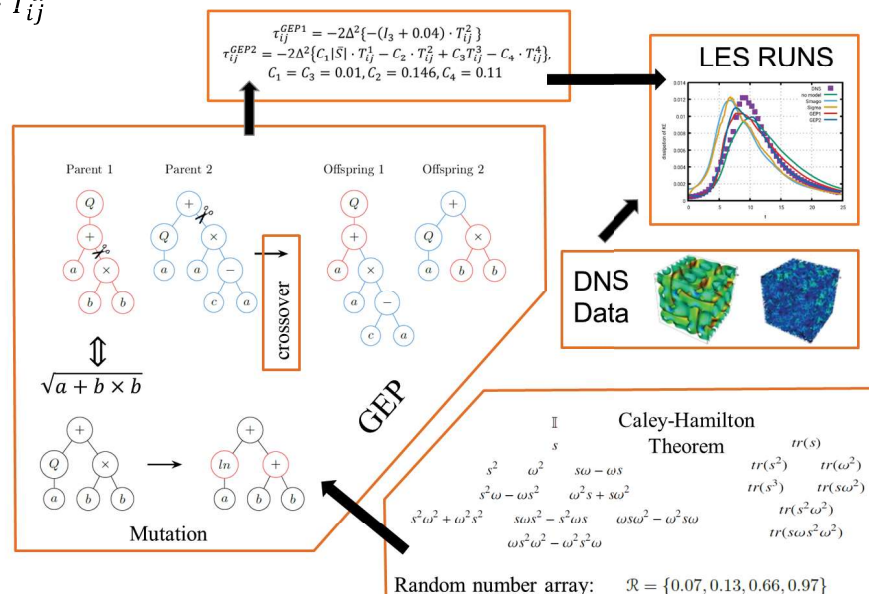
Gene Expression Programming

GEP tries to find optimal forms of the scalar coefficients G_α such that e.g. $\tau_{ij}^{sgs} \approx$

$$\rho \Delta^2 \sum_{\alpha} G_{\alpha}(I_1, \dots, I_m) \cdot T_{ij}^{\alpha}$$

T_{ij}^{α} = integrity basis

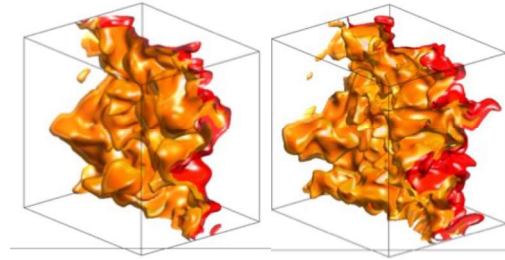
I_{α} = invariants



Closing the SGS stress [1]

Goal:

- Model the SGS tensor in turbulent Premixed combustion
- DNS data a-priori filtered for a range of filter width

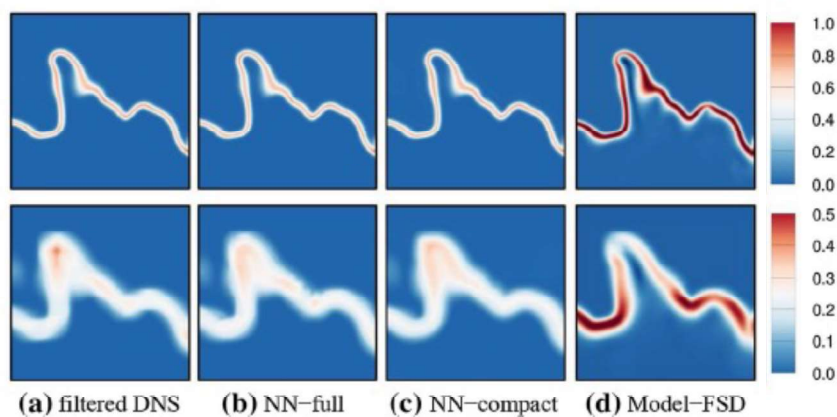


The best out of the 50 found models had the form

$$\tau_{ij}^{GSM} = \rho \Delta^2 \cdot C \cdot (T_{ij}^3 - T_{ij}^2 - T_{ij}^4) = \bar{\rho} \Delta^2 C \frac{\partial \tilde{u}_i}{\partial x_k} \frac{\partial \tilde{u}_j}{\partial x_k} \quad C = 8.21 \cdot 10^{-2} \approx \frac{1}{12}$$

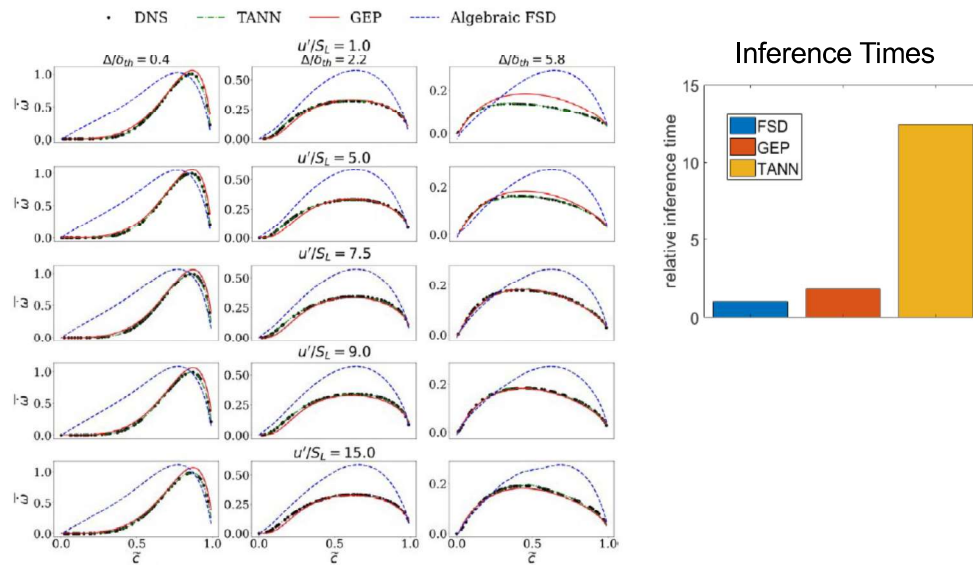
GEP recovered Clarks model including an appropriate model constant !

Closing the filtered reaction rate [2]



Instantaneous filtered reaction rate from DNS (left), full NN using 11 input parameters, compact NN using only 3 parameters (after feature importance analysis), and algebraic FSD model.

Closing the filtered reaction rate [3]

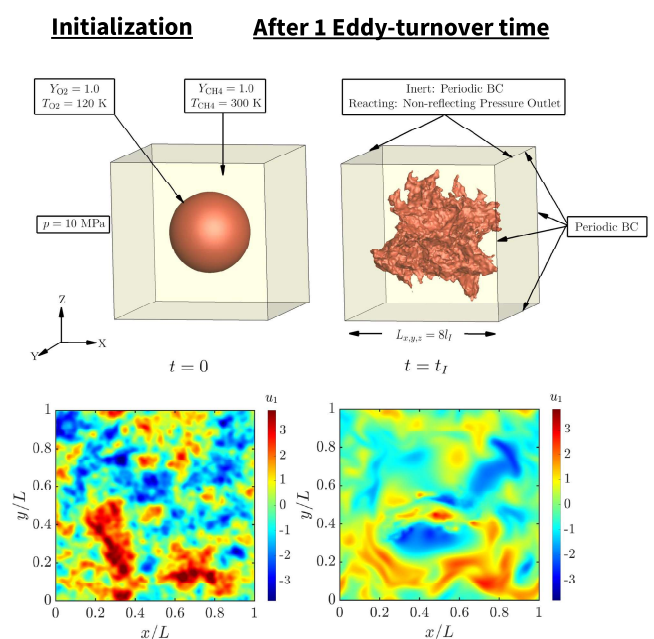


Normalised filtered reaction rate profiles from DNS, GEP, TANN (=Tiny ANN), and algebraic FSD model expressions for 3 Δ and 5 u'/S_L .

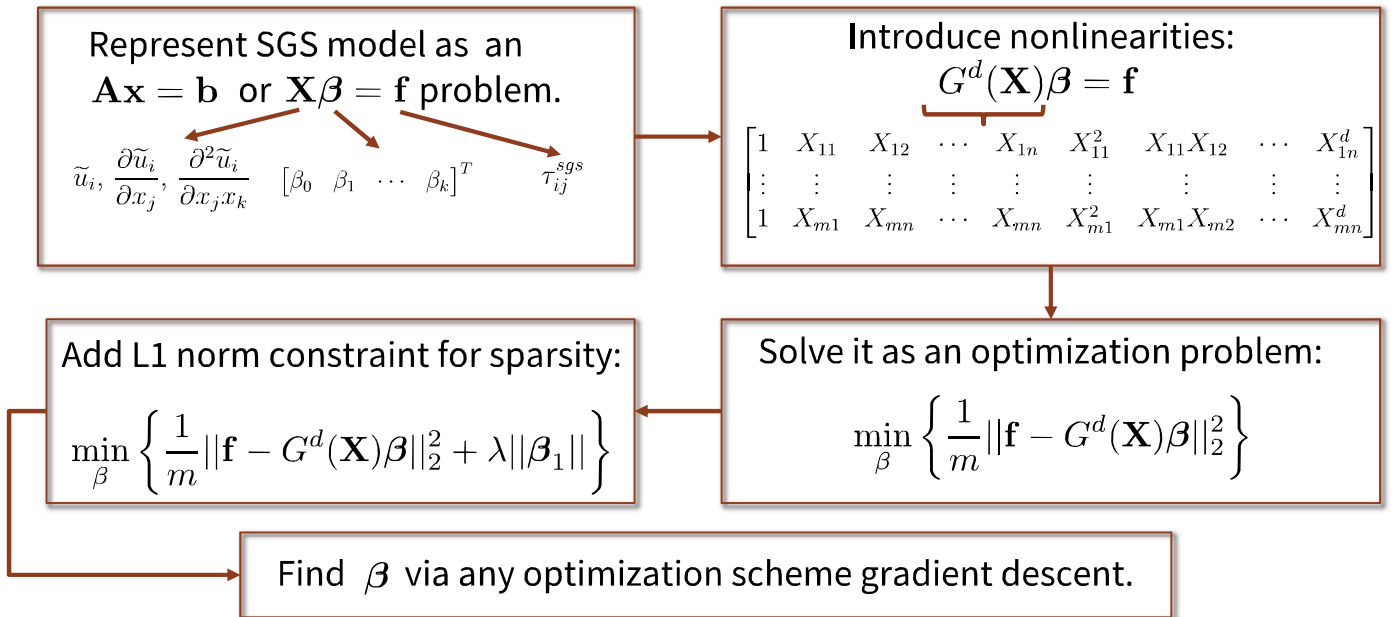
Problem formulation

Computational Setup

- DNS: 128^3 domain and $\Delta x = O(\eta_K)$
- Diffuse Interface Method
- Peng-Robinson Cubic EoS
- CH₄/O₂ chemistry: 5-species
- Initial conditions: von Karman/Pao spectrum and decaying turbulence
- Initial scalar flowfield initialized with 1D counterflow diffusion flame



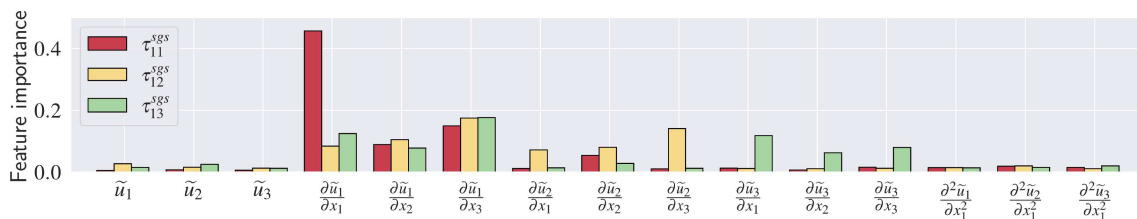
Sparse symbolic regression for model discovery



Stanford University

Sparse regression for model discovery

- Can be computationally expensive as cost scales with MN^d
- Feature importance is measured through mean decrease in node impurity



Feature importance simplifies sparse symbolic regression for model discovery

$$\frac{\tau_{ij}^{sgs}}{\rho u'^2} = f_{ij} \left[G^{d=2} \left(\frac{\tilde{u}_i}{u'}, \frac{\bar{\Delta}}{u'} \frac{\partial \tilde{u}_i}{\partial x_j}, \frac{\bar{\Delta}}{u'} \frac{\partial \tilde{u}_j}{\partial x_i}, \frac{\bar{\Delta}^2}{u'} \frac{\partial^2 \tilde{u}_i}{\partial x_j \partial x_k}, \frac{\bar{\Delta}^2}{u'} \frac{\partial^2 \tilde{u}_j}{\partial x_i \partial x_k}, \frac{\bar{\Delta}^2}{u'} \frac{\partial^2 \tilde{u}_k}{\partial x_i \partial x_i} \right) \right]$$



$$\frac{\tau_{ij}^{sgs}}{\rho u'^2} = f_{ij} \left[G^{d=2} \left(\frac{\bar{\Delta}}{u'} \frac{\partial \tilde{u}_i}{\partial x_k}, \frac{\bar{\Delta}}{u'} \frac{\partial \tilde{u}_j}{\partial x_k} \right) \right]$$

Stanford University

Sparse regression for model discovery

$$\frac{\tau_{ij}^{sgs}}{\bar{\rho} u'^2} = f_{ij} \left[G^{d=2} \left(\frac{\bar{\Delta}}{u'} \frac{\partial \tilde{u}_i}{\partial x_k}, \frac{\bar{\Delta}}{u'} \frac{\partial \tilde{u}_j}{\partial x_k} \right) \right]$$

↓ Apply sparse symbolic regression

$$\tau_{11}^{sgs} \simeq \bar{\rho} \bar{\Delta}^2 \left(0.116 \frac{\partial \tilde{u}_1}{\partial x_1} \frac{\partial \tilde{u}_1}{\partial x_1} + 0.191 \frac{\partial \tilde{u}_1}{\partial x_2} \frac{\partial \tilde{u}_1}{\partial x_2} + 0.207 \frac{\partial \tilde{u}_1}{\partial x_3} \frac{\partial \tilde{u}_1}{\partial x_3} \right)$$

$$\vdots$$

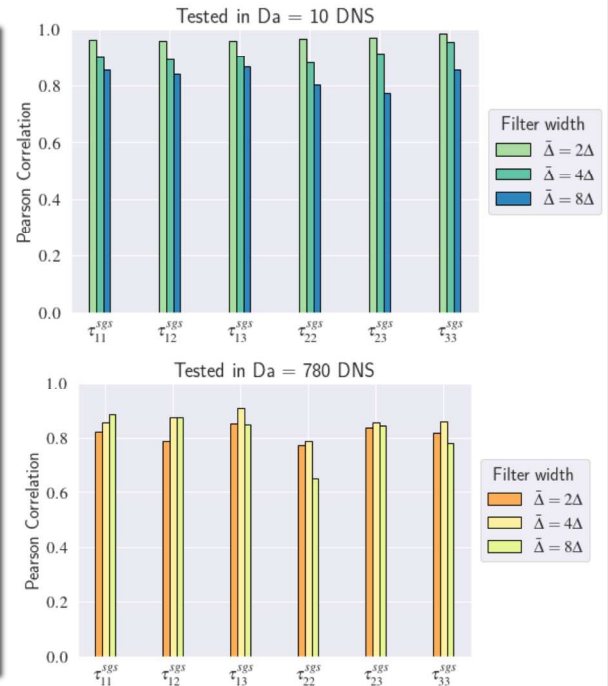
$$\tau_{33}^{sgs} \simeq \bar{\rho} \bar{\Delta}^2 \left(0.251 \frac{\partial \tilde{u}_3}{\partial x_1} \frac{\partial \tilde{u}_3}{\partial x_1} + 0.177 \frac{\partial \tilde{u}_3}{\partial x_2} \frac{\partial \tilde{u}_3}{\partial x_2} + 0.124 \frac{\partial \tilde{u}_3}{\partial x_3} \frac{\partial \tilde{u}_3}{\partial x_3} \right)$$

↓

$$\tau_{ij}^{sgs} \simeq \bar{\rho} C_x \bar{\Delta}^2 \frac{\partial \tilde{u}_i}{\partial x_k} \frac{\partial \tilde{u}_j}{\partial x_k}$$

~1/6

**Rediscovered
Clark and Ferziger's
Gradient Model!**



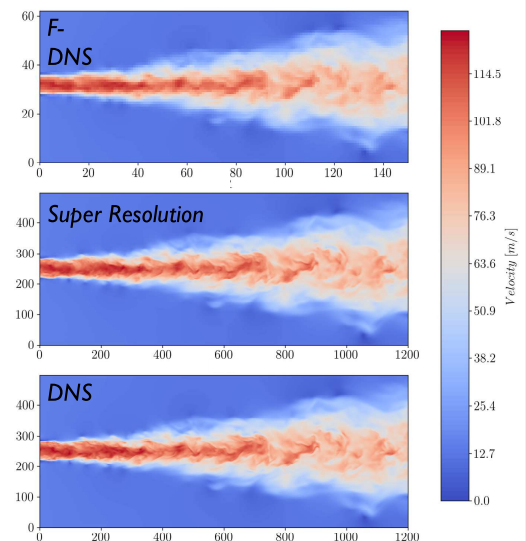
Generative model for LES of turbulent premixed reacting flows

L. Nista¹, C. Schumann¹, T. Grenga¹,
M. Bode¹, A. Attili², H. Pitsch¹

¹Institute for Combustion Technology, RWTH Aachen University, DE

²School of Engineering, University of Edinburgh, UK

Premixed Turbulent Flame workshop, 22-23 July 2022, Vancouver, CA



Introduction: data-driven closure modeling

Large Eddy Simulation and closure modeling

$$\frac{\partial \bar{\rho} \tilde{u}_j}{\partial t} + \frac{\partial \bar{\rho} \tilde{u}_i \tilde{u}_j}{\partial x_i} = - \frac{\partial \bar{p}}{\partial x_j} + \frac{\partial \bar{\tau}_{ij}}{\partial x_i} - \frac{\partial \bar{\rho} \tau_{ij}^r}{\partial x_i}$$

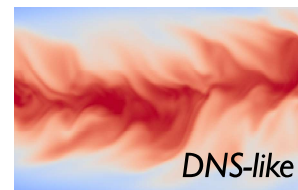
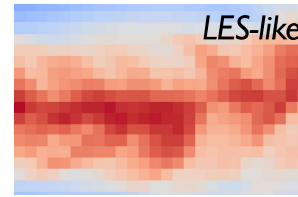
$$\frac{\partial \bar{\rho} \tilde{\Psi}_k}{\partial t} + \frac{\partial \bar{\rho} \tilde{u}_j \tilde{\Psi}_k}{\partial x_i} = - \frac{\partial \bar{\rho} \tau_j^T}{\partial x_j} + \frac{\partial}{\partial x_j} \left(\bar{\rho} D_k \frac{\partial \tilde{\Psi}_k}{\partial x_j} \right) + \bar{\Phi}_k$$

➤ **data-driven**: through **super-resolution**

$$\tau_{ij}^r = \overline{u_i u_j} - \tilde{u}_i \tilde{u}_j \text{ (unresolved stress tensor)}$$

$$\tau_j^T = \overline{u_j T} - \tilde{u}_j \tilde{T} \text{ (unresolved scalar flux)}$$

evaluated at DNS resolution



given
upsampling
factor

originally proposed by Bode et al.,
Proc. Combust. Inst., 2021^[1]

74

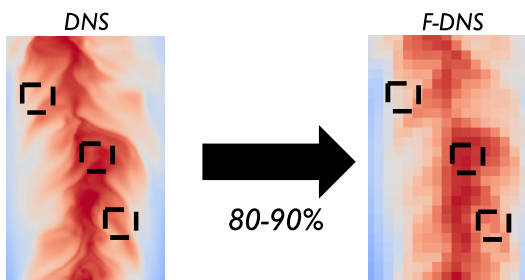
Institute for Combustion Technology | Ludovico Nista

[1]: M. Bode et al., "Using physics-informed enhanced super-resolution generative adversarial networks for subfilter modeling in turbulent reactive flows", Proc. Combust. Inst., 2021.



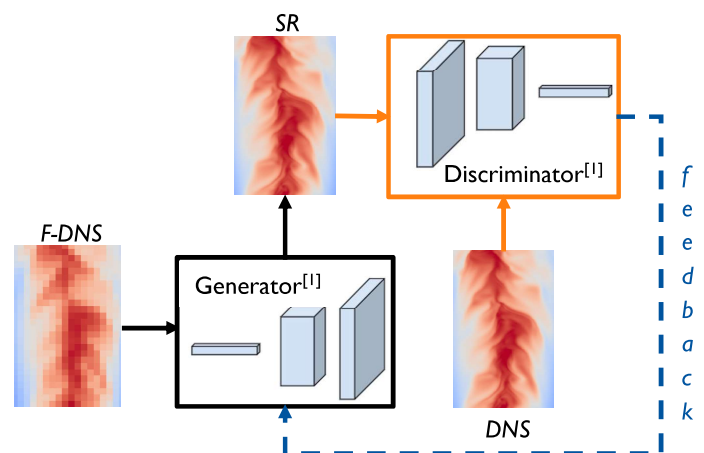
Methodology: Super-Resolution Generative Adversarial Network (SRGAN)

Preprocessing



- filtering the DNS dataset (e.g. *box* or *gaussian* kernel) to obtain the input data
- extracting sub-boxes to be used during the training
- normalizing input variables: $(u, v, w, T) \in [0, 1]$

GAN architecture



$$L_{gen} = \beta_1 L_{pixel} + \beta_2 L_{gradient} + \beta_3 L_{disc}$$

75

Institute for Combustion Technology | Ludovico Nista

[1]: Nista et al., "The influence of adversarial training on turbulence closure modelling", AIAA SciTech 2022 Forum, 2022.



CombML for experimental analysis

- Physical understanding and discovery
- Discovery of structures, combustion-regime, and coherent feature
- Construction of low-order models for control-oriented applications
- Data-generation

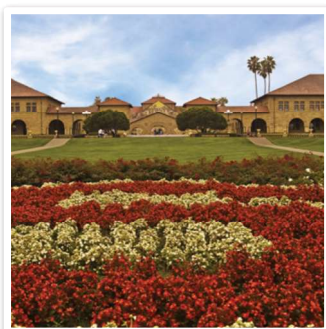
CombML for combustion modeling

- Parameterization of combustion manifolds
- Data augmentation and data generation
- Combustion-closure models
- Physical embedding to reduce computational cost

Stanford University

Shashank and Bruce

NREL



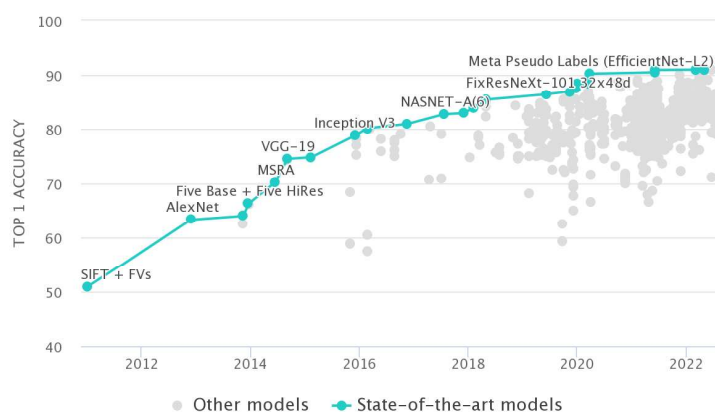
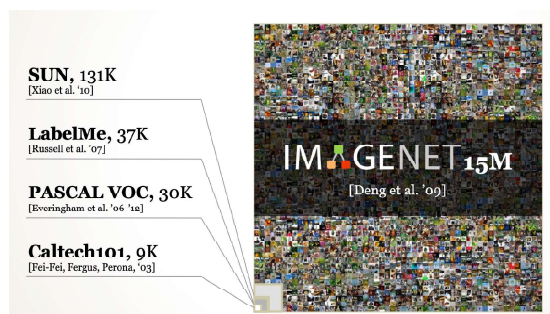
Stanford University

RESEARCH OPPORTUNITIES AND NEEDS



CombML @ TN/PF

Need for community effort



Stanford University

CombML @ TN/PF: Community-driven database

BLASTNet aims to **curate 100 different reacting DNS flow configurations**

- Extension to incorporate experimental data
- **Provides tutorials** for sharing and accessing data, ML-samples
- **Stores metadata** in consistent JSON format
- Compression and unstructured data to deal with large data sets (>100 GB)
- **Provides standards and guidelines** for shared data
- **Hosts discussion forum** for user support and community feedback
- Growing list-of-authors to include each contributor for **fair attribution**

BLASTNet

Bearable Large Accessible Scientific Training Network-of-Datasets

[About](#)
[Datasets](#)
[Tutorials](#)
[Contribute](#)
[Cite Us](#)
[Contact Us](#)

A Network-of-Datasets for Scientific Big Data

Step 1: Collect Data → **Step 2: Compress** → **Step 3: Upload to Kaggle** → **Step 4: Consolidate Kaggle Links and Important Metadata** → **Step 5: Training Data is now Accessible**

About

This Bearable Large Accessible Scientific Training Network-of-Datasets (BLASTNet) is composed of:

- Involvement from the scientific community
- Public Machine Learning (ML) repositories such as Kaggle
- Lossy compression techniques for managing >100 GB data
- An easily-accessible webpage. (You're browsing it right now!)

Right now, our efforts are focused on community outreach for **contributions** from 100 different reacting and non-reacting flow physics simulations.

We are also interested in experimental measurements and all kinds of data from other fields so please **contact us** if you're interested in collaborating.

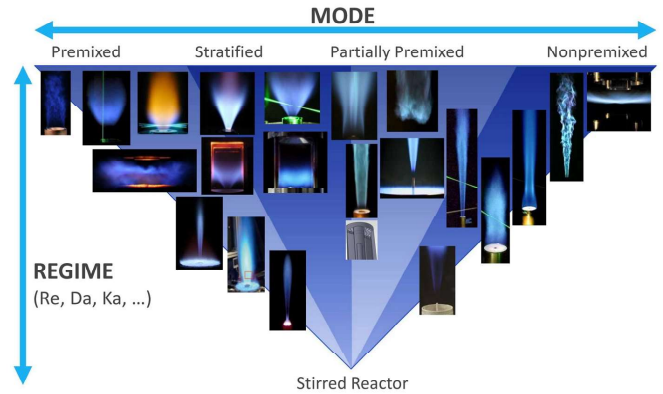
<https://blastnet.github.io>

Stanford University

CombML @ TN/PF

What experimental configurations to consider

- Driven by scientific questions
- Flame series with parametric variations in operating conditions, fuels, ...
- Scatter data
- Planar images
- High-speed image sequences
- Simultaneous measurements



Stanford University

CombML @ TN/PF

CombML-specific challenges

- Interpretability and explainability
- Quantifying uncertainties of CombML models
- Evaluation out-of-distribution predictions
- Integrating domain knowledge in CombML
- Computational complexity and accuracy

Stanford University

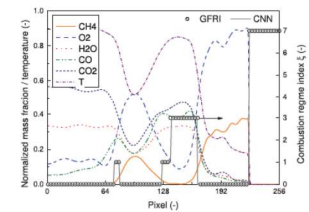
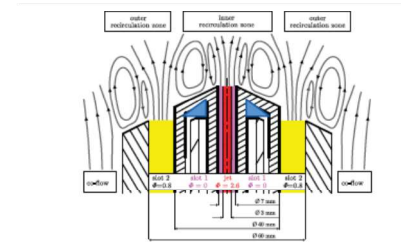
CombML @ TN/PF

Benchmark problems for ML-applications

- Combustion-regime identification
- Feature identification
- Manifold parameterization
- Combustion modeling

TN/PF participation

- ML-model benchmark
- Share ML-models through TN/PF infrastructure
- Establish best practice



Stanford University

CombML @ TN/PF

Want to contribute? send email to mihme@stanford.edu and wtchung@stanford.edu

Stanford University

TNF/PTF Workshops

Blank Page

Closing Panel Discussion Summary: Key Points, Opportunities, & Priorities

Ahmed, Dreizler, Hasse (chair), Ihme, Im

Initially, the scientific focus of the two workshops PTF (premixed flames) and TNF (non-premixed flames) was clearly distinguished from each other. In recent years, it has become apparent that the physical challenges as well as the experimental and numerical methods have converged more and more. The TNF workshop for some time also considers partially premixed and stratified flames, therefore "non-premixed" was dropped from the title.

However, the structure of the two workshops is fundamentally different. The PTF workshop is organized like a mini symposium with a series of presentations that reflect the richness of the community's work. The TNF workshop is more in the nature of a workshop. Historically, the talks have been grouped along particular flame configurations, e.g., for piloted partially premixed jet flames. For the experimental data sets, particular attention was paid to a well characterized set of boundary conditions (wall temperatures, inflow boundary conditions etc.). These experimental data were provided to interested groups for model development and simulation (initially RANS, now LES). The coordinator contacted all groups prior to the TNF workshop, and they provided selected simulation results, e.g., temperature or mixing fraction on specified lines. At the workshop, the numerical results of the different simulations were then plotted against each other and compared with the experiments. Progress on the models was discussed and unsolved challenges were identified. For the most part, this showed a common progress every two years. Models improved, experimental data became more complete, or additional flames/further metrics were provided. Future reference configurations were jointly discussed to explore the limits of the models ("break the models").

By combining the two workshops, there were PTF style presentations as well as discussions around flame configurations, in line with the previous TNF format. Other sessions, such as premixed H_2 , combined elements from both sides.

In the final discussion, we took up the key points of the two days. The challenges for the future are especially new fuels for CO_2 -neutral/ CO_2 -free combustion (H_2 , NH_3 , and blends, MeOH, EtOH, OME, DMC, SAF). Secondly, physical phenomena or conditions of turbulent flames, including high Ka, high pressure, turbulent flames close to the stability limit, flame wall interactions are of particular interest. As a starting point for the discussion, three possible targets for the next 2 years were formulated:

1. Consolidated chemistry for NH_3 – use in DNS and LES
2. Transport processes/differential diffusion in turbulent flames (esp. new fuels)
3. Experimental and DNS configurations that build on TNF heritage

The key outcomes of the discussion were:

There is a great need for NH_3 kinetics, so kinetics experts from our community should be integrated into the workshop. The goal is to have a common mechanism for DNS and LES.

Reference configurations for the new fuels will be defined, with two possible options

1. Some blends can probably be investigated in known reference burners. For this purpose, planning is currently underway at the various locations, including Darmstadt and KAUST. The big advantage for the modeling is that simulation setups are available, and several groups worldwide have experience regarding the specifics of the respective configurations. From previous TNF workshops there is extensive knowledge regarding the comparison of the simulations.
2. New burners, e.g. for pure H_2 or NH_3/H_2 mixtures, are currently under development. These can be either a new design or a modification of previous configurations. One example is the stratified/steam diluted H_2 burner (CORIA, EM2C) as a further evolution of the previous burner from T. Schuler. Depending on the funding opportunities in the respective countries, several new configurations are expected to become available in the next few years.

Regarding the quantities to be quantified experimentally, the discussion participants emphasized that NO is a crucial quantity for the validation of the model. This should be measured locally in laminar and turbulent flames.

DNS should be integrated into the investigations from the beginning and provide further information that the experiments and LES cannot deliver. As far as possible, phenomena such as flame stabilization and ignition should also be investigated. LES of the DNS configuration could become a part of the model comparisons like the reference experiments.

The participants in the discussion are in favor of having a TNF 15.5 in about a year's time, in preparation for TNF16 in Milan.